-i-

THE INTERACTION BETWEEN ROTARY VALVES
AND PNEUMATIC CONVEYING PIPELINES

by

Stephen Ronald Kessel

Thesis submitted for the degree of Doctor of Philosophy
to the Council for National Academic Awards

School of Engineering
Thames Polytechnic
London SE18 6PF

December 1985

ABSTRACT

THE INTERACTION BETWEEN ROTARY VALVES AND
PNEUMATIC CONVEYING PIPELINES

by

S R KESSEL

The object of this work was to investigate the interaction between rotary valves and pneumatic conveying pipelines and the effect which this can have on overall system performance.

A review of previous work and current industrial practice revealed that very little work has been published on this subject, although it was evident that some manufacturers of pneumatic conveying systems do have preferred entrainment configurations. Consequently, a preliminary experimental investigation was undertaken with a transparent model of a rotary valve and drop-out box in order to observe the air and solid flow patterns inside the drop-out box. This provided the most important outcome of this work, that is, the discovery that two distinctly different modes of flow can exist in the chamber of a conventional drop-out box. The first of these is a turbulent swirling motion caused by the conveying airstream and is the most desirable operating condition because it results in the most effective entrainment of material into the conveying line. The second is a situation where the drop-out box is effectively 'choked' with product.

Models to explain these two condidtions have been developed and subsequently tested against data obtained from a full size positive pressure conveying system specifically constructed for this purpose. An extensive experimental programme has been carried out in which the performance of this system was examined with a selection of different entrainment configurations and different test materials. The principal variables investigated were the height and volume of the drop-out box, the orientation of the rotary valve with respect to the pipeline and the conveying air velocity.

As a result of this work guidelines have been produced for inter-facing rotary valves with pneumatic conveying pieplines. These have been presented as a simple list of eight points and it is anticipated that they will enable systems to be designed with more confidence than has been possible previously.

Acknowledgements

I wish to thank Dr A R Reed for both instigating and supervising this research and Dr J S Mason for his assistance and guidance throughout.

The contribution of the technical staff of the School of Engineering was invaluable. In particular I would like to thank Mr W Churchill, Mr J Milton, Mr S Curtis and Mr J Wood. Without their assistance the construction of the experimental rig would have been impossible. My thanks also go to Mr G Smith and Mr G Gowers for their help with instrumentation.

The research was partically funded by collaboration with twelve different companies and acknowledgement is made for their contributions. These companies were, in alphabetical order:

Blue Circle Technical
B P Chemicals Ltd
Bush and Wilton Valves Ltd
Kemutec
MAS
National Coal Board
Rank Hovis Ltd
Rota Val Ltd
STB Engineering Ltd
Sturtevant Engineering Co Ltd
Wade Engineering Ltd
Westinghouse Systems Ltd

Apart from those immediately connected with this research I would also like to thank my other colleagues at Thames Polytechnic for their help and assistance. Particular thanks go to the staff of the Central Services Unit and to Dr R J Hitt, Dr P van Manen and Mr I R Bittle for many hours of stimulating conversation. Special thanks also go to Mrs A Pearson for the typing of this thesis.

Finally, I would like to thank my wife, Barbara, for her patient support during the writing of this thesis.

Author's Note

The contents of this thesis are the sole and original work of the author, except where stated otherwise by acknowlegement or reference. The views expressed are not necessarily those of the collaborating companies.

It has been the author's policy to publish some of the results of the research prior to writing this thesis. To date, four papers have been published which are, in order of publication:

'An investigation into the flow behaviour in the entrainment section of a rotary valve fed pneumatic conveying system.'
Proc Pneumatech I. International Conference on Pneumatic Conveying Technology, Stratford on Avon, UK, May 1982.

'The relationship between power consumption and pick-up velocity in a dilute phase pneumatic conveying system.'
Proc 9th Annual Powder and Bulk Solids Conference, Chicago, USA, 15th-17th May 1984.

'Current research into the performance of rotary valves.'
Proc Pneumatech II. International Conference on Pneumatic Conveying Technology, Canterbury UK, September 1984.

'A review of methods used for predicting the power requirements of dilute phase pneumatic transport systems.'
Proc International Symposium-Workshop and 16th Annual Meeting of the Fine Particle Society, Miami Beach, Florida USA, 22nd-26th April 1985.

CONTENTS

Chapter Four   Modelling of the Interaction between
     Rotary Valves and Pneumatic Conveying
     Pipelines

Chapter Five   Industrial Scale Experimental Rig

Chapter Six   Experimental Plan and Presentation of Data

Chapter Seven   Experimental Study

Chapter Eight   Conclusions

CHAPTER ONE

OUTLINE OF STUDY

1.1 Introduction

1.1.1 Rotary Valves and Feeders

Rotary valves are volumetric feeders used for the feeding and metering of particulate solid materials. They are simple devices in both concept and construction; basically consisting of a bladed rotor which turns in a fixed housing. On top of this housing is an inlet port and on the bottom an outlet port, see Figure 1.1. As the rotor turns, material supplied to the inlet is transferred through the valve, in the pockets formed between the rotor blades, and discharged from the outlet. Thus rotor speed is the principal means of controlling feed rate and is set by the valve capacity and the throughput required. Normal operating speeds range from 5 to 50 rev/min.

INLET PORT   MATERIAL IN

ROTOR   HOUSING

OUTLET PORT   MATERIAL OUT
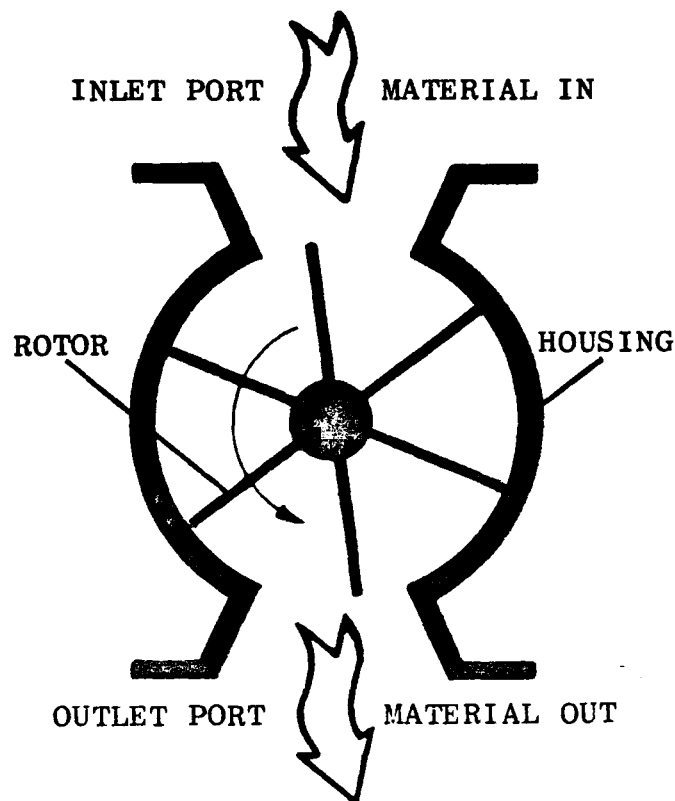
Figure 1.1   Schematic diagram of a drop-through rotary valve

Since they are volumetric devices the overall size of a valve is dictated by the maximum throughput needed. Rotors with capacities from 100 ml to more than 1000 l are produced; thus throughputs of a few kilogrammes per hour to several hundred tonnes per hour are possible. The rotor length is usually the same as its diameter and most manufacturers take the latter as the nominal size of the valve. The majority of valves made are between 150 and 300 mm. These are the sizes which are most compatible with the throughputs of systems used in the process industry, by far the largest users of rotary valves.

The detailed construction and operation of a valve depends upon two main factors. These are the condition and bulk characteristics of the material to be handled and the situation in which the valve is to be used. Material conditions and characteristics influence the choice of:

   i)   the shape and position of the inlet and outlet ports;

   ii)   the shape of the rotor pockets;

   iii)   the running clearances between the rotor and housing; and

   iv)   the materials of construction and surface finishes with respect to wear, corrosion and adhesion.

Consequently many variations to the basic design have been developed to cope with the diverse range of materials that are handled. Examples of some common valve configurations are shown in Figure 1.2.

The situations in which rotary valves are used can be categorised into three groups:

   a)   where the air pressure at the inlet and outlet ports is nominally the same;

   b)   where the air pressure at inlet is less than that at outlet, that is, where the valve is used to feed against an adverse pressure gradient; and

   c)   where the air pressure at inlet is greater than that at outlet, that is, where the valve is used to feed in the same direction as the pressure gradient.

These categories can be used to make a distinction between rotary valves and rotary feeders. Rotary feeder is the name commonly used for applications where the air pressure at the inlet and outlet ports

OFFSET INLET

OFFSET OUTLET

FLEXIBLE ROTOR BLADES

BRUSH OR SCRAPER

ADJUSTABLE BLADE TIPS

WATER COOLED HOUSING

LOW FRICTION COATINGS

SCALLOPED ROTOR

SPRING LOADED BLADE TIPS
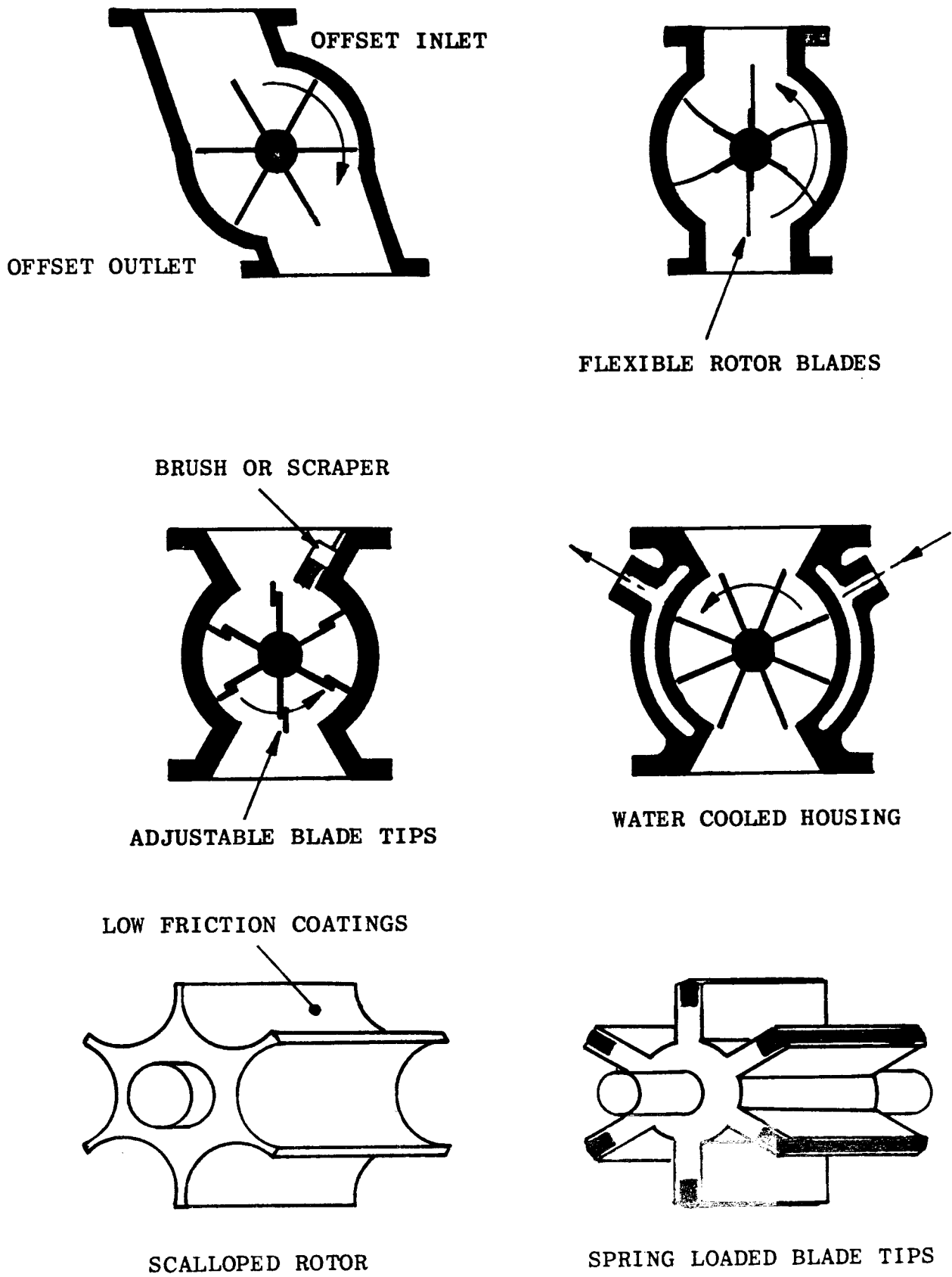
Figure 1.2   Some   Rotary Valve and Rotor Designs

is the same. In such circumstances, the feeder is simply a metering
device and is not required to function as an air seal. Conversely,
rotary valve is the name used in situations where the air pressures at
inlet and outlet are different. Rotary valves are essentially the same
as rotary feeders but perform the additional task of providing an air
seal. In reality a perfect seal is impossible to achieve because of
the running clearances which are necessary between the rotor blades and
housing; however if these are small enough (typically 0.1 mm in a
200 mm valve) the air leakage can usually be kept within acceptable
limits.

The practical maximum pressure ratio to which a single rotary valve
should be subjected is about 2. When feeding material from atmospheric
pressure against an adverse pressure gradient this corresponds to a
pressure at the outlet port of about 1 bar gauge. At pressures
greater than this the air leakage usually becomes excessive and can
cause problems with pocket filling.

1.1.2 Rotary Valves and Pneumatic Conveying Systems.

Pneumatic conveying systems are used extensively by industry for the
handling and transport of bulk particulate materials. As the name
implies, air or another gas is used as the medium to carry material
through a pipeline. This may be achieved by either suction, that is
negative pressure, or blowing, that is positive pressure, see Figure 1.3.
There are many different types of system but an important group are
those which use a rotary valve as the solids feeding device; these
account for about 50% of all pneumatic conveyors in current use.
Rotary valves are used in this application because of their ability to
transfer material between different pressures and at the same time
provide an effective air seal. This is essential, since, by definition,
the pressure in a pneumatic pipeline will be different to that of the
surrounding atmosphere.

Positive pressure systems work with pipeline pressures greater
than atmospheric. Consequently, valves used to feed such systems
operate in situation 'b' described in Section 1.1.1, that is, they
deliver material into the system against an adverse pressure gradient.
In this application the sealing characteristics of the valve are used
to restrict the air loss at the feed point. This minimises the
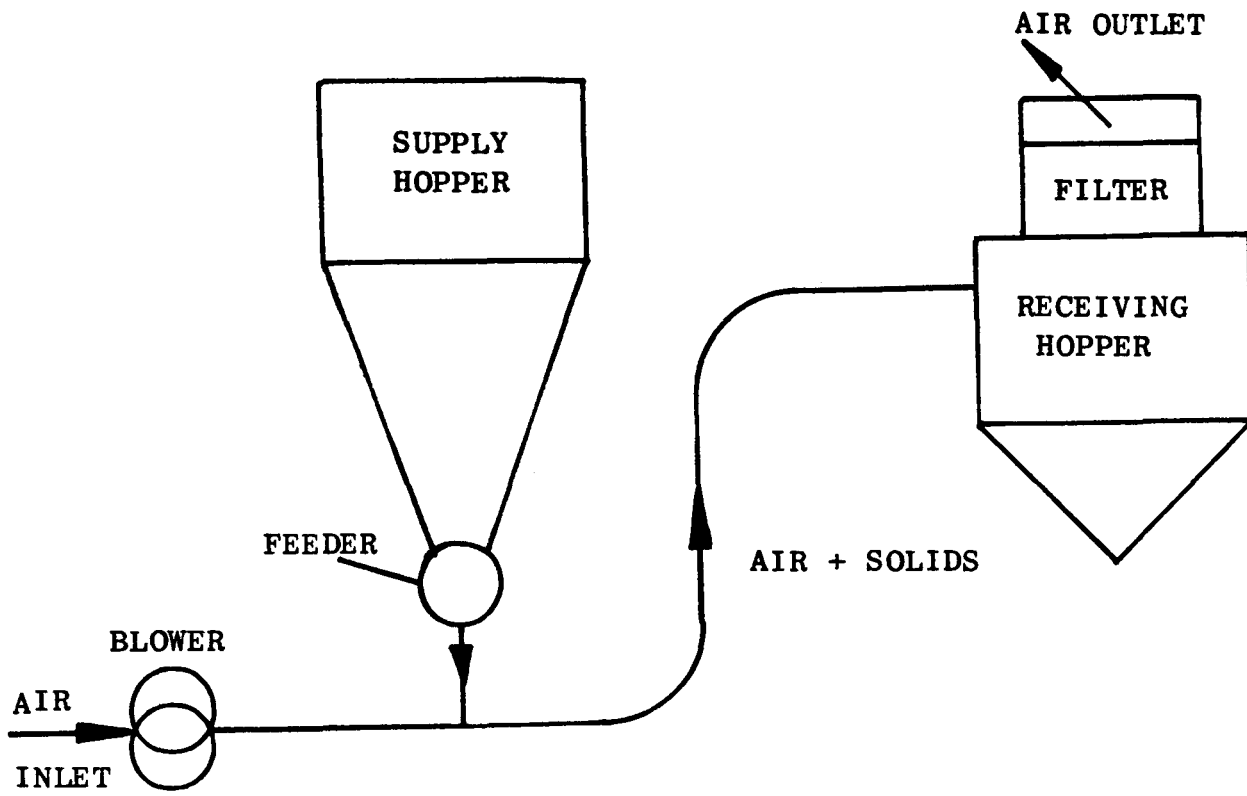
Figure 1.3a   Schematic Diagram of a Positive Pressure Pneumatic
               Conveying System
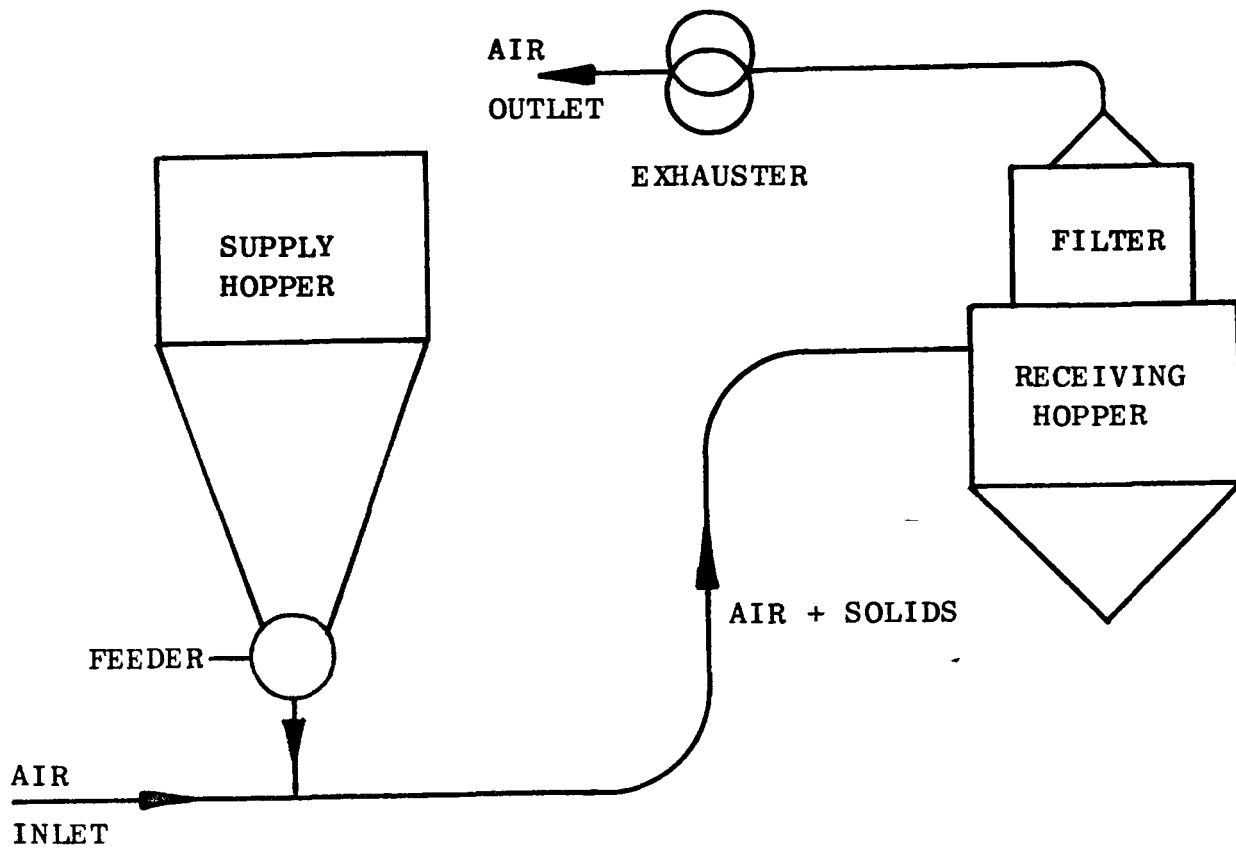
Figure 1.3b   Schematic Diagram of a Negative Pressure Pneumatic
               Conveying System

demand on the air supply and allows the pipeline pressure to be main-
tained.   Practical limitations usually restrict the pipeline pressure
to a maximum of about 1 barg.   However, operation at higher pressures
is sometimes achieved by using two valves connected in series, see
Figure 1.4.
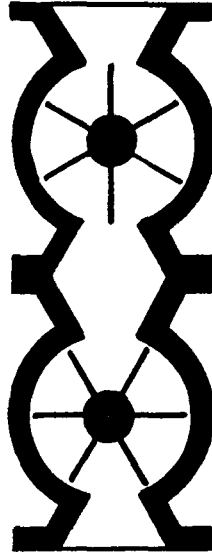
Figure 1.4   Two Rotary Valves Connected in Series

Rotary valves which are used to feed negative pressure systems
operate under conditions corresponding to situation 'c' described in
Section 1.1.1.   Since the pressure gradient in this case is in the
direction of product feed, the main function of the valve is simply to
regulate the feed rate.   Air leakage is not usually a problem in
vacuum systems unless there is more than one feed point.   In such
cases the sealing function of the valve is important in order to
maintain the depression in the pipeline.

Most rotary valves used for feeding pneumatic conveying systems
are of the conventional 'drop-through' type illustrated in Figure 1.1.
To enable them to feed a pipeline a discharge adaptor, commonly called
the 'drop-out box', is fitted to the outlet port.   This is a simple
transition section which forms a 'T' shaped junction with the pipeline
and provides a mixing chamber for the air and solids, see Figure 1.5.

As an alternative to this arrangement another type of rotary valve
is available, specifically for use in pneumatic conveying systems.   It
is called a 'blowing seal' or 'blow through' valve and is connected
directly into the pipeline, thus avoiding the need for a drop-out box.

This allows the conveying airstream to blow through the discharging
rotor pocket/s ensuring that they empty completely.   Figure 1.6
shows a typical example of such a valve.

Blowing seals are used for materials which will not readily
discharge from the pockets of a conventional drop-through valve.
They require less headroom than a drop-through valve but are not as
suitable for potentially abrasive products.
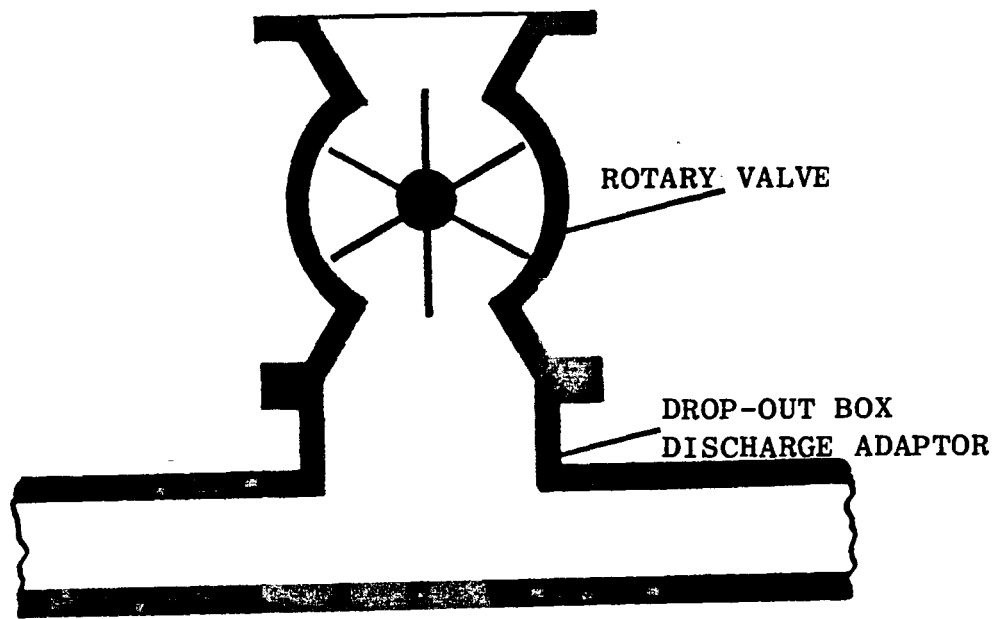
Figure 1.5   Rotary Valve and Drop-out Box
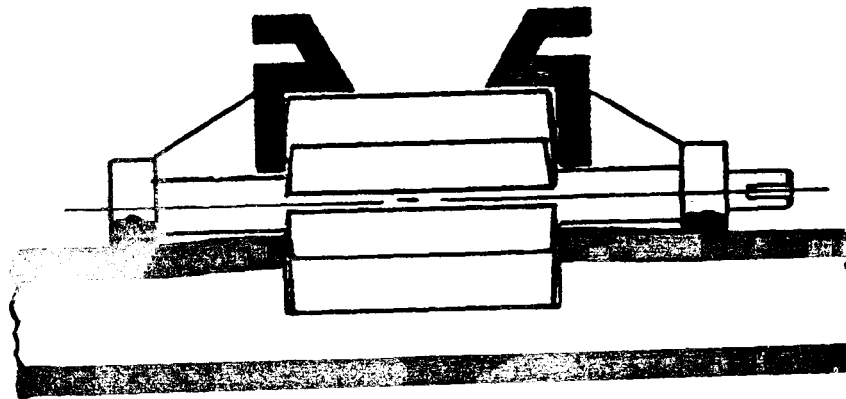
Figure 1.6   Blowing Seal or Blow Through Type of Rotary Valve

1.1.3 Industrial Problems and Reasons for the Research

Despite their widespread acceptance, industrial experience has shown that rotary valves used to feed pneumatic conveying systems commonly suffer from operating problems.   Indeed, this has prompted the Head of Research and Development of the largest industrial chemical company in the United Kingdom to remark: '.....rotary valves are often the Achille's heel of pneumatic conveying systems.'   Dobie (1).   Positive pressure systems are particularly troublesome because of the adverse pressure gradient in which the valve must work.   However, these problems are not always the fault of the valve itself but of the components it is connected to, and the way in which it interacts with them.   For convenience the feeding system of a pneumatic conveyor may be divided into three regions:

    i)   the interface of the supply hopper and valve;

    ii)   the rotary valve; and

    iii)   the interface of the valve and pipeline, commonly
        called the entrainment region.

In a well designed feeding system the performance of these must be matched such that each is capable of passing the required throughput under the particular conditions of airflow and pressure.   The interface of the valve and supply hopper and the valve itself have both been the subject of considerable previous research.   As a result, it is now possible to estimate the performance of these areas with a reasonable degree of certainty.   Unfortunately, this is not the case for the entrainment region about which there are many unanswered questions. These include:

    a)   Is there a 'best' orientation of the valve with
        respect to the pipeline?

    b)   Is the direction of rotation of the rotor in
        relation to the pipeline important?

    c)   Is the size and shape of the drop-out box important?

    d)   Does the air velocity in the entrainment region
        affect feeding performance?

    e)   In what way do the characteristics of the material
        to be handled affect answers to the preceeding questions?

.

With systems being 'designed' in the absence of satisfactory answers to these questions, it is not surprising to hear comments such as that quoted from Reference 1. Some system designers have their own preferred arrangements for the entrainment region, largely based upon practical experience. However, these are often contradictory and invariably based on rather dubious reasoning. Consequently, there is a clear need to investigate the interaction between valve and pipeline in order to provide an independent and co-ordinating assessment of the parameters which are believed to affect entrainment. The principal objective of this thesis is to describe the outcome of such an investigation.

1.2 Object of the Research

The object of the research is to provide an explanation of the process by which rotary valves feed particulate materials into positive pressure pneumatic conveying pipelines. In particular, attention is focussed on understanding the interaction between the air and solids which takes place at the interface of the valve and pipeline. This is a crucial part of a pneumatic conveyor because it can directly influence the over-all system performance.

It is envisaged that the research will ultimately lead to the formulation of guidelines for use by industry. These will allow systems to be designed with a greater degree of confidence than is currently possible.

1.3 Synopsis of Thesis

Recent investigations into rotary valve performance and current industrial practice regarding the interface of the valve and pipeline are reviewed in Chapter 2. The current 'state of the art' for predicting the performance of rotary valves is appraised, thus identifying areas requiring further investigation. This endorses the need for the research expressed in Section 1.1.3.

Some initial flow visualisation studies are described in Chapter 3. This work used a model rig to observe the nature of the air and solid flows in the entrainment region of a pneumatic conveyor. These observations were used to determine which parameters should be more

closely examined in further experiments and indicate approaches for modelling the interaction between the air and solids. Chapter 4 describes the models which were subsequently proposed.

On the basis of this initial work, further experimental investigations were conducted on an industrial size test rig. The significant features of this rig are described in Chapter 5 and the experimental plan and presentation of results are discussed in Chapter 6. Chapter 7 details the results of these investigations which are then used to appraise the mathematical models developed in Chapter 4.

The final chapter evaluates the contribution of this research to explaining the interaction between rotary valves and pneumatic conveying pipelines and discusses its value to industry. On the basis of this evaluation, guidelines are recommended for the selection of suitable entrainment configurations.

The thesis concludes with recommendations for further work.

CHAPTER TWO

REVIEW OF RECENT WORK AND CURRENT
INDUSTRIAL PRACTICE

2.1 Introduction

Although rotary valves have been in widespread use for many years,
research with a view to providing a rigorous understanding of how they
work has only taken place in comparatively recent times. This is
probably because they are essentially simple devices and as such were
considered unworthy of detailed investigation. However, with the use
of these valves in modern process plant and conveying systems it is
becoming more important to understand their characteristics and the
way in which they interact with other system components.

This chapter reviews the progress made by recent studies
in understanding the operation of rotary valves and their use for
feeding pneumatic conveying pipelines. Current industrial practice
regarding the interfacing of valves and pipelines is discussed with
examples of some proprietary drop-out box designs. The chapter
concludes with an appraisal of the current 'state of the art' for
predicting the performance of rotary valves.

2.2 The Performance of Rotary Valves

2.2.1 The Effect of Hopper Discharge Characteristics on Valve
Performance

The most simple concept of the way in which a rotary valve or feeder
works is that the rotor pockets completely fill and discharge at
regular intervals with material fed to them by a supply hopper. In
such circumstances the volumetric feed rate ($\dot{V}_s$) is directly
proportional to the rotor speed (n) and is given by:

$$\dot{V}_s = \frac{n}{60} V_o \qquad (2.1)$$

where n has the units of rev/min. This represents a measurable
quantity for any feeder, since the constant of proportionality (V_o)
is the volumetric capacity of the pockets per revolution of the rotor.
Alternatively, multiplication of this equation by a representative bulk
density (ρ_b) of the material filling the pockets gives the feed rate
on a mass basis $(\dot{m}_s)$, that is:

$$\dot{m}_s = \frac{n}{60} V_o \rho_b \qquad\qquad (2.2)$$

In practice the actual bulk density of the material in the rotor pockets
is difficult to determine and consequently the 'poured' value is
commonly used as an alternative.

Although this approach for predicting the feed rate suggests that
it increases continually with rotor speed, in practice it is limited
by the maximum discharge rate of product through the interface of the
supply hopper and the rotary valve, see Figure 2.1.
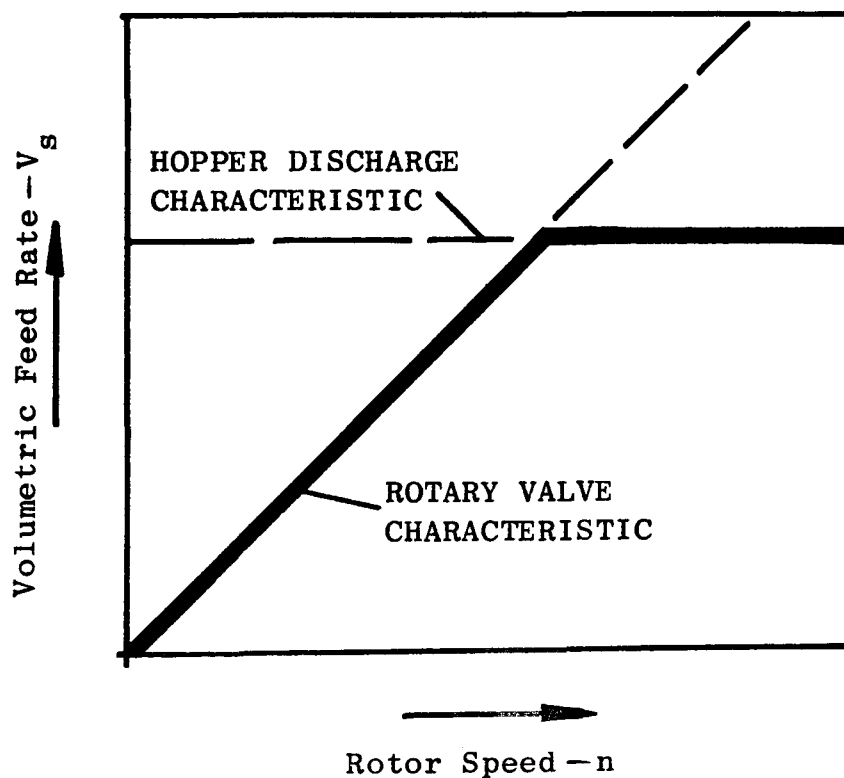
Figure 2.1   The Limiting Effect of the Hopper Discharge
             Characteristics on Volumetric Feed Rate

Since there are operational limitations to the rotor speed, the
maximum throughput of the valve is usually less than the unrestricted
discharge rate of the hopper, especially when the material being

handled is coarse and of a free flowing nature.   However, with fine
particle products this is not always so, particularly if the outlet of
the hopper is subjected to an adverse air pressure gradient.   Such
conditions can lead to a situation where the hopper discharge rate is
considerably lower than that obtained with coarser particles of the
same density, see Figure 2.2.   Whilst this is an area of considerable
ongoing research, a unified approach to predicting the discharge rate
from hoppers for all types of materials has yet to be developed.   Some
notable work in this field is given in References 2 to 8.
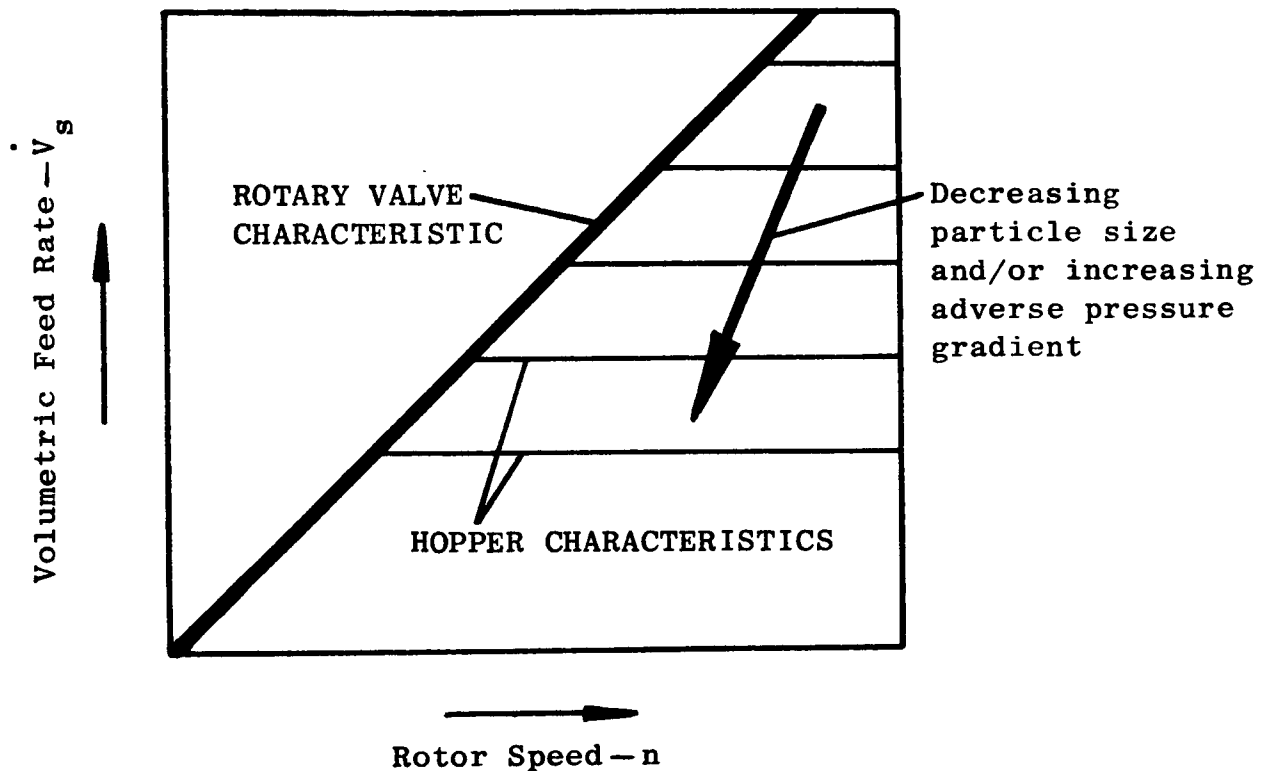
Figure 2.2   The Effect of Particle Size and Adverse
             Pressure Gradient on the Feed Rate
             Characteristics of a Hopper and Rotary
             Valve

Al-Din & Gunn (9) recognised that hopper discharge characteristics
could limit the maximum throughput of a rotary feeder and conducted a
series of small scale tests which demonstrated this.   Their results·
showed that the feed rate was dependent on the feeder characteristics
up to a certain rotor speed and dependent on the hopper characteristics
above this speed.   This may be taken as confirmation of the ideas
suggested earlier in Figure 2.1.   Furthermore, they showed that the
feed rate at high rotor speeds was dependent on the size of the inlet
port.   This is illustrated by Figure 2.3 which shows their results
for three different widths of the inlet port.   By using a modified
form of the Beverloo equation (5) for estimating the
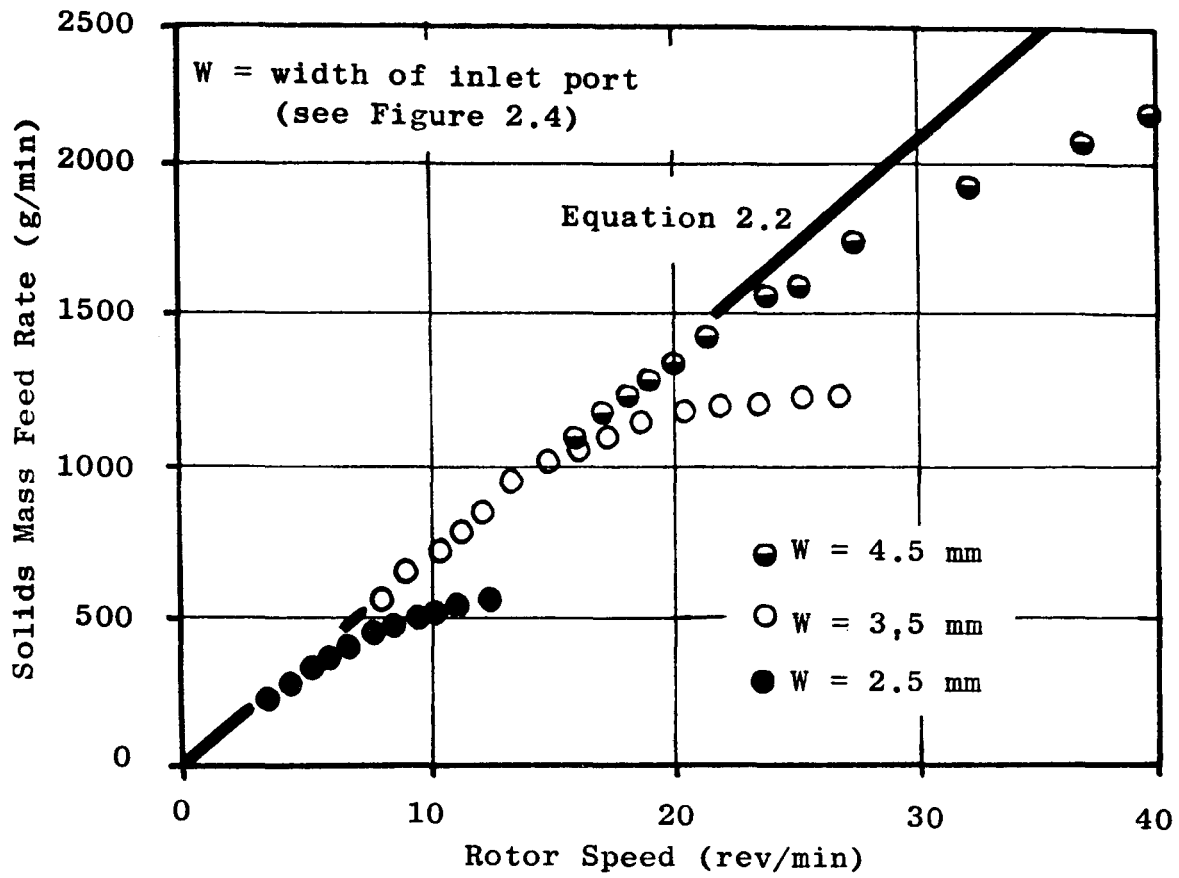
Figure 2.3   Experimental Results of Al-Din & Gunn (9) for 500 μm Glass Ballotini
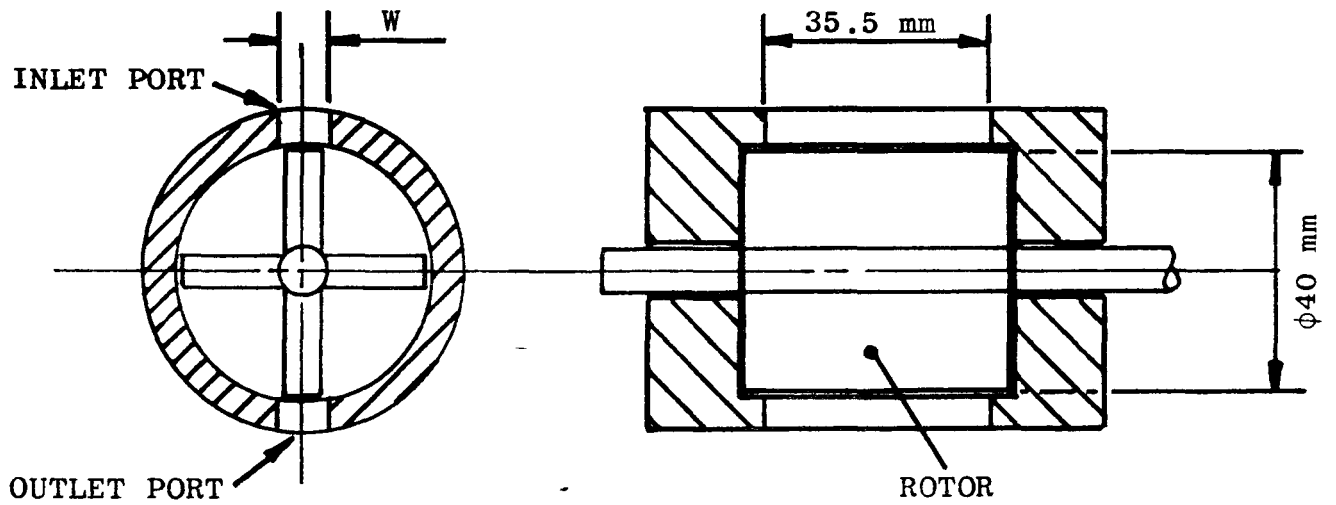
Figure 2.4   Rotary Feeder used by Al-Din & Gunn (9)

flow rate of solids through an orifice, they were able to correlate
their results for two materials and produce a general equation for the
performance of the feeder.　Unfortunately, the proportions of the
feeder which they used for their experimental work were very different
to those of the proprietary feeders which are used by industry.　In
particular, the length of the rotor and the angular size of the inlet
port were both very small compared with industrial feeders, see Figure
2.4.　Consequently, the application of their work to conventional
rotary feeders and valves is difficult to justify.　For instance, if
the dimensions of a typical 200 mm rotary feeder handling a free flowing
material of 1.0 mm mean particle size are substituted into their model,
it predicts that the maximum feed rate occurs at a rotor speed of only
10 rev/min.　However, it is known from work referred to in later
sections of this chapter that, in practice, the feed rate with such a
combination of valve and material would continue to increase up to
speeds of the order of 100 rev/min.　The significant implication of
this is that in the majority of industrial situations the discharge
rate of the hopper will be greater than the take-away rate of the
rotary feeder.　In such situations there are other factors which
limit the maximum feed rate and these will be discussed in the following
section.

2.2.2　Valve Filling Characteristics and the Concept of Critical Rotor Speed

The first notable academic study of rotary valves was published in
1970 by Jotaki & Tomita (10).　This was the first of a series of
papers by these authors specifically concerned with this subject.
The equipment they used for their investigation enabled them to examine
the performance of a rotary valve feeding against an adverse pressure
gradient.　The purpose of this was to simulate the conditions to which
these valves are often subjected when used in process plant and
pneumatic conveying systems.

　　　A diagram of their experimental rig is shown in Figure 2.5.　It
consisted of a 150 mm drop-through rotary valve mounted between a
supply hopper and receiving/weighing vessel.　The parameters which
could be varied were:　·　the head of material above the valve, the
pressure in the receiving vessel and the speed of the rotor.
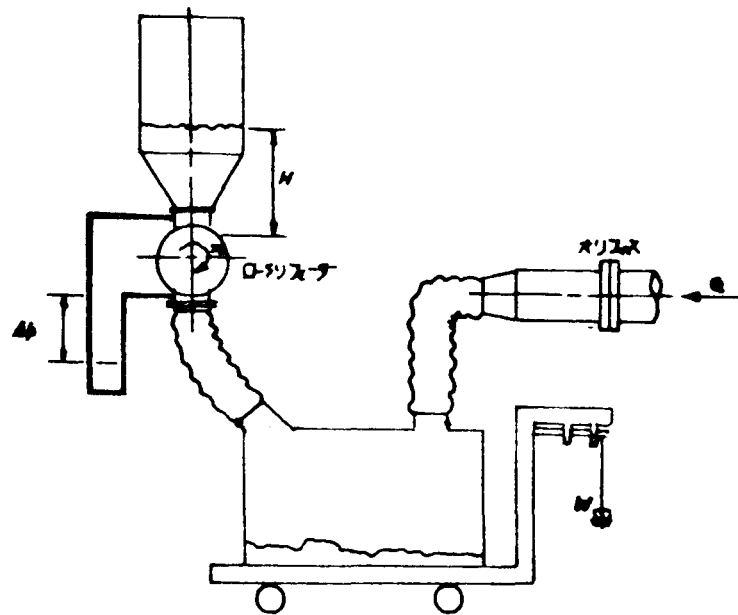
Figure 2.5   Experimental Apparatus used by Jotaki & Tomita

They investigated the relationship between throughput and rotor
speed both with and without an applied pressure gradient.   In each
case their results showed that there was a linear relationship between
these two variables up to a certain rotor speed.   Beyond this speed,
the throughput was observed to decrease in the manner shown by Figure
2.6.   They argued that this behaviour was the result of the reduced
time available for material to enter the rotor pockets and proposed
the concept of a 'maximum rotor speed'.   This being the speed at which
the pockets are exposed to the inlet port only just long enough to
allow complete filling.   In a later study Reed (11) called this the
'critical rotor speed' (n_{crit}) and this is the terminology which will be
used throughout this thesis.

To explain their reasoning Jotaki & Tomita used two mathematical
models of the pocket filling process; one applicable to speeds below the
critical value and the other applicable to speeds above this.   At
lower speeds they assumed that the pockets completely fill and calculated
the mass throughput simply as the product of rotor speed, volumetric
displacement of the rotor pockets per revolution and the bulk density of
the material.   That is, the relationship given by equation 2.2, namely:

REGION OF COMPLETE
POCKET FILLING

REGION OF
INCOMPLETE
POCKET FILLING

CRITICAL ROTOR
SPEED

(n_{crit})

Volumetric Feed Rate - $\overset{\circ}{V}_S$
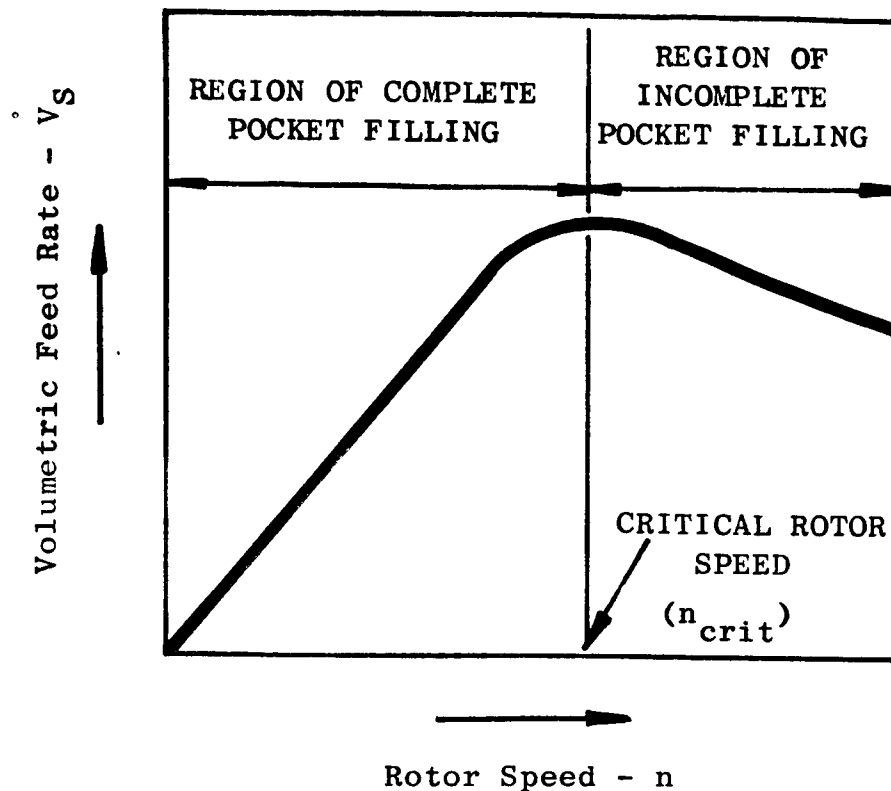
Rotor Speed - n

Figure 2.6   Typical Relationship Between the Volumetric Feed
             Rate and Rotor Speed for a Drop-through Rotary
             Valve

$$\dot{m}_s = \frac{n}{60} V_o \rho_b \qquad (2.2)$$

Above the critical speed they used the equation of motion for a single
particle in free fall to calculate the volume of material which can
enter a pocket during the time (t_o) that it is open to the inlet port.
This produced the following expression for the mass throughput:

$$\dot{m}_s = \frac{30}{n} \rho_b \frac{gw\ell}{Z} \qquad (2.3a)$$

where g is the gravitational constant, w is the width of the inlet port,
ℓ its length and Z the number of rotor blades as defined in Figure 2.7.

Unfortunately the value of t_o which Jotaki & Tomita used to
derive equation 2.3a is only correct for the particular case where the
angular size of the inlet port is equal to the rotor pocket pitch,
that is, $2\pi/Z$ radians.   They put t_o equal to 60/Zn seconds, which is
the time taken for the rotor to turn through an angle equal to the
pocket pitch.   However, if the angular size of the inlet port is not
equal to the pocket pitch, as is usually the case, t_o will be equal
to $60\ell/\pi d_r n$ seconds.   This is the time taken for the rotor to turn
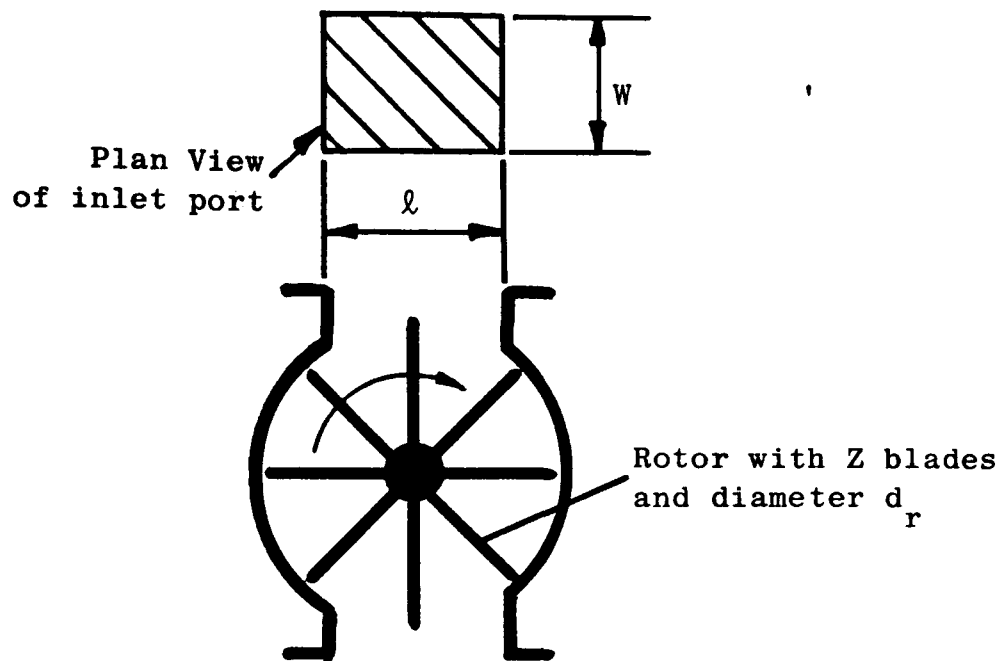
Figure 2.7   Dimensions of the Rotary Valve used in the Models
              Developed by Jotaki & Tomita

through an angle equal to the size of the inlet port and thus is the
effective duration for which the pocket is open to the inlet port.
Reed (11) realised this and proposed a pocket filling model based on
the free fall simplification in which he put t_o equal to $60\ell/\pi d_r n$
seconds.   Consequently, he proposed the following expression for the
mass throughput above the critical rotor speed:

$$\dot{m}_s = \frac{30}{n} \, \rho_b \, \frac{gw\ell^2}{\pi d_r}$$ (2.3b)

This is of more general applicability than the Jotaki & Tomita expression
because it does not presume that the dimensions of the inlet port and rotor
pocket pitch are the same.

Reasoning that both equation 2.2 and equation 2.3a are valid at
the critical rotor speed (n_{crit}), Jotaki & Tomita equated them and
solved for n to obtain an expression for that speed:

$$n_{crit} = \left(\frac{1800 \; gw\ell}{ZV_o}\right)^{\frac{1}{2}}$$ (2.4a)

Reed also proposed the same argument and hence produced the following
alternative expression for n_{crit} by the simultaneous solution of
equations 2.2 and 2.3b:

$$n_{crit} = \left(\frac{1800 \; gw\ell^2}{\pi d_r V_o}\right)^{\frac{1}{2}} \tag{2.4b}$$

Although these expressions suggest that n_{crit} is only a function of
valve geometry, Jotaki & Tomita's experiments showed it to vary with
the type of material being handled and the pressure difference across
the valve, see Figure 2.8. This discrepancy was the result of their
decision to use a free fall model for speeds greater than the critical
value. Realising this, they suggested that a coefficient be used to
take account of the effects of air drag on the falling solids and the
head of product above the valve. Consequently, they proposed the
following modified relationships:

$$\dot{m}_s = 30 \; C_1 \; \frac{\rho_s}{n} \; \frac{gw\ell}{Z} \; \ldots\ldots \; \text{for } n > n_{crit} \tag{2.5}$$

and

$$n_{crit} = \left(C_1 \; \frac{1800 \; gw\ell}{ZV_o}\right)^{\frac{1}{2}} \tag{2.6}$$

Figure 2.9 shows how the critical rotor speed and throughput predicted
by these relationships both vary with the coefficient C_1. Comparing
this with the experimental results shown in Figure 2.8 it can be seen
that the effect of reducing the value of C_1 is broadly the same as
increasing the pressure difference across the valve. However, the
precise shape of the characteristics is not predicted and the effect of
pressure difference on throughput in the complete filling region is not
modelled, for example, see the results for glass beads, Figure 2.8b.

   This last effect results from the air leakage dilating the material
entering the valve, thus reducing its bulk density and consequently the
mass throughput. As the pressure gradient is increased so the air
leakage increases, further exacerbating the problem. Jotaki & Tomita
noted this behaviour but did not make any attempt to model it. The
effect was not observed with soya beans, Figure 2.8a, presumably because
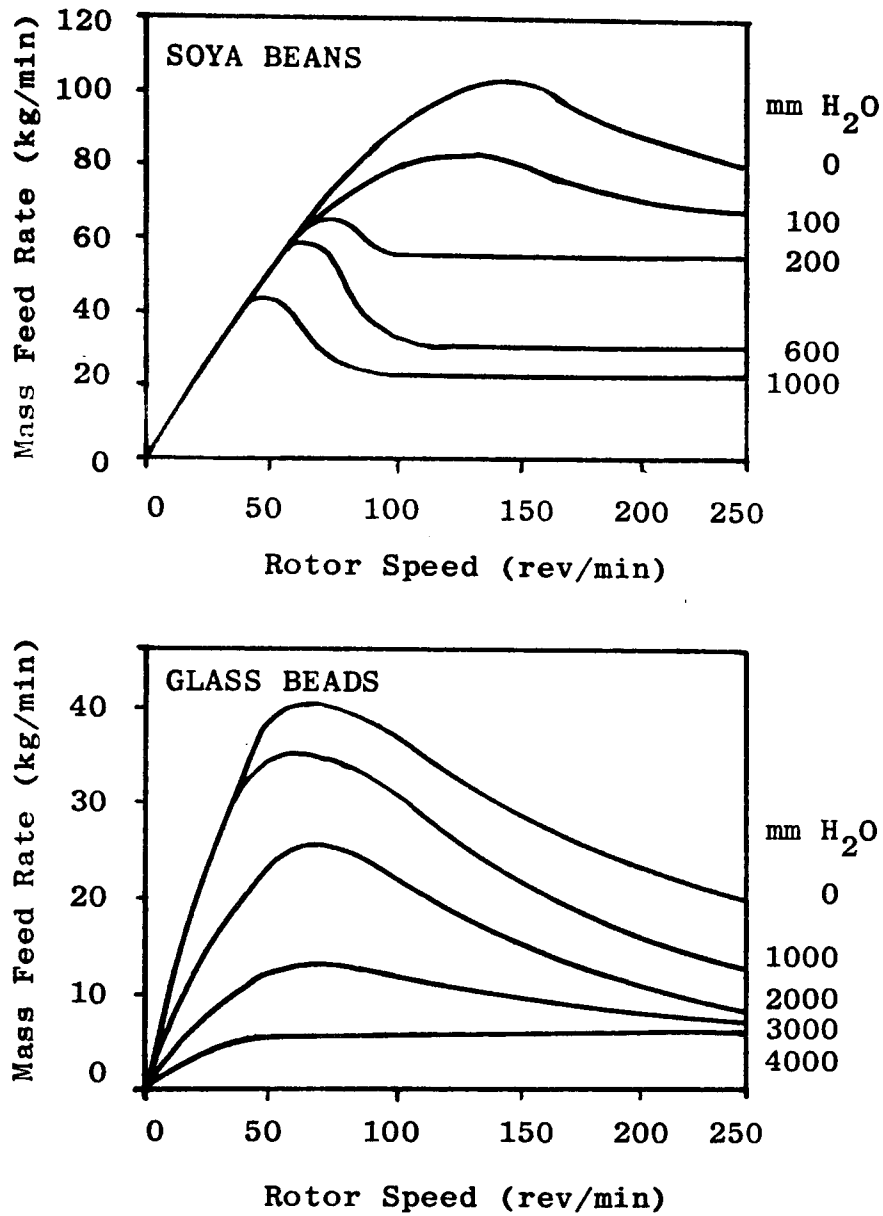
Figure 2.8   Experimental Results Obtained by Jotaki & Tomita (10) for Soya Beans and Glass Beads
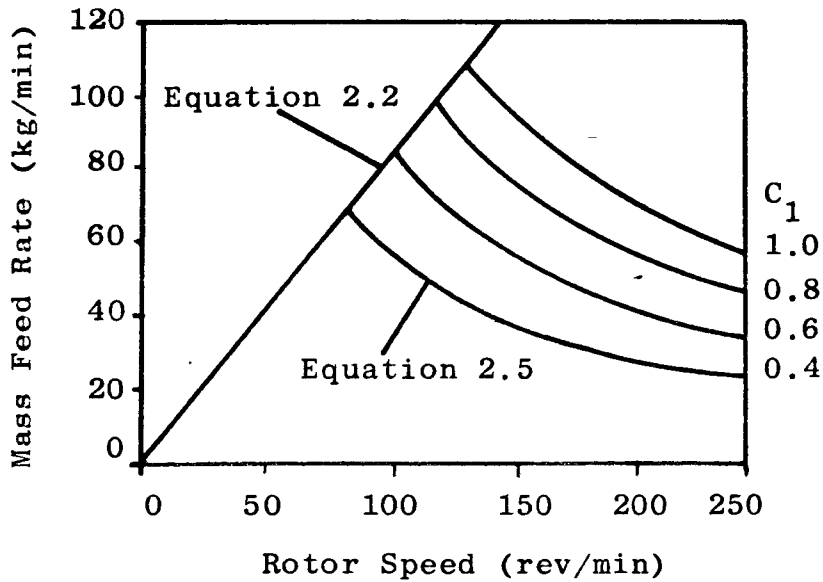
Figure 2.9   Feeding Characteristics Predicted by Jotaki & Tomita

the large interstices between the particles of this material permits
the air to escape without significant dilation.

The usefulness of Jotaki & Tomita's modelling depends on the
reliable determination of typical values for the coefficient C_1.
Unfortunately, this is virtually impossible because it is a rather crude,
all embracing factor, dependent on many variables. However, later work
by these authors, References 12 and 13, showed that the critical rotor
speed for granular materials is reasonably predicted by the simple free
fall model. That is, putting C_1 equal to unity in equation 2.6. This
was confirmed by Reed (11), who conducted a similar investigation to
Jotaki & Tomita. Reed's work suggested that the free fall model gives
an upper limit to the value of the critical rotor speed which can only be
attained with products having a mean particle size greater than about
3.0 mm. For finer products he argued that it is necessary to consider
the effect of other forces. In particular, that which results from
the displacement of air by material as it fills the rotor pockets.
This impedes pocket filling and thus reduces the critical rotor speed.
Subsequently Reed developed a model which attempted to allow for this
effect.

Jotaki & Tomita also recognised that the interaction between air
and solids could restrict pocket filling, as evident from their decision
to incorporate the coefficient C_1 into their model. However, realising
that this was an over simplistic approach, they later developed a
refined model which avoided the need for such a coefficient. The
following section describes this and also the model which was proposed
by Reed.

2.2.3 Pocket Filling Models which Consider the Interaction of Material with Air

Jotaki & Tomita (12 & 13) produced a pocket filling model which
considered the interaction of material and air by analysing the motion
of a single particle falling under its own weight, in still air, and
opposed only by air drag. The equation of motion for such a particle
is:

$$m_p \frac{d^2 y_p}{dt^2} = m_p g - \tfrac{1}{2}\rho_a \left(\frac{dy_p}{dt}\right)^2 \frac{\pi d_p^2}{4} C_d \qquad (2.7)$$

where m_p is the mass of the particle, d_p is the particle diameter and y_p is the vertical distance fallen. By assuming the Stokes' law relationship for the drag coefficient they integrated this to obtain an expression for the distance which a particle falls in time t, that is, $y_p(t)$:

$$y_p(t) = gt_* \left[t - t_*(1 - \exp(-t/t_*)) \right] \qquad (2.8)$$

The term t_* is a function of the particle size, its density (ρ_p) and the dynamic viscosity of air (μ). It is given by:

$$t_* = \frac{\rho_p d_p^2}{18\mu} \qquad (2.9)$$

Since this has the unit of seconds, Jotaki & Tomita called it the 'particle relaxation time.'

Making the questionable simplification that a body of particles will fall at the same rate as a single particle; they multiplied the expression for $y_p(t)$ by the area of the inlet port (wℓ) in order to calculate the volume (v) of material which enters a pocket as it passes the inlet. That is:

$$v = w\ell y_p(t_o) \qquad (2.10)$$

where t_o is the time that a pocket is open to the inlet port. Jotaki & Tomita put this equal to 60/Zn seconds[*]. Further multiplying by $Zn\rho_p/60$ they obtained the following expression for the filling rate, and hence the mass throughput, of a valve operating above the critical rotor speed:

$$\dot{m}_s = \frac{Zn}{60} \rho_b w\ell gt_* \left[\frac{60}{Zn} - t_*(1 - \exp(-60/Znt_*)) \right] \qquad (2.11)$$

---

* footnote: See discussion about t_o in section 2.2.2.

Unlike their previous model, all the terms in this expression are,
or can be derived from, measurable quantities.   The material
characteristics are taken into account by the particle relaxation
time.

Reed (11) used a similar method of analysis to Jotaki & Tomita
but chose to consider the motion of a bed of particles displacing the
air within a pocket rather than the air drag on a single particle.
This approach is much closer to the situation in the real system.   He
wrote the equation of motion of the bed of particles as:

$$P_b hA\frac{dC}{dt} = \rho_b hAg - \Delta P_h A \qquad (2.12a)$$

where C is the velocity of the bed of particles relative to a pocket
of stationary air, ΔP_h is the pressure difference across depth h of the
bed and A is the horizontal area of flow.   Re-arranging this equation
he obtained a relationship for the acceleration of the bed:

$$\frac{dC}{dt} = g = (\Delta P_h / h)\frac{1}{\rho_b} \qquad (2.12b)$$

Into this, Reed substituted an expression for the pressure drop per
unit length $(\Delta P_h / h)$, which had been formulated by Carman (14) for a
fluid flowing through a bed of granular solids.   This correlation was
initially derived from considerations of the Hagen-Poiseuille treatment
of laminar flow through circular ducts applied to the flow through
homogeneous beds of stationary, granular, mono-sized solids.   This
allowed the expression to be written in the integrateable form:

$$\frac{dC}{dt} = g - KC \qquad (2.13)$$

where K is a constant solely dependent on the characteristics of the
solids and the dynamic viscosity of air.   Reed called it the 'material
characteristic factor', and it has an equivalent role in his analysis
to that of the 'particle relaxation time' used by Jotaki & Tomita.
The factor has the unit of frequency and is given by:

$$K = \frac{180\mu}{\rho_p}\frac{(1 - \varepsilon)}{\varepsilon^3 (d_p \phi)^2} \qquad (2.14)$$

where ϵ is the voidage of the bed $(1 - \rho_b/\rho_p)$ and ϕ is a particle shape factor.

By integrating the equation for the acceleration of the bed, Reed was able to obtain an expression for the vertical distance it travels in time t, that is $y_b(t)$:

$$y_b(t) = \frac{g}{K} \left[t - \frac{1}{K} (1 - \exp(-Kt)) \right]$$ (2.15)

This is identical in form to the expression for $y_p(t)$, equation 2.8, which was developed by Jotaki and Tomita, but with t_* replaced by $1/K$. This difference is very important because it means that $y_b(t)$ can be used to estimate the pocket filling rate without making the highly questionable simplification that a body of particles will fall at the same rate as a single particle. Consequently, Reed calculated the volume of material which enters a single pocket as:

$$v = w \frac{\pi d_r}{Z} y_b (\frac{60\ell}{\pi d_r n})$$ (2.16)

where d_r is the rotor diameter, $\pi d_r/Z$ the rotor blade pitch and $60\ell/\pi d_r n$ is the length of time that a pocket is engaged with the inlet port. From this, he derived the following expression for the filling rate of a valve operating above the critical rotor speed:

$$\dot{m}_s = \frac{Zn}{60}\rho_b w \frac{\pi d_r}{Z} \frac{g}{K} \left[\frac{60\ell}{\pi d_r n} - \frac{1}{K} (1 - \exp(- \frac{60\ell}{\pi d_r n} K)) \right]$$ (2.17)

As with the free fall model, equating this or the equivalent Jotaki & Tomita expression, equation 2.11, with the complete filling model enables the critical rotor speed to be predicted. Figure 2.10 shows how the predicted feedrate and critical rotor speed change with the functions K and t_*. From this it can be seen that when K is small, or t_* is large, the critical rotor speed approaches that predicted by the free fall model. This is consistent with Reed's argument that the free fall model predicts an upper limit for the value of the critical rotor speed.

The difference between feedrates, and hence critical rotor speeds, which are predicted by the Reed and Jotaki & Tomita models can be large.

This is illustrated in Figure 2.11 which compares the predictions of
these models for similar materials.   This difference occurs because
t_* and $1/K$ are not the same for any given material.   This can easily
be demonstrated by comparing these two functions.

Reed proposed that K could be calculated as:

$$K = 1.296 \times 10^{-2}/d_p^2 \rho_p \qquad (2.18)$$

This is based on the expression given earlier with $\varepsilon = 0.5$, $\varsigma = 1$
and $\mu = 1.8 \times 10^{-5}$ Ns/m^2.   He justified this simplification on the
basis that these represent typical values which are reasonable
approximations for many different materials.   If this is accepted and
the same value of μ is used to calculate t_*, it can be shown that:

$$t_* = \rho_p d_p^2/3.24 \times 10^{-4} \qquad (2.19)$$

Hence, for any given material:

$$t_* = 40 \frac{1}{K} \qquad (2.20)$$

Consequently, for a given material, the critical rotor speed
predicted by the Jotaki & Tomita model will always be greater than that
which is predicted by the Reed model.

2.2.4   Critical Rotor Speed Ratio $(n_{crit}/n_{crit\ max})$

The 'critical rotor speed ratio' was suggested by Reed (11) as a means
of correlating experimental results obtained from different size
feeders.   It is the ratio of the actual or predicted critical rotor
speed to the maximum critical rotor speed which is obtained by equating
the free fall and complete pocket filling models.

Figure 2.12 shows the relationship between the critical rotor
speed ratio and the material characteristic factor.   Reed used this
diagram to compare his model with the experimental data of four
independent workers.   From this he concluded that the model adequately
predicts the critical rotor speed for coarse particle products which
have a value of K < 1.   That is, materials with a mean particle size
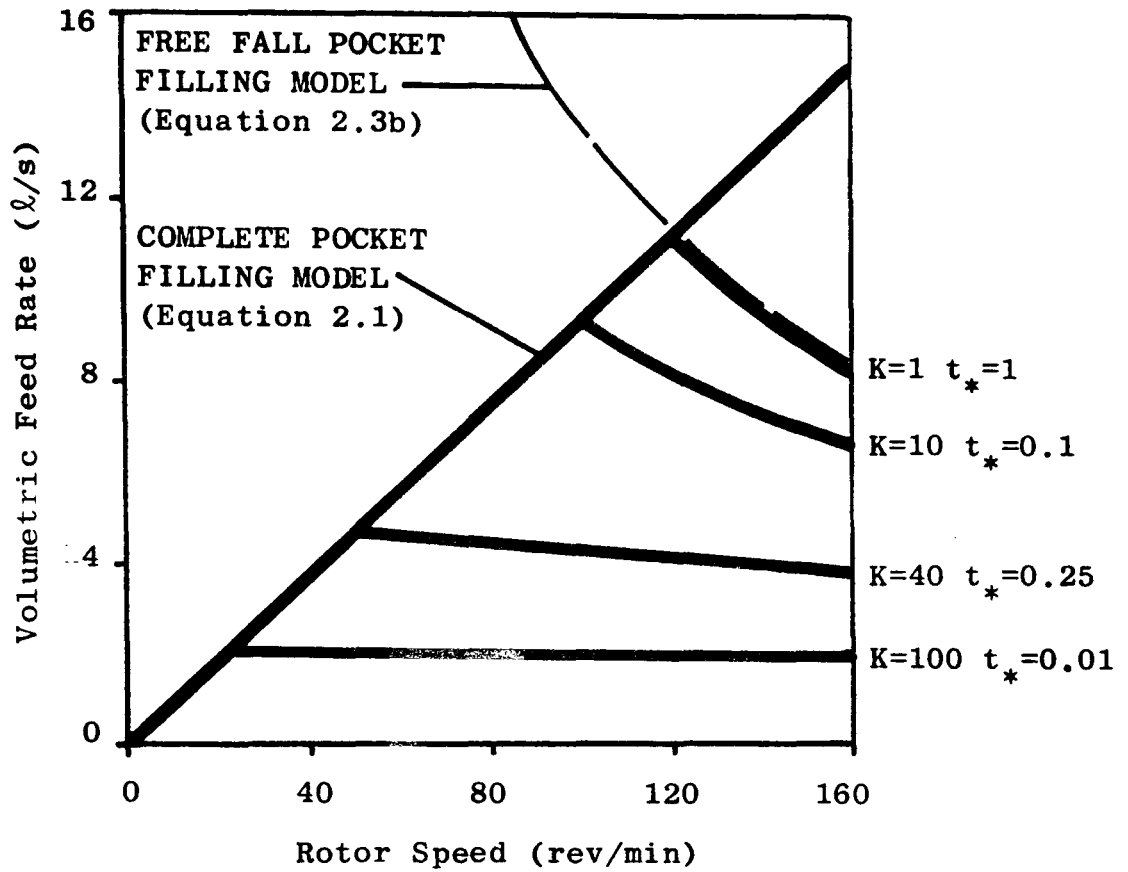
Figure 2.10   Typical Volumetric Feed Rate Characteristics as Predicted by the Models of Reed and Jotaki & Tomita
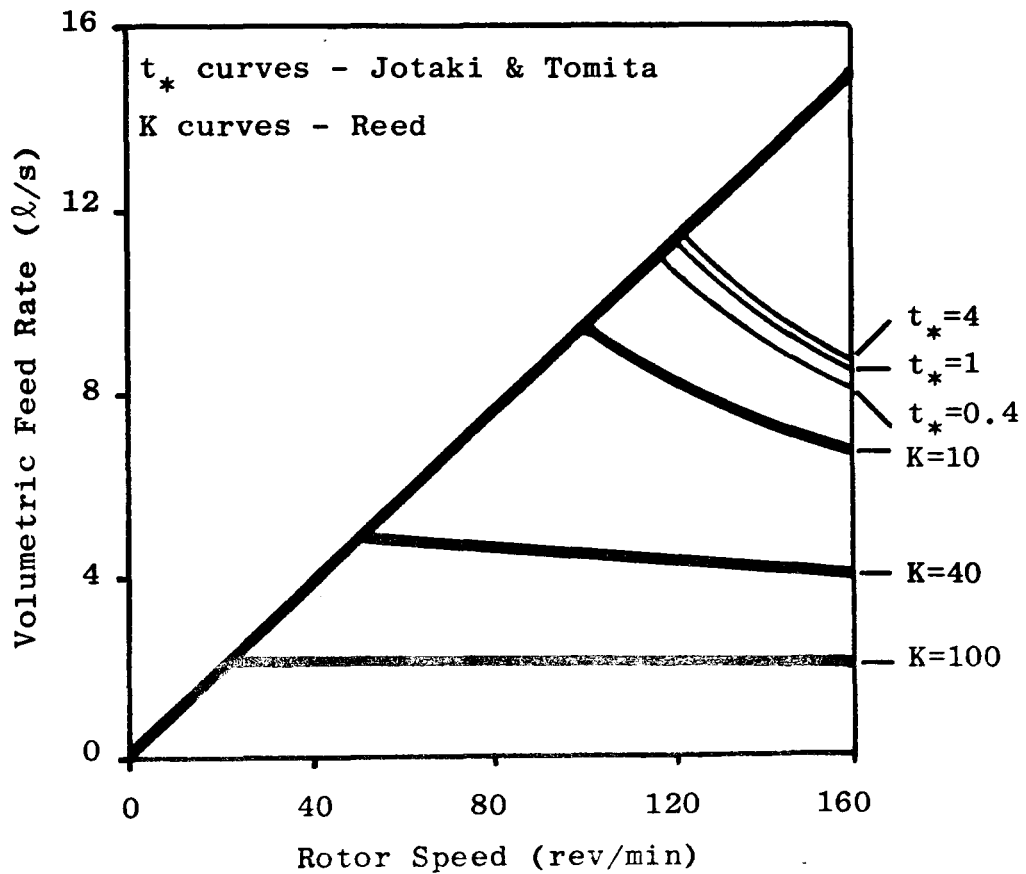
Figure 2.11   Comparison of the Feed Rates Predicted by the Reed and Jotaki & Tomita Models

larger than about 3.0 mm and a typical particle density of about
1500 kg/m^3.   For finer materials Figure 2.12 shows that the model
fails to predict the behaviour of the real system.   Reed attributed
this to his decision to use the Carman equation in the derivation of his
model.   This equation is strictly only valid for the laminar flow of
air through homogeneous beds of granular solids.   Thus, it may well be
considered to apply for materials with K < 10 but for finer products
with K > 10 such a decision is not justified.   In this case the
smaller interstices may only allow a limited amount of air to pass
uniformly through the material;   the excess air passing out of the
system either in the form of a 'bubble' or through a preferential
channel, depending on the cohesiveness of the material.   If this
happens, the resistance of the material to the displaced air would be
less than that allowed for by the model.   This, in turn, would result
in a critical rotor speed higher than that predicted by the model and
provide an explanation for the discrepancy between the experimental
and predicted behaviour as shown in Figure 2.12.

It is interesting to use a similar diagram to compare the model
of Jotaki & Tomita (12 and 13) with the same experimental data.
This is done in Figure 2.12, which shows the relationship between the
critical rotor speed ratio and the particle relaxation time t_*.   As
with the Reed model this shows that the agreement between the predicted
and experimental behaviour is only satisfactory for large particle
products.   The reason for this is undoubtedly due to the decision to
base the model on an analysis of single particle motion.   As noted
earlier such a simplification is highly questionable and Figure 2.13
justifies this doubt.

If Figures 2.12 and 2.13 are used to compare the predictions of
the two models it will be seen that the Reed model is more conservative
because it generally underestimates the actual critical rotor speed
whereas the Jotaki & Tomita model overestimates it.   This is further
confirmation of the earlier comment that the Jotaki & Tomita model
predicts a larger critical rotor speed than the Reed model.

Since neither of these models accurately describe the behaviour
of the real system for all particle sizes, their use in industrial
design is limited.   Consequently, Reed proposed that a least squares
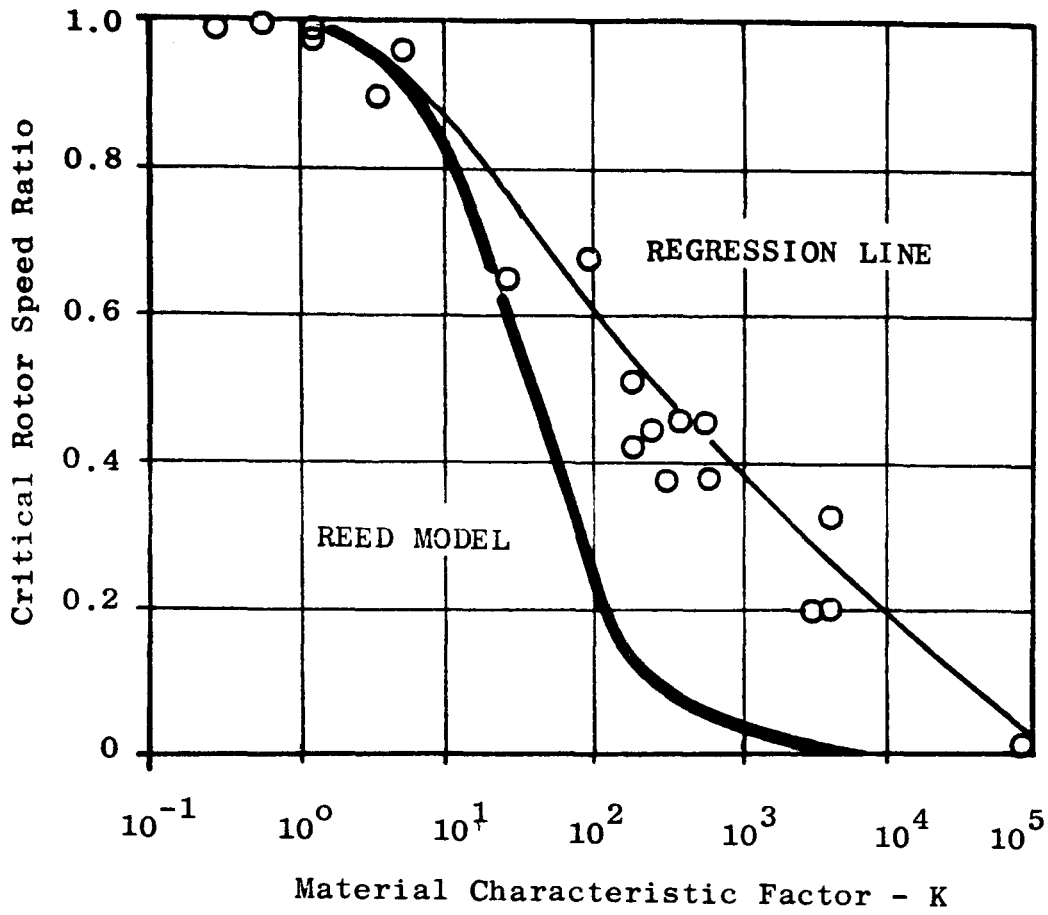
Figure 2.12   The Relationship between Critical Rotor Speed Ratio and the Material Characteristic Factor
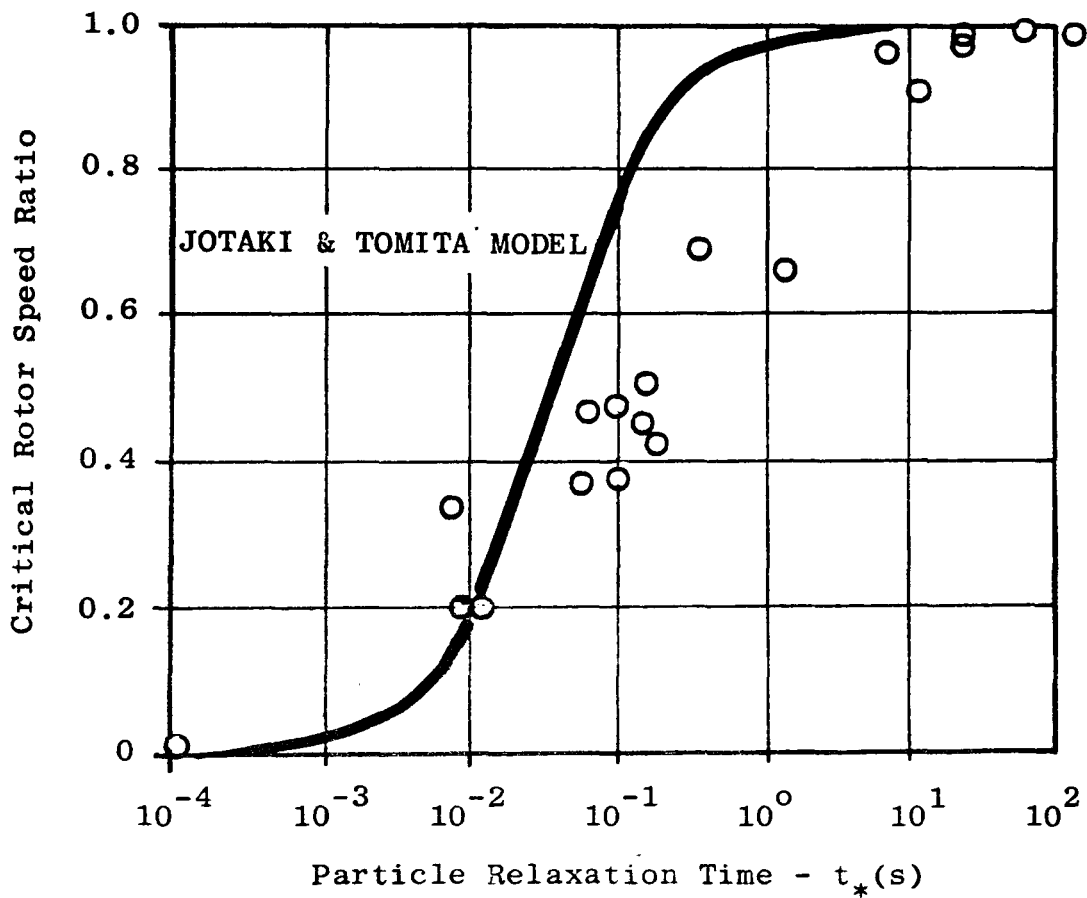
Figure 2.13   The Relationship between Critical Rotor Speed Ratio and the Particle Relaxation Time

regression line could be drawn through the data points to form the basis of a design curve, see Figure 2.12.   He argued that, if the experimental data is accepted as constituting a representative selection of materials, the curve can be used to predict the critical rotor speed ratio, and hence critical rotor speed, for any likely combination of rotary feeder[*] and material.

2.2.5   Feed Rate below the Critical Rotor Speed

Up to the critical rotor speed the feed rate characteristics of a rotary valve are broadly described by the complete pocket filling model.   However, the use of this model alone generally leads to an overestimate of the actual feed rate.   To obtain a better estimate, the usual method is to multiply the model by an empirical coefficient called the 'filling factor' (α), that is:

$$\dot{m}_s = \alpha \frac{n}{60} V_o \rho_b \tag{2.21}$$

The filling factor is essentially a volumetric efficiency and varies with both rotor speed and material characteristics.   Consequently, for equation 2.21   to be of any practical use it is necessary to understand the dependence of α on these variables.

Reed (11) showed that, in the case of rotary feeders, the filling factors for different materials could be correlated by plotting them against the rotor speed ratio (n/n_{crit}), see Figure 2.14.   This is the ratio of the actual rotor speed to the critical rotor speed for a particular combination of material and valve.   He proposed that this correlation could be used as a design curve to predict α for rotor speeds up to the critical value.

---

* footnote:

It should be noted that this design curve is strictly only applicable to rotary feeders.   This is because the original modelling only considered the displacement of air from the rotor pockets and did not allow for the additional retarding effect of the air leakage which occurs when the valve is used to feed across an adverse pressure gradient.   A possible method of allowing for the effect of air leakage will be discussed in Chapter 4.
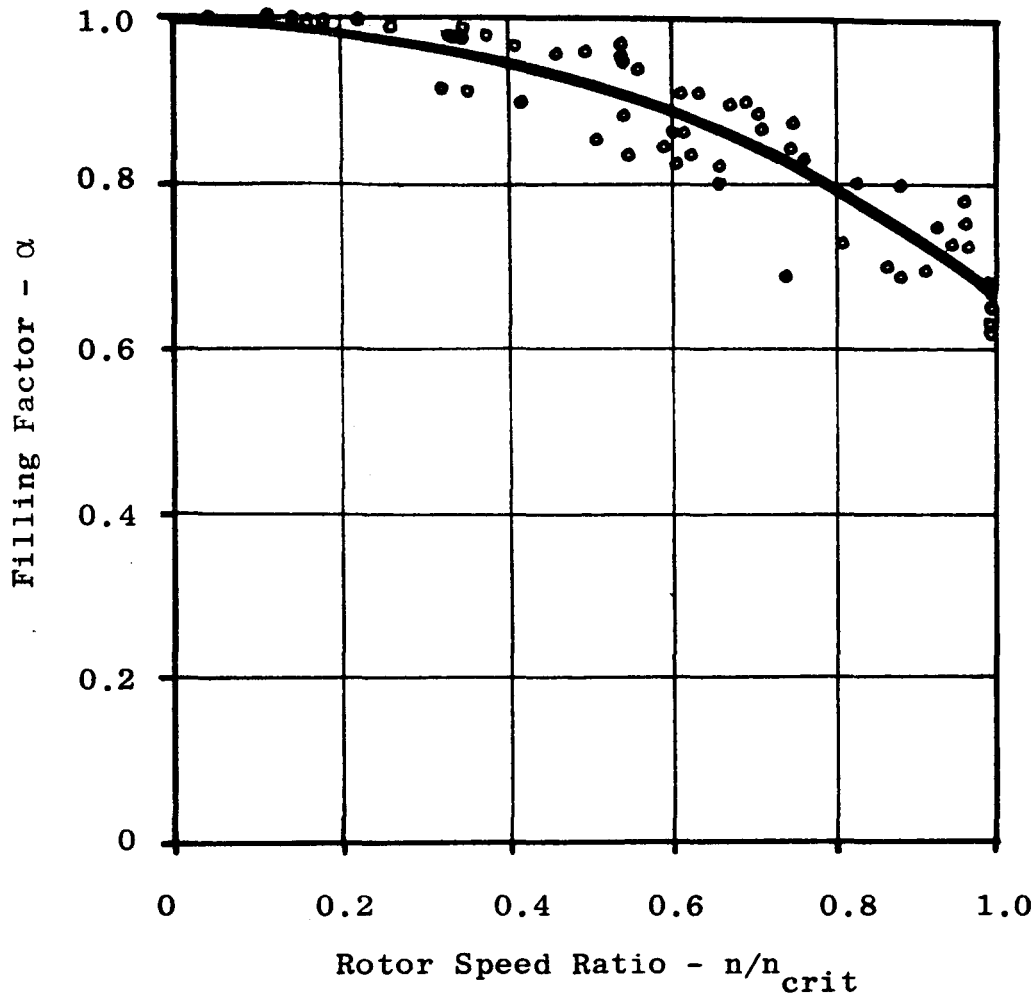
Fig 2.14　Reed's Correlation between the Filling Factor and Rotor
　　　　　Speed Ratio

For rotary valves the situation is more complicated because α is known to vary with the pressure ratio across the valve; for example, see Jotaki & Tomita's results for glass beads shown in Figure 2.8b. The relationship between filling factor and pressure ratio is complex and particularly dependent on material characteristics.　As a result, it is not possible to obtain a simple correlation such as that shown for rotary feeders in Figure 2.14.　However, Reed demonstrated by experiment that the feed rate for a representatove selection of materials is a maximum at unit pressure ratio.　Since the correlation curve of Figure 2.14 corresponds to this situation it may be taken as indicating the maximum likely performance of a rotary valve.

To estimate the filling factor of a valve operating at pressure ratios between 1.2 and 1.6 Reed proposed the use of the diagram shown in Figure 2.15.　This was constructed using test data which he obtained

from experiments on four different materials.   Arguing that similar
materials handle in a similar way, he suggested that this could be used
to estimate the filling factors of other materials by classifying them
by size and visual appearance against one of the test materials.
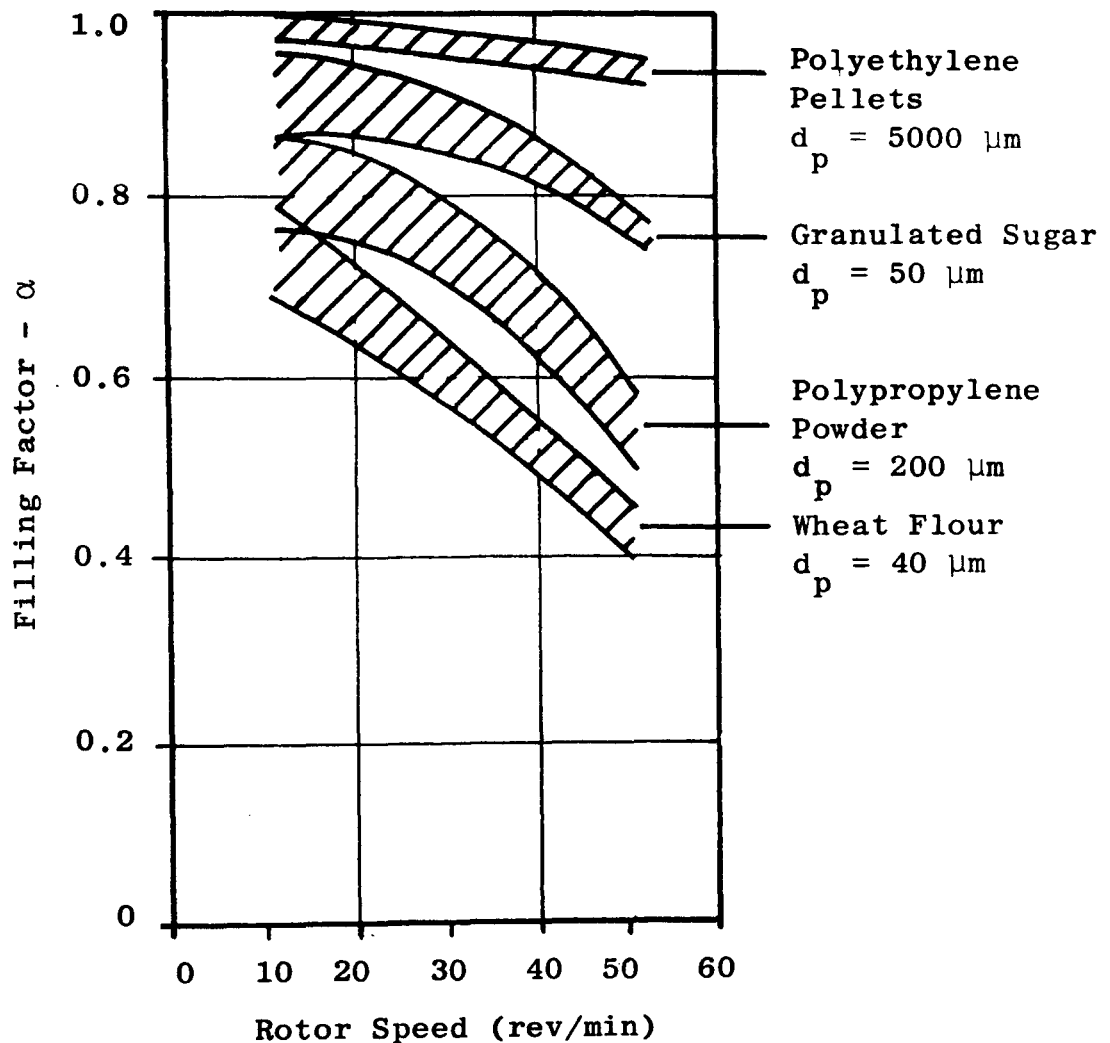
Figure 2.15   The Relationship between the Filling Factor and
               Rotor Speed for a Range of Materials as obtained
               by Reed (11)

In their trade literature, rotary valve manufacturers sometimes
show how to estimate the filling factor or their equivalent volumetric
efficiency term.   Often this is simply no more than an average
efficiency curve drawn on a throughput versus rotor speed diagram.   The
information published by Westinghouse Systems Ltd (15) for their range
of valves is a good example of this, see Figure 2.16.   This states
that: '.....The average efficiency curve is shown for guidance only and
is for an "average" powder which is neither sluggish nor very free
flowing and for a system with an adverse pressure differential across

CAPACITY/ SPEED CURVES FOR
AS 150 AND AS 175 VALVES
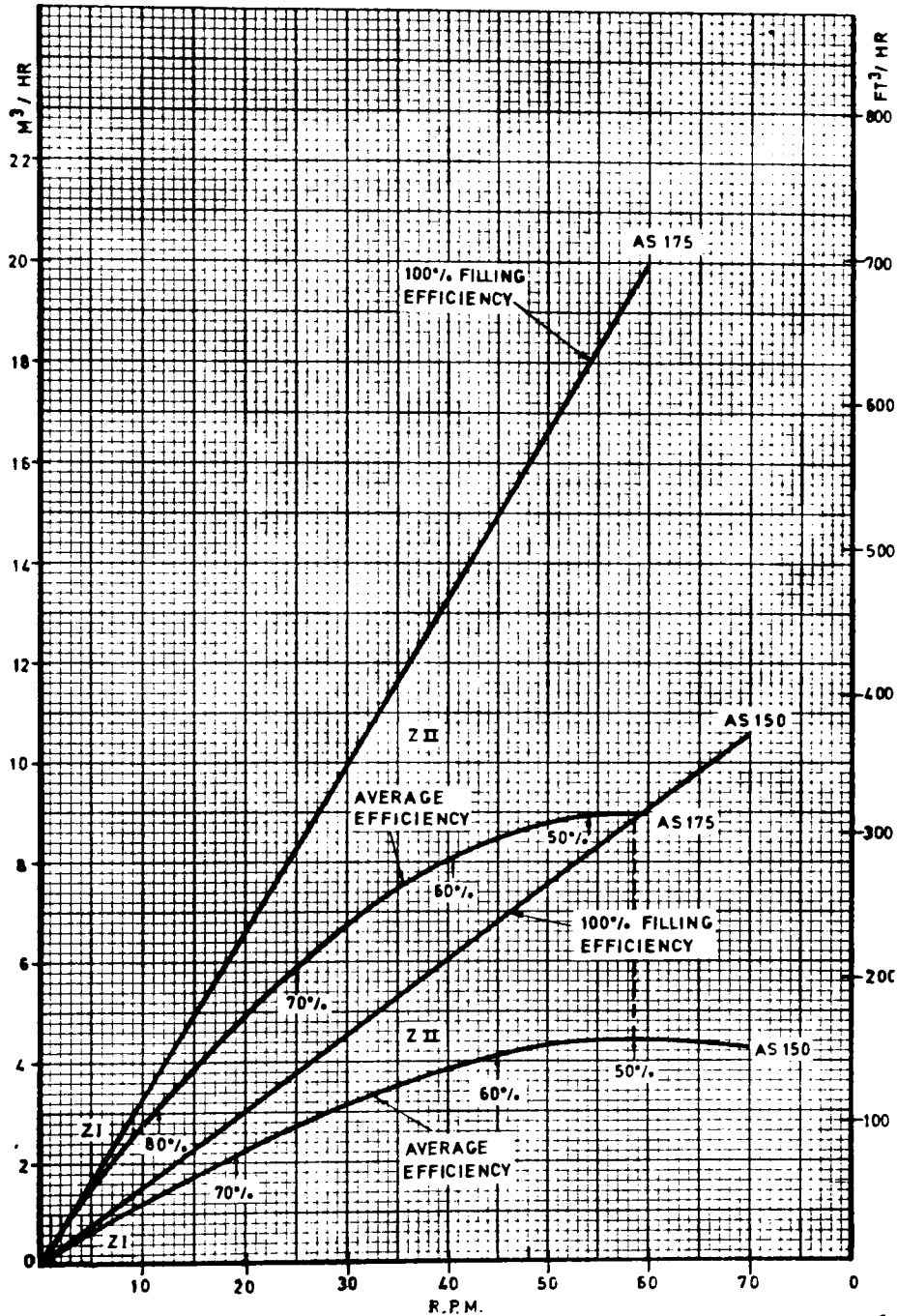
Figure 2.16   Performance Characteristics Published by
Westinghouse Systems Ltd for the 'Derion'
Range of Rotary Valves

the rotor of 5 $(lbf/in^2)^1$.

A more complicated, but not necessarily more accurate, method is used by the Smoot Co (16). They propose that the volumetric efficiency is calculated as the product of five different factors which are each dependent on one of the following parameters:

    i)   product flowability,

    ii)   pressure ratio,

   iii)   method of discharging product from the rotary valve,

    iv)   type of rotor, and

    v)   rotor speed.

The values of these factors are determined by the use of the design graphs and tables shown in Figure 2.17. Although this appears to be a very comprehensive method of evaluating the volumetric efficiency, the simplicity of the design graphs and tables is somewhat disconcerting and probably underestimates the actual performance. This suspicion is confirmed by Figure 2.18 which compares the filling factor predicted by the Smoot Co method against the experimental results obtained by Reed. Also drawn on this figure is a line corresponding to the average efficiency curve suggested by Westinghouse Systems Ltd. This corresponds reasonably well with the results obtained for fine particle products and, when taken with the 100% filling efficiency line, forms a band which encompasses most of the experimental results. However, because the band is very broad, its use for predicting the filling factor for any specific material and operating conditions is limited.

From the foregoing discussion it is apparent that although there are methods for estimating the filling factor of a rotary valve, it is very difficult to do this with any degree of precision. Consequently, the use of these methods must be treated with considerable caution. Furthermore, it must be concluded that the only certain method of accurately predicting the feed rate of a rotary valve below the critical rotor speed is to test the particular combination of material and valve in question at specific operating conditions.

V_1 = FLOWABILITY OF
PRODUCT FACTOR

FREE
FLOWING

AVERAGE
FLOWABILITY

SLUGGISH

1.0   .9   .8

FLOWABILITY (V_1)

V_2 = SYSTEM PRESSURE FACTOR

PRESSURE DROP IN
OPPOSITION TO PRODUCT
FLOW (PSIG)

0
2
4
6
8
10
12
14

1.0   .9   .8   .7   .6   .5

PRESSURE FACTOR (V_2)
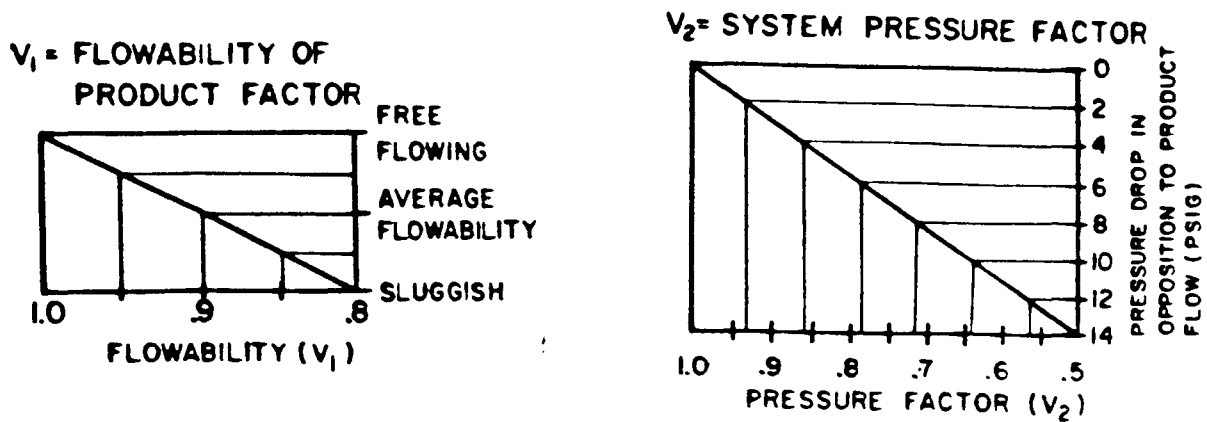
V_3 METHOD OF DISCHARGING PRODUCT FROM AIRLOCK FEEDER

	V_3
Blow-Thru Feeders	.95
Fall-Thru Feeders with Air Blast Discharge Adapter	.95
Fall-Thru Feeders with No Discharge Adapter	.95
Fall-Thru Feeders with Straight-Thru Discharge Adapter	.90

V_4 TYPE AIRLOCK FEEDER ROTOR

	V_4
Open End Rotor without Adjustable Tips	1.0
Closed End Rotor without Adjustable Tips	1.0
Closed End Rotor with Adjustable Tips	.95

V_5 = ROTOR RPM FACTOR

ROTOR RPM (N)

10
15
20
25
30
35
40

1.0   .9   .8   .7   .6   .5

RPM FACTOR (V_5)
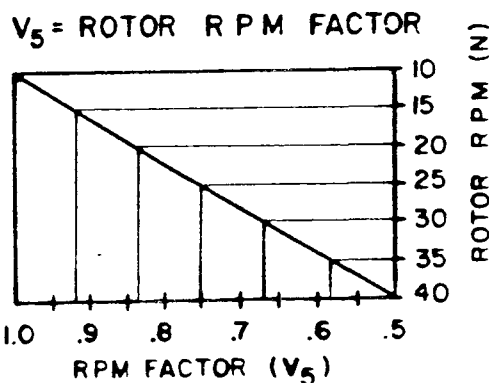
Figure 2.17   Tables used by the Smoot Co to size rotary valves
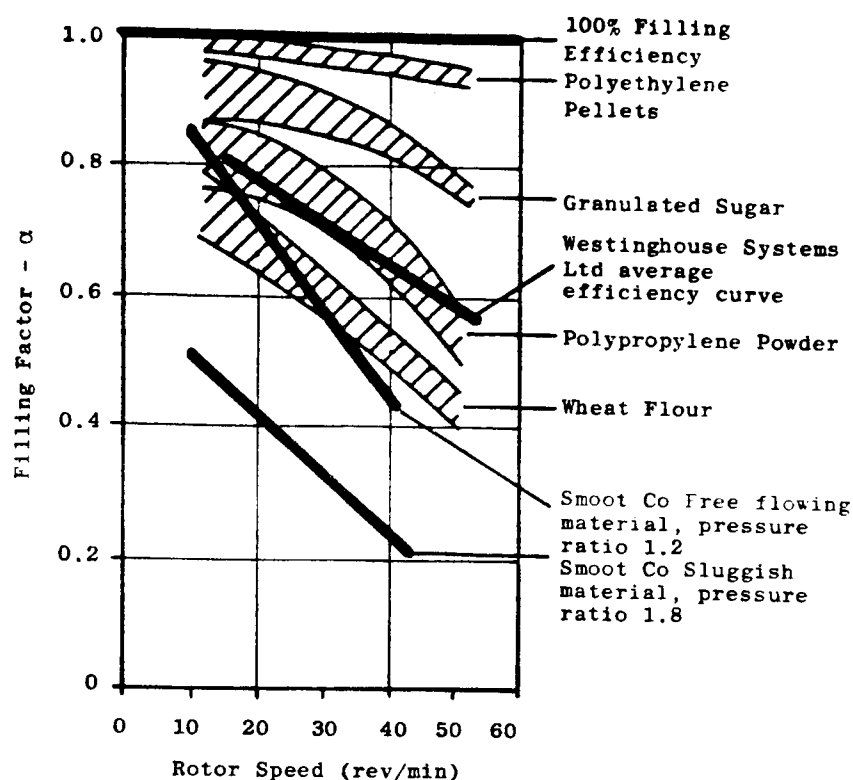
Figure 2.18   The Comparison of the Actual Filling Factors
obtained by Reed (11) and those Predicted using
the Method of Westinghouse Systems Ltd (15) and
the Method of the Smoot Co (16)

2.2.6   The Effect of Geometrical Configuration on Performance

Despite the many different shapes and sizes of rotary valves and feeders
which are available, only two published works have included any
information about the effect which geometrical configuration can have
on performance. One of these has already been discussed in section
2.2.1, that is, the work of Al-Din & Gunn (9) who investigated the
effect of changing the size of the inlet port. However, as stated in
that discussion, the proportions of the feeder which they used for their
work were not typical of those used by industry. The other work on
this subject was undertaken by Finkbeiner (17), who made and tested
several rotary feeders of similar capacity but with different geometries.
The main parameters which he investigated were the size and position of
the inlet port and the shape of the rotor blades.

The dimensions of the basic feeder which Finkbeiner used for his
work are shown in Figure 2.19. This shows that it was similar to the
feeder used by Al-Din & Gunn, Figure 2.4, in the respect that it had
a very short rotor; but in all other respects was of similar proportions

-35-

to the proprietary feeders used by industry.   To obtain different
configurations, the size and position of the inlet and outlet ports
were adjustable and the rotor was interchangeable.   The test material
which he used was Summer Rape Seed.   This is a free flowing material
with a mean particle size of 2.0 mm and a bulk density of 675 kg/m^3.
The purpose of using such a material was to minimise the effect of
material characteristics on the experimental results.
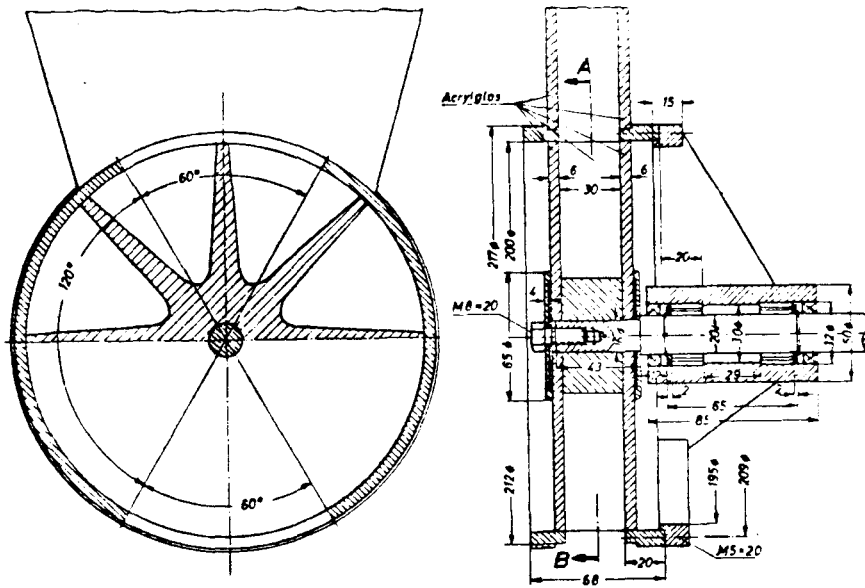
Figure 2.19   The Rotary Valve used by Finkbeiner

Finkbeiner's first experiments were designed to show how through-
put is affected by the size of the inlet port.   For these he used
the rotary feeder having a centrally positioned inlet.   By varying
the width of this inlet from 20 to 143 mm (12° to 90°) he was able
to demonstrate that the critical rotor speed, and hence the maximum
potential throughput, could be increased as shown in Figure 2.20.   This
diagram also shows that the feed rate for speeds greater than the crit-
ical value increases in approximate proportion with the size of the
inlet.   Both of these effects are consistent with the pocket filling
models of Reed and Jotaki & Tomita which predict a similar trend if the
term for the inlet port length (ℓ) is varied.   They are also consistent,
but not directly comparable, with the findings of Al-Din & Gunn.

Finkbeiner's experiments also demonstrated that the angular
position of the inlet port is important in determining the critical

Figure 2.20a
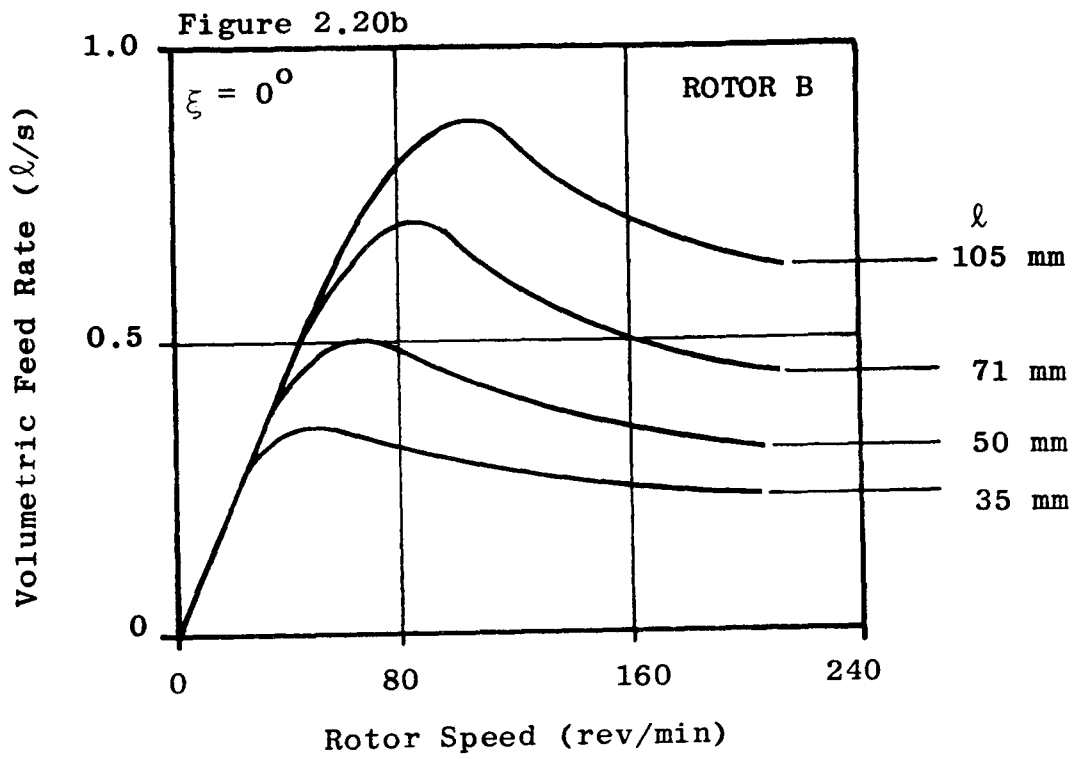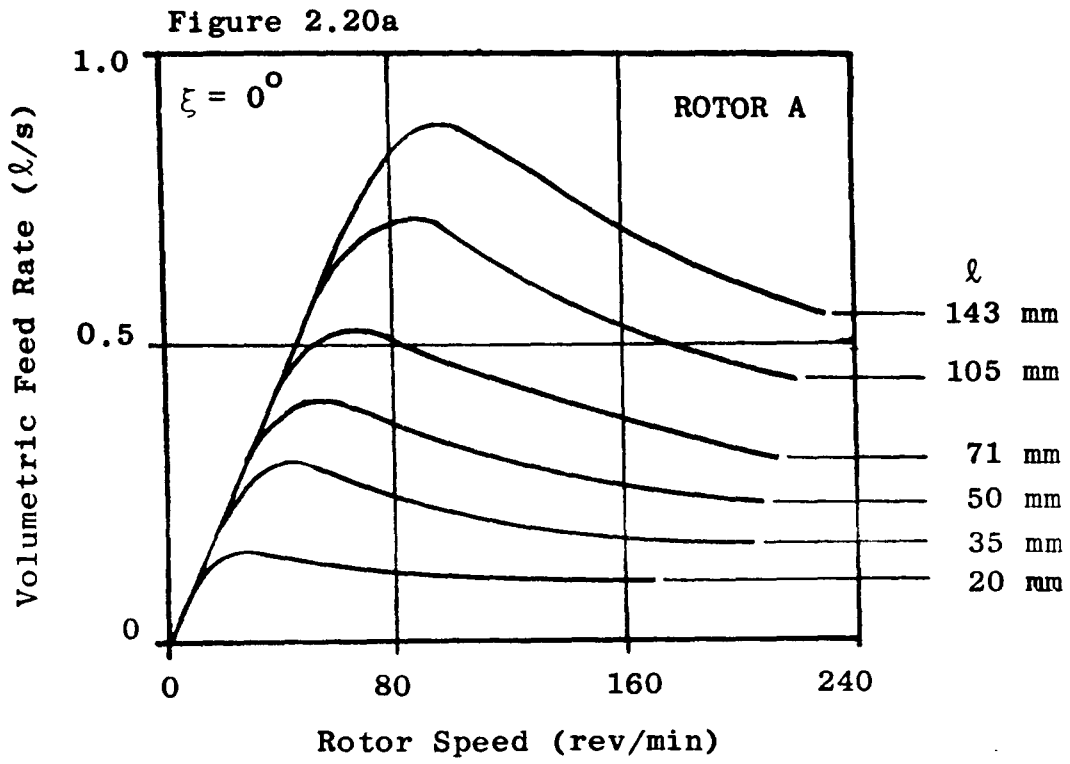
Figure 2.20b

Figure 2.20   The Variation of the Volumetric Feed Rate with
              Rotor Speed and Inlet Port Length as obtained
              by Finkbeiner (17)

rotor speed and the maximum potential throughput. Figure 2.21 shows
the effect of changing the angular position (ξ) of the inlet relative
to the vertical centreline of the valve. Positive values of ξ refer
to displacement of the inlet in the direction of rotation and negative
values to displacement in the opposite direction. From this figure it
is clear that the critical rotor speed and maximum throughput are both
increased significantly when the inlet is offset in the direction of
rotation. Finkbeiner attributed this improvement to a reduced level
of collisions between the particles and rotor blades and the smaller
acceleration forces needed to transfer material through a valve of
this configuration.

With regard to the shape of the rotor blades, Finkbeiner attempted
to determine their optimum form by analysing mathematically the paths
of single particles entering a rotor pocket. From this he concluded
that curved blades would maximise the filling rate by minimising their
obstruction to the material entering the pockets. To verify this he
undertook an experimental study to compare the performance of a
conventional straight bladed rotor and his curved bladed design, see
Figure 2.22.

Figures 2.20a and 2.20b compare the experimental results which he
obtained with these two rotors when fitted in a housing with a central
inlet ($\xi = 0^{o}$). These show that for any given inlet port length, the
critical rotor speed and maximum throughput are largest for the curved
bladed rotor. This is more clearly illustrated in Figures 2.23 and
2.24 which show respectively the variation of critical rotor speed and
the variation of maximum throughput with respect to the inlet port
length. From these figures it can be seen that, for an otherwise
identical valve, the critical rotor speed and maximum throughput
obtained with the curved bladed rotor are approximately 25% larger than
those obtained with the straight bladed rotor.

The comparative results which Finkbeiner obtained for the two
rotors when fitted in a housing having an offset inlet are shown in
Figures 2.21a and 2.21b. These show that although the feeder's
performance with the curved bladed rotor can be improved by offsetting
the inlet, the improvement is not as large as that obtained for a
straight bladed rotor with the same offset. For large offsets ($\xi > 30^{o}$)

Figure 2.21a
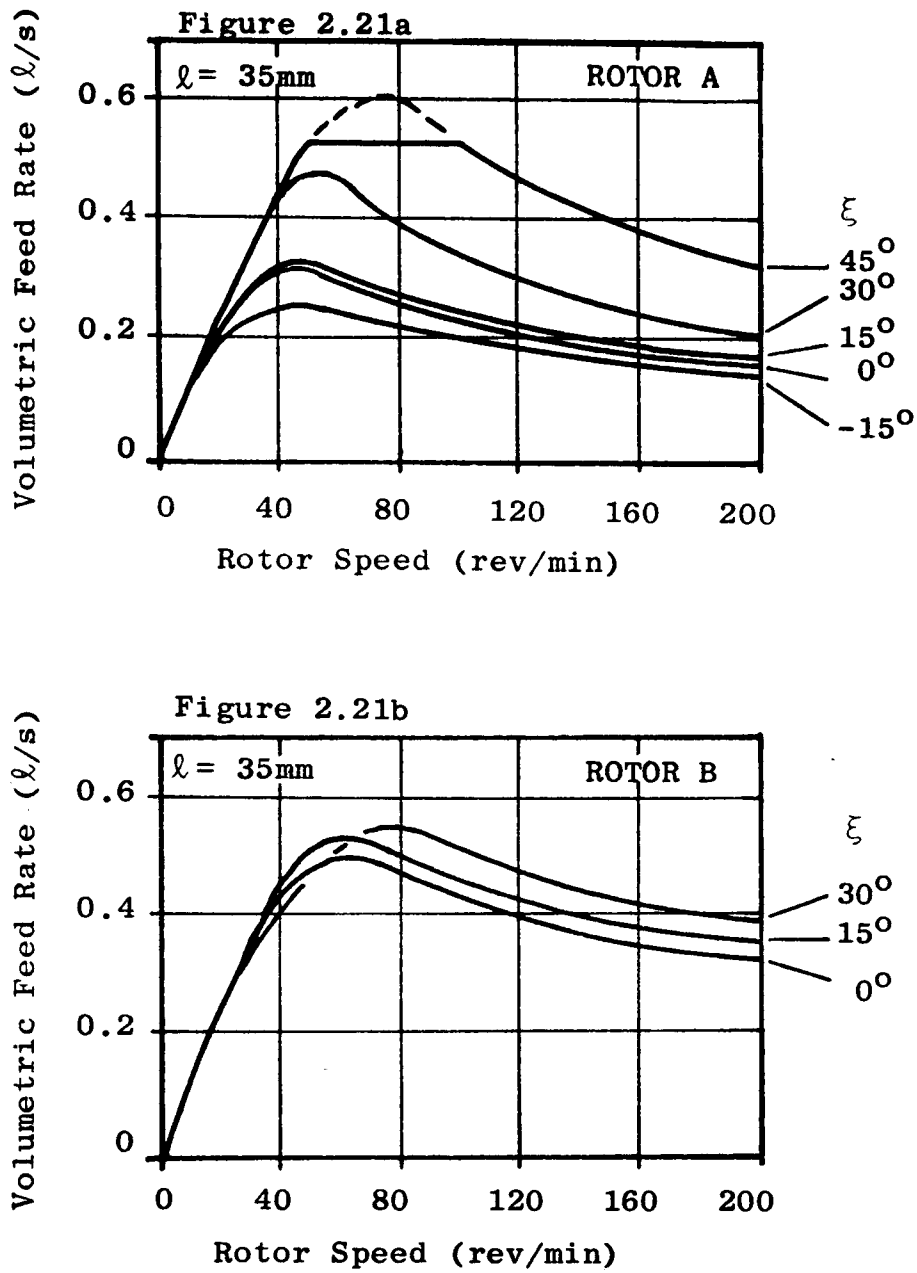
Figure 2.21b

Figure 2.21   The Variation of Volumetric Feed Rate with Rotor
Speed and Inlet Port Position as obtained by
Finkbeiner (17)
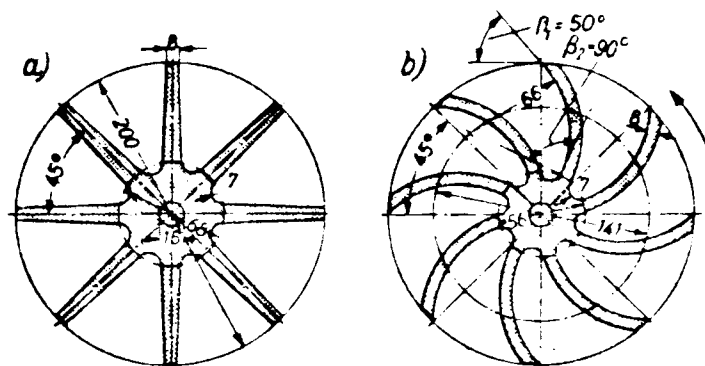
Figure 2.22   The Straight Bladed and Curved Bladed Rotor Designs
tested by Finkbeiner
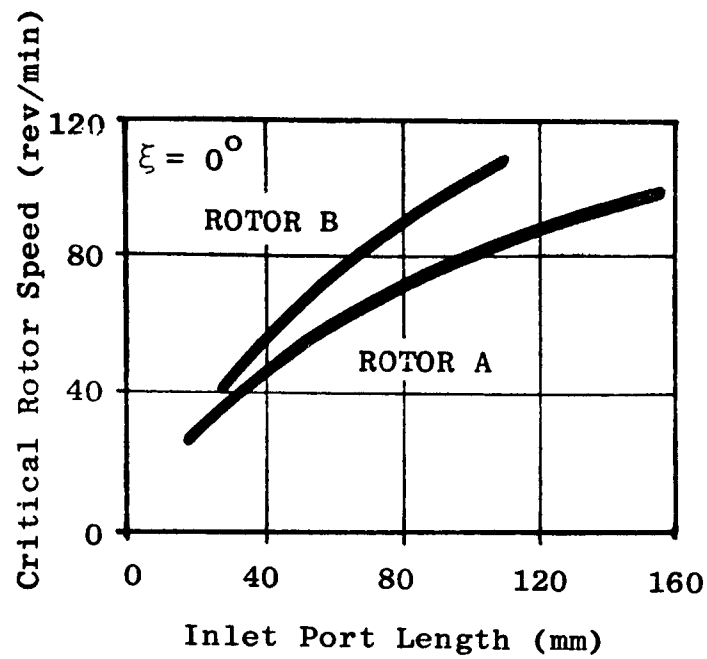
Figure 2.23   The Variation of Critical Rotor Speed with Inlet
              Port Length for Rotors A and B
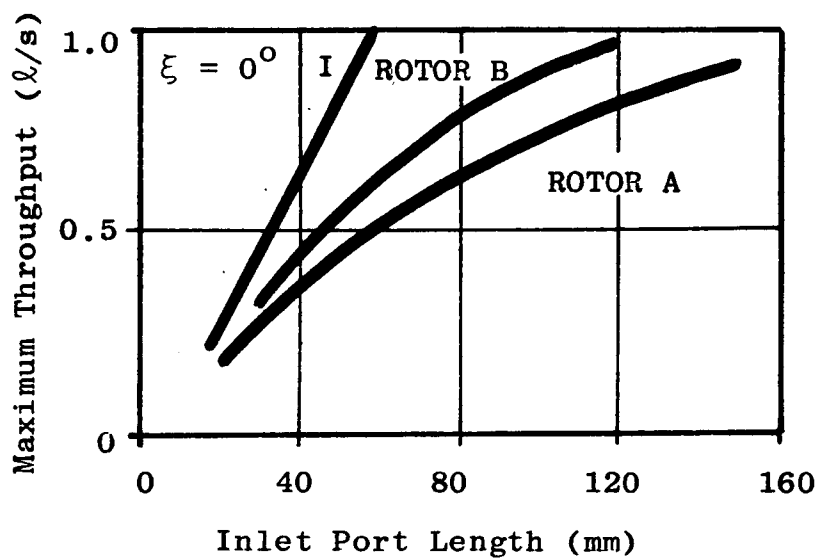
Figure 2.24   The Variation of Maximum Volumetric Throughput with
              Inlet Port Length for Rotors A and B.
              (The line I refers to the throughput of the inlet
              with the rotor removed).

this difference is such that there is little to choose between the performance of the two rotors.   This observation is interesting because it indicates a practical and cheaper alternative to the curved bladed rotor for maximising the performance of a rotary feeder or valve.

2.2.7 Air Leakage

As discussed briefly in Chapter 1, there will always be air leakage through rotary valves as a consequence of the pressure gradient to which they are subjected.   For valves which are used to feed positive pressure pneumatic conveying systems, this leakage represents a loss of air from the system.   Consequently, it is important to be able to predict the leakage so that the air supply equipment can be adequately sized.

Most rotary valve manufacturers publish figures for air leakage losses in their trade literature, but these are usually for one specific rotor speed and invariably for the valve running empty; that is, not transferring any product.   For the more usual situation, where the valve is not running empty, the information is far more vague.   A typical example is the trade literature of the Smoot Co (16) which states that the actual leakage may be between 50% and 100% of the figures they quote for the valve running empty, depending on the product being handled.

With the aim of providing a better general understanding of the parameters which affect air leakage, Reed (11 & 18) conducted an experimental investigation.   From this he concluded that the air leakage:

   i)   increases with increasing pressure ratio;

  ii)   may be considered independent of rotor speed;

 iii)   is a maximum when the valve is running empty;

  iv)   reduces if the number of rotor blades is increased;

   v)   reduces if the running clearances between the rotor
        and housing are made smaller.

As a result of his work Reed proposed a method for estimating the air leakage for any size of valve handling any product.   His approach was to define a parameter called the 'leakage velocity' (u).   This is

a notional velocity and is given by:

$$u = \frac{\dot{V}_L}{Lc}$$

(2.22a)

where $\dot{V}_L$ is the volumetric leakage rate for a valve running empty,
L is the rotor length and c is the clearance between rotor and
housing.   Using the leakage velocity, Reed was able to correlate his
results with the design data of two rotary valve manufacturers
(References 15 & 19) to produce the diagram shown in Figure 2.25.   From
this it can be seen that the leakage velocity is only dependent on
pressure ratio and the number of rotor blades.   Since the data from
which this diagram is constructed was obtained from three independent
sources and from many different sizes of valve with different internal
clearances, Reed proposed that it could be used as a general design
diagram for estimating valve leakage velocities.   If this is accepted
then the volumetric leakage rate for a valve running empty may be
calculated from:

$$\dot{V}_L = uLc$$

(2.22b)

This expression sets an upper limit to the leakage rate.   To
determine the actual leakage when the valve is transferring material
Reed suggested that an empirical coefficient, called the 'material
blockage factor' (b), be incorporated into the expression, that is:

$$\dot{V}_L = buLc$$

(2.23)

Figure 2.26 shows the relationship between the blockage factor and
particle size which Reed determined from his experimental results.   The
use of this, together with the leakage velocity diagram shown in Figure
2.25, probably represents the best general method for estimating air
leakage which is currently available.
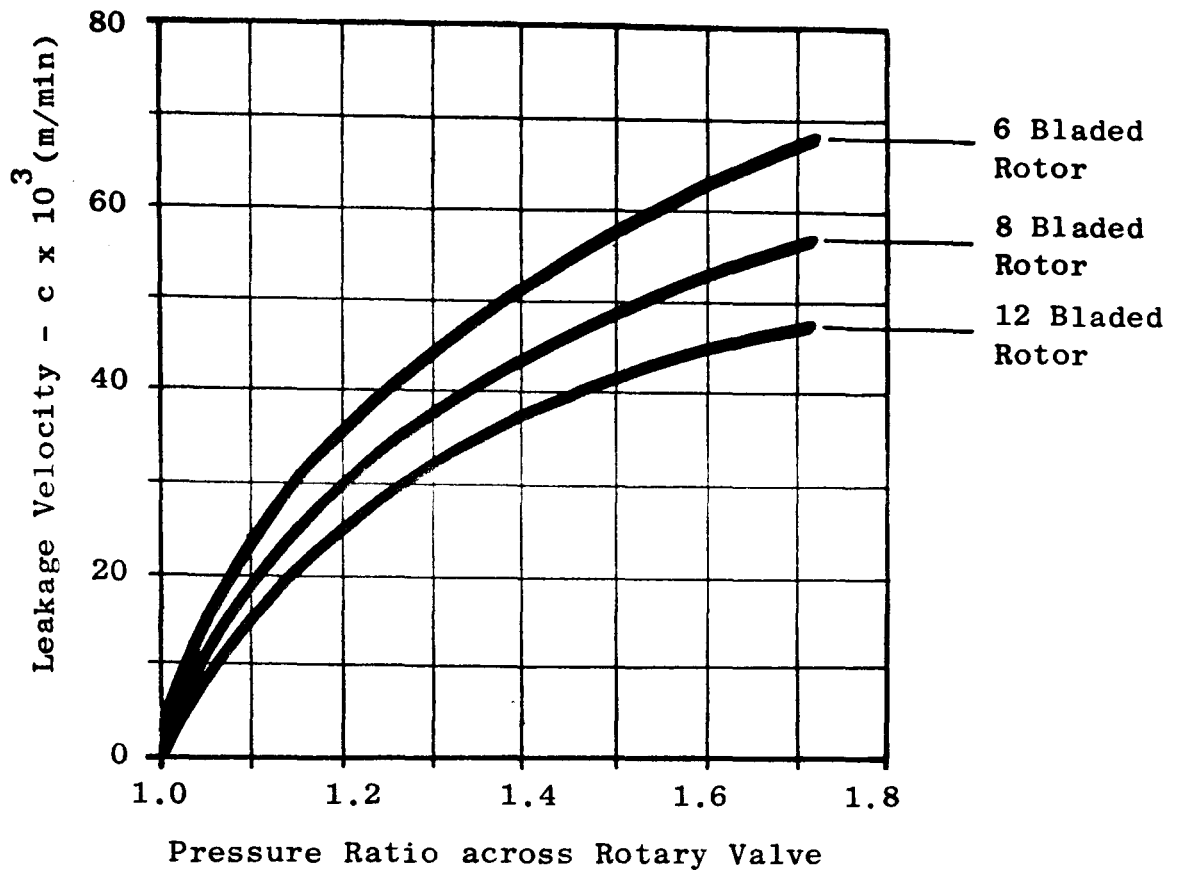
Figure 2.25   The Relationship between the Leakage Velocity and the
              Pressure Ratio across a Rotary Valve
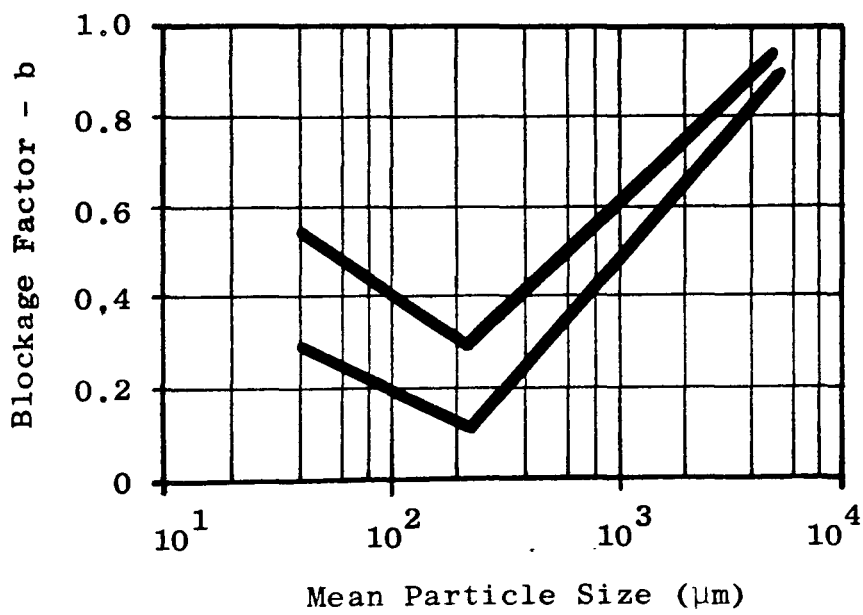
Figure 2.26   The Relationship between the Blockage Factor and the
              Mean Particle Size of a Product

2.3 The Performance of Rotary Valves used as Feeders for Pneumatic Conveying Systems

All of the research discussed in section 2.2 was concerned with explaining the isolated performance characteristics of rotary valves. That is, their performance when unrestricted by inlet and outlet conditions. However, when these valves are used as feeders for pneumatic conveying systems it seems reasonable to expect that their performance will be modified by the interaction with the supply hopper and with the conveying line.

With regard to the interaction with the supply hopper, this has already been discussed in section 2.2.1 where it was stated that, at the present time, there is no unified approach for predicting the discharge rate of hoppers with all materials. The situation is further complicated if the rotary valve is being used as a feeder for a positive pressure conveying system because of the air leakage through the valve, and hence through the interface with the supply hopper. Reed (11) and Jotaki & Tomita (12 & 13) considered the effect of the interaction between material and air with respect to the pocket filling process of rotary feeders, but did not extend their modelling to consider the case of a rotary valve operating in an adverse pressure gradient. In this situation it seems reasonable to argue that the air leakage will complicate the interaction between the material and air. A method for considering this effect will be discussed in Chapter 4.

The interaction of rotary valves with pneumatic conveying lines is even less well understood than the interaction with the supply hopper. The work of the authors previously mentioned did not consider this problem and their experimental rigs did not adequately simulate the feeding of a conveying line. For example, see Figure 2.5 which shows the rig used by Jotaki & Tomita.

Masuda et al (20) studied the mechanism of material discharge from a rotary feeder, but their analysis and experiments were only applicable to the case of a feeder discharging into free air space. Nevertheless, for this situation, they were able to demonstrate that the rotor pockets do not always discharge completely and proposed a method for estimating the discharge efficiency. It is interesting to compare this discharge efficiency, which is dependent on valve geometry

and material characteristics, with the 'filling factor' - 'rotor speed ratio' correlation obtained by Reed (11), see Figure 2.27. From this it can be seen that the agreement between the two is very good and this may be taken to indicate that below the critical rotor speed it is the discharge process which limits the performance of the valve. This is reasonable, since, by definition, there is time for the pockets to completely fill when the rotor speed is less than the critical value. Consequently, the Masuda model could be used as an alternative method to Reed's correlation (Figure 2.14) for estimating the volumetric efficiency of a rotary feeder operating below the critical rotor speed. If this is accepted then it seems reasonable to suggest that the filling factor would be more correctly termed the discharge efficiency or discharge factor. However, since the term filling factor is widely accepted, it is the terminology that will be used throughout this thesis.

Apart from published work by the author (21) the only other reported study which relates to the interaction between a rotary valve and a pneumatic conveying pipeline is that by Moseman & Bird (22). They were conducting tests on a new type of polypropylene powder which was to be pneumatically conveyed in a positive pressure system. In the course of this work they found that the interface of the rotary valve and conveying line was restricting the feed rate of the polypropylene. In order to quantify the magnitude of this problem they tested a range of different drop-out box configurations and rotary valve to conveying line orientations, see Figure 2.28.

The results of this investigation indicated that the depth of the drop-out box strongly influenced the throughput which could be achieved by the system. The deeper boxes giving greater potential throughput. Changing the orientation of the valve to the pipeline was found to have no perceptive influence on performance. In a private communication Moseman (23) stated that the throughput of the system with drop-out box 'C' was 7% better than with drop-out box 'B'. He also stated that the performance of drop-out box 'A' was considerably worse than either 'B' or 'C' although the difference was not quantified.

It is clear from this review that little research has been under-taken with the aim of understanding the interaction between rotary
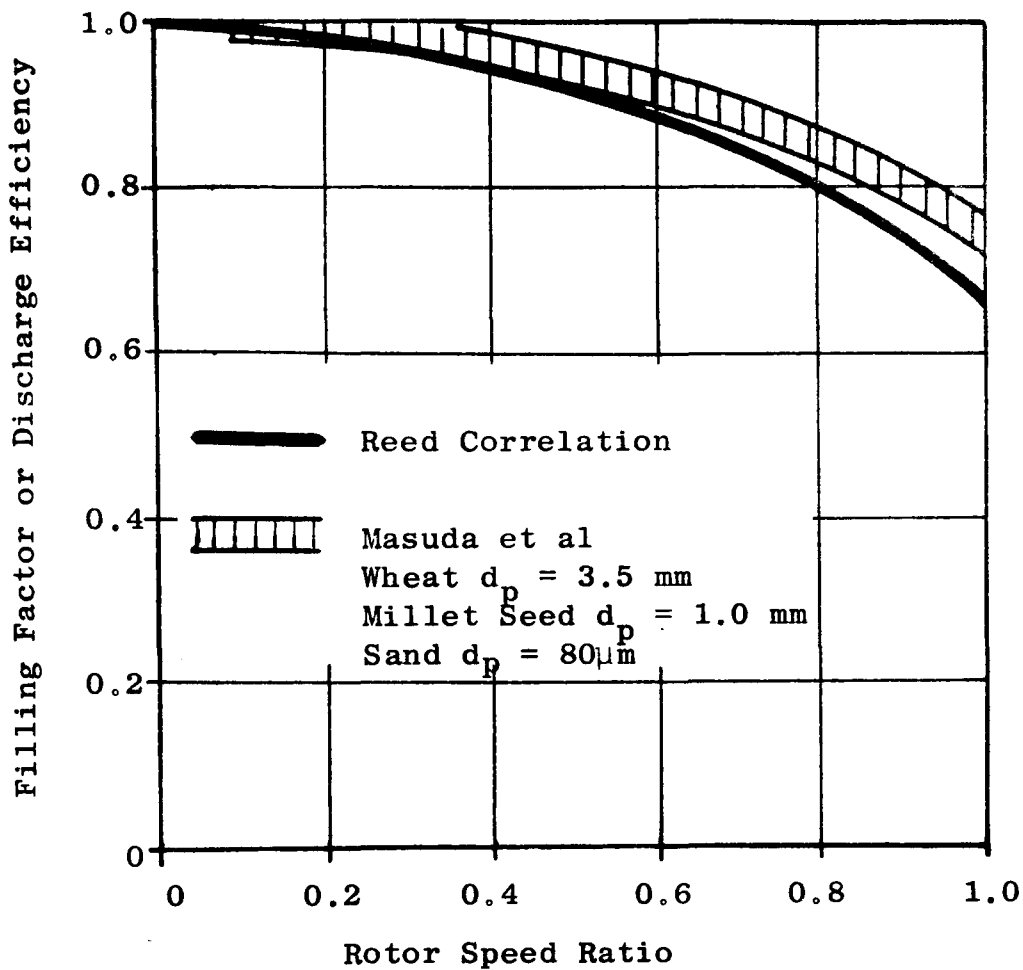
Figure 2.27 Comparison of the Discharge Efficiency Curve Predicted by Masuda's modelling with the Filling Factor Correlation obtained by Reed

valves and pneumatic conveying pipelines. Despite the lack of quantitative information, the work of Moseman & Bird is interesting because it confirms that the interface of the valve and pipeline is a potential problem area. This is also clear from the number of different drop-out box designs which are manufactured. Current industrial practice with regard to the interfacing of rotary valves with pneumatic conveying pipelines is discussed in the next section.
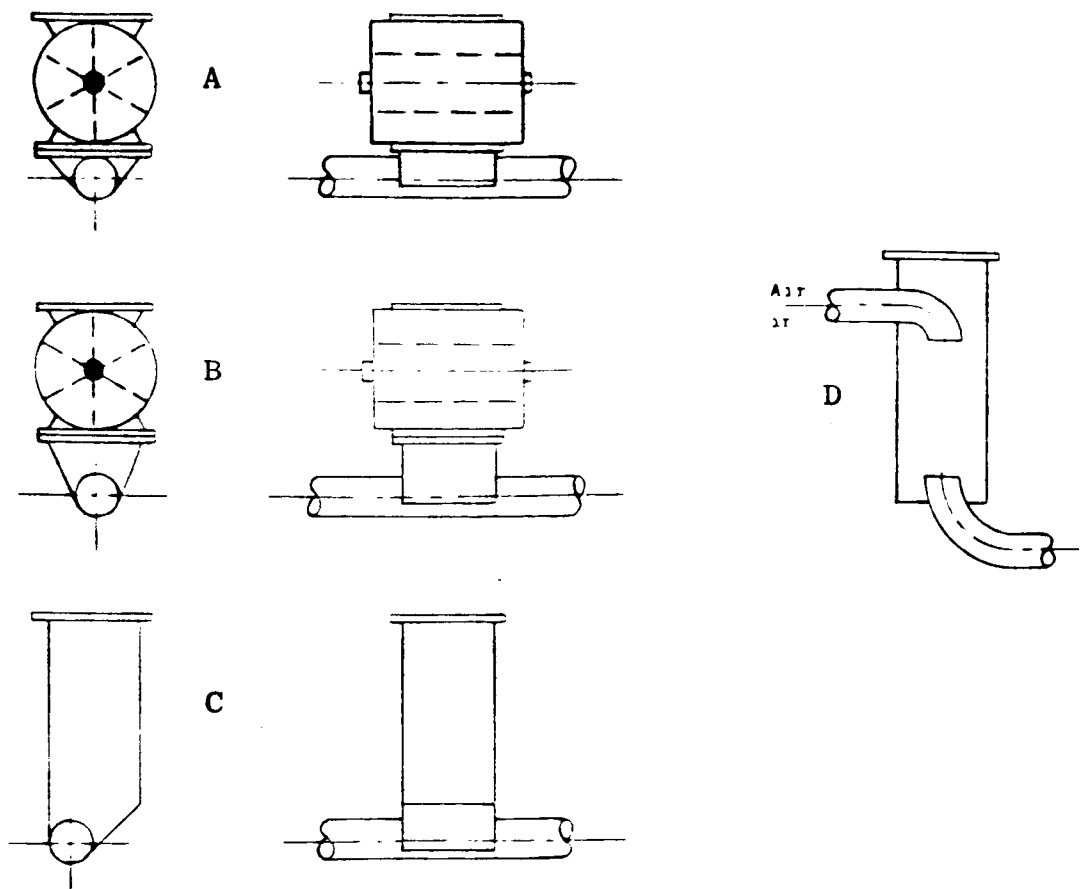
Figure 2.28a   Drop-out Boxes Tested by Moseman & Bird
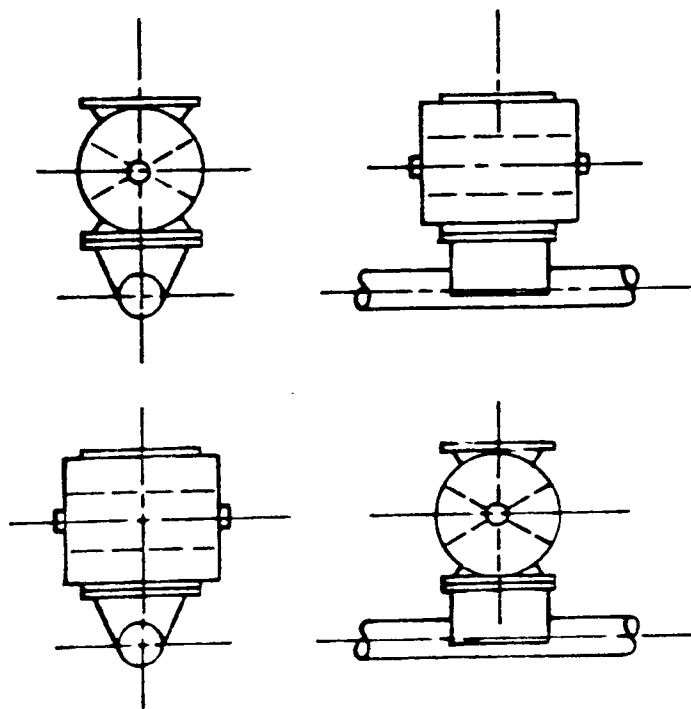
Figure 2.28b   Rotary Valve to Conveying Line Orientations
Tested by Moseman & Bird

2.4 Current Industrial Practice with respect to the Interfacing of Rotary Valves and Pneumatic Conveying Pipelines

Over the years many articles have been published by industrialists about the selection and application of rotary valves, see References 24 to 30.   However, these articles have generally contained very little information regarding the interfacing of these valves with pneumatic conveying pipelines.   Consequently, it is useful to examine current industrial practice in order to assess their approach to this problem.

The first, and most obvious, distinction which is apparent between the different methods of interfacing rotary valves with pipelines is the use of two different types of valves.   These are, the conventional 'drop-through' valve and the 'blowing seal'.   As described in Chapter 1, the drop-through valve must be fitted with a 'drop-out box' in order to make the junction between its outlet and the pipeline, whereas the blowing seal is connected directly into the pipeline, see Figures 2.29a and 2.29b.

The blowing seal is normally used for cohesive or adhesive products which will not readily fall out of the pockets of a drop-through valve. Since the airstream is directed through the rotor pockets, this type of valve can only be arranged with the rotor shaft parallel to the conveying pipeline.   However, there is at least one variant of the blowing seal in which the conveying air is supplied through the valve end plates.   Such a valve is the subject of a United States patent (Reference 31) originally held by the Atkinson Bulk Transport Co. The C.E.A. Carter Day Co (32) now manufacture a valve of this configuration and, as can be seen from Figure 2.29c, it could be considered as a combination of the blowing seal and drop-through valve.

An interesting variation between the blowing seals produced by different manufacturers is the level at which the pipeline intersects the rotor pocket chambers.   Figure 2.30 illustrates this point. Figure 2.30a shows a configuration where the complete cross-sectional area of the discharging rotor pockets are exposed to the airstream. This arrangement is used by Westinghouse Systems Ltd (15) for their range of valves and it has the obvious advantage that all the air blows through the pockets, thus maximising the chances of completely discharging the product.   However, it also has the disadvantage that high velocity air will pass over the internal surfaces of the valve.
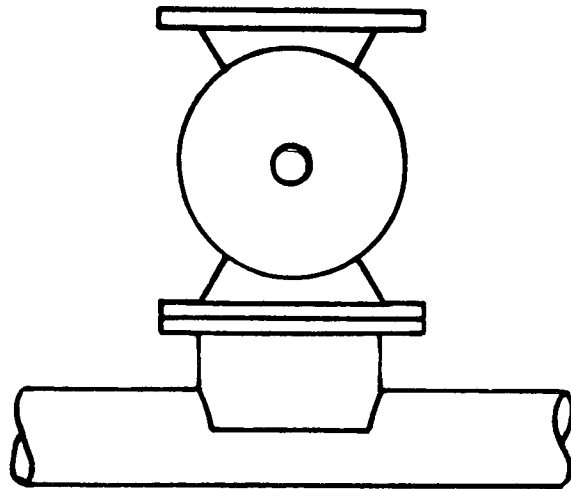
Figure 2.29a   Conventional Drop-through Rotary Valve and Drop-out
                Box
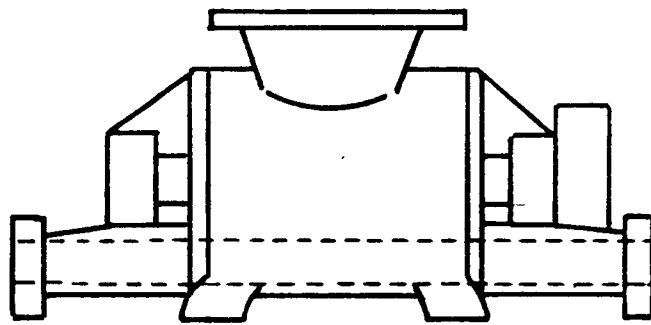
Figure 2.29b   Blowing Seal
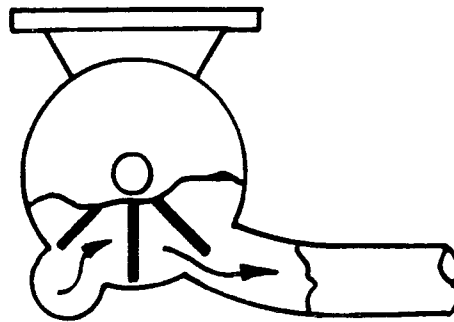
Figure 2.29c   Combination of the Drop-through and Blowing Seal
                Types

If abrasive products are being handled this could lead to severe wear problems, particularly on the end plates. Consequently, some other manufacturers prefer a compromise whereby not all the air passes through the pockets, see Figure 2.30b. The blowing seals produced by Rota-Val Ltd (33) are a good example of this. The other configuration which is sometimes seen is that shown in Figure 2.30c. In this arrangement the pipeline passes completely underneath the rotor and the airstream does not directly purge the pockets. Bush and Wilton Valves Ltd (34) produce a blowing seal of this design, which could be considered to be a drop-through valve with an integral drop-out box.

Blowing seals which are used for feeding abrasive products are sometimes designed with a rotor and connecting pipeline similar to that shown in Figure 2.30d. This arrangement has the advantage that the conveying air is kept clear from the end plates and shaft seals. Markham (35) use a valve of this type for their ash handling and pneumatic stowing equipment and a development of this has been used for a system which pumps structural concrete, (References 36 & 37). Tolmachev et al (38) have also produced a similar design for the handling of dry construction mixes.

While the mode by which material is discharged from the pockets of a blowing seal seems fairly obvious, that is by air purging, the same cannot be said for the drop-through valve. This uncertainty about the discharge and entrainment processes has led to a diverse range of drop-out boxes for use with these valves. For the same reason, the orientation of the valve with respect to the pipeline is also a matter about which there is little concensus of opinion.

Figure 2.31 shows some of the drop-out boxes which are currently produced. The most common of these is probably the simple transition section shown in Figure 2.31a. This is usually about two pipe diameters deep and is no more than a fabricated junction box between the valve and pipeline. An example of this type of box is that produced by the Mucon Co (39).

A variation to this basic design is to rake either or both the inlet and outlet faces of the box, Figure 2.31b. Presumably the reason for this design feature is to guide the material in the direction of the airflow. The 'F & R line loader' which is produced by Bush and Wilton

Configuration 'a'

Configuration 'b'

Configuration 'c'
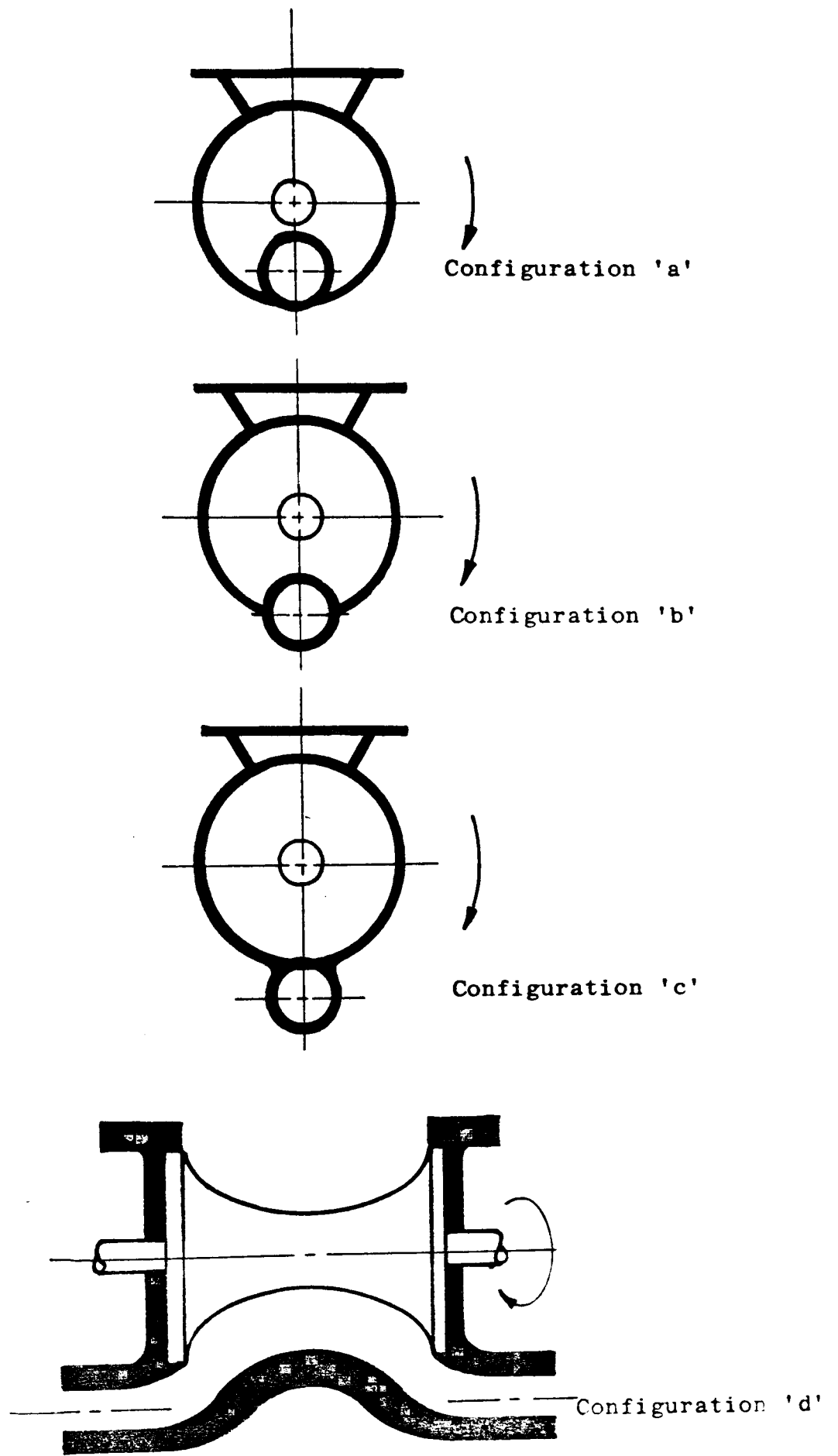
Configuration 'd'

Figure 2.30 Blowing Seal Configurations

a. Simple transition section   b. Raked inlet and outlet faces
    drop-out box
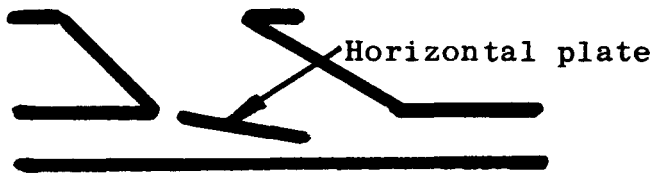
Horizontal plate

c. Buhler design with internal   d. Smoot design with deflector
    horizontal plate   plate

e. Waeshle design with angled
    pipe on inlet side

Box cross
sections
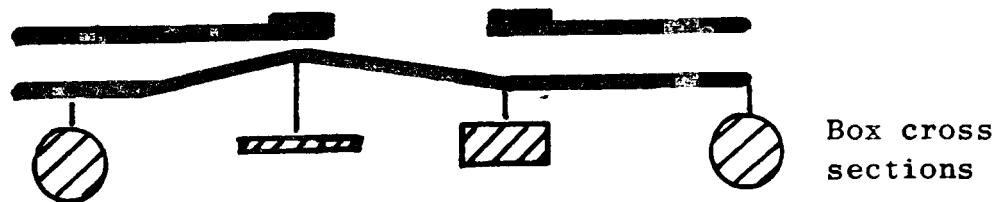
f. Bush and Wilton venturi type box

Figure 2.31 Some Common Types of Drop-Out Boxes

Valves Ltd (40) is a typical example.   Buhler Miag (41) also produce
a drop-out box of this configuration but with the addition of a
horizontal plate across half the length of the pipe opening, see
Figure 2.31c.   The reason for this plate is not clear and it must be
assumed that it has been developed as a result of practical experience.

Another interesting drop-out box is the 'air blast' design
produced by the Smoot Co (16), see Figure 2.31d.   This uses a deflector
plate to divert the airstream up into the rotor pockets.   They claim
that this improves the discharge of products which are sluggish and non-
free flowing.   Waeshle (42) also produce a drop-out box which seems to
have been designed through similar reasoning.   Instead of the deflector
plate they use a pipe to direct air towards the rotor pockets, see
Figure 2.31e.

If the air pressure at the outlet of the valve is considered to be
a problem, a drop-out box which is designed on the venturi principle
is often used.   The purpose of this is to cause a local reduction in
pressure in the drop-out box chamber and hence relieve the pressure on
the valve.   However, in practice, the reduction which can be obtained
is restricted if an acceptable pressure recovery is to be achieved.
Figure 2.31f shows a drop-out box produced by Bush and Wilton Valves Ltd
(34) which is loosely based on the venturi principle. Redmark UK Ltd (43)
also produce a drop-out box of this type for their coal handling
equipment.

With regard to the orientation of the valve with respect to the
pipeline and the direction of rotation of the rotor, individual
companies have their own preferred arrangements but there does not
appear to be any general agreement on this matter.   The three basic
orientations which are used are shown in Figure 2.32.   Obviously some
drop-out boxes are only intended for use in one particular configuration,
the Smoot Co 'air blast' box is an example of this, but for others the
best arrangement is not immediately clear.   This situation is
aggravated by the fact that there do not appear to be any methods for
predicting the effect on performance of changing the drop-out box
and/or the valve orientation.   The only published information on this
subject is that contained in the Smoot Co catalogue, see Figure 2.17.
In calculating the overall volumetric efficiency of their valves they
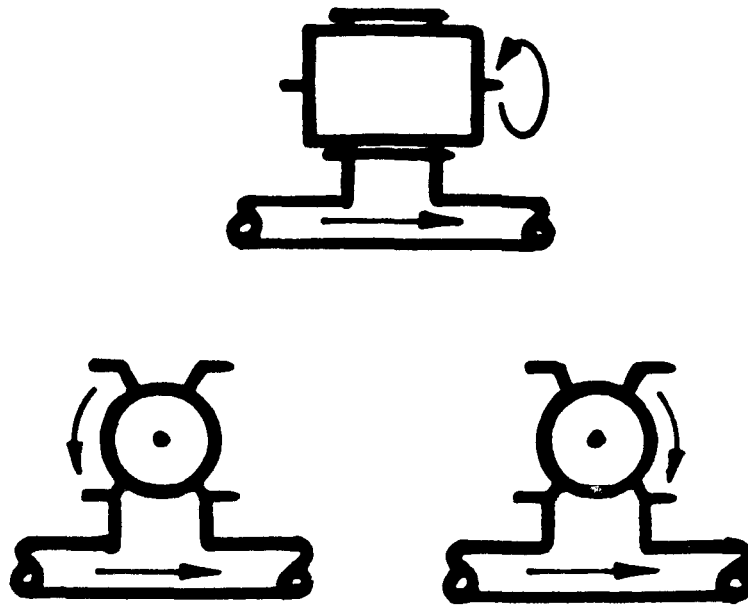
Figure 2.32   The Three Basic Rotary Valve Orientations
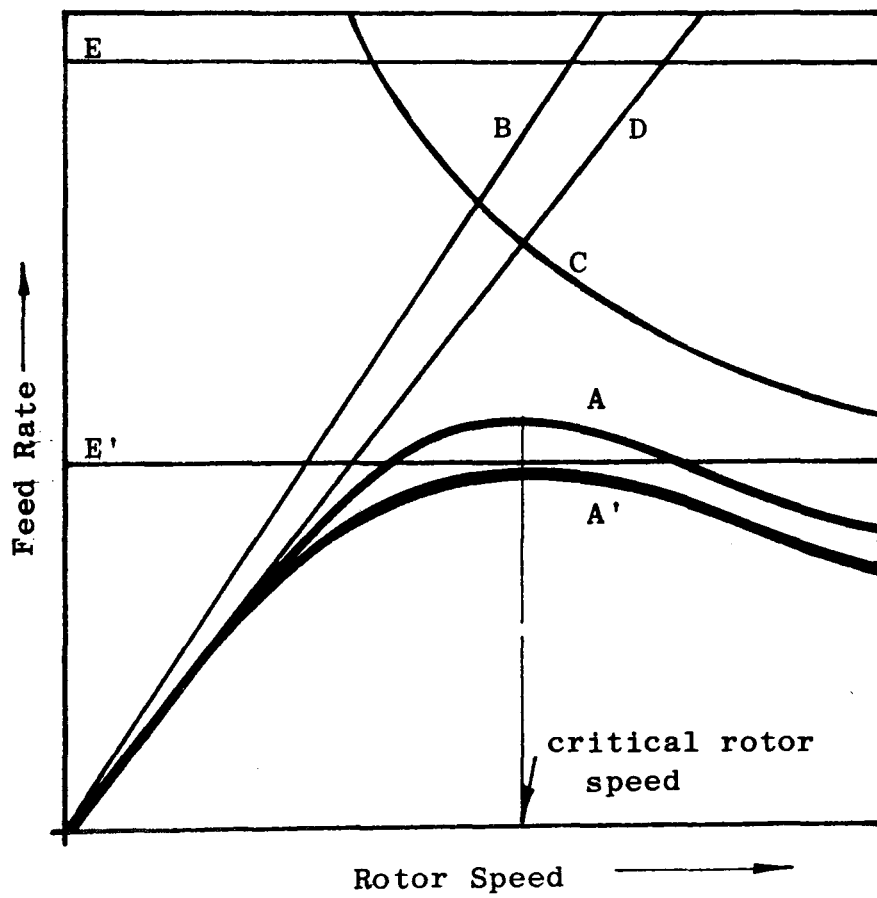
Figure 2.33   Current Models for Predicting the Performance of
              Rotary Valves

take into accout the method of discharging the product.   Figure 2.17,
Table V_3 shows that for: blowing seals; drop-through valves fitted with
their 'air blast' drop-out box; and drop-through valves with no drop-out
box they use a discharge efficiency of 95%.   For drop-through valves
fitted with a conventional drop-out box (Figure 2.13a) they use a
discharge efficiency of 90%.   These figures appear to be rather
arbitrary and the only other quantitative information which we have on
this subject is the previously quoted statement of Moseman (23) that a
deep drop-out box allowed a 7% higher throughput than a shorter design,
see section 2.3.   However, this finding is contradicted in a statement
by Perkins & Wood (29), who state in an article about operational
factors affecting rotary valves: 'Particularly when the material being
handled is a powder, the drop from the feeder into a pressure system
should be as short as possible.   An excessive drop encourages
entrainment of material and re-cycling to the rotor.'   These conflict-
ing opinions are typical of the disagreement among the manufacturers of
rotary valves and system designers.   Consequently, it must be concluded
that, in current industrial practice, there are no generally accepted
methods for evaluating the effect on performance of valve orientation
and drop-out box shape.

2.5   The Current 'State of the Art' for Predicting the Performance of Rotary Valves

From the discussions in the foregoing sections it is apparent that a
considerable amount of research has been undertaken with respect to
rotary valves and feeders.   However, the majority of this research
has concentrated on understanding the performance characteristics of
these valves in isolation from downstream conditions.   Their
performance when used as feeders for pneumatic conveying systems has not
been as extensively researched.   Since this is probably the most
common single use for these valves it is clear that there is a definite
need for further research in this area.

Figure 2.33 illustrates the current 'state of the art' for predict-
ing the performance of rotary valves and feeders using the throughput-
rotor speed diagram.   Curve A represents the typical characteristics
of a rotary feeder which is not restricted by inlet or outlet conditions.
From this it is clear that there is a maximum throughput which can be

achieved and two distinct operating regions; that is, where the
throughput is proportional to rotor speed and where the throughput is
inversely proportional to rotor speed. Line B represents the complete
pocket filling model and curve C the incomplete pocket filling models as
suggested by Reed (11) and Jotaki & Tomita (10, 12 & 13) for describing
the valve performance in these two regions. The intersection of these
two curves gives a prediction of the 'critical rotor speed' at which
the throughput is a maximum. As can be seen, the actual feedrate below
the critical rotor speed is overestimated by line B and curve D gives
a better model of the performance. This is obtained by multiplying
the complete pocket filling model by either the filling factor (α),
which can be obtained from Reed's correlation shown in Figure 2.14;
or the volumetric discharge efficiency determined by Masuda et al (20),
Figure 2.27. The intersection of curves D and C then gives a better
prediction of the critical rotor speed.

The typical performance characteristics of a rotary valve are
indicated by curve A' on Figure 2.33. As can be seen, this falls
below curve A which is the corresponding characteristic for a rotary
feeder. The difference between these two curves is the reduction in
performance due to the air leakage through the valve. This leakage
can be estimated by the method suggested by Reed, see section 2.2.7,
but its effect on throughput is more difficult to determine.

If the pressure ratio across the valve is in the range 1.2 to 1.6,
the filling factor below the critical rotor speed can be estimated by
Reed's design curves, see Figure 2.11. For other pressure ratios the
method of calculation suggested by the Smoot Co (16) could be used, but,
as has already been shown, this tends to underestimate the actual
performance, see Figure 2.18.

At present there is no adequate method for estimating the critical
rotor speed of a rotary valve because there is no reliable model for
predicting the feedrate above this speed. For large particle free
flowing products the pocket filling models for rotary feeders could be
used; but for finer products this will almost certainly lead to an
overestimate of the actual feedrate because these models do not allow
for the additional retardation effect which results from the air
leakage.

The effect of the hopper discharge characteristics on performance is shown by lines E and E' on Figure 2.33. If the discharge rate of the hopper is greater than the maximum take-away rate of the valve the hopper characteristic lies above the valve characteristic as indicated by line E. On the other hand, if the discharge rate of the hopper is less than the maximum take-away rate of the valve the feedrate will be restricted. This is represented in Figure 2.33 by the intersection of line E' and curve A'. At the present time there is no unified method for predicting the discharge rate of hoppers, consequently accurate determination of the relative positions of the hopper and valve characteristics is difficult. However, in most practical situations the unrestricted discharge rate of the hopper is usually several times greater than the maximum take away rate of the valve and thus does not restrict the feedrate.

The effect on performance of interfacing a rotary valve with a conveying pipeline is at present completely unknown. This, and a better understanding of the effects of air leakage on the pocket filling process, are the two areas which require further investigation before we can confidently predict the performance of a rotary valve used for feeding a pneumatic conveying pipeline.

CHAPTER THREE

FLOW VISUALISATION STUDY

3.1 Introduction

As a preliminary to any full scale test work and attempting to model
the process of entrainment, an experimental study of the air and solid
flows in a drop-out box was undertaken.   This was considered essential
because of the lack of published information and conflicting opinions
on the subject, as discussed in Chapter 2.   The presence of 'turbulence'
in the drop-out box has often been reported by engineers involved in the
installation and operation of rotary valves in pneumatic conveying
systems.   However, the exact nature of this turbulence and, more
importantly, its effect on the performance of the conveying system, has
never been quantified.

The investigation took the form of a series of flow visualisation
experiments.   A transparent Perspex rotary valve and a small pneumatic
conveying rig were specially constructed for this purpose.   The aim of
the investigation was to identify the nature of the air-solid flows in
a drop-out box with a view to understanding the mechanism(s) of
entrainment.   It was anticipated that this would indicate the parameters
which significantly influence the entrainment of material and thus
suggest approaches for modelling this process.

3.2 Description of the Experimental Rig

A photograph and schematic diagram of the experimental rig used for this
study are shown in Figure 3.1.   Essentially it consisted of a small
pneumatic conveyor incorporating a low pressure centrifugal fan to
provide the air supply and a rotary valve as the solids feeding device.
This valve was of the conventional 'drop-through' type and consisted of
a transparent Perspex housing with a six pocket aluminium rotor 140 mm
in diameter, see Figure 3.2.   The valve was supplied with
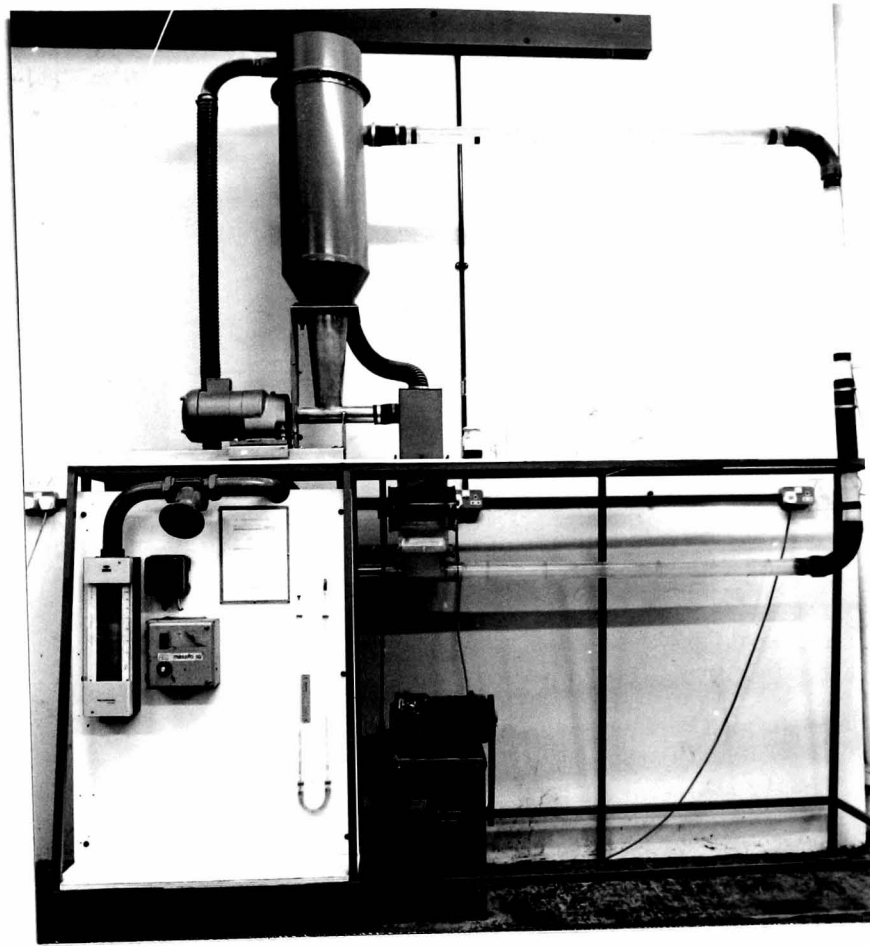
Figure 3.1a Photograph of Flow Visualisation Rig
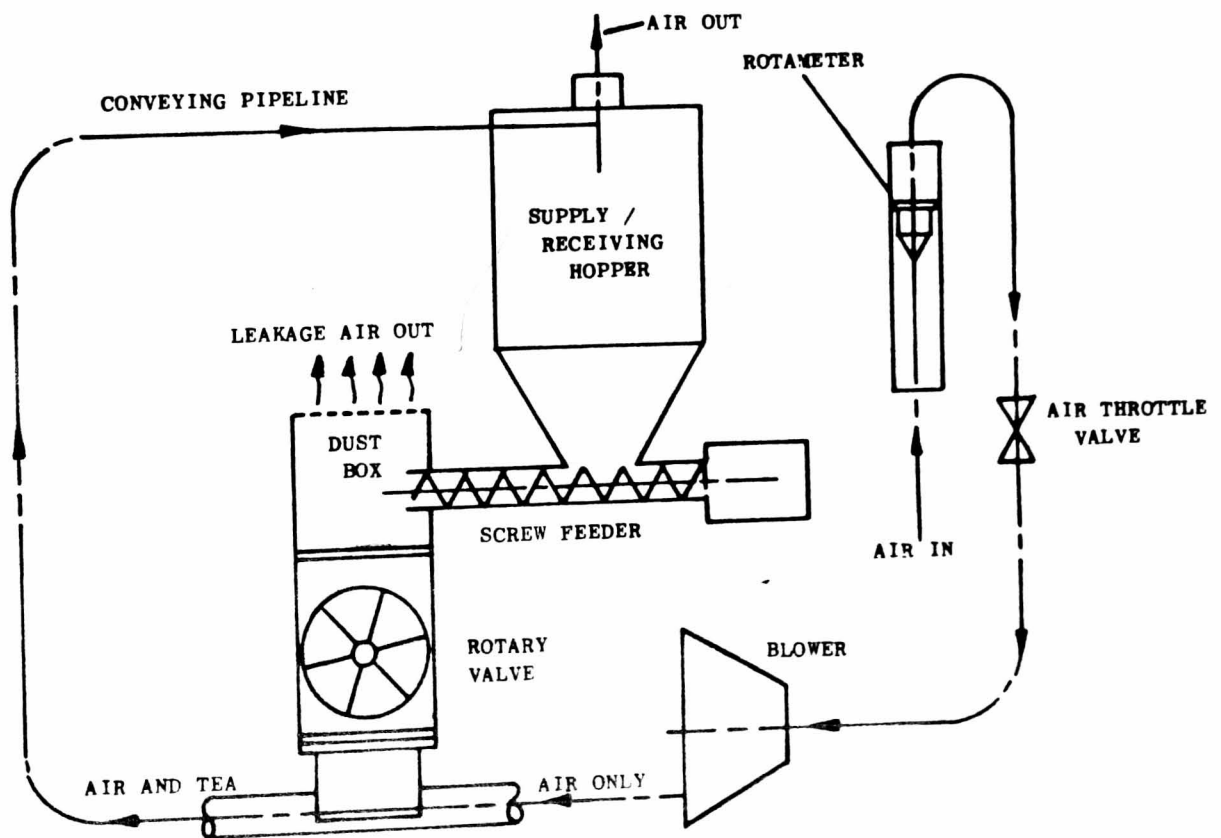
Figure 3.1b Schematic diagram of Flow Visualisation Rig
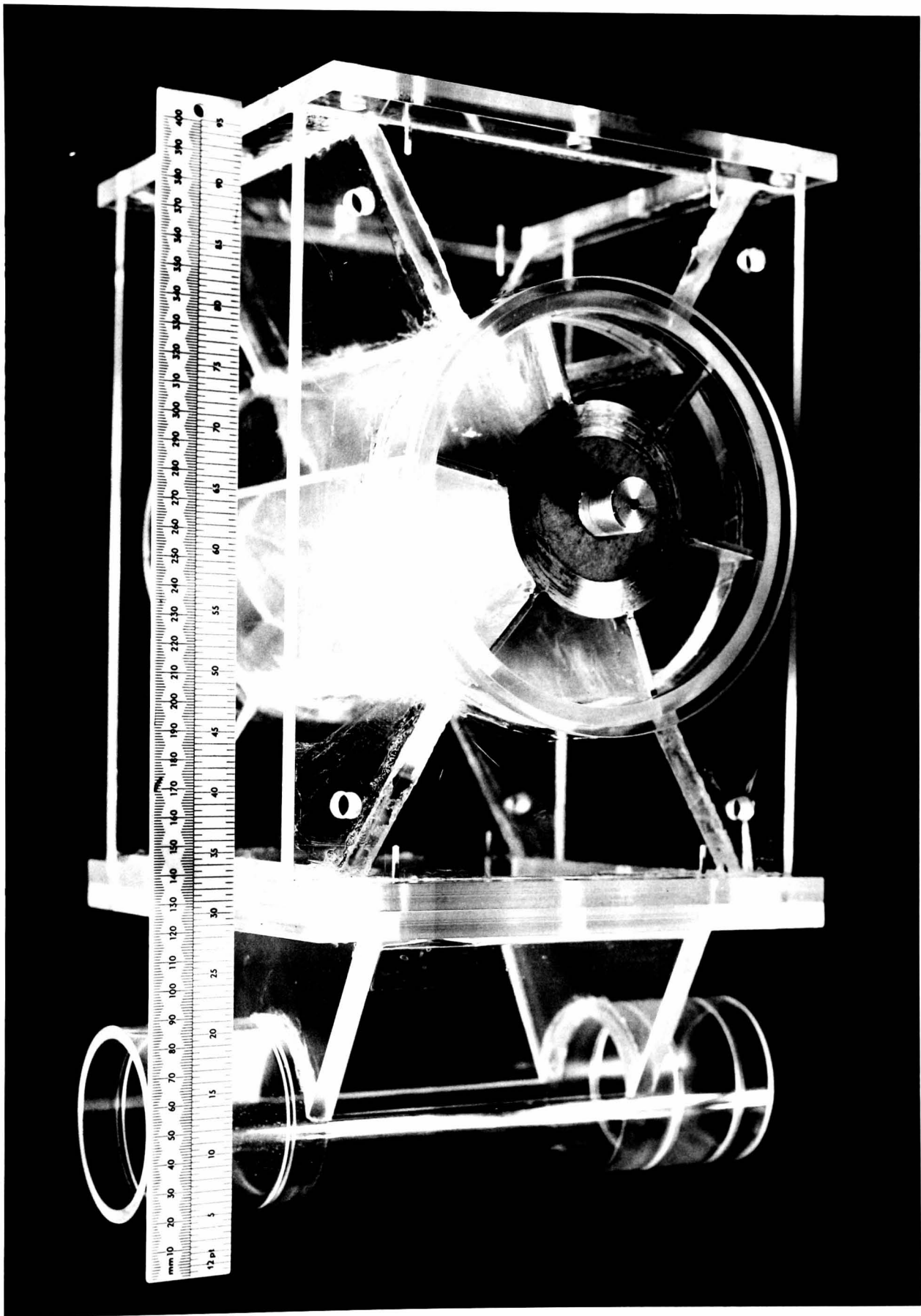
Figure 3.2 Photograph of the Rotary Valve used for the
Flow Visualisation Study

material from a variable speed screw feeder, which permitted the solids mass flow rate to be varied independently of the rotor speed. The material was fed into the conveying line through a drop-out box which fitted to the outlet of the rotary valve as shown in Figure 3.2. This was also constructed from transparent Perspex and was designed so thatit could be altered easily or changed to permit various entrainment configurations to be obtained. The conveying line was a 5.5 m circuit of 50 mm nominal bore Perspex pipeing, arranged in a closed-loop with two bends in the vertical plane. This allowed the conveyed material to be returned to the screw feeder, thereby enabling the system to operate continuously.

Tea leaves were used as the test material throughout all of the work. The principal characteristics of this product are shown in Figure 3.3. Being a soft material it minimised potential damage to the Perspex components. Also, its dark colour provided good contrast for video-tape recording of the flow patterns.

Particle Size Distribution 30-1000 μm
Mean Particle Size 450 μm
Particle Density 1420 kg/m^3
Poured Bulk Density 500 kg/m^3
Poured Angle of Repose 42°
Free Flow Handling Characteristics

Photomicrograph

Figure 3.3   Principal Characteristics of the Tea Leaves used
as the test material

Since the rig was primarily intended only for flow visualisation studies, the instrumentation was basic and did not allow accurate measurements of pressures and flow rates to be taken. However, the pick-up velocity could reasonably be determined to within ±0.5 m/s in a range of 0 to 20 m/s and the solids mass flow rate to within ±0.01 kg/s in a range of 0 to 0.15 kg/s

3.3 Description of the Entrainment Configurations Examined

Four basic configurations of drop-out box were used for this work and
these are illustrated in Figure 3.4. Box 'A' is the most simple of
these and probably represents the most common design in current
industrial use.   It is a straightforward transition section with an
overall depth of two conveying pipe diameters.   Box 'B' is also a
design which is in widespread use.   It is similar to 'A' except for
the 45° rake on the downstream face.   By the introduction of a
partition into box 'B' , box 'C' could be produced.   Again, this is
representative of designs which are in common use.   Box 'D' was
obtained by fitting an extension piece between the flanges of the
rotary valve and the drop-out box, thereby increasing the box depth
to 5.5 pipe diameters.   The inclusion of this arrangement in the
experimental programme was prompted by the work of Moseman & Bird
(22 & 23), who reported that the drop-out box depth was an important
variable with regard to maximising the throughput of their particular
conveying system.

   By using drop-out boxes A, B, C and D with the three basic rotary
valve to conveying line orientations, see Figure 2.32, the nine
different entrainment configurations shown in Figure 3.5 were
obtainable.   The flow patterns in each of these configurations were
examined for a range of pick-up velocities (0 to 20 m/sec), rotor
speeds (0 to 50 rev/min) and solids feed rates (0 to 0.15 kg/sec).

3.4 Experimental Observations

3.4.1 Air Swirl

Entrainment flow patterns were recorded on video-tape and then studied
in slow motion for the purpose of analysis.   This revealed that
although there are small differences between the flows in the different
configurations, there is one dominant feature common to them all, that
is, the presence of a very strong air swirl in the drop-out box chamber.
Figure 3.6 shows a photograph illustrating this point.   It is proposed
that this swirl results from the shearing action of the fast moving
airstream in the bottom of the chamber interacting with the captive air
volume above it.   If this is accepted, then it follows that the strength
of the swirl will depend upon the magnitude of the air velocity in the
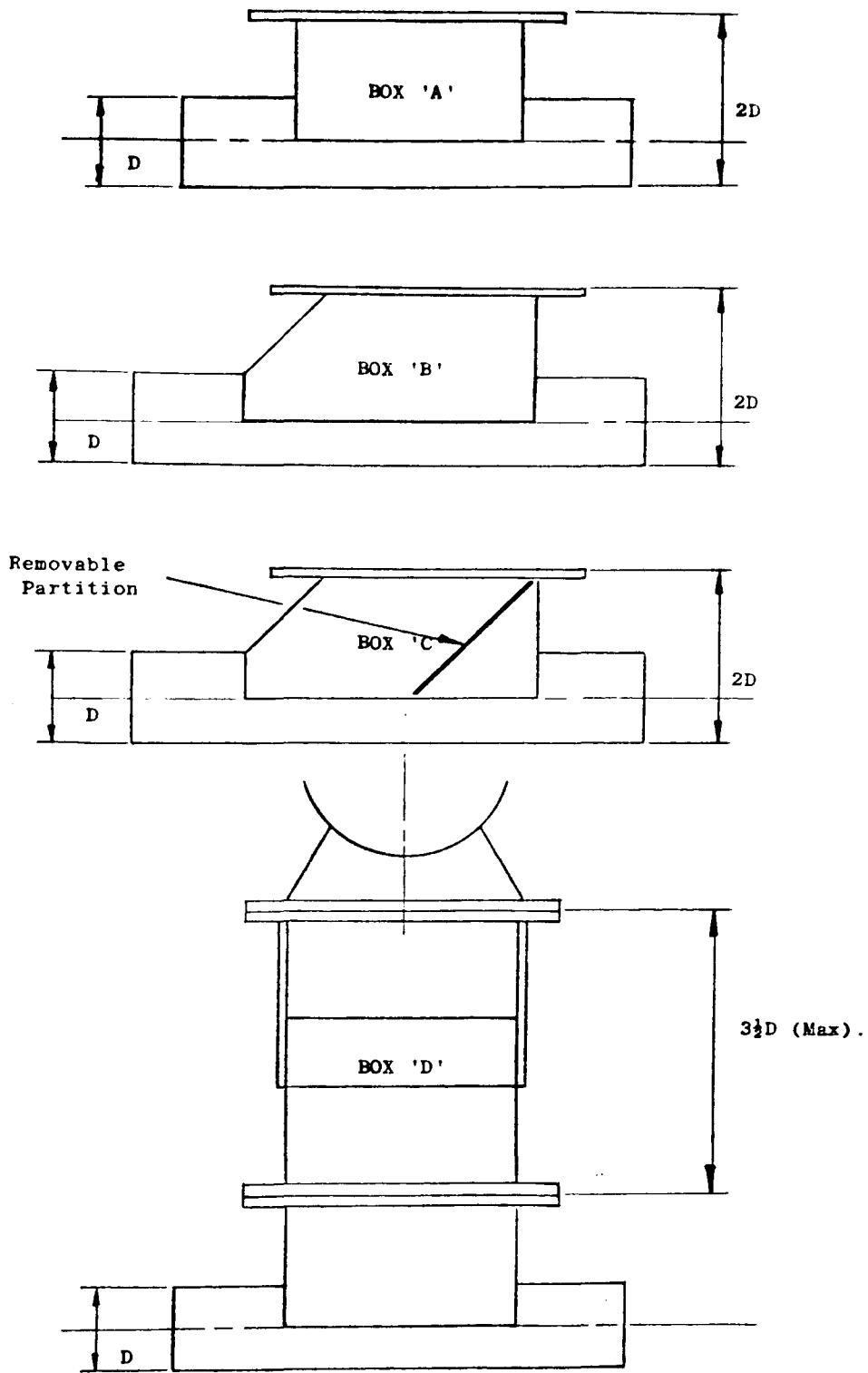
Figure 3.4   Drop-out boxes used for flow
visualisation study
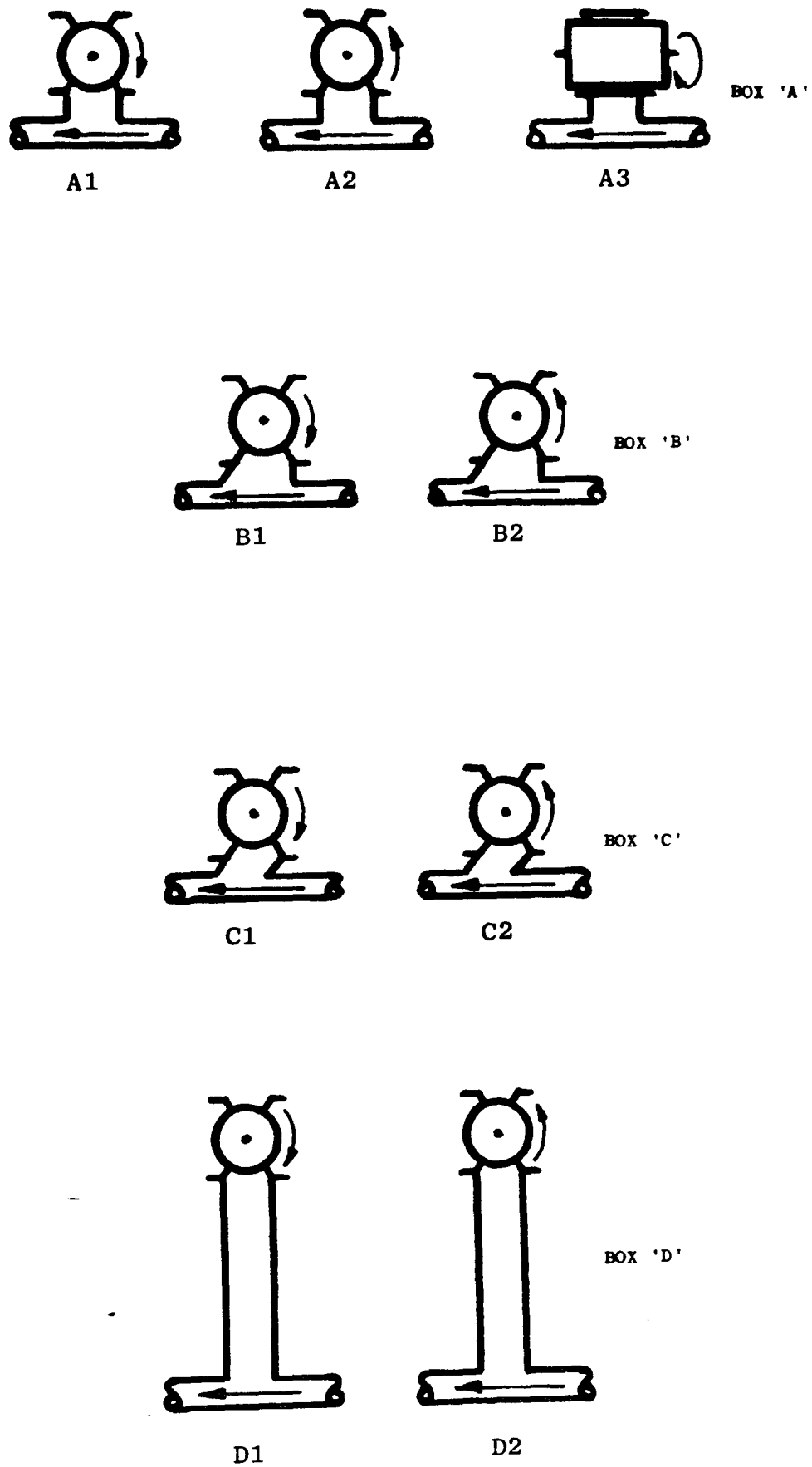
Figure 3.5 Entrainment configurations examined in flow
visualisation experiments
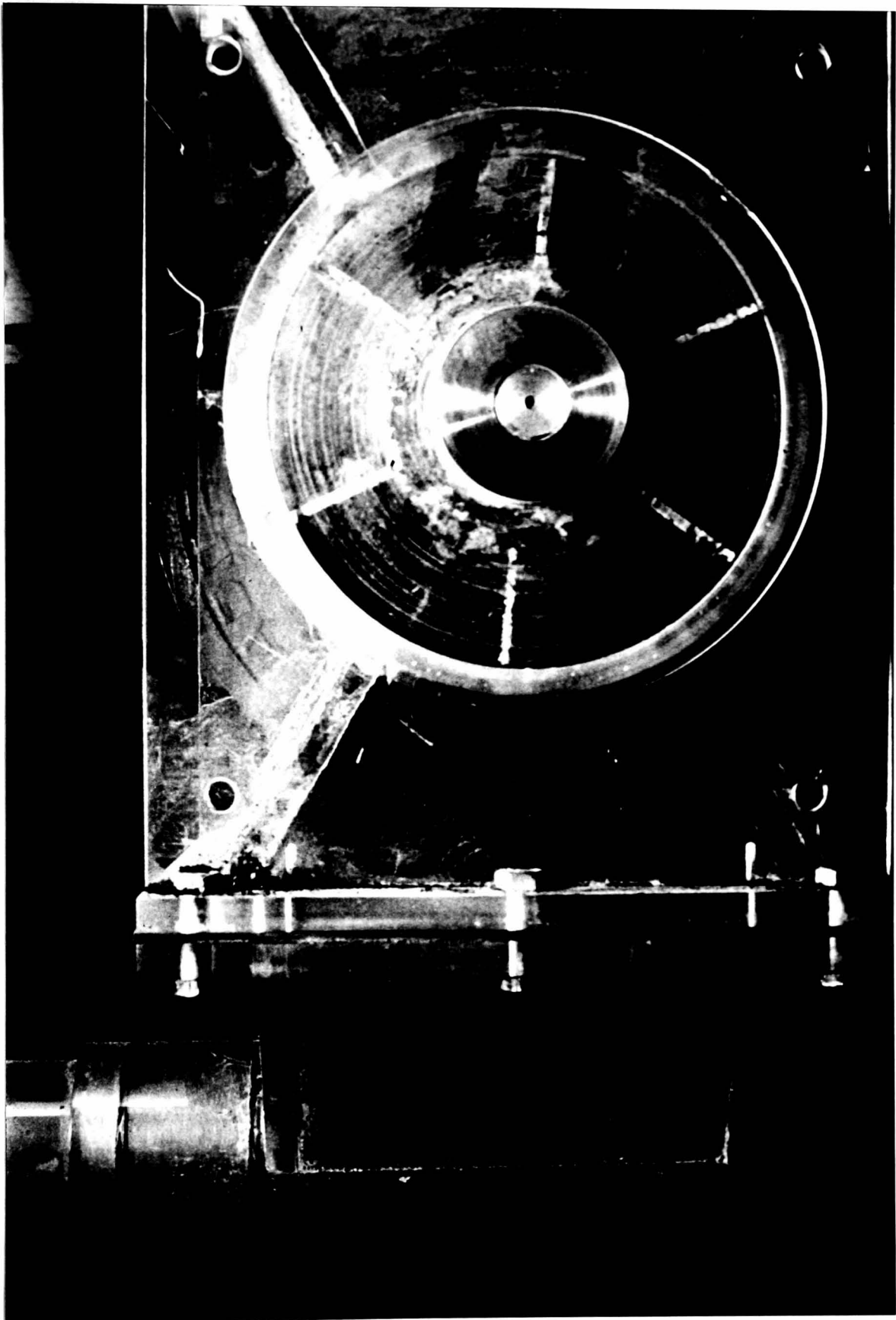
Figure 3.6 Photograph of flow pattern in drop-out box.

pipeline just upstream of the drop-out box; commonly referred to as the 'actual pick-up' velocity, see Figure 3.7a.   This can be considered to be analagous to a constrained wheel in contact with a moving belt as shown in Figure 3.7b.   This concept of the method by which the air swirl is driven appeared to be confirmed by the experimental observations, which revealed that the flow pattern of the tea leaves was more strongly influenced by the air swirl as the pick-up velocity was increased.

The presence of the air swirl is significant because it suggests that the conditions beneath a rotary valve which is used to feed a pneumatic conveyor are complex.   Certainly it is clear that they are very different from the conditions in the experimental apparatus used to obtain most of the previous research data.   That is, the rigs of Jotaki & Tomita Reed, Finkbeiner and Masuda (References 10, 11, 12, 13, 17 & 20).   The swirl may also be an explanation for the 'turbulence' reported by industrialists and referred to in the introduction to this chapter.

3.4.2   Observations - Box A

The flow patterns observed in drop-out box A are shown in Figure 3.8. As previously mentioned the entrainment process was dominated by a strong air swirl.   Even at low pick-up velocities (less than 12 m/s), this swirl was strong enough to recirculate and hold tea leaves in the box chamber for a significant period of time.   The swirl was not significantly influenced by the direction of rotation of the rotor when the valve was mounted in configurations A1 and A2.   However, in configuration A3 a twist was imparted to the swirl as shown in Figure 3.9.   The sense of this twist was found to be dependent on the direction of rotation of the rotor.   It is proposed that it is induced because the air leaks preferentially through the returning 'empty' rotor pockets.

At pick-up velocities between 15 and 20 m/s the air swirl was strong enough to lift large quantities of tea into the upper regions of the drop-out box.   With certain configurations, especially A1 and A3, this led to recapture of tea in the returning empty pockets as shown in Figure 3.10.   This reduces the volumetric efficiency of the valve and results in less material being supplied to the conveying line.   Recapture was not observed with configuration A2, that is, where the valve is arranged so that it initially discharges tea over the downstream half of the drop-out box.   A possible reason for this is that in this arrangement the

AIR IN DROP-OUT BOX
CHAMBER TURNED BY
CONVEYING AIR IN
PIPELINE BELOW.

AIR

SWIRL

CONVEYING AIR

Figure 3.7a

WHEEL IN CONTACT WITH
MOVING BELT MADE TO
ROTATE

MOVING BELT
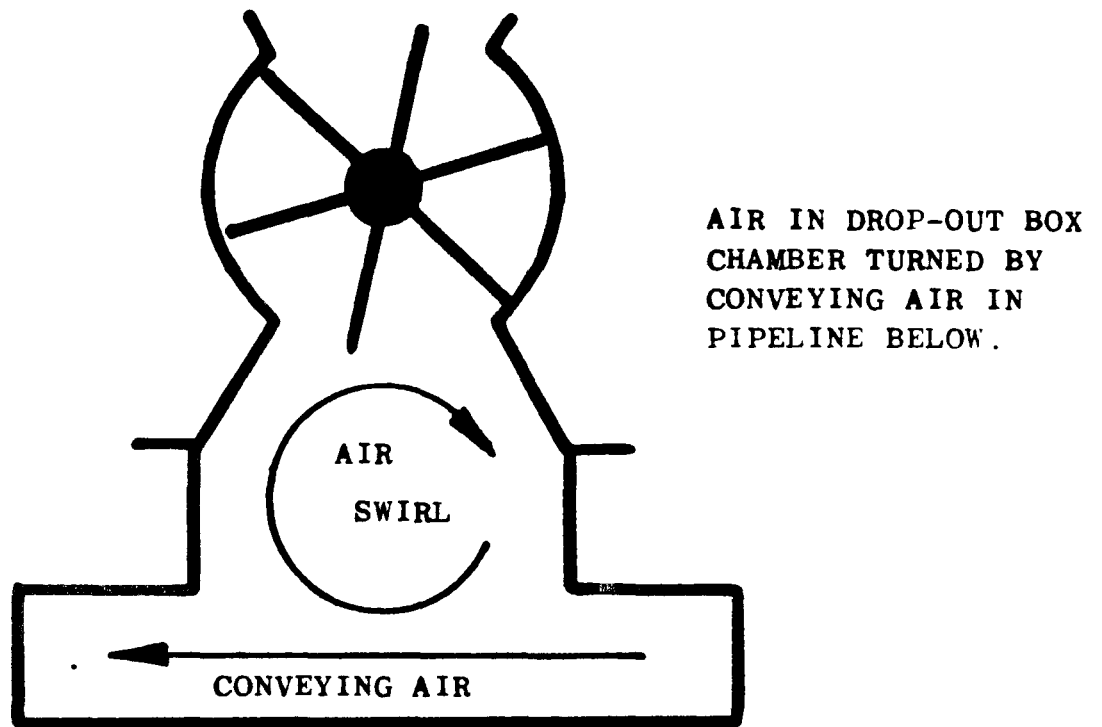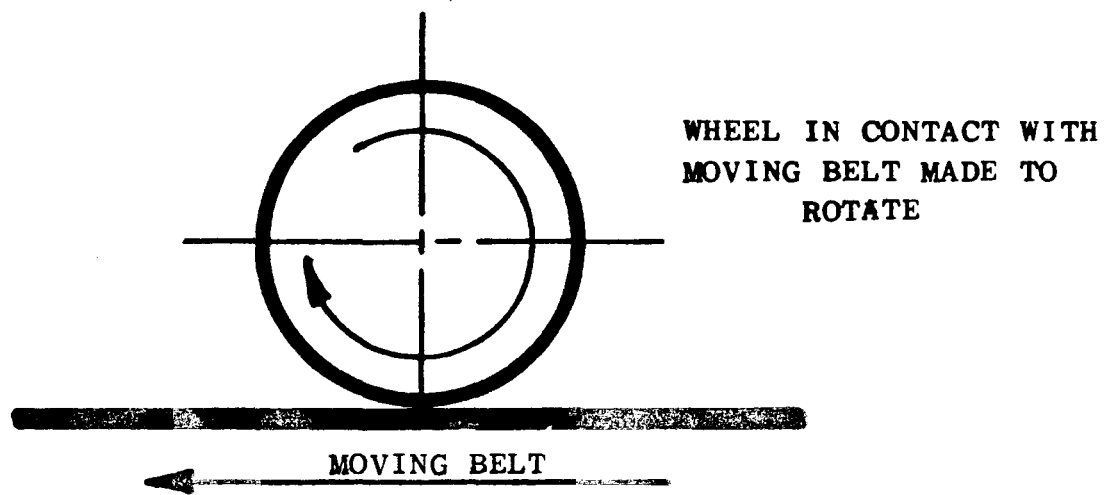
Figure 3.7b

Figure 3.7 Air Swirl in the Drop-out Box
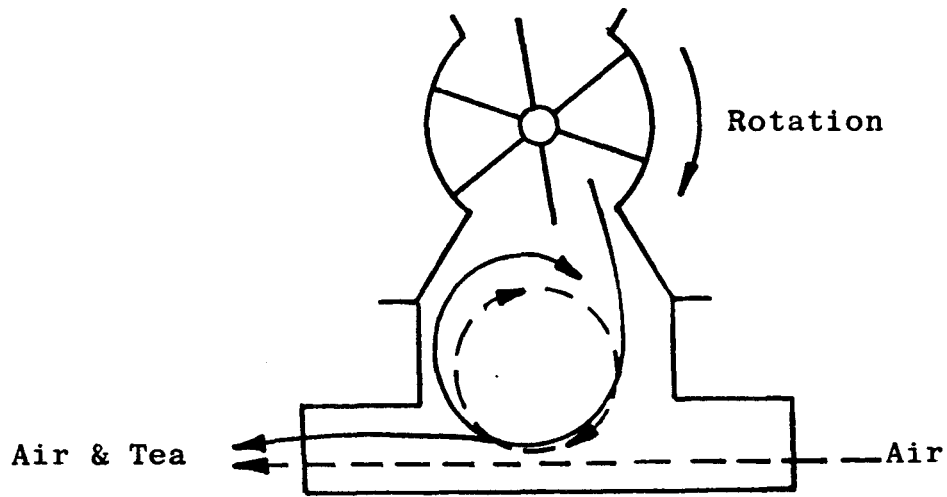
A1

Figure 3.8a
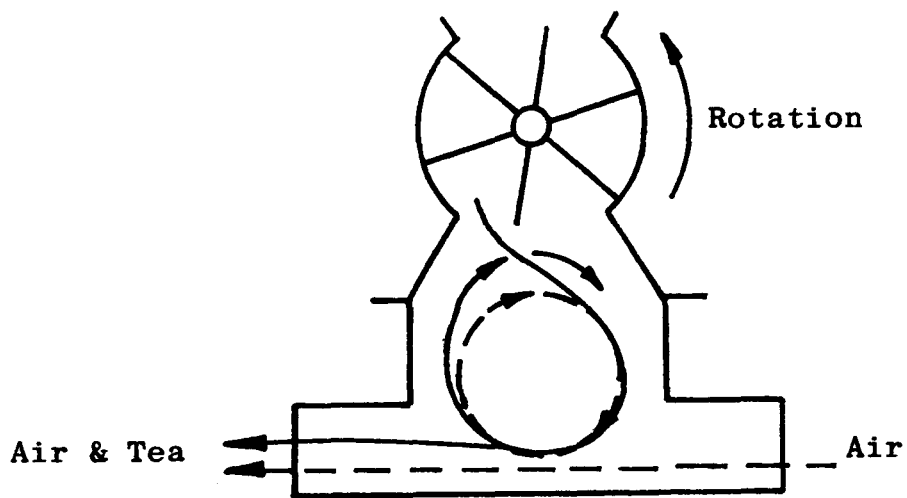
A2

Figure 3.8b

Figure 3.8   Air and Solids Flow Patterns observed
in Drop-out Box A

Tea caught by
returning pocket

Rotation

Twist
imparted
to air
swirl
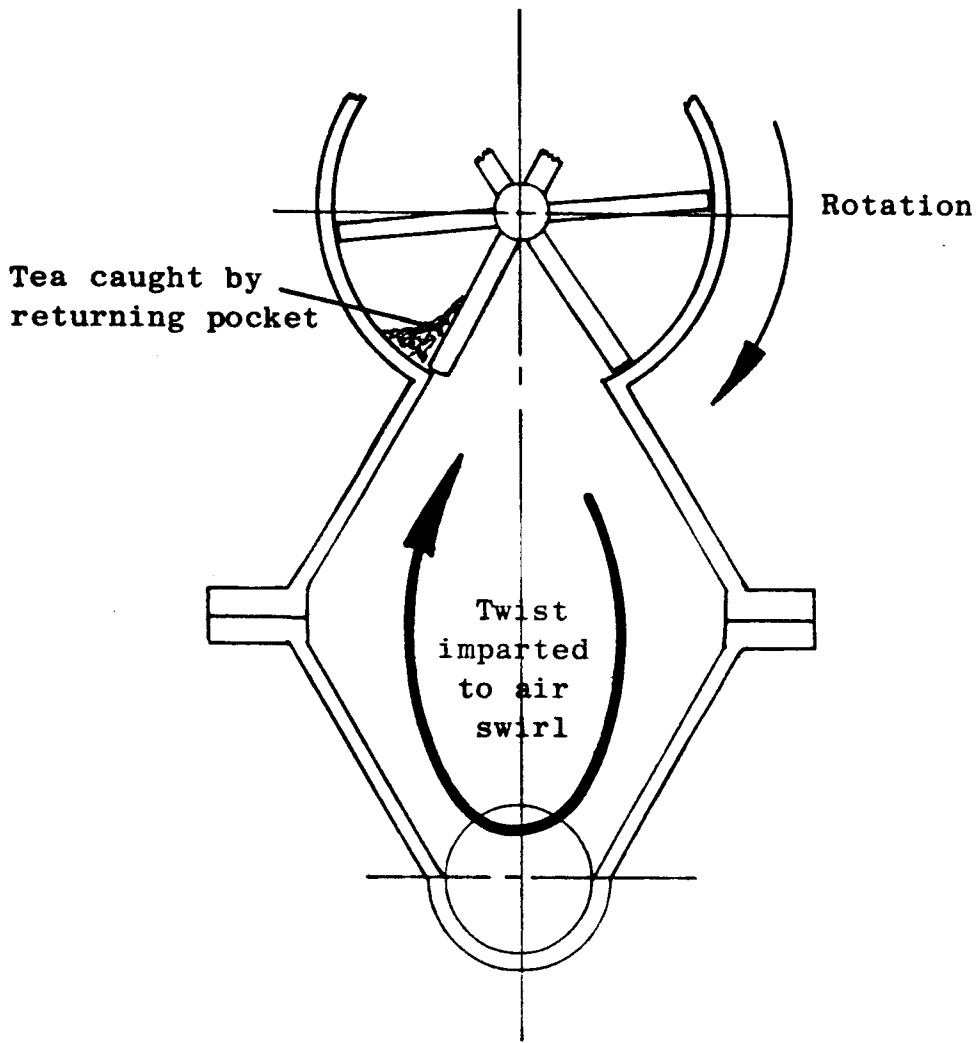
Figure 3.9 Twist imparted to air swirl in configuration A3.

Tea thrown
back into
pocket by
air swirl

Rotation

Tea & air
swirl

Tea caught
in pocket

Rotation

Tea & air
swirl
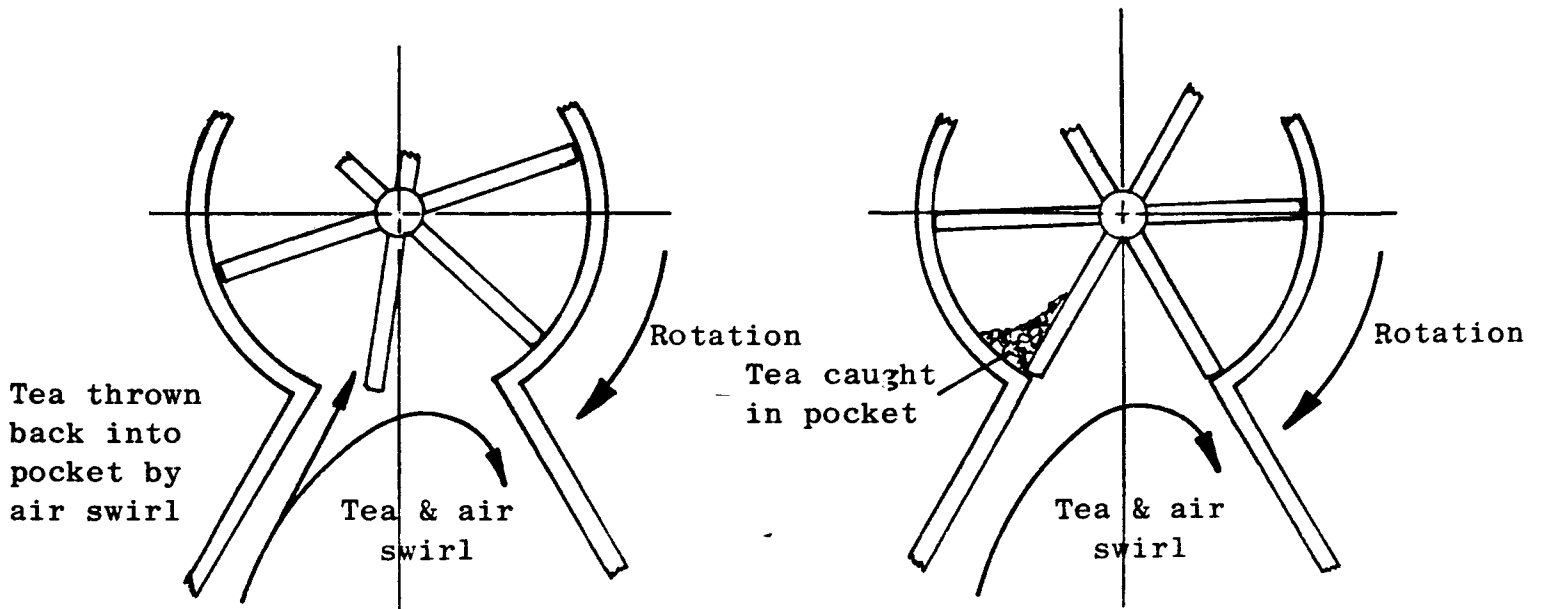
Figure 3.10 Recapture of tea in rotor pockets.

swirling airstream tends to carry the tea leaves away from the rotor pockets.   Also the tea flows into the box chamber in the form of a sheet, see Figure 3.8b, thus effectively shielding the returning rotor pockets from particles in the air swirl.

3.4.3   Observations - Box B

The flow patterns observed in the entrainment configurations using drop-out box B were essentially similar to those already described for box A.   The only significant difference was that the angled outlet face distorted the air swirl and caused the tea to be deflected back across the box at an acute angle.   As a result of this it appeared that less material was recaptured by the returning rotor pockets.   However, because of the limited instrumentation, this observation could not be quantified.

3.4.4   Observations - Box C

The flows observed in configurations C1 and C2 proved to be very interesting.   At solids feed rates less than about 0.05 kg/sec the air was observed to set up a swirl in the drop-out box chamber similar to that previously described for the other configurations, see Figure 3.11a. However, at solids feed rates above 0.05 kg/sec and pick-up velocities greater than 15 m/s the method of entrainment was quite different. Under these conditions the tea leaves were observed to build-up on the ramp formed by the raked inlet face, eventually filling the drop-out box chamber and forming a bridge across the box outlet.   In this situation the mode of entrainment is for small quantities of material to break-away from the underside of the bridge as shown in Figure 3.11c. The feed rate of the valve is then restricted because the material in the box obstructs the discharge of that in the rotor pockets.   In this situation, reducing the rotor speed and/or the pick-up velocity was found to cause the drop-out box to blow clear.   The mode of entrainment then reverts to that where the air swirl is dominant as illustrated in Figure 3.11a.   These observations are interesting because they indicate that, in some circumstances, a drop-out box can restrict the throughput of a rotary valve.   If this happens, the performance of the conveying system as a whole will suffer.
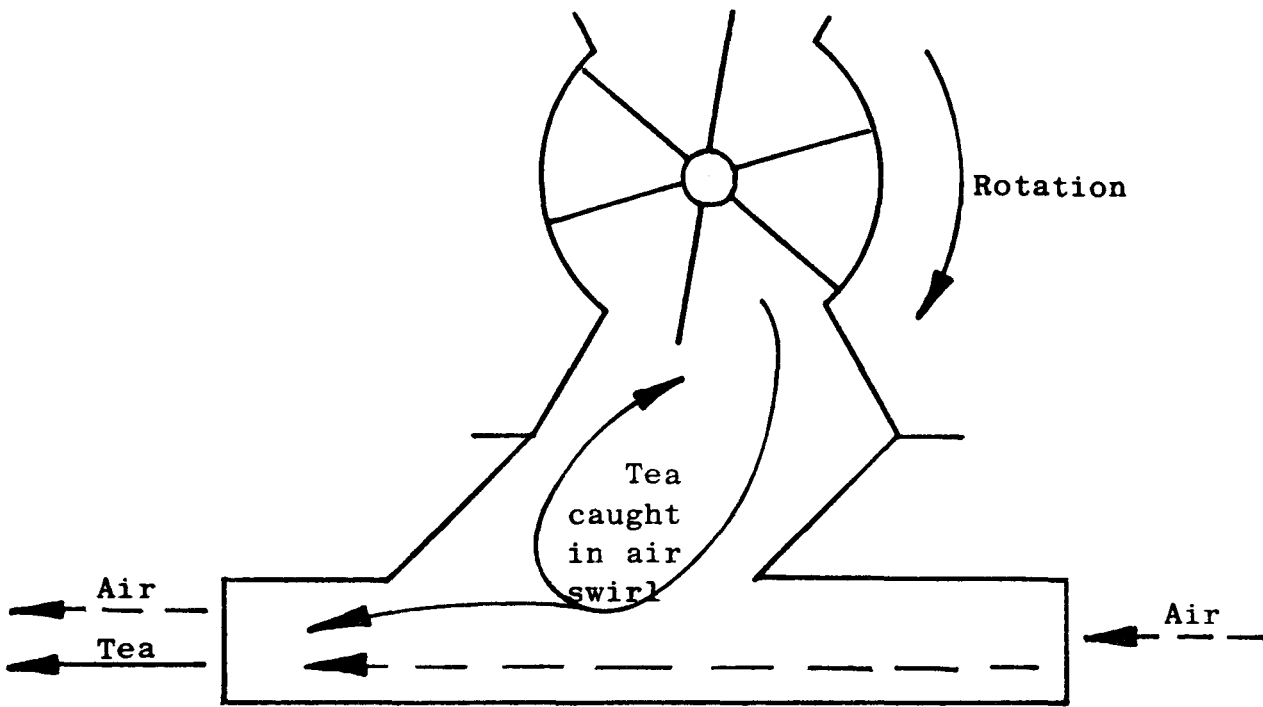
Figure 3.11a
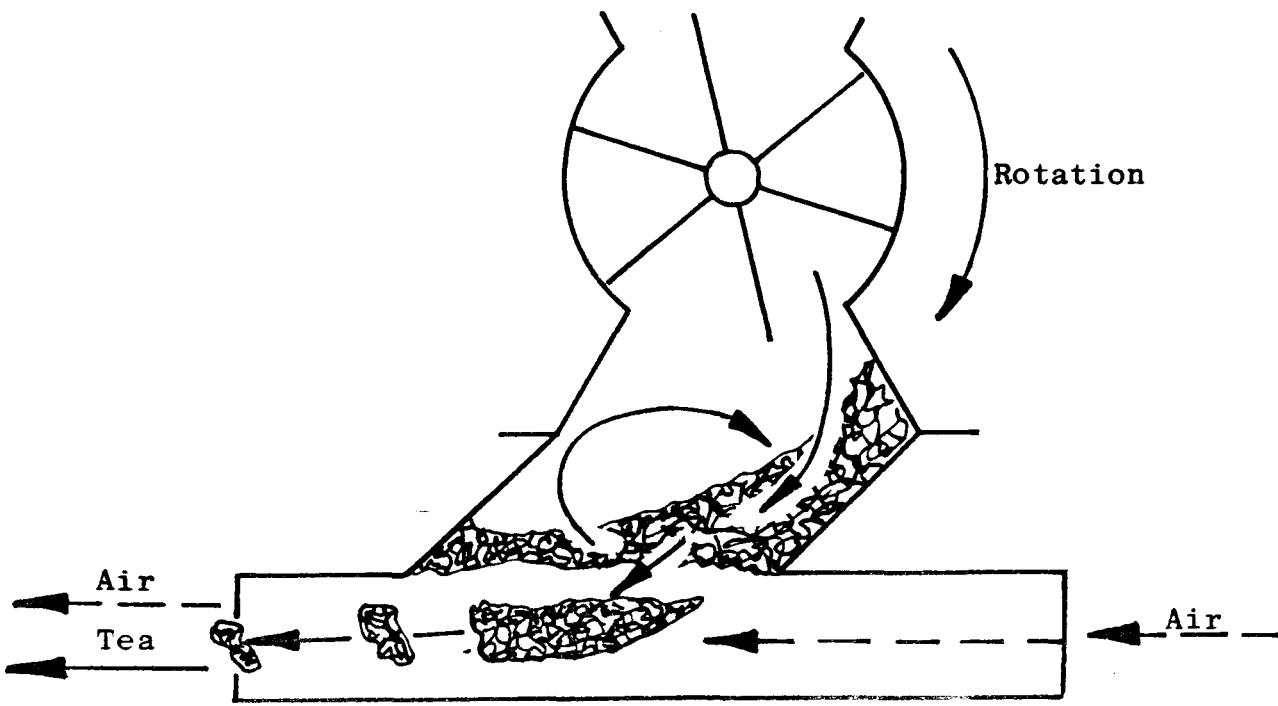
Figure 3.11b

Figure 3.11   Flow Patterns in Drop-out Box C

An indication that this situation may sometimes arise in industrial systems is contained in a communication from Tyrrell (44). He stated that during commissioning trials of a rotary valve system for handling sugar, the required feed rate could not be initially achieved. Subsequent investigation suggested that the pick-up velocity being used was too high. When this was reduced the feed rate was found to increase. Tyrrell went on to say that in his mind there is:'..little doubt that material can indeed be held up inside a drop-out box if the air velocity in the pipe beneath the box is too high'. While this is by no means conclusive evidence that the conditions in a drop-out box can restrict the performance of a conveying system, it is certainly consistent with the behaviour observed in drop-out box C.

3.4.5 Observations - Box D

When the deep drop-out box configurations, D1 and D2, were tested the dominant air swirl was still found to be present. However, the flow patterns differed slightly from that observed in the shorter boxes because the air swirl was removed from the immediate vicinity of the valve discharge port, as illustrated in Figure 3.12. This had the effect of minimising the quantity of tea recaptured by the valve pockets. As previously mentioned, Moseman & Bird (22 & 23) found that a deep drop-out box was more effective than shorter designs and these observations provide a possible explanation for this.

3.4.6 Valve Orientation and Direction of Rotor Rotation

The effect of these variables has been briefly mentioned in the foregoing sections. Nevertheless, because they were observed to have a significant influence on the entrainment process they will now be discussed individually.

For the deep drop-out box the observations revealed that valve orientation and direction of rotation had no apparent effect on throughput. This was also the conclusion reached by Moseman & Bird with regard to short drop-out boxes. However, the visual observations of this study appear to contradict their findings and suggest that there is a 'best' configuration for short boxes which can optimise the
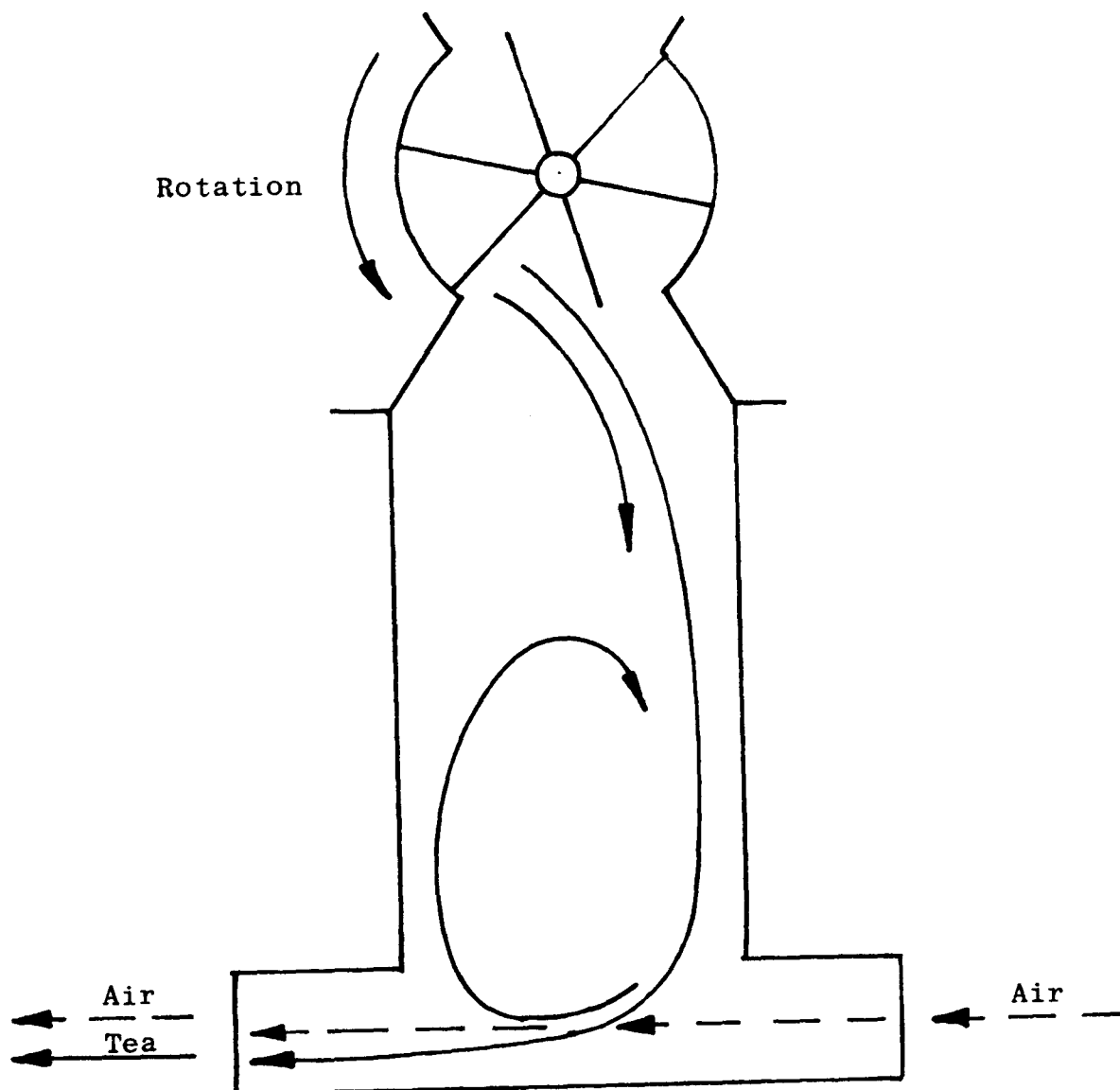
Figure 3.12   Flow Pattern in Drop-out Box D

feeding capacity of the system. To illustrate this point consider the diagrams shown in Figures 3.8 and 3.9.

When the rotary valve was mounted with the rotor pockets parallel to the conveying line, Figure 3.9, there was no preferred direction of rotation and product was easily recaptured in the rotor pockets. However, when the valve was mounted with its axis at 90° to the conveying line the preferred direction of rotation was as shown in Figure 3.8a, that is, configurations A2 and B2. This appeared to minimise the amount of product recaptured, for the reasons discussed in section 3.4.2. It is interesting to note here that an experienced designer of pneumatic conveying systems for a leading American company also favours this configuration, Gerchow (45 & 46). Gerchow does not give any reasons for this preference, but it is reasonable to assume that it has been arrived at through practical experience.

3.4.7 Rotor Speed

It is clear from the work discussed in Chapter 2 that rotor speed is the principal means of controlling throughput. However, in terms of entrainment performance it was found to be of little importance. In the case of the tea leaves used in this study, it was clear that the momentum imparted to the particles by the rotational motion of the valve rotor was swamped by the aerodynamic forces resulting from the swirling air. Consequently, the rotor speed had little effect on the material flow pattern in the drop-out box chamber. The following analysis demonstrates that this is likely to be the case for all materials if they are discharged from the rotor pockets as discrete particles. (The analysis is not valid for materials which discharge 'en masse').

Consider a particle of mass m_p in a valve pocket rotating at an angular velocity of ω_r as shown in Figure 3.13. On falling free from the constraints of the pocket and surrounding material the particle will have a component of kinetic energy equal to $\frac{1}{2}m_p\omega_r^2 r^2$ resulting from the rotational motion. Now, the largest radius at which the particle could still have been influenced by the motion of the pocket is that of the rotor (r_r). Therefore, the maximum kinetic energy which could be imparted to a particle by the valve rotor is given by:

$$(K.E.)_r = \frac{1}{2}m_p\omega_r^2 r_r^2 \qquad (3.1)$$
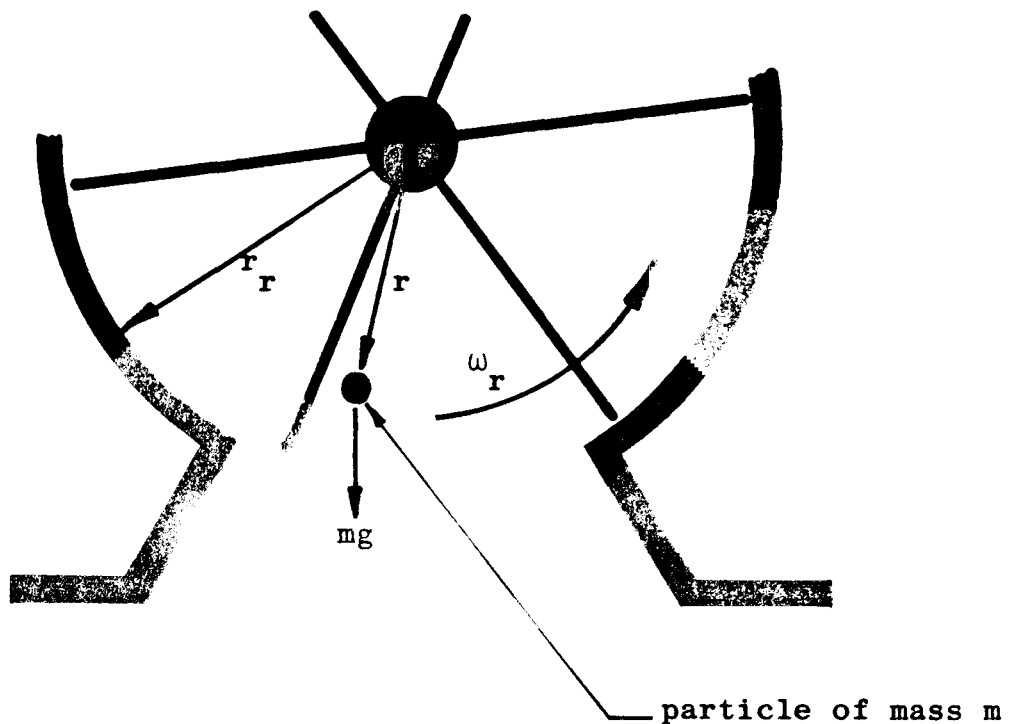
Figure 3.13 Analysis of a single particle falling from a rotary
            valve pocket.

The kinetic energy of the same particle when it has become
entrained into the swirling air of the drop-out box is:

$$(K.E.)_b = \tfrac{1}{2}m_p v_p^2 \tag{3.2a}$$

where v_p is a typical particle velocity in the air swirl.   It is
clear that v_p is difficult to determine exactly but it seems reasonable
to assume that it must have the same order of magnitude as the pick-up
velocity.   Therefore, for the sake of simplicity, let $v_p = sV_{pu}$,
where V_{pu} is the nominal pick-up velocity and s is the slip ratio, that
is, the particle to air velocity ratio.   We can then write:

$$(K.E.)_b = \tfrac{1}{2}ms^2 V_{pu}^2 \tag{3.2b}$$

The ratio of the kinetic energies $(K.E.)_r$ and $(K.E.)_b$ will give an
indication of the relative magnitudes of the forces acting on the
solid particles in the valve pocket and in the drop-out box chamber.

That is:

$$\frac{(K.E.)_b}{(K.E.)_r} = \left[\frac{sV_{pu}}{\omega_r r_r}\right]^2 \qquad (3.3a)$$

or alternatively:

$$\frac{(K.E.)_b}{(K.E.)_r} = \left[\frac{60sV_{pu}}{2\pi n r_r}\right]^2 \qquad (3.3b)$$

where n = valve rotor speed in rev/min.

For the rotary valve used in this work r_r = 70 mm. Substituting this into equation 3.3b and using a conservative value for the slip ratio of 0.1, the graph shown in Figure 3.14 was constructed. This shows how the kinetic energy ratio $(K.E.)_b/(K.E.)_r$ varies with rotor speed and pick-up velocity. Despite the fact that the value used for the slip ratio is smaller than might be anticipated, the diagram shows clearly that, for the majority of conditions examined in the flow visualisation rig, the kinetic energy of a particle in the air swirl is at least an order of magnitude greater than that imparted to the particle by the rotor blades. Using a higher value for the slip ratio, say 0.8 as measured by Birchenough (47) for alumina particles in a vertical pipeline, would suggest that the difference is at least two orders of magnitude. Consequently, it is not surprising to find that the rotor speed has little effect on the material flow pattern in the drop-out box chamber.

If similar calculations are performed for a size of valve commonly used in industry, say 200 mm, it can be shown that the kinetic energy ratio would be about 2000:1 for a typical rotor speed of 30 rev/min and a pick-up velocity of 20 m/s. Therefore, it is reasonable to conclude that the effect of rotor speed on the material flow pattern in drop-out boxes fitted to such valves will be minimal, as was observed in the flow visualisation rig.

This work, although simplistic in its approach, demonstrates conclusively that the forces acting on the product in the drop-out box chamber are overwhelmingly due to the interaction with the air swirl. Thus, it follows that it is not practicable to utilise the momentum

imparted by the rotor to 'throw' material in a preferential direction.
The practical implication of this is that rotor speed cannot be used
to significantly influence the trajectory of materials which are fine
and easily entrained by the air swirl.   However, this may not be the
case with products that consist of large dense particles.
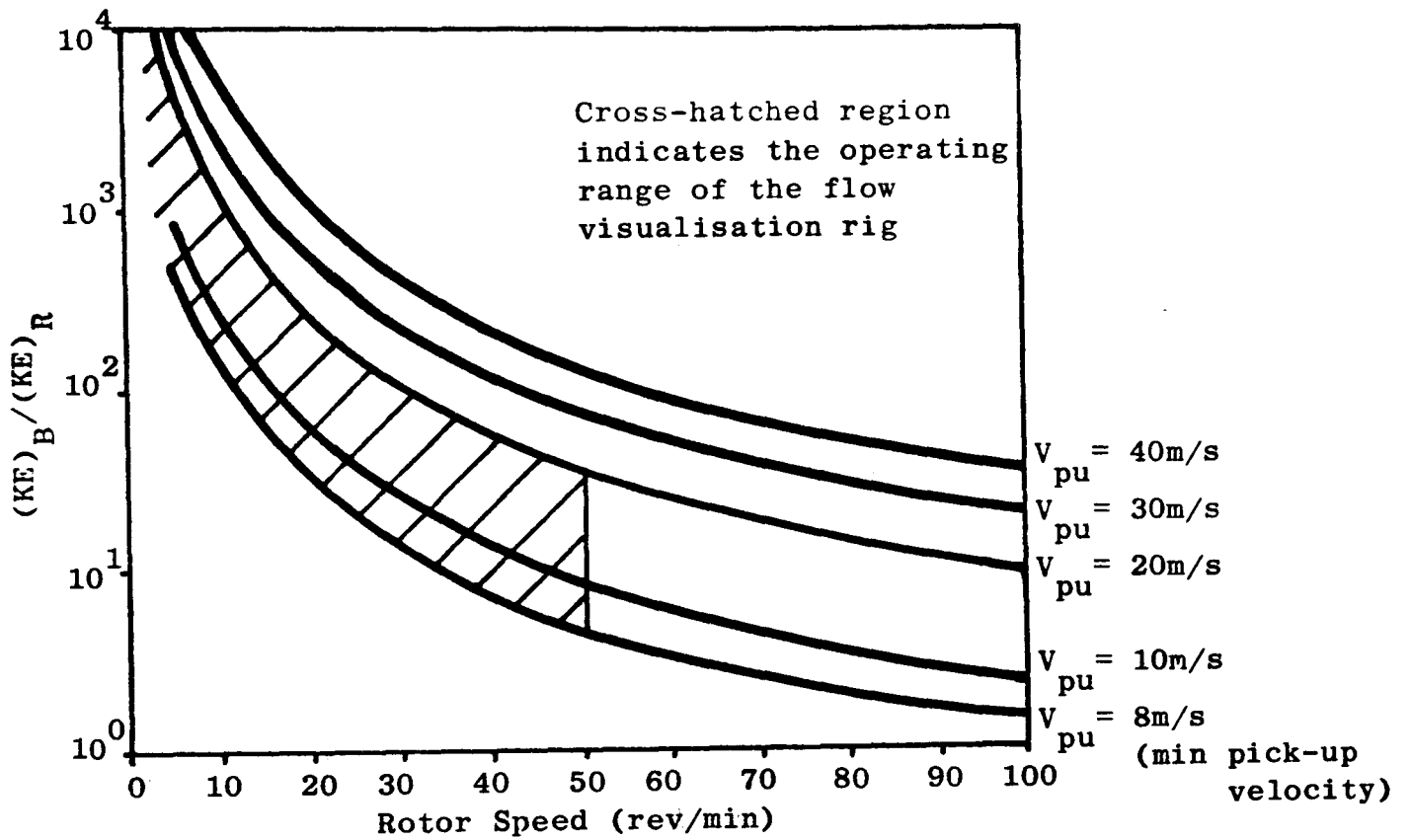
Figure 3.14   Variation of Kinetic Energy Ratio $(K.E.)_B/(K.E.)_R$
with Rotor Speed and Pick-up Velocity for Rotary
Valve used in Flow Visualisation Rig.

3.4.8 Air Velocity

The 'pick-up' velocity of the conveying airstream was observed to influence both the product and the air flows within the drop-out box in two distinct ways.   Firstly, when the velocity was less than about 8 m/s the material was not entrained properly into the airstream. Operation below this velocity led to a build up of material in the box chamber, eventually causing a blockage.   This behaviour is not surprising since the prediction of minimum air velocities for pneumatic conveying has long been the subject of considerable research.   Some recent papers on this subject are given in References 48, 49 and 50.

The second effect of 'pick-up' velocity is its direct influence on the strength of the air swirl in the box chamber.   As the velocity was increased so the strength of the air swirl was also observed to increase.   At high velocities it was noted that some of the tea particles collected in the extremities of the box chamber as a result of the swirl.   In the case of drop-out box C this eventually led to the box becoming choked as was previously described in section 3.4.4. A possible explanation for this is discussed in Chapter 4.

3.5 Concluding Remarks on and Implications of the Entrainment Flow Observations

The most significant outcome of these experiments was the discovery of the swirling air flow pattern which dominates the entrainment of material into the conveying line.   This swirl was present in all of the drop-out box configurations tested and its strength was found to be dependent on the 'pick-up velocity' of the air.   In some cases it was found to cause recapture of product in the returning 'empty' valve pockets.   However, the observations suggested that this could be minimised by the correct choice of drop-out box, valve orientation and direction of rotation.   With the deep drop-out box recapture could be avoided almost completely.

The implication of these observations is that both the geometry of the entrainment section and the conditions within it can have a significant effect on product feed rate and hence on the performance of the conveying system as a whole.   This was taken as a justification for extending the research in order to quantify the effect of these

parameters on the performance of industrial systems. To achieve this, mathematical models of the entrainment process have been developed and further experiments performed using an industrial size rig capable of handling a wide range of materials. This work and the subsequent conclusions are detailed in the following chapters.

CHAPTER FOUR

MODELLING OF THE INTERACTION BETWEEN ROTARY VALVES AND PNEUMATIC CONVEYING PIPELINES

4.1 Introduction and Synopsis of Chapter

This chapter proposes some methods for modelling the interaction between rotary valves and pneumatic conveying pipelines. The purpose of these models is to provide a means of quantifying the effect of this interaction on the performance of rotary valves and hence on the performance of the conveying system as a whole; thereby enabling the feed rate to be predicted with more confidence than is currently possible. A method of accounting for the effect of air leakage on the pocket filling character-istics of rotary valves is also proposed. This is important to consider because valves which are used to feed positive pressure conveying systems are subject to an adverse pressure gradient. As discussed in Chapter 1, this gives rise to an air leakage which opposes the transfer of product and, therefore, should be taken into account when predicting the feed rate.

The chapter is divided into three main sections. The effect of air leakage on the pocket filling characteristics of a rotary valve is discussed in section 4.2. This is considered first because it determines the maximum feed rate which can be achieved assuming that all the material which enters the pockets can be completely discharged.

The performance of a conventional drop-through valve used with a drop-out box transition section is considered in section 4.3. The reasoning behind much of this work is based on the flow visualisation experiments described in Chapter 3. A simple model is proposed for estimating the volumetric entrainment efficiency of a given combination of rotary valve and drop-out box and a method for determining the conditions that lead to the drop-out box becoming choked is developed. Section 4.4 deals briefly with the interaction between the blow-through type of rotary valve and pneumatic conveying pipelines.

The chapter concludes with section 4.5 which summarises the models that have been proposed and their contribution to understanding the interaction between rotary valves and pneumatic conveying pipelines.

4.2   The Effect of Air Leakage on the Pocket Filling Characteristics of a Rotary Valve

4.2.1   The Problem

Air leakage has long been recognised as having a limiting effect on the performance of rotary valves.   However, to date, there are no accepted methods for evaluating this effect and consequently valves are often oversized in order to ensure that the desired feed rate can be achieved. For instance, Fischer (23) states that: 'In selecting a feeder which must serve as an airlock it should be sized so as to be capable of carrying out at least twice its theoretical rate.'   This is obviously a very simplistic approach, but it serves to illustrate the lack of confidence which system designers have in predicting the performance of rotary valves.   To emphasise this point, Stoess (51) gives an example which shows that even a valve 'oversized' by 100% will not necessarily guarantee an adequate feed rate.

Reed (11) and Jotaki & Tomita (12 & 13) have both proposed models for the pocket filling characteristics of rotary feeders and these have been already discussed in detail in Chapter 2.   Unfortunately, these models cannot be applied to rotary valves because they do not consider the situation where there is an adverse pressure gradient to cause an air leakage opposing the transfer of solids.   In this section a method of evaluating the effect of air leakage on the pocket filling characteristics of a rotary valve is proposed. Essentially it is a more general form of the model which was developed by Reed for a rotary feeder.   The important difference being the inclusion of a term which allows for the effect of air leakage.   The implication of the model is that, depending upon the characteristics of the material being handled, increasing the pressure ratio across a rotary valve can significantly reduce the maximum potential feed rate and even cause a feed stoppage. This is consistent with the experience of industry and is the reason why proprietary rotary valves are often fitted with vents to divert the leakage air away from the inlet port.

4.2.2 The Model

It is known that when a rotary valve is used to feed material against an adverse pressure gradient, there is an inevitable flow of leakage air through the internal clearances. If the rotor shaft seals are effective and there is no means of diverting the air by venting, then it seems reasonable to assume that it will pass out of the system at the inlet port by percolating through the interstices of the material in this region. Furthermore, it is reasonable to envisage that this flow of air will impede the flow of solids into the rotor pockets and hence impede the pocket filling process.

In an attempt to model this situation, the simplifying decision is made that the air leakage is the only restriction to the flow of solids. The equation of motion for a bed of solids entering a rotary valve can then be written as:

$$\rho_b h A \frac{dS}{dt} = \rho_b g A g - \Delta P_h A \qquad (4.1a)$$

where ΔP_h is the pressure difference across depth h of the bed and A is the horizontal area of flow as defined in Figure 4.1

$$\Delta P_h \quad h$$

Pressure drop ΔP_h across
bed of solids of height h

Horizontal area
of flow A

G   S

Rotation

C = G + S
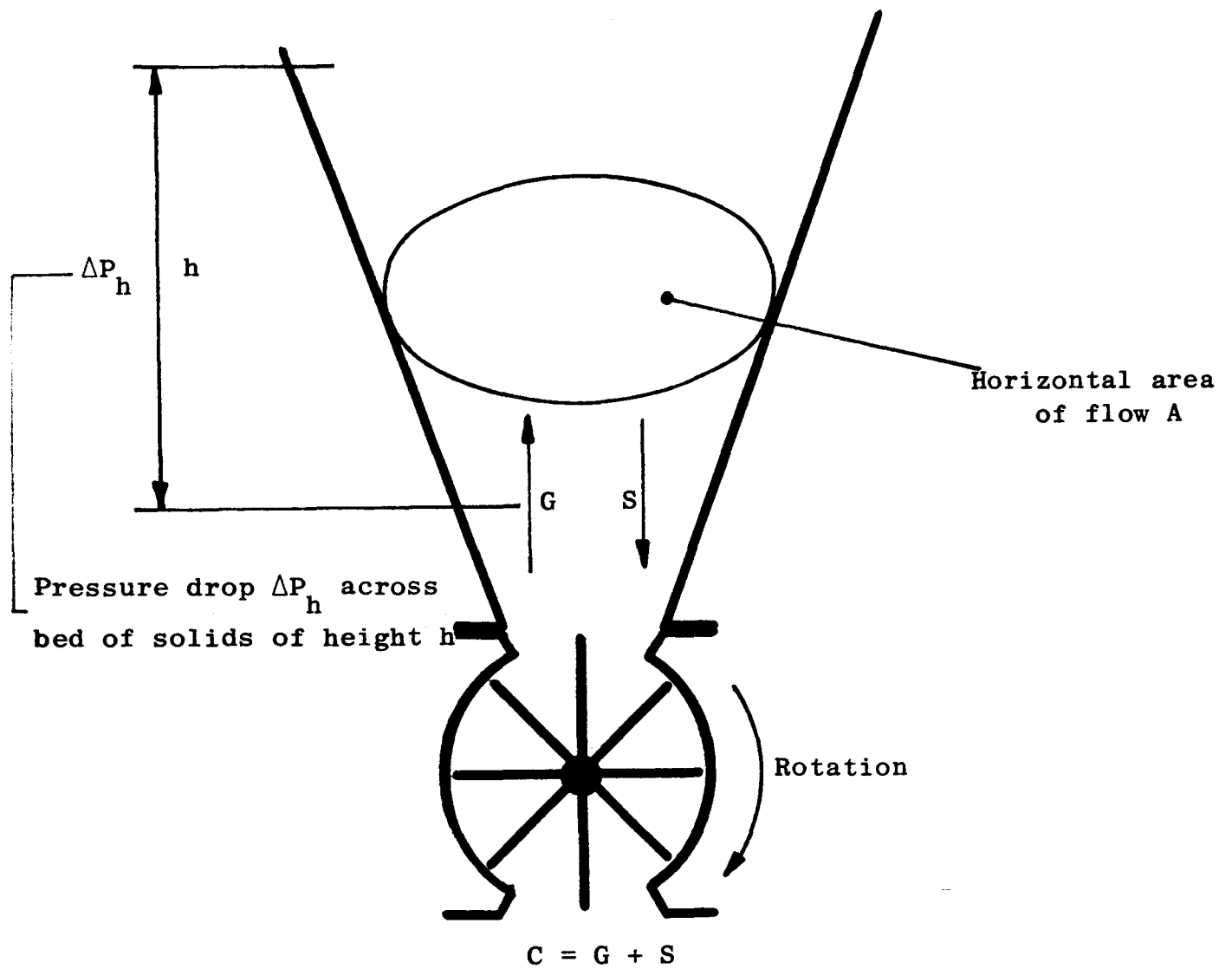
S = Velocity of solids towards pockets

G = Velocity of air relative to pockets

C = Relative velocity of air and solids

Figure 4.1 The Pocket Filling process of a Rotary
Valve

By re-arranging equation 4.1a a relationship for the acceleration of the bed with respect to the pocket can be obtained:

$$\frac{dS}{dt} = g - (\Delta P_h/h) \frac{1}{\rho_p} \qquad (4.1b)$$

These two equations are the same in form as equations 2.12a and 2.12b which were used by Reed.   The difference being that S, the velocity of the solids bed relative to the pocket, is used instead of C, the relative velocity of the air and solids.   This difference is important because it distinguishes the present general model from the version derived by Reed specifically for rotary feeders.   Since there is no air leakage through a rotary feeder, Reed made the simplifying decision that the bed of solids could be considered as falling through stationary air in which case G = 0 and hence C = S.   Consequently, it is clear to see that equations 2.12a and 2.12b are special cases of the general equations 4.1a and 4.1b.

As previously discussed in Chapter 2, Reed substituted an expression for the pressure drop per unit length ($\Delta P_h/h$) into equation 2.12b in order to put it into an integrable form.   The expression which he used was derived by Carman (14) for a flow flowing through a bed of granular solids.   That is:

$$\frac{\Delta P_h}{h} = 180\mu \frac{(1 - \varepsilon)^2}{\varepsilon^3 (d_p\phi)^2} C' \qquad (4.2)$$

where ε is the voidage of the bed $(1 - \rho_b/\rho_p)$, μ is the dynamic viscosity of the interstitial air and ϕ is a particle shape factor which is unity for a sphere and less than unity for all non-spherical particles.   Since this correlation was initially derived for fluid flow through homogeneous beds of stationary particles, the term C' refers to the velocity of the fluid relative to a fixed bed.   However, for the purpose of this analysis C' may be considered to be the same as the relative velocity of the air and solids in the moving bed above the inlet of the rotary valve.   If this simplification is accepted then the Carman expression may also be used to write equation 4.1b in an integrable form, which then gives:

$$\frac{dS}{dt} = g - K(G + S) \qquad (4.3)$$

where (G + S) is the relative velocity of the air and solids above the inlet port and K is the 'material characteristic factor' which was defined by Reed as:

$$K = \frac{180\mu}{\rho_p} \frac{(1 - \varepsilon)}{\varepsilon^3 (d_p \phi)^2} \qquad (2.14)$$

or alternatively in the simplified form,

$$K = 1.296 \times 10^{-2}/d_p^2 \rho_p \qquad (2.18)$$

From these expressions it can be seen that K is solely dependent on the characteristics of the bulk solid and the interstitial fluid. Therefore, provided that the air temperature, and hence the dynamic viscosity (μ), are constant, K may be treated as a constant in equation 4.3. The velocity of the air relative to the rotor pockets (G) may also be treated as a constant because it is dependent on the air leakage through the valve; which itself is constant for a given material, rotary valve, applied pressure ratio and head of solids. G can be estimated by dividing the equation proposed by Reed (11) for the air leakage rate, equation 2.23, by the effective horizontal area of flow, that is, the product Aε. Thus:

$$G = buLc/A\varepsilon \qquad (4.4)$$

Integrating equation 4.3 twice, with the boundary conditions[*]:

    i) t = 0, S = 0 and

    ii) t = 0, y_b = 0

gives the vertical distance $y_b(t)$ travelled by the bed of solids in time t.   That is:

$$y_b(t) = \frac{g}{K} K_\ell \left[t - \frac{1}{K}(1 - \exp(-Kt)) \right] \qquad (4.5)$$

If this is compared with the equivalent expression derived by Reed for a rotary feeder, equation 2.15, it can be seen that they are identical except for the term K_ℓ.   This is the term which allows for the effect

* footnote: See Appendix II

of air leakage and is given by the relationship:

$$K_\ell = 1 - GK/g \qquad (4.6a)$$

or substituting for G from equation 4.4

$$K_\ell = 1 - buLcK/A\epsilon g \qquad (4.6b)$$

If equation 4.6b is analysed it can be seen that the air leakage factor K_ℓ is dependent on the characteristics of the material being handled (b, ϵ and K), the dimensions of the valve (L, c and A) and the notional leakage velocity (u) which is a function of the pressure ratio across the valve, see Figure 2.25. Since all of these parameters are readily obtainable it is a simple matter to calculate K_ℓ for any particular combination of material, valve and pressure ratio.

For a pressure ratio of unity, which is the operating condition for a rotary feeder, Figure 2.25 shows that the notional leakage velocity is zero. Substituting this into equation 4.6b gives the value of K_ℓ as unity. Equation 4.5 then becomes equal to Reed's expression for a rotary feeder, that is, equation 2.15. This agreement between the two models is to be expected because of the similarity between the original propositions from which they are derived. It is also confirmation of the earlier statement that the Reed model is a special case of that proposed here.

Having obtained equation 4.5 for determining $y_b(t)$, the volume of material which enters a rotor pocket may be calculated using equation 2.16, that is:

$$v = w \frac{\pi d_r}{Z} y_b \left[\frac{60\ell}{\pi d_r n} \right] \qquad (2.16)$$

From this, the following expression for the filling rate of a rotary valve operating above its critical rotor speed may be derived:

$$\dot{m}_s = \frac{Zn}{60} \rho_b w \frac{\pi d_r}{Z} \frac{g}{K_\ell} K \left[\frac{60\ell}{\pi d_r n} - \frac{1}{K} \left(1 - \exp - \frac{60\ell}{\pi d_r n} K \right) \right] \qquad (4.7)$$

Below the critical rotor speed $\dot{m}_s$ can be estimated by the following relationship:

$$\dot{m}_s = \alpha \frac{n}{60} V_o \rho_b \tag{2.21}$$

The use of these expressions then enables the relationship between feed rate and rotor speed to be predicted for any given combination of rotary valve, material and pressure ratio. Equating the expressions leads to a prediction of the critical rotor speed.

4.2.3   Discussion

Figure 4.2 shows how the relationship between feed rate and rotor speed varies with the leakage factor (K_ℓ), as predicted by equation 4.7. Also shown on this figure is the relationship between feed rate and rotor speed as predicted by equation 2.21 for various values of the filling factor (α). Since, for a given rotary valve and bulk solid, K_ℓ is only a function of the air pressure ratio across the valve and α is only a function of the pressure ratio and rotor speed; Figure 4.2 may also be regarded as showing how the feeding characteristics of a rotary valve vary with the adverse pressure gradient imposed by a positive pressure conveying system. From Figure 2.25 it can be seen that as the pressure ratio is increased so the notional leakage velocity increases. The effect of this is to reduce the value of K_ℓ and hence the critical rotor speed as shown by Figure 4.2.

Ultimately, if the pressure ratio is continually increased, K_ℓ will become equal to zero and eventually take a negative value. The implication of this is that there is a critical pressure ratio at which the air leakage through the valve is sufficient to maintain a stationary bed of solids above the inlet port and thus stop the pocket filling process altogether, see the line for $K_\ell = 0$ in Figure 4.2. This is consistent with the experience of Stacey (52), who has stated that feed stoppages in rotary valve systems handling P.V.C. powder and Soda Ash are not uncommon.

Experimental evidence that such a situation can occur is contained in a paper published by Jotaki et al (53). In this paper the authors report that a feed stoppage occurred in a rotary valve system handling
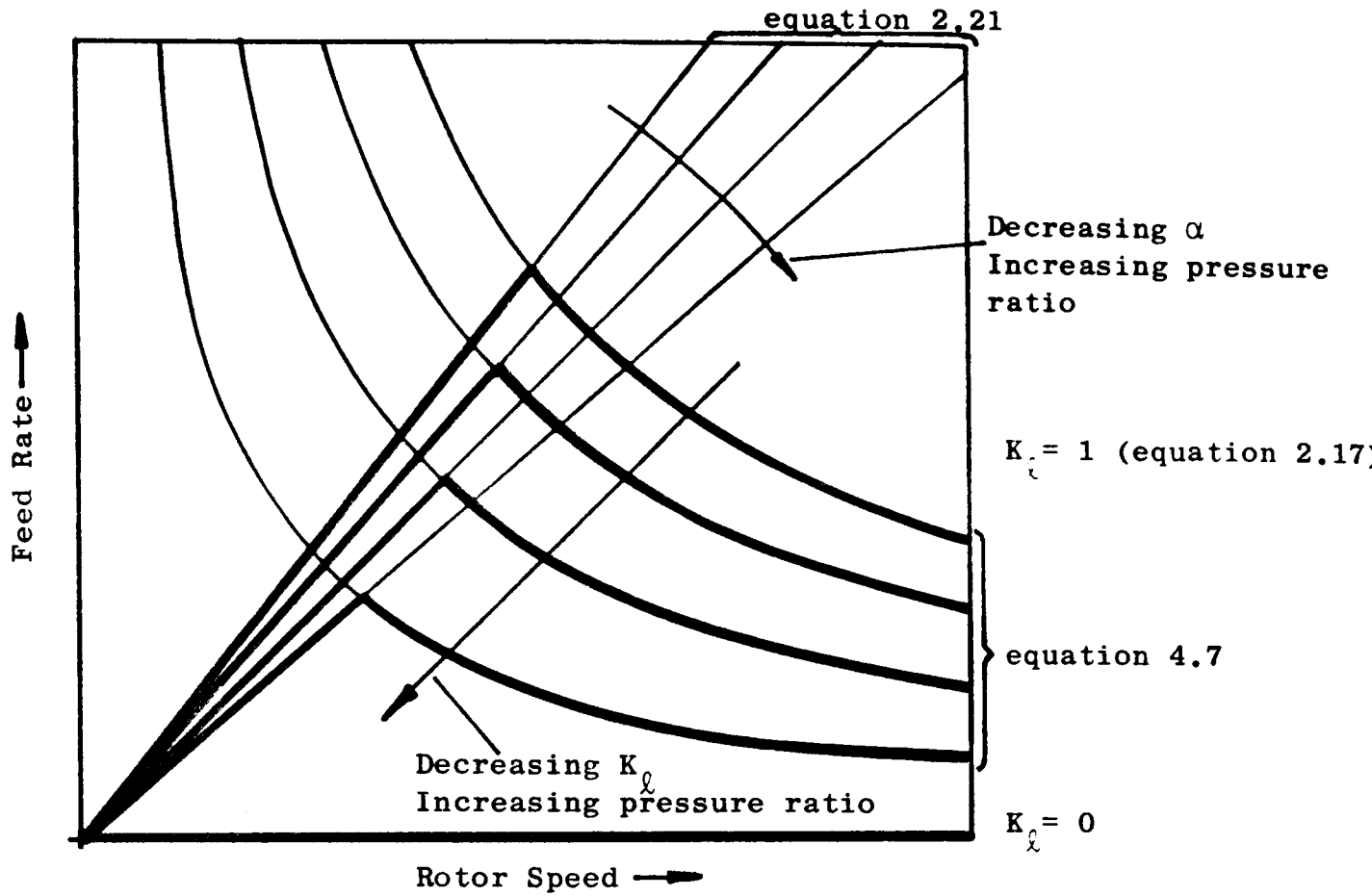
Figure 4.2   Variation of ratoary valve feeding
characteristics with pressure ratio
as predicted by equations 2.21 and 4.7
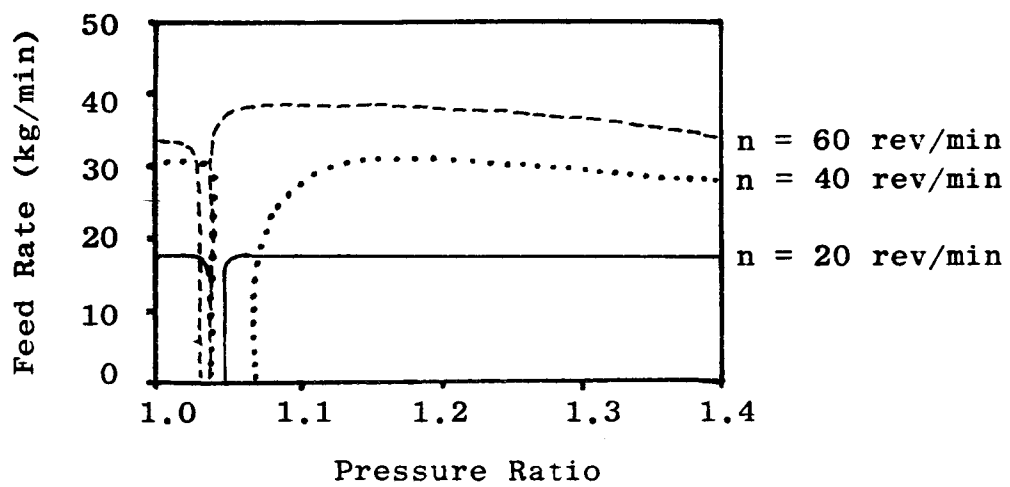
Figure 4.3   Feedrate v's pressure ratio characteristics
for a rotary valve as obtained by Jotaki
et al (53)

P.V.C. powder (d_p = 166 µm) when the pressure ratio reached a critical value. Figure 4.3 illustrates the actual relationship between feed rate and pressure ratio which they obtained. From this it can be seen that the feed rate was only zero at one particular pressure ratio, that is, approximately 1.05. Increasing the pressure ratio beyond this caused the feed rate to recover. A possible reason for the recovery is that the increased air leakage associated with the increased pressure ratio was sufficient to fluidize the P.V.C. and thus render it more free-flowing. If this is the case, it might also explain why the results indicate that the feed rates at pressure ratios above that corresponding to the stoppage condition are generally higher than those which were obtained at lower pressure ratios. In this situation the model proposed in section 4.2.2 is no longer applicable because the premise on which it was based is not valid; that is, that the air leakage impedes the flow of solids into the rotor pockets.

Jotaki et al state that when the feed stoppage occurred the superficial air velocity through the cross-sectional area of the supply hopper was 0.017 m/s. They also give information about the bulk and particle characteristics of the P.V.C. from which it is possible to calculate the minimum fluidising velocity (U_{mf}). For materials with a mean particle size between 50 and 500 µm Woodcock (54) has suggested the following simple correlation for the minimum fluidising velocity:

$$U_{mf} = 420 \, \rho_p d_p^2$$

where U_{mf} is measured in m/s, ρ_p in kg/m^3 and d_p in m. Using this correlation the calculated value of U_{mf} for the P.V.C. is 0.016 m/s[*]. Since this is almost exactly the same as the superficial air velocity measured by Jotaki et al at the feed stoppage condition, it suggests that fluidization was almost certainly the reason for the observed recovery of feed rate. This argument is strengthened by the fact that the P.V.C. is on the borderline between groups A and B in the Geldart classification for fluidization (55), which suggests that it will fluidize readily.

* footnote: See Appendix III.

From the information given by Jotaki et al it is also possible to calculate the value of K_ℓ for their system at the feed stoppage condition.* This should be equal to zero if the model accurately predicts the performance of the system. When the calculation is performed it shows that the value of K_ℓ is approximately 0.05. Consequently, it may be argued that the model is in reasonable agreement with the actual performance of the system for this condition because 0.1 is close to the lower limit of the range of values which K_ℓ may take, that is, $0 < K_\ell < 1$. However, it is evident from Figure 4.3 that this is not the case for other conditions because the characteristics of the P.V.C. are such that the actual variation of feed rate with pressure ratio is very abrupt and not gradual as the model suggests.

To assess the usefulness of the model for materials which exhibit a more gradual variation of feed rate with pressure ratio Figure 4.4 has been constructed. This compares the model predictions with experimental data obtained by Jotaki & Tomita (10) for soya beans.

To determine the predicted characteristics the following procedure was used. Firstly, line A was constructed using equation 2.21. The feeding factor was taken as being 0.7, which is the value suggested by the work of Reed (11) and Masuda et al (20) for unit pressure ratio and unit rotor speed ratio, see Figure 2.27. Consequently, the intersection of this with curve B, which was obtained from equation 4.7 with $K_\ell = 1.0$, gives a prediction of the critical rotor speed at unit pressure ratio. For rotor speeds up to this critical value the throughput is predicted by curve C. This was constructed with the use of Figure 2.27 which shows how the filling factor varies with rotor speed ratio. Thus, the curve C-B is the predicted characteristic for unit pressure ratio.

For other pressure ratios the characteristics are obtained by putting the appropriate values of α and K_ℓ into equations 2.21 and 4.7. However, as discussed in Chapter 2, there are no proven methods for determining α at pressure ratios other than unity. Consequently, curve C has been used for all the pressure ratios considered in Figure 4.4. It is argued that this is justified because the experimental data with which the models are being compared was only obtained for relatively low pressure ratios, that is 1.1 or less.

---

* footnote: See Appendix III.
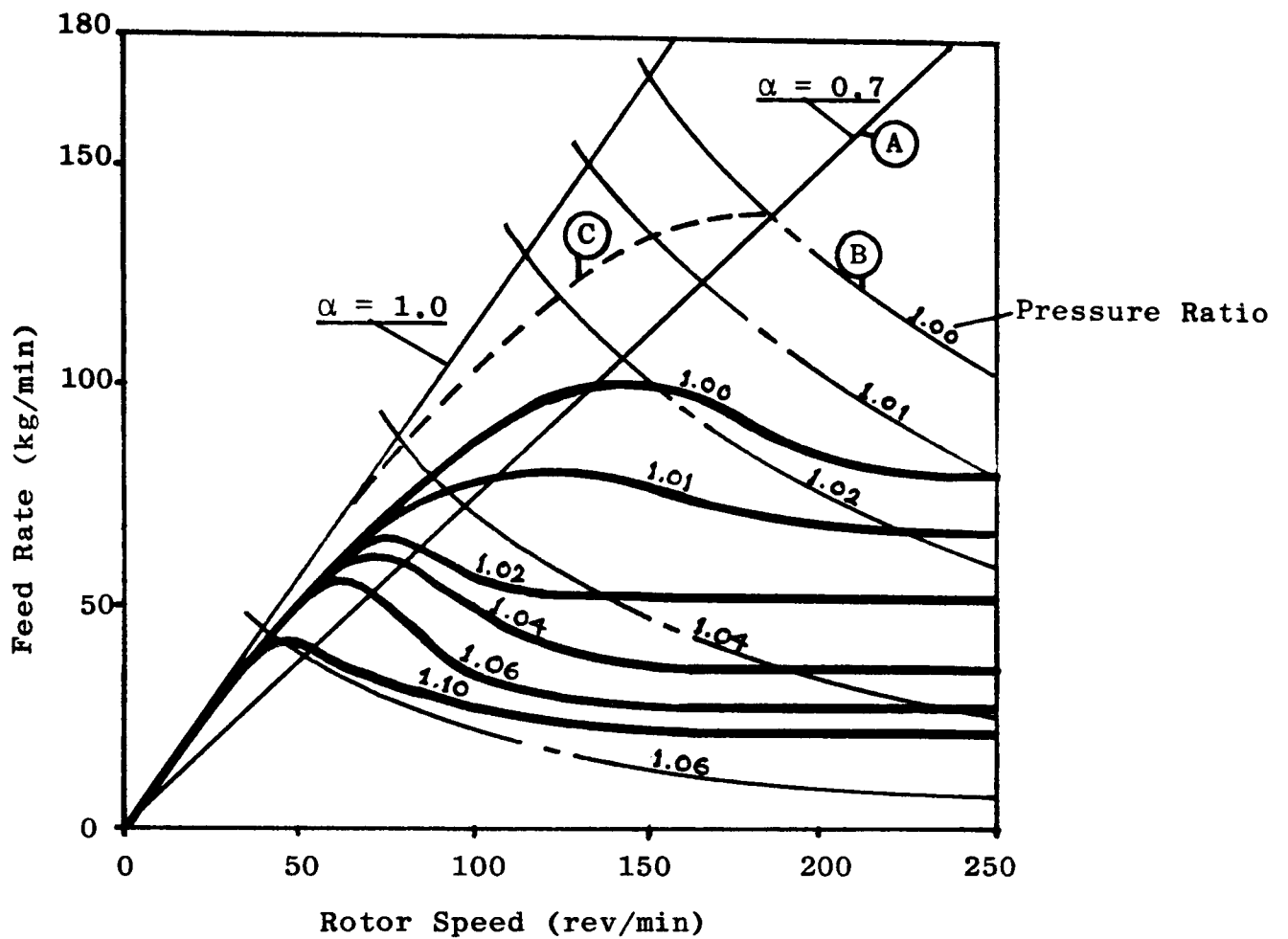
Material: Soya Beans
ρ_p = 1200 kg/m^3
ρ_b = 688 kg/m^3
d_p = 6330 µm

Material Characteristic Factor K = 0.272 -/s
Blockage Factor b = 0.95

Rotary Valve: Drop-through type, 8 bladed rotor
A = 0.012 m^3
c = 0.0001 m
L = 0.15 m
w = 0.15 m
ℓ = 0.082 m
d_r = 0.15 m
V_o^r = 1.6 litre

Pressure Ratio	K_ℓ
1.00	1.00
1.01	0.80
1.02	0.60
1.04	0.28
1.06	0.08

━━━━━━━━ Jotaki & Tomita Data
═ ═ ═ ═ ═ Predicted Curves

Figure 4.4 Comparison of model predictions with experimental
data obtained by Jotaki & Tomita (10) for soya
beans

It is immediately obvious from Figure 4.4 that, for pressure ratios
up to about 1.05, the overall magnitude of the predicted characteristics
is larger than that of the actual characteristics.   This discrepancy is
not surprising because it is consistent with predictions of the pocket
filling model developed by Reed (11), equation 2.17, on which the present
model is based.   Reed's model overestimated the actual maximum feed
rate by as much as 50% for large particle products.   At pressure ratios
greater than 1.05, Figure 4.7 shows that the leakage factor over-
compensates for the effect of air leakage.   Consequently, the model
underestimates the actual feed rate and predicts a feed stoppage at a
pressure ratio of about 1.08.

This inconsistency between the predicted and actual results suggests
that the inclusion of the leakage factor into the pocket filling analysis
does not produce an accurate model of the variation of feed rate with
pressure ratio.   However, if the relationship which defines the leakage
factor, equation 4.6, is examined it will be seen that it includes two
terms which are difficult to quantify with any degree of certainty;
these are, the horizontal area of flow (A) and the voidage of the material
entering the valve (ε).   The horizontal area of flow is difficult to determine
because the junction between the supply hopper and valve does not usually
have a uniform cross-section.   It is interesting to note here that, in
the case quoted previously for P.V.C. powder, the supply hopper used was
a cylinder only slightly larger in diameter than the inlet port of the
valve.   This might explain why the model was in satisfactory agreement
with the actual performance at the feed stoppage conditions.   The
voidage is important to determine precisely because the variation of the
leakage factor with this parameter is significant.   Unfortunately this
is difficult to do because it is an implicit function of the air pressure
gradient over the material and the interstitial air velocity, see
equation 4.2.

The evaluation of the leakage factor is further complicated because
it is a function of the material characteristic factor (K).   In Chapter
2 it was explained that the Carman equation, from which the material
characteristic factor is derived, can only be considered valid for
material which have a value of K < 10.   That is, those which have a
mean particle size greater than about 1.0 mm and a typical particle

density of about 1500 kg/m^3. The implication of this is that there is
a limit to the range of materials for which the leakage factor can be
determined.   A possible means of overcoming this limitation is to use
a more generally applicable equation for the pressure drop per unit
length in a bed of solids in the development of the pocket filling model;
for instance, that proposed by Ergun (56).

$$\frac{\Delta P_h}{h} = 150 \frac{(1 - \varepsilon)^2}{\varepsilon^3} \frac{\mu U_{mf}}{d_p^2} + 1.75 \frac{(1 - \varepsilon)}{\varepsilon^3} \frac{\rho_a U_{mf}^2}{d_p}$$

The problem with using such an equation is that it would not lead to a
single simple material characteristic factor such as that obtained when
the Carman equation is used.

The inevitable conclusion of the foregoing discussion is that the
present model cannot be used to reliably evaluate the effect of air
leakage on the performance of rotary valves.   Nevertheless, the trends
which it predicts appear to be in good agreement with the observed
performance of actual systems, see Figures 4.2 and 4.4.   This may be
taken as an indication that the form of the model is a reasonable and
sound basis for further development.   The derivation of alternative
expressions for the material characteristic factor (K) and the leakage
factor (K$_\ell$) are seen as the most likely methods of achieving this;
possibly by using the Ergun equation as suggested above.   However,
further development of the model will not be discussed here because it
falls outside the scope of this thesis.   The justification for
including the work presented so far is that the influence of air leakage
on the filling characteristics of a rotary valve is a secondary effect
of the interaction with a pneumatic conveying line and, under some
circumstances, will be the limiting effect on system performance.
This is particularly the case for the blow-through type of rotary valve,
as will be discussed in section 4.4.   Consequently, the development of
an understanding in this subject is closely allied to the aims of the
research, as stated in Chapter 1.

4.3   The Interaction between Air and Solids in a Drop-out Box

4.3.1   The Two Different Modes of Entrainment

When a drop-through rotary valve is used as a feeder for a pneumatic
conveying system the initial mixing of the air and solids takes place
in the chamber formed by the drop-out box.   In Chapter 3 experiments
to identify the nature of the air and solid flow patterns in this
chamber were discussed.   These established that there are two distinctly
different processes by which solids are entrained into the conveying air-
stream.   These are:

    i)   where a strong swirl dominates the interaction between
         air and solids; and

    ii)   where the drop-out box becomes 'choked' with material
         and thus restricts the discharge rate of the rotary
         valve.

Since many proprietary drop-out boxes are of similar design to those
examined in this study, it is reasonable to assume that these modes of
entrainment are typical of those which occur in many industrial
systems.   If this is accepted then it is important to quantify their
effect on system performance.   In this section two models are proposed
which attempt to do this.   The first proposes a method of quantifying
the effect of the drop-out box volume on performance when the air
swirl dominates the entrainment process.   The second explains why the
drop-out box can become 'choked' with material and provides a method
of determining the conditions that lead to this situation.

4.3.2   The Effect of Drop-out Box Volume on the Entrainment Process

As a result of the flow visualisation experiments it is now known that,
for a wide range of operating conditions and drop-out box configurations,
the flow pattern in the drop-out box is dominated by a strong air swirl.
In this situation material is entrained by the swirl and distributed
throughout the box chamber.   If the simplification is made that this
distribution is uniform, it is possible to estimate an entrainment
efficiency which is based on the comparative volumes of the drop-out
box and of the comparative volumes of the drop-out box and of the rotor

pocket(s) which are open to the drop-out box when material is being
discharged.
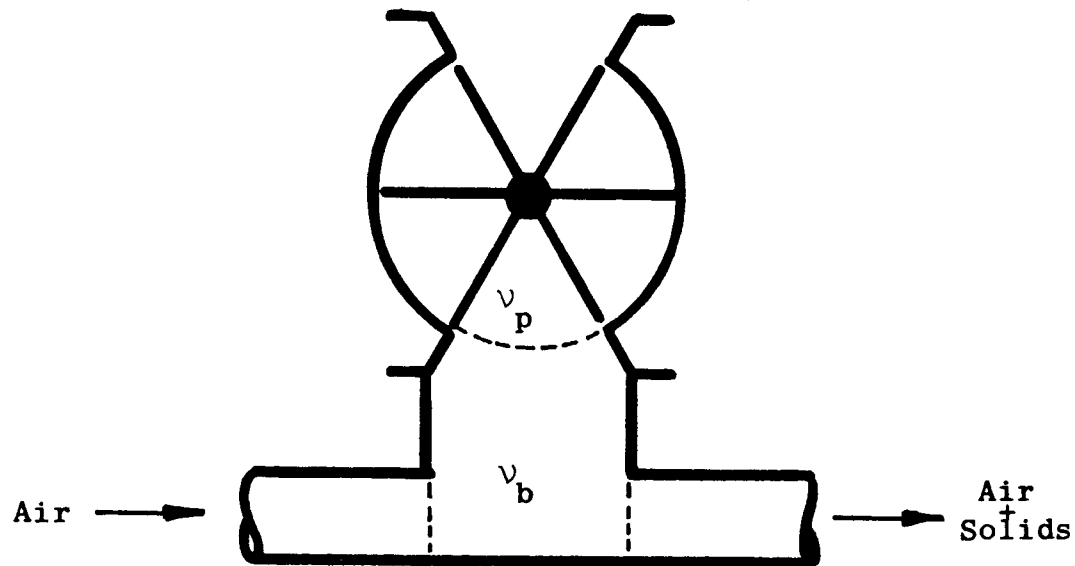
Figure 4.5   Comparative volumes of the drop-out box
and the rotor pockets open to the drop-
out box

Consider Figure 4.5, which shows a section through a typical
rotary valve and drop-out box.   Two volumes, ν_b and ν_p are defined
in this figure, ν_b as the volume of the drop-out box and ν_p as the
volume of the rotor pocket(s) which are open to the drop-out box.
The total volume of the drop-out box chamber is given by the sum of
these individual volumes, that is, $(\nu_p + \nu_b)$.

When the system is operating ideally, the contents of each rotor
pocket are completely entrained into the airstream before the pocket
closes.   However, in practice this is unlikely to happen because
material is held inside the drop-out box chamber by the air swirl.
Furthermore, since the rotor pockets form part of this chamber, some of
the material will be retained in them when they close.   If the
simplification is made that the distribution of material is uniform,
then it follows that the quantity which is retained in the pockets, as
a proportion of the total amount in the drop-out box chamber, will be

given by:

$$\nu_R = \frac{\nu_p}{\nu_p + \nu_b} \qquad (4.8)$$

where ν_R is the 'volume ratio' of the rotary valve and drop-out box
combination. If the further simplification is made that steady state
conditions exist in the drop-out box, the entrainment efficiency (η_e)
may be calculated as:

$$\eta_e = (1 - \nu_R)\ 100\% \qquad (4.9a)$$

or alternatively,

$$\eta_e = \frac{\nu_b}{\nu_p + \nu_b}\ 100\% \qquad (4.9b)$$

If steady state conditions do not exist, because the concentration of
material in the drop-out box fluctuates significantly, this model will
probably give an underestimate of the actual entrainment efficiency.
It may also underestimate the performance of systems which have very deep
drop-out boxes. In such cases it seems reasonable that gravity will
cause a higher concentration of material in the bottom of the box chamber.
Consequently, the decision to assume a uniform distribution of material
is then questionable and less material is likely to be retained in the
rotor pockets than the model predicts. Furthermore, the model can only
be justified for those materials which are easily entrained by the air
currents in the drop-out box. For other materials the initial premise
is unlikely to be correct.

Despite these limitations the significant implication of this
analysis is that the rotary valve and drop-out box must be considered as
one unit as far as the entrainment process is concerned. A possible means
of classifying rotary valve and drop-out box combinations is provided by
the volume ratio (ν_R), which is defined by equation 4.8. For a typical
rotary valve and drop-out box two pipe diameters in depth, ν_R usually has
a value of 0.1 and thus the entrainment efficiency which can be expected
is about 90%.

Another important implication of this analysis is that, for a
given size of rotary valve, the throughput can be maximised by making
the volume of the drop-out box (v_b) as large as possible; see equation
4.9b.   This is consistent with the observations of the flow visualisation
study, Chapter 3, and the results obtained by Moseman & Bird (22 & 23).
Indeed, it is interesting to use equation 4.9b to determine the
entrainment efficiencies of the rotary valve and drop-out box combinations
which were examined by Moseman & Bird.   Illustrations of these are shown
in Figure 4.6 along with their calculated volume ratios and entrainment
efficiencies.   As previously discussed in Chapter 2, Moseman & Bird
found that the throughput of their system was improved by increasing the
depth of the drop-out box.   Thus, box 'C' was better than box 'B' and
box 'B' was better than box 'A', which is in agreement with the predicted
trend.   Furthermore, Moseman (23) stated that the throughput obtained
with box 'C' was 7% better than that obtained with box 'B'.   This
figure is very interesting because it is exactly the difference between
the calculated entrainment efficiencies of these two arrangements.
Unfortunately, Moseman did not quantify the performance obtained with box
'A', only to say that it was considerably worse than with either box 'B'
or box 'C'.   On the basis of the analysis this comment is surprising,
because there is only a 3% difference between the calculated entrainment
efficiencies of boxes 'A' and 'B'.   However, there are other factors
which could make box 'A' a poor arrangement and these will be discussed
in the next section.

In conclusion, the proposed model appears to provide a simple method
for estimating the discharge efficiency of a rotary valve and drop-out
box combination.   The only information which is needed in order to use
the model are the volumes of the drop-out box and the rotor pockets.
Despite this simplicity, the agreement with the only available
experimental data, that is Reference 23, is very encouraging.   However,
this alone is not sufficient evidence to justify confidence in the model
and hence further experimental data is needed for comparison.   The
results of an investigation to provide such information will be discussed
in Chapter 7.

Rotation

Air swirl dominates
the flow pattern

Air
Solids

Air

Figure 4.7a

Rotation

As above but a higher
concentration of solids

Air
Solids

Air

Figure 4.7b

Rotation

Almost static condition
'CHOKED'

Air
Solids

Air
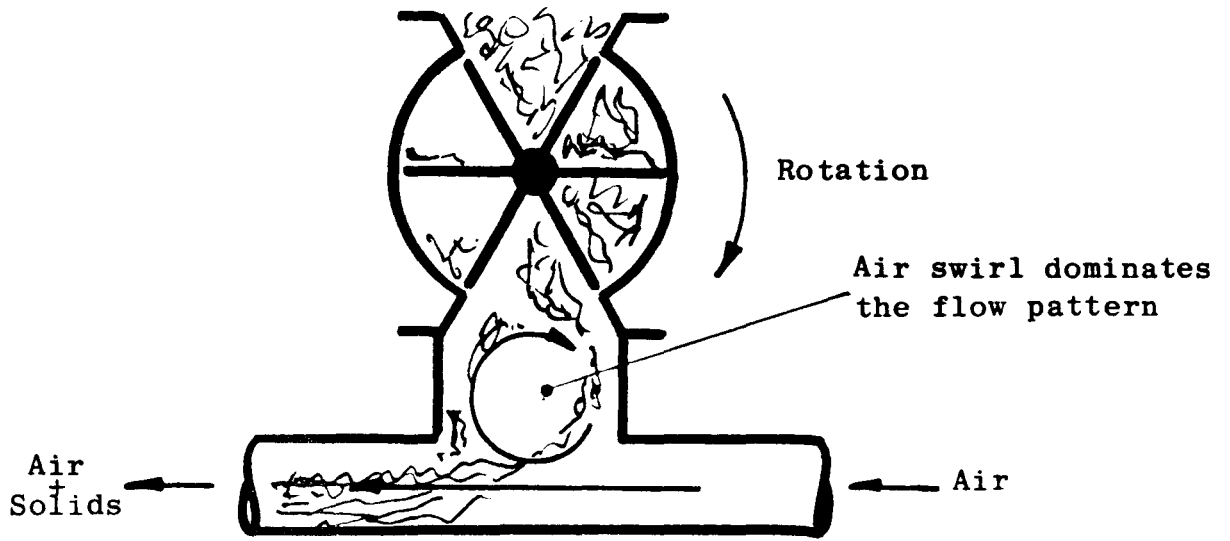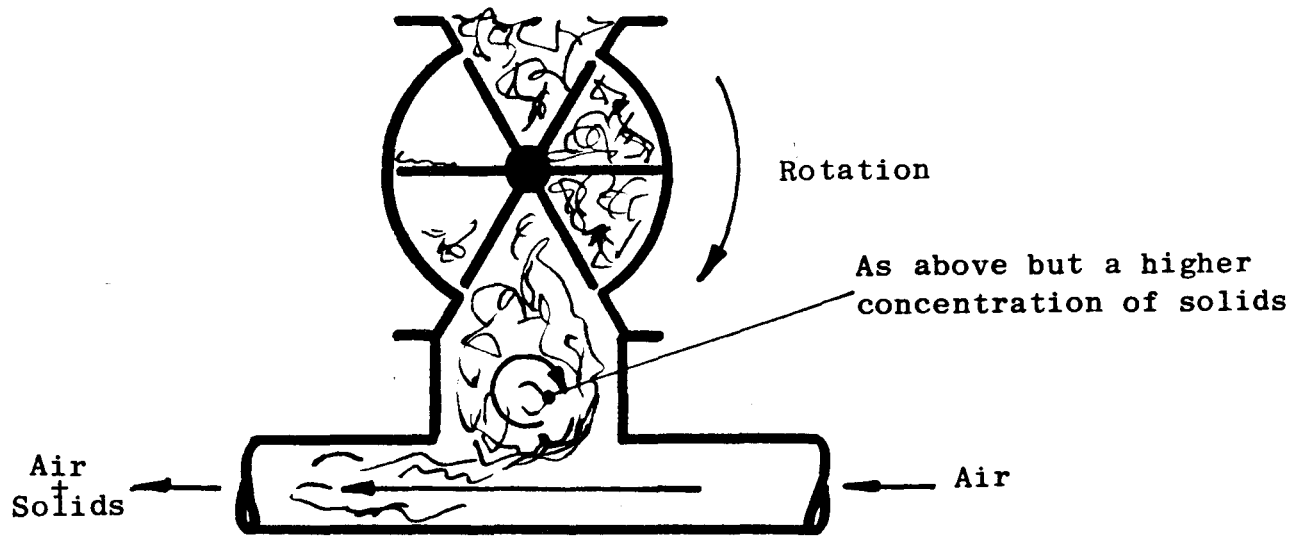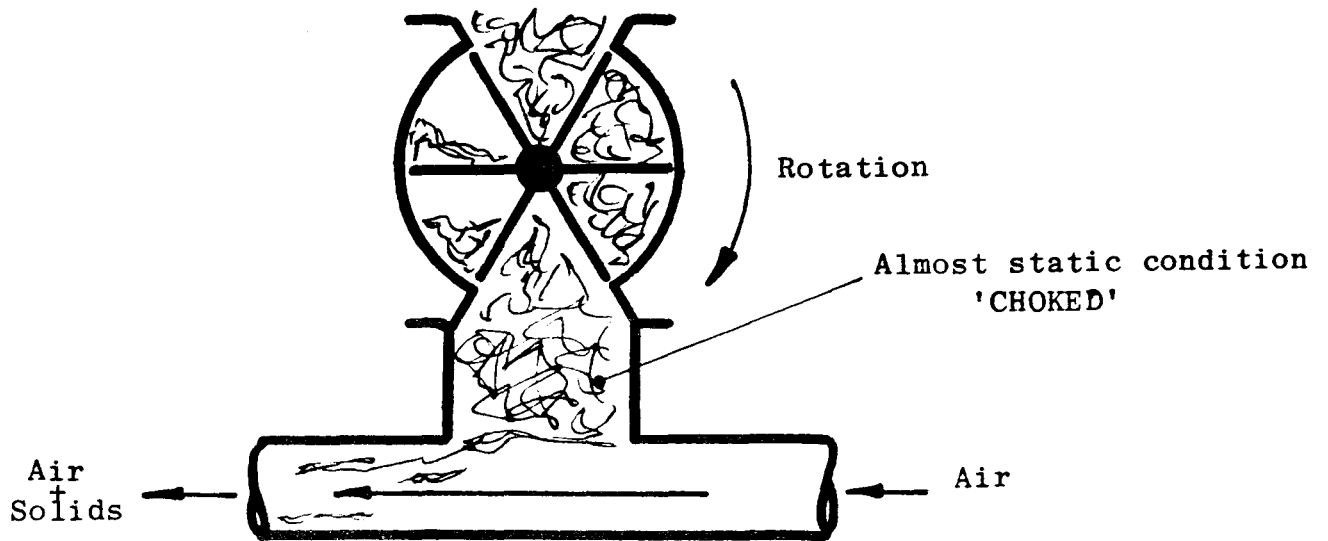
Figure 4.7c

Figure 4.7   The Transition to choked flow

4.3.3 Explanation and Model for the Choked Flow Mode of Entrainment

The flow visualisation work discussed in Chapter 3 showed that, under certain conditions, it is possible for the drop-out box to become 'choked' with material and thus restrict the discharge rate of the rotary valve. The initial operating conditions which were found to result in this situation were a combination of high solids feed rate and high air velocity. Under these conditions the previously discussed air swirl was observed to restrict the rate at which material could be entrained into the airstream. Consequently, the material collected inside the drop-out box chamber and eventually led to the box becoming choked. In the discussion that follows a model is proposed to explain this behaviour and provide a method for determining the minimum air velocity which will cause choking.

To explain the phenomenon of choking, take as a starting point the situation shown in Figure 4.7a, that is, where an air swirl dominates the flow pattern in the drop-out box.   In Chapter 3 it was proposed that the interaction between this swirl and the conveying airstream could be likened to a constrained wheel in contact with a moving belt. Thus, increasing the velocity of the airstream will increase the angular velocity of the swirl. If this analogy is accepted, then it seems reasonable to propose that there will be an air velocity at which the centripetal force acting on the particles in the swirl will be sufficient to hold them in suspension. This will restrict the rate at which material is entrained into the airstream and thus result in a higher concentration of particles in the drop-out box, as shown in Figure 4.7b. If the concentration increases sufficiently this may lead to the drop-out box becoming choked. However, for this to happen there must be a transition from the rotational motion to a relatively* static condition, see Figure 4.7c. Consequently, the material must either have sufficient interparticulate strength to hold up inside the drop-out box, or, the air which percolates through the material as a consequence of the pressure difference across the valve must be sufficient to hold it in suspension. This point is important because it suggests a means of

---

* footnote: The word 'relatively' is used because the material is not
              completely static in the choked condition.

classifying materials into two groups; that is, those which are, and those which are not, capable of choking.

If the above reasoning is accepted as the correct explanation for why a drop-out box can become choked, then it is of value to know the minimum air velocity at which this will happen. The following analysis proposes a method of calculating this for any given drop-out box and bulk material.

Consider a particle of mass m_p rotating with the air swirl inside a drop-out box as shown in Figure 4.8. The forces acting on the particle will be:

i)   the centripetal force (F_c) resulting from the rotational motion;

ii)   the air drag force (F_d); and

iii)   the weight of the particle (W_p).

Figure 4.9 shows the two alternative paths of the particle when it crosses the boundary between the drop-out box and pipeline. If the resultant force acting on it is sufficient to hold it in suspension, it will follow path A and be lifted back into the drop-out box. However, if the resultant force is insufficient to hold it in suspension, then it will follow a path similar to B and become entrained into the conveying airstream. Mathematically, the conditions for these two alternatives may be written as:

a)   to follow path A,

$$\int_{-\theta_A}^{\theta_A} F_c \cos\theta.d\theta + \int_{-\theta_A}^{\theta_A} F_d \sin\theta.d\theta > \int_{-\theta_A}^{\theta_A} W_p.d\theta \qquad (4.10a)$$

b)   to follow path B,

$$\int_{-\theta_A}^{\theta_A} F_c \cos\theta.d\theta + \int_{-\theta_A}^{\theta_A} F_d \sin\theta.d\theta < \int_{-\theta_A}^{\theta_A} W_p.d\theta \qquad (4.10b)$$
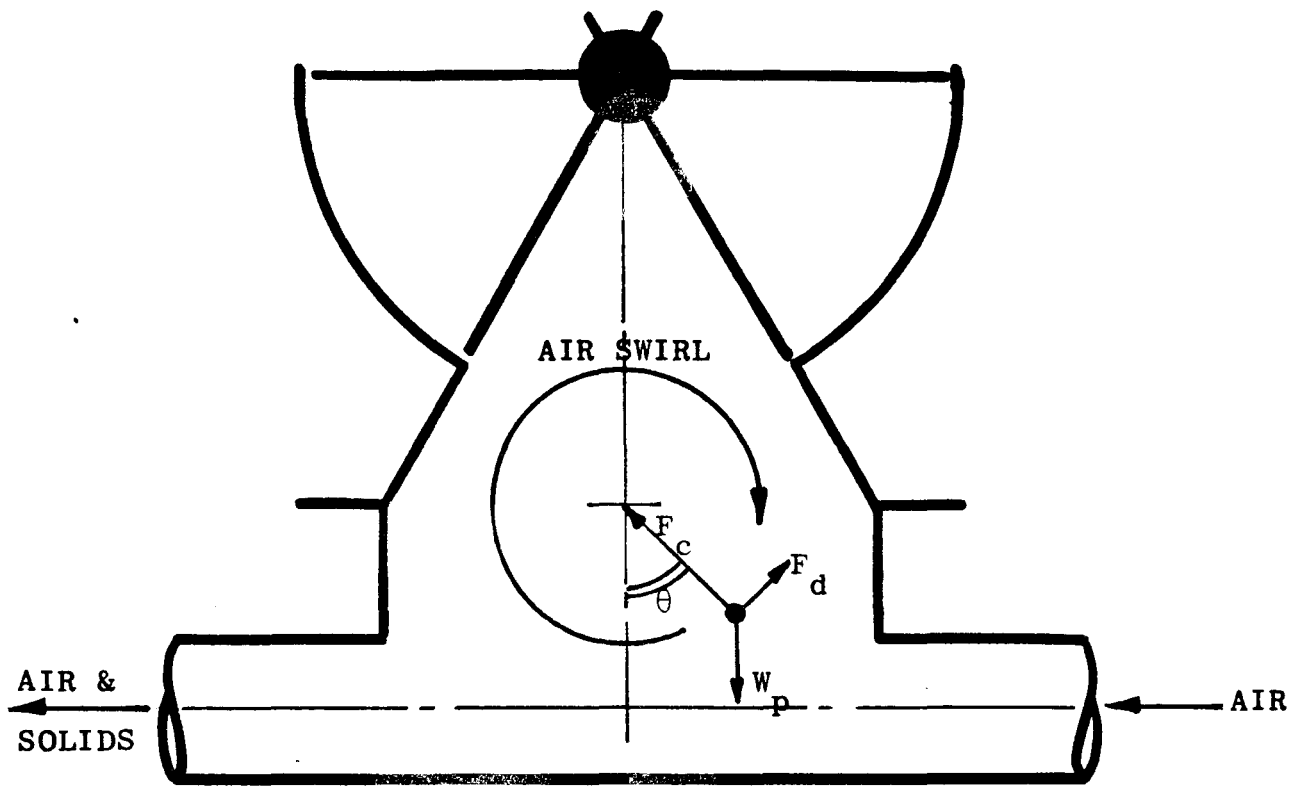
Figure 4.8   Forces acting on a particle in the drop-out box
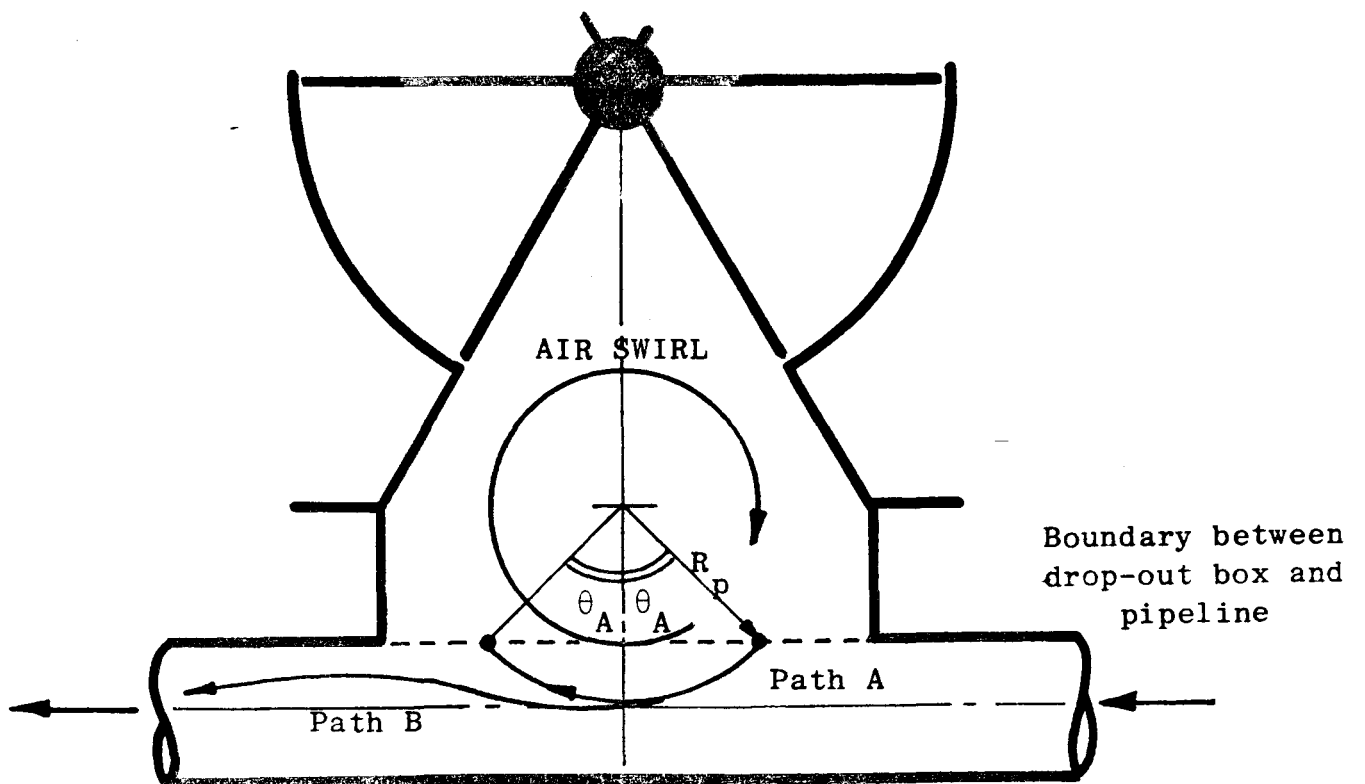
Figure 4.9   Alternative paths of a particle which crosses the
imaginary boundary between drop-out box and pipe-
line

These conditions are derived by resolving the forces acting on the particle in the vertical direction and integrating to sum the effect of the resultant along path A; θ is the angle between the particle and the radius vector R_p, as defined in Figure 4.9.

Now, since the particle is rotating with the air swirl, its velocity relative to the air will be very small and hence the drag term in the above expressions will be at least one order of magnitude smaller than the other two terms. Consequently, the following simplified conditions may be written:

a)   to follow path A,

$$\int_{-\theta_A}^{\theta_A} F_c \cos\theta . d\theta > \int_{-\theta_A}^{\theta_A} W_p . d\theta \qquad (4.11a)$$

b)   to follow path B,

$$\int_{-\theta_A}^{\theta_A} F_c \cos\theta . d\theta < \int_{-\theta_A}^{\theta_A} W_p . d\theta \qquad (4.11b)$$

If the integrations are now performed with F_c replaced by $m_p R_p \omega_p^2$ and W_p replaced by $m_p g$ the conditions become:

a)   to follow path **A**,

$$R_p \omega_p^2 \sin \theta_A > g\theta_A \qquad (4.12a)$$

b)   to follow path B,

$$R_p \omega_p^2 \sin \theta_A < g\theta_A \qquad (4.12b)$$

where ω_p is the angular velocity of the particle. Re-arranging condition 4.12a will give a relationship for the angular velocity needed to make a particle follow path A, that is:

$$\omega_p > (g\theta_A / R_p \sin \theta_A)^{\frac{1}{2}} \qquad (4.13)$$

From the above expression it is clear that ω_p is dependent on the radial position (R_p) of the particle. For choking to occur, all the particles crossing the boundary between the drop-out box and pipeline must follow path A. Therefore, in order to determine the minimum angular velocity required for the drop-out box to choke (ω_c) it is necessary to consider the case where ω_p is a maximum. This will occur when the particle only just crosses the boundary between the drop-out box and pipeline, as shown in Figure 4.10. R_p is then a minimum and $\theta_A/\sin \theta_A$ is unity. Consequently, ω_c is given by:

$$\omega_c = (g/R_{p\ min})^{\frac{1}{2}} \qquad\qquad (4.14)$$

where $R_{p\ min}$ is as defined in Figure 4.10.

$$R_{pmin} = H/2$$

$$R_{pmax} = \left[\frac{H^2 + a^2}{4}\right]^{\frac{1}{2}}$$
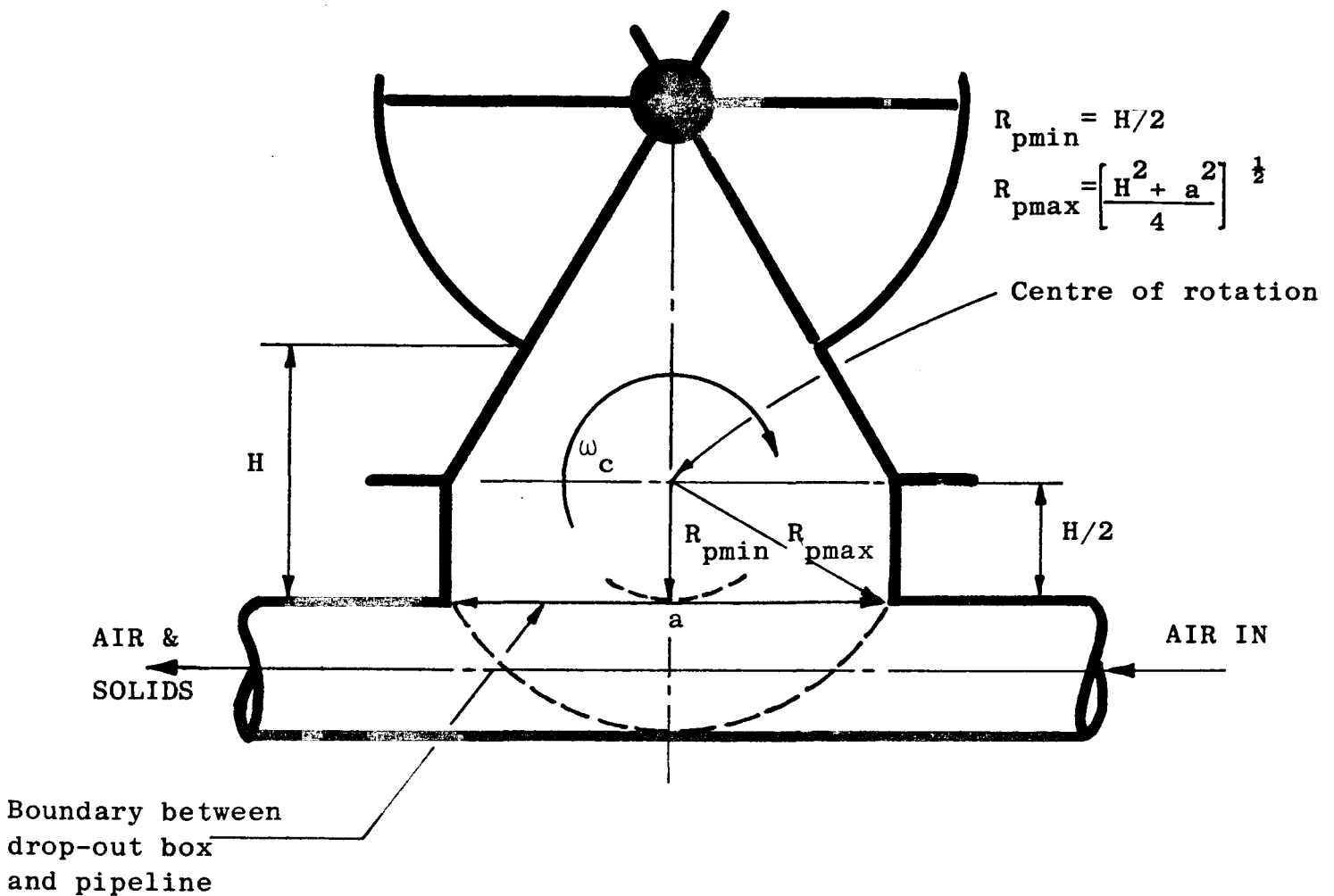
Figure 4.10   Definition of drop-out box dimensions

To determine the conveying air velocity which is required to drive
the mixture of air and solids at an angular velocity of ω_c, it is
necessary to consider the geometry of the drop-out box and the energy
transfer from the conveying airstream to the rotating mixture.   The
geometry of the box dictates where the centre of rotation will be and
hence the maximum radius of rotation.   If these are known, the kinetic
energy of the rotating mixture may be calculated for any given angular
velocity.   Thus, by considering the energy transfer from the conveying
airstream to the rotating mixture, the conveying air velocity which is
needed to maintain an angular velocity of ω_c may then be determined.

For simple drop-out boxes of the type shown in Figure 4.10 it is
reasonable to suppose that the centre of rotation will be close to the
intersection of the horizontal and vertical centrelines.   If this is
accepted, the maximum radius of the rotating mixture will be:

$$R_{p\ max} = \left(\frac{H^2 + a^2}{4}\right)^{\frac{1}{2}} \qquad (4.15)$$

where H is the height of the drop-out box and a is its length, as
defined in Figure 4.10.   At this radius the peripheral velocity of the
rotating mixture must be equal to $\omega_c R_{p\ max}$ if choking is to occur.
Thus, for any given drop-out box there will be a critical peripheral
velocity (P_c), above which the box will choke, that is:

$$P_c = g \frac{R_{p\ max}^2}{R_{p\ min}}^{\frac{1}{2}} \qquad (4.16a)$$

or

$$P_c = \frac{g}{2} \frac{(H^2 + a^2)}{H}^{\frac{1}{2}} \qquad (4.16b)$$

From these equations it can be seen that P_c is solely dependent on the
dimensions of the drop-out box.   Consequently, it provides a means of
comparing different shaped drop-out boxes in respect of their tendency
to choke.   In Chapter 3 it was proposed that the rotating mixture and
conveying airstream could be likened to a constrained wheel in contact
with a moving belt.   If this analogy is accepted then it follows that
a drop-out box with a high value of P_c will need a higher conveying
air velocity to cause it to choke than will a box with a low value of
P_c.

Figure 4.11 shows the variation of P_c with drop-out box height
(H) and length (a).   This clearly shows that, for any given box
height, P_c increases with increasing box length.   Furthermore, it is
clear that there is a minimum value of P_c for any given box length.
By integrating equation 4.16b with respect to H and equating the
resultant to zero, it can be shown that this minimum occurs when the
box height and length are the same, that is, H = a.   Therefore, the
analysis suggests that boxes of this shape will choke at lower conveying
air velocities than boxes of other shapes.   For any given box length
the minimum value of P_c ($P_{c\ min}$) will be given by putting H equal to a
in equation 4.16b, hence:

$$P_{c\ min} = (ga)^{\frac{1}{2}} \tag{4.17}$$

Figure 4.12 shows the variation of $P_{c\ min}$ with the drop-out box length
(a) as predicted by the above equation.   This definition of $P_{c\ min}$ is
useful because it can be used to normalize equation 4.16b.   Consequently,
a dimensionless form of the critical peripheral velocity may be defined:

$$P_* = \frac{1}{\sqrt{2}} (\frac{H}{a} + \frac{a}{H})^{\frac{1}{2}} \tag{4.18}$$

where P_* is the dimensionless critical peripheral velocity and is equal
to $P_c/P_{c\ min}$.   From this equation it can be seen that P_* is only a
function of the ratio H/a, which could be thought of as a shape factor
or aspect ratio for drop-out boxes.   Figure 4.13 shows the variation
of P_* with the ratio H/a and provides confirmation of the earlier
statement that the conveying air velocity which is needed to cause
choking will be a minimum when H is equal to a.   This diagram is useful
because it provides a basis for comparison of experimental data obtained
with different size drop-out boxes.

From the definition of P_*, it follows that:

$$P_c = P_* P_{c\ min} \tag{4.16c}$$

This expression is interesting because it shows that P_c can be regarded
as the product of two different terms, one of which is dependent on the
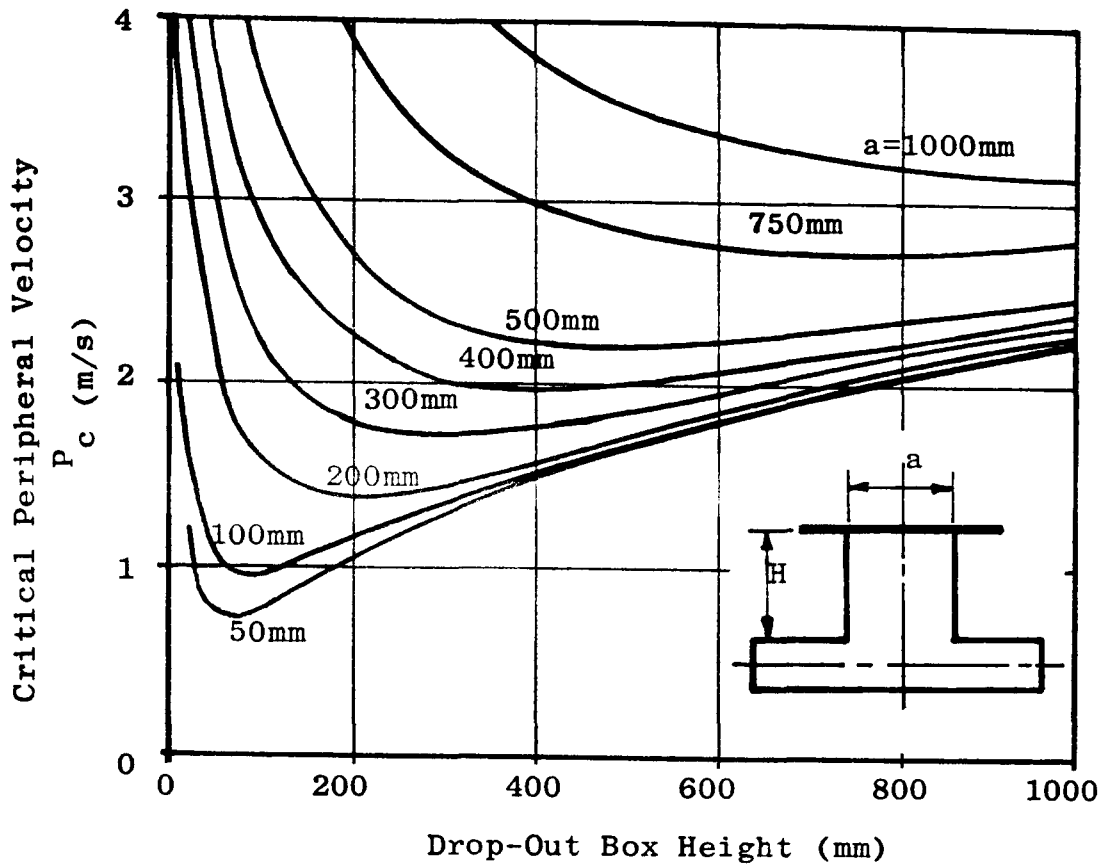
Figure 4.11   Variation of critical periferal velocity (P_c) with drop-out box height (H) and length (a)
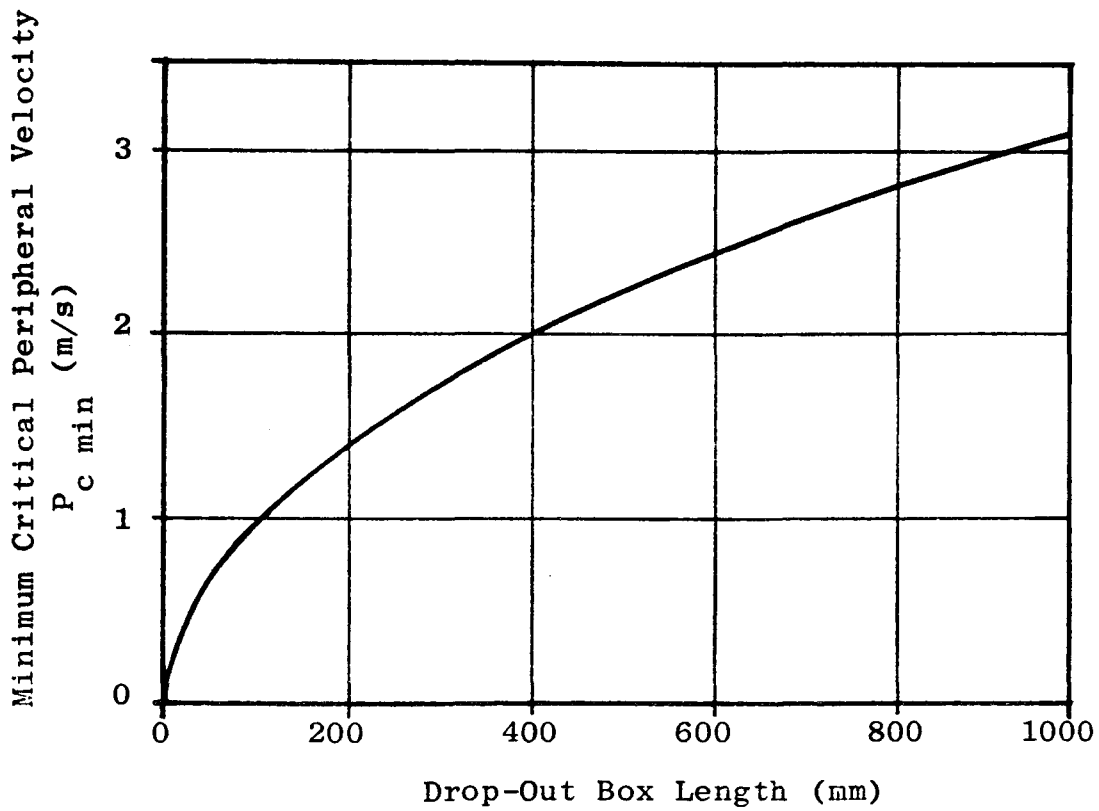
Figure 4.12   Variation of the minimum critical peripheral velocity with drop-out box length
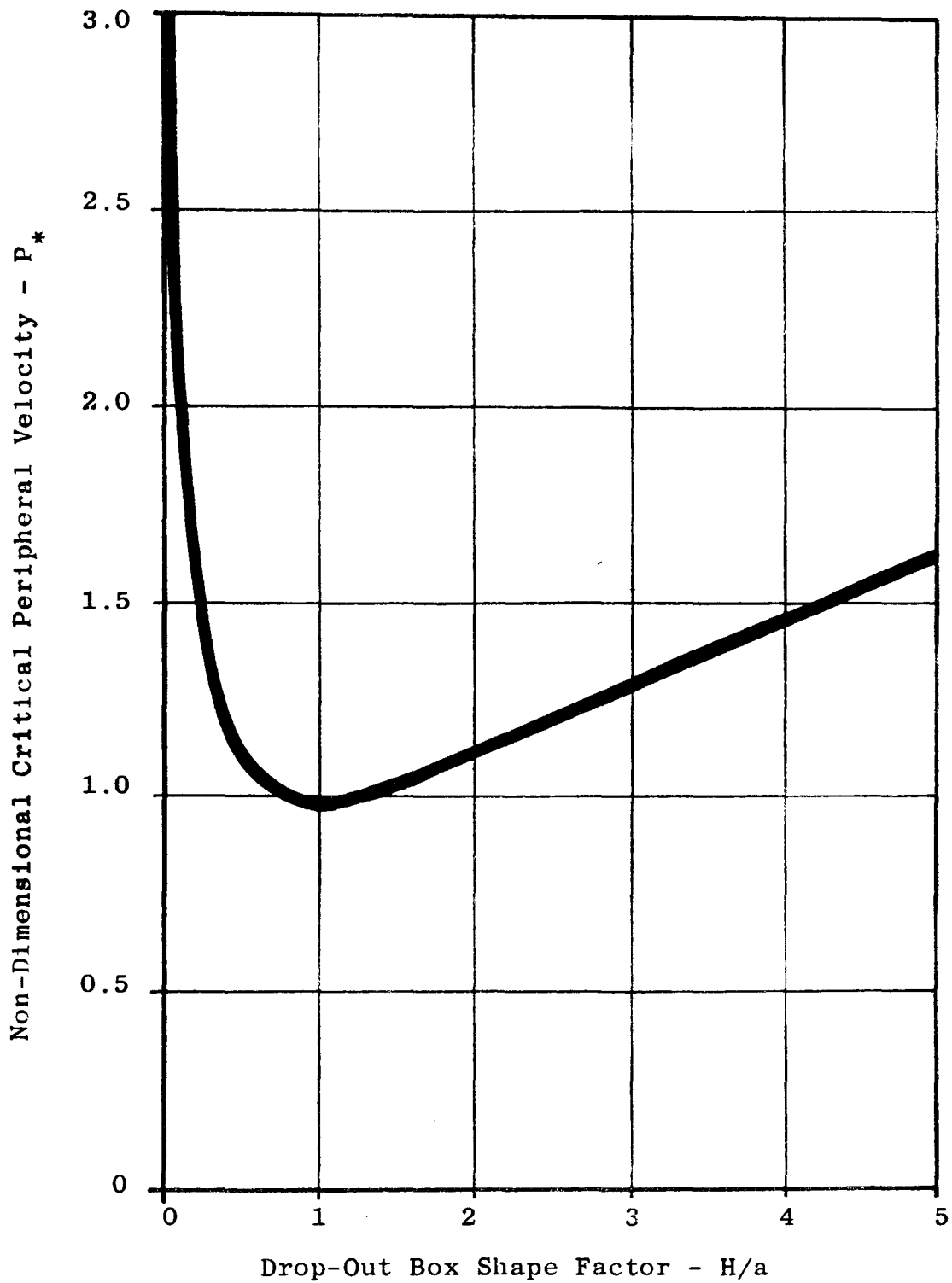
Figure 4.13   Variation of the non-dimensional critical
peripheral velocity with drop-out box
shape factor

shape of the drop-out box (P_*) and the other dependent on the size of
the box ($P_{c\ min}$).   The implication of this is that it should be possible
to scale experimentally obtained values of P_c for identically shaped
drop-out boxes.

As a function of the critical peripheral velocity (P_c) and the
maximum radius of rotation ($R_{p\ max}$) the kinetic energy of the air-solids
mixture rotating at an angular velocity of ω_c is:

$$K.E._{as} = \frac{1}{2}I_{as} \frac{P_c^2}{R_{p\ max}^2} \qquad (4.19a)$$

where I_{as} is the moment of inertia of the rotating mixture.   However,

$$I_{as} = M_{as} K_{as}^2$$

and

$$K_{as} = N_{as} R_{p\ max}^2$$

where M_{as} is the mass of the rotating mixture, K_{as} is the radius of
gyration of the same and N_{as} is a numerical constant dependent on the
shape of the rotating mixture.   Consequently, equation 4.19a can be
simplified to:

$$K.E._{as} = \frac{1}{2}M_{as} N_{as} P_c^2 \qquad (4.19b)$$

Similarly, when air only is flowing through the drop-out box, it can be
shown that the kinetic energy of the resultant air swirl is given by:

$$K.E._a = \frac{1}{2}I_a \frac{s^2 V_{p.u.}^2}{R_{p\ max}^2} \qquad (4.20a)$$

or

$$K.E._a = \frac{1}{2} M_a N_a s^2 V_{p.u.}^2 \qquad (4.20b)$$

where I_a is the moment of inertia of the air swirl, M_a is the mass of

the same, N_a is a numerical constant dependent on the shape of the air swirl, $V_{p.u.}$ is the conveying air velocity and s is a slip ratio relating the peripheral velocity of the air swirl to $V_{p.u.}$

In order to determine the conveying air velocity at which the transfer of energy to the rotating air-solids mixture is sufficient to maintain an angular velocity ω_c, the following simplification is proposed. For any given conveying air velocity, the energy transferred from the conveying airstream to the contents of the drop-out box chamber is always the same, regardless of whether the contents are an air-solids mixture or air only. If this is accepted, then it can be argued that the conveying air velocity at which $K.E._a$ is equal to $K.E._{as}$ is that which is needed to rotate the air solids mixture at an angular velocity of ω_c. Equating the right hand sides of equations 4.19b and 4.20b and re-arranging gives the following expression for this value of the conveying air velocity (V_c):

$$V_c = \frac{P_c}{s}\left[\frac{M_{as}}{M_a}\frac{N_{as}}{N_a}\right]^{\frac{1}{2}}$$ (4.21a)

In most cases the mass ratio M_{as}/M_a will be satisfactorily approximated by the density ratio ρ_{as}/ρ_a because the size and shape of the air-only swirl and the rotating air-solids mixture will be similar. Unfortunately, it is not easy to see how the value of ρ_{as} could be determined and therefore it is suggested that the poured bulk density (ρ_b) be used as an alternative. This is not unreasonable because the drop-out box must be closely packed with material in order to choke. Consequently, the expression for V_c may be written:

$$V_c = \frac{P_c}{s}\left[\frac{\rho_b}{\rho_a}\frac{N_{as}}{N_a}\right]^{\frac{1}{2}}$$ (4.21b)

It could be argued that the expression be further simplified by assuming that the ratio N_{as}/N_a is unity. At first sight this seems reasonable if the size and shape of the air-only swirl and rotating air-solids mixtures are similar. However, because the rotating masses are not rigid bodies, there may be significant internal shearing taking place; particularly if the shape of the drop-out box chamber is not

square, that is, $H \neq a$. The effect of this would be to increase the
energy required to maintain the rotational motion. Since the energy
dissipated in the shearing will undoubtedly be greater in the air-
solids case than the air-only situation, the ratio N_{as}/N_a will probably
be greater than unity. However, it is very difficult to see how its
value could be determined with any degree of certainty. Consequently,
the simplification that N_{as}/N_a is equal to unity cannot be justified,
except perhaps for the case of a 'square' drop-out box ($H = a$) which
would minimise the internal shearing.

Since the value of the slip ratio (s) is also difficult to
determine and the simplification of putting $\rho_{a/s}$ equal to ρ_b may not be
completely correct, the following expression for V_c is suggested:

$$V_c = C_c P_c (\rho_b/\rho_a)^{\frac{1}{2}}$$

(4.21c)

where C_c is a dimensionless coefficient which allows for the internal
shearing in the rotating air-solids, the slip between the conveying
airstream and the air swirl and the discrepancy in substituting ρ_b for
ρ_{as}. It is proposed that if typical values of C_c can be determined
experimentally for different shaped drop-out boxes and bulk materials,
then equation 4.21c could be used to predict V_c for similar
arrangements. For the drop-out box which was found to choke during
the flow visualisation experiments, that is box C in Figure 3.4, C_c is
approximately 0.9. To ascertain whether or not this is a typical
value for C_c further experimental data is needed. In Chapter 7
experiments to provide more data will be discussed as well as further
development of the model proposed here.

4.4 Blowing Seals

The interaction between a blowing seal and a pneumatic conveying pipeline
will be, in most cases, completely different to that previously discussed
for the drop-through type of rotary valve. This is because the inter-
face between the rotor and pipeline is such that the conveying airstream
is directed through the length of the rotor pockets rather than underneath
them. There are a few exceptions to this, for instance the configuration
shown in Figure 4.14c. This type of blowing seal could be considered
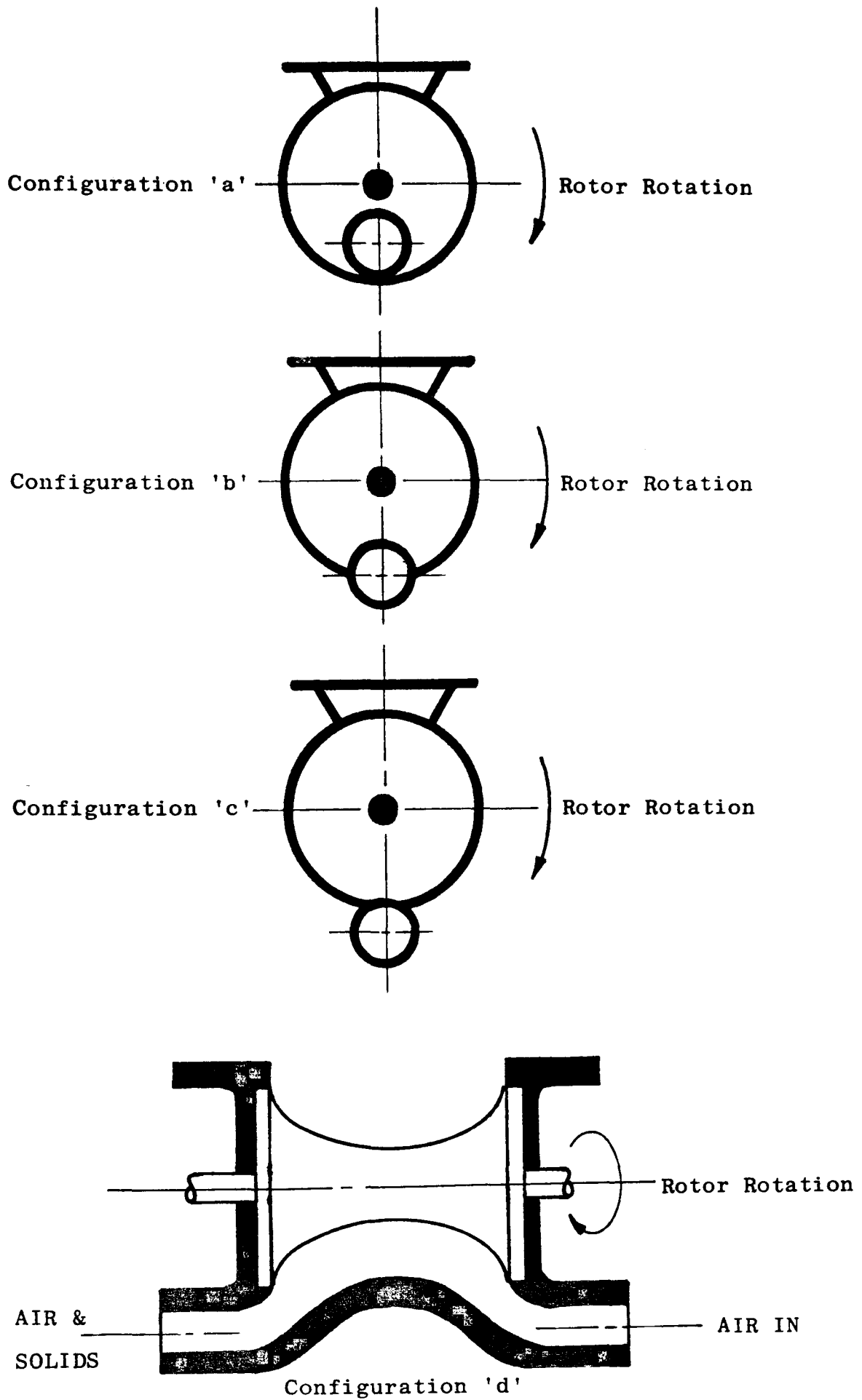
Figure 4.14 Blowing Seal Configurations

as a drop-through type with an integral drop-out box.   Therefore, the method proposed in section 4.3.2 for determining the entrainment efficiency of drop-through valve/drop-out box configurations could be reasonably applied to estimate the discharge efficiency of this type of blowing seal.   For the more conventional types of blowing seal, Figures 4.14a, b and d, this model cannot be used because the rotor pocket is part of the pipeline.   Consequently, the drop-out box chamber volume (v_b) is effectively zero and hence the entrainment efficiency (η_e) predicted by equation 4.19 will be zero.   This is obviously not the case and hence some other method of predicting the discharge efficiency must be found.

One approach is to consider the distance which a pocket full of material moves during the time that it is engaged with the conveying pipeline, see Figure 4.15.   If this is more than the length of the pocket the discharge efficiency will be 100%.   If it is less, the discharge efficiency (η_d) will be given by:

$$\eta_d = \frac{1 - x}{L} \ 100\% \qquad\qquad (4.22)$$

where L is the length of the rotor pockets and x is the distance which the material moves during the time interval that one pocket is engaged with the pipeline.
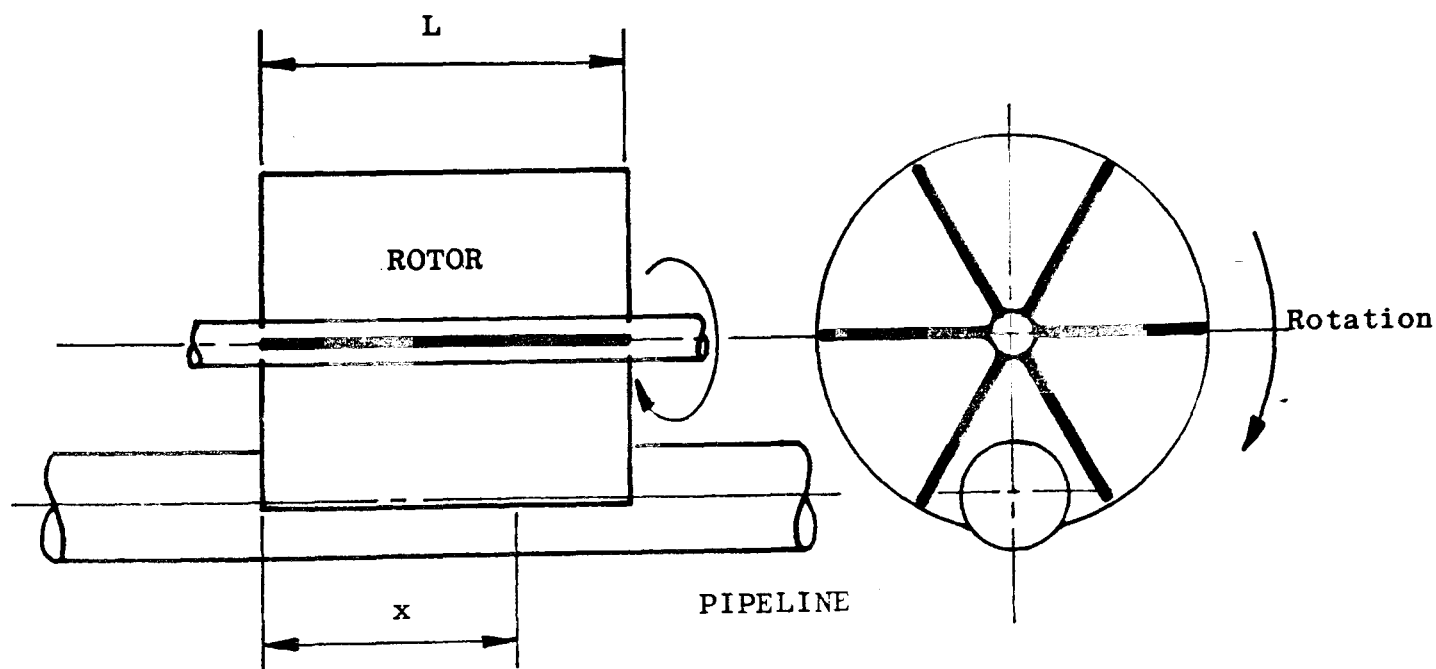
Figure 4.15 Simple discharge model for a blowing seal

Unfortunately x is difficult to determine because it is unlikely that the material will move as a solid slug. Also, the pocket is not exposed to the pipeline instantaneously, but progressively as the rotor turns. Nevertheless, the following simple analysis is proposed to demonstrate that for most operating conditions η_d is likely to be very close to 100%.

First of all the simplification is made that the material will be instantaneously accelerated to the pick-up velocity of the conveying air $(V_{p.u})$ when the pocket is engaged with the pipeline. The minimum time which a pocket must be engaged with the pipeline in order to discharge all its contents (t_{min}) can then be estimated by dividing the length of the rotor by the pick-up velocity, that is:

$$t_{min} = \frac{L}{V_{p.u}} \qquad (4.23)$$

The duration which a pocket is engaged with the pipeline (t_e) can be determined by considering the geometry of the valve and the rotor speed. For most proprietary blowing seals the angular size of the outlet port is between 10° and 30^0. Consequently a conservative estimate for t_e will be given by:

$$t_e = \frac{60}{n} \cdot \frac{30}{360} \qquad (4.24)$$

where n is the rotor speed in rev/min.

Equating these expressions for t_{min} and t_e will give an expression for the maximum rotor speed that can be used if complete discharge is to be achieved (n_{max}) as a function of the pick-up velocity, that is:

$$n_{max} = \frac{5V_{p.u}}{L} \qquad (4.25)$$

Now, the minimum safe pick-up velocity for many materials is usually greater than 15 m/s. Therefore for a very large blowing seal with a length of say 1.0 m, n_{max} would be of the order of 75 rev/min. This is far in excess of normal operating speeds because of pocket filling considerations. For the more common smaller sizes n_{max} is even larger, for instance 375 rev/min for a 200 mm seal. Consequently, despite the

very simplified approach used in this analysis, it can be safely
concluded that in most normal situations the discharge efficiency of
a blowing seal will be very close to 100%.   If this is the case, other
factors will limit the performance characteristics; for instance, the
effect of air leakage on the pocket filling process as previously
discussed in section 4.2.   In Chapter 7 experimental results which
confirm this conclusion will be discussed.

4.5 Summary

In this chapter various models have been proposed for describing the
interaction between rotary valves and positive pressure pneumatic
conveying pipelines.   On the whole these are rather simplistic in
approach because of the simplifying decisions which are used in their
derivation.   These decisions were necessary in order to make any
progress in modelling the complicated flow patterns revealed by the flow
visualisation experiments.   Even then the resulting expressions
incorporate terms for which it will be very difficult to obtain any
realistic values.   However, despite these obvious limitations, the
models indicate trends which appear to be in reasonable agreement with
the limited amount of experimental data that is available and provide
plausible explanations for some hitherto unexplained observations.   As
such it is considered that they provide a positive contribution to
understanding the interaction between rotary valves and pneumatic
conveying pipelines.

In Chapter 7 the models will be examined further in the light of
the results obtained from a purpose built experimental rig and in Chapter
8 the application of the models to practical system design will be
discussed.

CHAPTER FIVE

INDUSTRIAL SCALE EXPERIMENTAL RIG

5.1 Basic Concept

In order to obtain reliable quantitative data on the interaction between rotary valves and positive pressure pneumatic conveying systems an experimental rig of industrial proportions was constructed. The need to use a rig of this size was considered essential because the results of the experimental work were intended to be of direct use to industry. A smaller rig would have necessitated scaling the experimental results in order to render them useful, but this was not regarded to be a satisfactory approach because the application of scaling factors to the entrainment process is not an established procedure. Although the models proposed in Chapter 4 suggested ways in which results could be scaled, these procedures cannot be applied until the validity of the models is proven.

Following discussions with the industrial organisations collaborating in the research programme, it was decided that the rig should be a positive pressure conveying system* with the air supplied by a Roots-type blower. This is probably the most common type of system in which rotary valves are used as the solids feeding device. Other requirements of the rig were versatility, in order to permit a range of entrainment configurations and operating conditions to be examined and, reliable comprehensive instrumentation. This chapter contains the salient details of the rig which was finally constructed.

---

* footnote: See definition in Chapter 1

5.2 General Description of Rig

The rig which was constructed for the experimental part of this research was of a small industrial size, see Figures 5.1 and 5.2.   The essential elements were a 175 mm rotary valve feeding a 70 mm bore pipeline 52 m long.

At the point where air is drawn into the system a paper cartridge filter was used to prevent the ingestion of dust into the Roots-type blower.   Between this filter and the inlet silencer of the blower was a 100 mm diameter pipeline containing two orifice plate flow meters. These were used to measure the air flow into the system and are described in detail in section 5.4.1.

The blower was driven by a 37 kW DC motor, the speed of which could be controlled by a proprietary thyristor rectified/controller unit. This enabled the air mass flow rate to be set to any required level within the performance range of the blower.   The air was ducted from the blower through an outlet silencer into a small tank which was used as a distribution manifold.   From this manifold the air could be routed in one of three ways:

a)   to supply air to a short conveying system which was used to load the supply hopper with new materials, line A in Figure 5.3;

b)   to supply air to a pipeline which was used to return material from the receiving hopper to the supply hopper after a test run, line B on Figure 5.3; and

c)   to supply the main conveying line, line C on Figure 5.3.

Air entering the main conveying line flows through a non-return valve and then into a short length of pipe which connects with the inlet side of the drop-out box.   Bulk solids are introduced into the drop-out box by the rotary valve which is mounted beneath the supply hopper. These solids mix with the air in the drop-out box chamber and are then entrained into the conveying line.

The overall length of the conveying line was 52m.   This was made up of a 12 m horizontal acceleration run followed by a 4 m vertical lift and a further 36 m of horizontal pipe, see Figure 5.2.   There were six bends in the system, two in the vertical and four in the horizontal plane.   These were all right angled bends with a bend radius to pipe
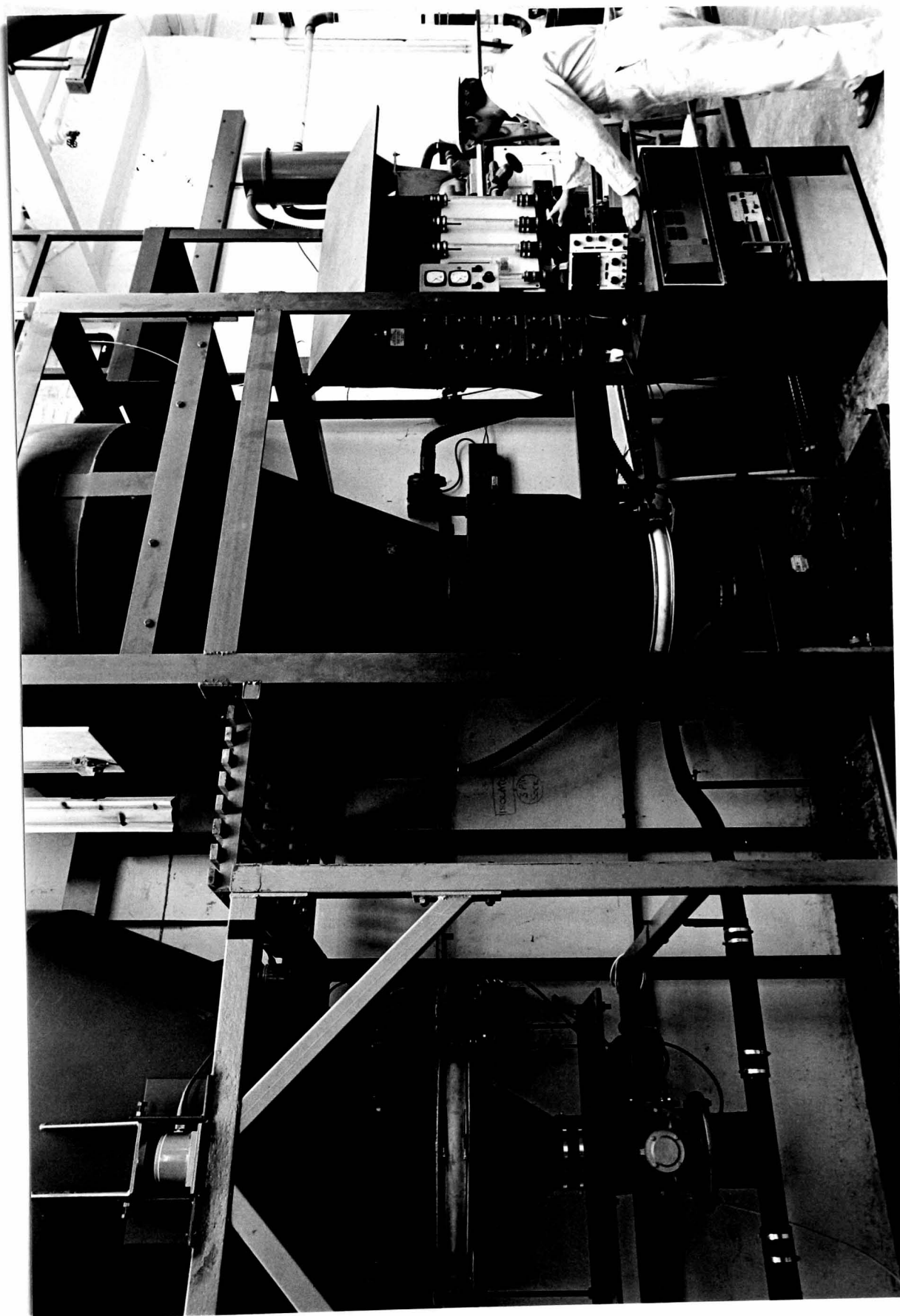
Figure 5.1 Photograph of experimental rig.
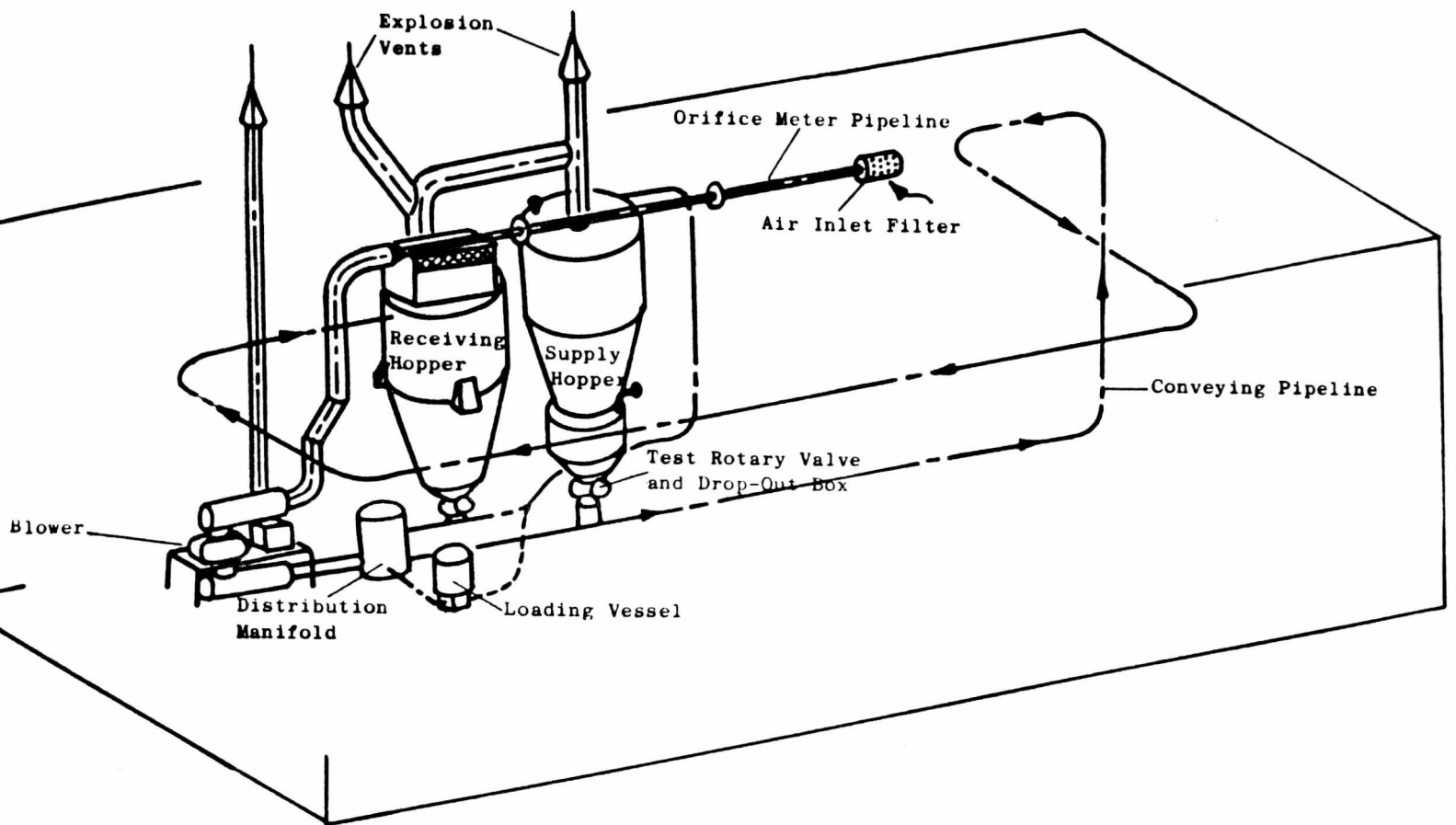
Figure 5.2   Schematic diagram of rig
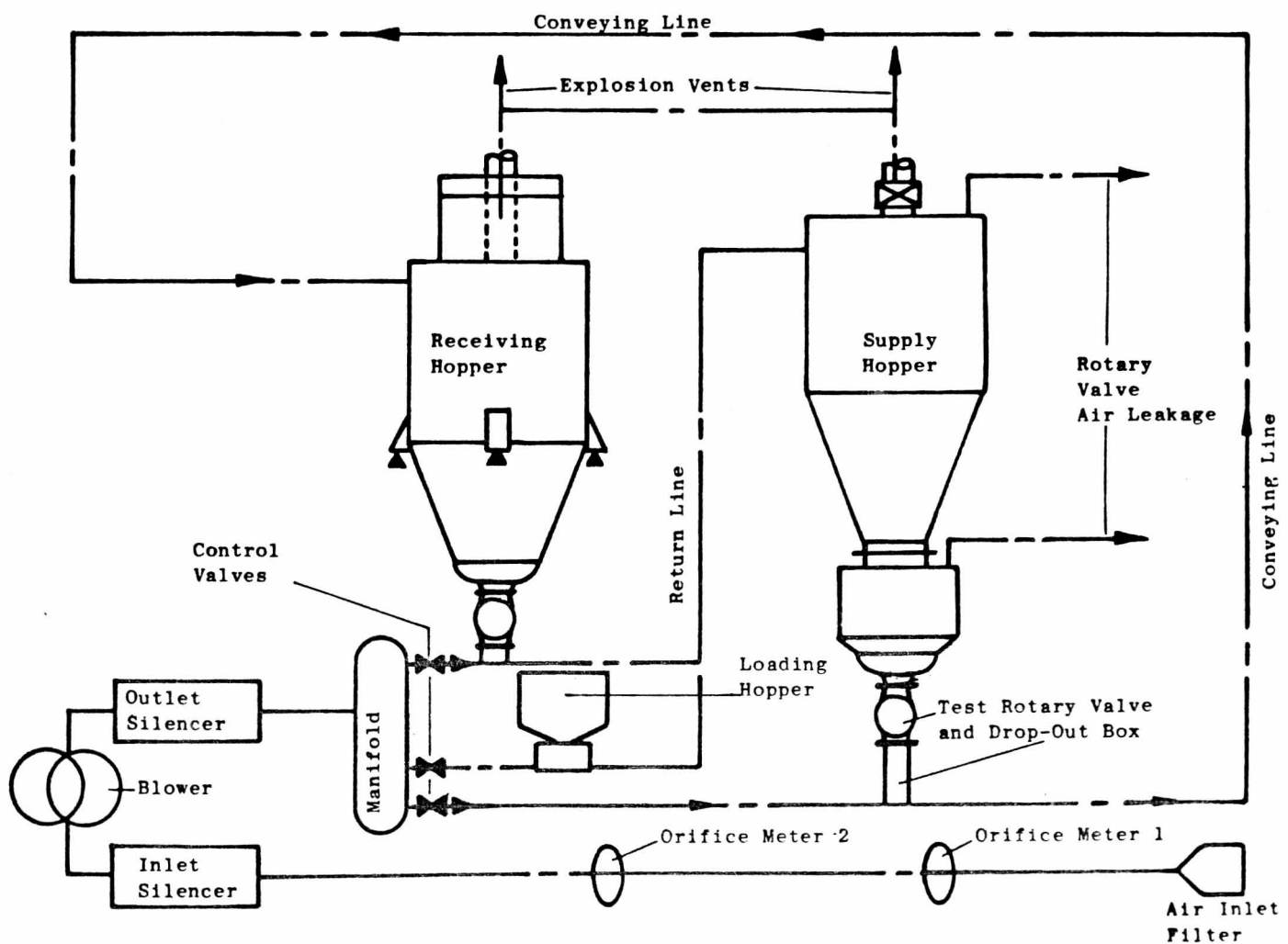
Figure 5.3   Air circuit diagram of experimental rig

bore ratio of approximately 11.

At the end of the conveying line the air and material were discharged into a receiving hopper. This was mounted on load cells to enable the total mass of solids conveyed to be monitored. The output from these load cells was recorded by a pen recorder and the solids mass flow rate ($\dot{m}_s$) was determined by measuring the slope of the resulting trace. The conveying air was exhausted to atmosphere through a bag filter unit which was mounted on top of the receiving hopper.

At the end of an experimental run the test material was transferred from the receiving hopper back into the supply hopper by means of a short conveying line. A rotary valve on the bottom of the receiving hopper was used to feed the material into this pipeline, see Figures 5.1, 5.2 and 5.3.

5.3   Detailed Description of Key Components

5.3.1   The Supply Hopper and Constant Head Tank

The supply hopper for the rotary valve and drop-out box under test was a composite device. It consisted of a conventional cylindrical/ conical hopper on to which was bolted a smaller cylindrical bin. The hopper was used to hold the main bulk of the test material (approximately 2 m^3) and had an included cone angle of 40°. This angle was chosen so as to encourage a mass flow type discharge pattern for a wide range of materials. The smaller bin was a device called the 'constant head tank'. As its name suggests its purpose was to provide an effectively constant head of material above the rotary valve. Jotaki & Tomita (51) demonstrated that the air leakage through a rotary valve is dependent on both the type of material being handled and the head of material above the valve. For this work it was decided that the air leakage should, if possible, be made invariant of the quantity of material in the hopper; thereby eliminating a variable which would otherwise complicate the analysis of the experimental results. This requirement led to the necessity for a constant head device.

The concept of the constant head tank was quite simple. Where it was attached to the main hopper the diameter of the truncated cone was 500 mm, see Figure 5.4. From this junction a cylindrical section, also 500 mm diameter, extended into the constant head tank to a depth
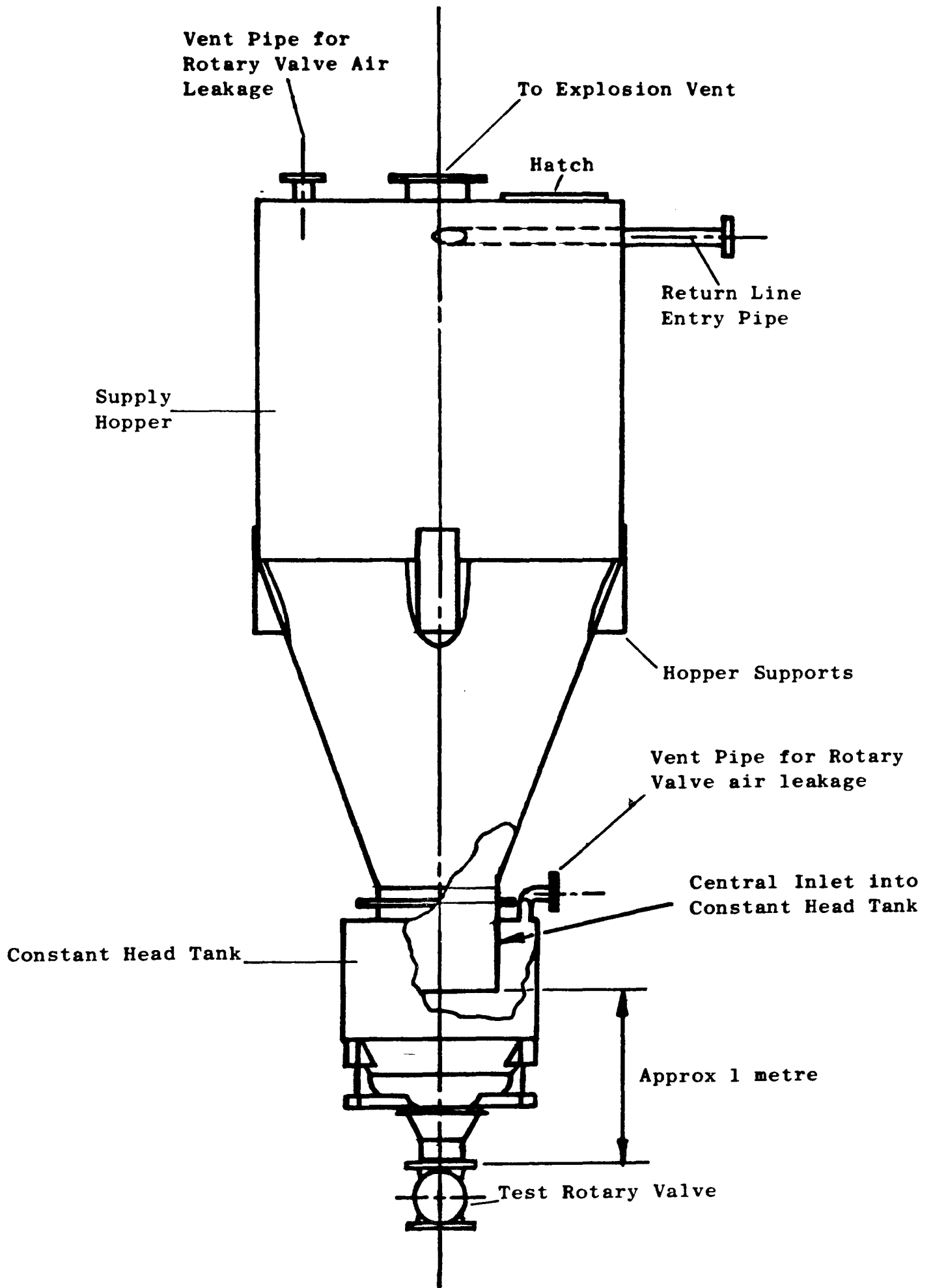
Figure 5.4   Diagram of supply hopper and constant head tank

of 300 mm where it was cut off square.   The purpose of this was to make the material flowing out of the cylindrical section dilate and expand to the 800 mm diameter of the constant head tank.   This produced an annulus of material, the surface of which was approximately one metre above the rotary valve inlet.   Since the air which leaks through the rotary valve will seek the line of least resistance through the head of material above it, it was argued that the preferential leakage path would be through the annulus in the constant head tank, rather than through the main bulk of material in the supply hopper, see Figure 5.4. Consequently, it was argued that this would enable an apparently constant head of material to be maintained throughout the duration of an experiment.   The ratio of the annulus area to that of the outlet from the supply hopper was 1.2:1.

A hose connected the space above the annulus to a bank of rotameters. This enabled the air leakage through this head of product to be measured. Another hose connected the air volume in the top of the main hopper to the rotameters.   The purpose of this was to measure the small amount of air which inevitably will leak through the main core of the material. Thus, the sum of these two air flows was the total air leakage through the rotary valve.

At the base of the constant head tank was a hopper discharge device of the vibrating cone type (Reference 57).   The purpose of this was to ensure a consistent supply of material to the rotary valve.   The design of this device also contributes to the effectiveness of the constant head tank because the vibrating cone forces leakage air to flow radially outwards before it can percolate up through the material, see Figure 5.4

Another important feature of the supply hopper and constant head tank assembly was that it could be jacked up or down to accommodate different combinations of rotary valves and drop-out boxes without the necessity to alter the configuration of the conveying pipeline.   This was achieved by the use of four screwjacks in the legs of the supporting framework. The total vertical movement was 680 mm.

5.3.2   The Receiving Hopper

The receiving hopper was of similar geometry to the cylindrical/conical section of the supply hopper.   In common with the supply hopper it was

designed to accept a vibrating cone discharge device to ensure a
consistent supply of material to the rotary valve used for discharging,
see Figure 5.1.   On the top of the hopper was mounted a bag filter unit.
This discharged to atmosphere inside the laboratory and had a nominal
filtration area of 22.7 m^2, which was more than adequate to handle the
maximum capacity of the blower (18.5 m^3/min at 1.013 bar absolute, 15°C) [*]

Both the supply and receiving hoppers were fitted with dust explosion
vents.   These consisted of large diameter ducts which extended out
through the roof of the laboratory.   In each of these ducts was a cork
tile, the purpose of which were to act as sacrificial membranes in the
event of a dust explosion.

5.3.3   The Blower

The air supply for the conveying system was provided by a Roots-type
blower, manufactured Wade Engineering Ltd (59); type number SVR 113/
6369/HP, serial number 5400.   This was driven by a 37 kW DC motor which
allowed a maximum volumetric capacity of approximately 18.5 m^3/min at
1.013 bar absolute and 15°C to be achieved at a pressure ratio of 1.8 : 1.

The speed of the blower could be infinitely varied between 0 and
2200 rev/min by means of a proprietary thyristor rectified/controller
unit.   This enabled the blower to be operated at any point within its
normal operating envelope, thus permitting specific conveying conditions
to be set up and examined.

Figure 5.5 shows the performance characteristics for the blower
which were obtained by the author during quality control trials at
Wade Engineering Ltd.

5.3.4   The Rotary Valves

Two types of rotary valve were used for the experimental work.   One of
these was a conventional drop-through valve, the other was a blowing
seal, as shown in Figures 5.6 and 5.7 respectively.   These two valves
were selected because, apart from the obvious differences between a
blowing seal and drop-through type, they have identical internal

---

[*] footnote: This gives a maximum air to cloth ratio of 0.81 m^3/min/m^2
            which is within the maximum values usually recommended by
            the manufacturers of filter units; that is, 1 m^3 min/m^2
            for fine particles and dusty materials and 2 m^3/min/m^2
            for coarse particles and granular materials (Reference
            58).
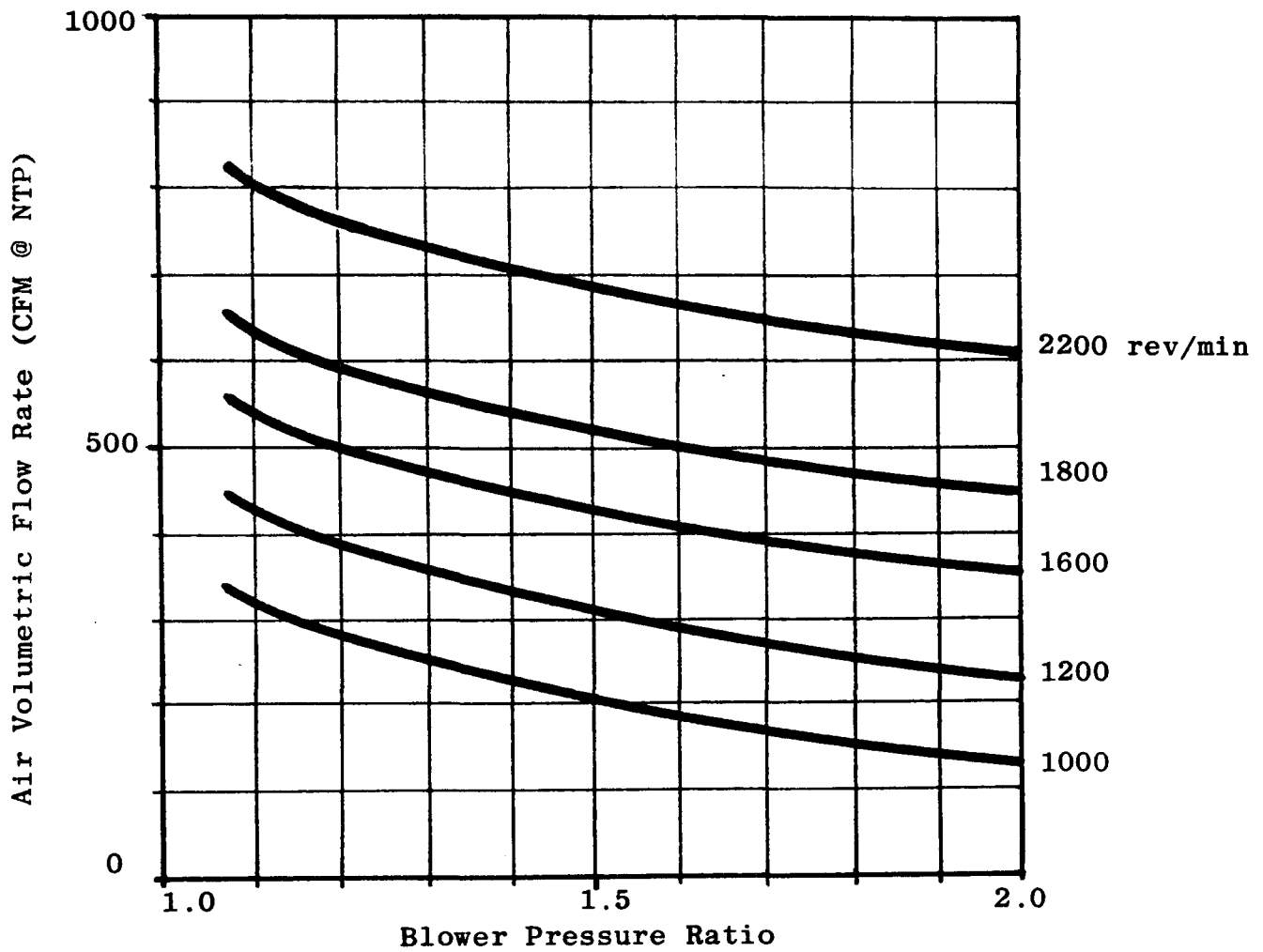
Figure 5.4　Air volumetric flowrate-pressure ratio
　　　　　　characteristics for the 'Roots type' blower
　　　　　　used for the experimental work
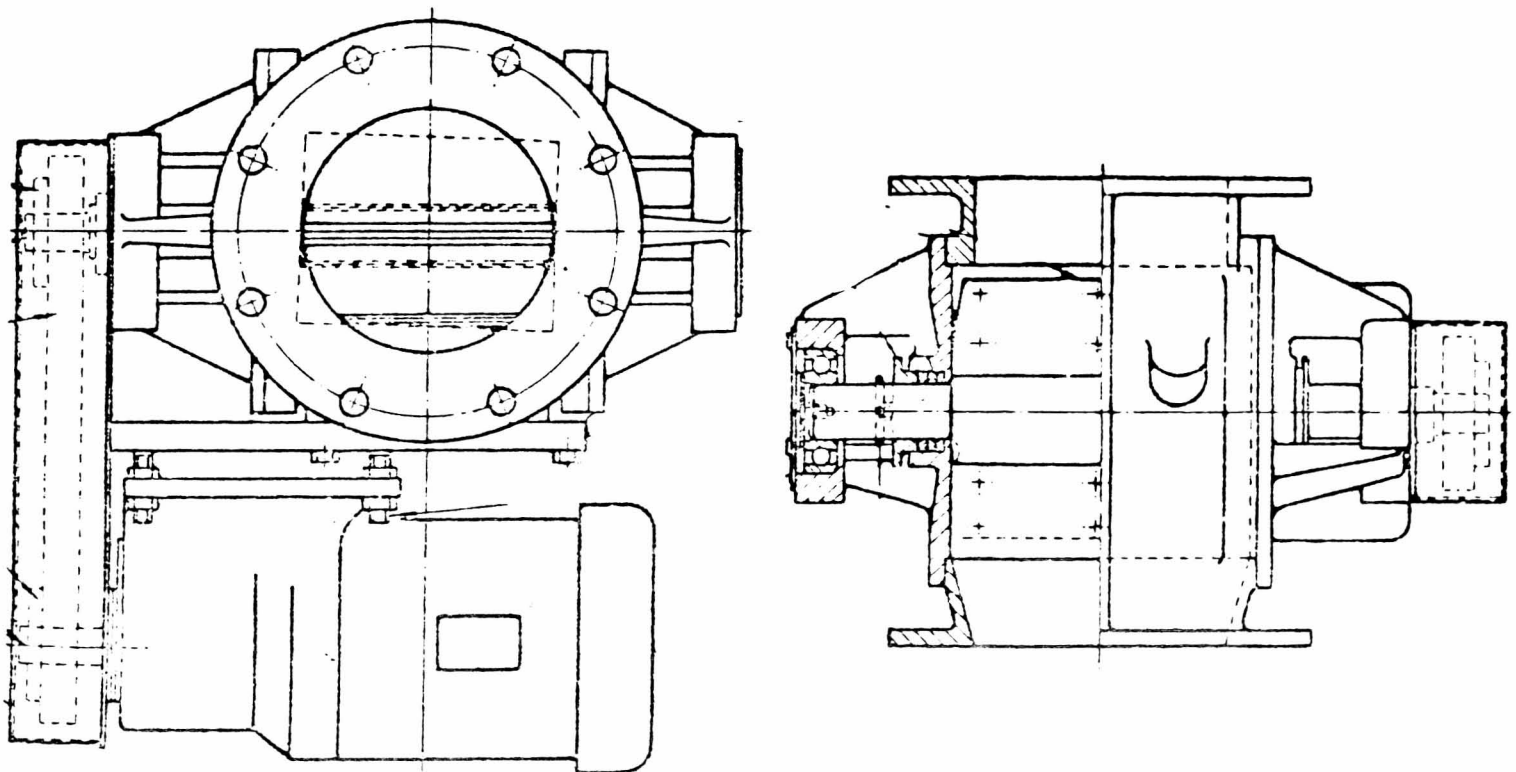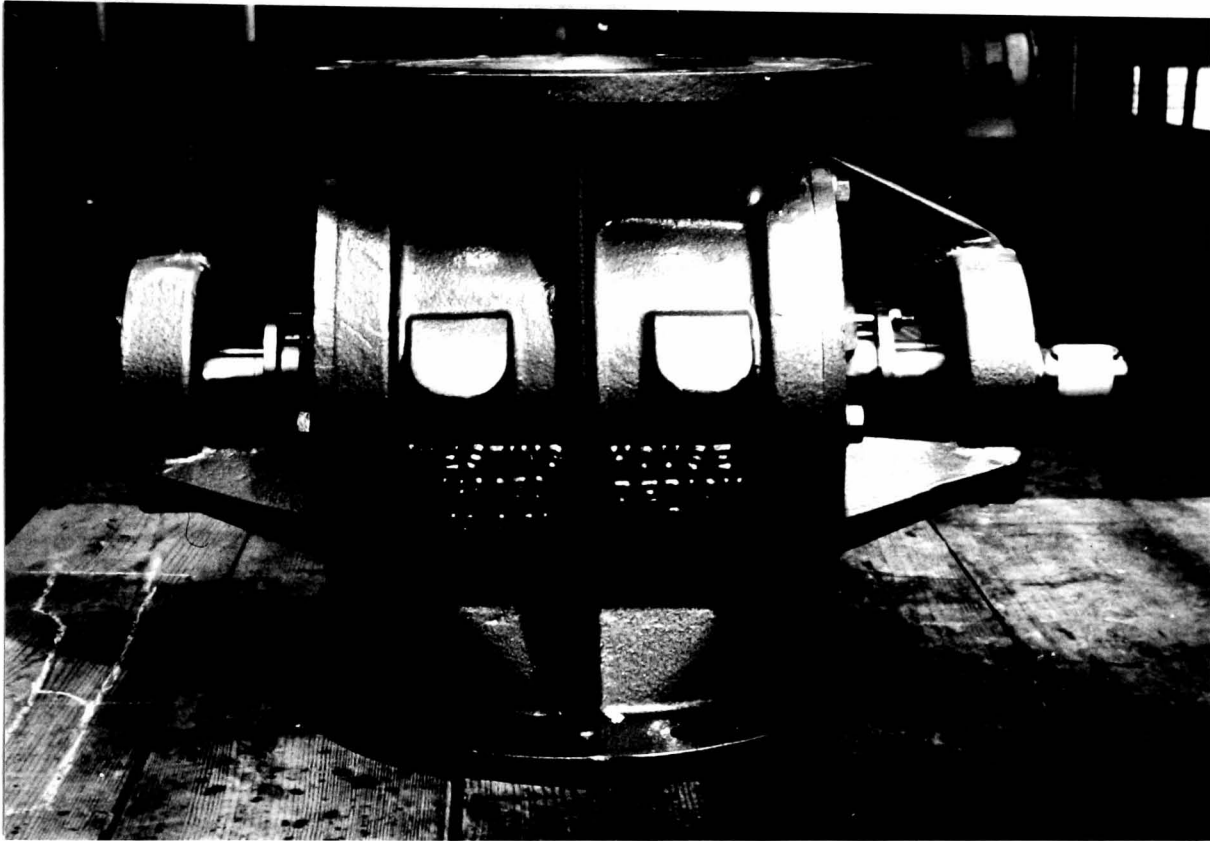
Figure 5.6   Photograph and drawings of drop-through type rotary
             valve used for experimental studies
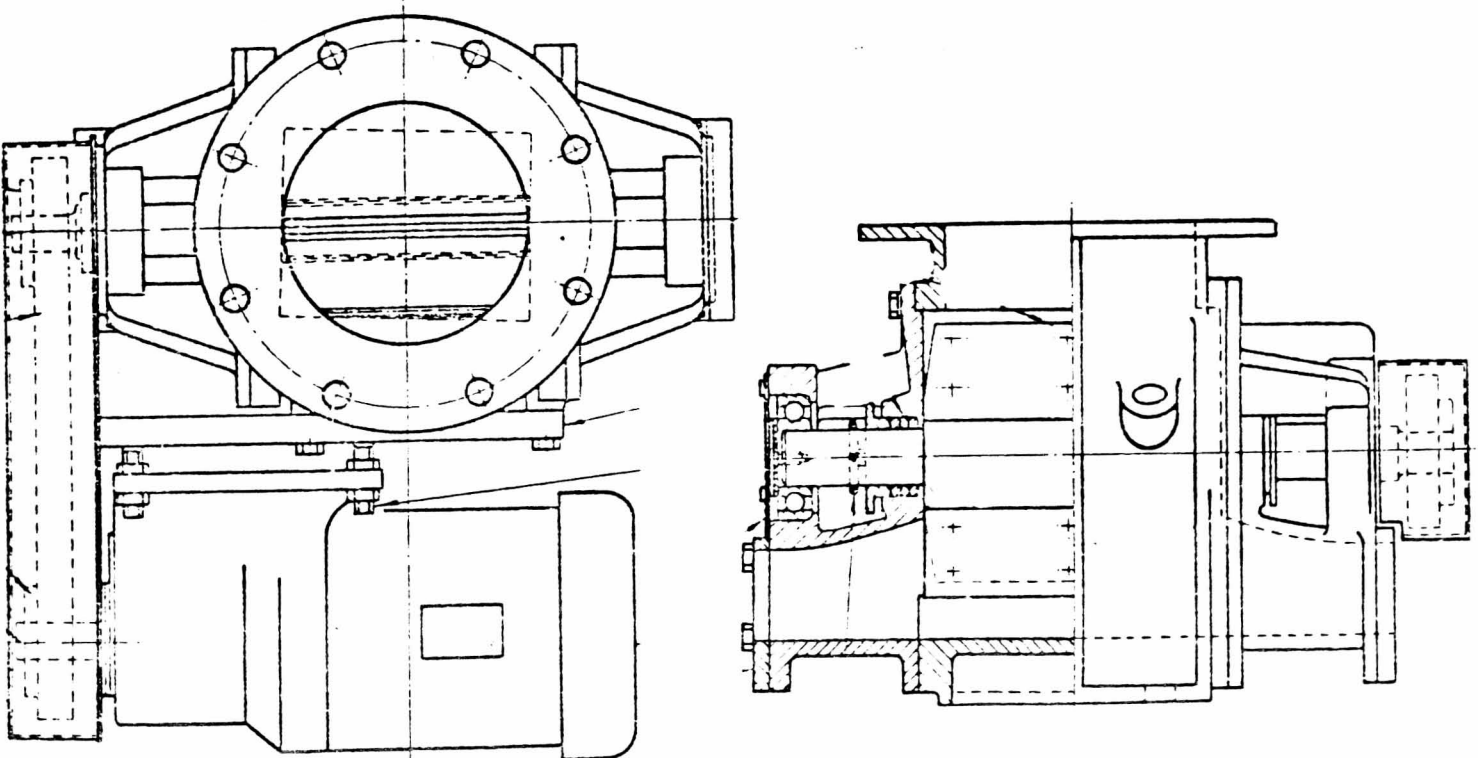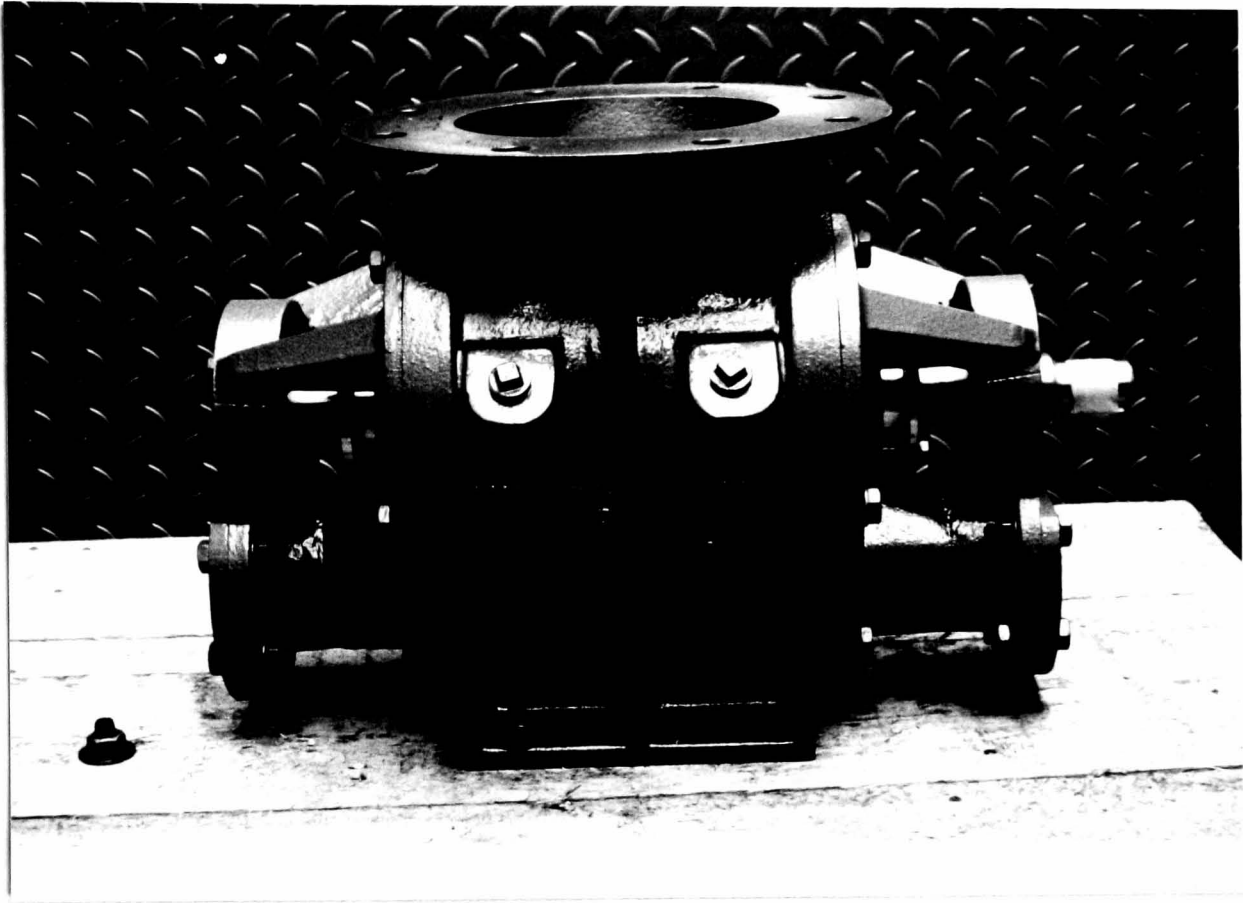
Figure 5.7　Photograph and drawings of blow seal used for
experimental studies

dimensions. They were both standard proprietary designs manufactured by Westinghouse Systems Ltd (15). The drop-through valve was a type AS-175, serial number HSO782 and the blowing seal was a type AS-175, serial number HSO782. The drive for these valves was provided by a 550W electric motor fitted with a mechanical variable ratio reduction gearbox. Rotor speeds in the range 7 to 42 rev/min were obtainable with this arrangement.

5.4 Instrumentation

5.4.1 The Measurement of Air Mass Flow

The measurement of air mass flow ($\dot{m}_a$) was achieved by the use of two orifice plate, differential pressure meters. These were only chosen after careful deliberation. The reason for concern being the presence of pressure fluctuations in the air flow. These fluctuations are a result of the mechanical operation of the Roots type blower which causes four pressure fluctuations per revolution. It is well known that such disturbances affect the operation of orifice plate meters and can lead to erroneous results (References 60 & 61). However, after studying the available alternatives it was decided that orifice plates would be no less reliable than any other device used in this situation.

Rallis & Marcus (62) reported the presence of two pressure pulses in a Roots-type blower/rotary valve conveying system. These were a low frequency, high amplitude pulse generated by the rotary valve and a high frequency, low amplitude pulse generated by the blower. For this reason it was decided to place the orifice meters on the inlet side of the blower. This effectively shielded them from the disturbances generated by the rotary valve, although they still had to operate in the presence of the disturbances generated by the blower.

Jeffery (63) suggested the method of using two orifice plate meters of different area ratios and mounted in series. He said that if the disturbances generated by the blower were going to be a problem then there would be a significant difference between the flow rates indicated by these two meters. Consequently, it was decided to incorporate such a system into the experimental rig in order to assess the degree of confidence in the measurement of the air flow rate.

The use of two orifice plate meters with different area ratios also permitted a wider range of flow rates to be measured. To extend the measurement range further three orifice plates were made with orifice sizes of 40, 70 and 80 mm. These had area ratios of 0.155, 0.475 and 0.620 respectively when fitted in the 101.6 mm (4 inch) bore inlet pipe. The orifice plates were of the corner tapping type and were manufactured and installed according to BS 1042 (64).

Initial results showed a wide discrepancy between the flow rates indicated by the two meters. However, experimentation revealed that this was attributable to the use of long connecting tubes between the orifice plates and their respective manometers. These tubes were subsequently shortened and as a consequence the disagreement between the indicated flow rates was reduced to 5% or less over the useful range of air flows. Figures 5.8a and 5.8b illustrate the improved results. These are a plot of the percentage difference between the indicated mass flow rates of the two orifice plates as a function of the arithmetic mean of the two indicated flows. Figure 5.8a compares the 40 mm and 70 mm meters which are intended for the range 1 to 6 m^3/min and Figure 5.8b compares the 70 mm and 80 mm meters which are intended for the range 5 to 15 m^3/min.

5.4.2   The Measurement of Solids Mass Flow

The solids mass flow rate ($\dot{m}_s$) was not obtained by direct measurement but by monitoring the mass of product in the receiving hopper. This was achieved by recording the output of the load cell system on a displacement - time pen recorder. The solids mass flow rate over a given time interval was obtained by measuring the slope of the resulting trace. Since the load cells were fitted to the receiving hopper the time delay between any change in feed rate at the rotary valve and that subsequently recorded at the receiving hopper had to be allowed for.

5.4.3   The Measurement of Rotary Valve Air Leakage

The air leakage through the rotary valve was measured by means of a bank of rotameters. The air was ducted from the constant head tank and supply hopper to a manifold which distributed it to four rotameters, as shown in Figure 5.9. By opening and closing valves in this manifold,
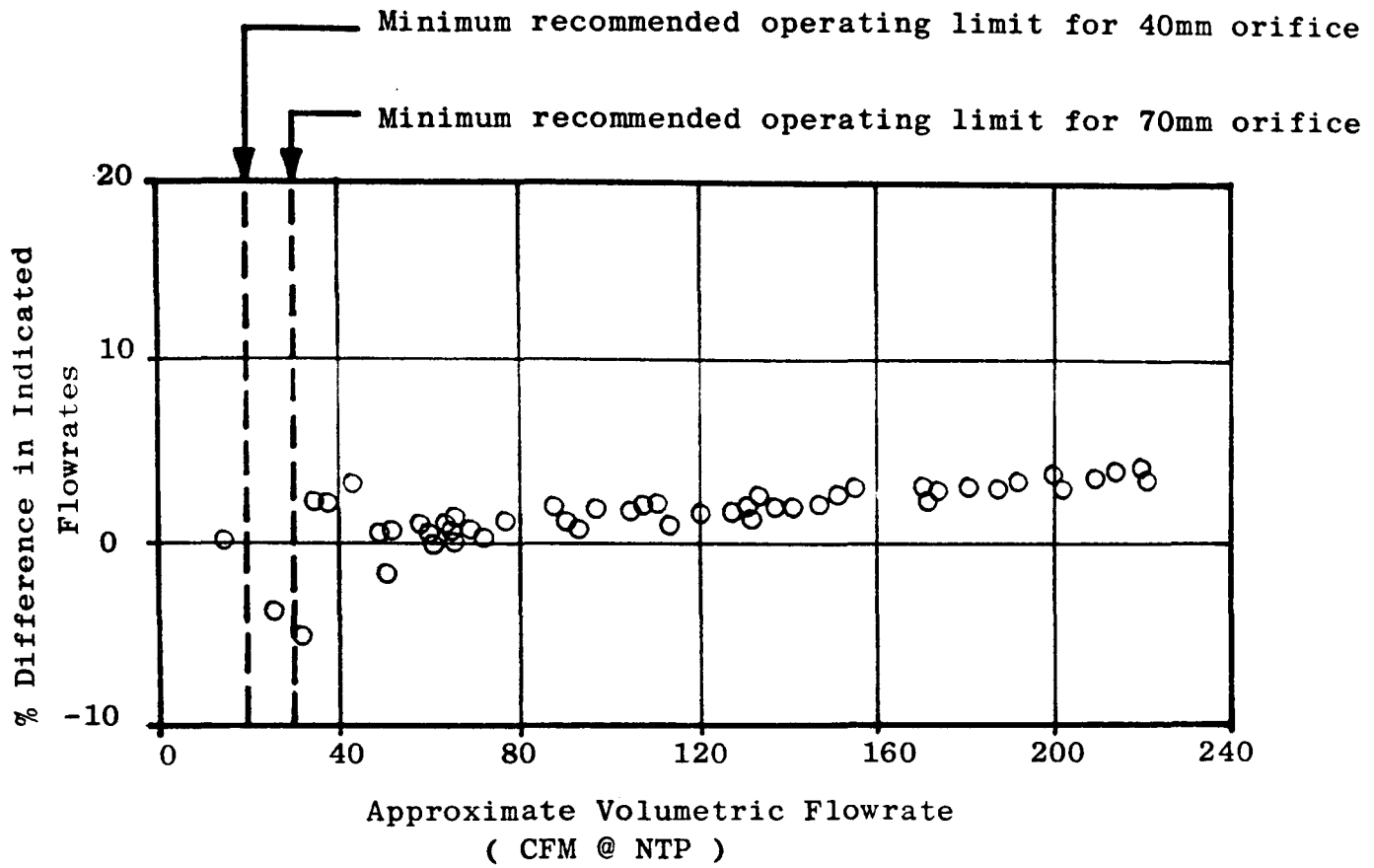
Figure 5.8a   Percentage difference in indicated volumetric
flowrate versus approximate volumetric flowrate
for the 40 mm and 70 mm orifice plate meters
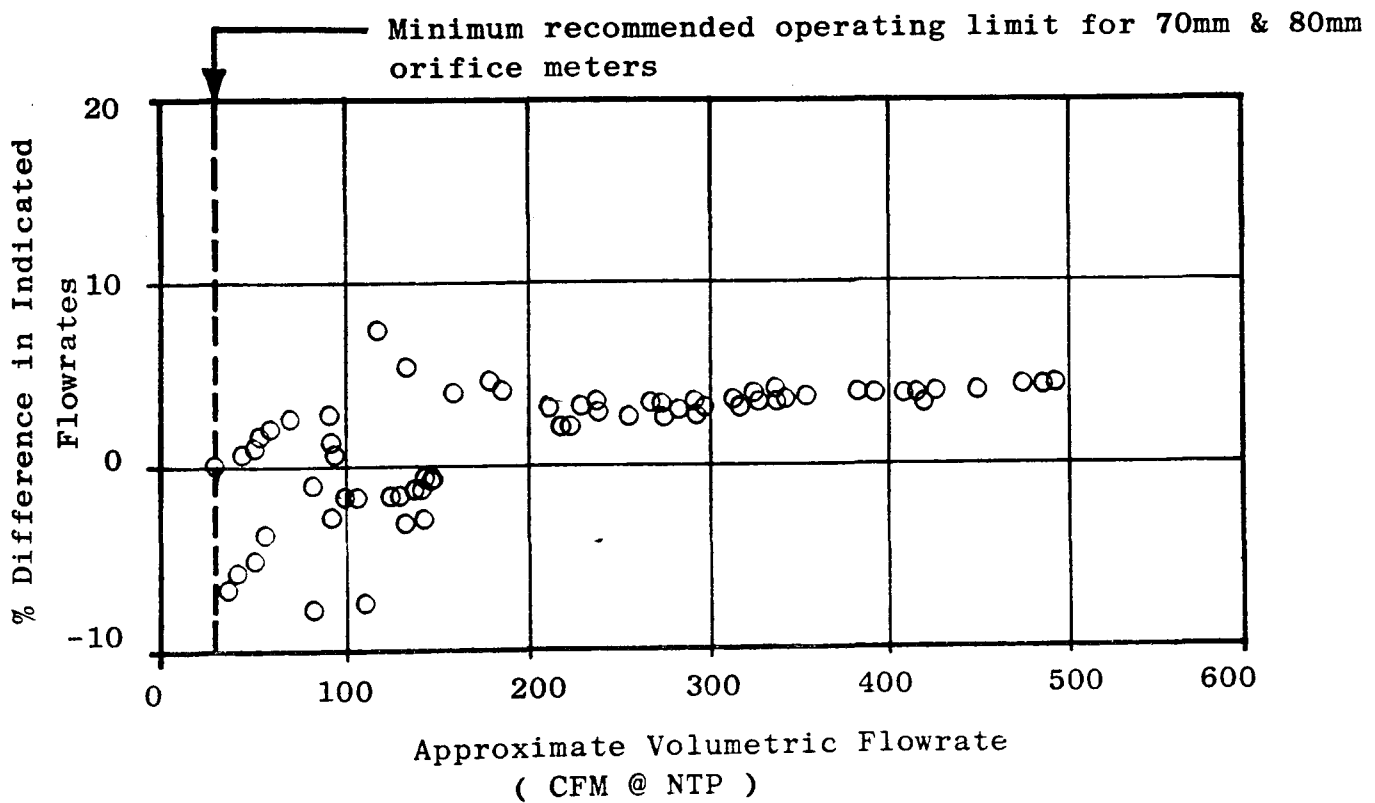
Figure 5.8b   Percentage difference in indicated volumetric
flowrate versus approximate volumentric flowrate
for the 70 mm and 80 mm orifice plate meters

PLUGS TO STOP FLOW THOUGH THESE
ROTAMETERS IF REQUIRED

ON/OFF VALVES

AIR LEAKAGE FROM C.H.T.   AIR LEAKAGE FROM SUPPLY HOPPER
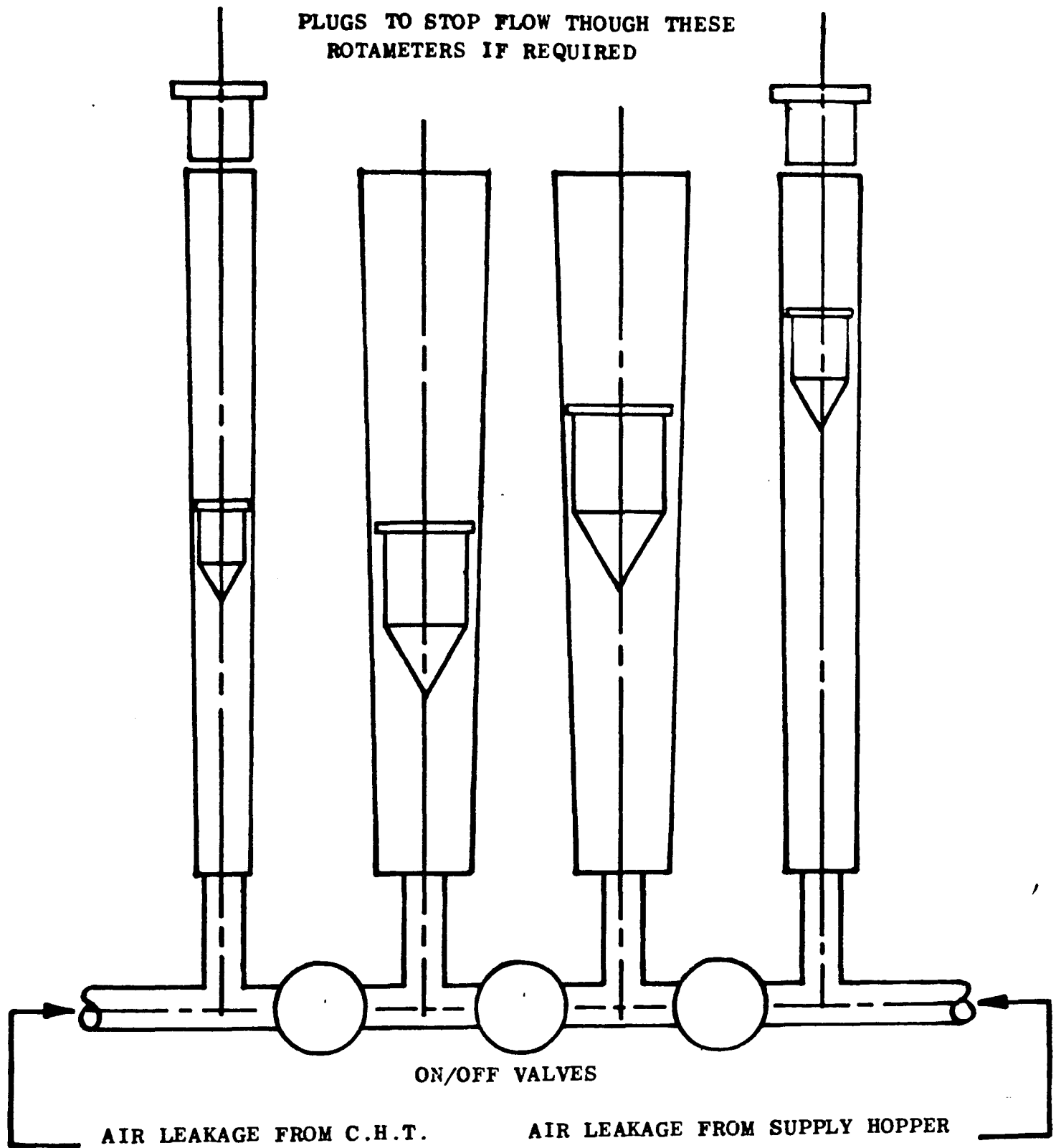
Figure 5.9   Rotameters and manofold assembley for measurement
              of rotary valve air leakage

the required combination of rotameters for the expected leakage flow could be used.

5.4.4 Other Measurements

Instrumentation for measurements other than those already discussed was quite conventional. Pressure measurements were made with both manometers and electronic transducers. Initial measurements of the rotary valve speed were made with a stopwatch and then later by means of an optical switch and incremental encoder disc fitted to the output shaft of the variable speed gearbox. Temperature measurements were made with both mercury-in-glass and thermocouple instruments.

An interesting measurement was that of the electrical power consumed by the blower drive motor. This was achieved by the use of a pair of galvanometers to measure the voltage and current being drawn by the drive motor for the blower. While strictly outside the scope of this thesis, this has resulted in the accumulation of a considerable amount of interesting data regarding the specific power consumption in pneumatic conveying systems. Some of this information has been published in two separate papers (References 65 and 66).

CHAPTER SIX

EXPERIMENTAL PLAN AND PRESENTATION OF DATA

6.1 Introduction

The principal objectives of the experimental work using the industrial size rig were:

a) to assess whether or not the flow patterns and modes of entrainment observed in the flow visualisation rig are also typical of those which occur in industrial systems; and, if so,

b) to provide reliable quantitative data for testing the models developed in Chapter 4; and also

c) to provide a set of reference data for estimating the performance of similar systems.

To achieve these objectives, eight basic entrainment configurations and six different bulk materials were selected for experimentation. The plan was to examine the performance of the conveying system for each combination of material and entrainment configuration. The purpose of incorporating six different materials into the experimental programme was to obtain information about the effect of material characteristics on the entrainment process. This was essential if the work was to be of any practical value because of the diverse range of materials which are handled in industrial pneumatic conveying systems. A serious shortcoming of the flow visualisation work was that only one test material had been used.

This chapter describes the entrainment configurations and materials used for the experimental work; outlines the experimental procedure; and explains the methods used for the presentation of the resulting data.

6.2 Description of the Entrainment Configiurations Used in the Experimental Programme

The eight basic entrainment configurations which were selected for experimentation were:

A. conventional drop-through type of rotary valve which feeds material into the conveying line via a simple transition shaped drop-out box one pipe diameter in depth, Figure 6.1a;

B. as configuration A but with a simple transition shaped drop-out box two pipe diameters in depth, Figure 6.1b;

C. as configuration A but with a simple transition shaped drop-out box three pipe diameters in depth, Figure 6.1c;

D. as configuration A but with an extension tube added between the flanges of the rotary valve and drop-out box to give a total depth of nine pipe diameters, Figure 6.1d;

E. a conventional drop-through type of rotary valve which feeds material into the conveying line via a drop-out box consisting of a cylindrical chamber 110 mm in diameter and two pipe diameters deep, Figure 6.1e;

F. as configuration E but with a cylindrical chamber 150 mm in diameter, Figure 6.1f;

G. as configuration E but with a cylindrical chamber 180 mm in diameter, Figure 6.1g; amd

H. a blowing seal type of rotary valve as shown in Figure 6.1h.
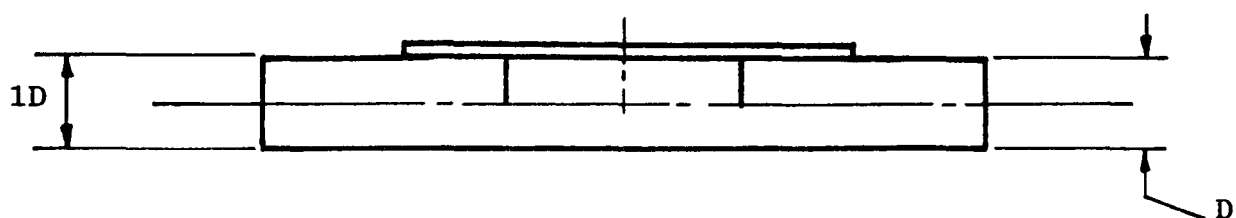
Figure 6.1a
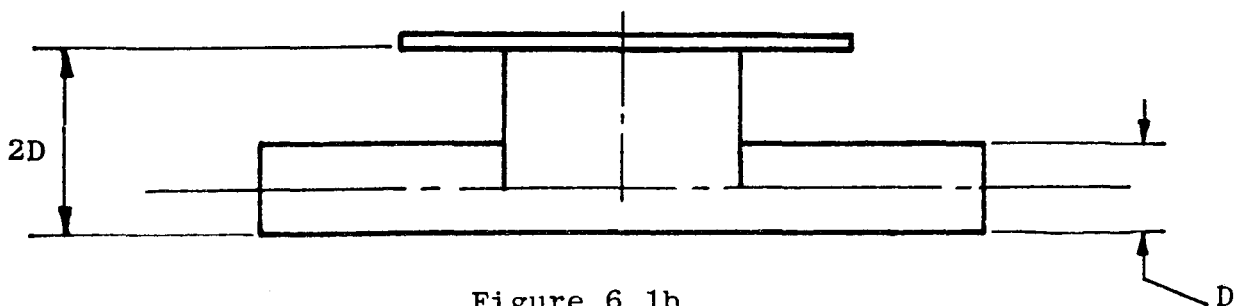
Figure 6.1b

Figure 6.1 Experimental drop out boxes
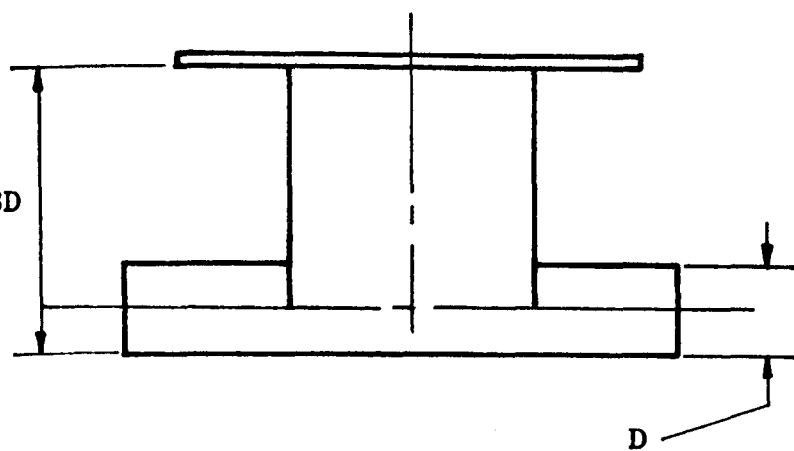
Figure 6.1c
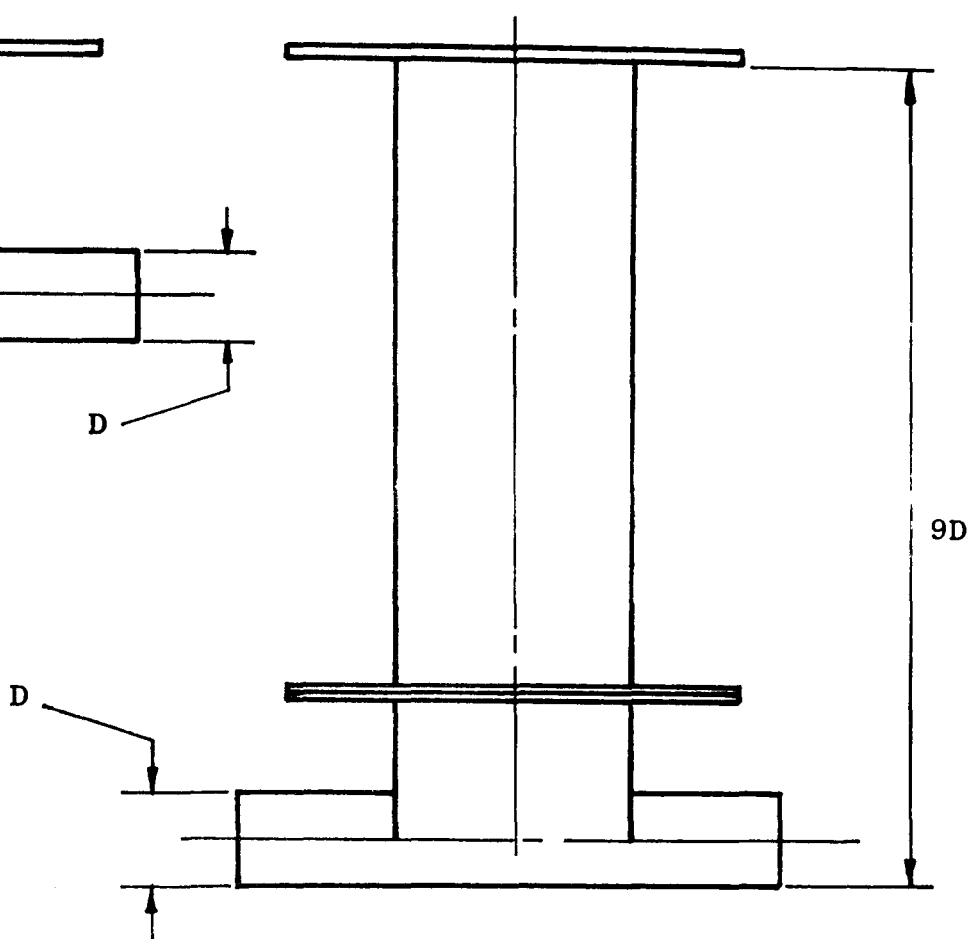
Figure 6.1d
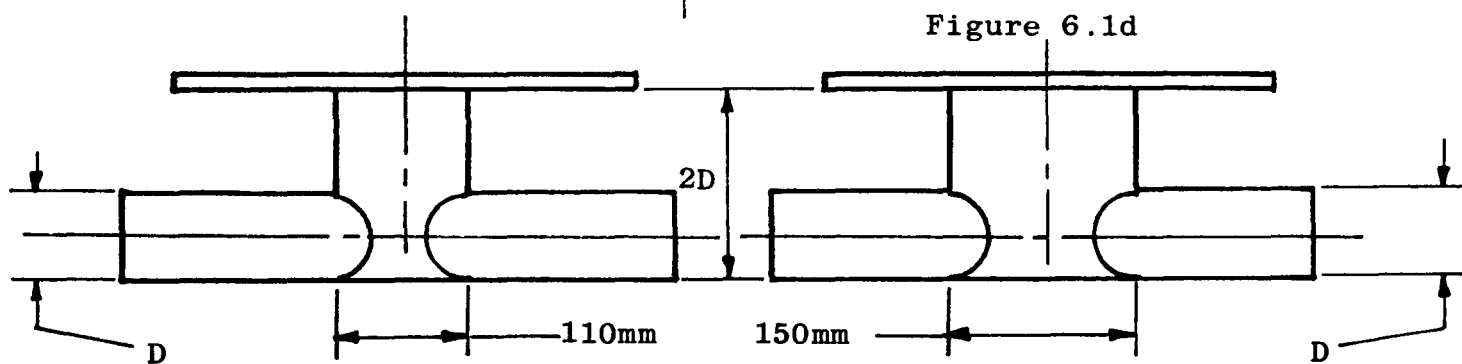
Figure 6.1e

Figure 6.1f
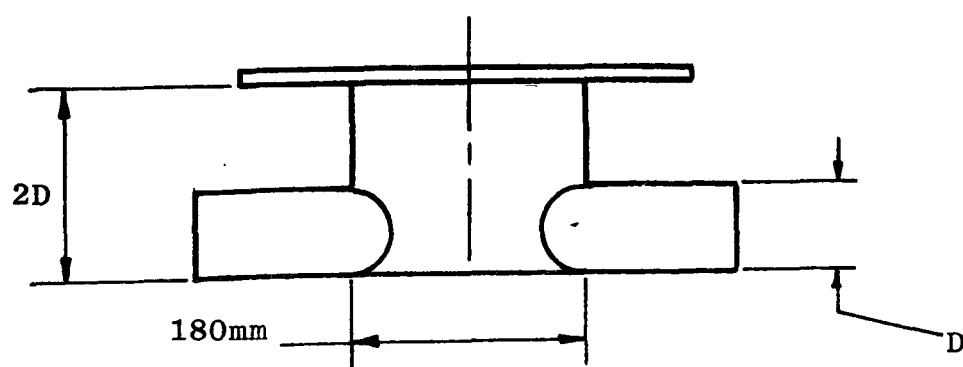
Figure 6.1g

Figure 6.1 Experimental drop-out boxes
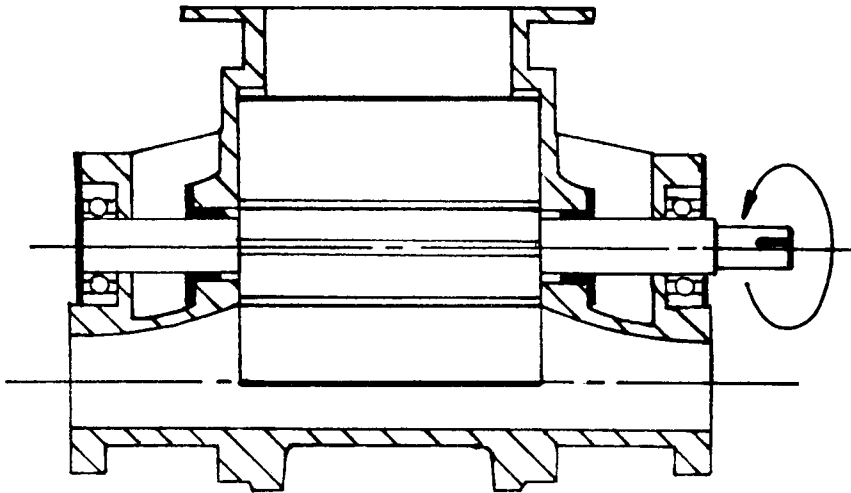
Figure 6.1h Blowing Seal

Drop-out box config.	Box Length	Box Height	Aspect Ratio	Box Volume	Volume Ratio	Entrainment Efficiency	Critical Peripheral Velocity
	a (mm)	H (mm)	H/a (-)	V_b (mL)	V_R (-)	η_e (%)	P_* (m/s)
A	180	60	0.33	2590	0.29	71	1.72
B	180	130	0.72	4020	0.23	77	1.36
C	180	260	1.44	7100	0.15	85	1.37
D	180	560	3.11	16740	0.07	93	1.74
E	110	130	1.18	2930	0.29	71	1.05
F	150	130	0.87	4070	0.23	77	1.22
G	180	130	0.72	5160	0.19	81	1.36
H	n/a	n/a	n/a	n/a	n/a	n/a	n/a

Figure 6.2   Table of defining parameters for the eight drop-out
box configurations used in the experimental programme.

Figure 6.2 tabulates the defining parameters of these eight configurations
as proposed in Chapter 4.   For configurations A to G the rotary valve
used was the 175 mm drop-through type described in Chapter 5 and
illustrated in Figure 5.5.   The blowing seal which was used for

configuration H is also described in Chapter 5 and illustrated in Figure 5.6.

The blowing seal and configurations A, B and C probably represent the most common arrangements in current industrial use, hence the reason for their selection. In addition to this, configurations B and C are similar to those used for the flow visualisation study and thus enable a direct comparison to be made with that work. Also in keeping with the flow visualisation work, the rotary valve could be mounted in one of three different orientations as shown by Figure 6.3. With the exception of the blowing seal, this enabled three variations to each of the basic configurations to be obtained which allowed the effect of different valve orientations to be investigated.

Configuration D was obtained by fitting a 500 mm long tube between the flanges of the rotary valve and drop-out box. This gave an overall drop-out box depth of about nine pipe diameters and an aspect ratio of 3.11. The reason for selecting this particular configuration was that it is approximately the same as that which maximised the performance of the system tested by Moseman & Bird (22 & 23); see drop-out box 'C' in Figure 2.28a of Chapter 2.

The drop-out boxes used for configurations E, F and G were significantly different in shape from those used for the other configurations described above. Instead of being a transition section they consisted of a simple cylindrical chamber two pipe diameters in depth. The purpose of testing these was to obtain information about the effect of changing the volume of the drop-out box chamber (ν_b) while keeping the depth of the box (H) constant. By comparing this with the information obtained from the experiments with configurations A, B, C and D, which have different volumes by virtue of their different depths, it was argued that the relative importance of ν_b and H with regard to the entrainment efficiency could be established.

6.3 Description of the Test Materials Used in the Experimental Programme

The test materials used in the experimental programme were chosen to be a representative selection of the type of products that are typically handled in pneumatic conveying systems which use a rotary valve as the solids feeding device. In order to ensure that this objective was

Rotation

Direction of Flow

Rotation   Rotation

Direction of Flow   Direction of Flow
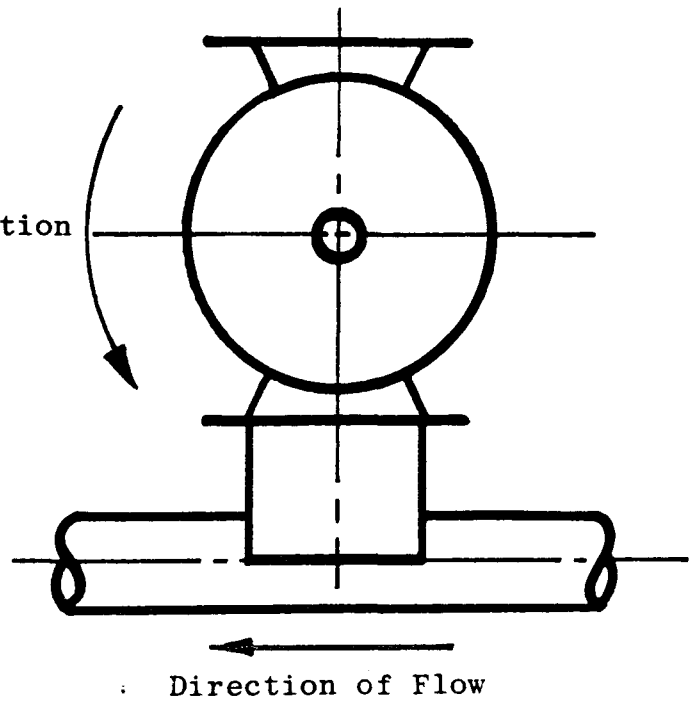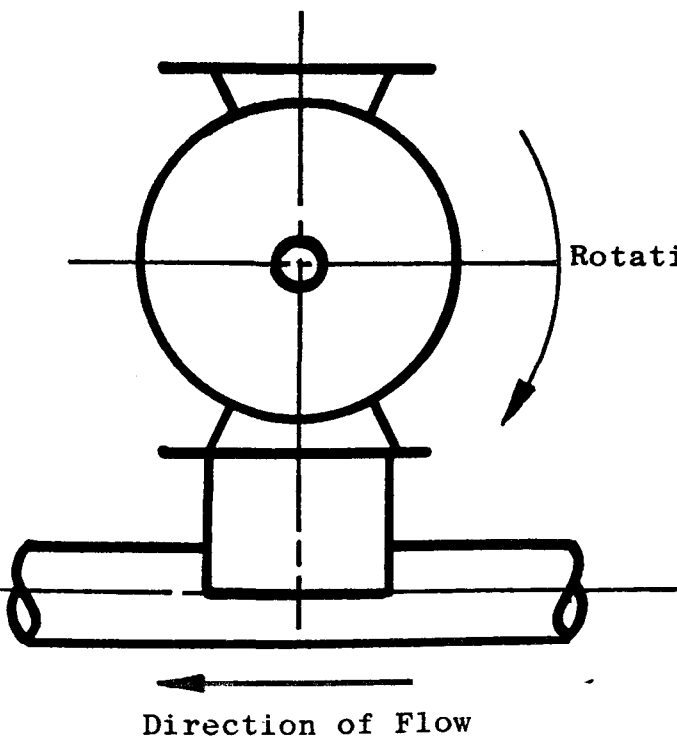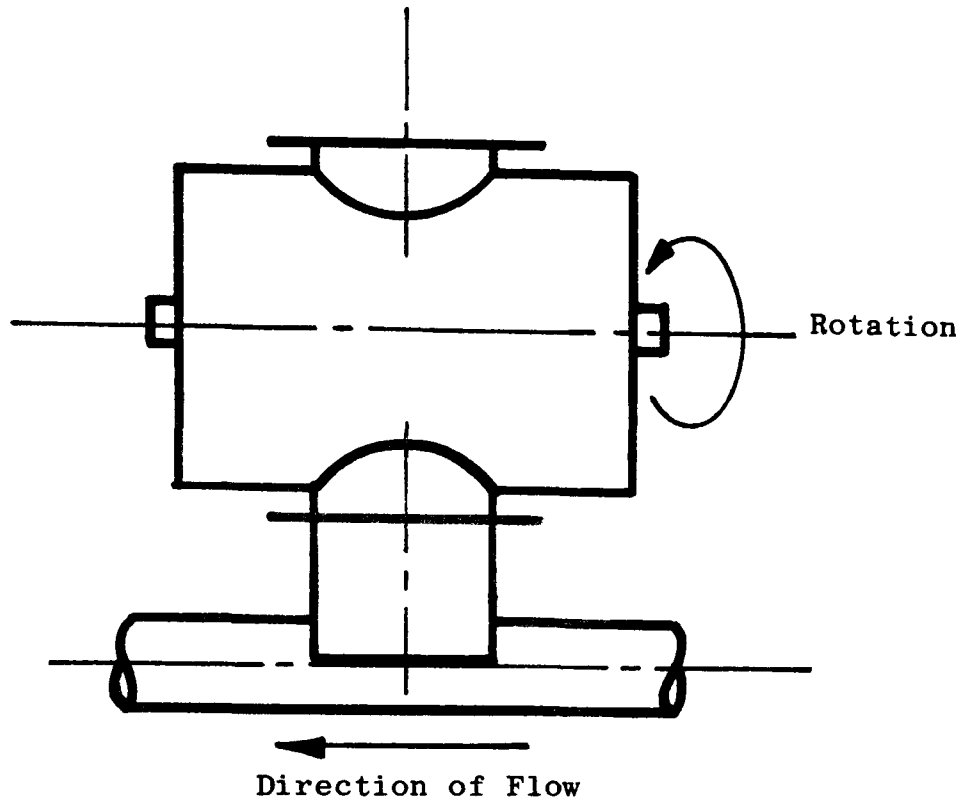
Figure 6.3   The three basic rotary valve orientations

achieved the industrial companies supporting the research were consulted. On the basis of their advice the following group of materials were selected:

    a)   Polyethylene Pellets

    b)   Polyethylene Powder

    c)   Wheat Flour

    d)   Ordinary Portland Cement

    e)   Coal - 'singles' grade, and

    f)   Coal - 'pulverised' grade

All of these materials are well known and as a group probably represent the range of physical characteristics which are likely to be encountered with materials that are handled pneumatically. Consequently it was argued that the incorporation of these into the experimental programme would enable a comprehensive set of reference data to be established. If presented in a suitable way this would then enable the performance of similar systems handling other products to be estimated by inter-polation. However, in order to do this it is essential that both the bulk and the particle characteristics of the six reference products are known. To satisfy this requirement photomicrographs and details about the bulk and particle characteristics of these products are given in Figures 6.4 to 6.9.

6.4 Experimental Procedure

The experimental plan was to test each combination of material and entrainment configuration for a range of rotor speeds and pick-up velocities. To achieve this five set rotor speeds were used, 7, 15, 20, 30 and 40 rev/min and the pick-up velocity was varied between the minimum required to prevent the pipeline from blocking and a maximum of about 50 m/s. The procedure which was used is shown by the flow chart in Figure 6.10. By following this a complete set of measurements was obtained for each combination of material, entrainment configuration, rotor speed and pick-up velocity. The measurements recorded were:

    i)   the conveying air mass flow rate ($\dot{m}_a$);

    ii)   the solids mass flow rate ($\dot{m}_s$);

iii)   the rotary valve speed (n);

iv)   the conveying line pressure drop (ΔP_ℓ);

v)   the conveying air temperature at the solids pick-up point (Ta); and

vi)   the air leakage through the rotary valve ($\dot{V}_L$)

To process these measurements a computer programme was written. This ensured consistency in the calculations and enabled the procedure recommended in B.S. 1042 (64) for the calculation of the air mass flow rate to be followed exactly.

6.5   Presentation of the Experimental Data

In considering the most appropriate method for presenting the experimental data attention was paid to the methods used by the manufacturers of rotary valves and blowing seals.   They invariably present the performance characteristics of their valves in the form of graphs which show the relationship between the volumetric throughput and the valve rotor speed.   This is also the approach which has been used by previous researchers; for example, see the experimental results of Jotaki & Tomita (10) which are shown in Figure 2.8 of Chapter 2.

Figure 6.11 shows an example of the performance characteristics which are published by Westinghouse Systems Ltd (15) for their range of valves. These are quoted as an example because the AS-175 and GS-175 curves on these diagrams refer respectively to the rotary valve and blowing seal used in this investigation.   A 100% filling efficiency line and an average filling efficiency curve are shown for each size of valve.   The 100% lines are based on the assumption of complete pocket filling and emptying as modelled by equation 2.1 in Chapter 2, that is:

$$\dot{V} = V_o n \tag{2.1}$$

The purpose of showing the average efficiency curves is to indicate the likely effect of the material characteristics and operating conditions on the performance of the valve.   However, as explained in Chapter 2, these curves should be treated with considerable caution because the actual efficiency is dependent on many factors which are not adequately represented by a single curve of the type shown in Figure 6.11

From the relationship between the volumetric throughput and rotor speed another diagram may be derived. This is the relationship between the filling factor and rotor speed as used by Reed (11). The filling factor (α) is sometimes called the volumetric efficiency and as such is always equal to or less than unity. It is the ratio of the actual volumetric throughput to the maximum capacity of the valve at the same rotor speed. In other words, it is the outcome of dividing the average efficiency curve by the 100% efficiency line shown in Figure 6.11.

Figure 6.12 shows the filling factor versus rotor speed curves for a range of different materials. This figure was produced by Reed for a 200 mm drop-through rotary valve. It indicates clearly that rotary valves do not handle all materials with equal effectiveness and emphasises the point made earlier that manufacturers' average efficiency curves should be treated with caution.

In Chapter 7 the results obtained from the experimental work conducted with the industrial scale rig are presented in a similar way to those shown in Figure 6.12. The significant difference being that the term 'feeding' factor (γ) is used instead of the term filling factor (α). The reason for this difference is that these results reflect the overall effectiveness with which material can be entrained into the conveying line. This distinguishes it from previous studies (References 10, 11, 12, 13, 17 & 53) which concentrated only on understanding the pocket filling process and looked at this aspect of performance in isolation. Consequently, the feeding factor is a function of the entrainment configuration and conditions existing in the drop-out box as well as the parameters which determine the filling factor; namely, material characteristics, rotor speed and the air pressure ratio across the valve. Graphs which show the variation of the feeding factor with entrainment configuration and pick-up velocity are also used in the analysis of the experimental results.

Another important aspect regarding the presentation of results which must be clearly understood, is that the volumetric throughput of the rotary valve was not obtained by direct measurement. To obtain the volumetric throughput for any given set of conditions the solids mass flow rate ($\dot{m}_s$) must be divided by the appropriate bulk density for the material in question. This step is not as straightforward as it first appears because the appropriate bulk density, that near the inlet region

of the rotary valve, is not known and not easily measured.   To overcome
this problem the 'poured' value of the bulk density was used to calculate
the volumetric throughput.   As a consequence of this decision the
feeding factors which were subsequently calculated are almost certainly
in error.   However, this approach is justified because the derived data
is readily usable; the 'poured' bulk density being a quantity which is
easily measured using simple equipment.   With the exception of the Singles
Coal, the poured bulk densities quoted in Figures 6.4 to 6.9 were
determined by pouring the material through a funnel into a one litre
measuring flask.   The poured bulk density was then calculated from the
measured weight and volume of this sample.   In the case of the Singles
Coal the figure quoted was obtained from the National Coal Board.   Their
method of determining the bulk density is to fill a $1m^3$ box with coal and
then measure its weight.

The final method which is used for the presentation of the
experimental results is as shown in Figures 6.13 to 6.18, that is, the
conveying system characteristics for each material.   Since these were
to be independent of the entrainment configuration, they may be
considered as further information characterising the test materials;
thus complementing the details given in Figures 6.4 to 6.9.   The
envelopes shown by broken lines on these diagrams indicate the range of
conveying conditions that were examined with each material.

As a consequence of the experimental procedure which was used, that
is, fixing the rotor speed and then varying the air mass flow rate, the
curves on the graphs relating the conveying line pressure drop and the
air mass flow rate were obtained directly.   An example of such a
graph is shown in Figure 6.13a.

The graphs relating the solids mass throughput and the air mass
flow rate, for example Figure 6.13b, were obtained by interpolating
the data to draw curves which represent a constant conveying line
pressure drop.   This method of presentation is useful because it shows
the range of solids loading ratios which were examined with each material.
The solids loading ratio ($\dot{m}_s/\dot{m}_a$) is a useful parameter because it
indicates the nature of the gas-solid flow in a pipeline.
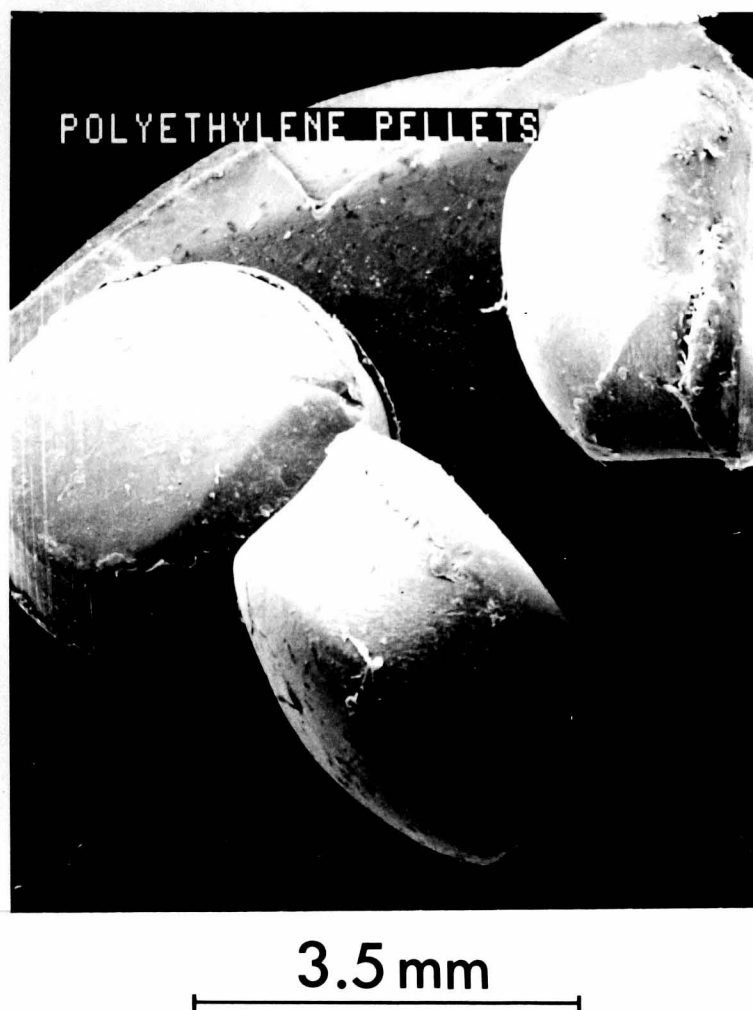
3.5 mm

Figure 6.4

B P RIGIDEX POLYETHYLENE PELLETS

MATERIAL CHARACTERISTICS

Bulk density 529 kg/m^3

Packed density 573 kg/m^3

Particle density 909 kg/m^3

Monosized 3.5 mm particles

HANDLING CHARACTERISTICS - Free flowing

Figure 6.5

B.P CHEMICALS RIGIDEX
POLYETHYLENE POWDER

Bulk density 504 kg/m^3

Packed density 567 kg/m^3

Particle density 951 kg/m^3

Mean particle size 1.0 mm

HANDLING CHARACTERISTICS

Free flowing, prone to
static charging

POLYETHYLENE POWDER
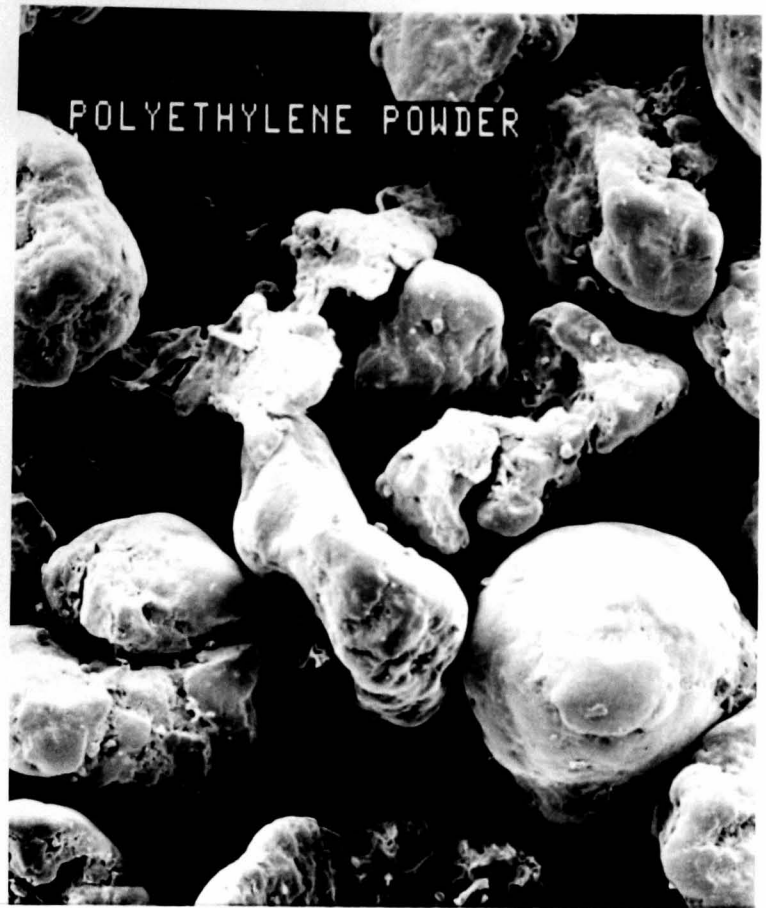
2.0 mm

Size analysis technique: Stack Sieving
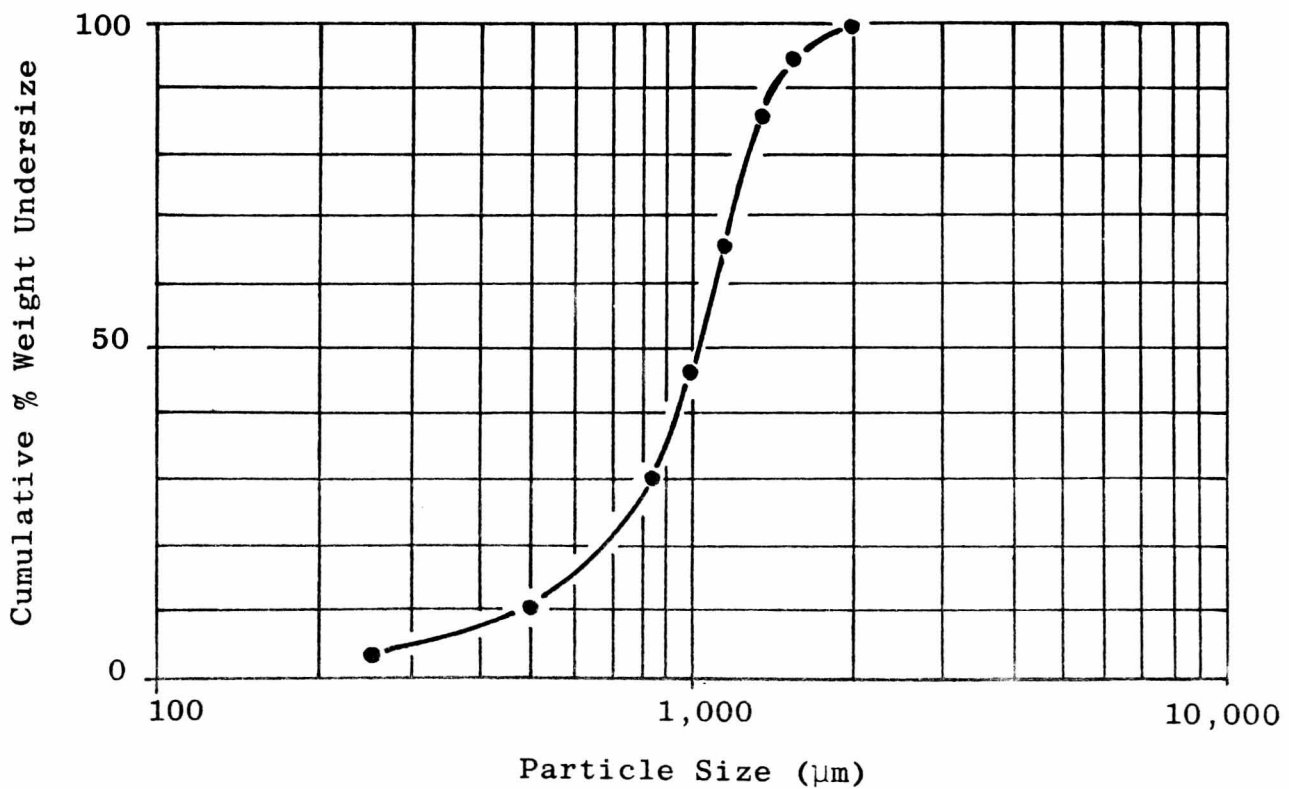
Particle Size (μm)

Figure 6.6

RANK HOVIS MINARET WHEAT FLOUR

MATERIAL CHARACTERISTICS

Bulk density 440 kg/m^3

Packed density 644 kg/m^3

Particle density 1461 kg/m^3

Mean particle size 65 µm

HANDLING CHARACTERISTICS

Cohesive

500 µm

Size analysis techniques: Malvern Laser Diffractometer ●
Alpine Jet Sieve ○
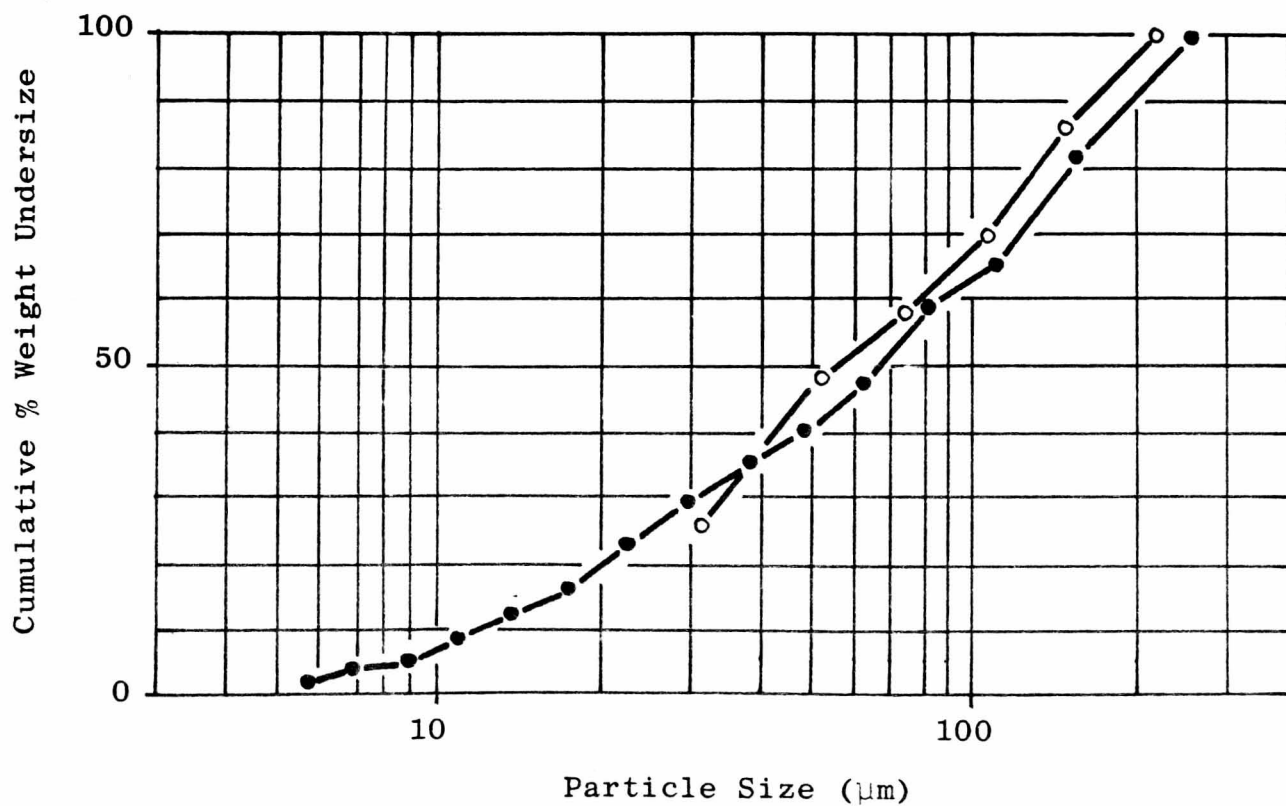
Particle Size (µm)

Figure 6.7

BLUE CIRCLE ORDINARY PORTLAND
CEMENT

MATERIAL CHARACTERISTICS

Bulk density 1138 kg/m^3

Packed density 1563 kg/m^3

Particle density 3166 kg/m^3

Mean particle size 12.5 μm

HANDLING CHARACTERISTICS

Free flowing when aerated,
cohesive when compacted

50 µm

Size analysis technique: Malvern Laser Diffractometer
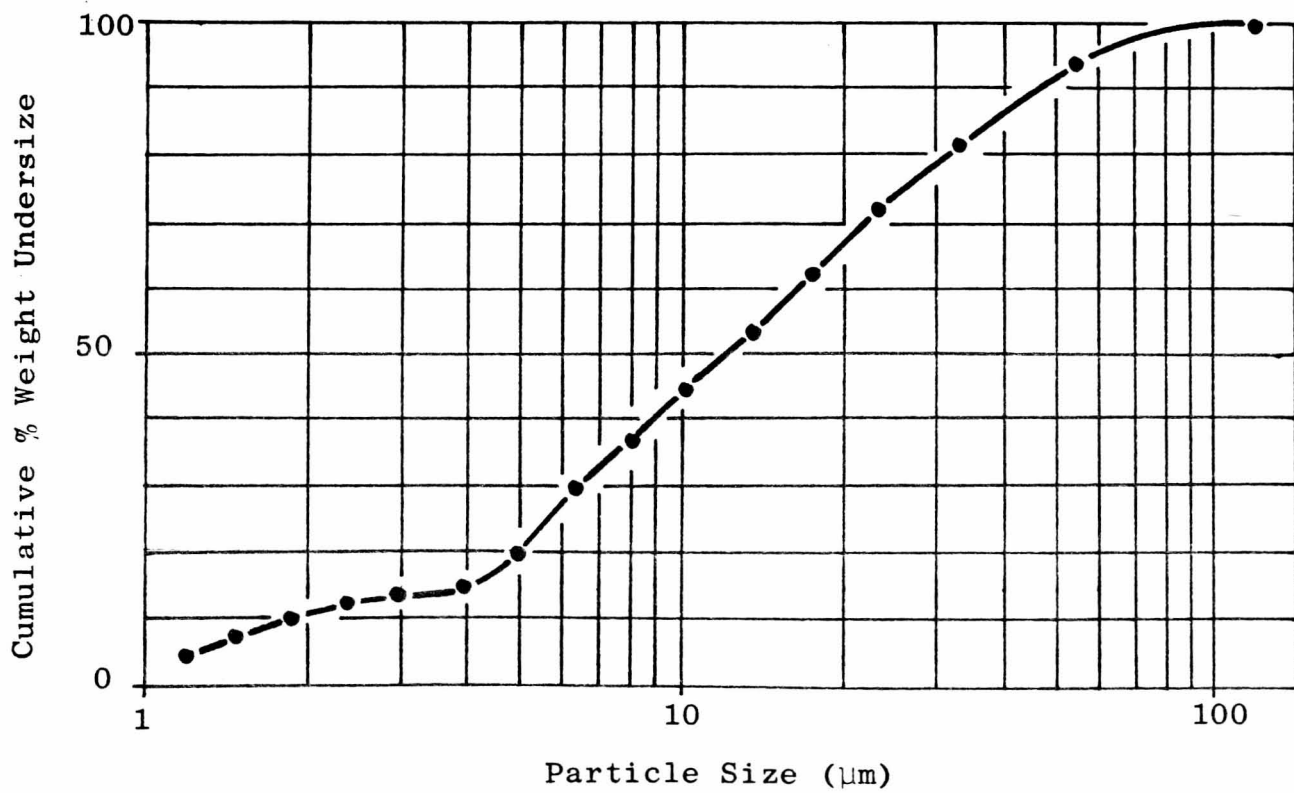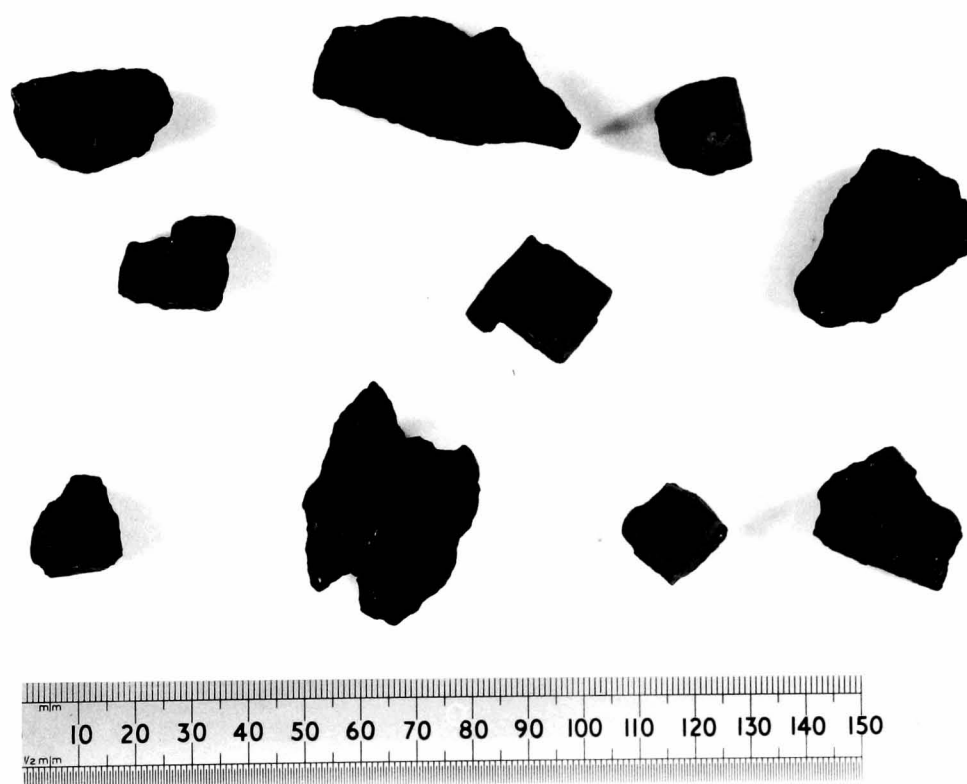
Figure 6.8

NATIONAL COAL BOARD 'SINGLES' GRADE COAL

Bulk density 641 kg/m^3

Particle density 1295 kg/m^3

Size range: Maximum 25mm Minimum 12.5mm
            (everything that will pass through
             a 25mm sieve and be retained on a
             12.5mm sieve)

Figure 6.9

<u>PULVERISED COAL</u>

Supplied but not milled
by Blue Circle.

<u>MATERIAL CHARACTERISTICS</u>

Bulk density 587 kg/m^3
Particle density 1457 kg/m^3

Mean particle size 44µm

<u>HANDLING CHARACTERISTICS</u>

Free flowing when aerated
Very cohesive when compacted
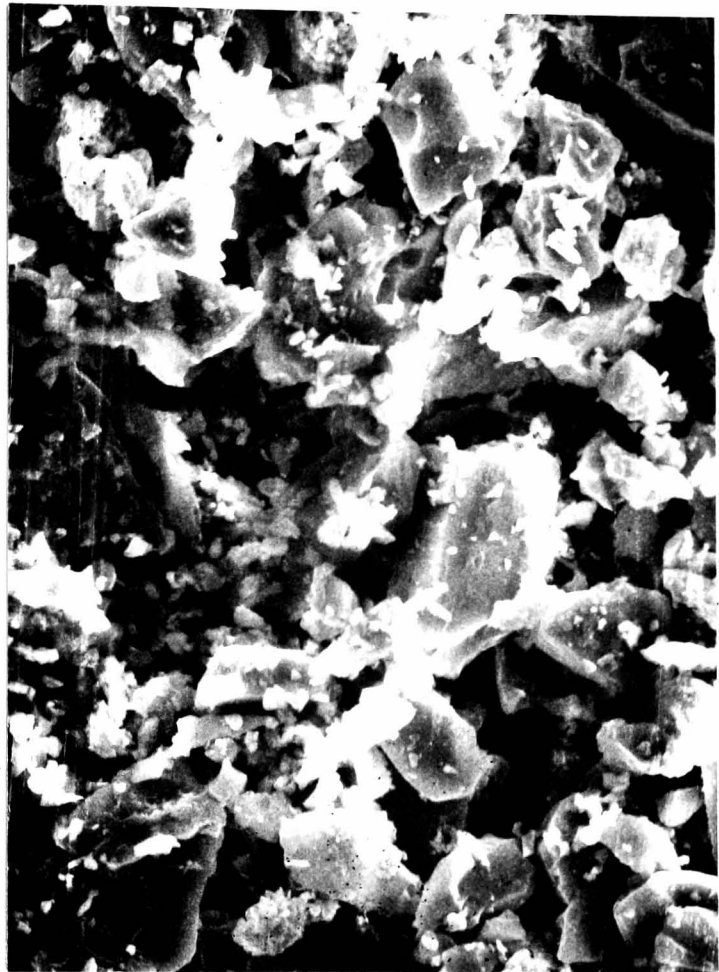
100 µm

Size analysis technique: Wide Angle Scanning Photosedimentometer
Blue Circle (suppliers) data ●

Particle Size (µm)
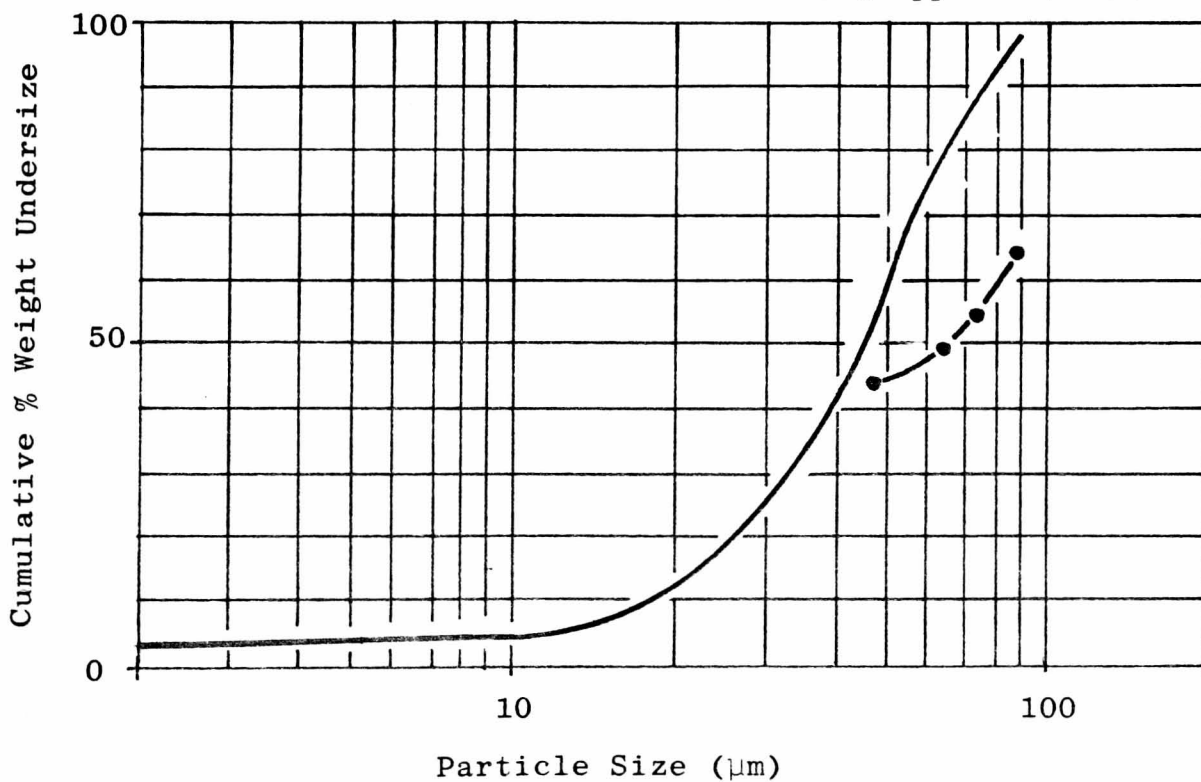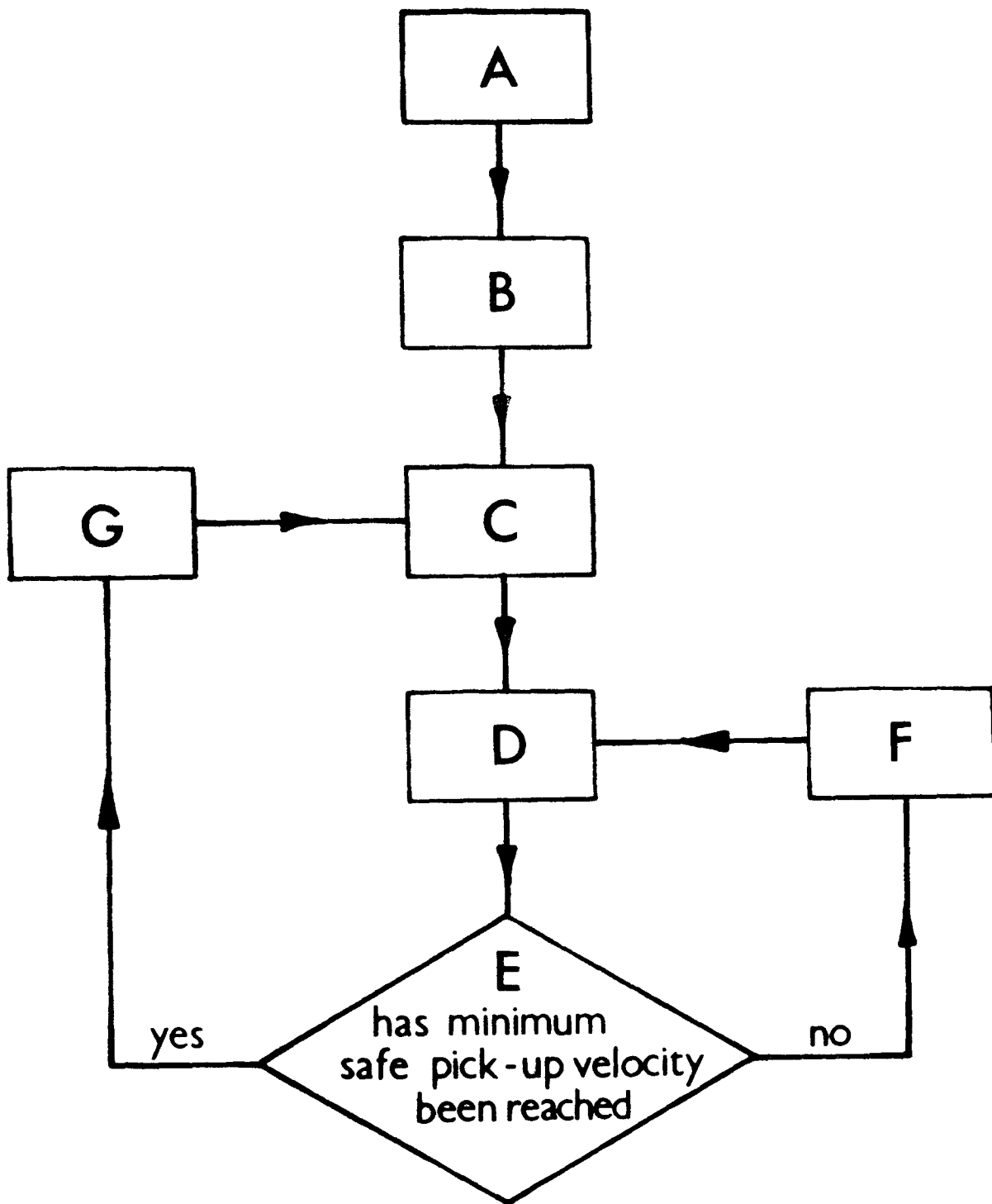
A - Select rotary valve/drop-out box configuration
B - Select valve rotor speed
C - Start test - Initially at high air flowrate
                         (i.e. at high pick-up velocity)
D - Allow conditions to settle and then take measurements
E - Repeat cycle D-E-F until minimum safe pick-up velocity
    has been reached
F - Reduce air flow rate
G - Change rotor speed and repeat cycle C-D-E-F etc.

Figure 6.10 Experimental procedure

CAPACITY / SPEED CURVES FOR
AS 150 AND AS 175 VALVES
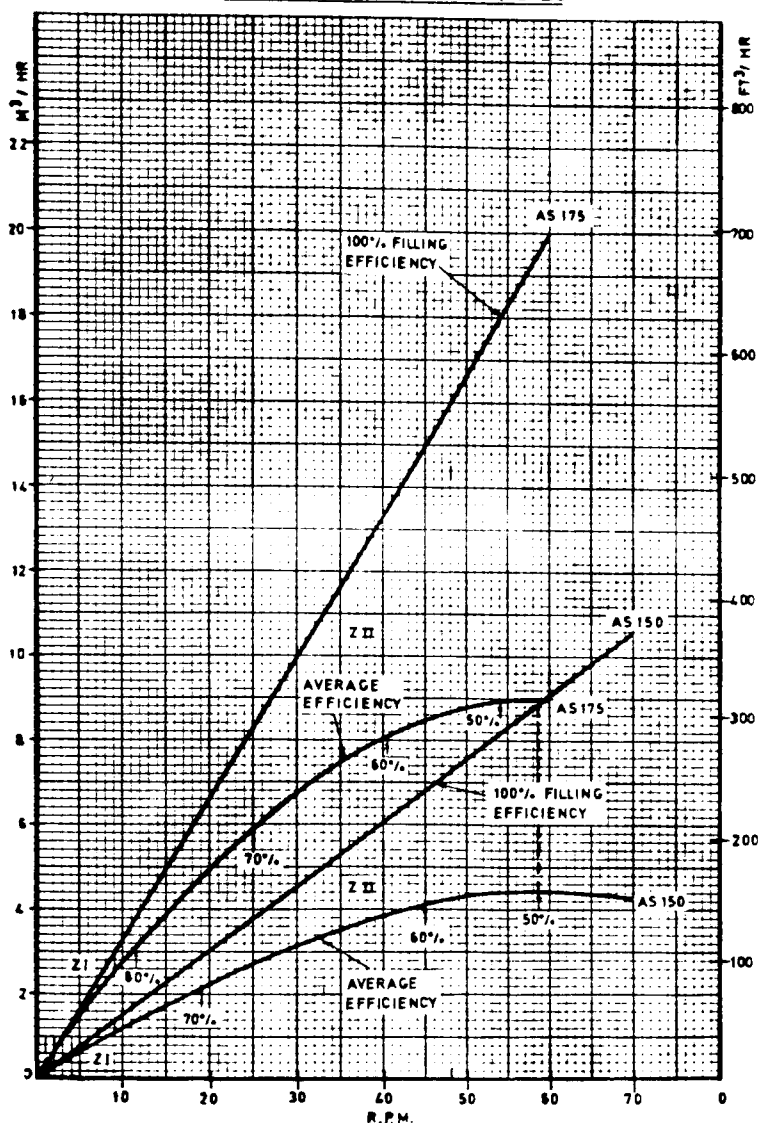
Figure 6.11   Performance characteristics published
by Westinghouse Systems Ltd
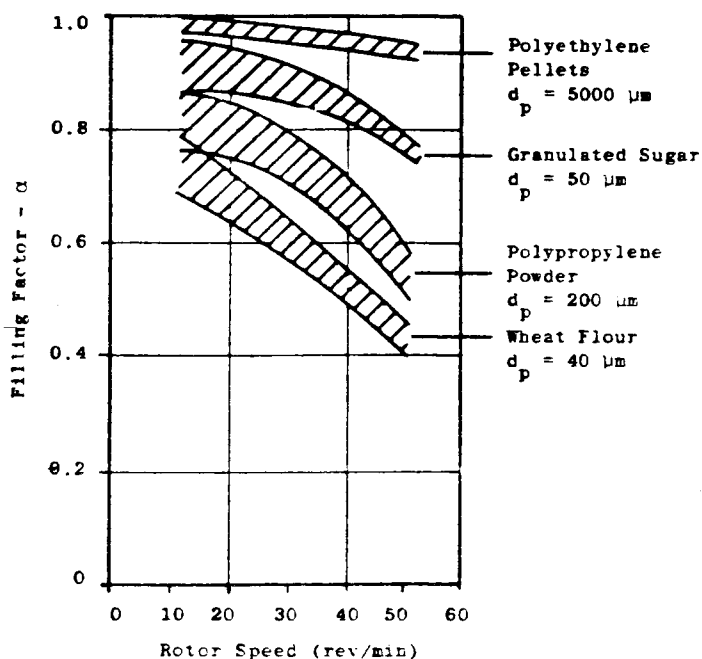
Figure 6.12   The relationship between the filling factor
and rotor speed for a range of materials as
obtained by Reed (11)
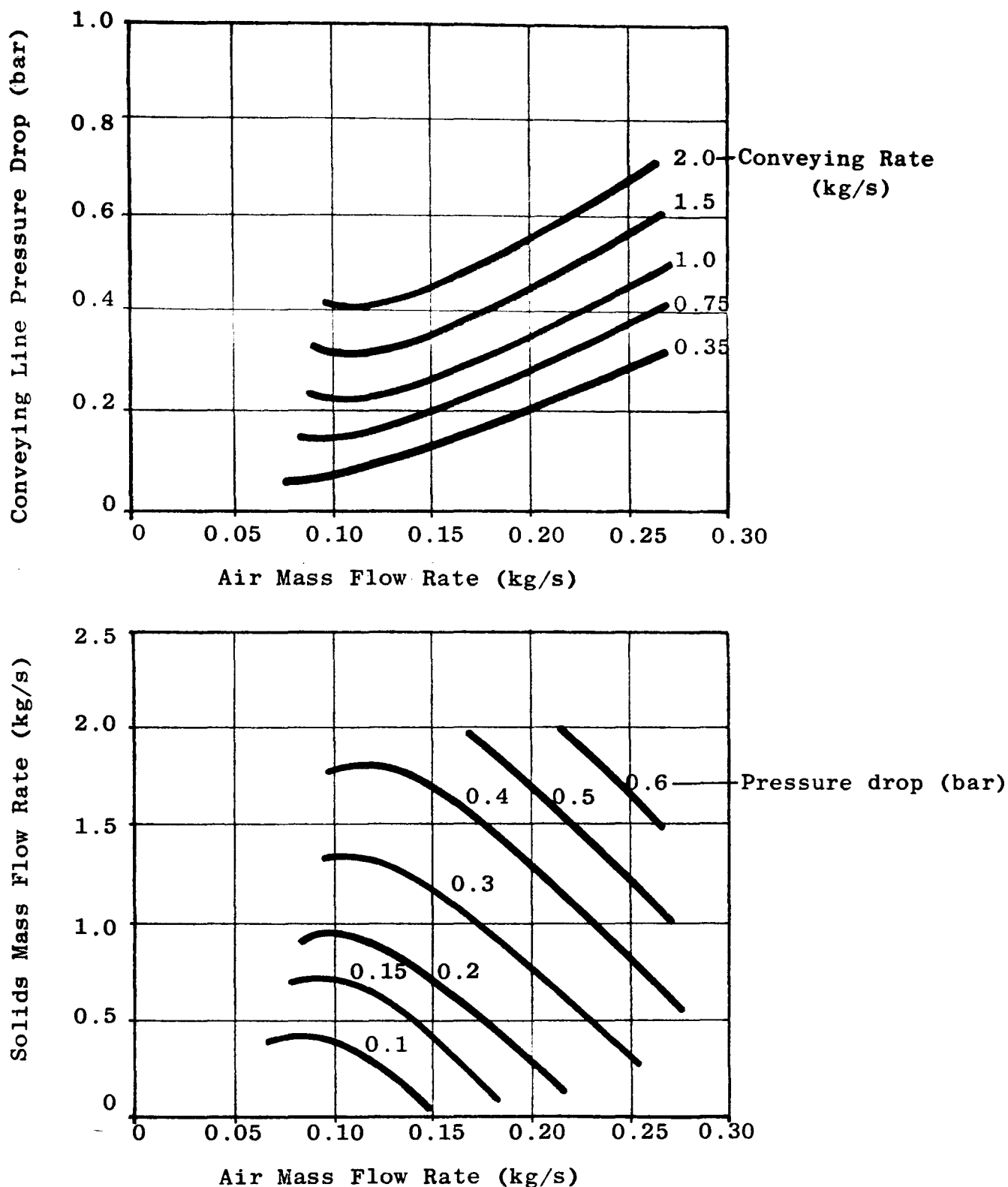
Figure 6.13   Conveying characteristics of polyethylene pellets
              as obtained from testwork using rotary valve
              research rig. Pipeline configuration :
              70 mm bore x 52 metre long x 6 bends
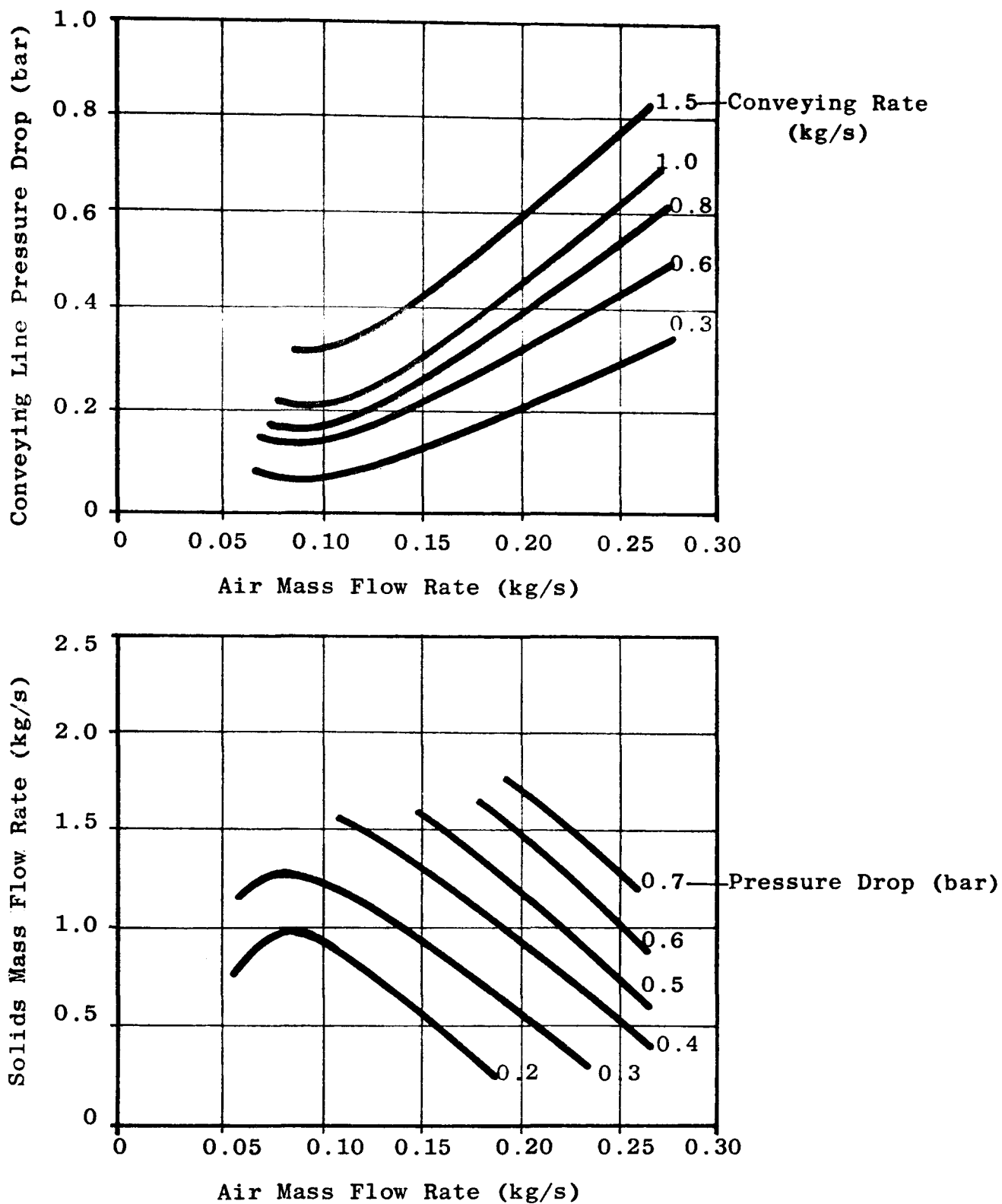
Figure 6.14   Conveying characteristics of polyethylene powder
as obtained from testwork using rotary valve
research rig.   Pipeline configuration :
70 mm bore x 52 metre long x 6 bends
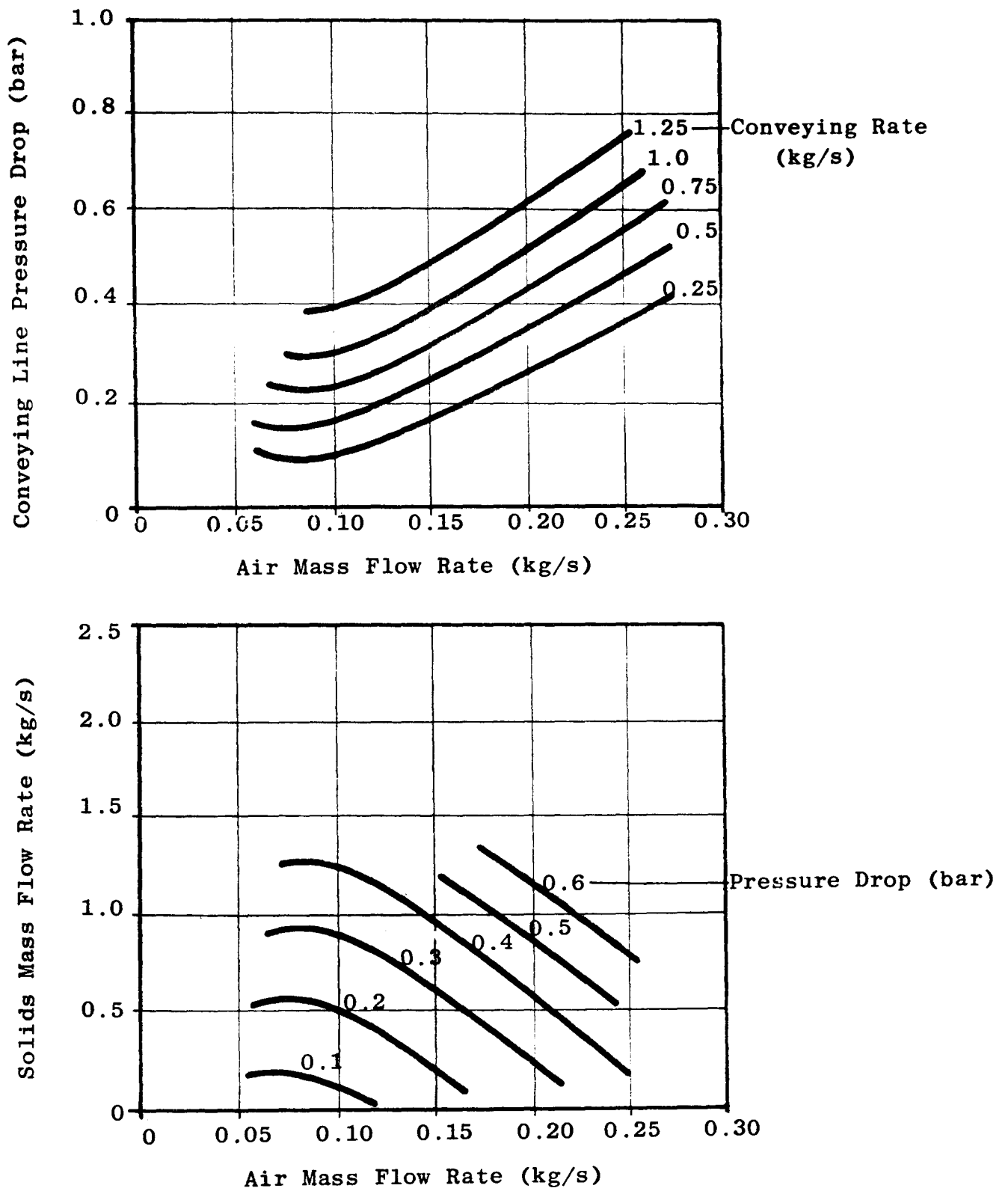
Figure 6.15　Conveying characteristics of 'Minaret' wheat
flour as obtained from testwork using rotary
valve rsearch rig.　Pipeline configuration :
70 mm bore x 52 metre long x 6 bends
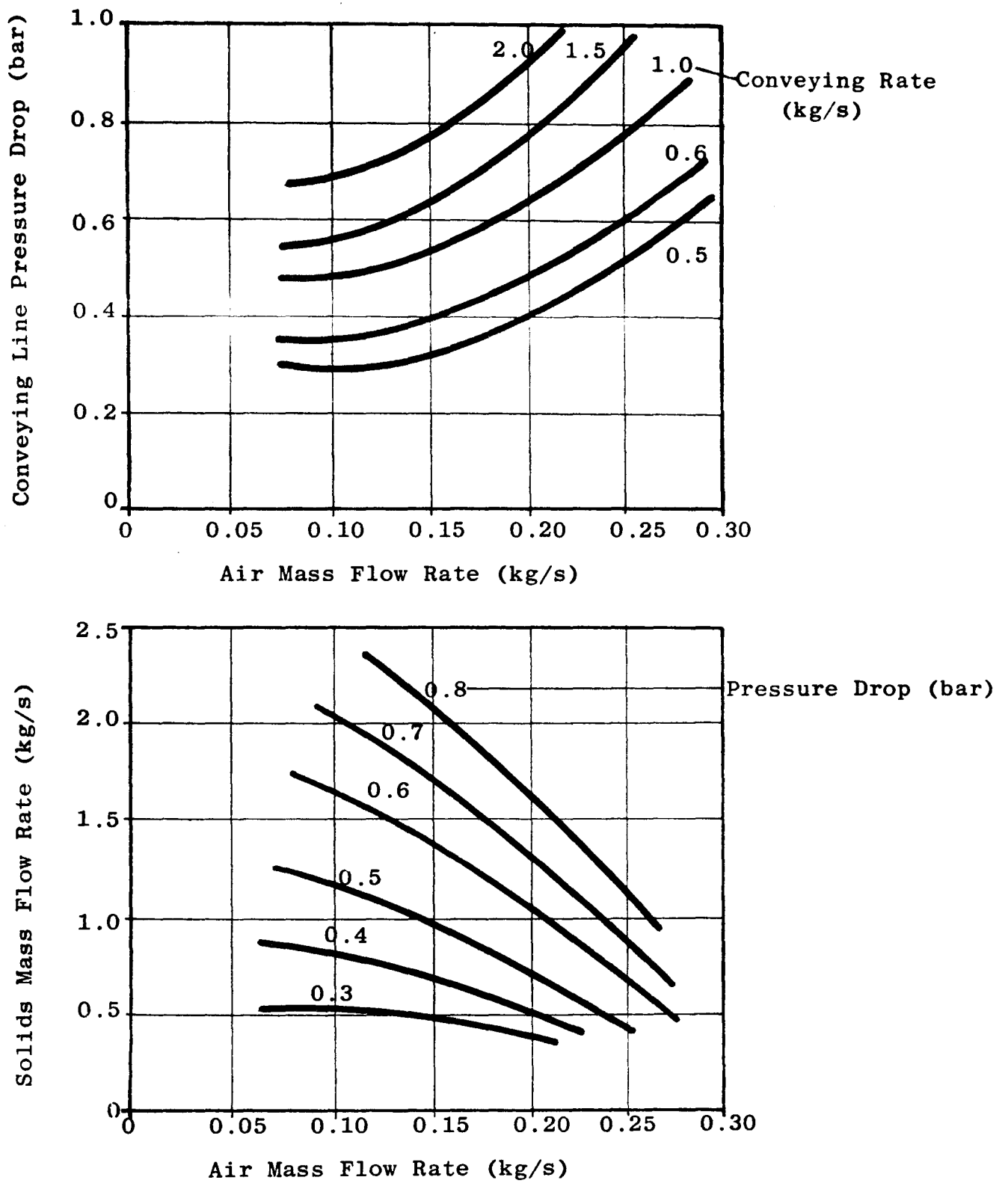
Figure 6.16   Conveying characteristics of ordinary portland
cement as obtained from testwork using rotary
valve research rig.   Pipeline configuration :
70 mm bore x 52 metre long x 6 bends
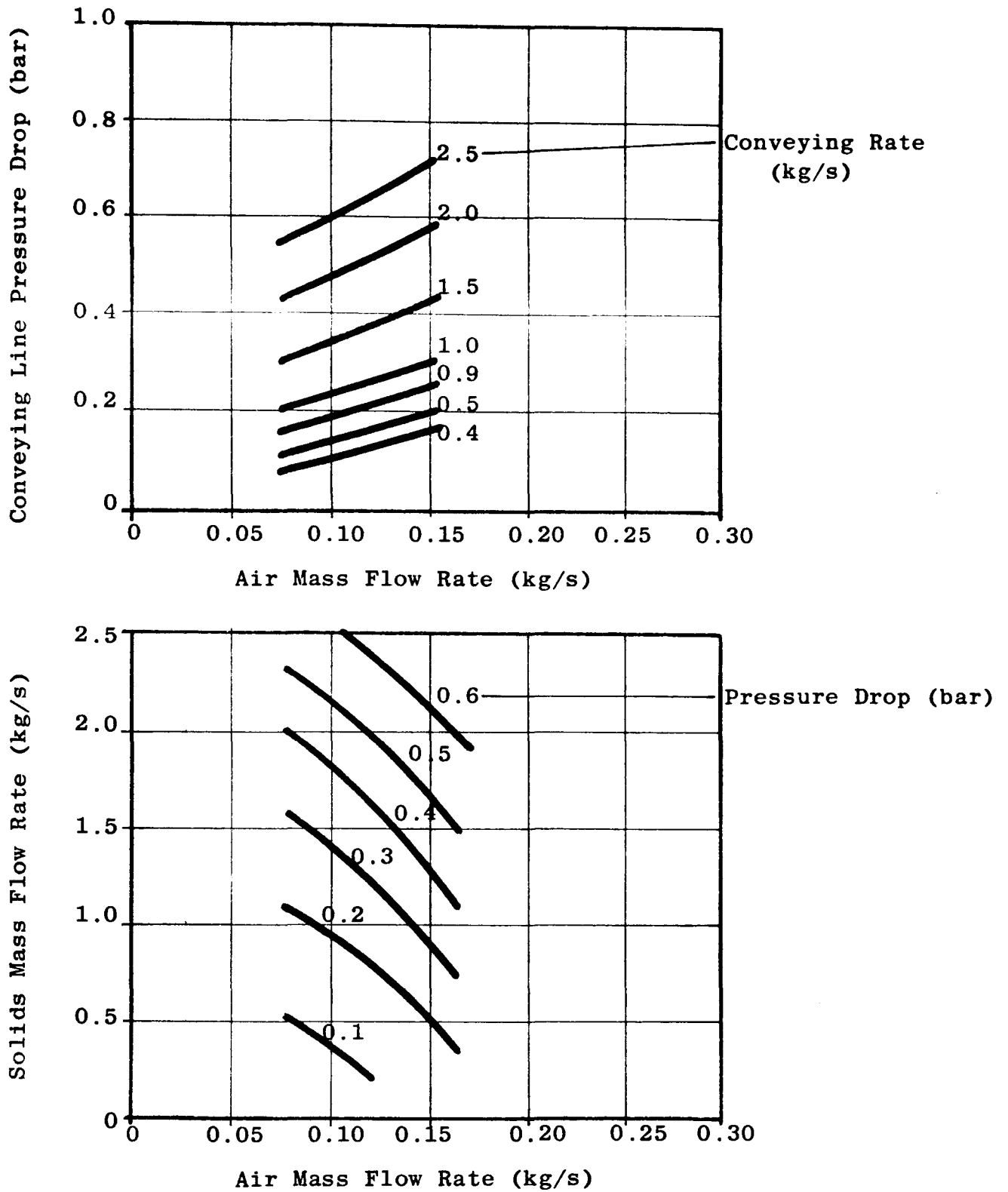
Figure 6.17   Conveying characteristics of singles coal as
              obtained from testwork using rotary valve
              research rig.   Pipeline configuration :
              70 mm bore x 52 metre long x 6 bends
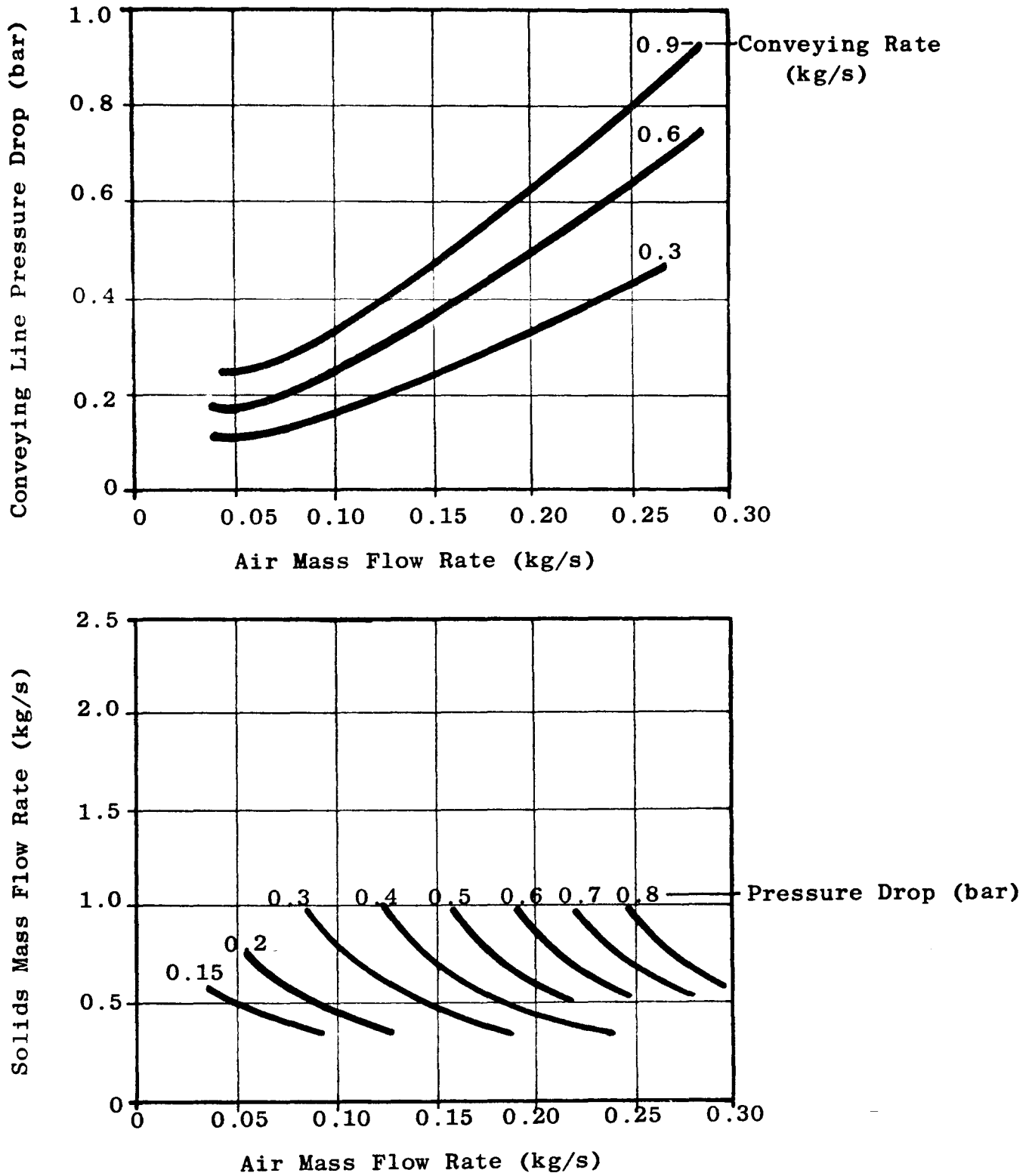
Figure 6.18   Conveying characteristics of pulverised coal as
              obtained in rotary valve research rig.
              Pipeline configuration : 70 mm bore x 52 metre long
              x 6 bends

CHAPTER SEVEN

EXPERIMENTAL STUDY

7.1 Introduction and Synopsis of Chapter

This chapter presents the results of the experimental work undertaken with the industrial sized rig described in Chapter 5. For the purpose of analysis the discussion of these results has been divided into five sections; each of which is concerned with one particular aspect of the interaction between rotary valves and pneumatic conveying pipelines.

Sections 7.2 to 7.4 discuss the performance of a system consisting of a conventional drop-through rotary valve and fabricated drop-out box. Section 7.2 looks specifically at rotary valve orientation and its effect on the material entrainment process. The purpose of this is to establish whether or not the orientation of the valve relative to the pipeline is an important parameter. The effects of changing the drop-out box size and shape are discussed in section 7.3. The results of this work are used to assess the validity of the model proposed in Chapter 4 for estimating the entrainment efficiency of a given rotary valve and drop-out box combination. An investigation of the choked flow condition is discussed in section 7.4. This confirms the relationship between choking and the conveying air velocity and compares the predicted and actual results.

An investigation into the performance of the blow-through type of rotary valve is described in section 7.5. This compares the performance of a blow-through valve with that of a conventional drop-through type of similar internal dimensions and shows that, for the range of materials and conveying conditions that were examined, the performance of the blowing seal was at least as good as and generally better than that of the drop-through type of rotary valve.

Air leakage and its effect on rotary valve performance are
discussed in section 7.6.   Evidence is presented which indicates that,
for a given pressure ratio, the air leakage through a rotary valve used
to feed a pneumatic conveying line is less than that through a valve
which is used to feed a simple pressurised container.

7.2   Rotary Valve Orientation

7.2.1   Purpose of Experiments

The purpose of this work was to obtain experimental data to enable the
effect of rotary valve orientation on the material entrainment process
to be investigated.   The objective was to determine whether or not
there is an 'optimum' orientation and, if so, whether the difference
in performance between this and other orientations is significant.   The
work was a development from that undertaken with the flow visualisation
rig which had indicated that orientation may be significant.

7.2.2   Experimental Plan and Method

The experimental plan was to examine the performance of the conveying
systems with the rotary valve mounted in the three different orientations
shown in Figure 7.1.   These are the orientations which are most commonly
used in industry and are the three most different arrangements which can
be obtained with a conventional rotary valve and drop-out box.   In
each case the drop-out box used was a simple transition section two
pipe diameters in depth, as shown in Figure 7.2.   The primary reason
for using this drop-out box was that it is typical of the most common
type in current industrial use and therefore of immediate practical
interest.   Also, the use of such a box gives a relatively short
entrainment configuration.   This last point is important because if the
orientation of the valve does have a significant effect on the entrainment
process, then it is reasonable to expect that this will be
most noticeable in configurations where the valve discharge port and
the conveying pipeline are in close proximity to one another.   The
flow visualisation work discussed in Chapter 3 provided some evidence
to support this reasoning.

The initial experiments were conducted using the Polyethylene
Pellets and the Wheat Flour as the test products.   These are,
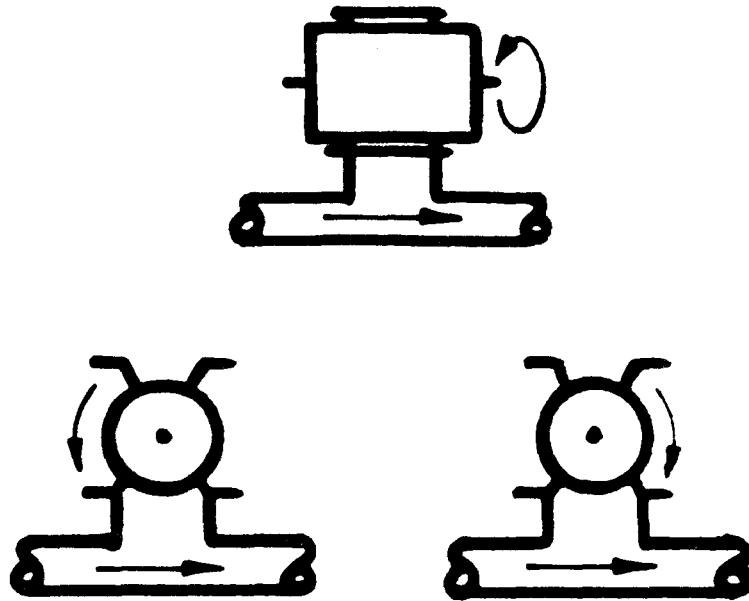
Figure 7.1 The Three Basic Rotary Valve Orientations
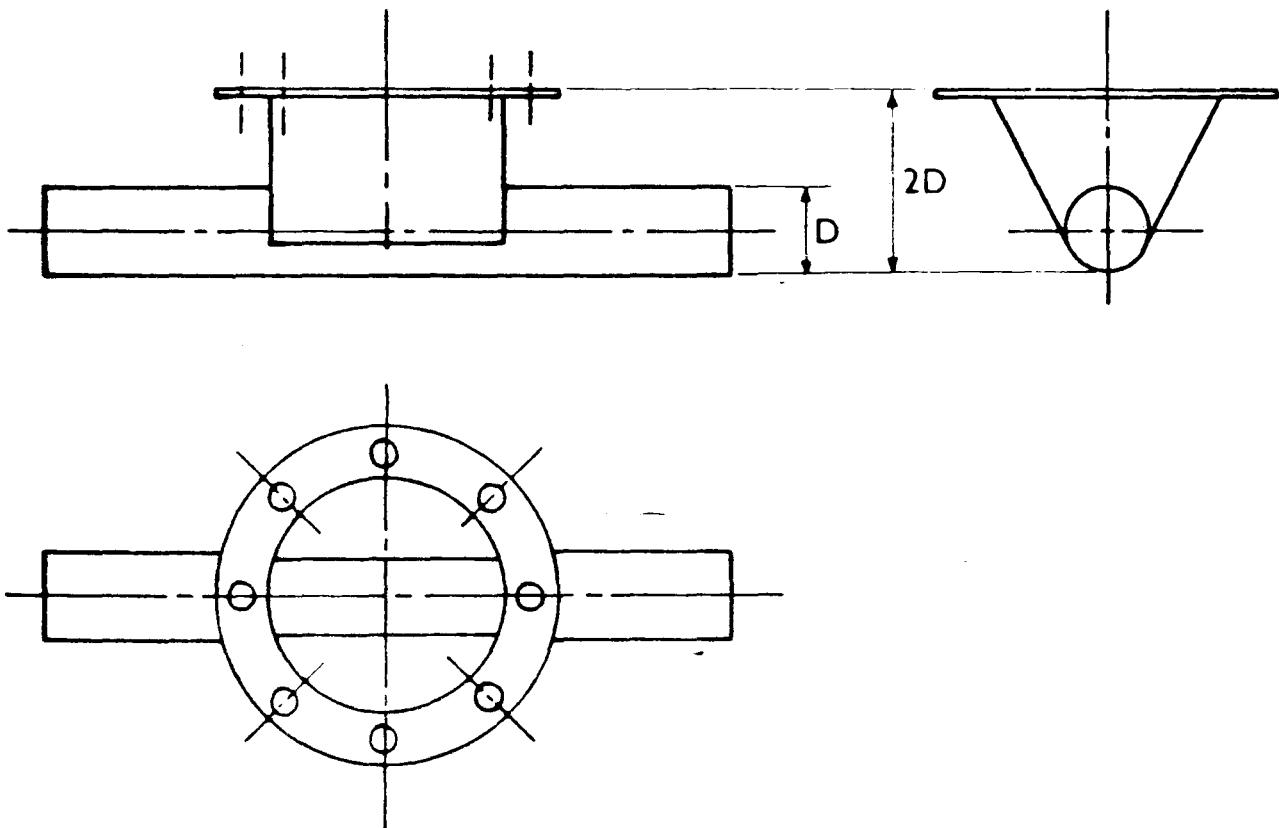
Figure 7.2 Typical Drop-Out Box Two Pipe Diameters
in Depth.

respectively, the most free-flowing and the most cohesive of the six selected test materials.   Consequently, it was argued that experiments using these two materials would indicate the range of performances to be expected.   Then, on the basis of the results obtained from these experiments, a judgement could be made whether or not to include any of the other four materials in this part of the experimental programme. As a result only one other material was tested in all three orientations. This was the Polyethylene Powder.

The actual experimental method used was that outlined in Chapter 6. This enabled a complete set of data to be obtained for the envelope of conveying conditions which are indicated on the conveying characteristics shown in Figures 6.13, 6.14 and 6.15.

7.2.3 Results

The experimental results obtained from following the plan described in section 7.2.2 are presented in Figures 7.3 to 7.14.   Each of these figures consists of two graphs.   The upper graph shows the relationship between the measured solids mass feed rate ($\dot{m}_s$) and the valve rotor speed (n) and was derived from the raw data.

The lower graph shows the relationship between the feeding factor (γ) and the valve rotor speed (n).   The feeding factor indicates the overall effectiveness with which material is fed into the conveying line and this can be used to compare the performance of different feeding/ entrainment configurations.-   It is obtained by dividing the actual volumetric feed rate of solids, based upon the poured bulk density of the material, by the maximum theoretical volumetric throughput of the valve, that is:

$$\gamma \; = \; \frac{60 \dot{V}_s}{n V_o} \tag{7.1}$$

To provide a simple quantitative means of comparing the experimental results obtained with the three rotary valve orientations, the arithmetic mean of the ffeding factor ($\bar{\gamma}$) and the standard deviation

of the experimental points about this mean (σ_γ) were calculated. The appropriate values of $\overline{\gamma}$ and σ_γ for each combination of valve orientation and test material are given in Figures 7.3 to 7.14.

Figures 7.3 to 7.5 show the results obtained for the Polyethylene Pellets which each of the three rotary valve orientations. Figure 7.6 then compares these on one diagram. A similar set of results for the Wheat Flour are shown in Figures 7.7 to 7.10 and for the Polyethylene Powder in Figures 7.11 to 7.14. The analysis and discussion of these results is given in the following section.

7.2.4 Analysis and Discussion of Results

Figures 7.3 to 7.6 present the experimental results which were obtained with the Polyethylene Pellets. These show that the ability of the rotary valve to feed material into the conveying system was, in all practical respects, identical for each of the three orientations. Also, for the range of rotor speeds and conveying conditions which were examined, the solids throughput was approximately the same as the theoretical maximum based upon the volumetric capacity of the rotor pockets and the poured bulk density of the Polyethylene Pellets. In one respect this last result is not surprising because the Polyethylene Pellets are very free flowing, however, compared with the results obtained by Reed (11) for a similar grade of polyethylene[*], the performance was slightly better than might have been expected, see Figure 7.6. It seems reasonable to propose that the disagreement between the two sets of results is due to the differences between the two rigs. The most significant of these differences being that in the present rig the rotary valve interfaces with a pneumatic conveying line, whereas in the rig used by Reed the rotary valve interfaced with a pressurised weighing vessel. This implies that the comparatively better performance of the current rig is a consequence of the interaction between the rotary valve and the conveying line. This would be consistent with the argument expressed in Chapter 2[**], that below the critical rotor speed it is the pocket discharge process which limits the performance of a rotary valve.

---

* footnote: 5.5 mm pellets

** footnote: See section 2.3 of Chapter 2; comparison of the work of
                Reed (11) and Masuda et Al (20)

Furthermore, it would appear that in the case of the Polyethylene Pellets the interaction between the rotary valve and the conveying line has a positive effect on the pocket discharge process.

The experimental results forthe Wheat Flour are shown in Figures 7.7 to 7.10. As with the results for the Polyethylene Pellets, these do not show a clearly identifiable difference between the performance of the system with each of the three rotary valve orientations. This similarity between the results is significant because of the very different characteristics of the Wheat Flour and Polyethylene Pellets. This implies that the effect of rotary valve orientation on system performance is not likely to be significant for most materials. In order to confirm this implication a further series of experiments were conducted with Polyethylene Powder. The results which were subsequently obtained are shown in Figures 7.11 to 7.14 and these confirm that the effect of valve orientation on system performance is negligible.

Further evidence to support this conclusion is given in the previously quoted paper of Mosemand & Bird (22), who examined the performance of a rotary valve system handling Polypropylene Powder. They reported that no perceptive change in throughput could be obtained by changing the rotary valve orientation. Furthermore, they also showed that this was the case for three different designs of drop-out box, see Figure 2.28 boxes A, B and C.

7.3 The Size and Shape of the Drop-out Box

7.3.1 Purpose of Experiments

The purpose of this part of the experimental programme was to investigate the effect of the size and shape of the drop-out box on the entrainment process. The intention was to determine whether or not these are significant parameters with regard to entrainment and, if so, to quantity their effect. Also, it was reasoned that this would provide data with which to assess the ideas and model proposed in Chapter 4 for estimating the volumetric entrainment efficiency (η_e) of a given combination of rotary valve and drop-out boxes. This model proposed that
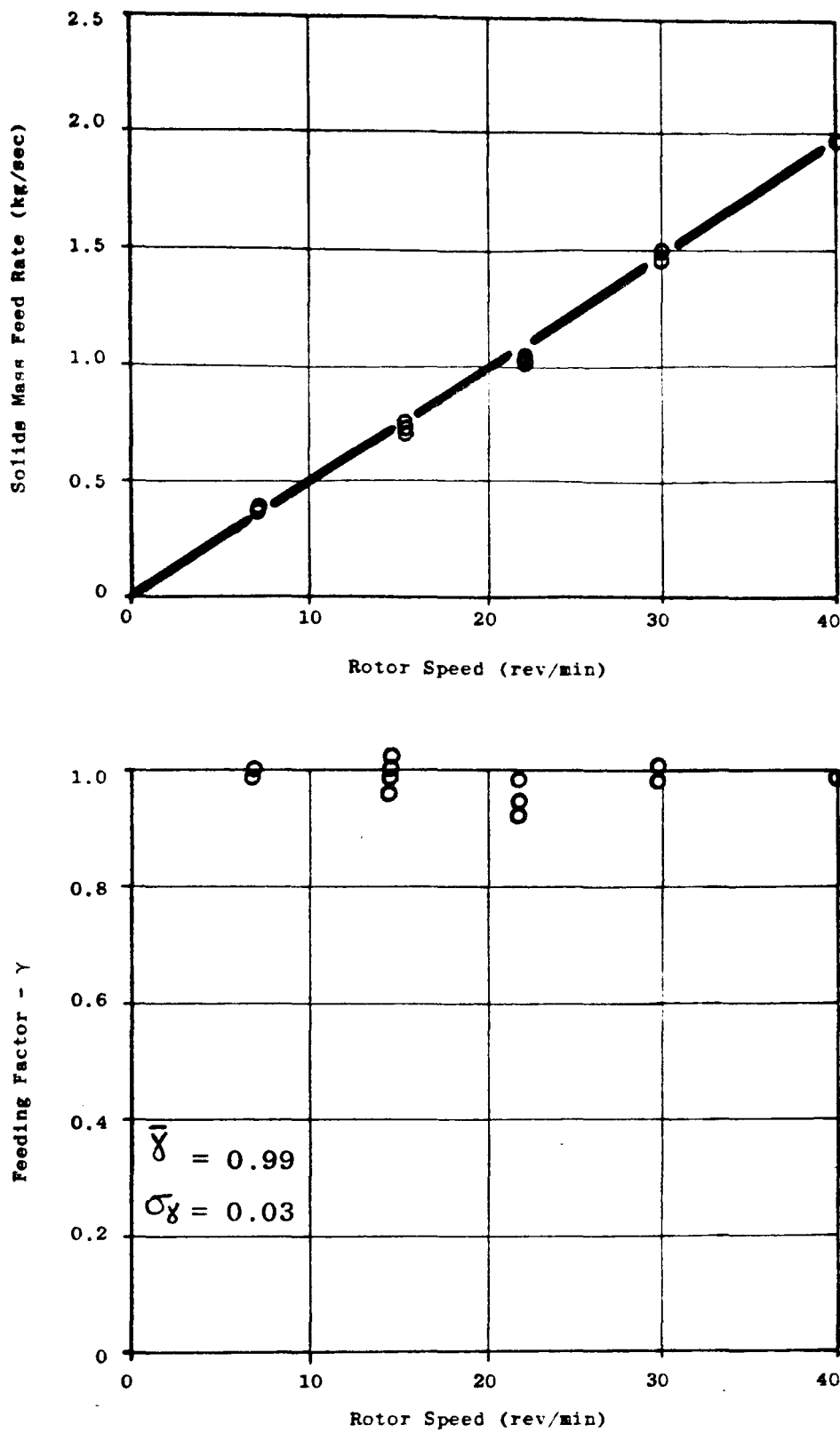
Figure 7.3   Feeding Characteristics of Polyethylene Pellets
             with Drop-Out Box B and Rotary Valve Orientation a.
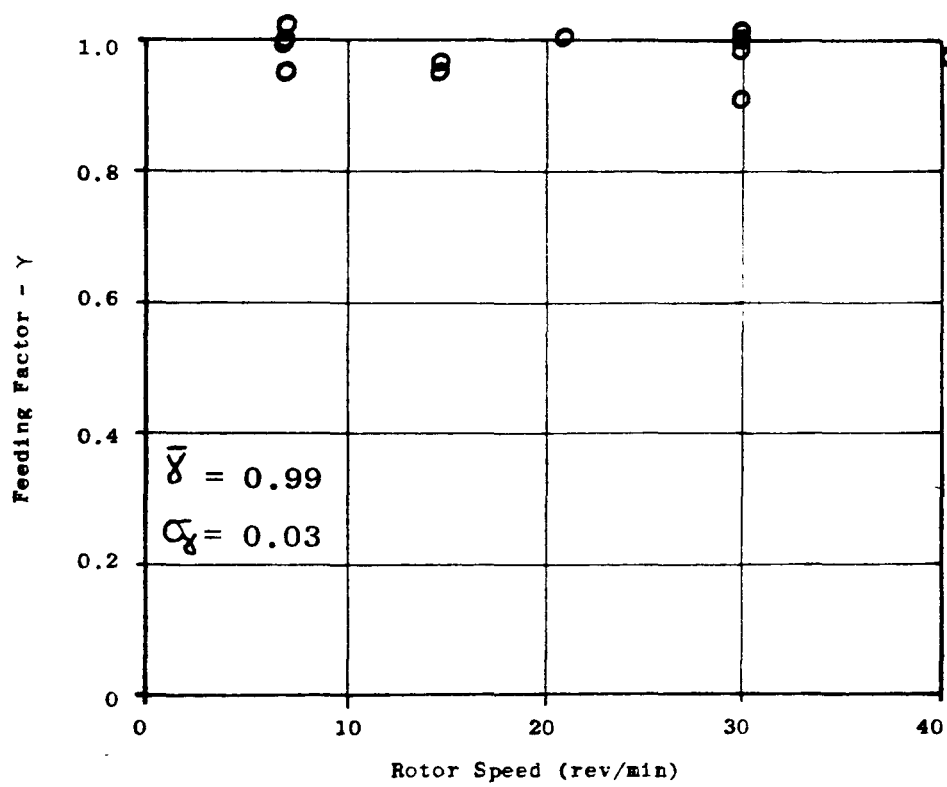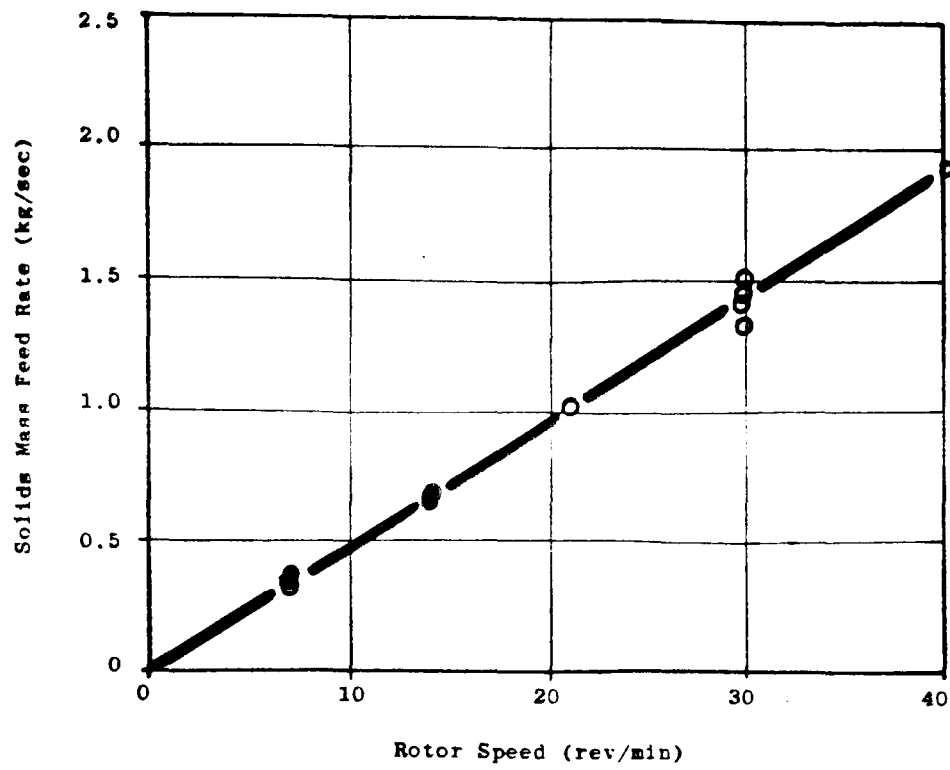
Figure 7.4 Feeding Characteristics of Polyethlene Pellets
with Drop-Out Box B and Rotary Valve Orientation b.
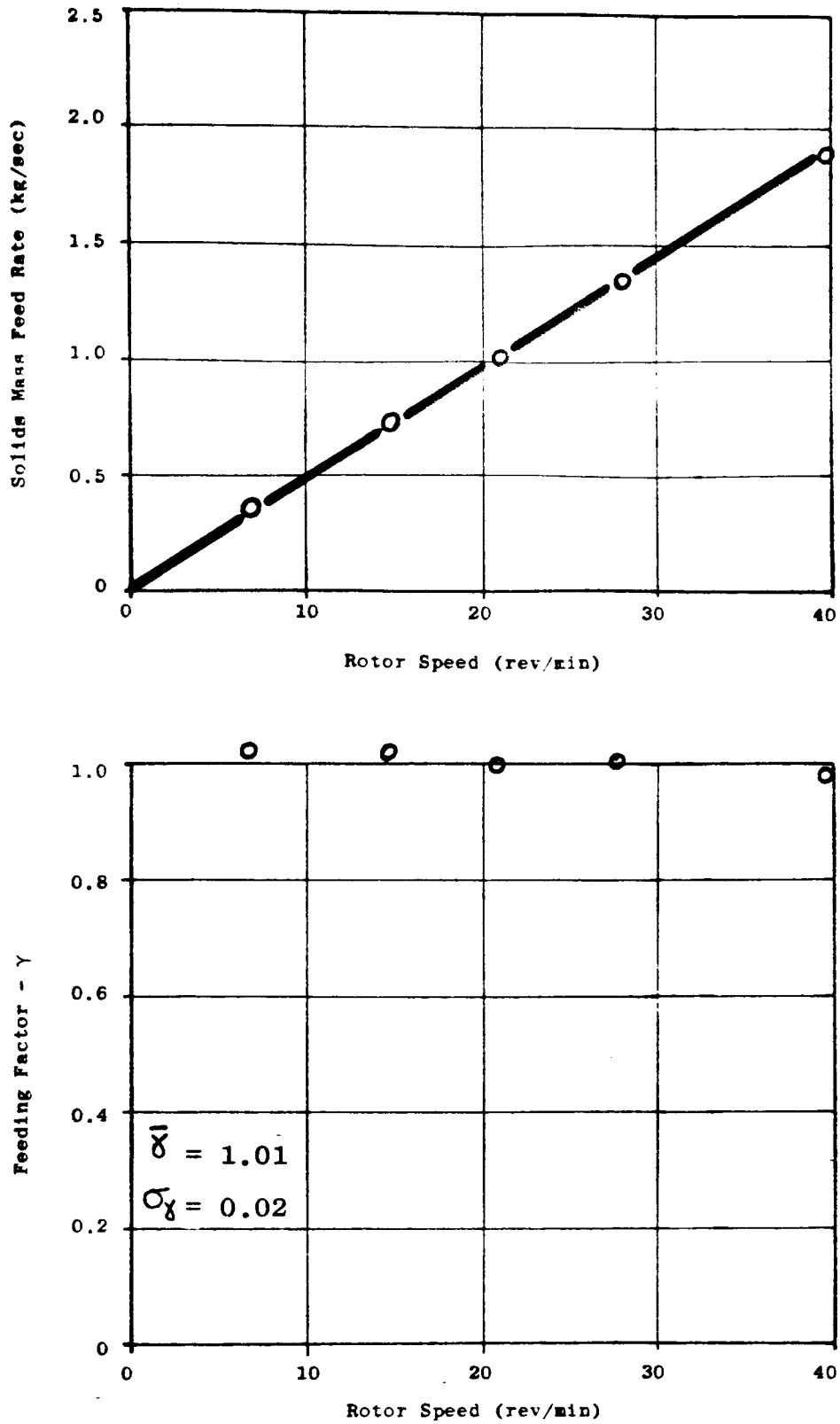
Figure 7.5 Feeding Characteristics of Polyethlene Pellets with Drop-Out Box B and Rotary Valve Orientation c.
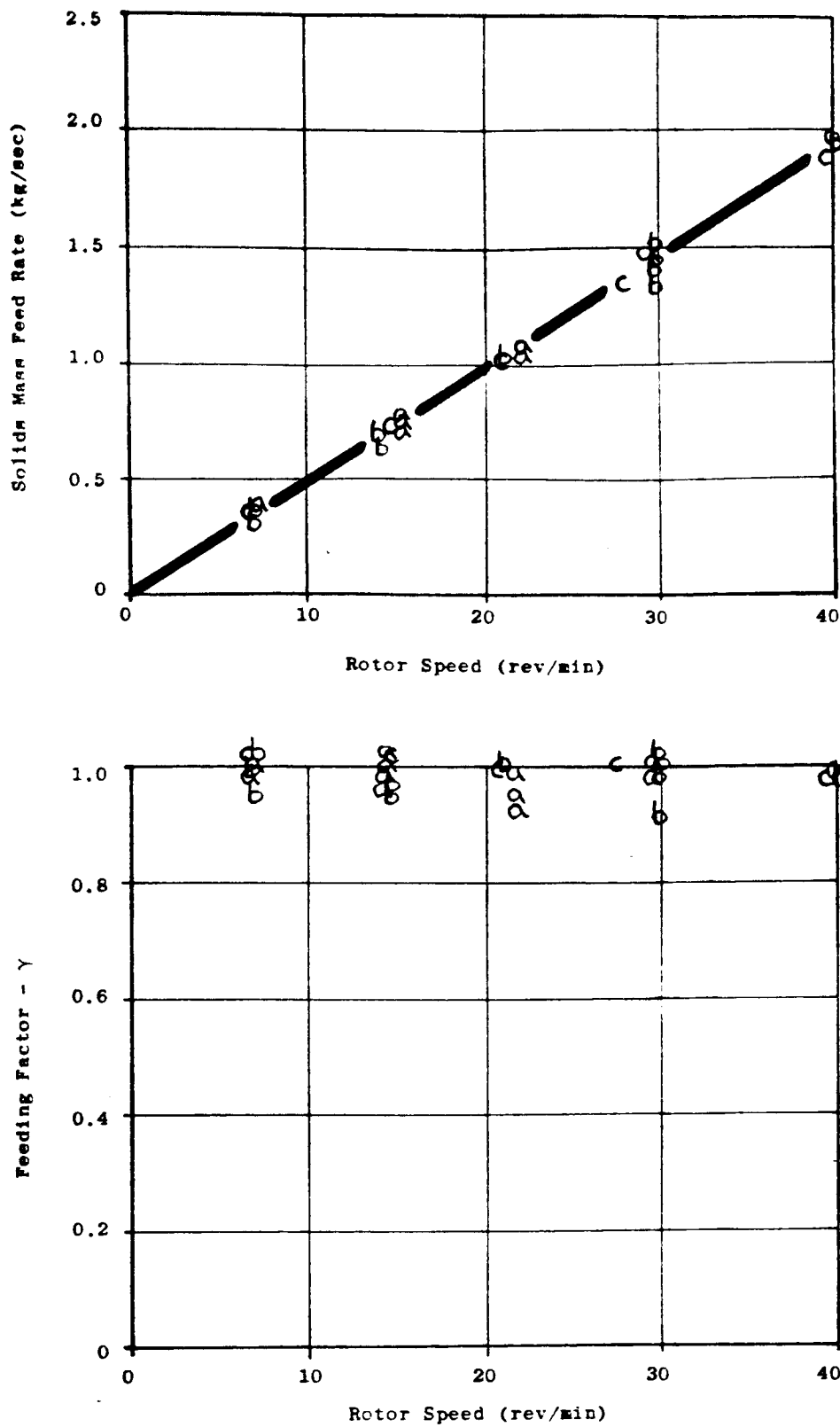
Figure 7.6   Feeding Characteristics of Polyethylene Pellets.
Comparison of results obtained with Drop-Out Box
B and Rotary Valve Orientations a, b and c.
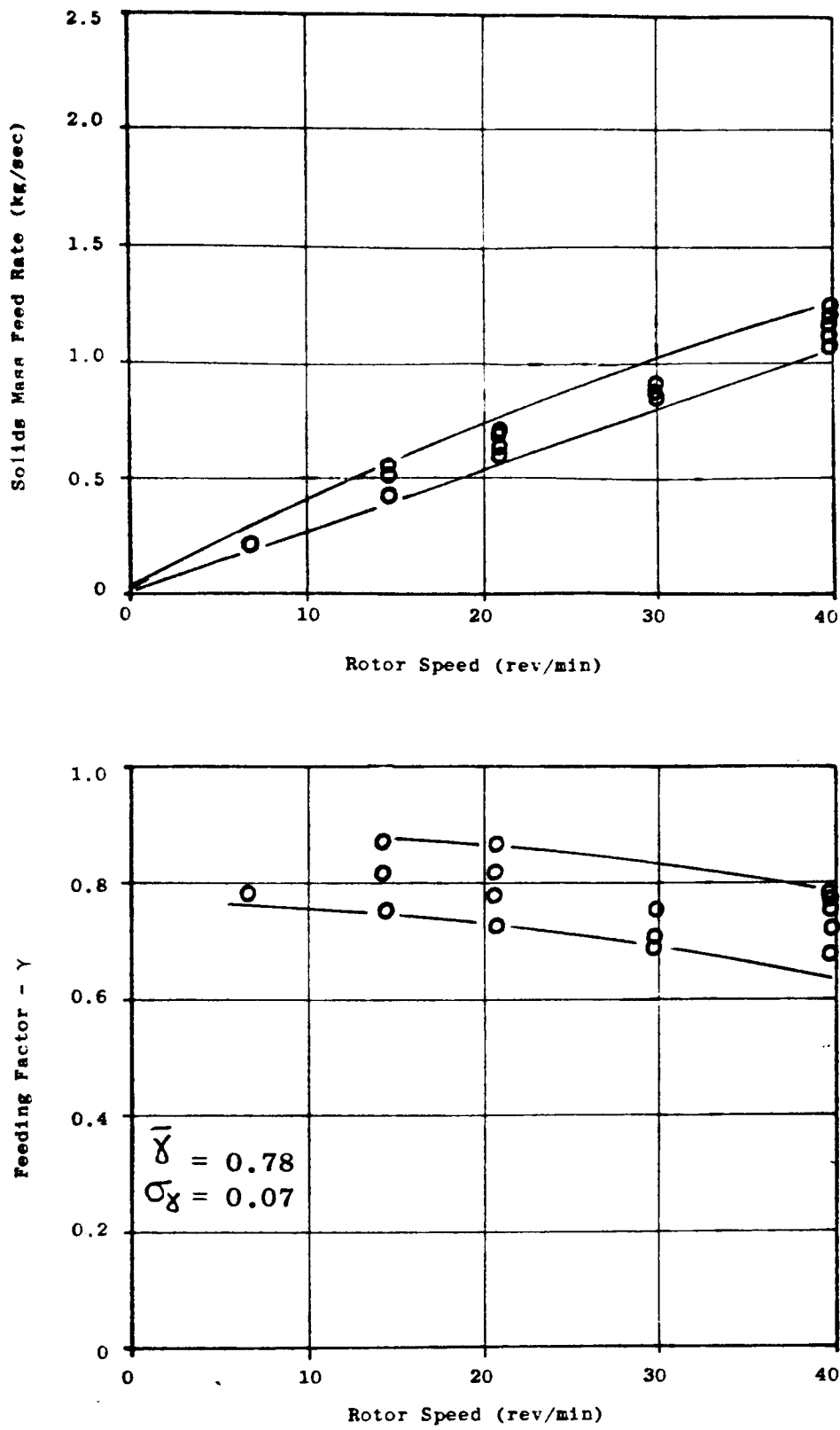
Figure 7.7 Feeding Characteristics of Wheat Flour
         with Drop-Out Box B and Rotary Valve Orientation a.
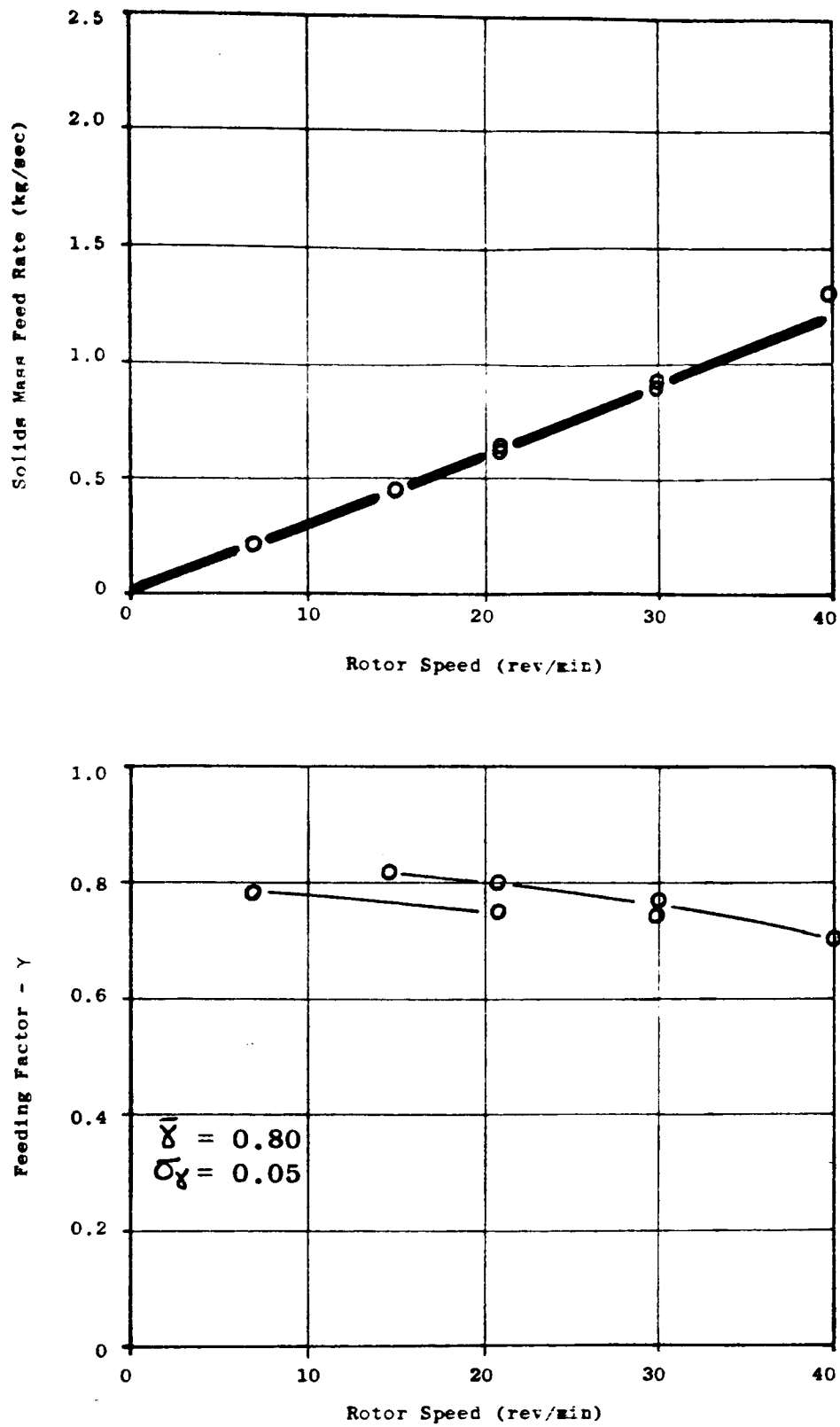
Figure 7.8   Feeding Characteristics of Wheat Flour
              with Drop-Out Box B and Rotary Valve Orientation b .
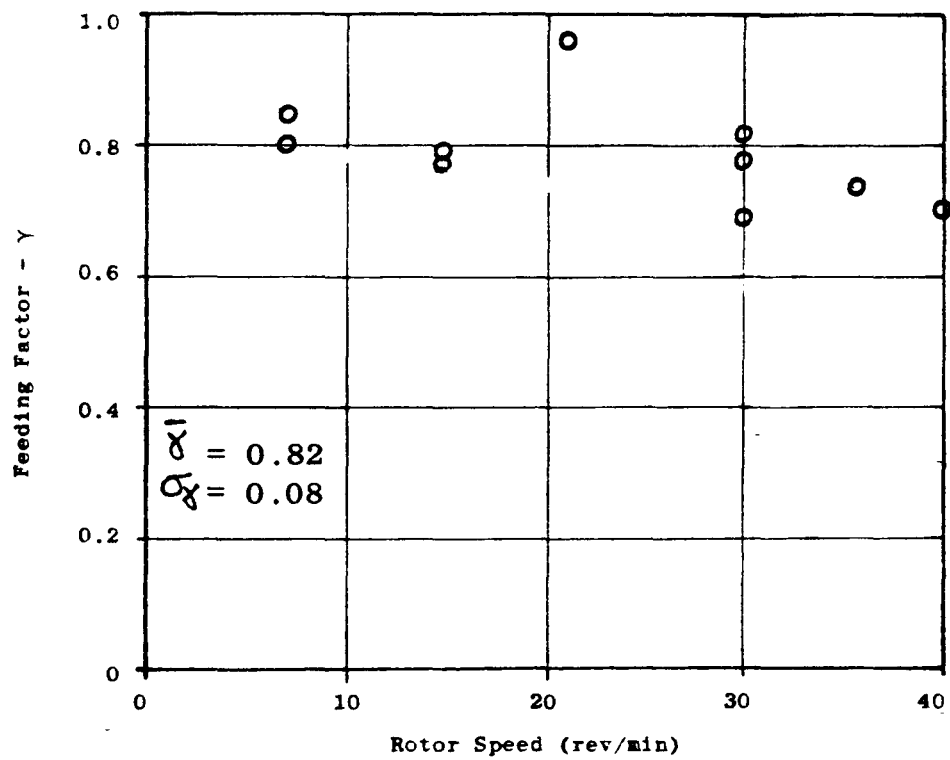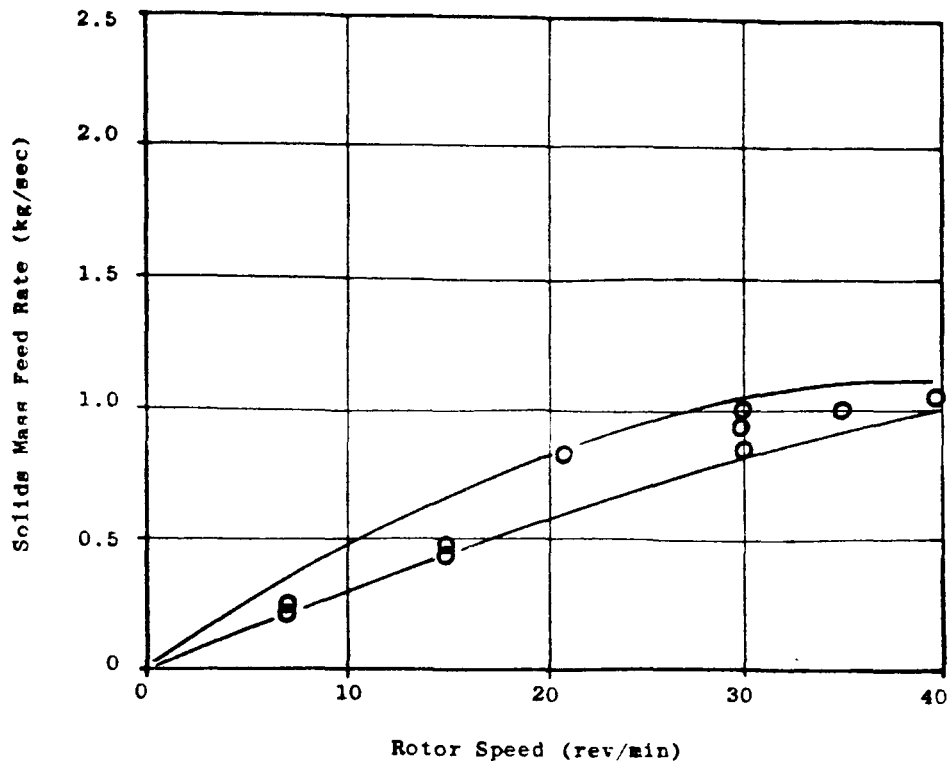
Figure 7.9 Feeding Characteristics of Wheat Flour
with Drop-Out Box B and Rotary Valve Orientation c.
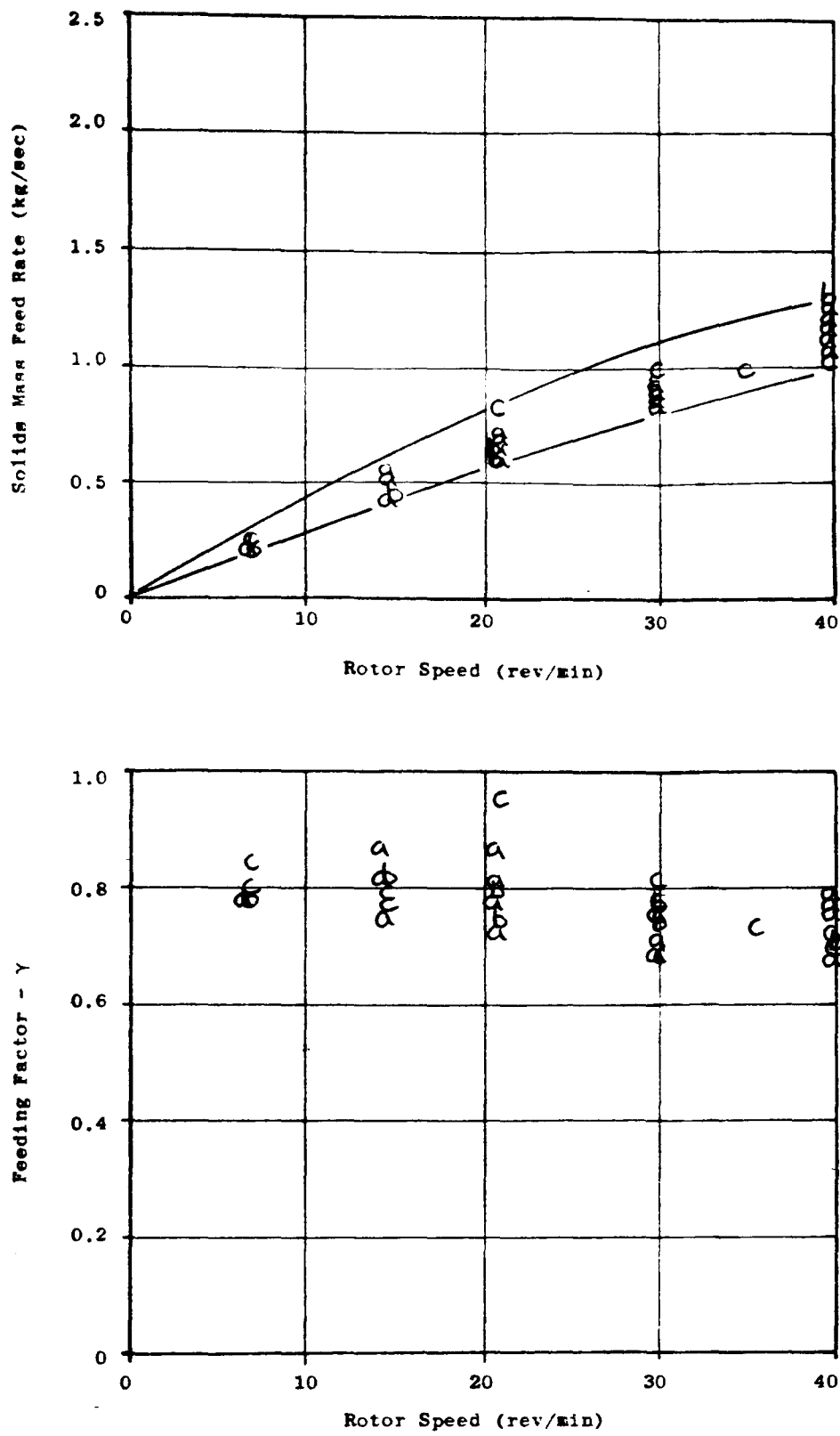
Figure 7.10 Feeding Characteristics of Wheat Flour.
Comparison of results obtained with Drop-Out Box
B and Rotary Valve Orientations a, b and c.
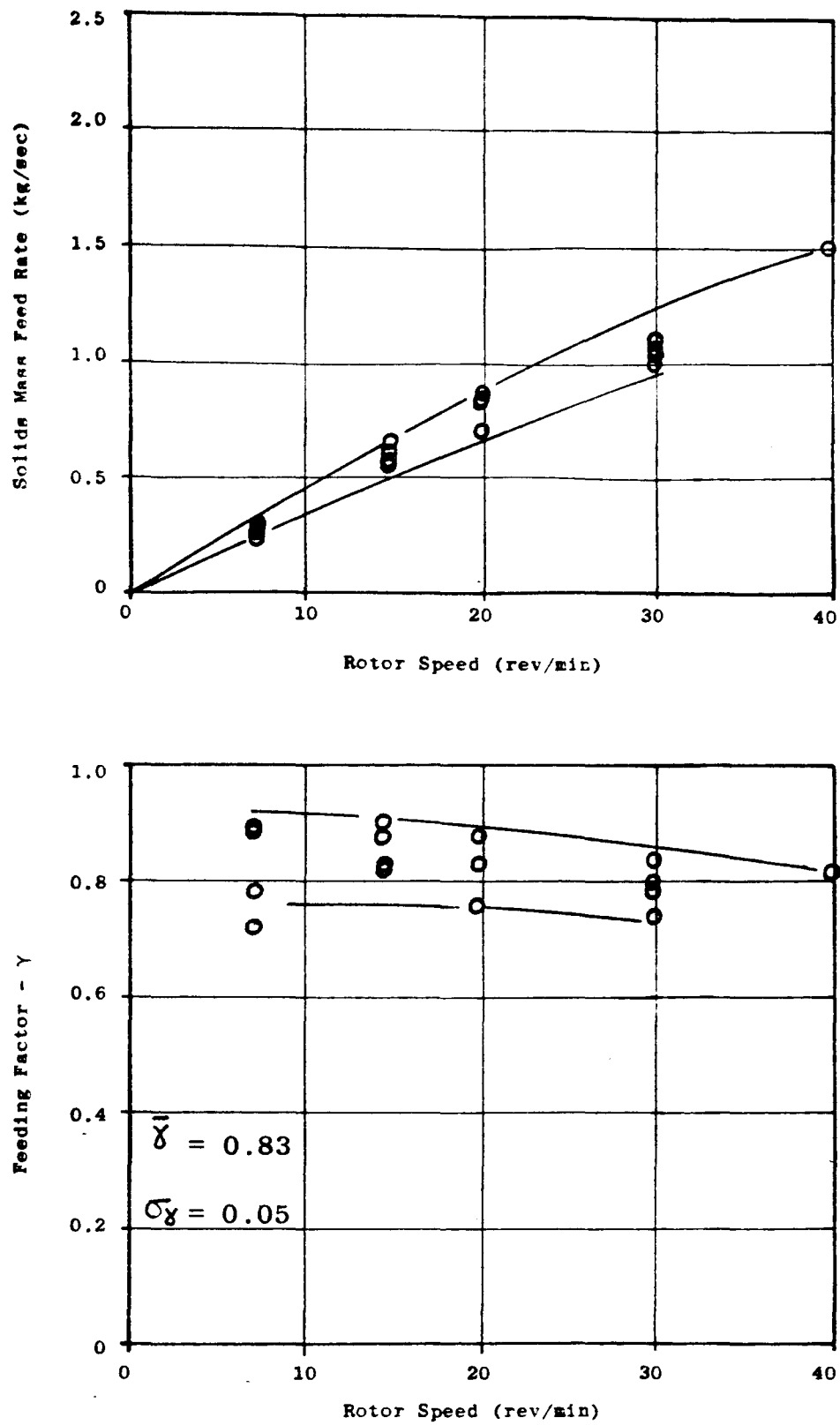
Figure 7.11 Feeding Characteristics of Polyethylene Powder
with Drop-Out Box B and Rotary Valve Orientation a.
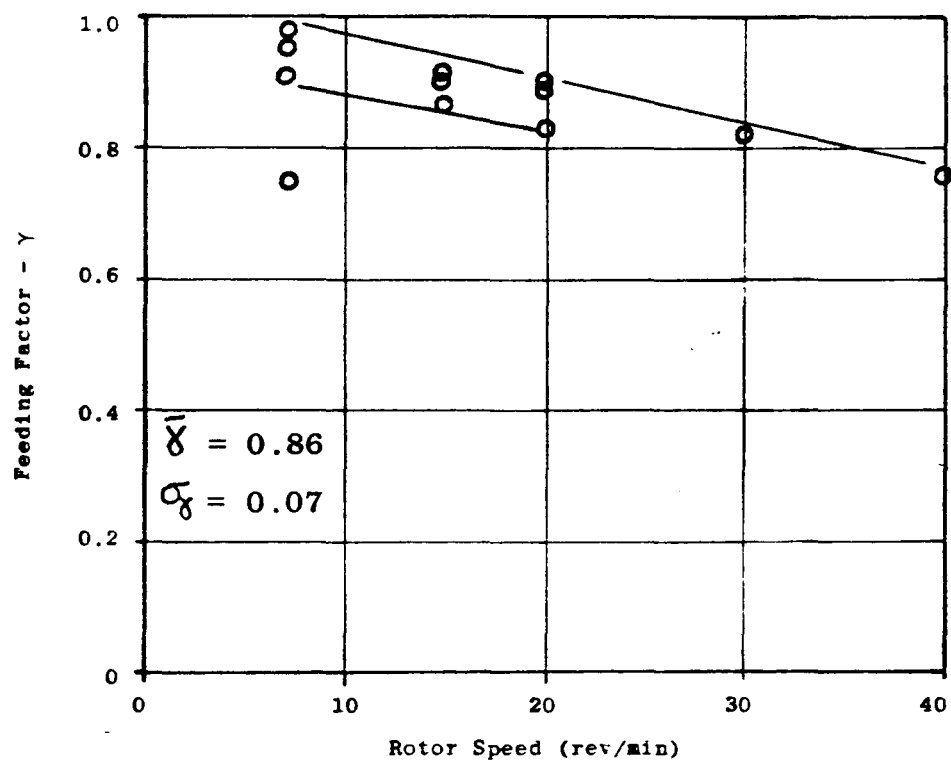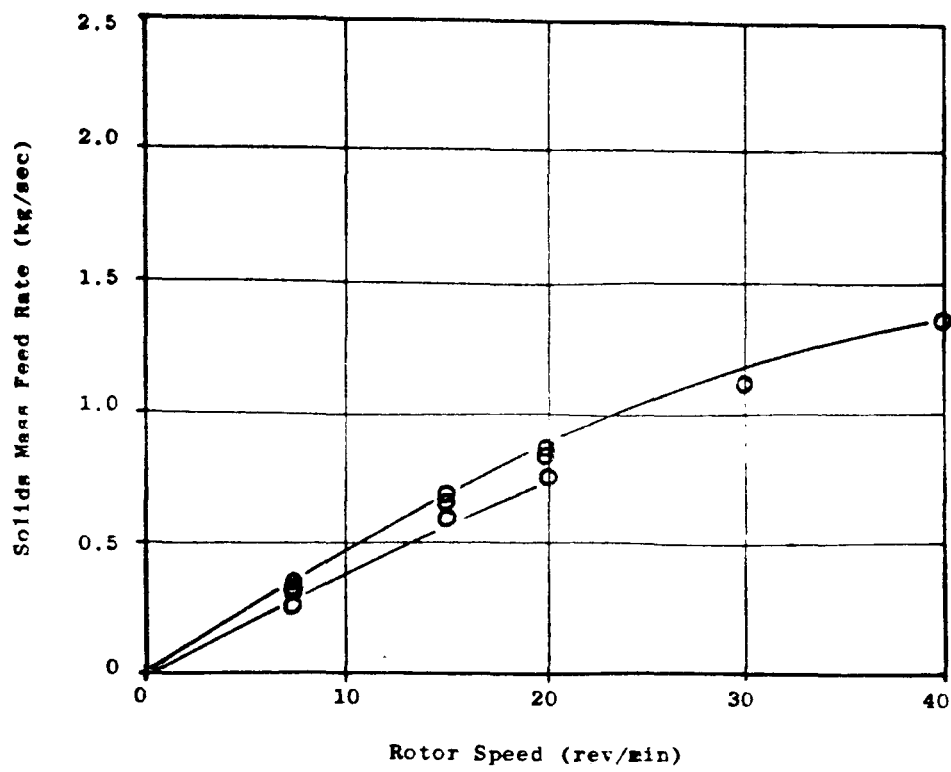
Figure 7.12　Feeding Characteristics of Polyethylene Powder
with Drop-Out Box B and Rotary Valve Orientation b.
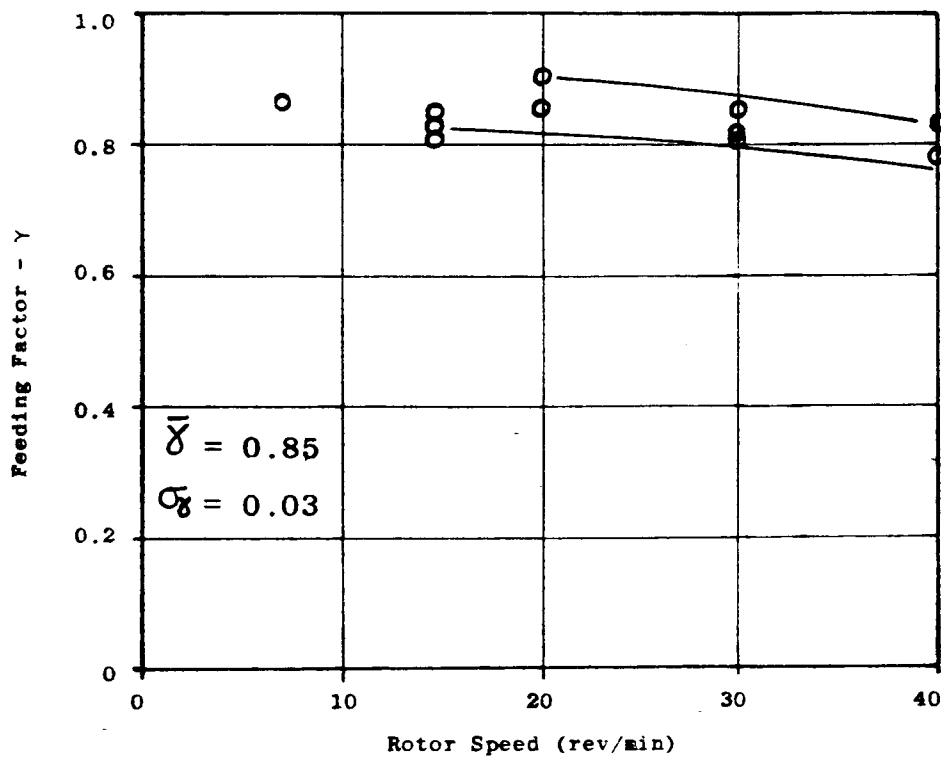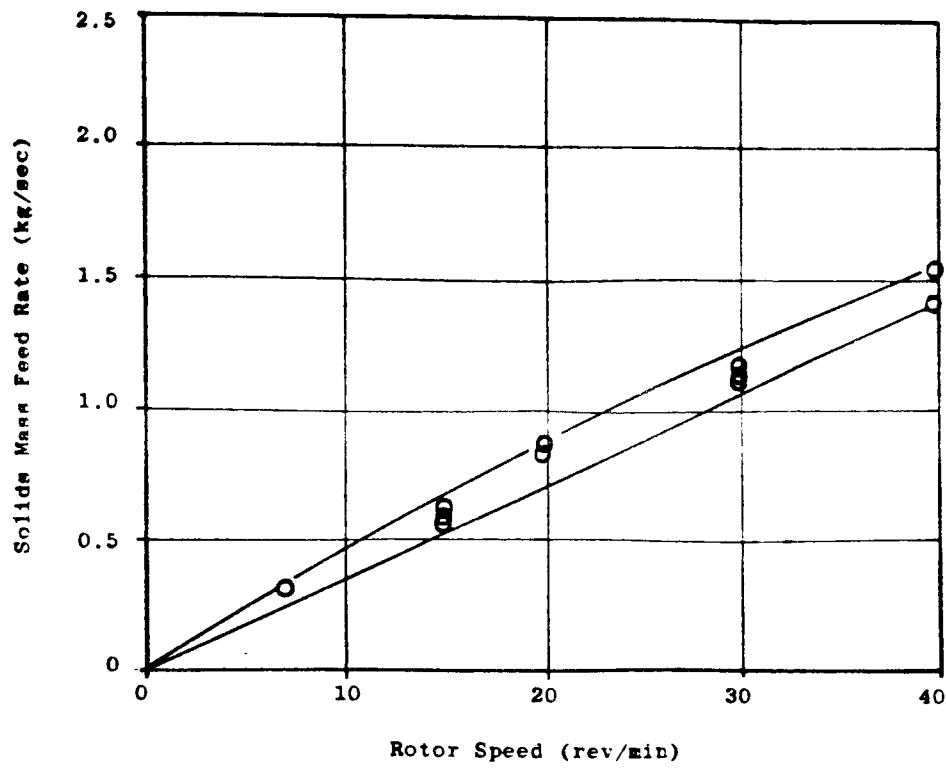
Figure 7.13 Feeding Characteristics of Polyethylene Powder
with Drop-Out Box B and Rotary Valve Orientation c.
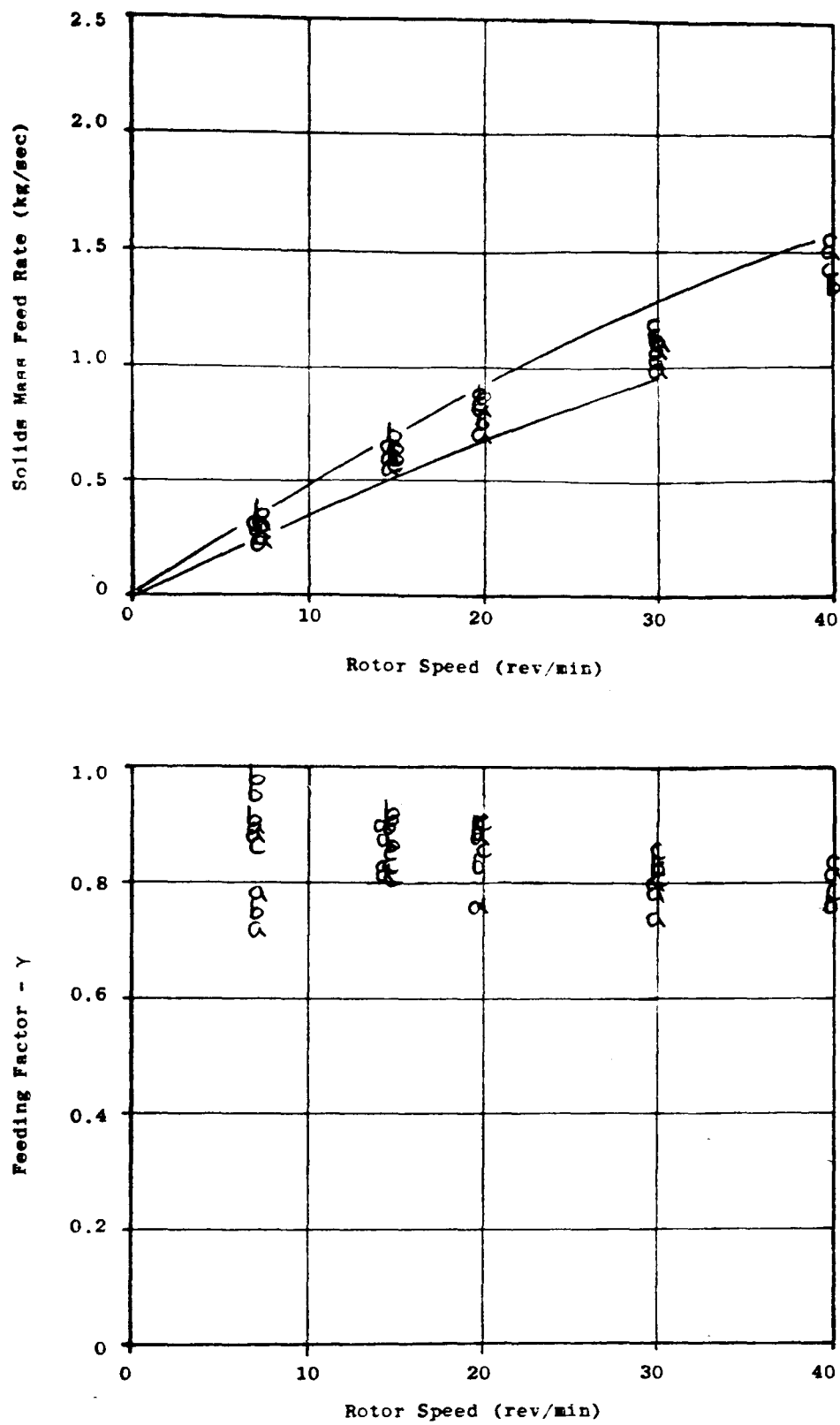
Figure 7.14 Feeding Characteristics of Polyethylene Powder.
             Comparison of results obtained with Drop-Out Box
             B and Rotary Valve Orientations a, b and c.

the entrainment efficiency was a function of the relative volumes of the rotor pockets and the drop-out box chamber.

7.3.2   Experimental Plan and Method

The experimental plan was to examine the performance of the conveying system with seven different drop-out boxes and six different materials. Three of these drop-out boxes, see Figures 7.15 a, b and c, are similar in shape to many which are used in industry, essentially consisting of a simple transition between the flange of the outlet port and the inter- section with the pipeline. Box A had a depth of one pipe diameter, box B two pipe diameters and box C three pipe diameters. The drop- out box shown in Figure 7.15d was obtained by using box B with an extension tube. This resulted in a box having a very large chamber volume and an overall depth of nine pipe diameters.

The purpose of examining the performance of the system with boxes A, B, C and D was to investigate the effect of changing the volume of the drop-out box chamber by changing the depth of the drop-out box. To complement this work another series of experiments were undertaken using three drop-out boxes of the same depth but different internal volumes; these are illustrated in Figures 7.15 e, f and g. It was reasoned that comparison of the results obtained from these two sets of experiments would enable the relative importance of the depth and volume of the drop-out box to be established.

The six different materials which were used for this work were those described in Chapter 6, that is: Polyethylene Pellets, Polyethylene Powder, Wheat Flour, Ordinary Portland Cement, 'Singles' Coal, 'Pulverised' Coal.

The actual experimental method which was used was that outlined in Chapter 6. This enabled a complete set of data to be obtained for the envelope of conveying conditions which are indicated in Figures 6.13 to 6.18. The rotary valve orientation used for all of these experiments was that shown in Figure 7.1c, that is, with the rotor pockets parallel to the conveying pipeline.

7.3.3   Results

The experimental results are presented in Figures 7.16 to 7.47. These follow the same format as the figures used to present the results in
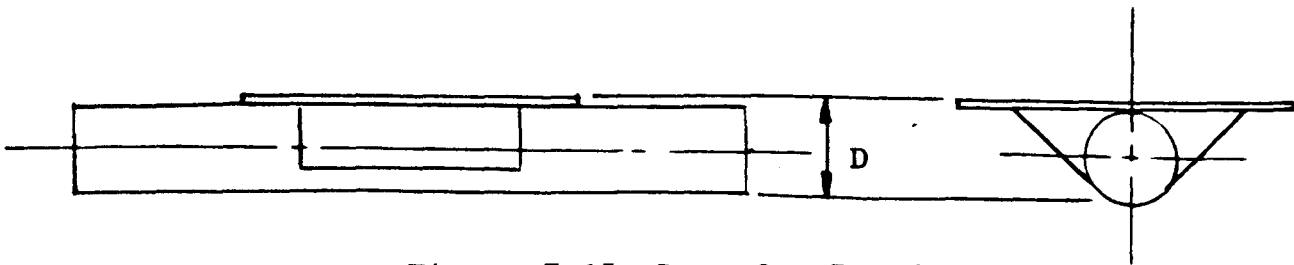
Figure 7.15a Drop-Out Box A
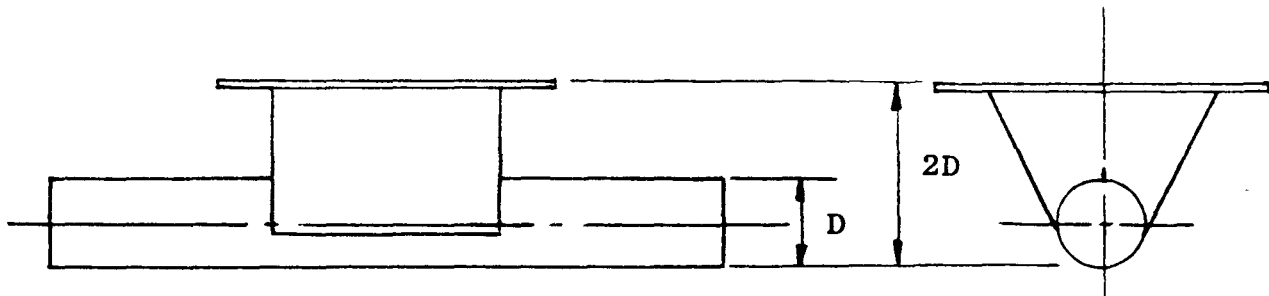
Figure 7.15b Drop-Out Box B
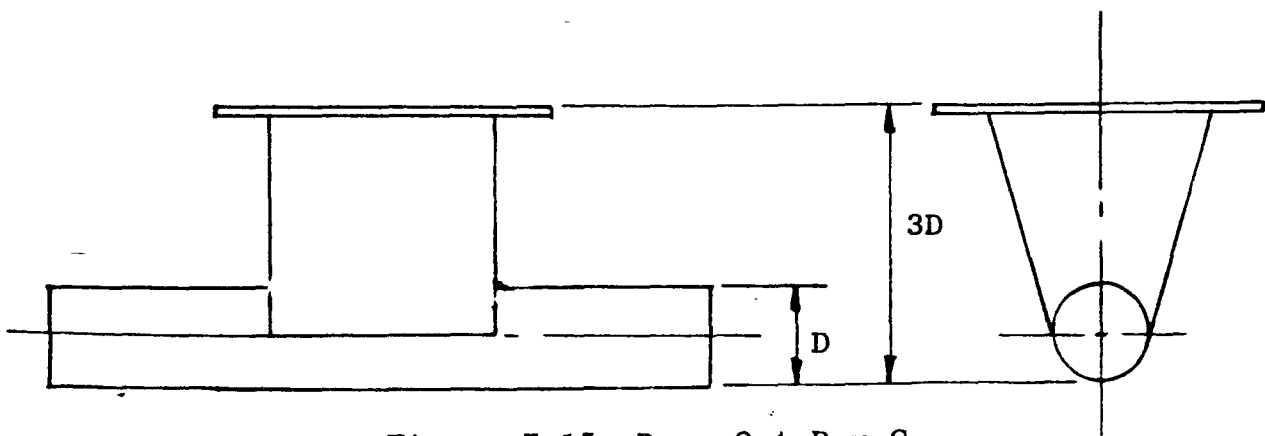
Figure 7.15c Drop-Out Box C

section 7.2. Each figure shows the results obtained for one particular combination of material and drop-out box. Where necessary, these are complemented by figures which compare the performance of the system with the different drop-out boxes. An analysis and discussion of these results is given in the following section.

7.3.4. Analysis and Discussion of Results

Figures 7.16 and 7.17 show the results obtained for the Polyethylene Pellets with drop-out boxes B and D. This was the first material to be tested and, at the time, these were the only two drop-out boxes available. However, because these boxes represent the opposite extremes in respect of volume and depth, it was reasoned that the results obtained with them should indicate the range of performance for the Polyethylene Pellets.

Figures 7.16 and 7.17 show that the performance of the system with these two drop-out boxes was, in all practical respects, identical. The implication of this is that for materials like Polyethylene Pellets, the volume and depth of the drop-out box are not significant parameters with regard to entrainment. Probable reasons for this are:

    i)   that the Polyethylene Pellets are free-flowing and so discharge easily from the pockets of the rotary valve; and

    ii)   that the size and mass of the pellets are sufficient for gravitational force acting on them to be significant.

A consequence of this last point is that such materials would not be uniformly distributed by the air currents, but concentrated towards the bottom of the drop-out box. From this it follows that very little material would be retained in the rotor pockets when they close on the outlet port; and thus the volume and depth of the drop-out box would not be significant parameters with regard to entrainment.

If the above reasoning is sound then similar results should also be obtained with other products consisting of large, heavy particles. This was confirmed by the limited number of results obtained with the Singles Coal. However, before discussing these results in detail they require some explanation.

Because coal is a very friable product it was easily degraded by the action of the rotary valve and by attrition in the pipeline.
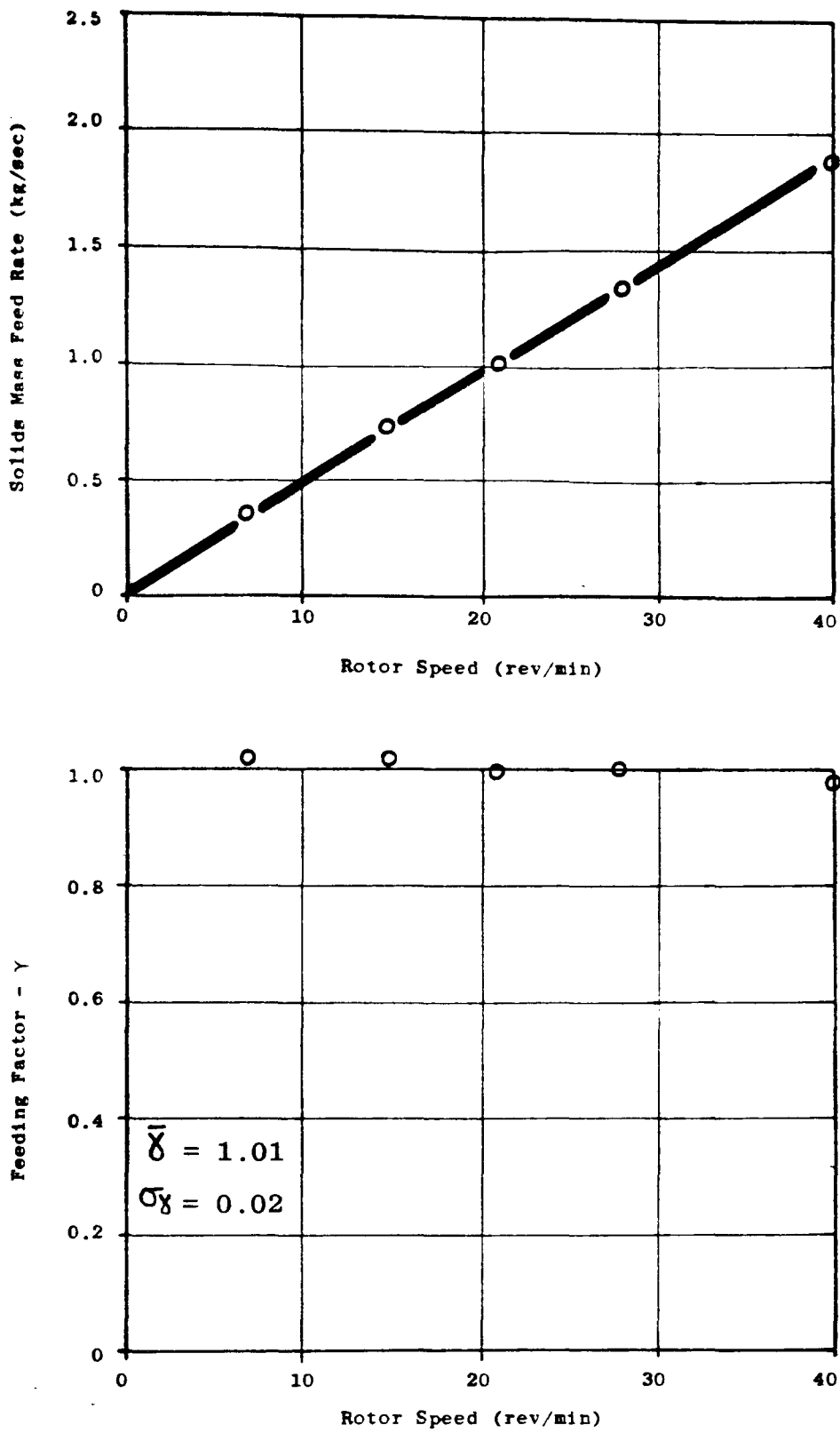
Figure 7.16 Feeding Characteristics of Polyethylene Pellets
            with Drop-Out Box B and Rotary Valve Orientation c.
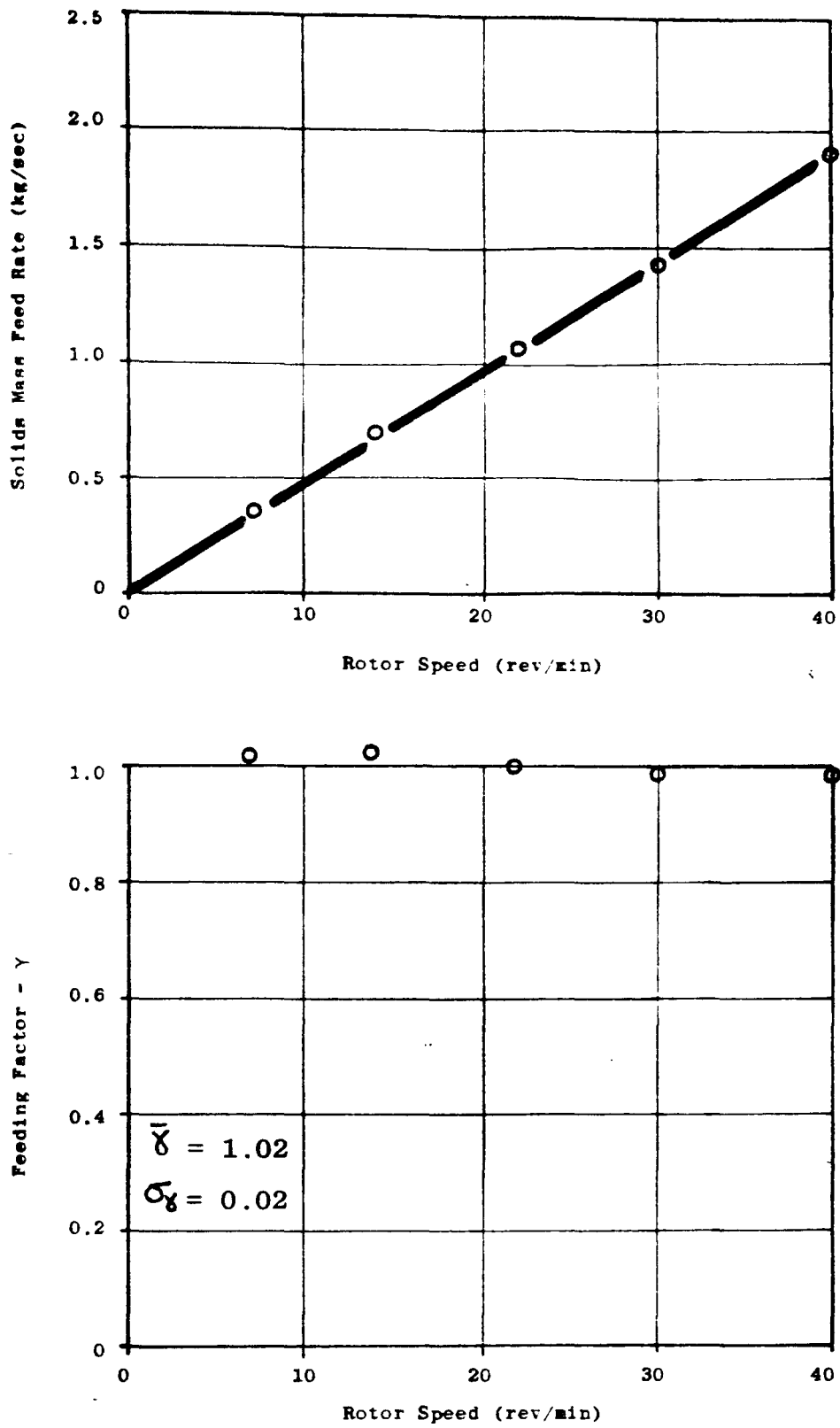
Figure 7.17 Feeding Characteristics of Polyethylene Pellets
with Drop-Out Box D and Rotary Valve Orientation c .
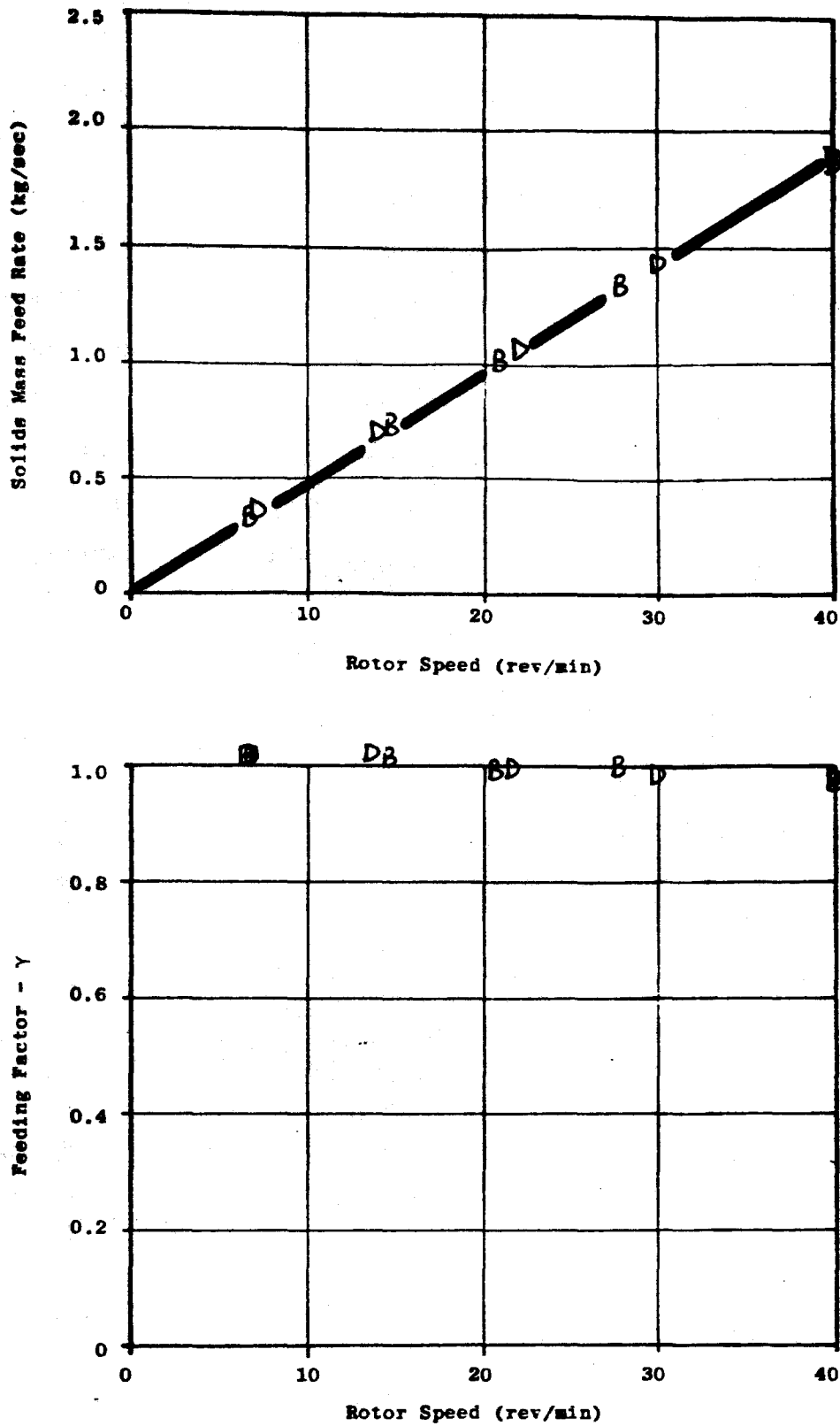
Figure 7.18 Feeding Characteristics of Polyethylene Pellets.
Comparison of the results obtained with Drop-Out
Boxes B and D.

Consequently, only a limited number of experiments could be made with each batch before it had to be changed. As a result of this and the limited quantity of coal which was available, only three entrainment configurations were examined. These were drop-out boxes A and B and the blowing seal. Even then the rate of degradation was such that little useful information was obtained. This is illustrated by Figure 7.19 which shows how the poured bulk density of the coal changed with both the number of passes through the rotary valve and the distance conveyed. This information enabled the feeding factor - valve rotor speed relationships shown in Figures 7.20 and 7.21 to be constructed by selecting the value of the bulk density relevant to the previous number of passes of the coal through a rotary valve and the previous
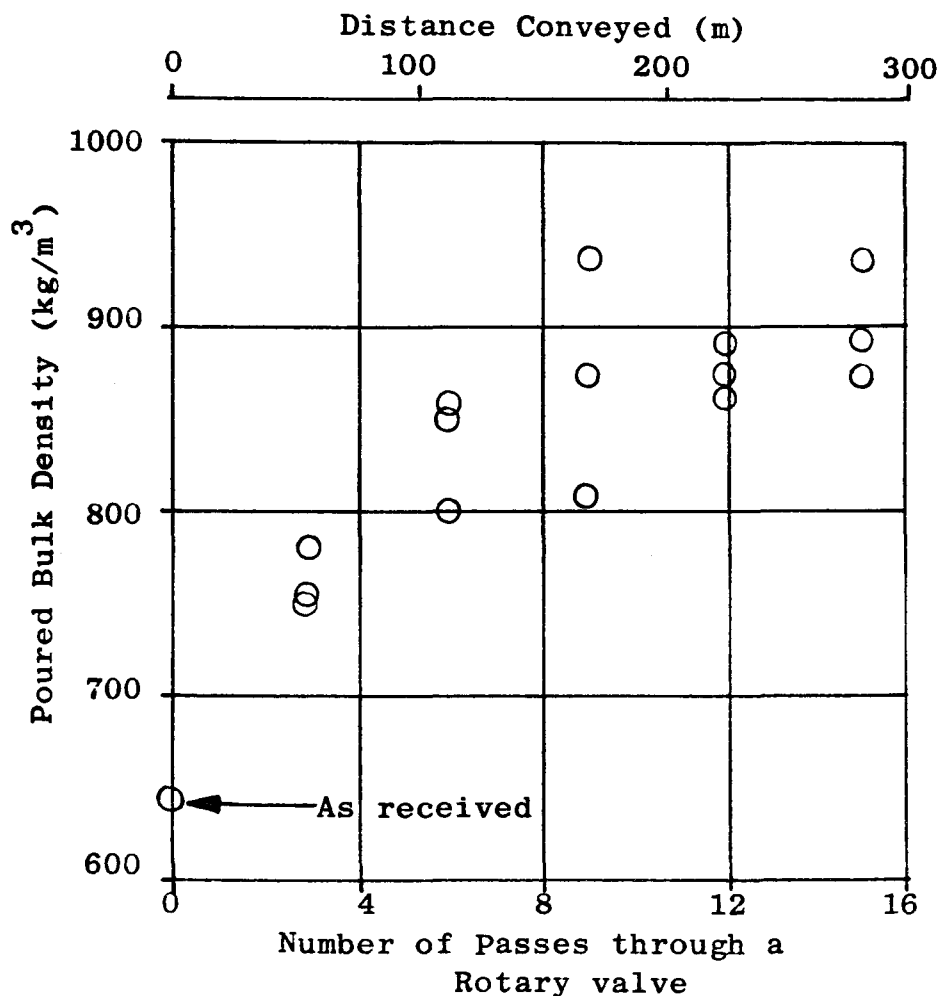
Figure 7.19 The Change in Density of the Singles Coal
with Distance Conveyed and Number of
Passes through a Rotary Valve.
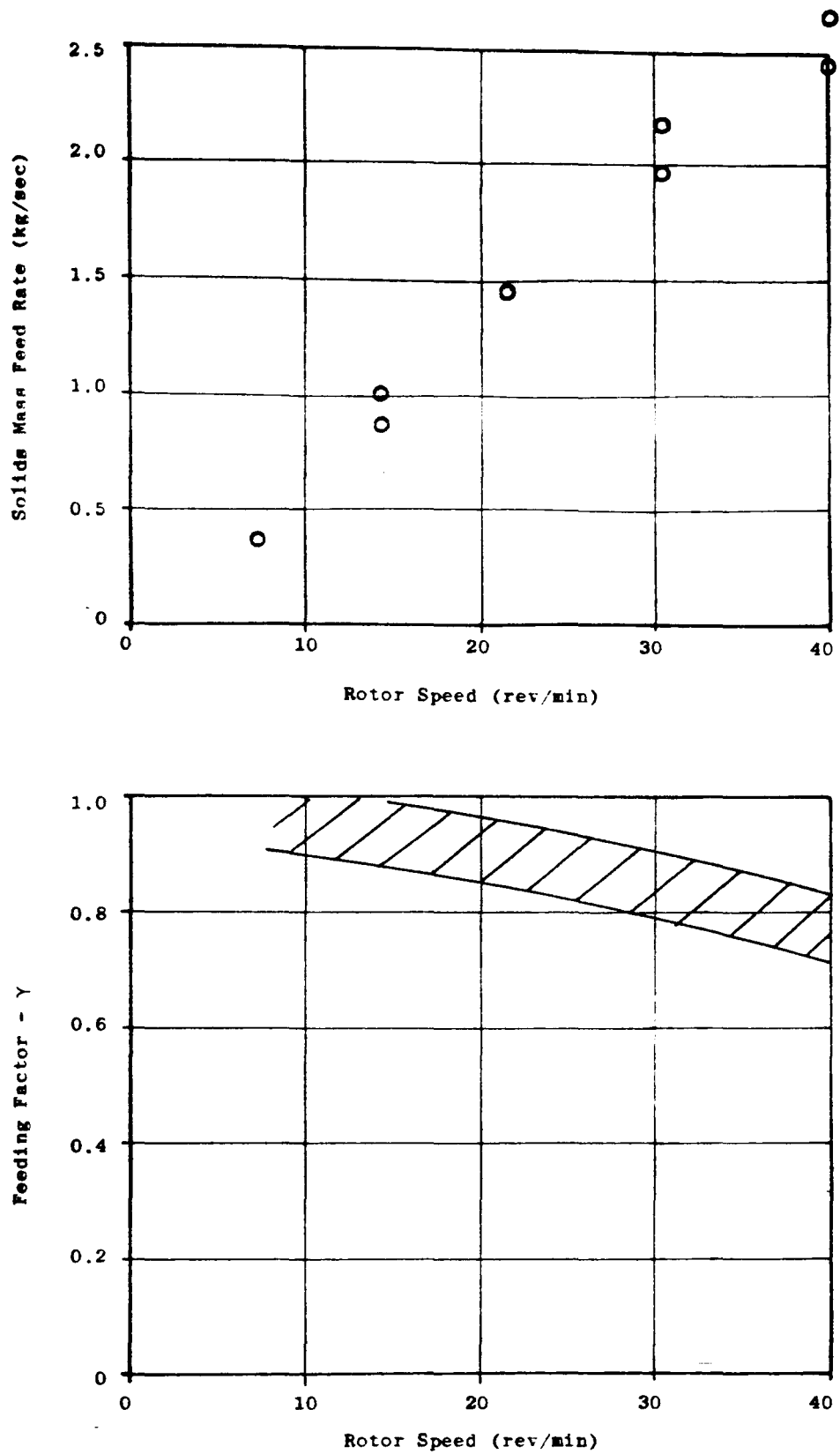
Figure 7.20 Feeding Characteristics of Singles Coal
         with Drop-Out Box A and Rotary Valve Orientation c .
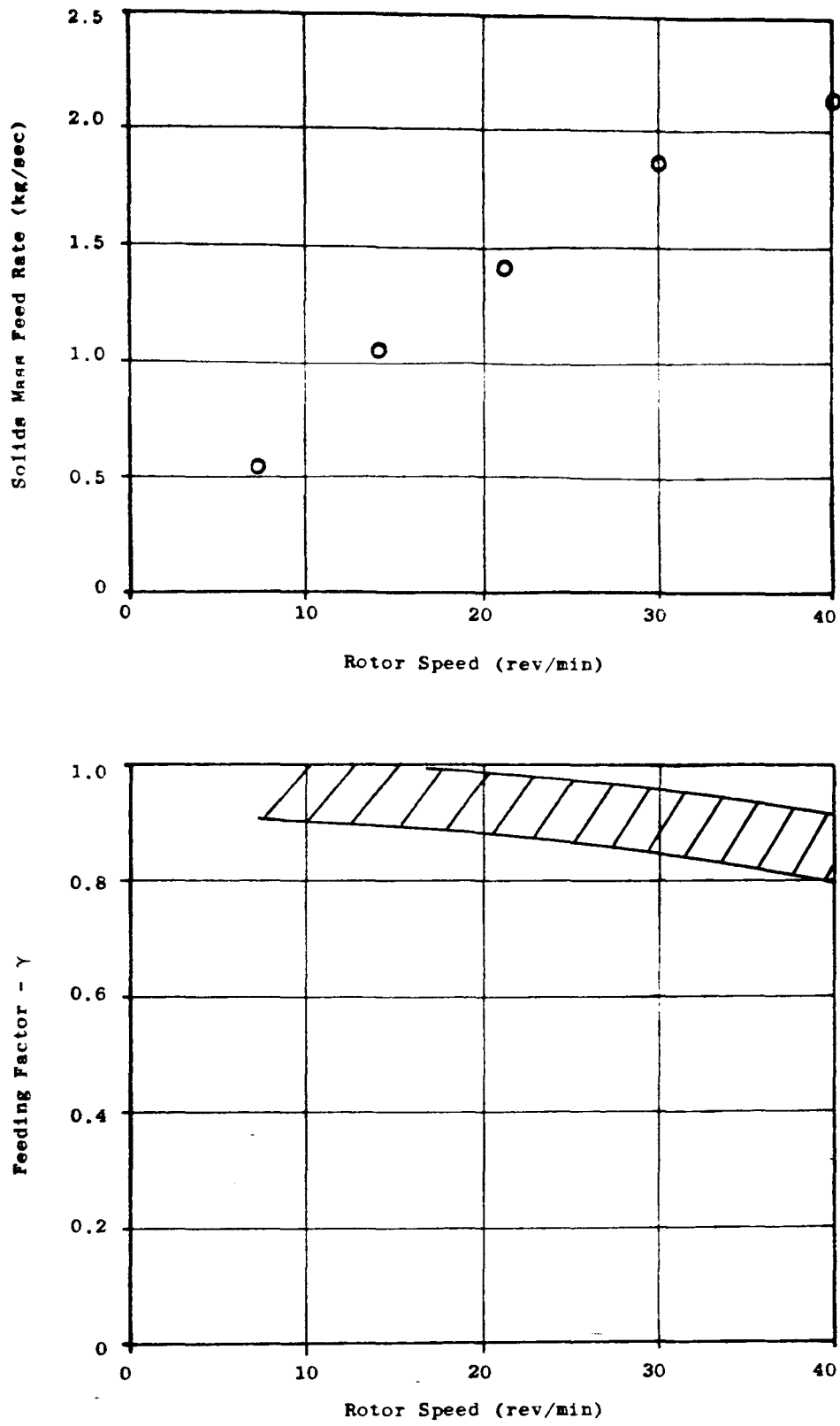
Figure 7.21 Feeding Characteristics of Singles Coal
         with Drop-Out Box B and Rotary Valve Orientation c.

distance conveyed. The resulting relationships are shown as bands rather than individual data points in order to indicate the degree of uncertainty which is associated with using this method of analysis. Furthermore, it is important to realise that because of the rapid degradation, the results presented in Figures 7.20 and 7.21 represent the performance of the system with degraded coal and not with virgin material.

In view of the above mentioned limitations, comparison of Figures 7.20 and 7.21 show that the performance of the system with drop-out boxes A and B was identical. This result supports the argument expressed earlier that for large particle products the volume and depth of the drop-out box are not significant parameters with regard to entrainment. However, this is not the case with finer particle products as demonstrated by the results for Wheat Flour, Cement and Polyethylene Powder.

Consider first of all the results obtained with the Wheat Flour which are shown in Figures 7.22 to 7.29. The experiments with the Wheat Flour were conducted at two separate times because of the availability of the drop-out boxes. The performance of the system with drop-out boxes B and D were examined first and then later the experiments were repeated with boxes A, B and C. Unfortunately, as a result of unloading and then reloading, the flour became contaminated and the bulk density increased from 440 kg/m^3 to 470 kg/m^3. Although this did not alter the general trend of the results, it did have the effect of reducing the overall magnitude of the feeding factor for any given rotor speed. This can be seen from Figure 7.22 which compares the results obtained from the two sets of experiments cannot be compared directly, but only with respect to those obtained for drop-out box B.

Figures 7.23 and 7.24 show the results obtained from the first set of experiments with drop-out boxes B and D respectively. These results are combined in Figure 7.25 to compare the performances obtained with these two boxes. This shows that the feeding factor characteristic for drop-out box D is approximately 7% greater than that for drop-out box B. While this result is consistent with the idea postulated in Chapter 4, that the entrainment efficiency of a drop-out box with a large volume will be better than that of a drop-out box with a small
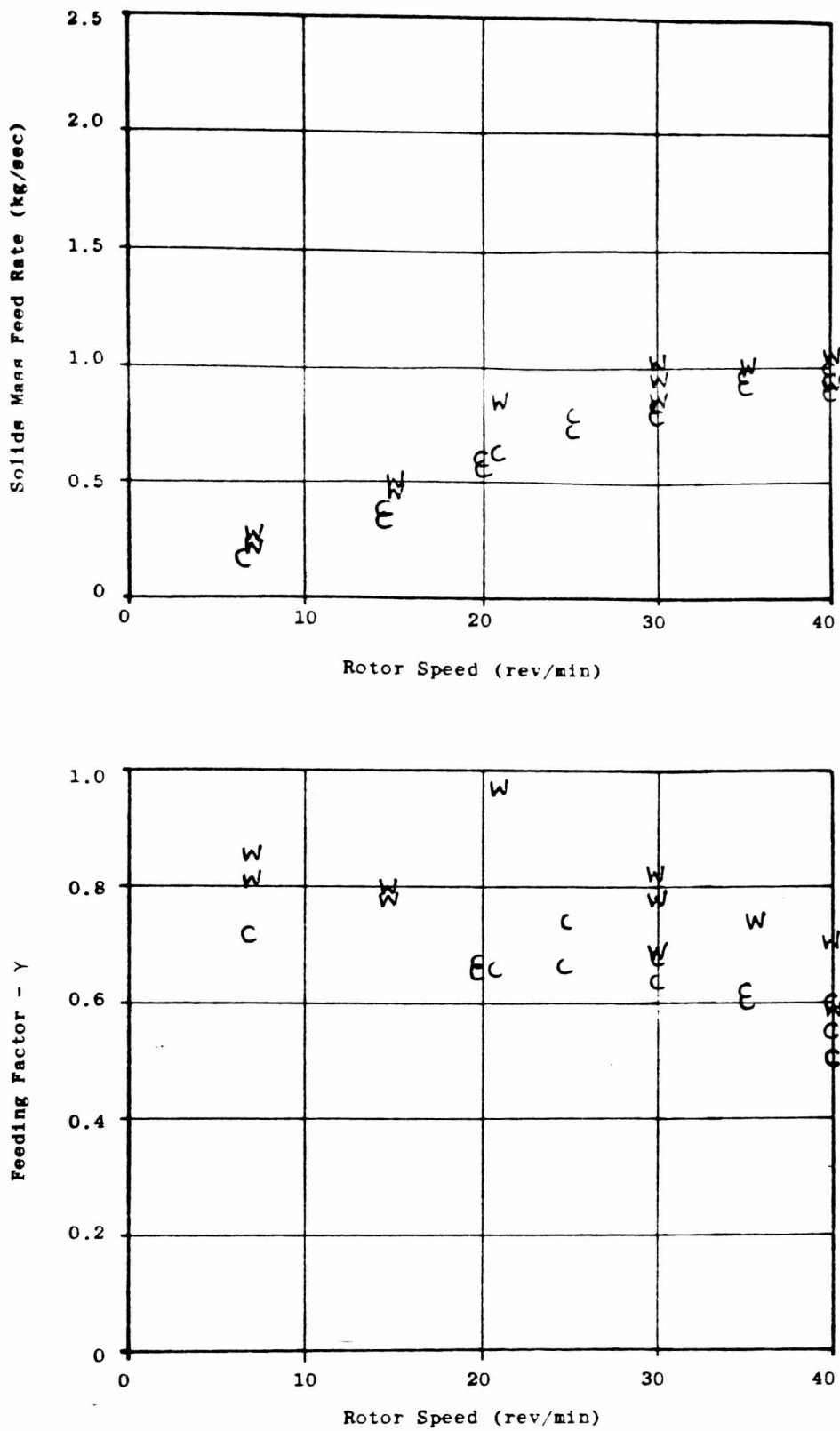
Figure 7.22   Comparison of the feeding characteristics obtained
with the Wheat Flour and the Contaminated Wheat
Flour in Drop-Out Box B.
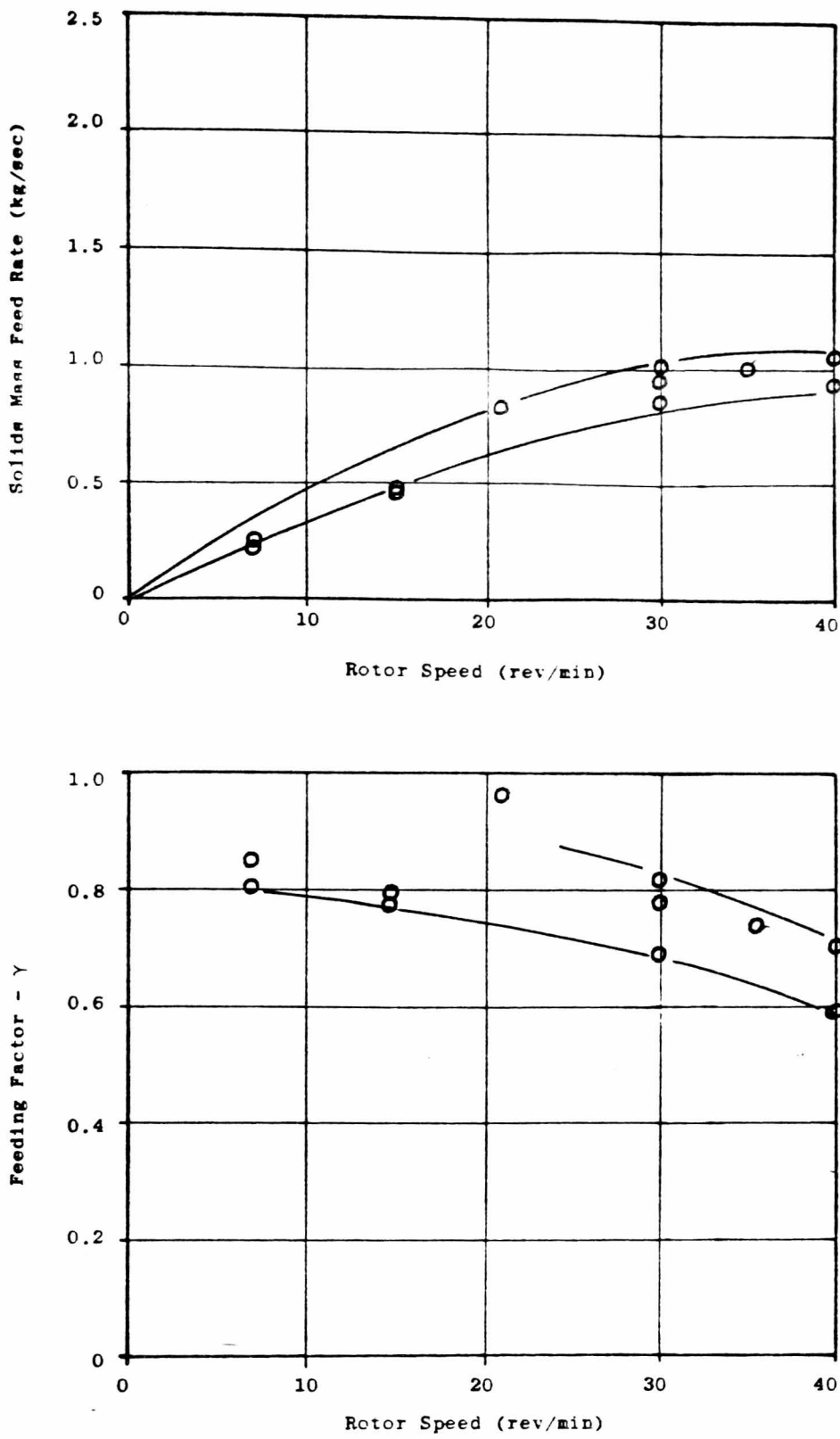
Figure 7.23 Feeding Characteristics of Wheat Flour
            with Drop-Out Box B and Rotary Valve Orientation c.
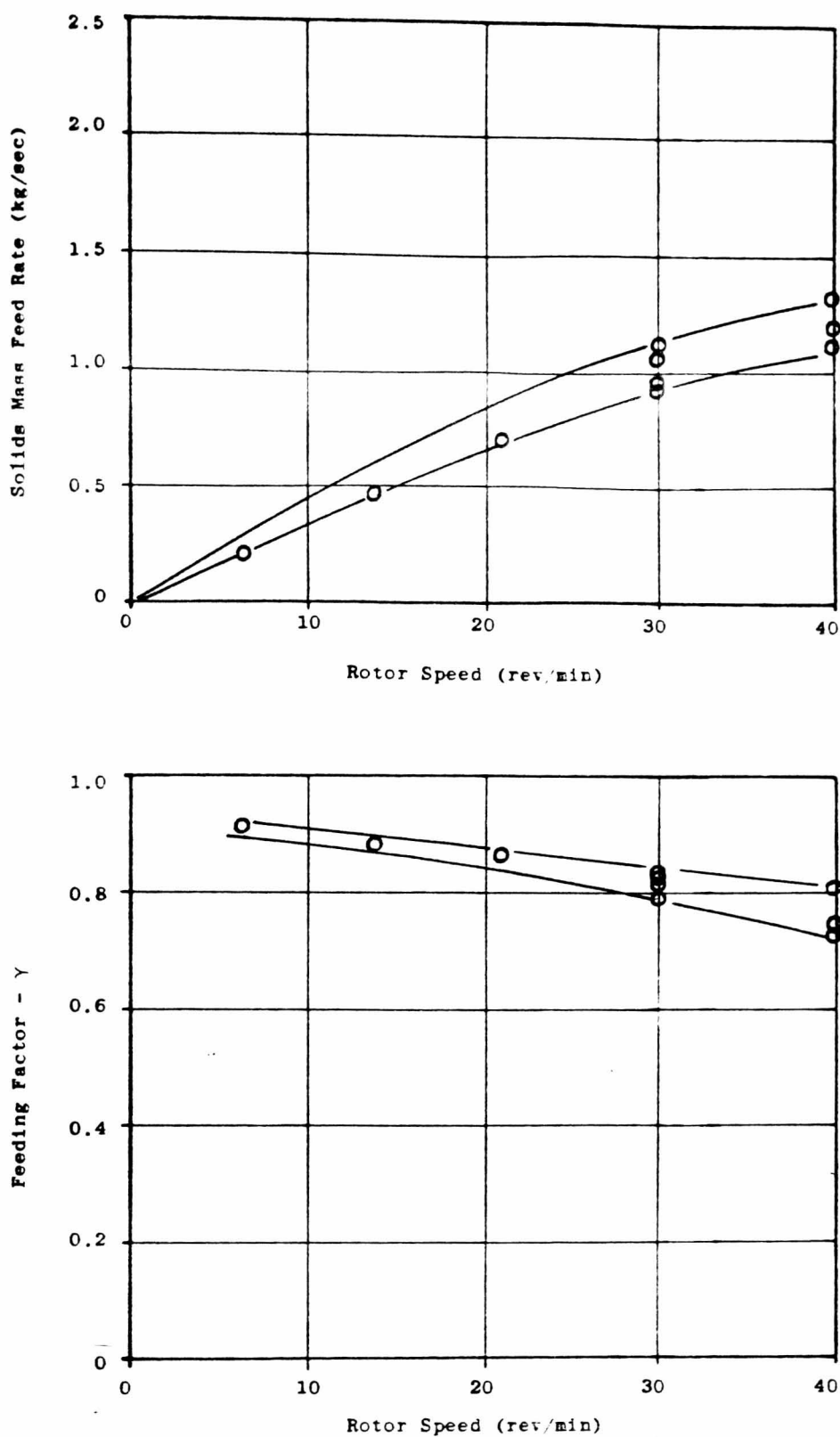
Figure 7.24 Feeding Characteristics of Wheat Flour
            with Drop-Out Box D and Rotary Valve Orientation c.
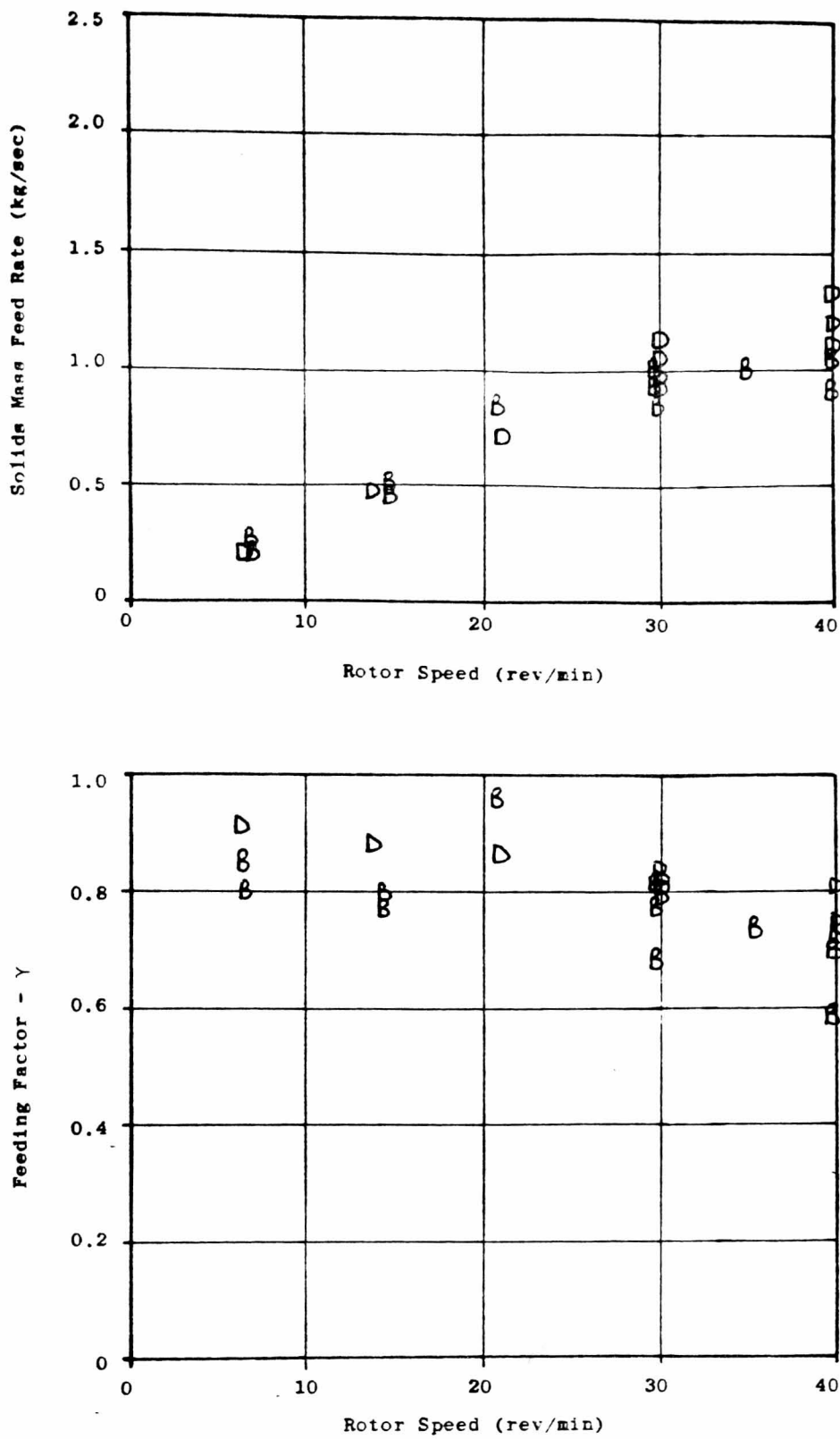
Figure 7.25 Feeding Characteristics of Wheat Flour.
Comparison of the results obtained with Drop-Out
Boxes B and D.
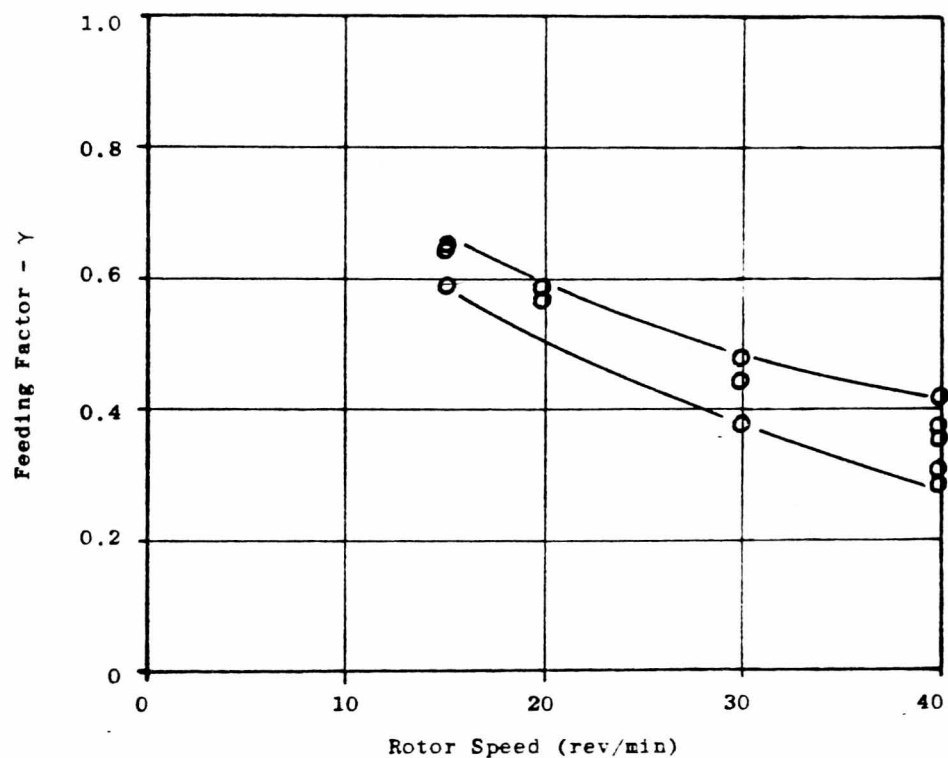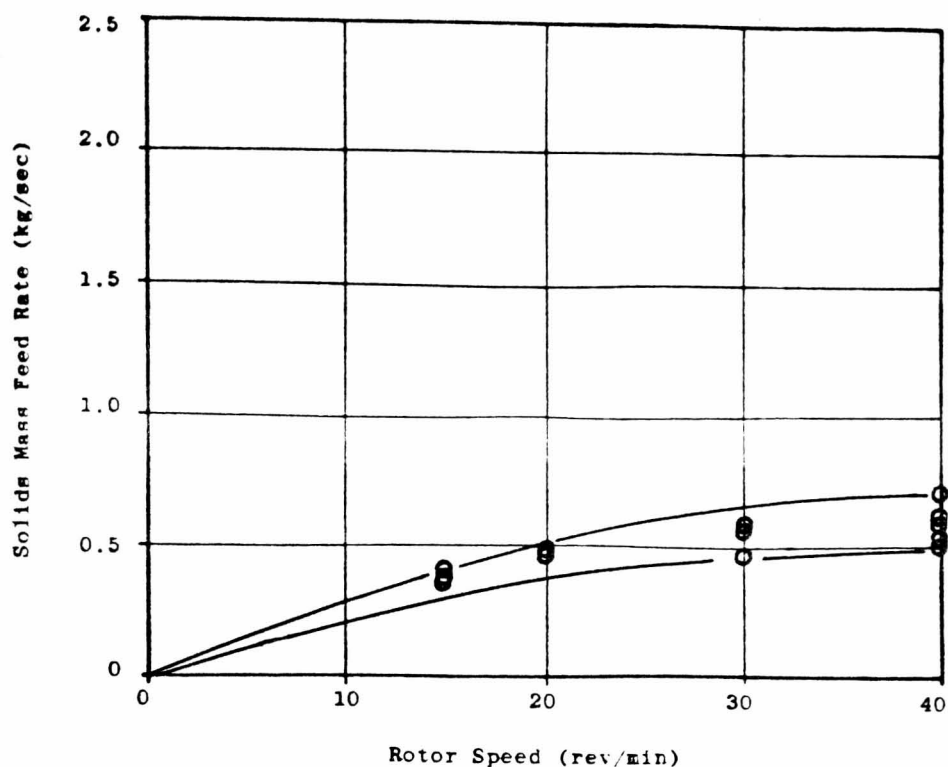
Figure 7.26 Feeding Characteristics of Wheat Flour (contaminated) with Drop-Out Box A and Rotary Valve Orientation c.
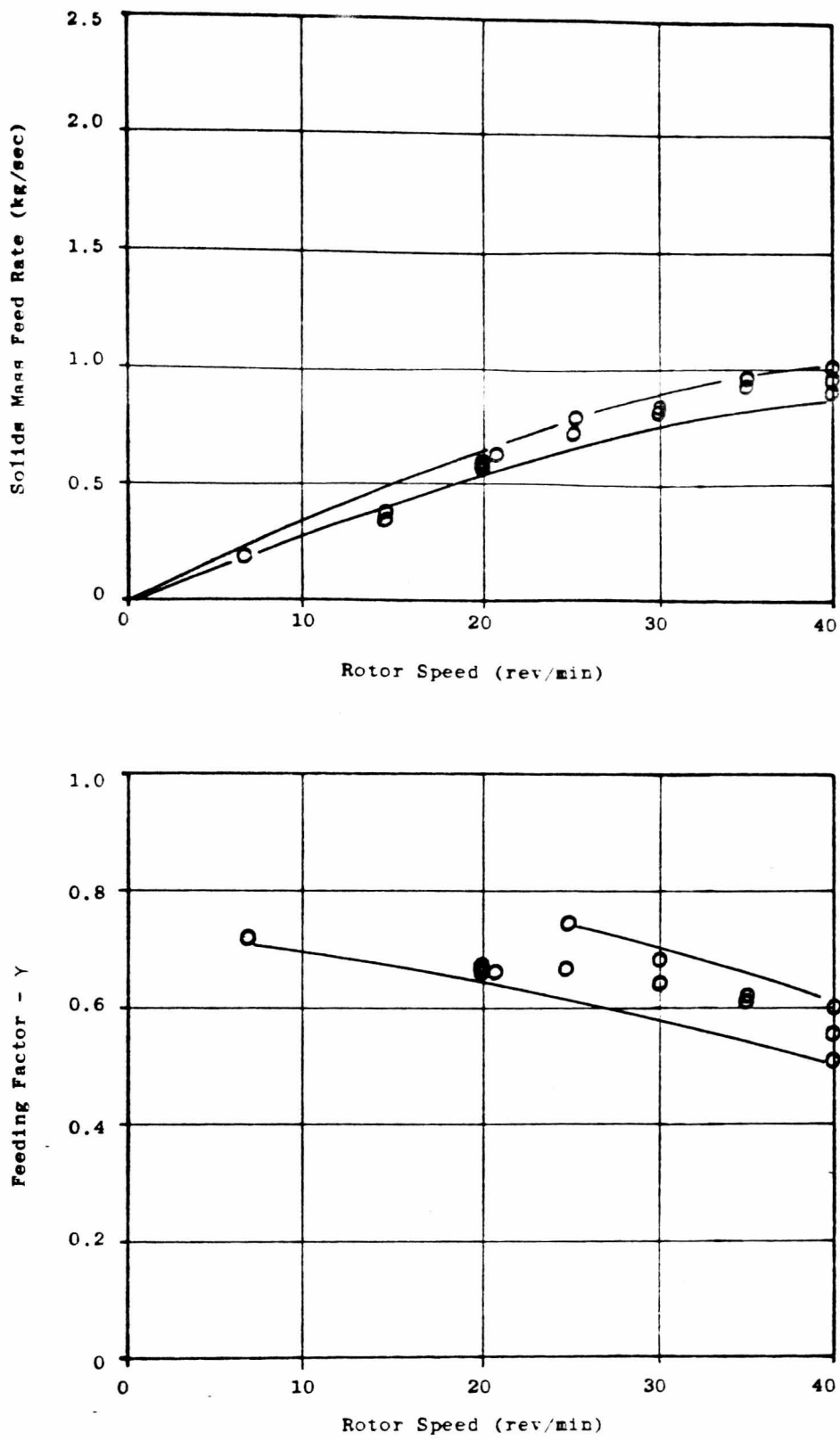
Figure 7.27 Feeding Characteristics of Wheat Flour (contaminated)
with Drop-Out Box B and Rotary Valve Orientation c.
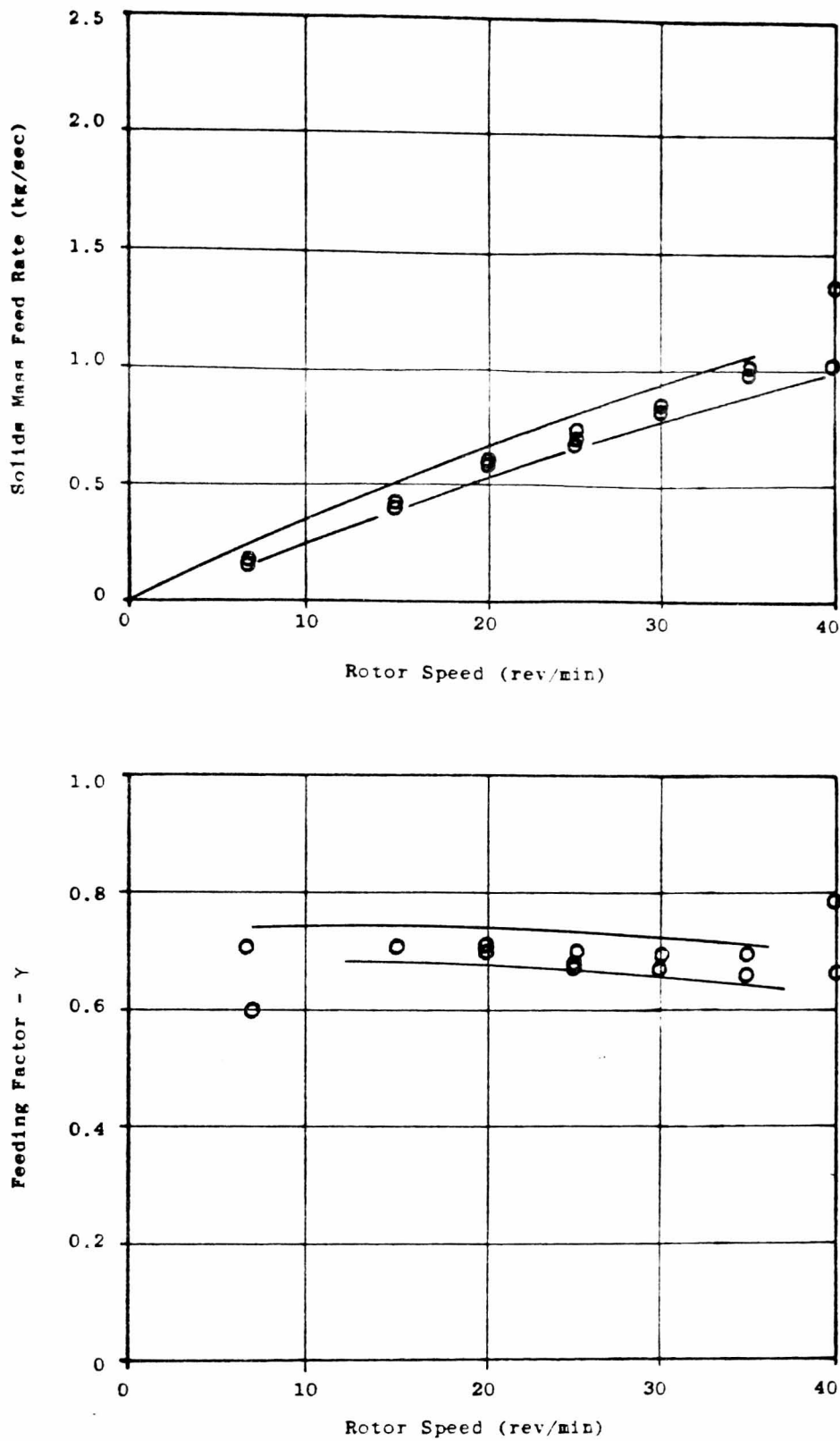
Figure 7.28 Feeding Characteristics of Wheat Flour (contaminated)
with Drop-Out Box C and Rotary Valve Orientation c.
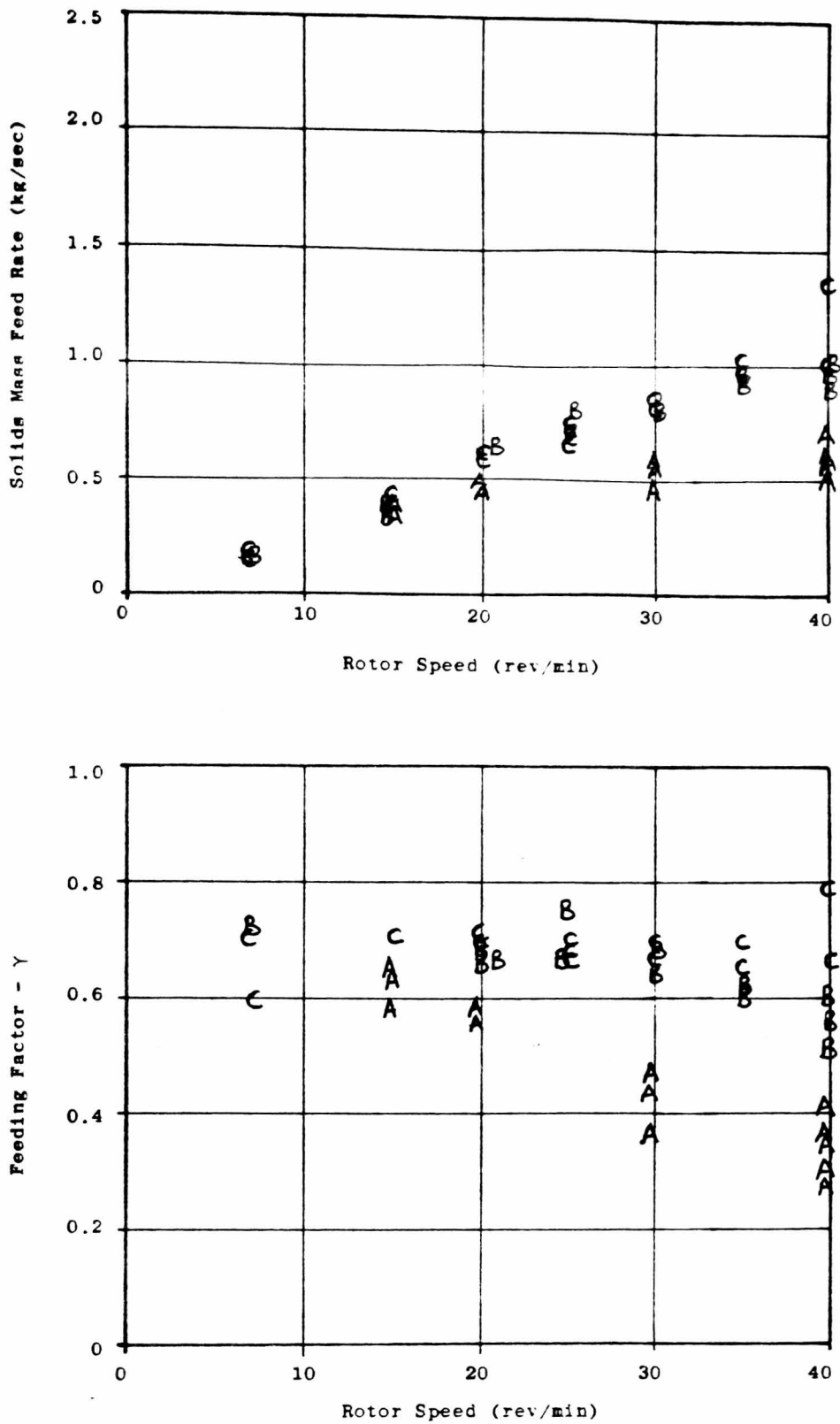
Figure 7.29 Feeding Characteristics of Wheat Flour (contaminated).
Comparison of the results obtained with Drop-Out Boxes
A, B and C.
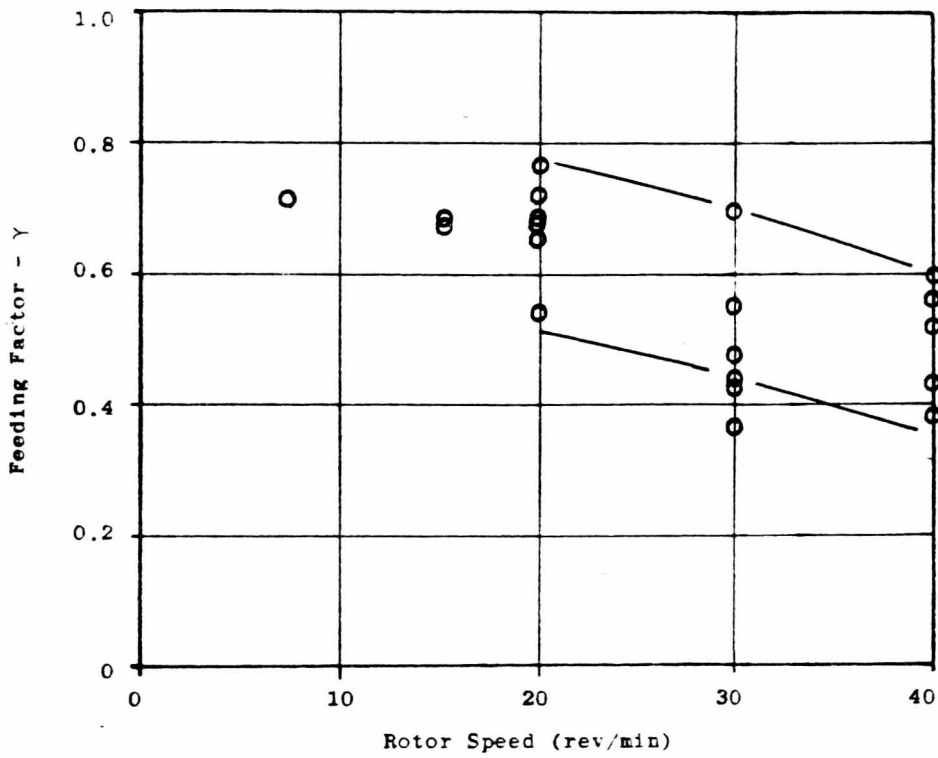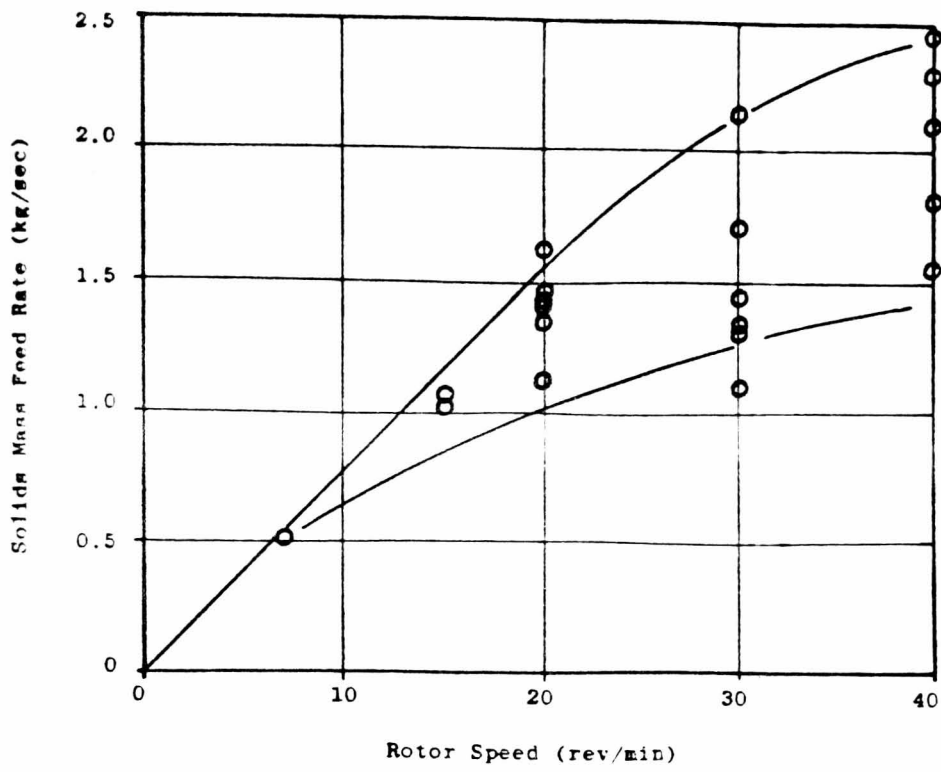
Figure 7.30 Feeding Characteristics of Cement
with Drop-Out Box A and Rotary Valve Orientation c.
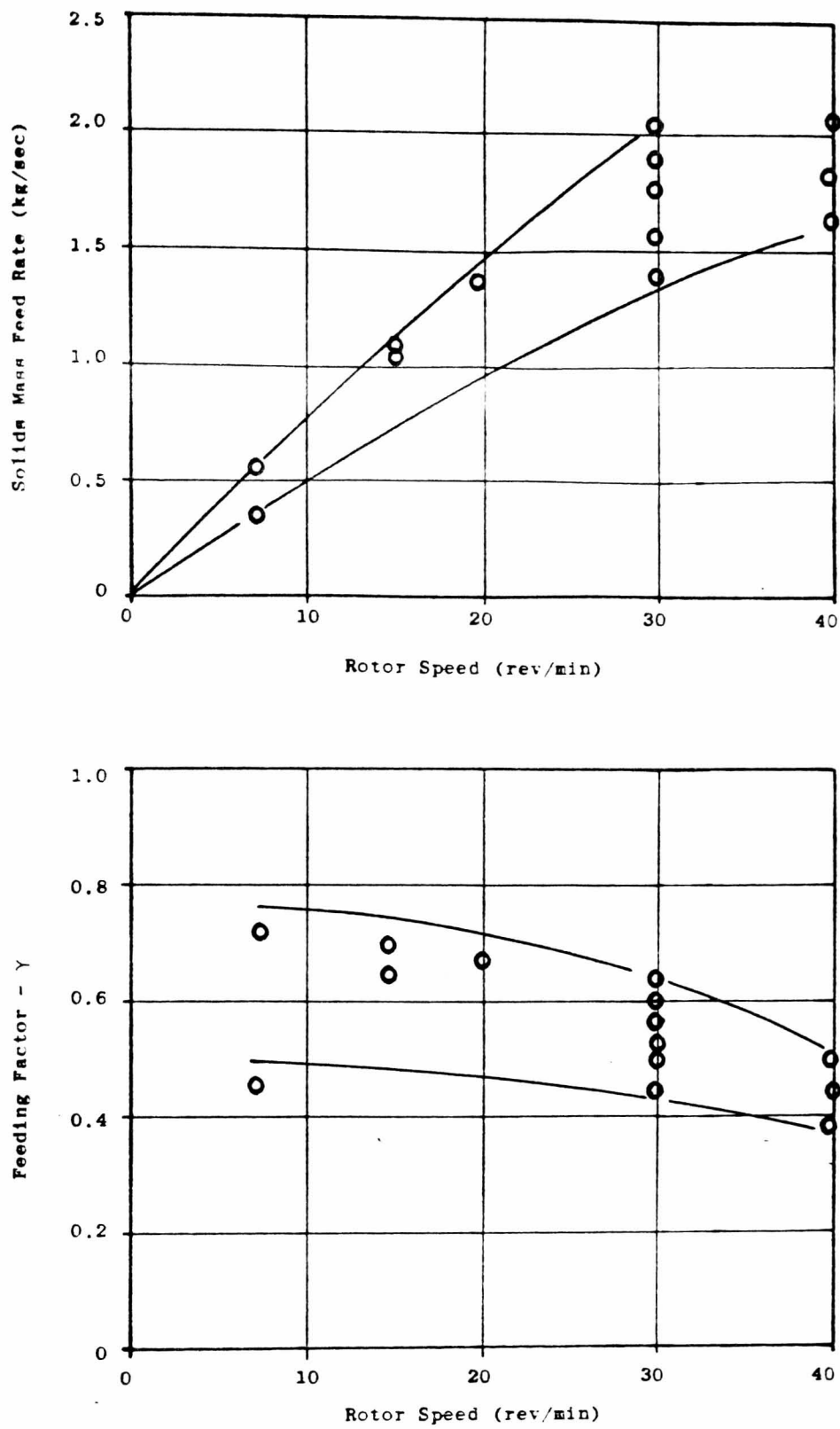
Figure 7.31 Feeding Characteristics of Cement
              with Drop-Out Box B and Rotary Valve Orientation c.
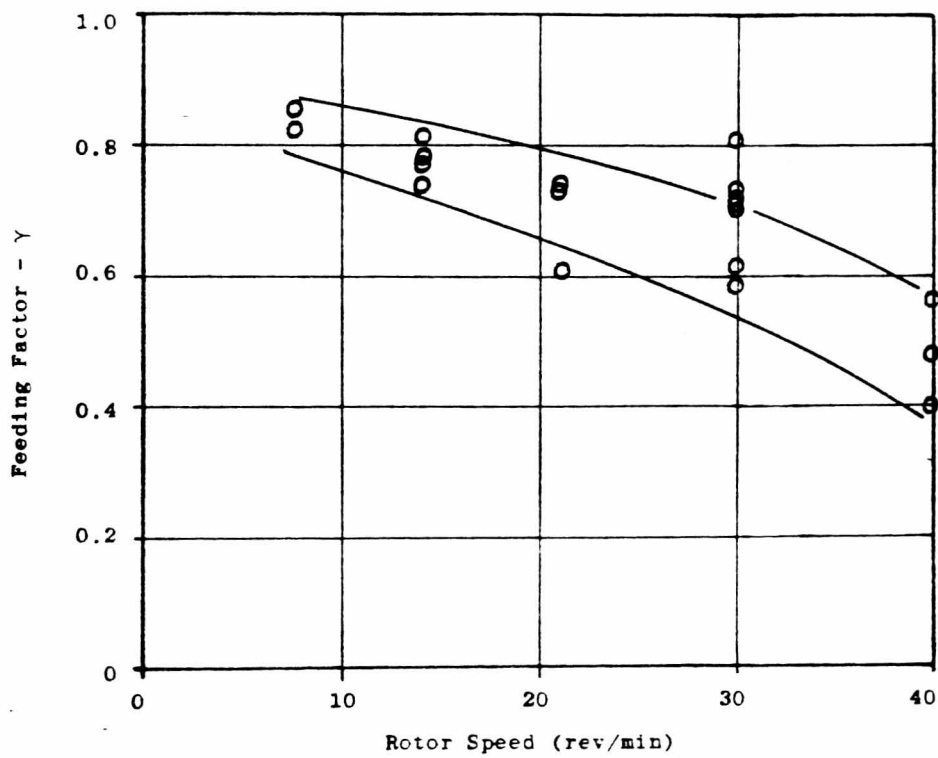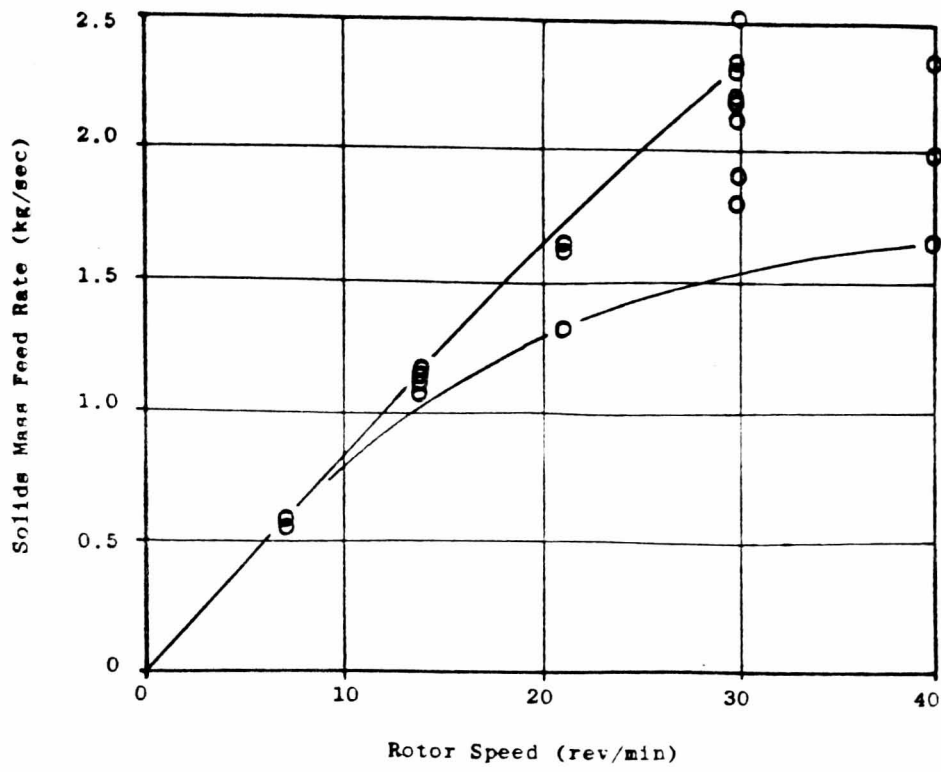
Figure 7.32 Feeding Characteristics of Cement
            with Drop-Out Box C and Rotary Valve Orientation c.
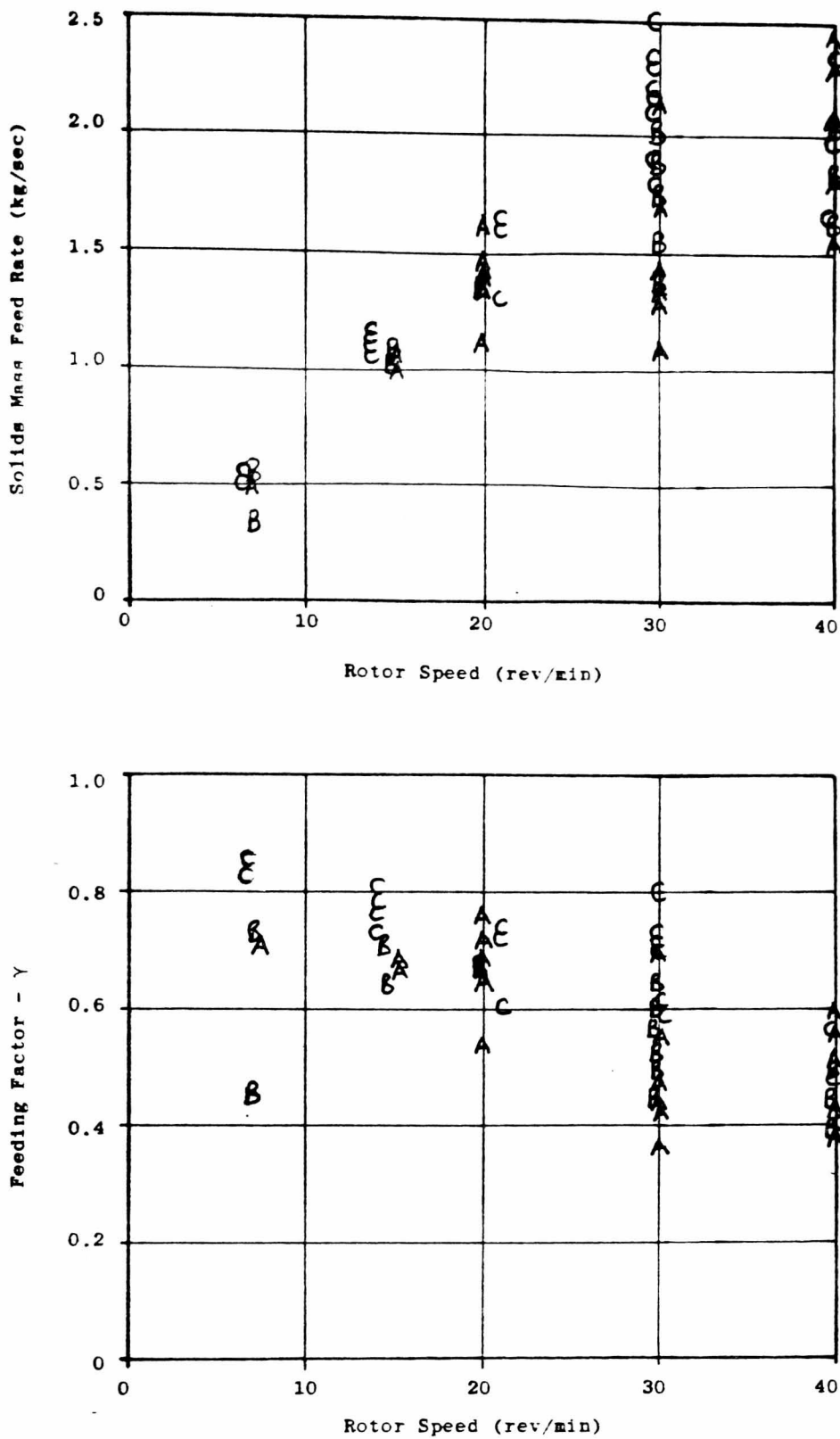
Figure 7.33 Feeding Characteristics of Cement.
Comparison of the results obtained with Drop-Out
Boxes A, B and C.
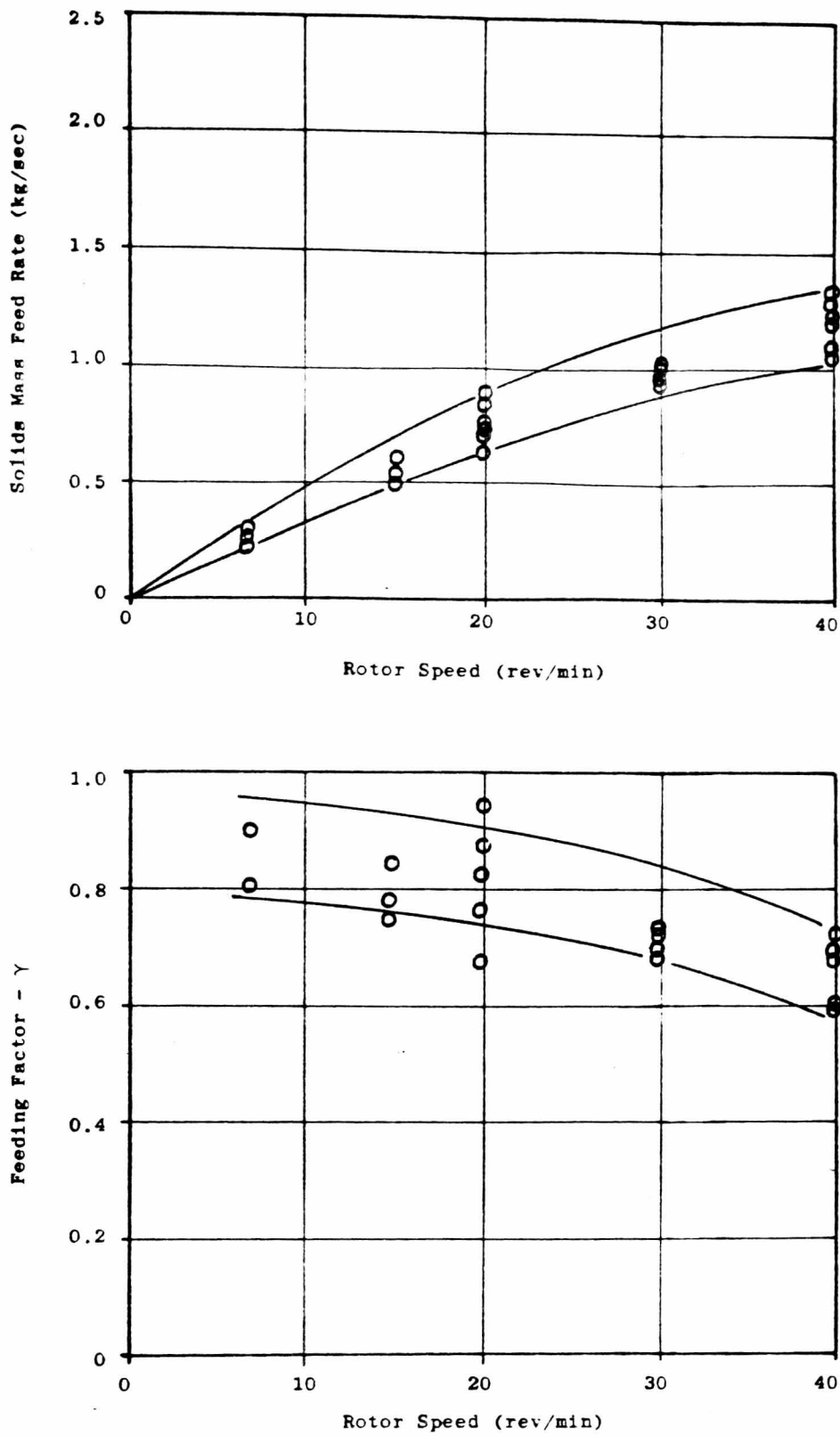
Figure 7.34 Feeding Characteristics of Polyethylene Powder
with Drop-Out Box A and Rotary Valve Orientation c.
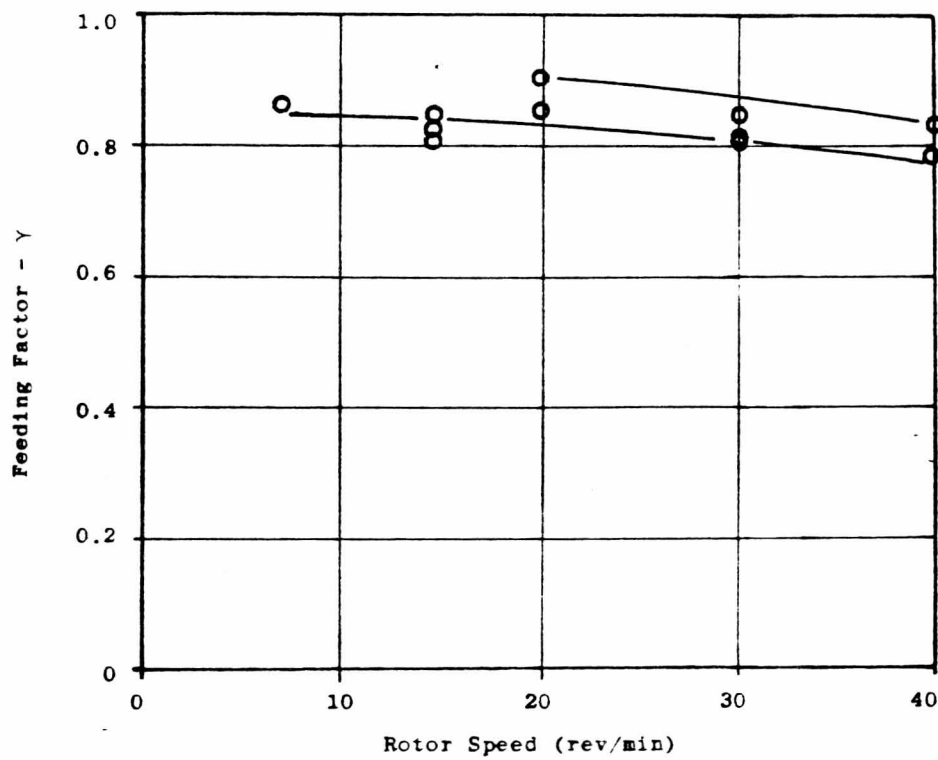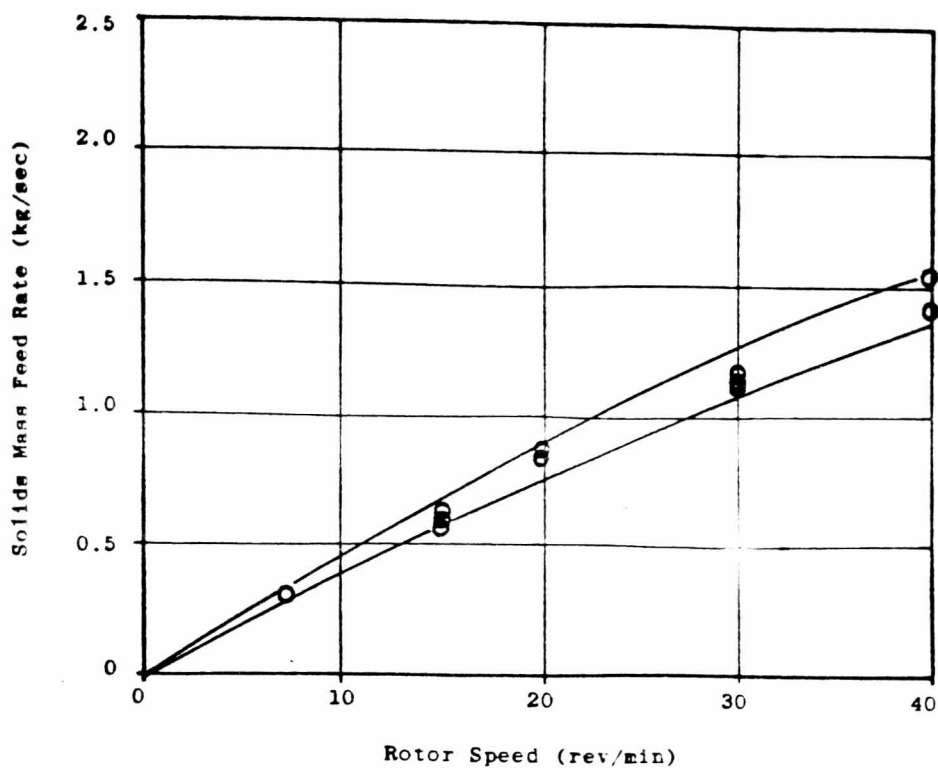
Figure 7.35 Feeding Characteristics of Polyethylene Powder
with Drop-Out Box B and Rotary Valve Orientation c.
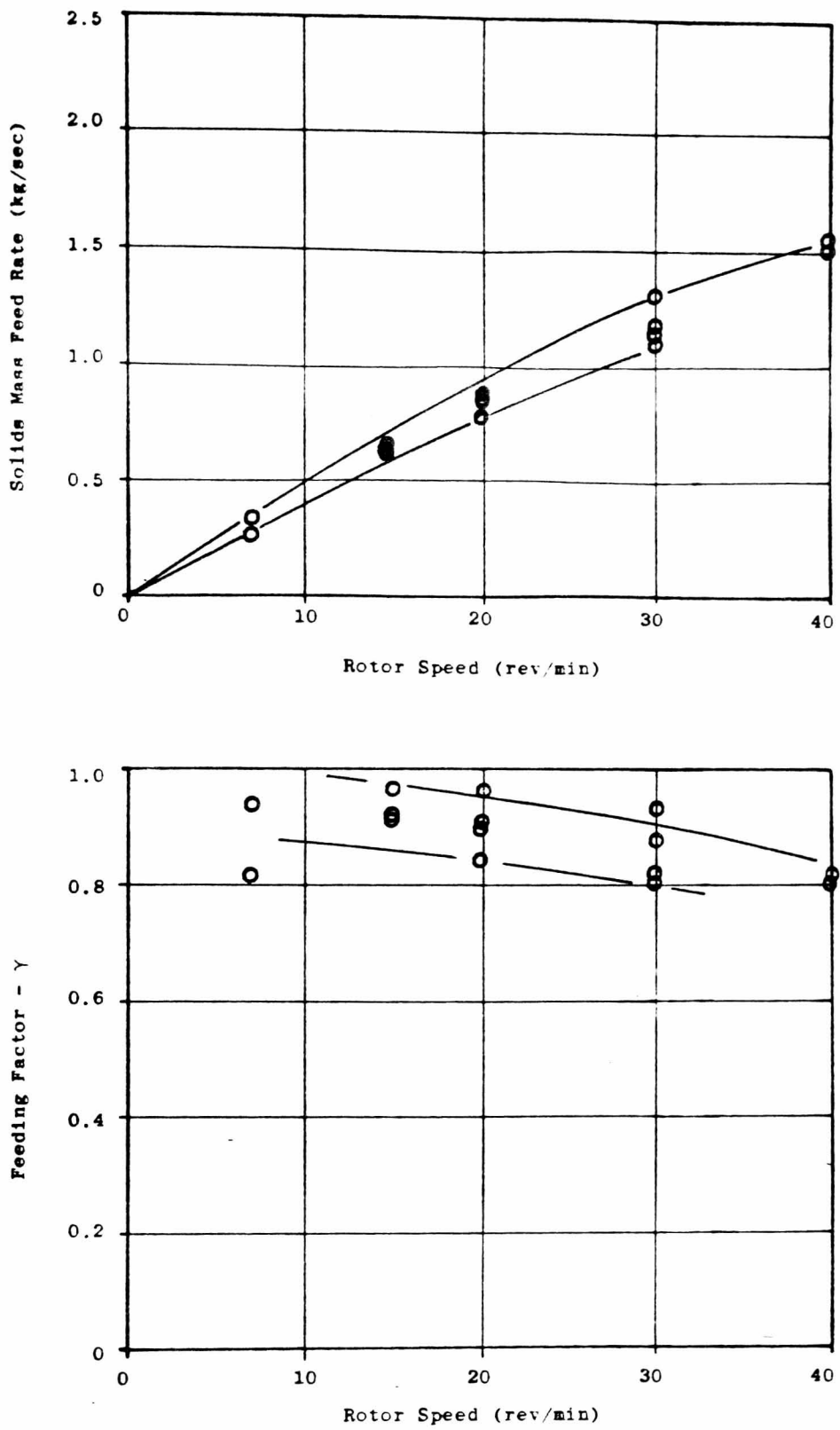
Figure 7.36 Feeding Characteristics of Polyethylene Powder
with Drop-Out Box D and Rotary Valve Orientation c.
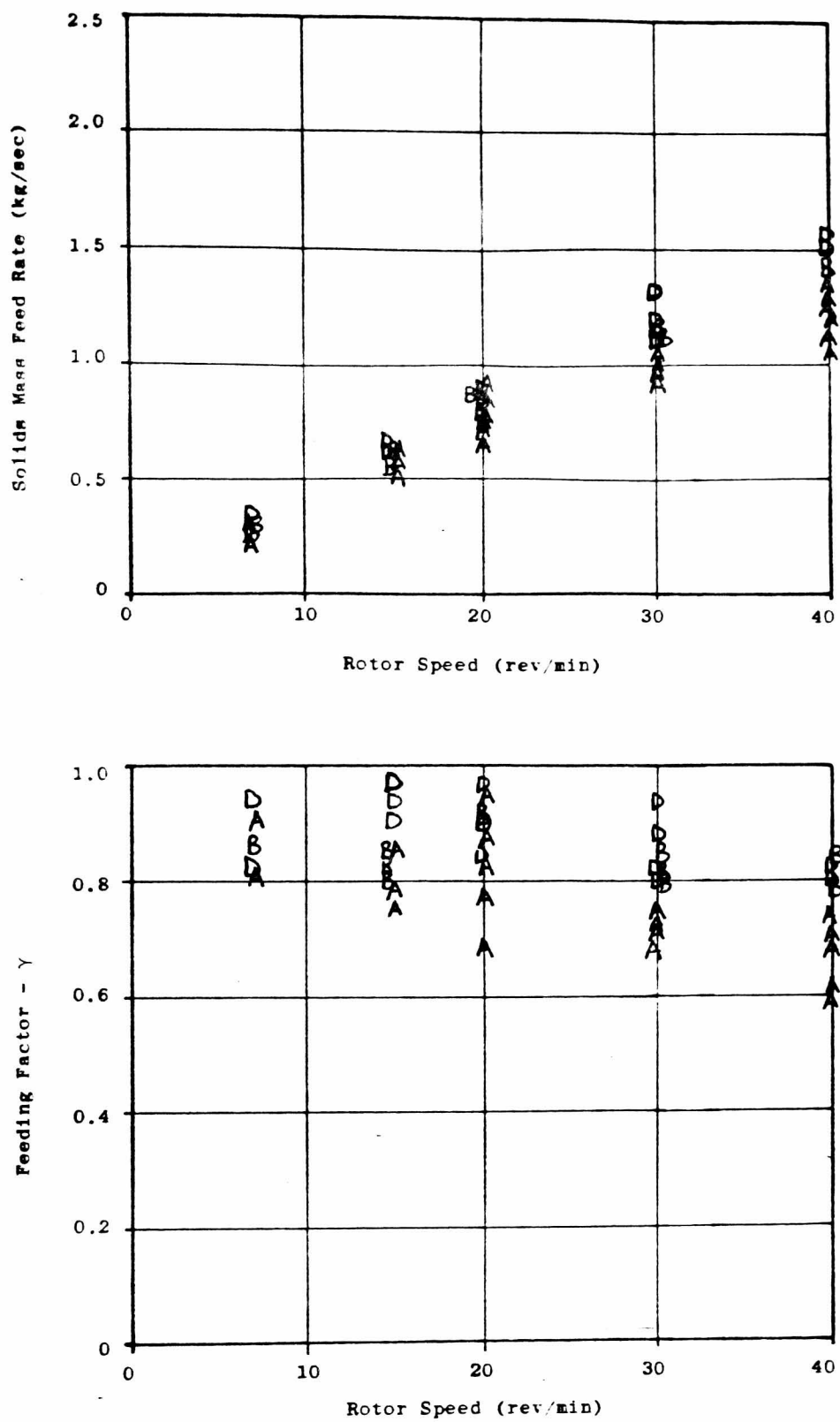
Figure 7.37 Feeding Characteristics of Polyethylene Powder.
Comparison of the results obtained with Drop-Out
Boxes A, B and C.
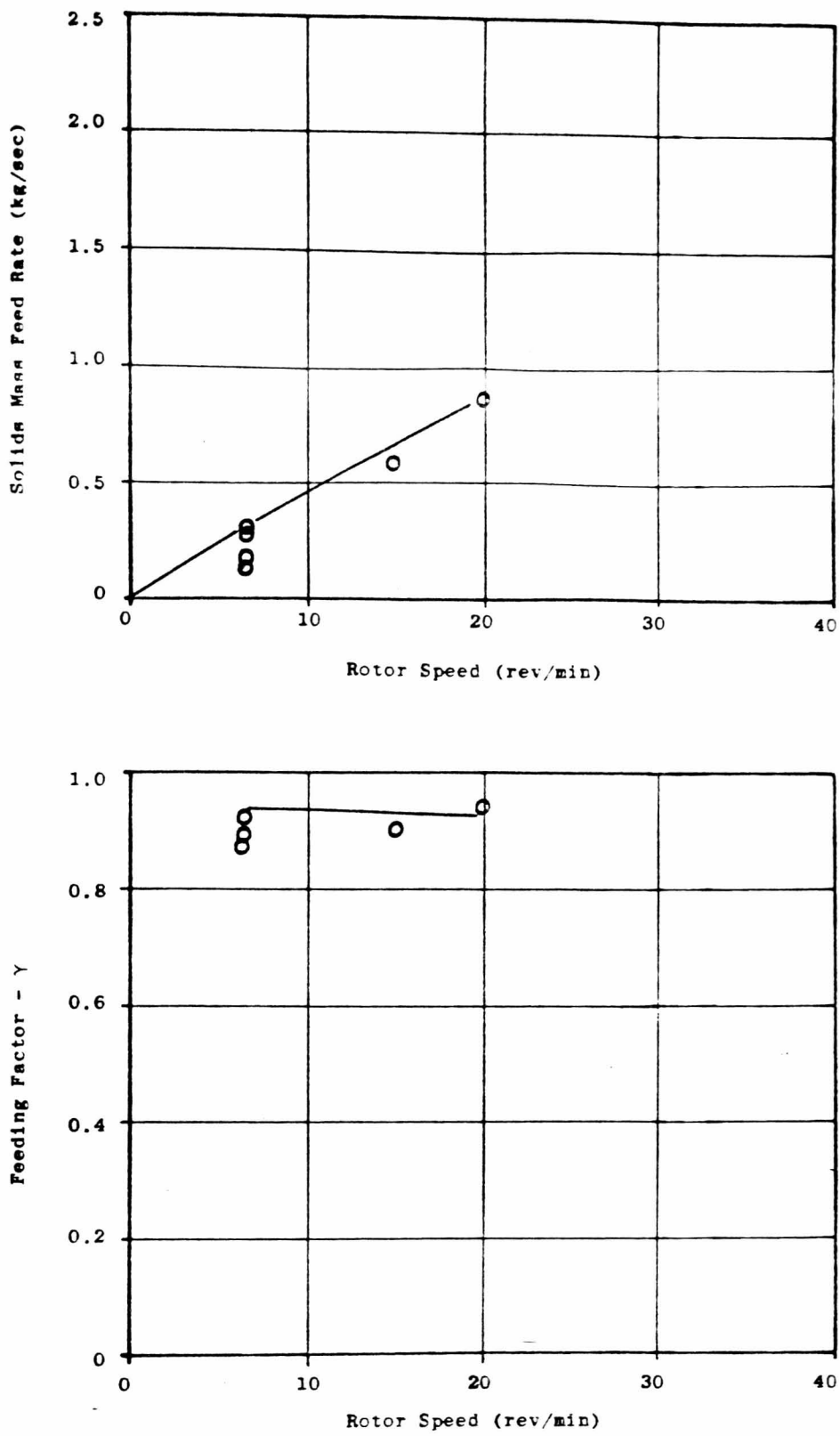
Figure 7.38 Feeding Characteristics of Polyethylene Powder
            with Drop-Out Box E and Rotary Valve Orientation c.
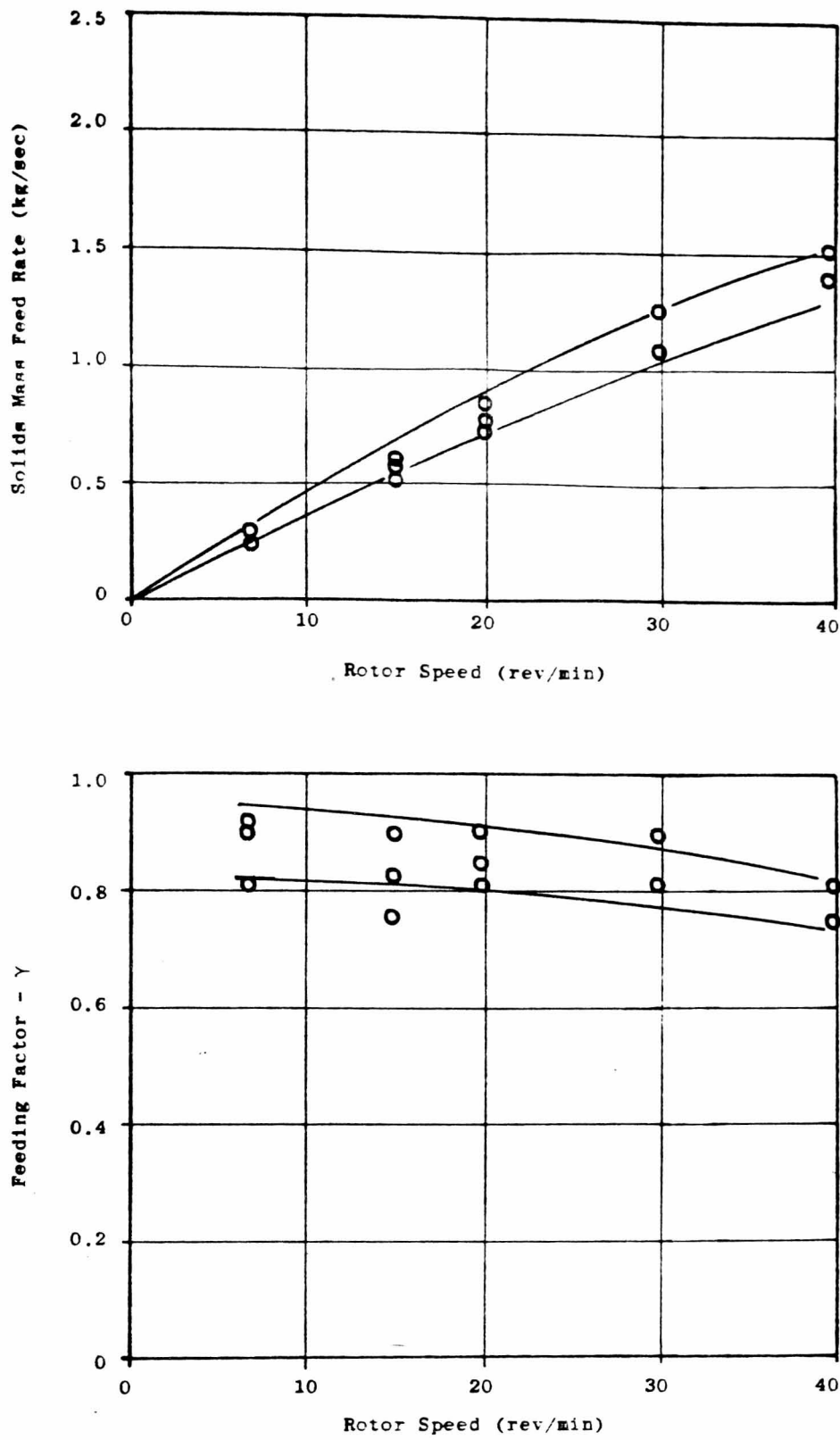
Figure 7.39 Feeding Characteristics of Polyethylene Powder
          with Drop-Out Box F and Rotary Valve Orientation c.
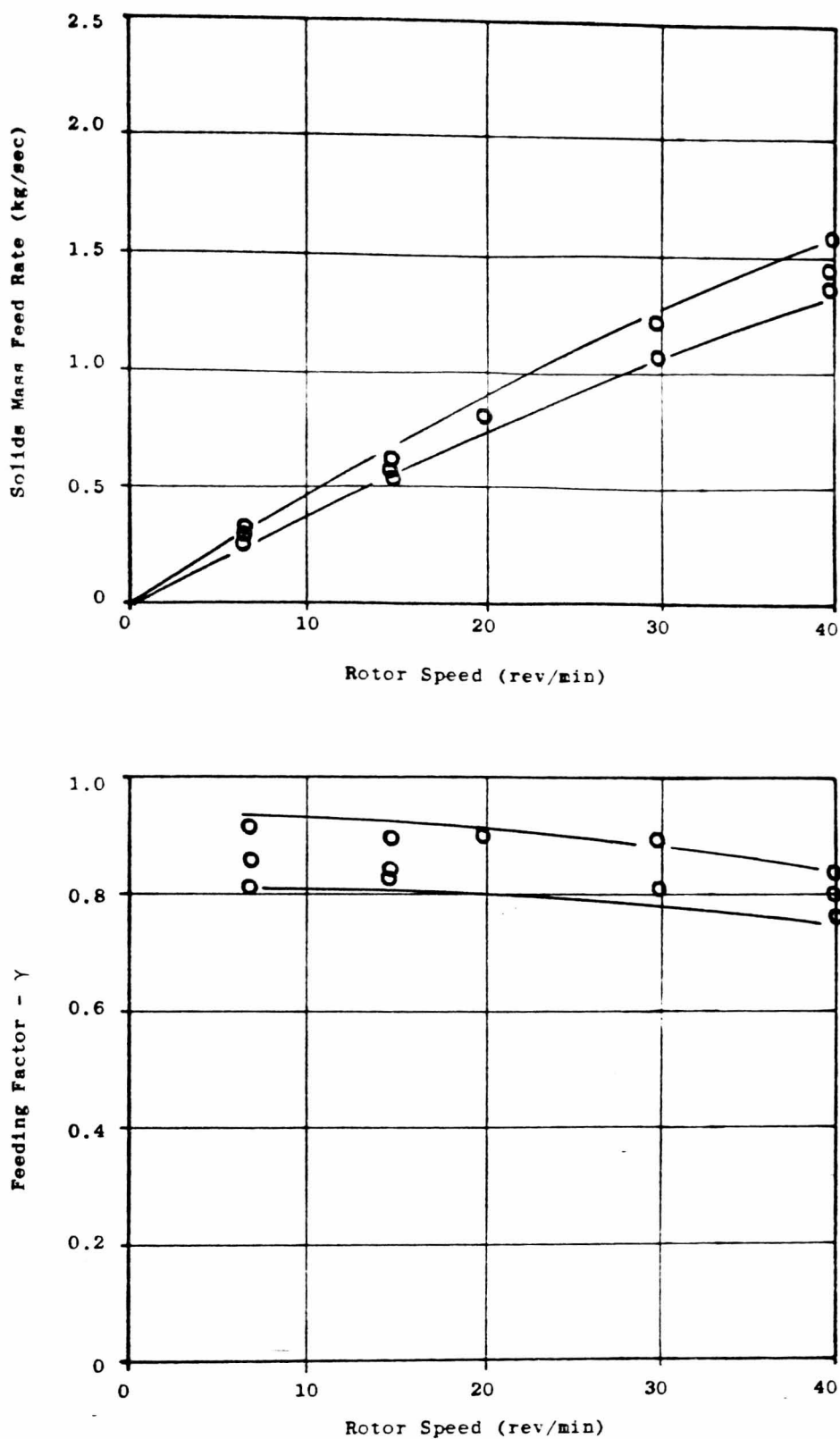
Figure 7.40 Feeding Characteristics of Polyethylene Powder
with Drop-Out Box G and Rotary Valve Orientation c.
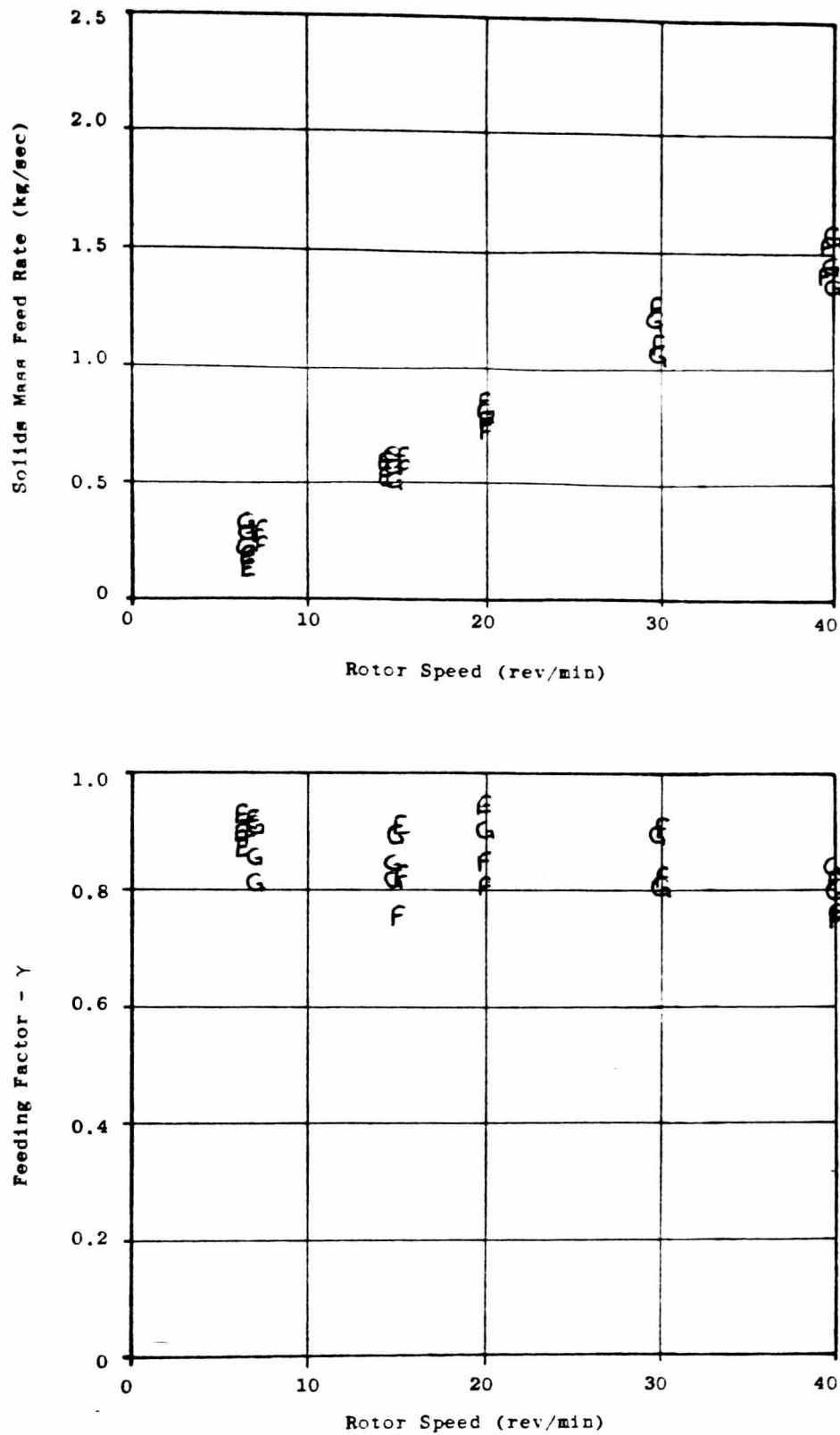
Figure 7.41 Feeding Characteristics of Polyethylene Powder.
Comparison of the results obtained with Drop-Out
Boxes E, F and G.

volume, the actual difference in performance is less than expected.
Equation 4.9, which is the model proposed for determining the entrain-
ment efficiency of a given combination of valve and drop-out box (η_e),
gives the value of η_e for box B as 77% and for box D as 93%; that is,
a 16% difference. This discrepancy is undoubtedly due to the over
simplistic decisions made to derive this model.

$$\eta_e = \frac{\nu_b}{\nu_p + \nu_b} \; 100\% \qquad\qquad (4.9b)$$

The results of the second set of experiments with the Wheat Flour
are presented in Figures 7.26 to 7.29. These show respectively the
individual performances obtained with drop-out boxes A, B and C and
their comparative performances. From Figure 7.29 it is clear that the
throughputs obtained with drop-out boxes B and C were similar and
significantly better than those obtained with box A, particularly at
high rotor speeds. However, as with the comparison between boxes
B and D, the differences in performance were not in the same proportion
as the entrainment efficiencies of these configurations calculated from
equation 4.9.

Similar results were obtained with drop-out boxes A, B and C when
Cement was used as the test material, see Figures 7.30 to 7.33. As
with the flour, the largest throughput was obtained with box C, but
there was no significant difference betwen the performance of boxes
A and B.

The results obtained with the Polyethylene Powder are presented in
Figures 7.34 to 7.40. As with the results for the Wheat Flour and
Cement, these show that increasing the volume of the drop-out box by
increasing the depth did lead to a small improvement in throughput
over the range of rotor speeds examined. This is shown most clearly
by Figure 7.37 which compares the performance of the system with drop-
out boxes A, B and D.

In view of these findings it is interesting to look at the results
obtained for the Polyethylene Powder with drop-out boxes E, F and G;
that is, Figures 7.38[*], 7.39 and 7.40 respectively. Each of these boxes

* footnote: Results were only obtained for a limited range of rotor
             speeds with drop-out box E because of its tendency to
             become choked. This point will be discussed further in
             section 7.4.

are the same depth but different internal volumes as shown by Figure
7.15. Thus, they provide a means of assessing how the throughput of
the system is affected by changing the volume of the drop-out box with-
out also changing the box depth. Figure 7.41, which compares the
feeding factor characteristics obtained for boxes E, F and G, clearly
shows that the performance of the system with each of these boxes was,
in all practical respects, identical.

The only reasonable conclusion to draw from these results is that,
for Polyethylene Powder, the depth of the drop-out box is a more
important parameter with regard to entrainment than the volume of the
drop-out box. This is consistent with the argument that the gravitational
force acting on the particles in the drop-out box is significant; which
was the supposition proposed to explain the results obtained with both
Polyethylene Pellets and Singles Coal.

To provide further information about the effect of the depth and
volume of the drop-out box on system performance, the experiments
conducted with the Polyethylene Powder were repeated with the
Pulverised Coal. However, unfortunately the pocket filling characteristics
restricted the throughput which could be achieved with this material and
thus prevented any meaningful comparison of the performances obtained with
the different drop-out boxes. Despite this the results are presented in
Figures 7.42 to 7.47 becuase they do highlight the importance of consider-
ing every aspect of the design of a rotary valve feeding system. They
also justify the inclusion in Chapter 4 of the model for estimating the
effect of air leakage on the pocket filling characteristics of a rotary
valve.

In conclusion, the results presented in this section show that:

i)   for coarse particle products the depth and volume of the
     drop-out box are not significant parameters with regard
     to entrainment; and

ii) for fine particle products, increasing the volume of the
     drop-out box by increasing its depth leads to a general
     improvement in throughput.

Furthermore, there is evidence which suggests that the depth of the
drop-out box is a more important parameter than the volume in maximising
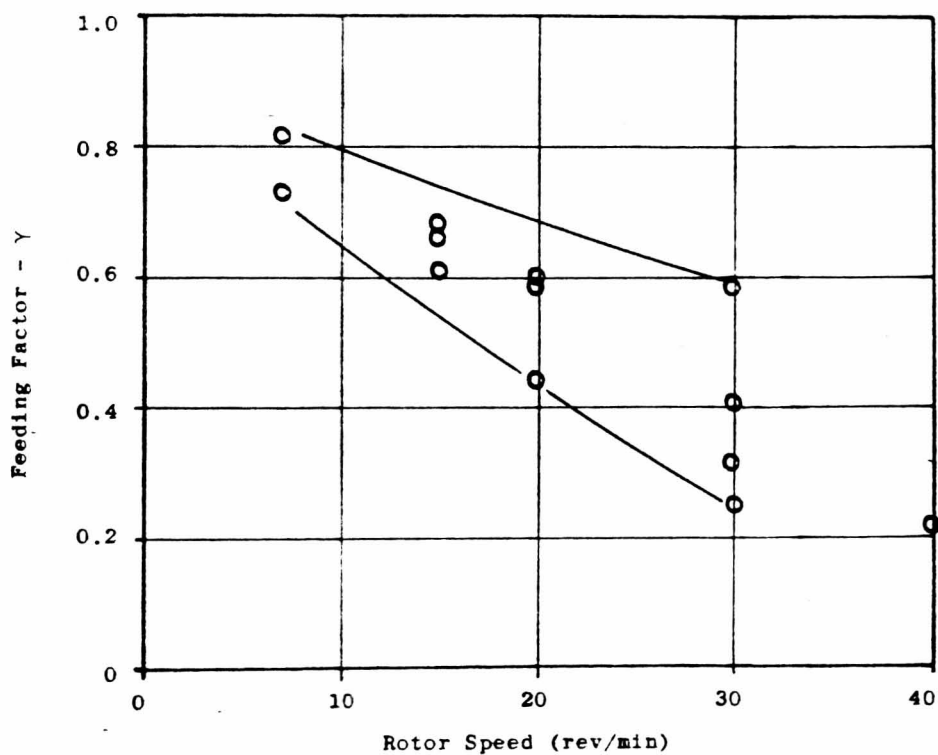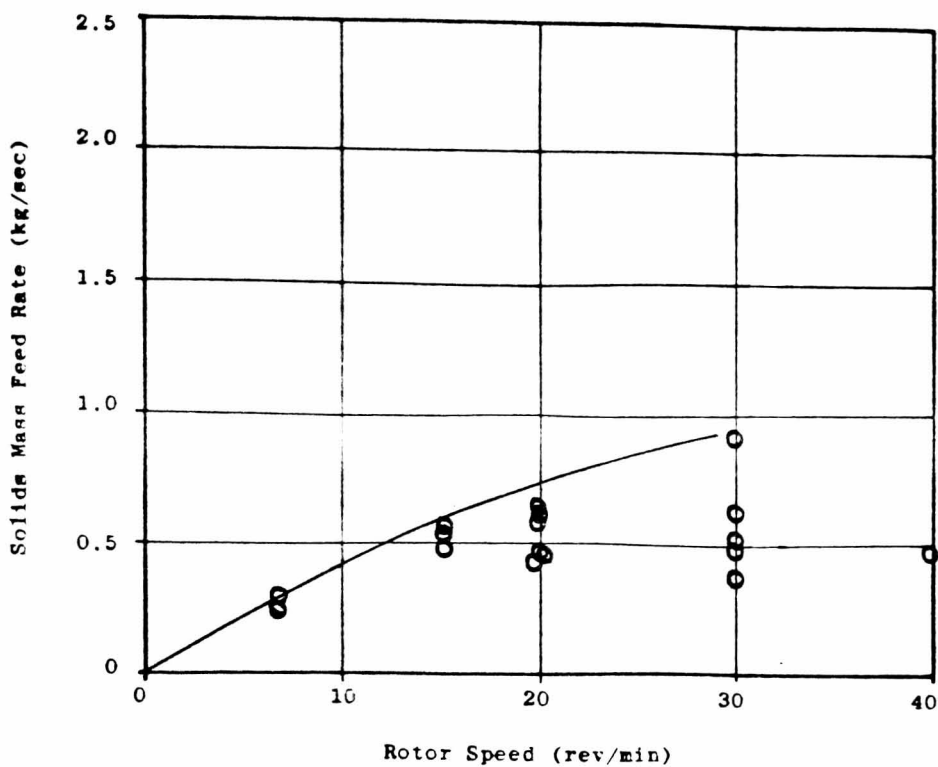
Figure 7.42   Feeding Characteristics of Pulverised Coal
              with Drop-Out Box A and Rotary Valve Orientation c.
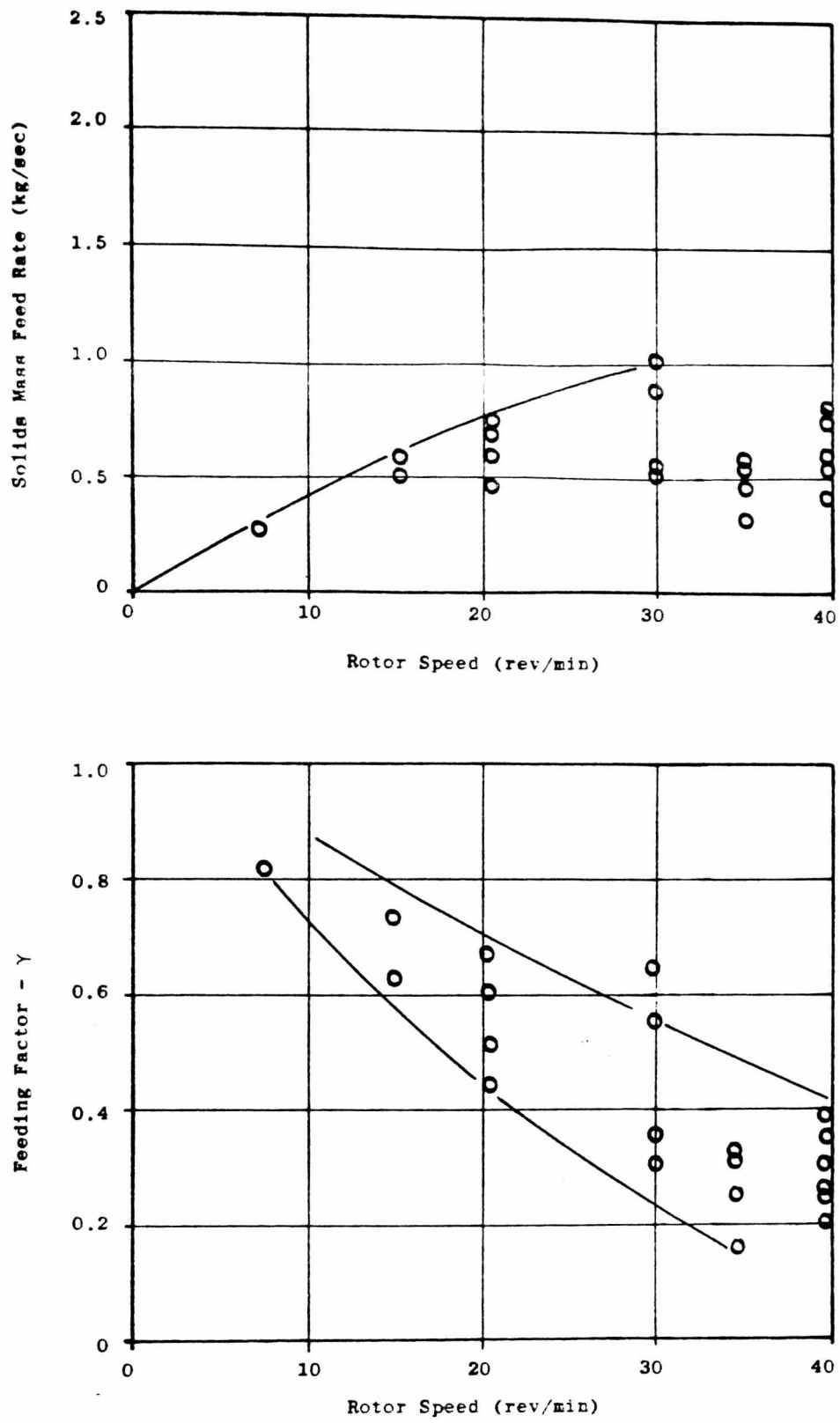
Figure 7.43 Feeding Characteristics of Pulverised Coal
with Drop-Out Box B and Rotary Valve Orientation c .
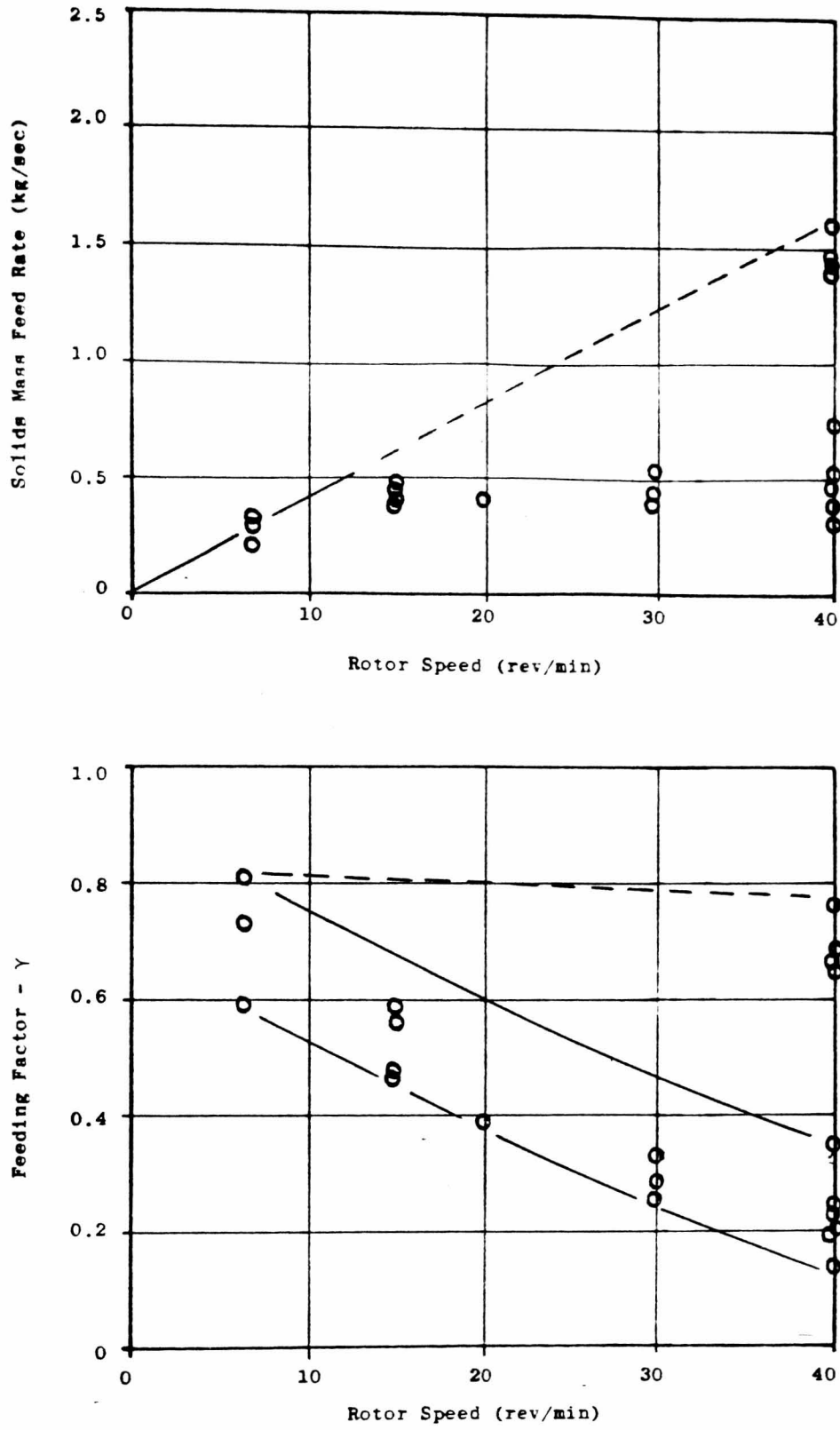
Figure 7.44 Feeding Characteristics of Pulverised Coal
           with Drop-Out Box D and Rotary Valve Orientation c.
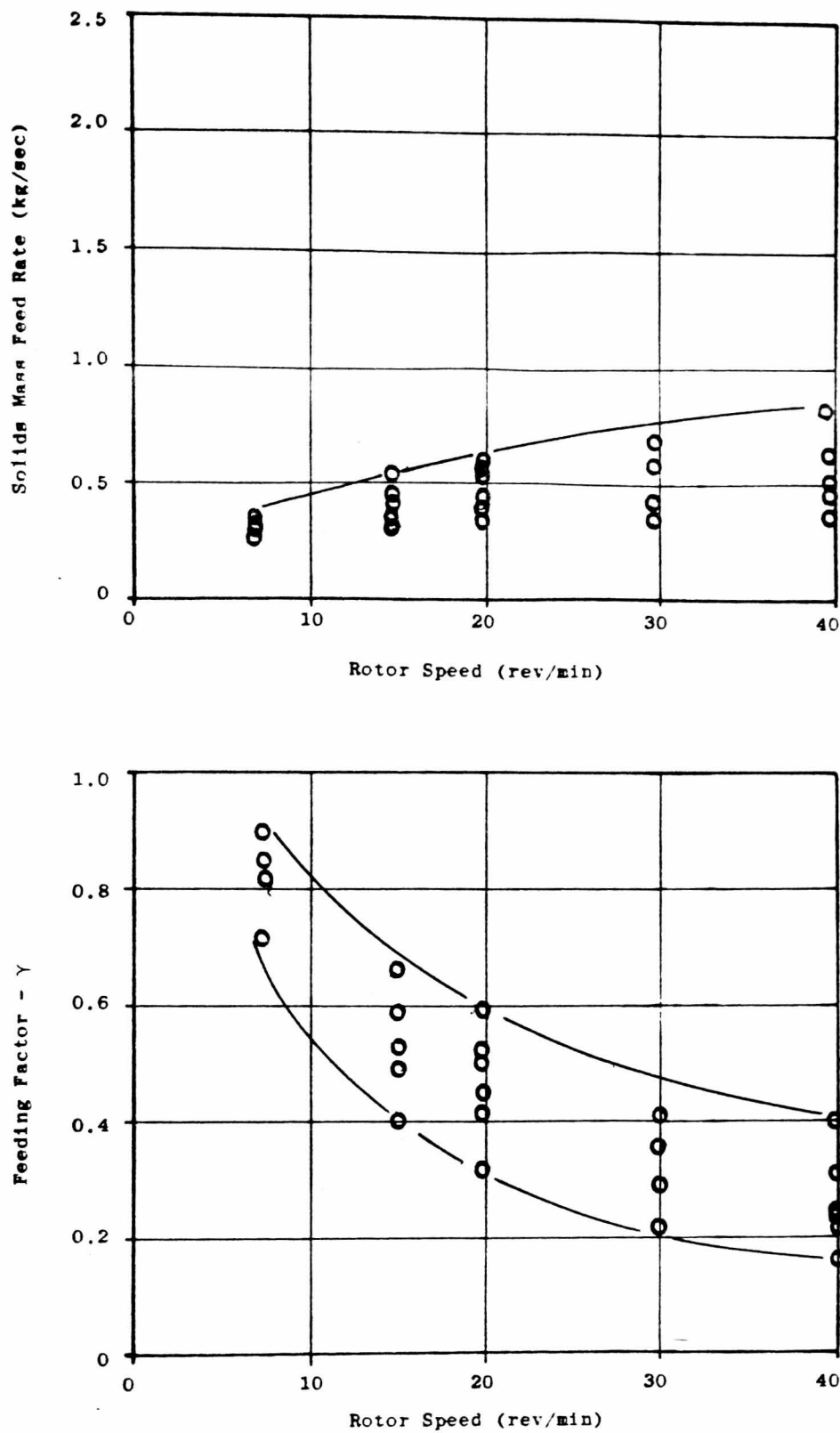
Figure 7.45 Feeding Characteristics of Pulverised Coal
            with Drop-Out Box E and Rotary Valve Orientation c.
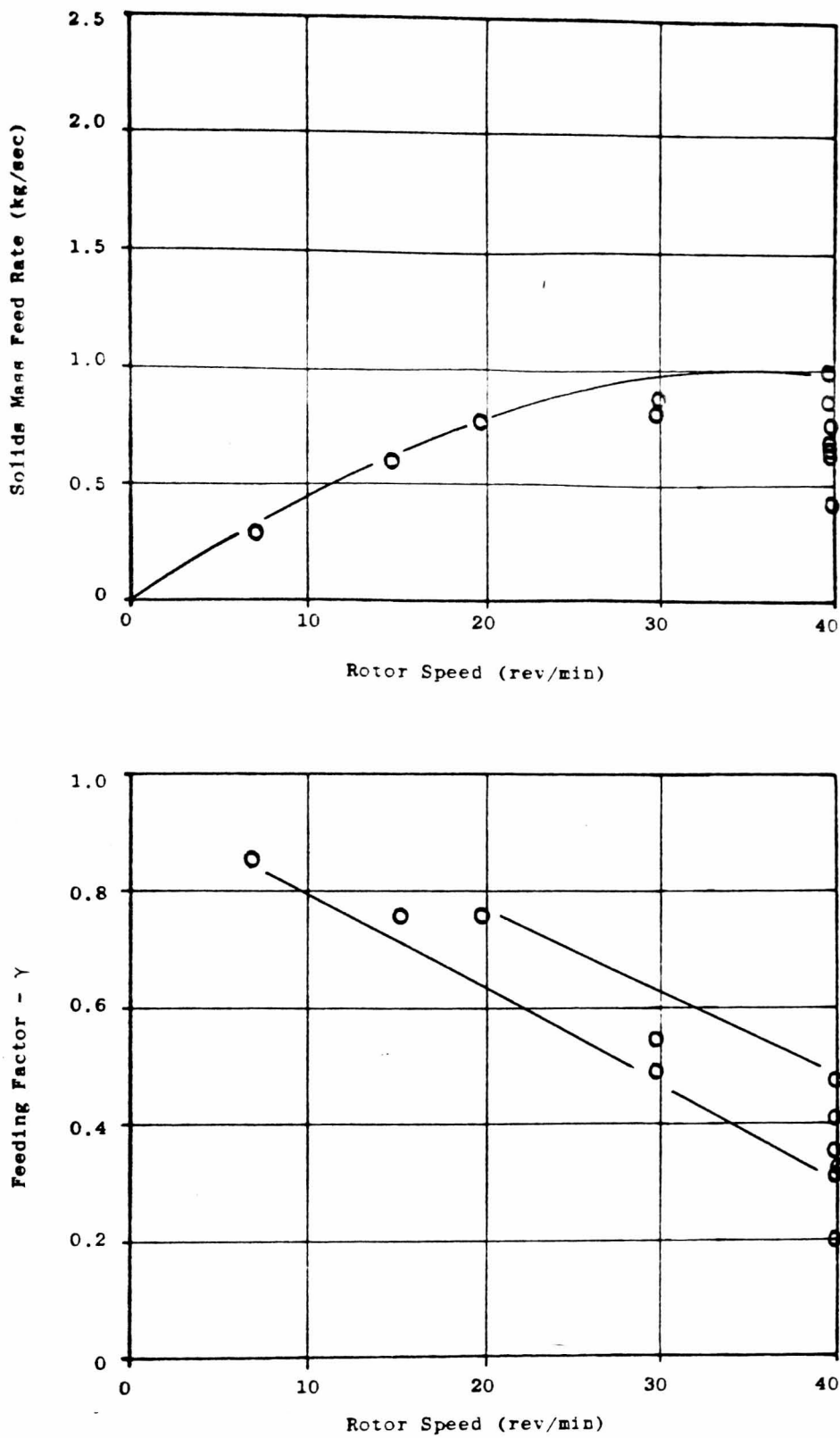
Figure 7.46 Feeding Characteristics of Pulverised Coal
         with Drop-Out Box F and Rotary Valve Orientation c.
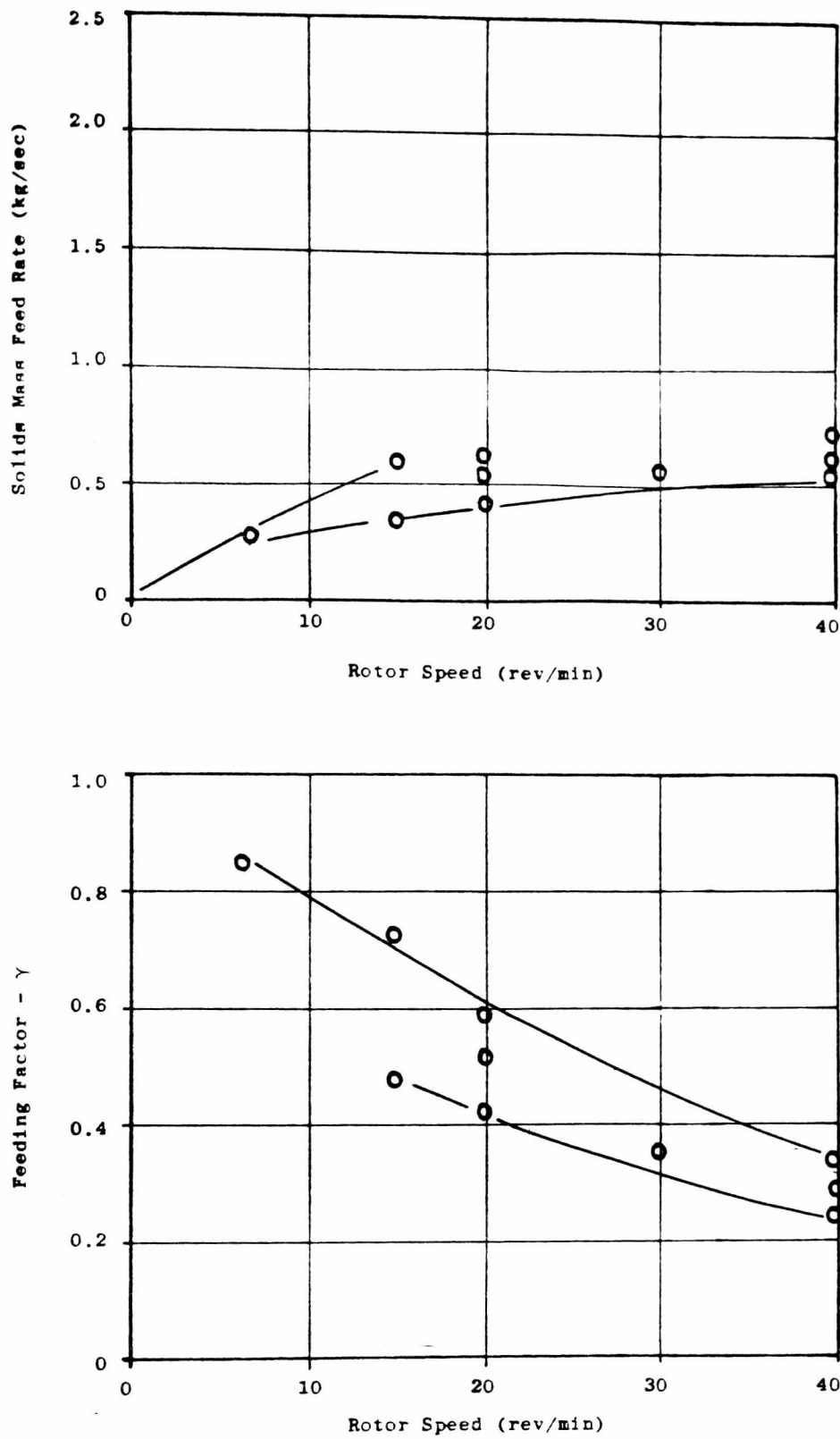
Figure 7.47 Feeding Characteristics of Pulverised Coal
with Drop-Out Box G and Rotary Valve Orientation c .

the entrainment efficiency. Also, it is evident from the results that
the model proposed in Chapter 4 for estimating the entrainment efficiency
of a given combination of rotary valve and drop-out box, does not
accurately predict the difference in throughput obtained with different
drop-out boxes. A more accurate model would need to take account of
the characteristics of the material being handled as well as the geometry
of the rotary valve and drop-out box. However, it is difficult to see
how this could be done and any such model would certainly be very
complicated.

In view of these difficulties it is suggested that the most practical
approach to the design of a pneumatic conveyor is to make the depth and
volume of the drop-out box as large as is possible within the constraints
of the system. The results of this work suggest that the normal
transition shaped drop-out box between two and three pipe diameters in
depth is adequate for most materials.

7.4 Investigation of the Choked Flow Condition

7.4.1 Purpose of Experiments

The purpose of the experiments described in this section was to investigate the choked flow condition which had been observed previously in the flow visualisation rig. It was considered important to ascertain whether or not choking is likely to occur in conventional industrial systems and, if so, to quantify the consequences of this with regard to overall system performance. In addition, data was needed to assess the ideas and model proposed in Chapter 4 for determining the conditions likely to lead to choking. These were based upon the supposition that choking occurs because material is held up inside the drop-out box by an air swirl[*] which is induced by the conveying airstream. The development of this led to the concept of a critical pick-up velocity at which the transfer of energy to the mixture of air and solids within the drop-out box is just sufficient to hold the solids in suspension (V_c). The following expression was proposed for evaluation (V_c) for any given combination of rotary valve, drop-out box and material:

$$V_c = C_c P_c (\rho_b / \rho_a)^{\frac{1}{2}}$$

(4.21c)

where ρ_b and ρ_a are respectively the poured bulk density of the material and the air density in the drop-out box chamber; P_c is the 'critical peripheral velocity' which is a function of the drop-out box size and shape; and C_c is a dimensionless constant requiring empirical evaluation. One of the reasons for the experiments described here was to determine typical values for the constant C_c and thus allow equation 4.21c to be used for predicting the value of V_c for similar entrainment configurations.

7.4.2 Experimental Plan and Method

The experimental plan was to see if choking occurred during the experiments described in sections 7.2 and 7.3, and if so, to investigate each occurence more thoroughly. This was argued to be the best approach because these experiments covered the range of conveying conditions

* footnote: Evidence for the existence of this air swirl was reported
             in Chapter 3.

normally used in industrial systems.   Hence, if choking was found to occur, it would be reasonable to assume that it could be a genuine industrial problem and hence worthy of further investigation.

As a result of using this procedure two of the test materials were found to choke in the conventional transition shaped drop-out boxes; these were the Wheat Flour and the Polyethylene Powder.   Having established this, further experiments were conducted to investigate specifically the phenomenon of choking.   To do this the system was operated at a fixed rotor speed and the pick-up velocity was increased gradually until the drop-out box became choked.   During this procedure the conveying conditions were monitored regularly and the output from the load cells was recorded continuously on a chart recorder.   This permitted the change in feed rate to be identfied when the drop-out box became choked.   A typical trace from the chart recorder is shown in Figure 7.48; this was obtained for the Wheat Flour being handled in drop-out box B at a valve rotor speed of 30 rev/min.   After repeating this procedure several times in order to obtain sufficient data and confidence in the repeatability of the results, the experiment was repeated at other valve rotor speeds.   As with the previous work, rotor speeds of 7, 15, 20, 30 and 40 rev/min were used.

Drop-Out Box B   Wheat Flour

$\dot{m}_s = 0.386$ kg/s; $V_{pu} > 35$ m/s

$\dot{m}_s = 0.835$ kg/s; $V_{pu} < 35$ m/s

CHOKED FLOW

Change of Feed Rate

NON-CHOKED FLOW

n = 30 rev/min

Mass Conveyed (3.71 kg/mm)

Time (10mm/min)
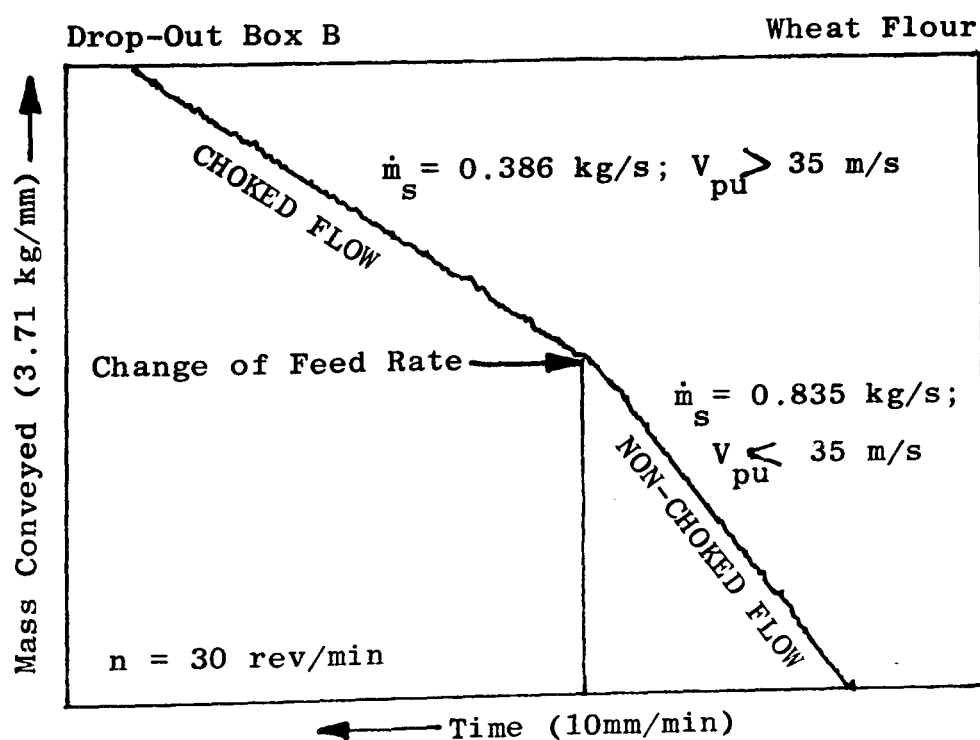
Figure 7.48 A Typical Chart Recorder Trace of the Load Cell Output.

The data obtained by this method were used to plot graphs showing the relationship between the feeding factor (γ) and the pick-up velocity $(V_{p.u.})$ for each combination of rotary valve, drop-out box and test material at each of the five set rotor speeds. It was reasoned that these graphs would provide a means of determining the actual values of V_c which could be used to evaluate the coefficient C_c in equation 4.21c.

In parallel with this work the nature of the air and solid flow patterns inside a drop-out box, just before and just after choking, were investigated. To do this one of the drop-out boxes was fitted with Perspex Windows. A photograph of this drop-out box is shown in Figure 7.49.

7.4.3 Visual Observations of the Entrainment Process

It has already been stated that choking was only found to occur with the Wheat Flour and Polyethylene Powder, and even this only happened when the simple transition shaped drop-out boxes A, B and C were used. Of these, box B probably represents the most common type of drop-out box in current industrial use. Consequently, the drop-out box fitted with Perspex windows was made to the same dimensions as this, see Figures 7.2 and 7.49.

Figure 7.50 shows a series of graphs which represent the feeding characteristics typically obtained with drop-out boxes A, B and C for the Wheat Flour and Polyethylene Powder. When conveying at the conditions represented by point A on these graphs the flow pattern was very complicated. The swirling motion previously seen in the flow visualisation experiments* was present, but difficult to see because of the large quantity of material in the drop-out box chamber. The most significant feature of the flow for these conditions was that the material and air were thoroughly mixed and there were no air pockets or regions of stagnant material. An illustration of this flow pattern is shown in Figure 7.51a.

Changing the conditions to those represented by point A' did not alter the flow pattern or feed rate. The flow pattern also remained the same when the feed rate was increased by increasing the rotor speed to follow the path A to B. The only noticeable change was the denser nature of the flow as a result of the higher solids loading ratio

* footnote: See Chapter 3.
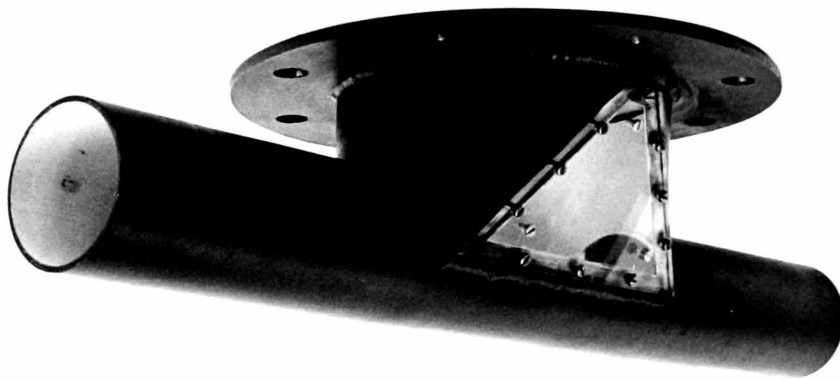
Figure 7.49 Photographs of the Drop-Out Box fitted
with Perspex windows.
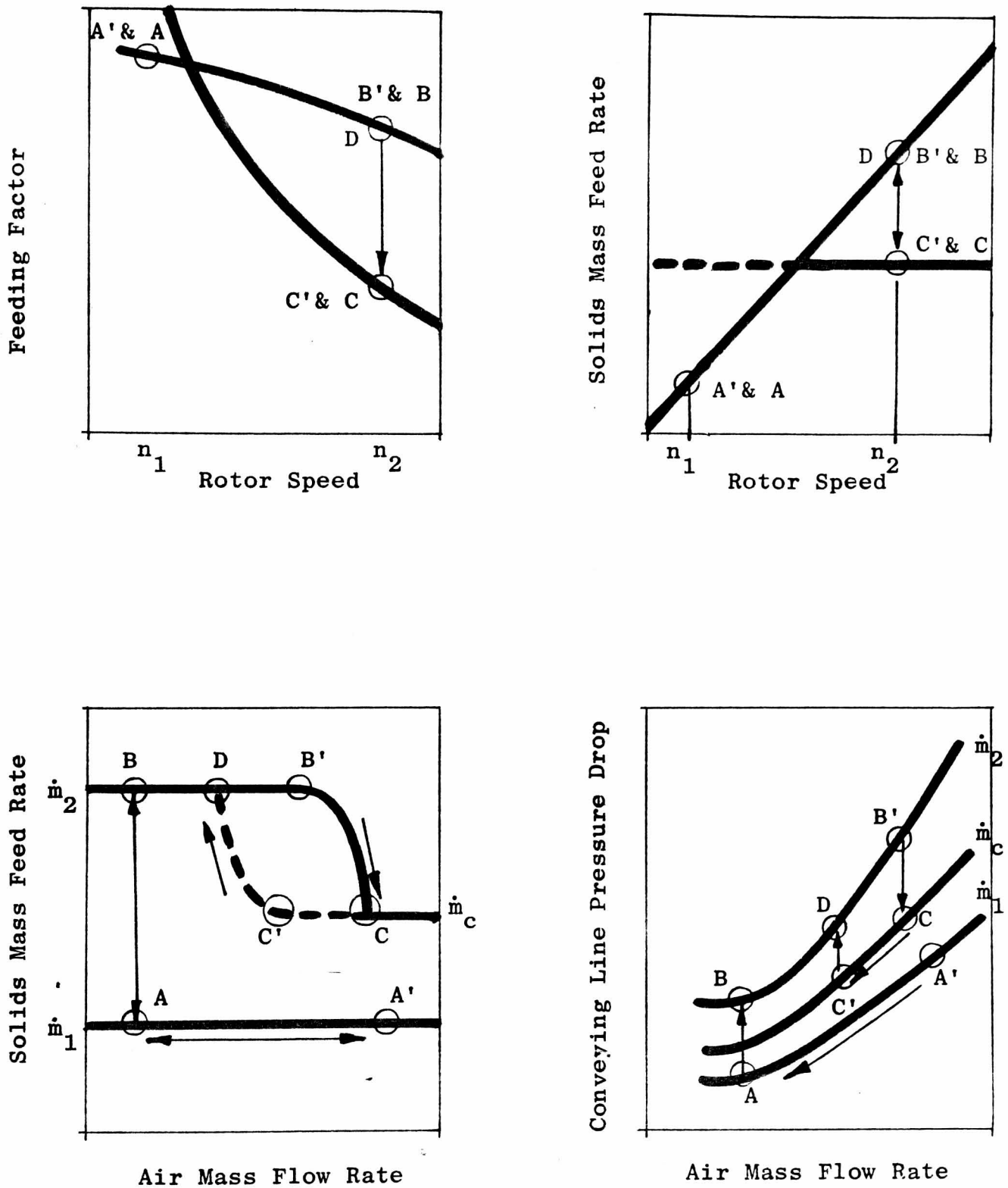
Figure 7.50 Diagrams illustrating the choked feed conditions.

PERSPEX OBSERVATION WINDOW

AIR IN

AIR + SOLIDS
OUT

Turbulent mixing of
air and solids

NORMAL FLOW PATTERN

Hardly any mixing of the
air and solids in this
region of the drop-out
box.

CHOKED FLOW PATTERN

Material arches over
conveying air.Entrainment
isachieved by arched layers
breaking down into airstream.

CHOKED FLOW PATTERN ON X-X
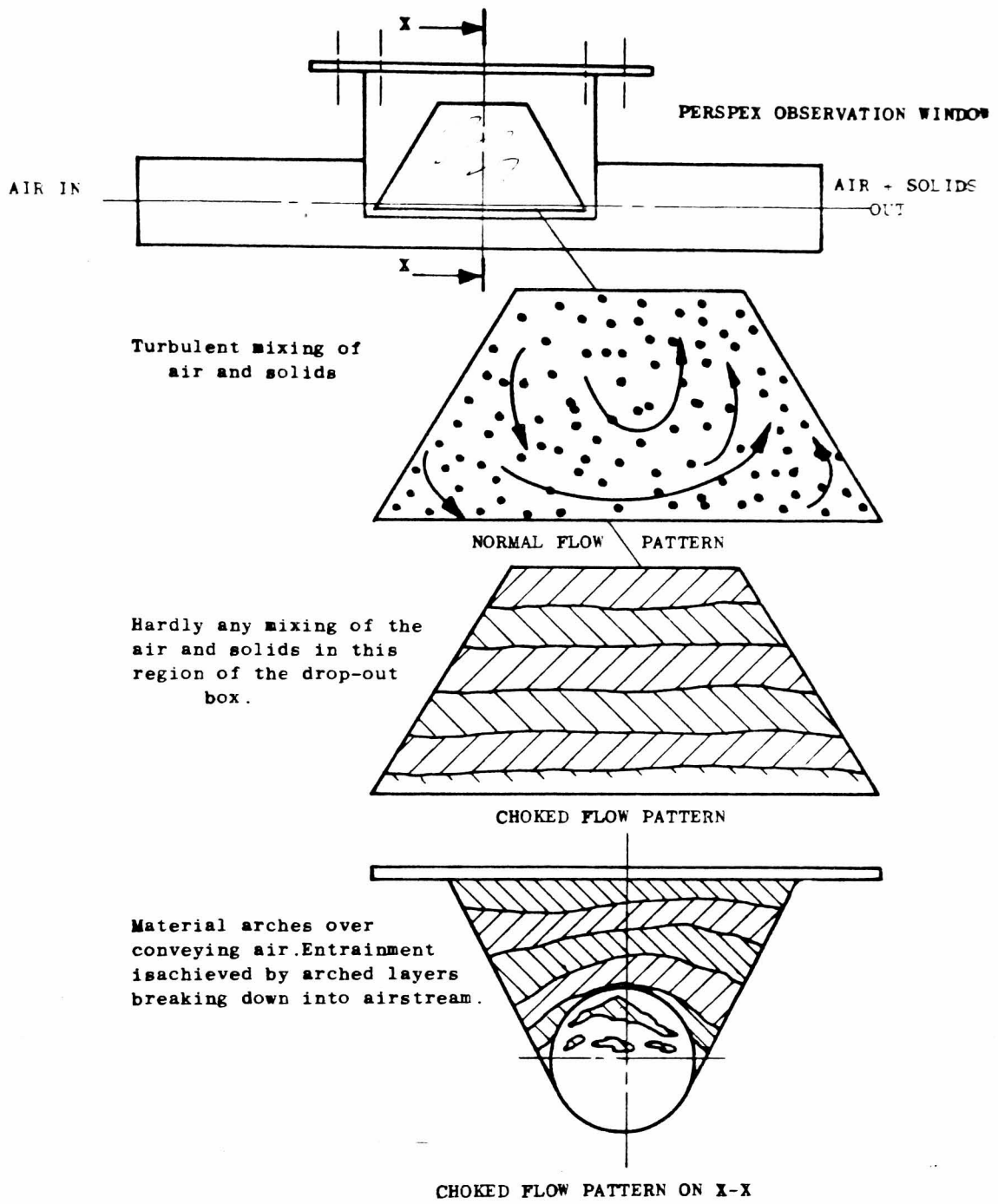
Figure 7.51 Flow Patterns Observed in the Drop-Out Box Chamber.
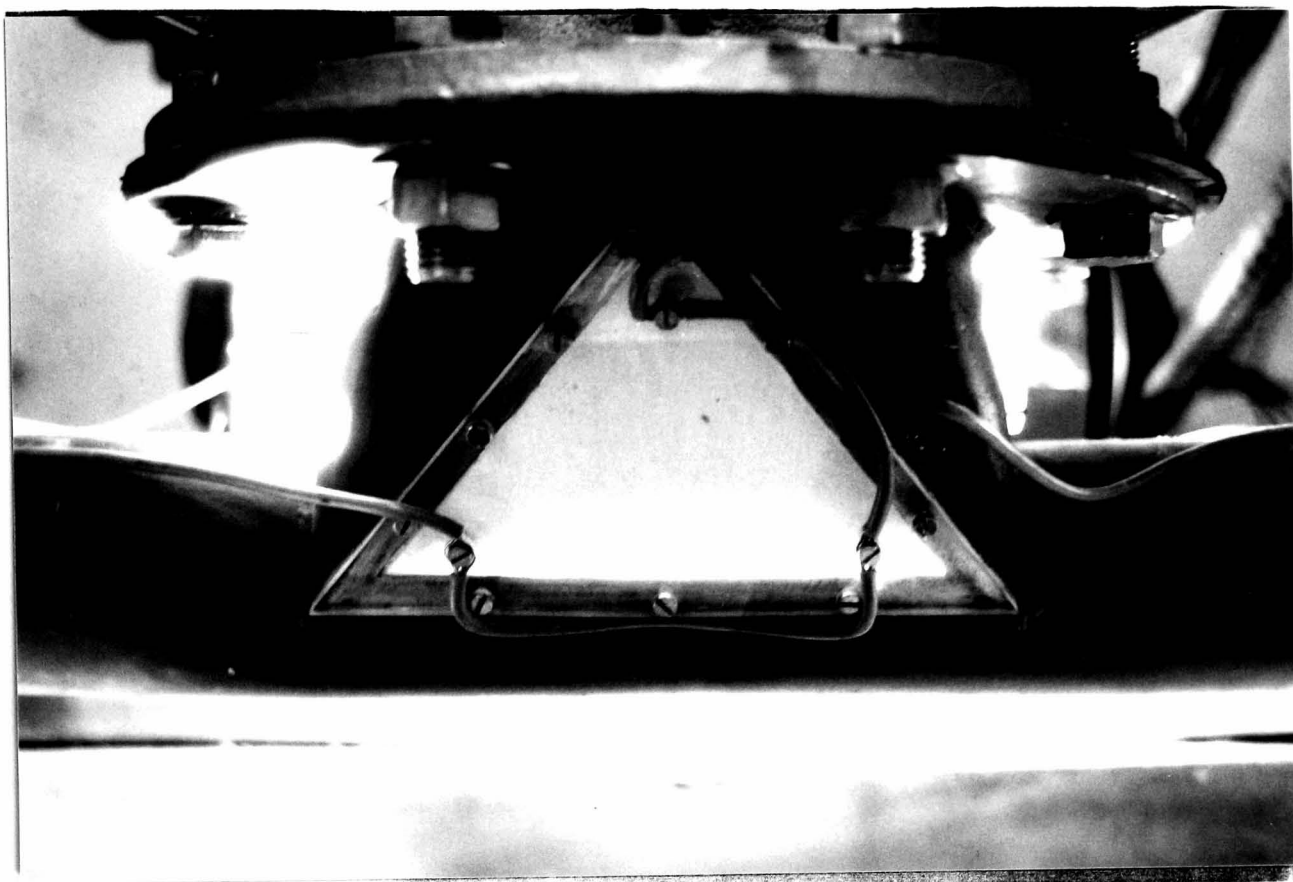
Figure 7.52 Photograph of the choked flow condition.
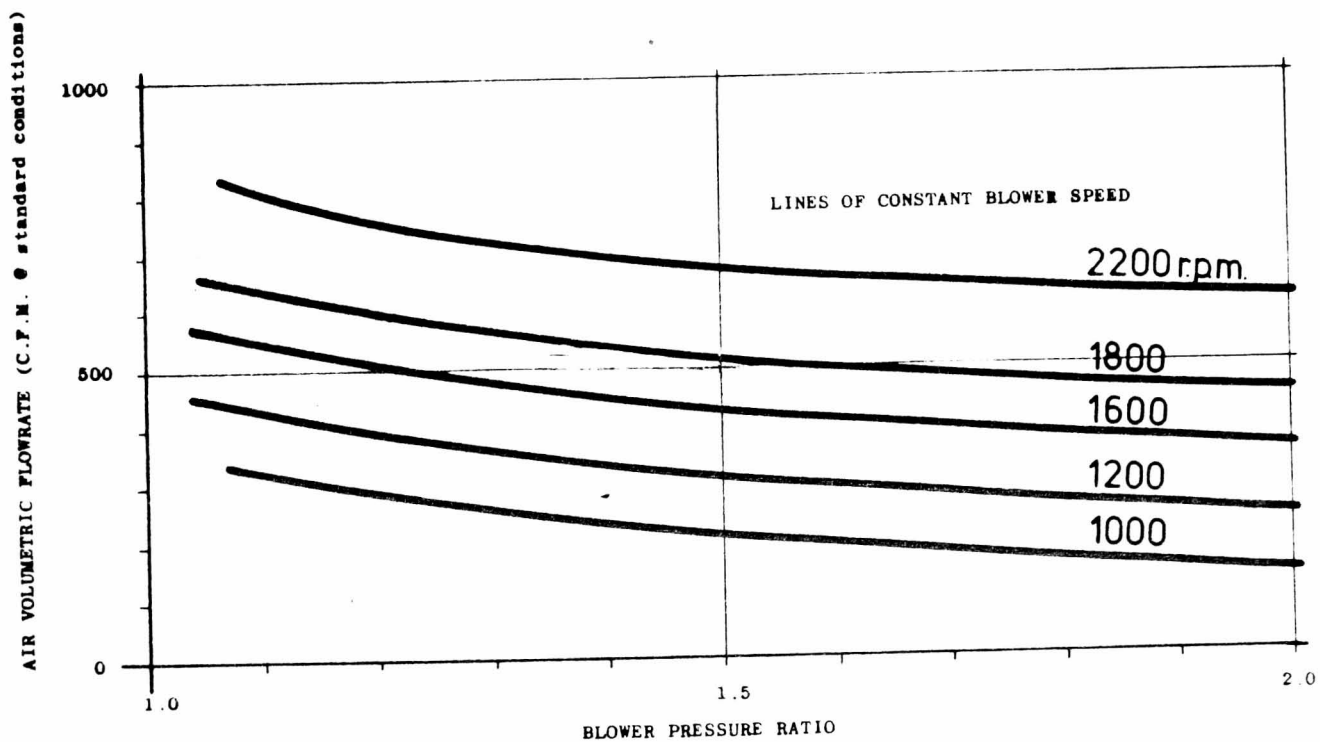
Figure 7.53 Performance Characteristics of a'Roots' type blower.

$(\dot{m}_s/\dot{m}_a)$.   However, when the air mass flow rate $(\dot{m}_a)$ was increased from initial conditions at point B to follow the path B-B'-C then changes were observed in both the flow pattern and the solids feed rate.   From B to B' there was no change, but increasing $\dot{m}_a$ a small amount further caused the conditions to change to those represented by point C.   When this happened a new stable flow pattern was established in the drop-out box chamber; that is, the choked flow condition previously observed in the flow visualisation rig.   This change in conditons occurred within a second or so, as indicated by the specimen chart recorder trace reproduced in Figure 7.48.

In contrast to the highly turbulent flow that was seen before, the drop-out box became choked with material and there was very little mixing, particularly in the top half of the box chamber, see Figure 7.51b. The conveying air appeared to tunnel underneath the material which formed a stable arch between the inside surfaces of the drop-out box, as shown in Figure 7.51c.   Subsequently the method of entrainment was for material to fall away from the underside of the arch into the conveying airstream.   This always resulted in a reduced solids feed rate, as shown by Figure 7.50.   In this condition the geometry of the drop-out box and the characteristics of the material dictated the feed rate and not the rotary valve speed.

Figure 7.52 is a photograph of the flow pattern in the drop-out box in the choked condition · in this particular case the material being handled was Wheat Flour and the pick-up velocity was approximately 40 m/s.   From this it can be seen that the material is being held in the top half of the drop-out box.   This situation could be considered analogous to that of a hopper outlet in which a stable arch has formed.   However, it is more complicated than this because the air beneath the arch in the drop-out box is not static.   Also, the reasons for the arch forming are not clear, but the most probable are that it is held in place by the leakage air which percolates through it and subsequently, through the internal clearances of the valve; and/or it is held in place by interparticulate forces.

An explanation for the arching may be obtained by considering the behaviour of the system in the choked condition.   In all cases it was found that the choked condition was very stable and there was no tendency

for the system to revert back to the turbulent mode of entrainment, as illustrated in Figure 7.51a. In order to make the system return to the turbulent mode of entrainment the air mass flow rate had to be reduced to below that which was needed for the initial change to the choked condition. This is shown by the path C-C'D on Figure 7.50.

From this and the previous observations it is clear that the air mass flow rate is an important factor in determining the mode of entrainment which will prevail. The two parameters which vary significantly with the air mass flow rate and which are most likely to affect the entrainment process are the pick-up velocity of the conveying airstream and the pressure of the air in the drop-out box.

The pressure of the air in the drop-out box will almost certainly influence the performance of the feeding system because, as discussed in Chapter 2 and 3, the difference between this and the pressure at the inlet side of the rotary valve causes a leakage of air through the valve clearances. Both Jotaki & Tomita (10, 12, 13 & 53) and Reed (11) have demonstrated that this leakage can affect the flow of material into the rotor pockets and, in Chapter 4 of the present study a model was proposed for estimating this effect. However, with regard to the entrainment process, it seems unlikely that air leakage is the cause of choking or is responsible for maintaining the arch of material in the drop-out box. To explain this it is necessary to consider the conveying characteristics shown in Figure 7.50 and the performance characteristics of the Roots-type blower given in Figure 7.53.

From the conveying characteristics it can be seen that for a given air mass flow rate the conveying line pressure drop (ΔP_ℓ), and hence the pressure difference across the rotary valve, will decrease if the solids mass flow rate is decreased. This point is important because of its implication with regard to the response of the Roots-type blower to a step change in solids feed rate, such as that which occurs when a drop-out box chokes. For a fixed operating speed these machines have a relatively flat relationship between volumetric air flow rate and pressure ratio. Therefore, when the drop-out box chokes and the solids feed rate reduces, the air flow rate will remain approximately the same. Consequently, the conveying line pressure drop will then reduce and so will the pressure difference across the rotary valve.

Now, if it was a high air leakage, resulting from a high pressure difference, which initially caused the drop-out box to choke, then it would be logical to expect the system to revert back to the turbulent mode of entrainment as soon as the pressure difference reduces. Since, the above analysis shows that the pressure difference will reduce when the drop-out box chokes, this would lead us to expect the solids feed rate to hunt between two levels, as indicated by the diagram shown in Figure 7.54. However, the experimental observations shows that this does not happen and that the performance of the system in the choked condition is stable. Consequently, it is reasonable to conclude that choking is not a result of the pressure change in the drop-out box when the air mass flow rate is increased; and that air leakage cannot be solely responsible for maintaining the arch of material which forms when the drop-out box chokes.

The implication of this conclusion is that the pick-up velocity of the conveying air must be the factor which determines the mode of entrainment, because it is the only other parameter which varies siginificantly with the air mass flow rate. This agrees with the interpretation of the results obtained from the flow visualisation rig which were discussed in Chapter 3 and justifies the approach used in Chapter 4 for developing a model which could be used to predict the minimum pickup velocity at which choking can occur (V_c). In the following section the experimental results relating to the choked condition are analysed in order to obtain actual values of V_c. These results are used to explain why choking did not occur with all the materials that were tested.

However, before examining the results in detail, the following general observations are made about the solids feed rate corresponding to the choked condition. These help to explain the distribution of data points on the graphs presented in Figures 7.56 to 7.71 which relate the solids mass feed rate $(\dot{m}_s)$ to the valve rotor speed (n) and the feeding factor (γ) to the valve rotor speed (n).

The experiments showed that the solids feed rate in the choked condition was always the same for any given combination of drop-out box and material. Furthermore, this was completely independent of the initial solids feed rate that was obtained before choking occurred. This

indicates that the solids feed rate in the choked condition was primarily dependent on both the characteristics of the material being handled and the geometry of the drop-out box. If this is accepted then curves representing the solids feed rate of a drop-out box in the choked condition, the 'choked feed characteristics', can be superimposed on the feed rate and feeding factor characteristics of a rotary valve in order to determine the combined performance of that particular rotary valve and drop-out box. An example of this is shown in Figure 7.55. From this it can be seen that the choked feed characteristic is a straight horizontal line on the feed rate - rotor speed graph and a curve on the feeding factor - rotor speed graph. For operating conditions which correspond to points below the choked feed characteristics, the choked condition cannot occur because the potential feed rate of the rotary valve is less than the choked feed rate of the drop-out box. However, for operating conditions corresponding to points above the choked feed characteristics the choked condition can occur. Whether or not it does depends on the magnitude of the pick-up velocity.

The observations suggest that if the pick-up velocity is less than the minimum needed to cause choking (V_c), then the system will operate at conditions corresponding to a point on the rotary valve characteristics. Consequently, the feed rate will then be proportional to the valve rotor speed. Alternatively, if the pick-up velocity is higher than V_c the drop-out box will choke and the resulting operating conditions will correspond to a point on the choked feed characteristic.   The results presented in Figures 7.56 to 7.71 show the data points to be concentrated in bands corresponding to the shapes of the rotary valve characteristics and drop-out box choked feed characteristics proposed in Figure 7.55.

7.4.4 Analysis and Discussion of Results
The results presented in Figures 7.56 to 7.59 and 7.68 to 7.71 show respectively the performance of the system with Wheat Flour and Polyethylene Powder for each of the three rotary valve orientations shown in Figure 7.1. Drop-out box B was used in each case. From these figures it can be seen that the choked feed characteristics of this drop-out box were not affected by the orientation of the rotary valve. This result is consistent with the conclusion that the choked feed
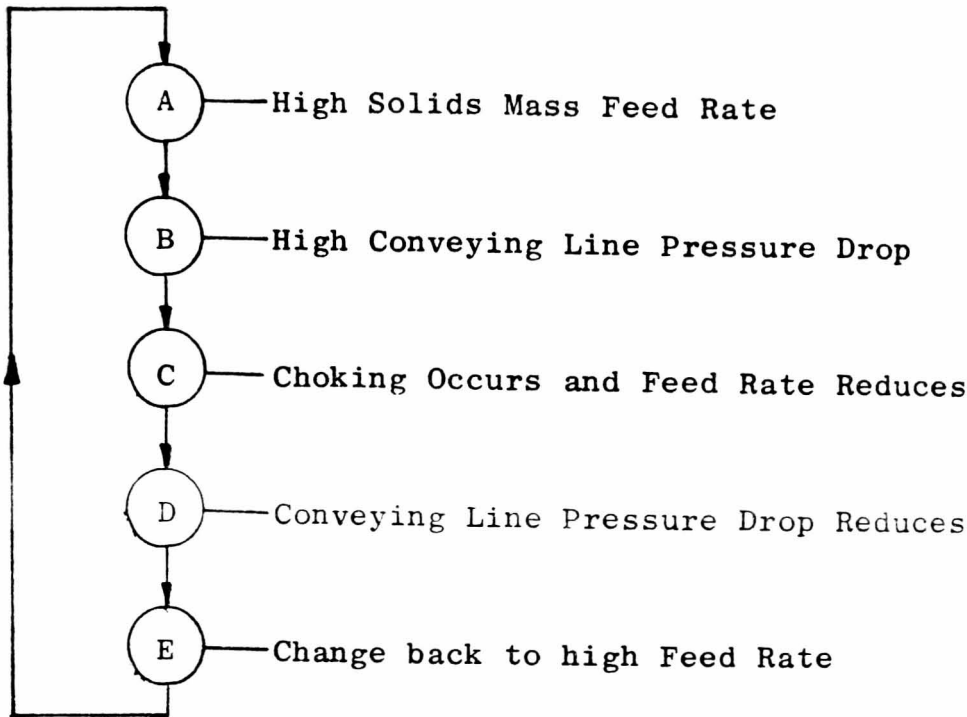
Figure 7.54 Diagram to illustrate Hunting of the Feed Rate.
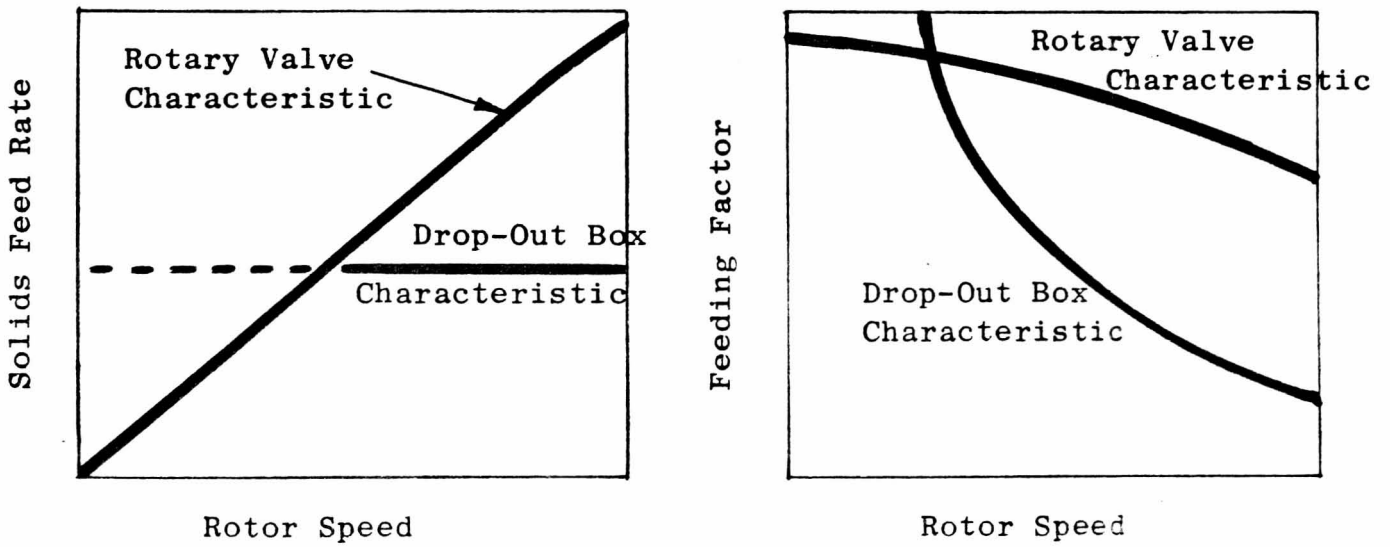
Figure 7.55 The Drop-Out Box Characteristics Overlayed on the
Rotary Valve Characteristics.
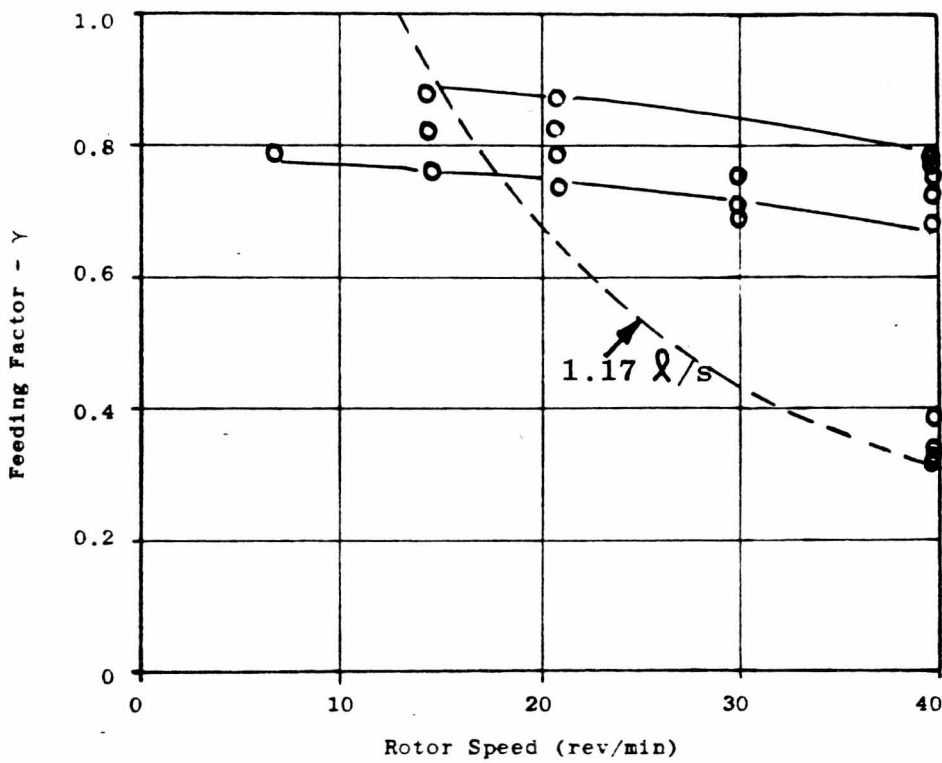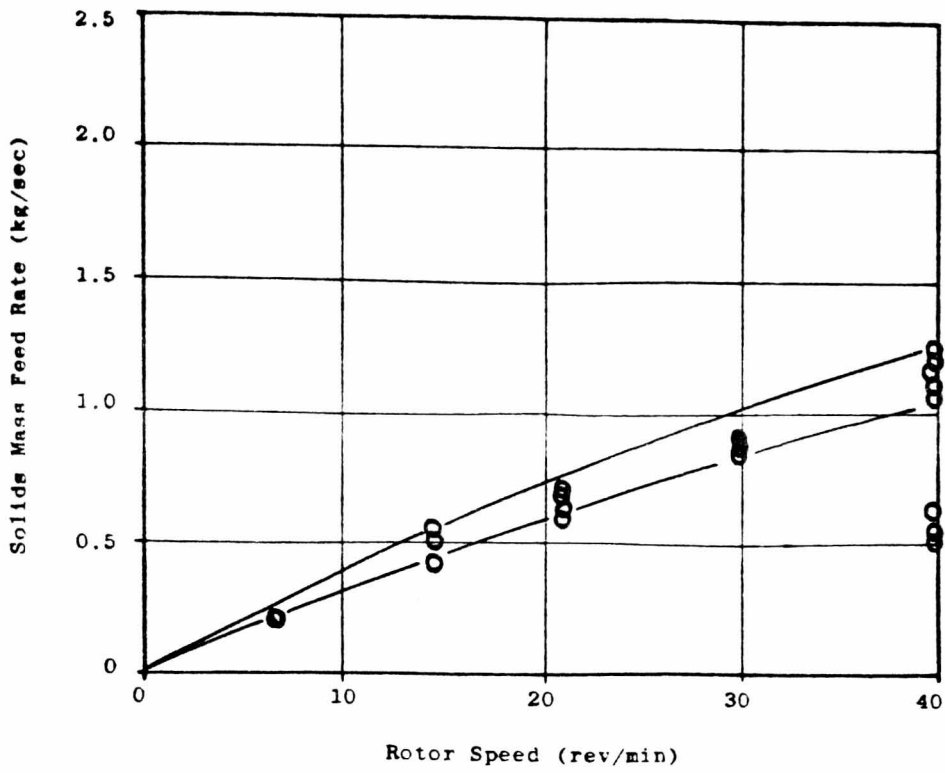
Figure 7.56 Feeding Characteristics of Wheat Flour
with Drop-Out Box B and Rotary Valve Orientation a.
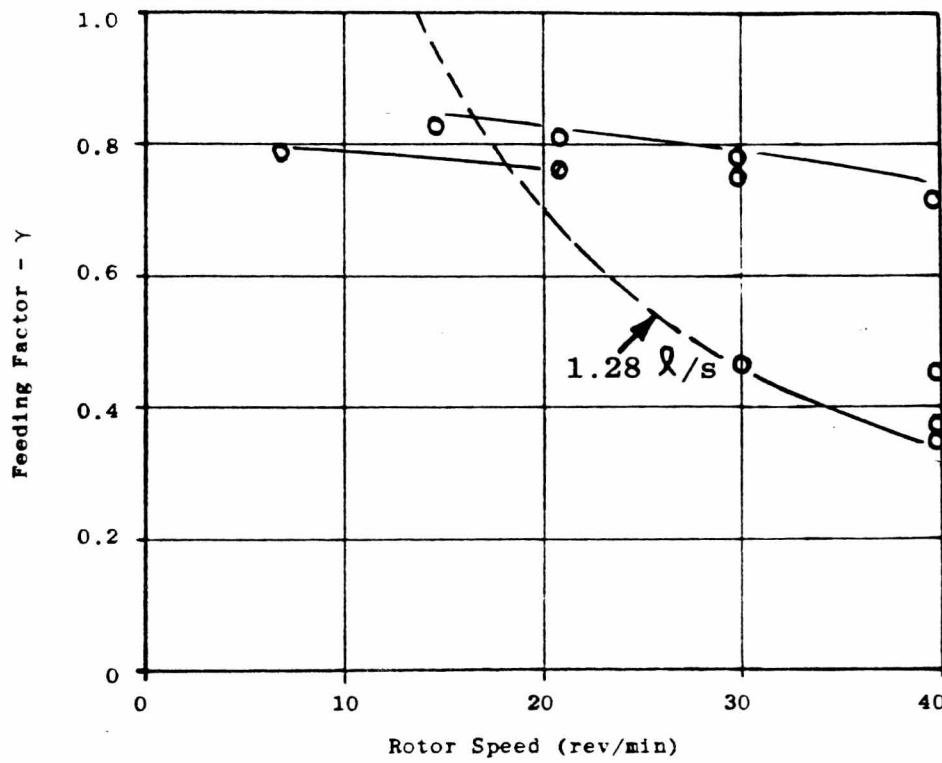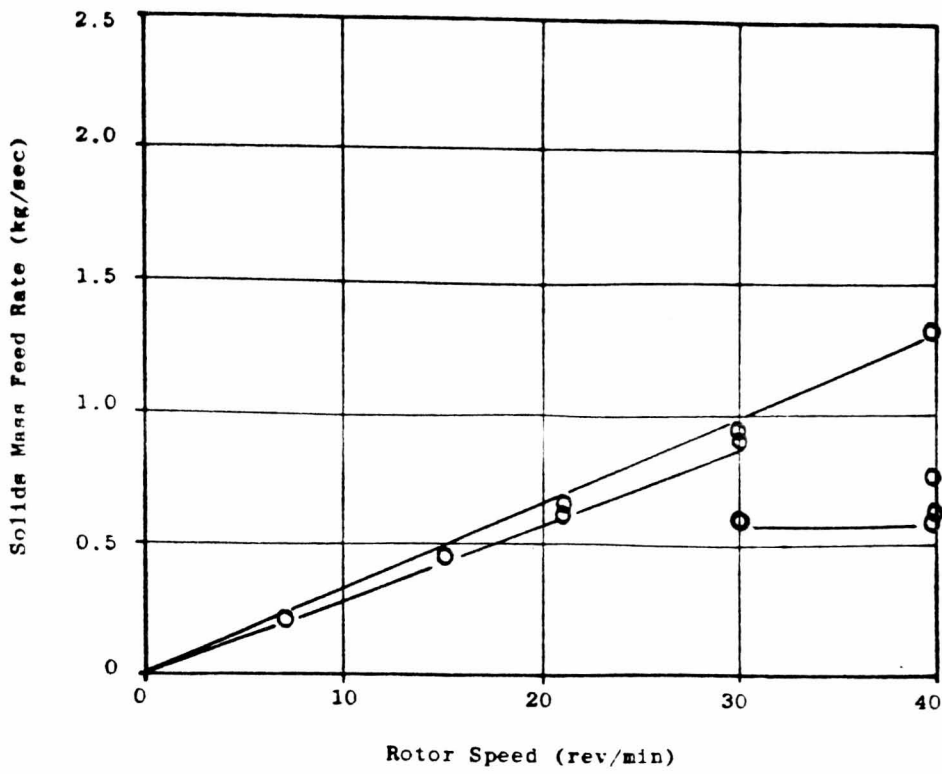
Figure 7.57 Feeding Characteristics of Wheat Flour
            with Drop-Out Box B and Rotary Valve Orientation b.
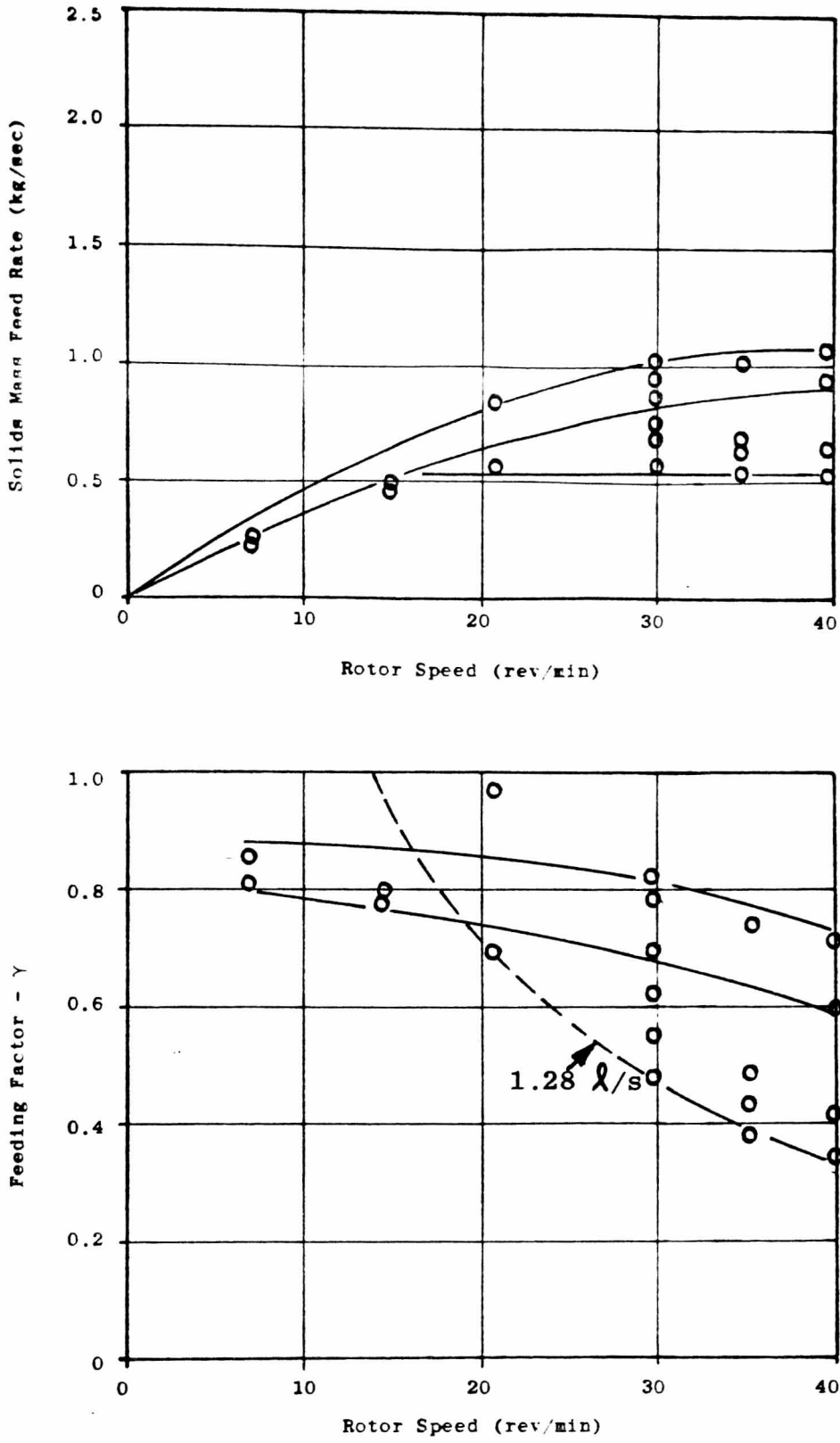
Figure 7.58 Feeding Characteristics of Wheat Flour
with Drop-Out Box B and Rotary Valve Orientation c .
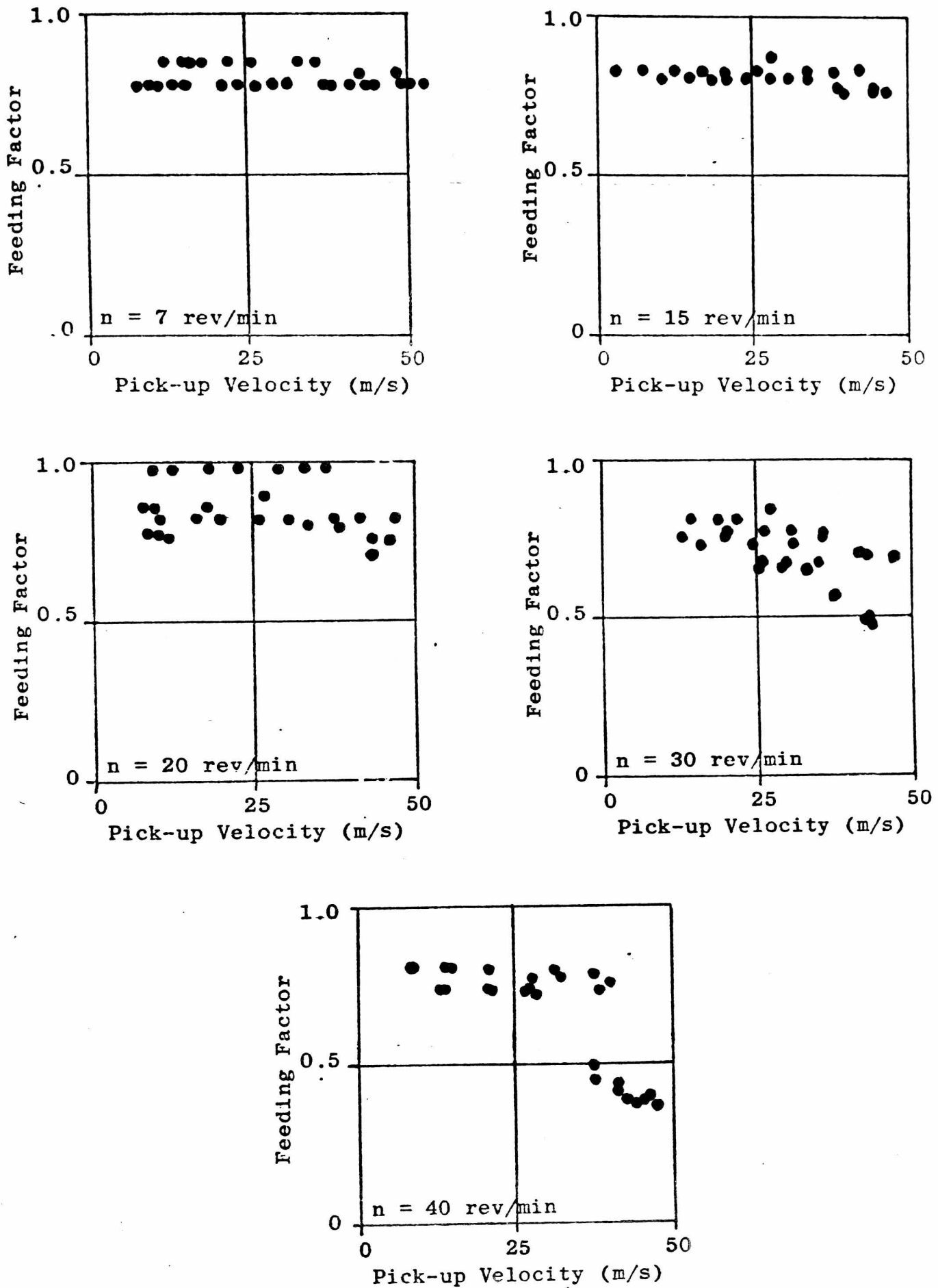
Figure 7.59 The Relationship between the Feeding Factor and the
             Pick-up Velocity for Wheat Flour   with
             Drop-Out Box B.
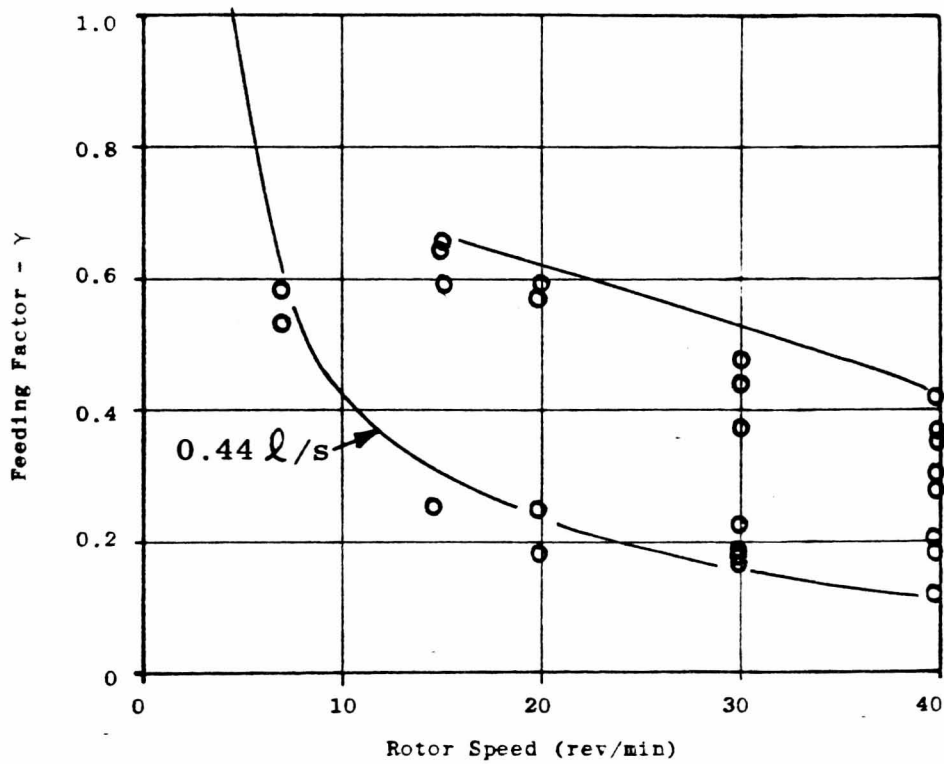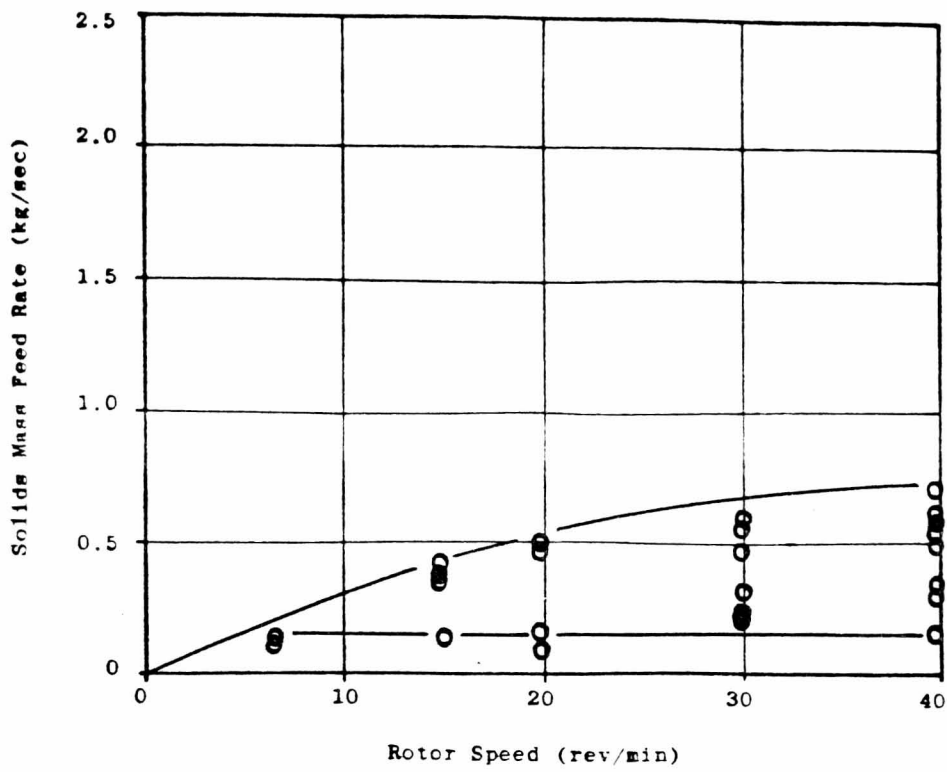
Figure 7.60 Feeding Characteristics of Wheat Flour (contaminated)
             with Drop-Out Box A and Rotary Valve Orientation c.
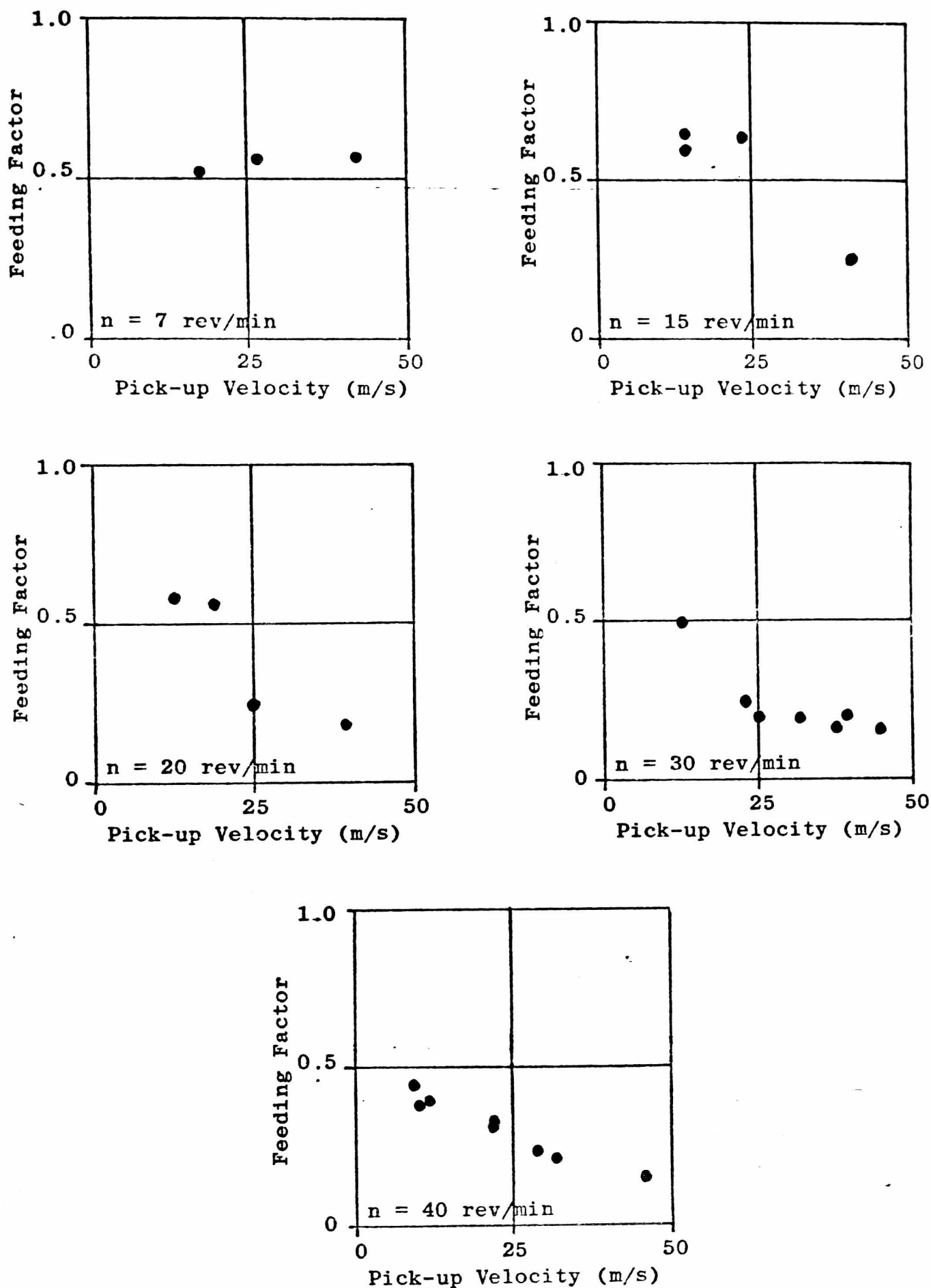
Figure 7.61 The Relationship between the Feeding Factor and the Pick-up Velocity for Contaminated Wheat Flour with Drop-Out Box A.
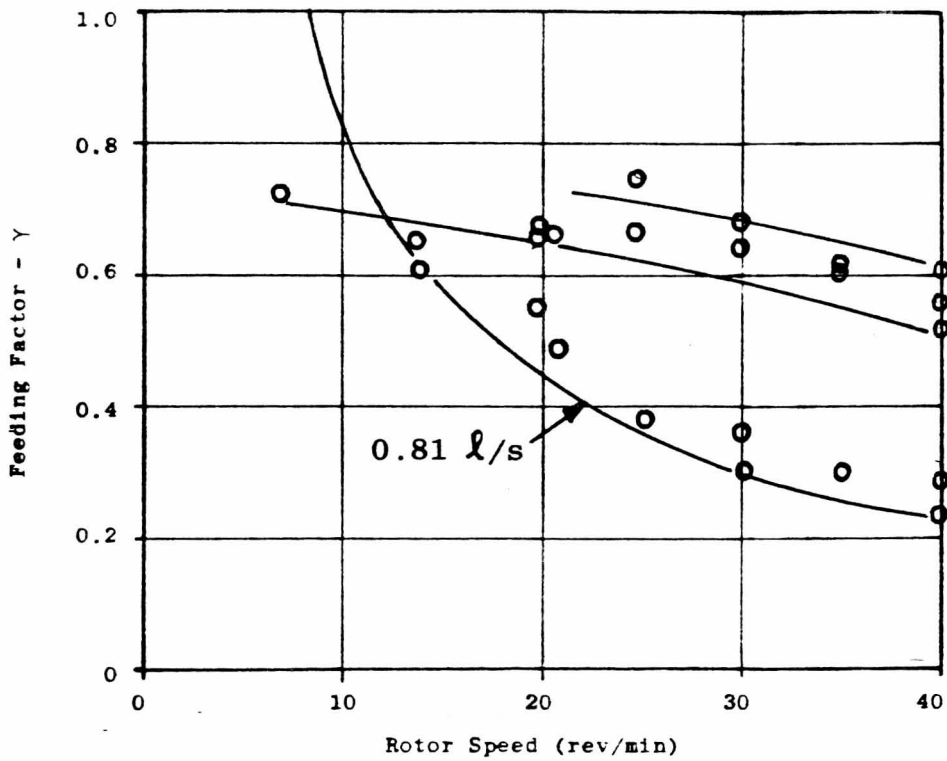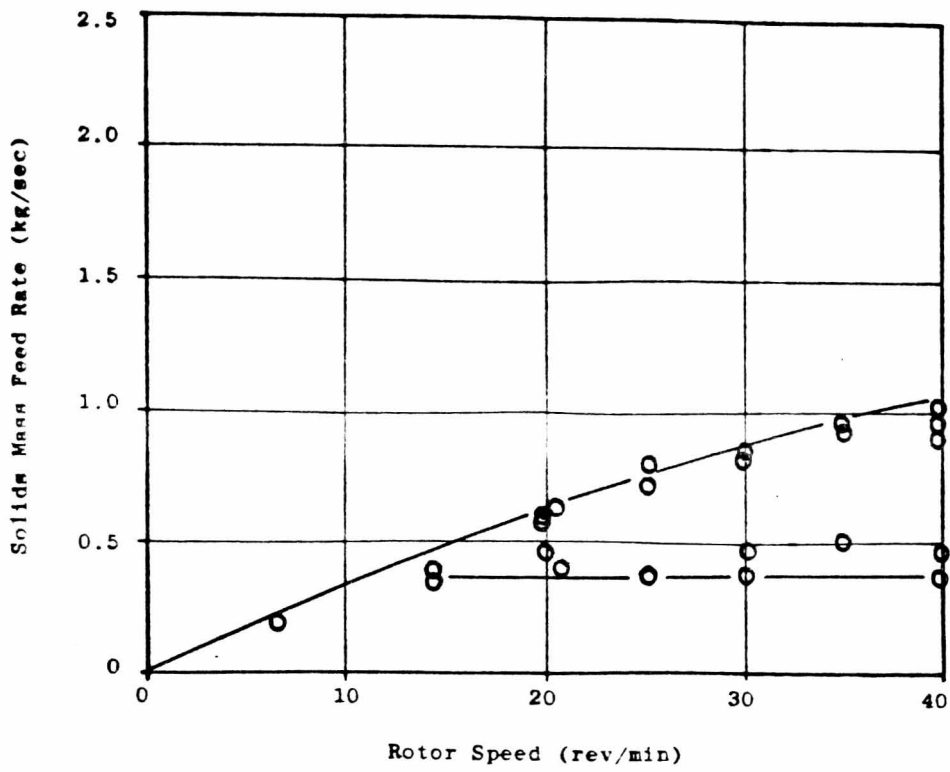
Figure 7.62 Feeding Characteristics of Wheat Flour (contaminated)
with Drop-Out Box B and Rotary Valve Orientation c .
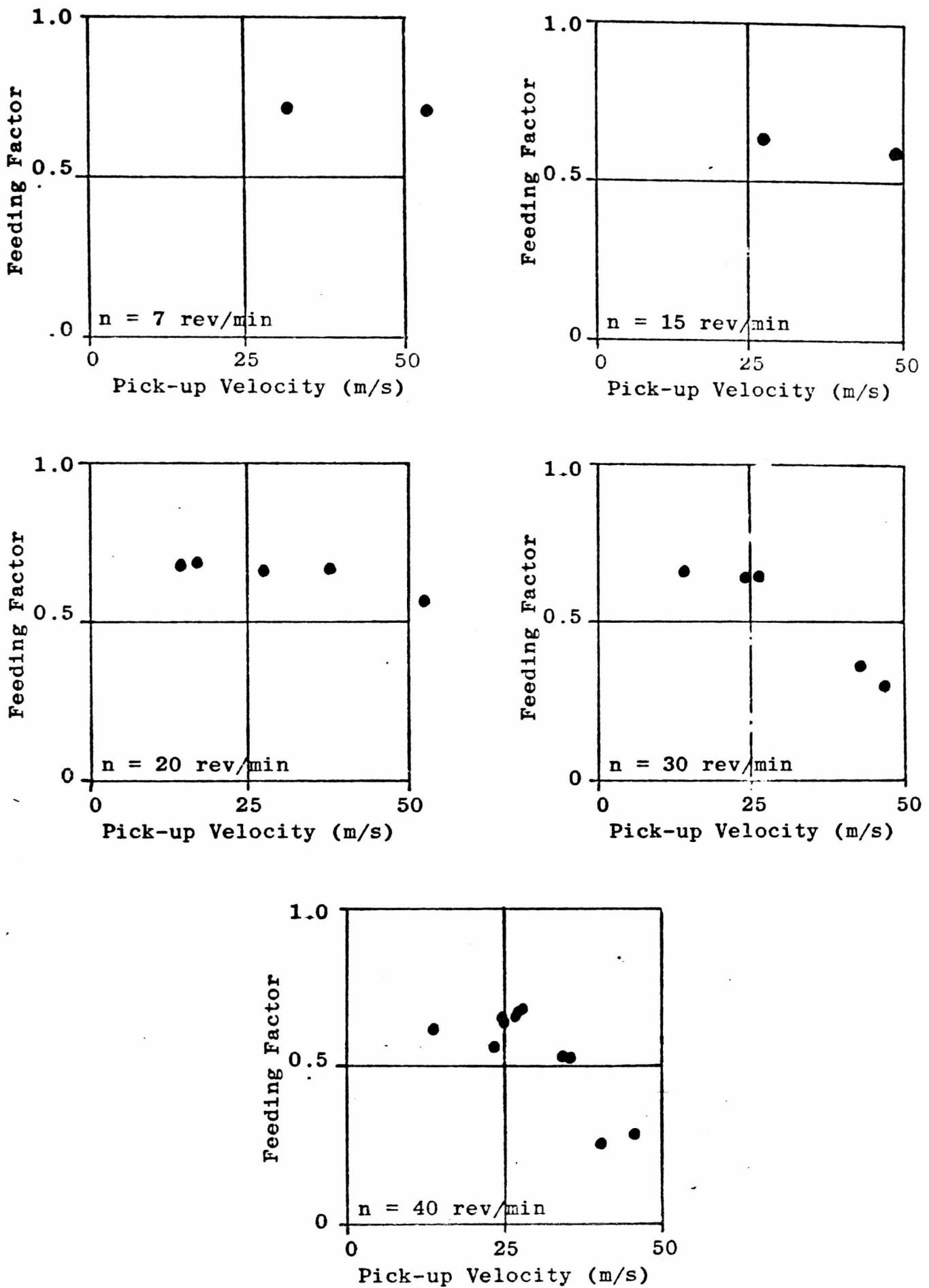
Figure 7.63 The Relationship between the Feeding Factor and the Pick-up Velocity for Contaminated Wheat Flour with Drop-Out Box .
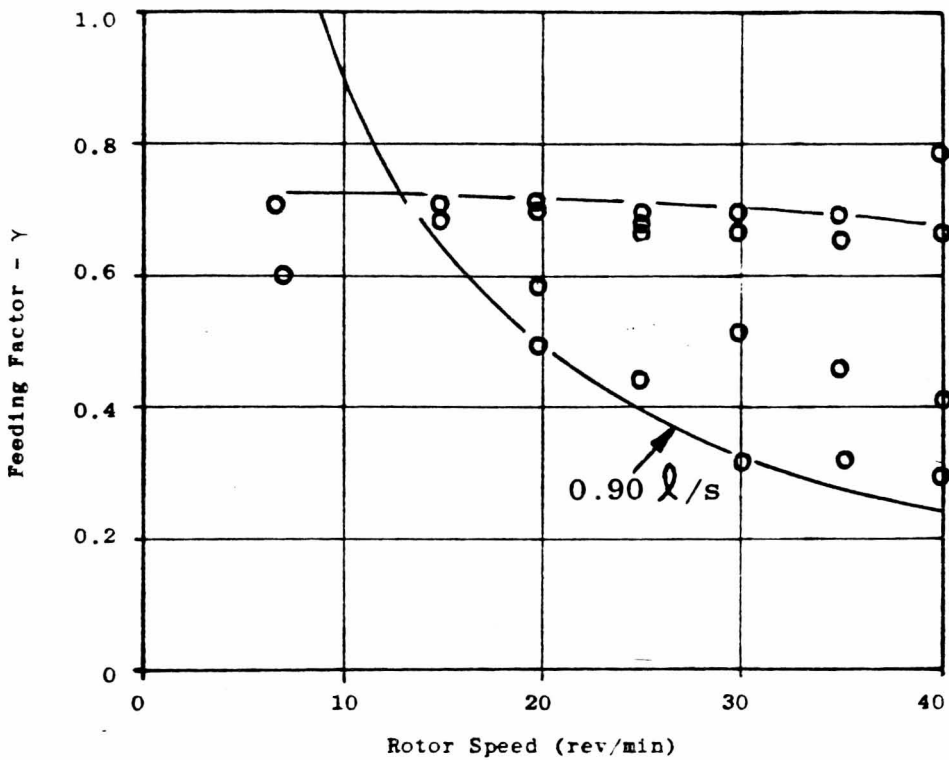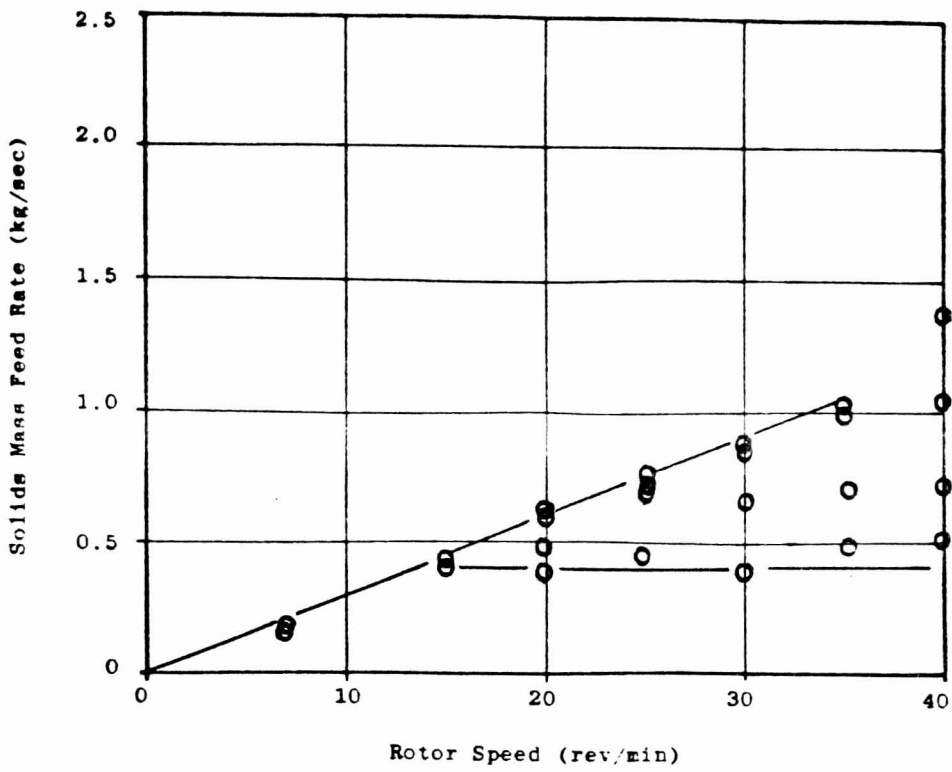
Figure 7.64   Feeding Characteristics of Wheat Flour (contaminated)
with Drop-Out Box C and Rotary Valve Orientation c.
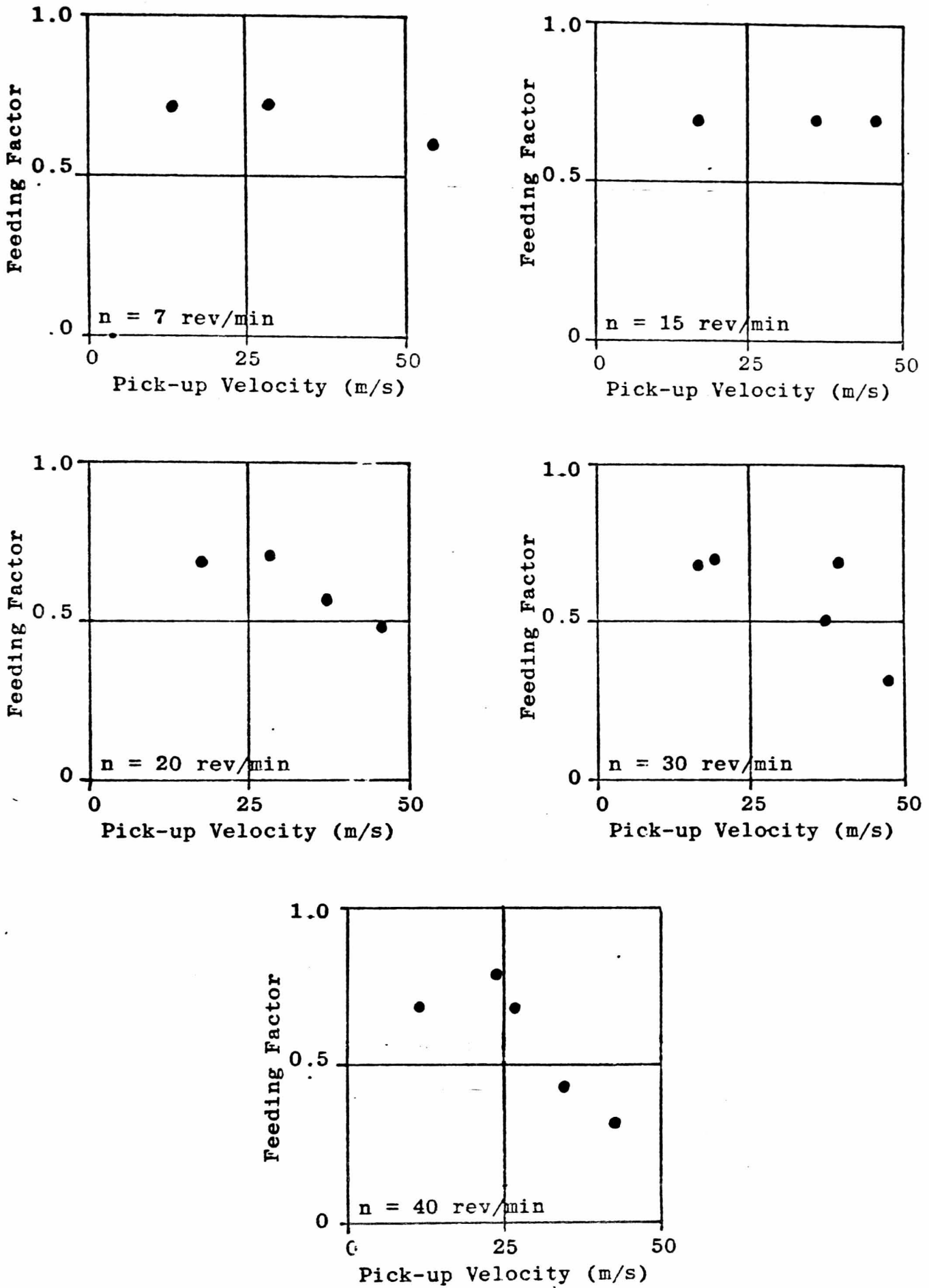
Figure 7.65 The Relationship between the Feeding Factor and the
Pick-up Velocity for Contaminated Wheat Flour with
Drop-Out Box C .
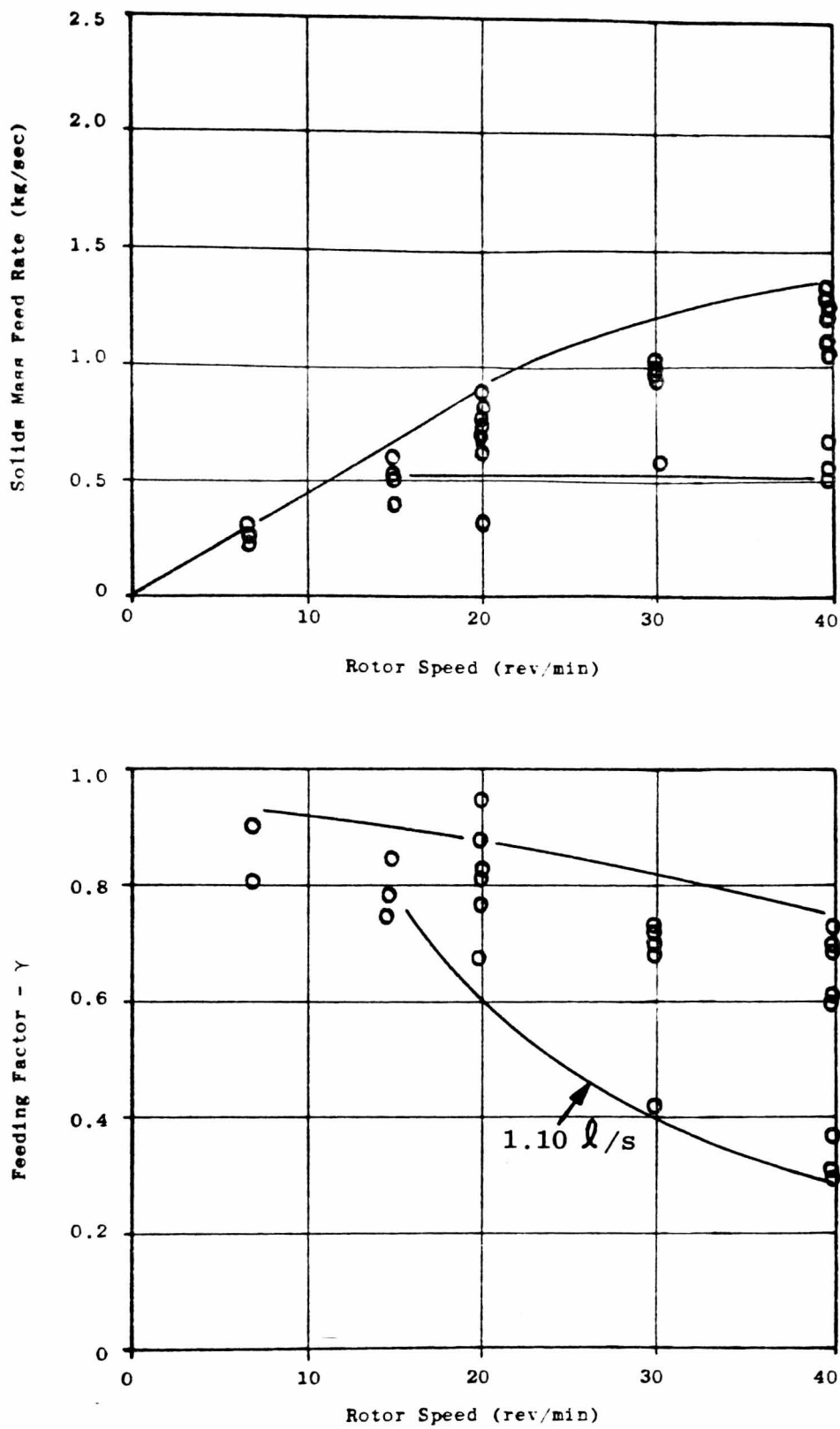
Figure 7.66 Feeding Characteristics of Polyethylene Powder
with Drop-Out Box A and Rotary Valve Orientation c.
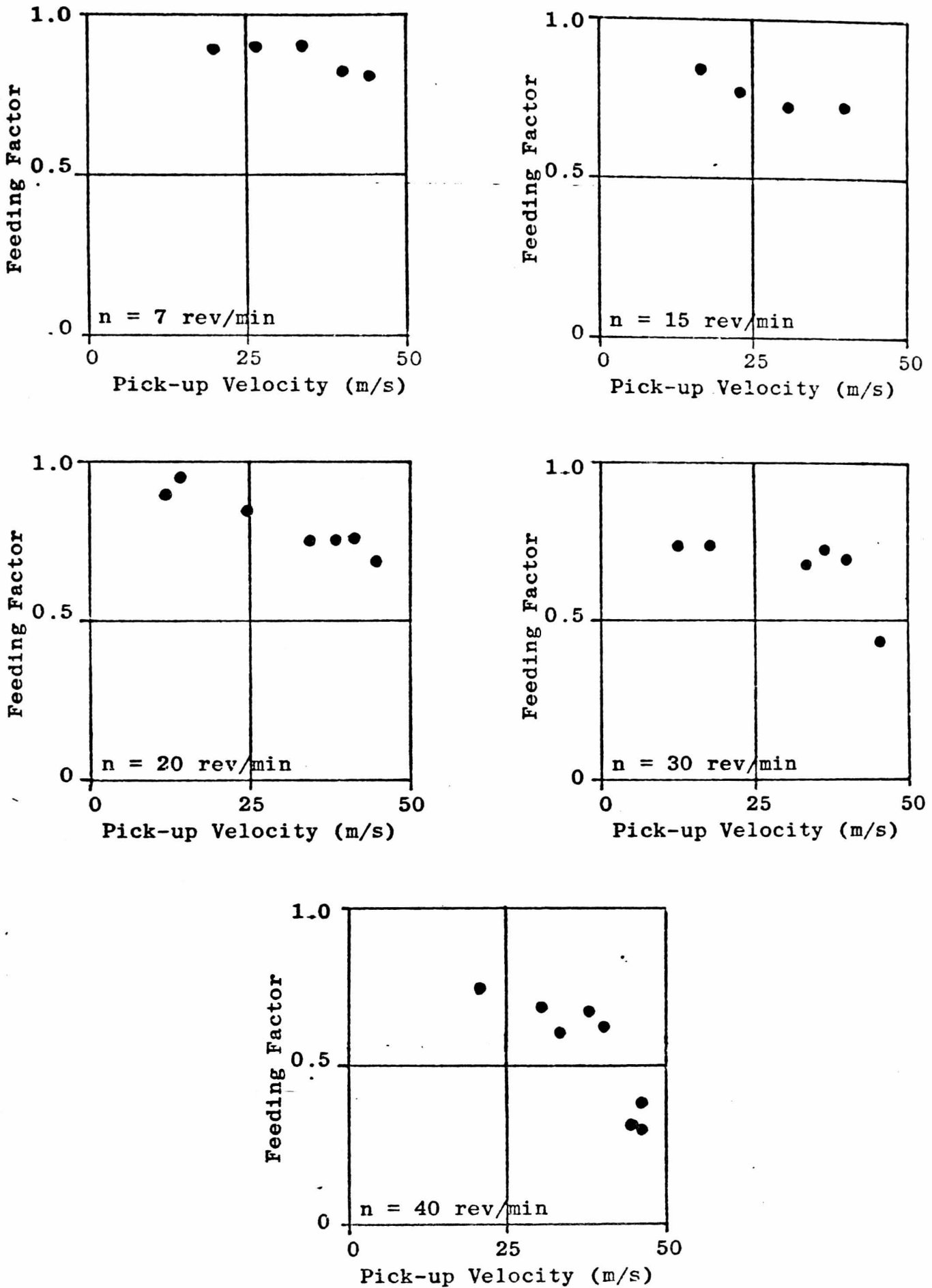
Figure 7.67 The Relationship between the Feeding Factor and the
             Pick-up Velocity for Polyethylene Powder   with
             Drop-Out Box A.
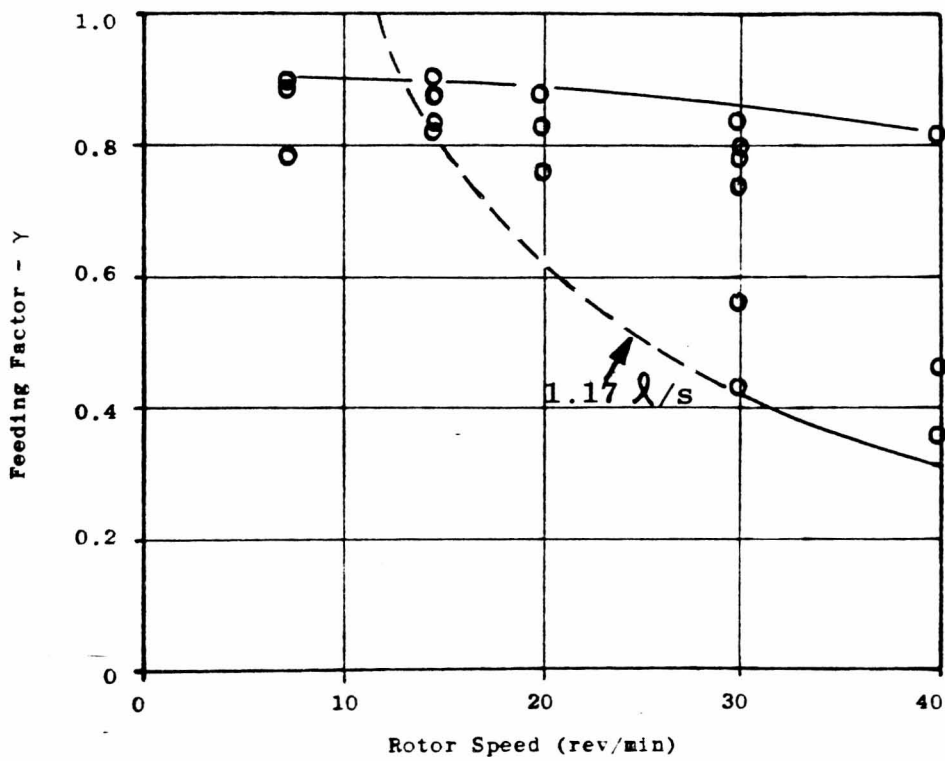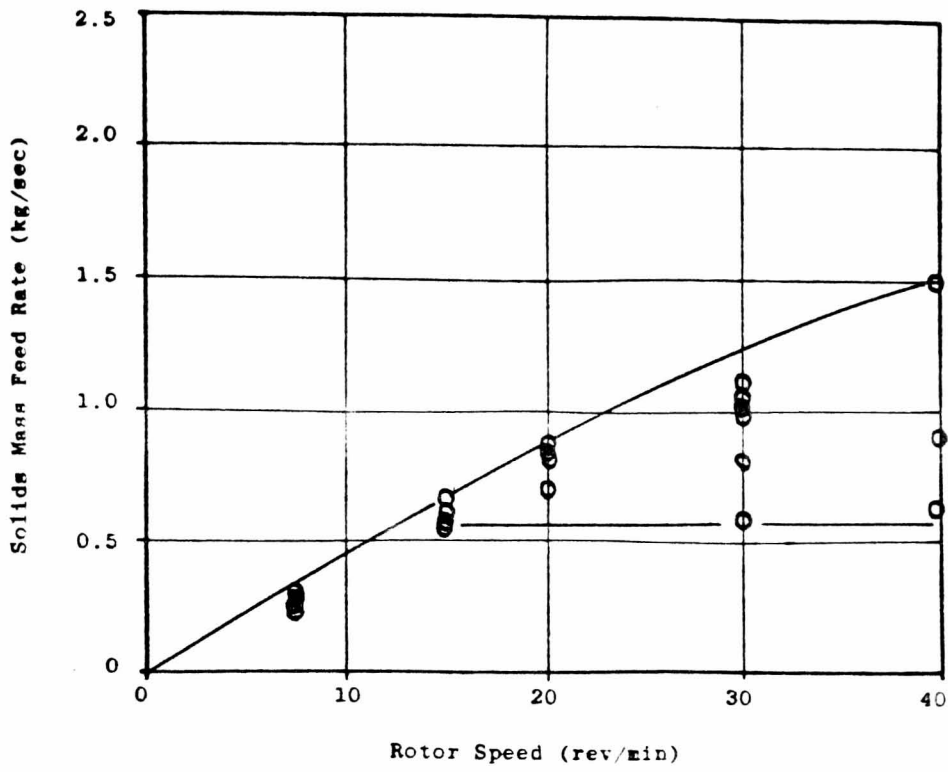
Figure 7.68 Feeding Characteristics of Polyethylene Powder
with Drop-Out Box B and Rotary Valve Orientation a.
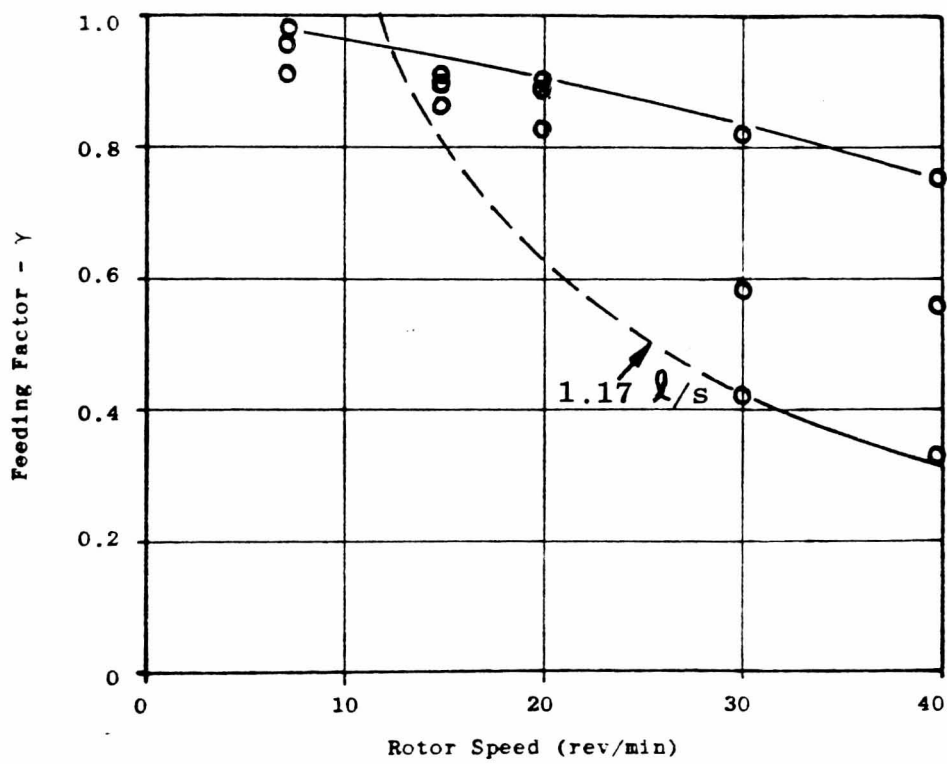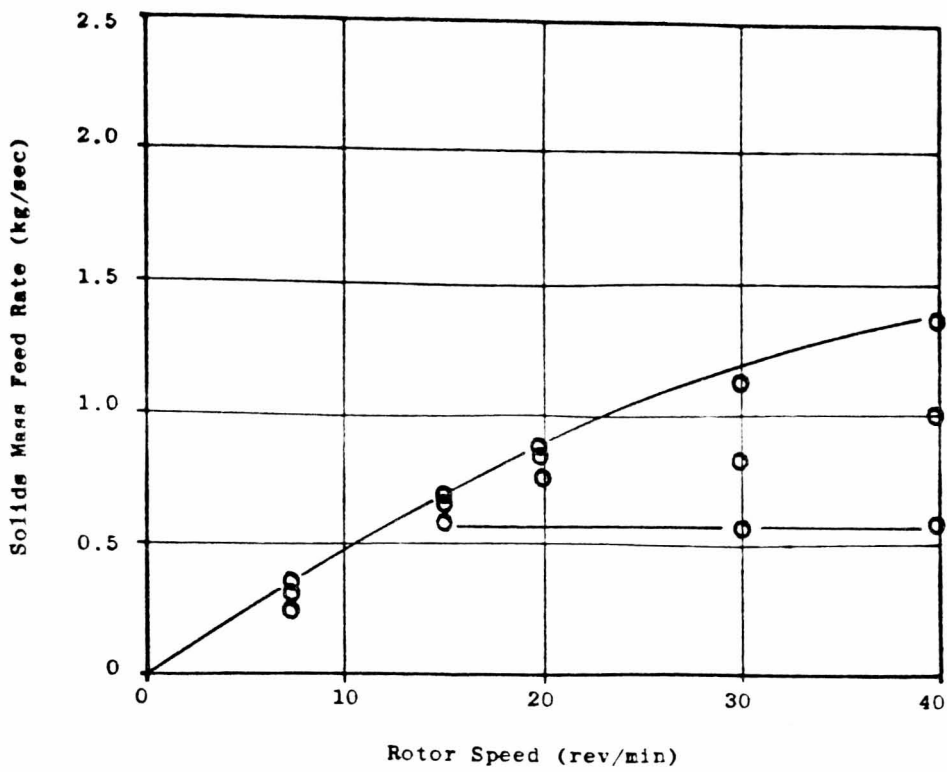
Figure 7.69 Feeding Characteristics of Polyethylene Powder
with Drop-Out Box B and Rotary Valve Orientation b.
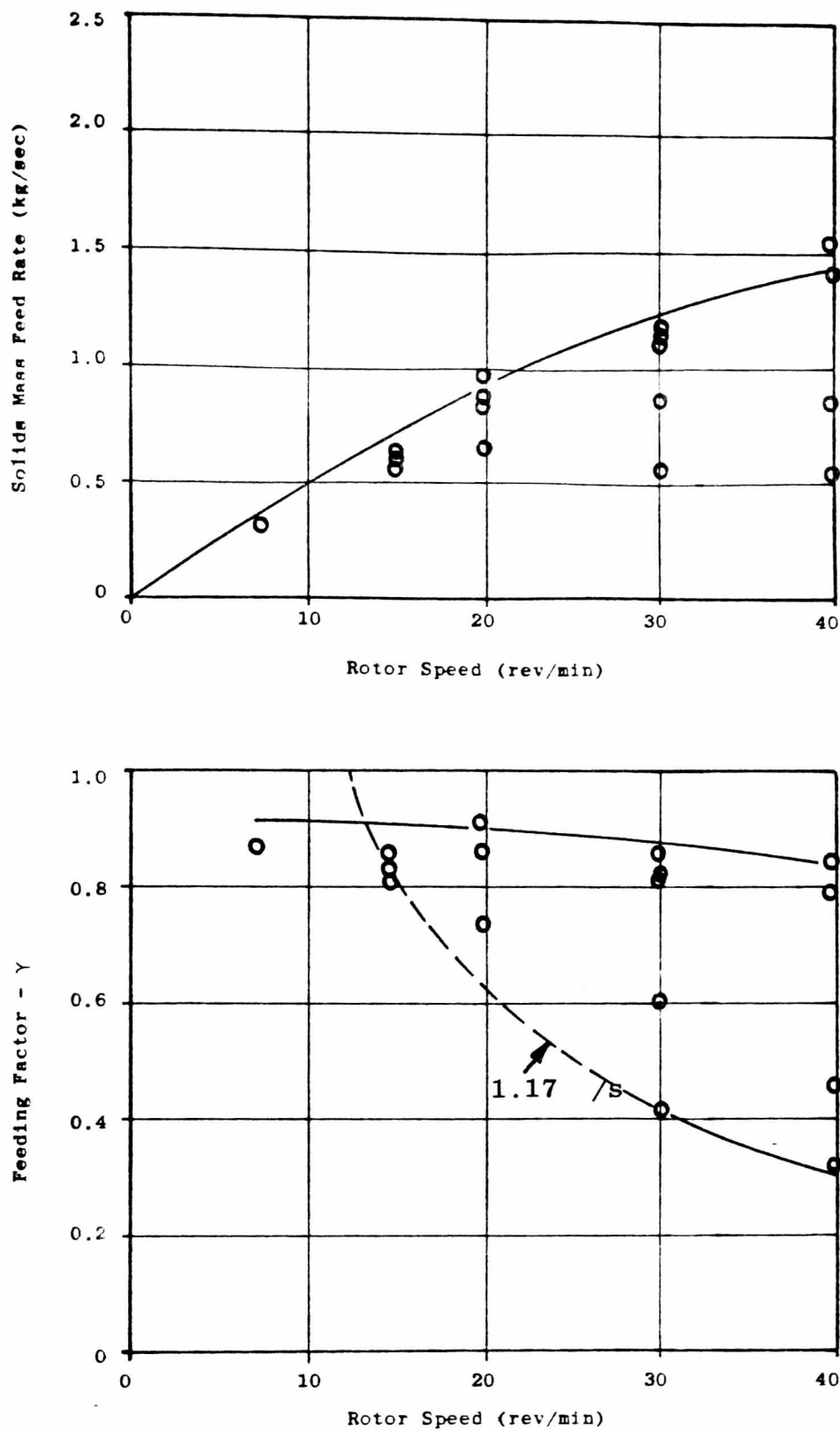
Figure 7.70 Feeding Characteristics of Polyethylene Powder
with Drop-Out Box B and Rotary Valve Orientation c.
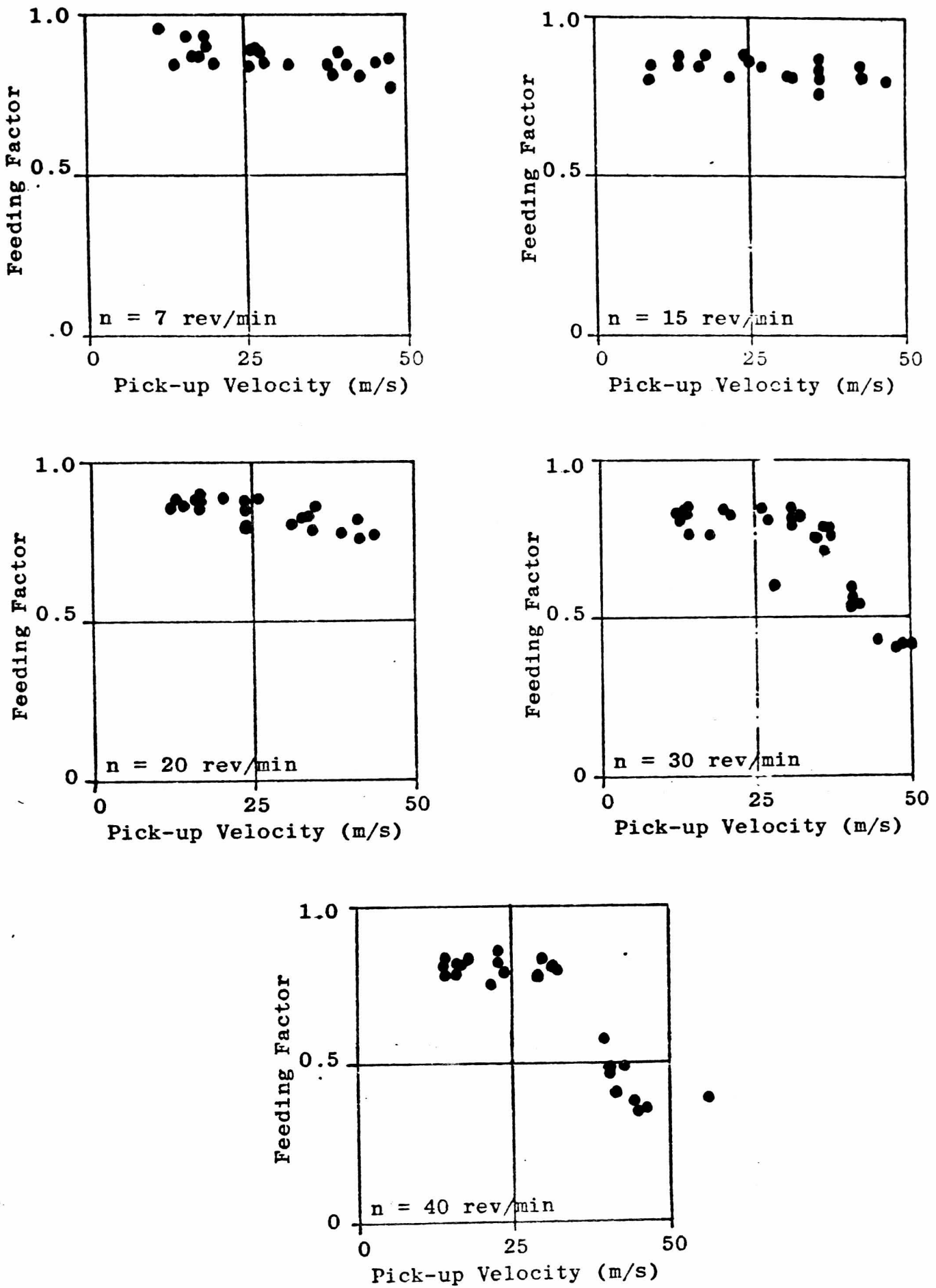
Figure 7.71 The Relationship between the Feeding Factor and the Pick-up Velocity for Polyethylene Powder   with Drop-Out Box B .

characteristics of a drop-out box are primarily dependent on the geometry of the box and the characteristics of the material being handled.

Figure 7.59 shows the relationship betwen the feeding factor and the pick-up velocity for the Wheat Flour in drop-out box B.   Individual graphs are drawn for each of the five set rotor speeds which were examined, that is, 7, 15, 20, 30 and 40 rev/min.   These graphs were constructed by combining the results obtained from the experiments with the three rotary valve orientations.   Figure 7.71 is a similar series of results for the Polyethylene Powder.   Both of these figures show that the choked condition only occurred when there was a combination of high pick-up velocity and high valve rotor speed.   The significance of the high rotor speed being a potentially high solids feed rate.

From these figures the actual value of V_c can be determined.   It is the pick-up velocity at which there is a step change in the value of the feeding factor.   This can be seen most clearly in the graph for 40 rev/ min with the Wheat Flour and the graphs for both 30 and 40 rev/min for the Polyethylene Powder.   For both these materials the value of V_c was approximately 40 m/s in drop-out box B.

Figures 7.60 to 7.65 show the results obtained for the Contaminated Wheat Flour[*] with drop-out boxes A, B and C.   From these figures it can be seen that the feed rate obtained with boxes B and C in the choked condition were similar, but that obtained with box A was very much smaller.   This is consistent with the idea that the geometry of the drop-out box is one of the primary factors dictating the feed rate in the choked condition.   However, in the case of the Polyethylene Powder the results do not show such a clear difference between the choked feed rates of drop-out boxes A and B, see Figures 7.66 to 7.71.   The reason for this is probably due to the Polyethylene Powder being more free-flowing than the Wheat Flour and therefore the shape of the drop-out box was less important.

The results given in Figures 7.72 to 7.76 were obtained for the Polyethylene Powder with drop-out boxes E and F.   The performance of these drop-out boxes showed characteristics similar to but not exactly the same as for choking.   The difference was that the feed rate did not

---

* footnote: See section 7.3.4 for the reasons why the flour was
             contaminated.
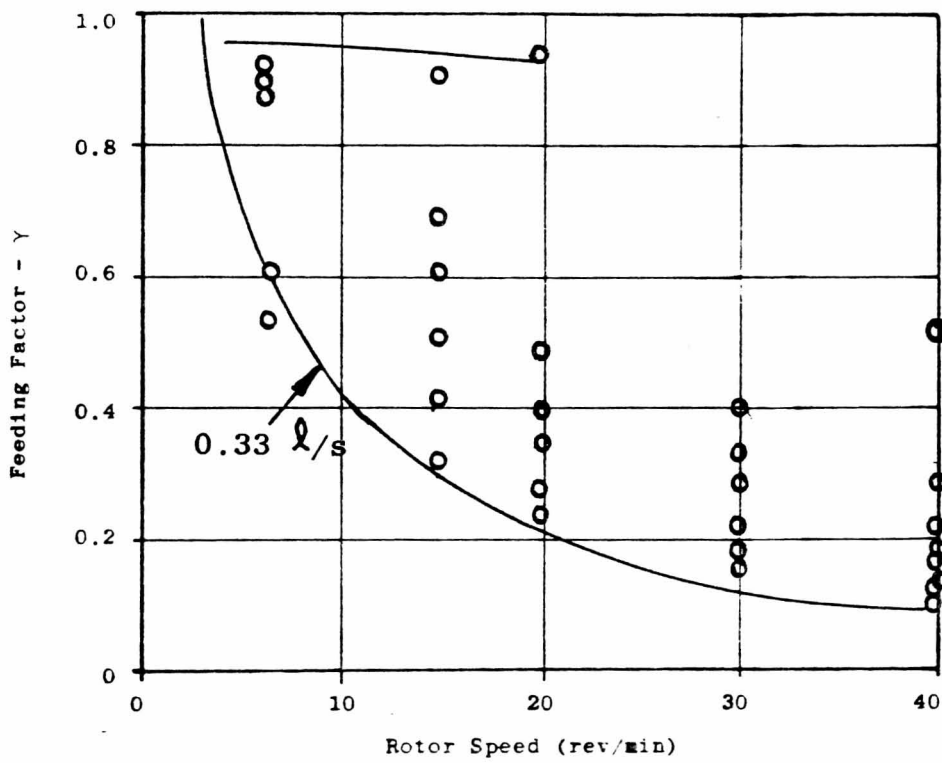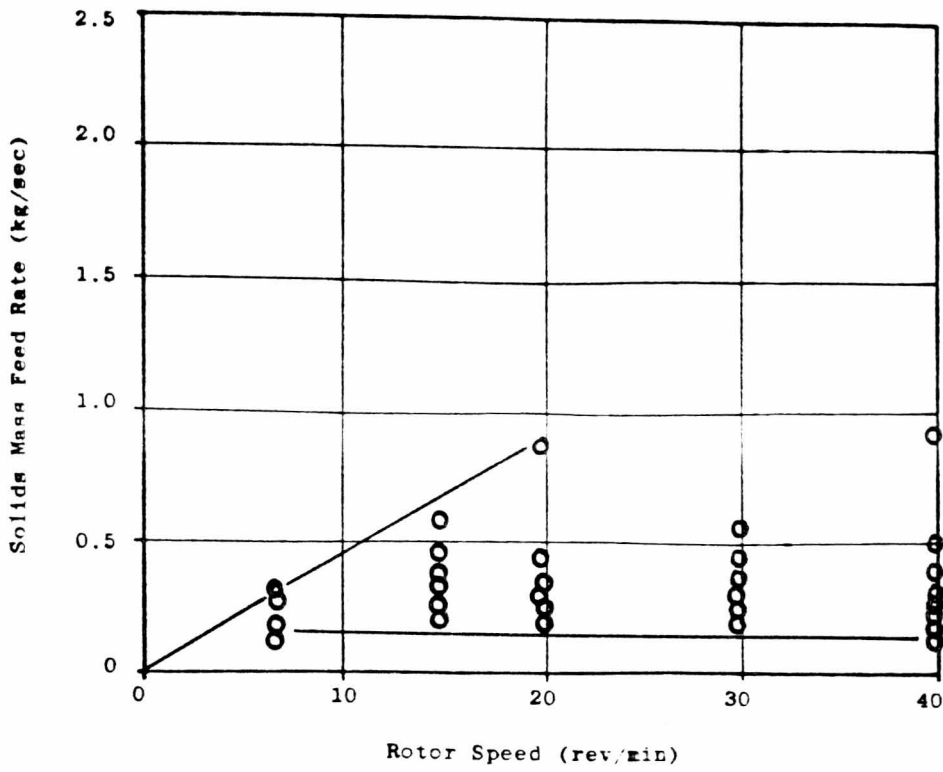
Figure 7.72 Feeding Characteristics of Polyethylene Powder
with Drop-Out Box E and Rotary Valve Orientation c.
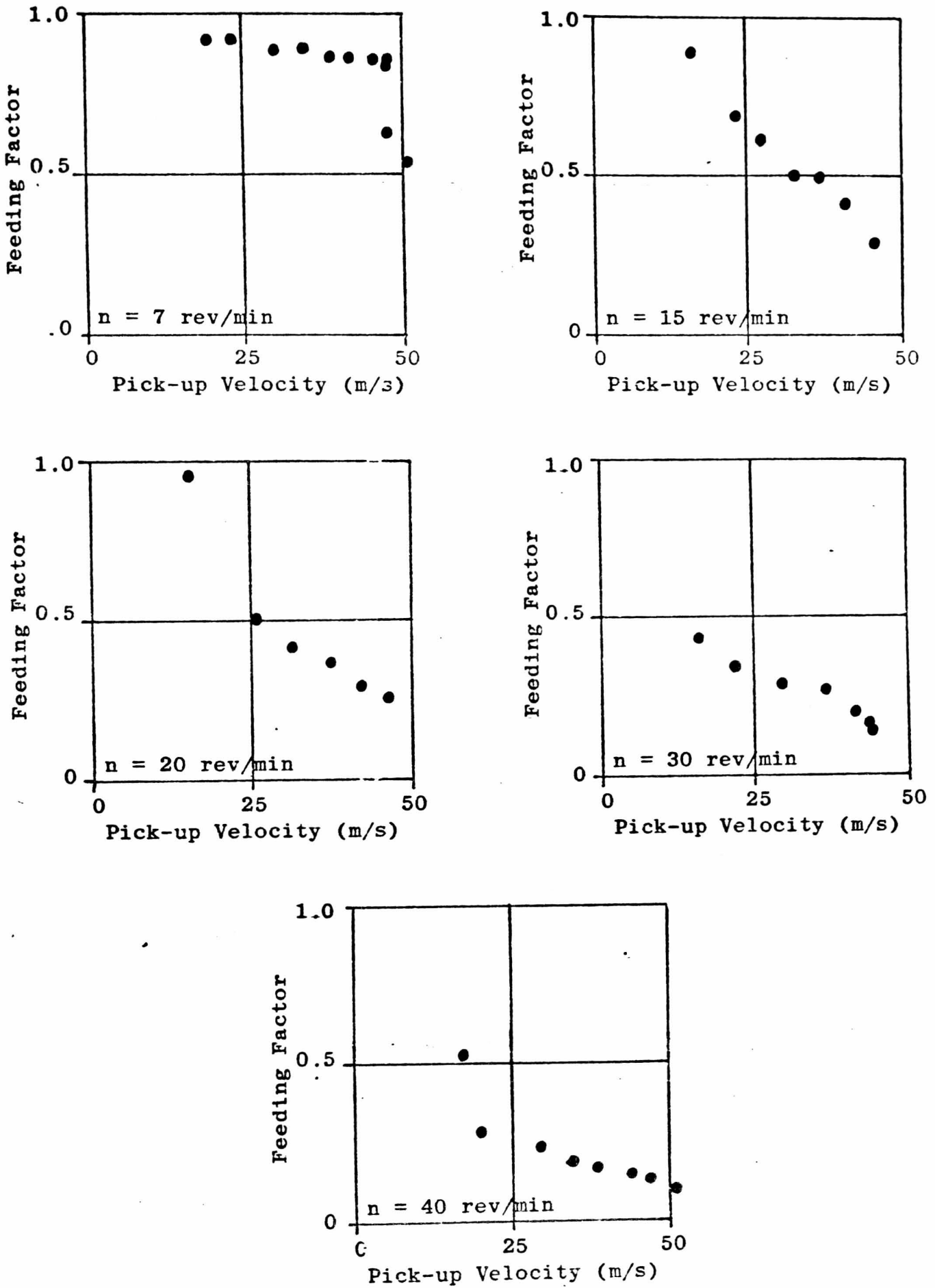
Figure 7.73 The Relationship between the Feeding Factor and the
           Pick-up Velocity for Polyethylene Powder   with
           Drop-Out Box E .
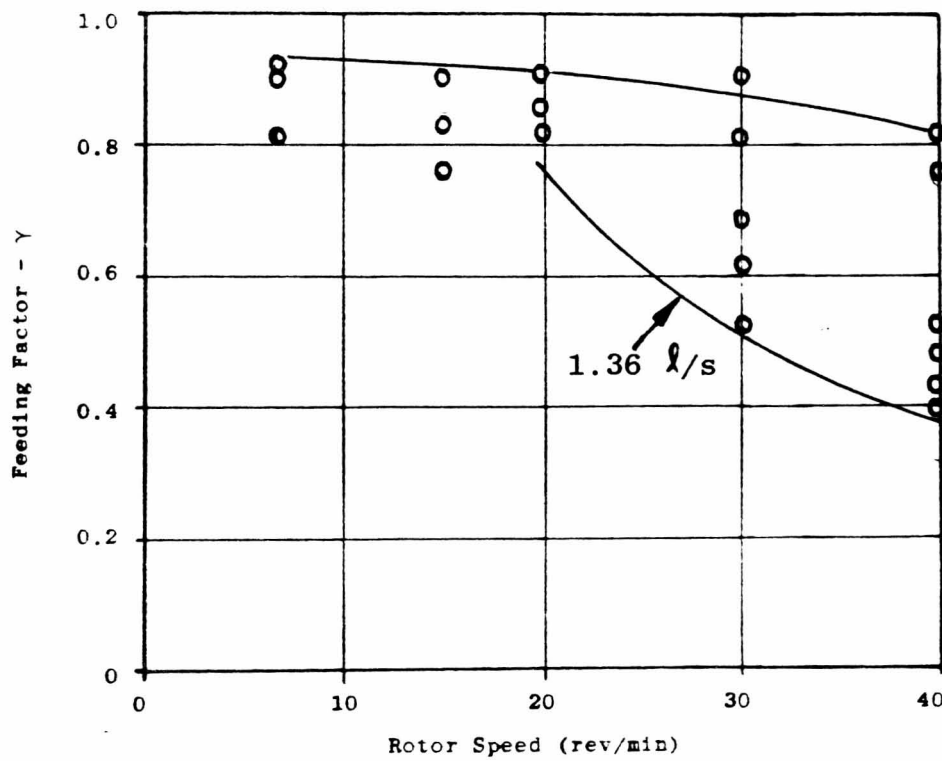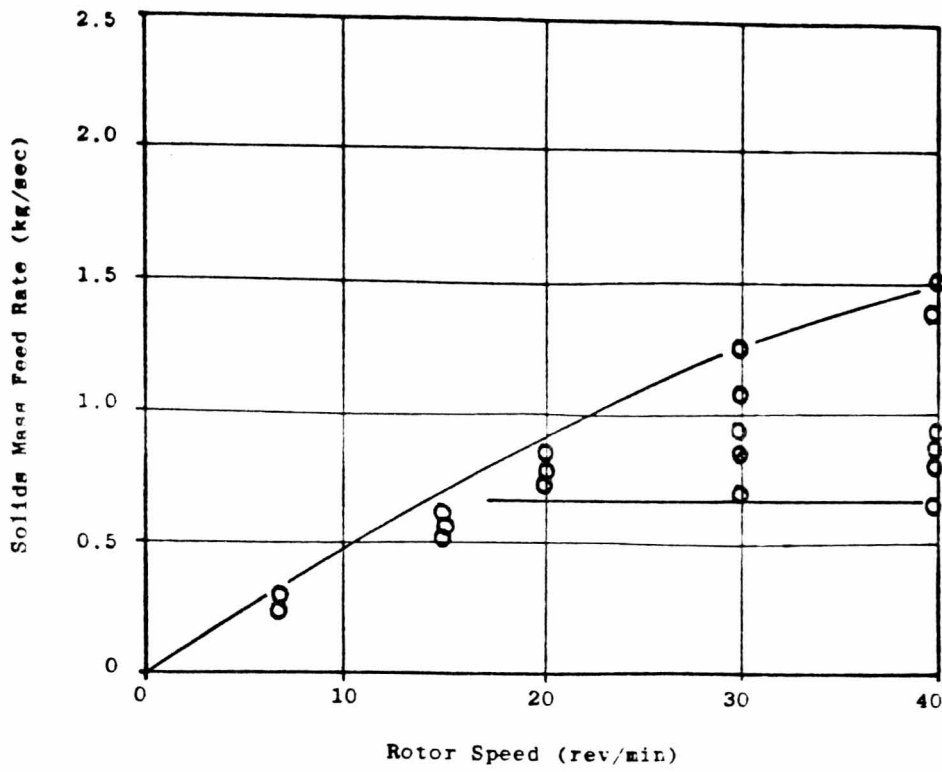
Figure 7.74 Feeding Characteristics of Polyethylene Powder
with Drop-Out Box F and Rotary Valve Orientation c.
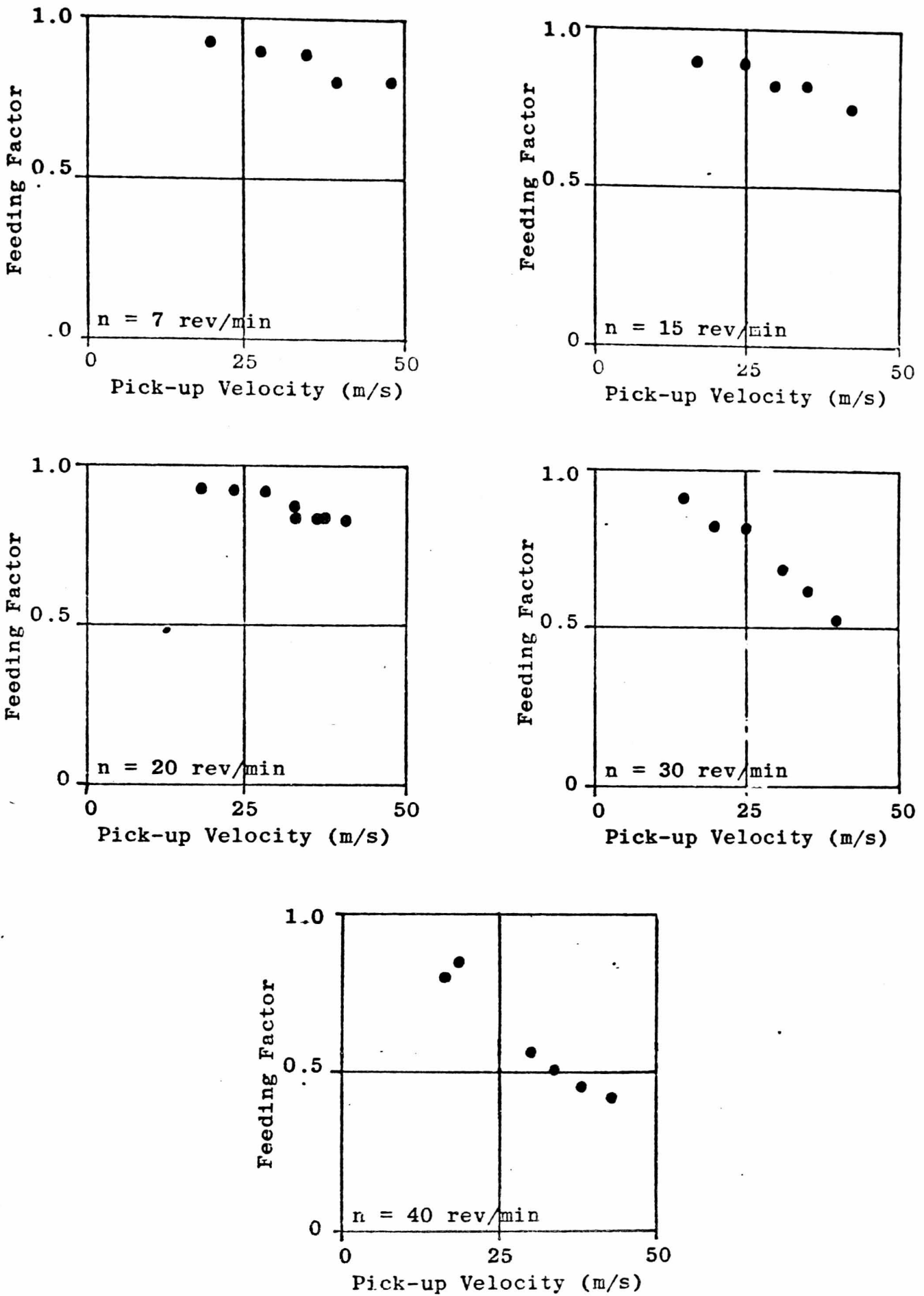
Figure 7.75 The Relationship between the Feeding Factor and the
Pick-up Velocity for Polyethylene Powder   with
Drop-Out Box F .
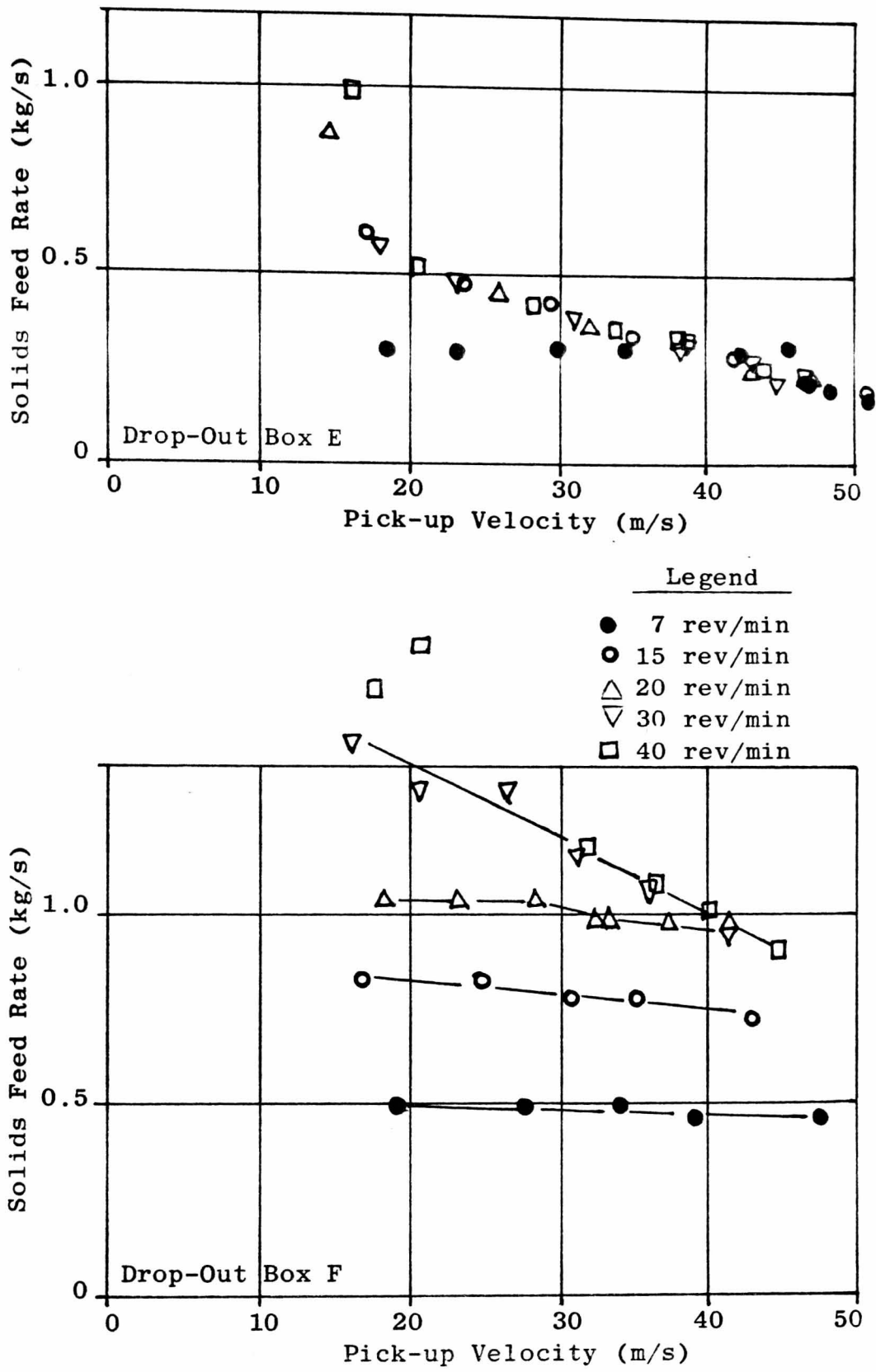
Figure 7.76 The Relationship between Solids Feed Rate and
Pick-up Velocity for Polyethylene Powder with
Drop-Out Boxes E and F.

'switch' distinctly from one value to another, but was restricted
progressively as the pick-up velocity was increased.   This is
illustrated by Figures 7.73, 7.75 and 7.76.   Figure 7.76 also shows
that this effect was more severe for drop-out box E than F.   This is
to be expected because the cross-sectional area of box E is smaller than
that of box F and therefore it is reasonable to expect it to offer a
greater restriction to the feed rate.

The tables shown in Figures 7.77 to 7.79 show the values of V_c
obtained experimentally for drop-out boxes A, B and C respectively.   Also
shown in these tables are the predicted values of V_c/C_c obtained from
equation 4.21c.   Dividing the experimental values of V_c by the predicted
values of V_c/C_c gives empirical values of C_c for each combination of
material and drop-out box which was found to choke.   In Chapter 4 it was
proposed that such empirical values of C_c would provide useful reference
data which together with equation 4.21c could be used to estimate V_c for
other systems.   However, since choking did not happen with all of the
materials which were tested, only a limited amount of data regarding
typical values for C_c was obtained.

The graphs shown in Figure 7.80 were constructed to present the results
in a more useful manner.   These are similar to the graphs in Figure 4.3
of Chapter 4 which showed the relationship between the dimensionless
critical peripheral velocity (P_*) and the drop-out box shape factor
(H/a), and which were proposed as a means of comparing the choking
characteristics of different sized and different shaped drop-out boxes.
Figure 7.80 differs slightly from this because the product of the terms
C_c and P_*, rather than P_* alone, is plotted against the shape factor.
The reason for doing this is that the product of these terms can be obtained
directly from experiment whereas their individual values cannot.   The
values of C_c given in Figures 7.77 to 7.79 were obtained by assuming the
value of P_* to be equal to that predicted by equation 4.18, that is:

$$P_* = \frac{1}{\sqrt{2}} \left(\frac{H}{a} + \frac{a}{H}\right)^{\frac{1}{2}}$$

(4.18)

However, this approach can only be justified in the respect that it
enables empirical values of C_c to be obtained.   The more correct approach
would be to quote experimentally determined values of the product $C_c P_*$

DROP-OUT BOX A		P_c = 1.72 m/s H/a = 0.33			
MATERIAL	ρ_s Bulk Density (kg/m^2)	V_c/C_c Predicted From Eq 4.21c (m/s)	V_c Actual (m/s)	C_C (P_*=1.30 (-)	$C_c P_*$ (-)
POLYETHYLENE PELLETS	529	25-36	Not Tested	-	-
POLYETHYLENE POWDER	504	25-35	40-44	1.45-1.60	1.88-2.07
WHEAT FLOUR	440	23-33	Not Tested	-	-
CONTAMINATED WHEAT FLOUR	470	24-34	20-44	0.94-1.13	1.22-1.46
ORDINARY PORTLAND CEMENT	1138	37-52	Did not choke	-	-
SINGLES COAL	641	28-39	Did not choke	-	-
PULVERISED COAL	587	27-38	Did not choke	-	-

Figure 7.77   Comparison of Predicted and Actual Characteristics for Drop-Out Box A

DROP-OUT BOX B		P_c = 1.36 m/s H/a = 0.72			
MATERIAL	ρ_s Bulk Density (kg/m^2)	V_c/C_c Predicted From Eq 4.21c (m/s)	V_c Actual (m/s)	C_c (P_*=1.30) (-)	$C_c P_*$ (-)
POLYETHYLENE PELLETS	529	20-28	Did not choke	-	-
POLYETHYLENE POWDER	504	20-38	40-45	1.84-2.07	1.88-2.11
WHEAT FLOUR	440	18-26	38-42	1.87-2.07	1.91-2.11
CONTAMINATED WHEAT FLOUR	470	19-27	28-42	1.81-2.00	1.85-2.05
ORDINARY PORTLAND CEMENT	1138	29-41	Did not choke	-	-
SINGLES COAL	641	22-31	Did not choke	-	-
PULVERISED COAL	587	21-30	Did not choke	-	-

Figure 7.78   Comparison of Predicted and Actual Characteristics
for Drop-Out Box B

DROP-OUT BOX C		$P_c = 1.37$ m/s H/a = 1.44			
	ρ_s Bulk Density (kg/m^2)	V_c/C_c Predicted From Eq 4.21c (m/s)	V_c Actual (m/s)	C_c (P_*=1.30) (-)	$C_c P_*$ (-)
POLYETHYLENE PELLETS	529	20-28	Not Tested	-	-
POLYETHYLENE POWDER	504	20-28	Not Tested	-	-
WHEAT FLOUR	440	18-26	Not Tested	-	-
CONTAMINATED WHEAT FLOUR	470	19-27	35-40	1.65-1.89	1.70-1.95
ORDINARY PORTLAND CEMENT	1138	29-52	Did not choke	-	-
SINGLES COAL	641	22-31	Not Tested	-	-
PULVERISED COAL	587	21-30	Not Tested	-	-

Figure 7.79   Comparison of Predicted and Actual Characteristics
for Drop-Out Box C
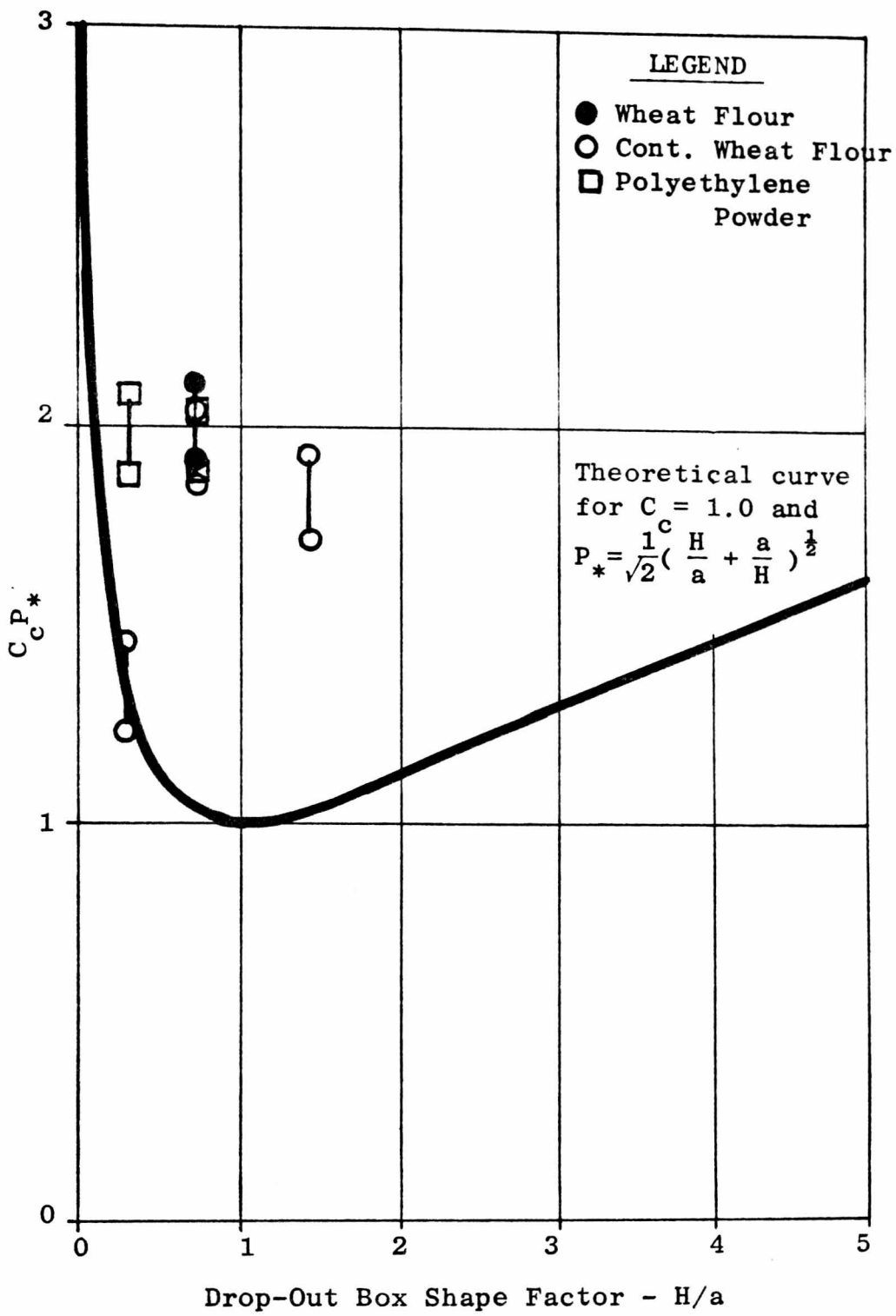
Figure 7.80 The Relationship between $C_c P_*$ and H/a.

and then use these with the following modified form of equation 4.21c
in order to esimate V_c for other systems:

$$V_c = C_c P_* \left(ga \frac{\rho_s}{\rho_a} \right)^{\frac{1}{2}}$$ (7.1)

which is obtained by substituting $P_*(ga)^{\frac{1}{2}}$ for P_c in equation 4.21c.

Unfortunately, it is not possible to identify the actual relation-
ship between $C_c P_*$ and H/a from the graphs shown in Figure 7.80 because
of the limited number of data points. However, it is clear from the
results obtained with the Contaminated Wheat Flour that it does not
necessarily follow the same trend as that predicted by equation 4.18
for the relationship between P_* and H/a.

Clearly, more experimental data is needed if the graphs shown in
Figure 7.80 are to be used as reliable reference information from which
the choking characteristics of other systems can be estimated. However,
it is equally valuable to understand why the drop-out boxes did not choke
with all the materials which were examined because this would enable us to
identify the types of material for which choking is not a problem.

The tables shown in Figure 7.77 to 7.79 indicate why one of the
materials did not choke. This was the Cement, which was considered to
be a likely candidate for choking before the experiments were conducted.
However, the Cement had a much greater bulk density than the other test
materials and consequently a significantly higher value of V_c/C_c. The
implication of this is that the Cement would require a very high pick-up
velocity to cause it to choke. For instance, consider drop-out box B,
for which C_c was determined to be approximately 2.0 with each of the
three materials that did choke. Using this value of C_c gives a
predicted value of V_c for Cement between 76 and 84 m/s; which is far in
excess of the pick-up velocities used in the experimental work and much
greater than those used in industrial conveying systems. Consequently,
for materials like Cement choking is not a practical problem. However,
the converse argument is that materials with a low bulk density will be
very prone to choking.

The other materials which did not choke were the Polyethylene
Pellets and the two grades of Coal. In the case of the Polyethylene
Pellets the reason for the drop-out boxes not choking was due to the

free-flowing nature of this material, which prevents the formation of a
stable arch.   However, the same argument could be pplied to the
Polyethylene Powder which did choke.   This apparent inconsistency may
have been due to electrostatic charging of the Polyethylene Powder which
would undoubtedly change its handling characteristics.   The ability of
this material to take a charge was first noted when its bulk density was
being measured.   If care was not taken to prevent the material acquiring
a charge the poured bulk density was found to decrease by up to 20%.

The ability of the system to handle the Single Coal was surprising.
Blockages in both the drop-out box and the pipeline had been anticipated
as a problem because of physical interlocking of the large particles.
However, in practice this was not found to be a problem and the coal
conveyed reliably.   Choking did not occur with the Single Coal because
its mode of entrainment was quite different from that of all the other
materials.   Using the drop-out box with the Perspex windows it could be
seen that the pieces of coal were not recirculated inside the drop-out
box by an air swirl but simply moved 'en masse'.   Consequently, choking
did not occur because the lumps of coal were not held in suspension.

The other material which did not choke was the Pulversised Coal.
In this case the air leakage through the rotary valve restricted the
pocket filling process, as discussed in section 7.3.4.   As a result of
this the rotary valve was not able to feed material into the drop-out box
at a sufficient rate to cause it to choke.

In conclusion, the materials which are most likely to choke a drop-
out box are those which have a low bulk density and thus a low inertia.
This enables the air swirl in the drop-out box to entrain the material
easily and, because of the low-inertia, the pick-up velocity needed to
choke the box will be low.   In addition, those materials which have a
significant interparticulate strength will choke easily because they will
be able to form a stable arch in the drop-out box; that is, provided that
they can be fed into the drop-out box at a sufficiently high rate.

7.5 Blowing Seal Investigation

7.5.1 Purpose of Experiments

The purpose of this part of the experimental programme was to compare the performance of the blowing seal with that of a similar sized drop-through rotary valve. In Chapter 4 the performance of a blowing seal was analysed simplistically and this indicated that for most normal operating conditions the discharge efficiency will be very high. If this is so, the primary factor limiting the performance of a blowing seal will be the pocket filling process. The results presented here show that this was the case with at least one of the test materials.

7.5.2 Experimental Plan and Method

The experimental plan was to examine the performance of a blowing seal with each of the six test materials described in Chapter 6. The blowing seal used was the Westinghouse GS-175 previously described in Chapter 5, see Figure 5.7. This particular blowing seal had the same internal dimensions as the drop-through rotary valve used for the previous work.

The experimental method which was used was exactly the same as that followed for the experiments with the drop-through valve. This enabled a complete set of data to be obtained for the envelope of conveying conditions indicated on the conveying characteristics shown in Figures 6.13 to 6.18.

7.5.3 Results

The results obtained with the blowing seal are compared with those for the drop-through rotary valve in Figures 7.81 to 7.92. The results presented for the drop-through valve are those obtained with drop-out box B.

7.5.4 Analysis and Discussion of Results

The solids mass throughputs obtained with the blowing seal were at least as good, and in most cases better than those which were achieved with the drop-through rotary valve and drop-out box.

Figure 7.81 shows that in the case of the Polyethylene Pellets the feeding factor was unity for the range of rotor speeds examined. The implication of this is that both the pocket filling and discharge processes were complete, as suggested by the analysis given in Chapter 4. However, Figure 7.82 shows that a similar performance was also obtained
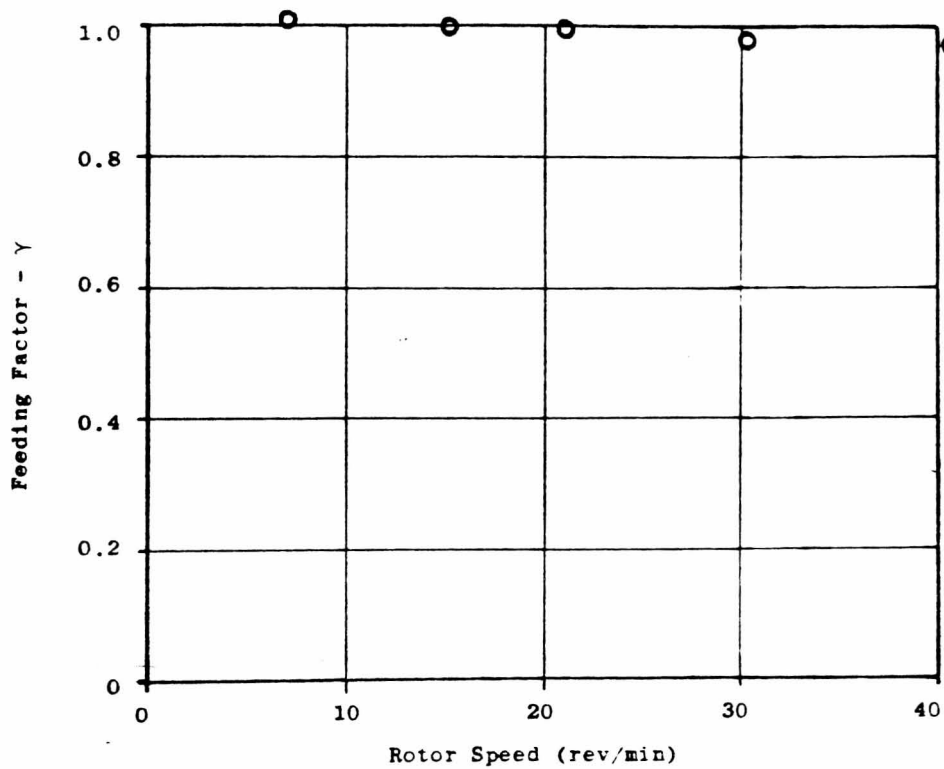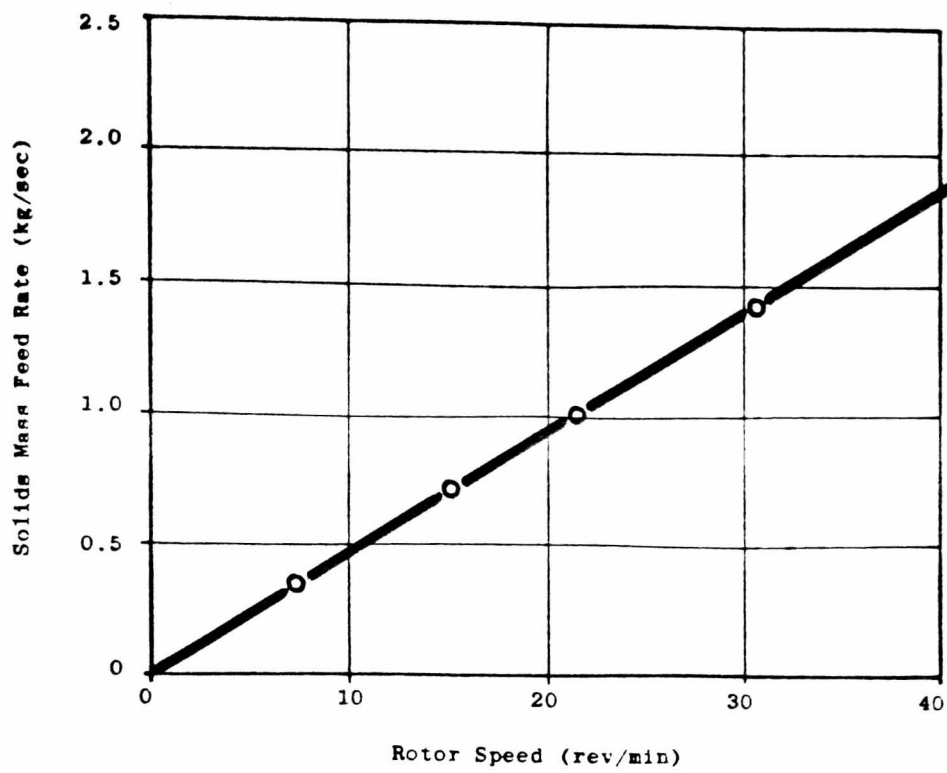
Figure 7.81 Feeding Characteristics of Polyethylene Pellets
with the Blowing Seal.
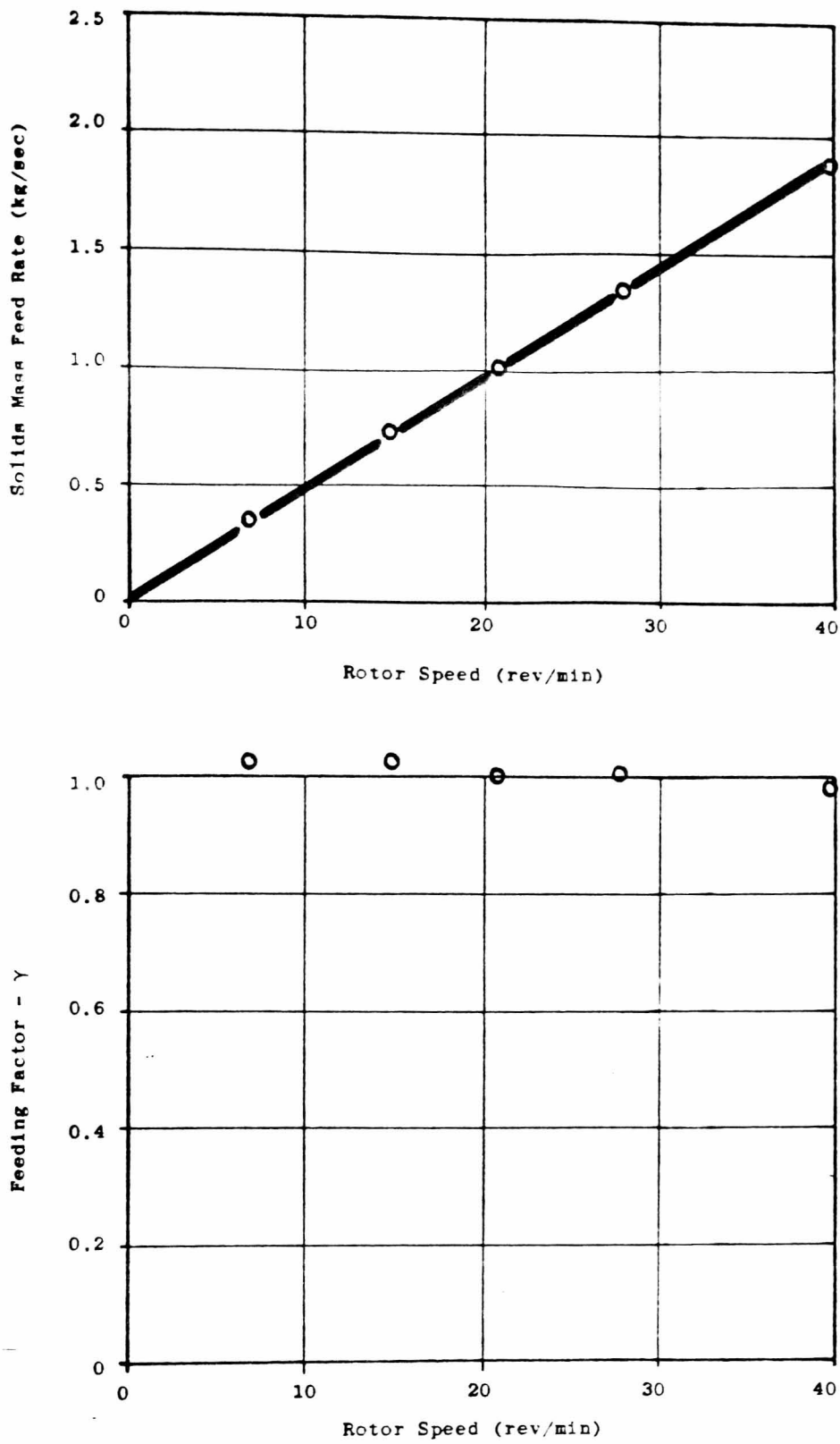
Figure 7.82 Feeding Characteristics of Polyethylene Pellets
            with Drop-Out Box B and Rotary Valve Orientation c.

with the drop-through rotary valve and drop-out box.   Consequently,
for this particular material, there is no advantage to be gained in using
a blowing seal instead of a drop-through valve.

Similarly with the Polyethylene Powder there was very little
difference between the performance of the blowing seal and the 'best'
performance obtained with the drop-through valve, see Figures 7.83 and
7.84.   However, in this case there was considerably less scatter in the
results obtained for the blowing seal and this could be a significant
advantage in some process systems where it is important to control the
feed rate within close limits.

The most distinct difference between the performance of the blowing seal
and the drop-through valve was obtained with the Wheat Flour and Cement.
In the case of the Wheat Flour the throughput of the blowing seal was
approximately 5% better than that obtained with the drop-through valve,
see Figures 7.85 and 7.86; and in the case of the Cement the difference
was approximately 10%.   Both of these two materials are more cohesive in
nature than the two grades of Polyethylene and this may be the reason why
they were handled more efficiently by the blowing seal.

As mentioned in section 7.3.4, the results obtained with the Singles
Coal had to be processed differently from those obtained with the other
materials because of severe degradation.   Despite the uncertainty which
this imposes on the calculated values of the feeding factor, it can be
seen from Figures 7.89 and 7.90 that the performance of the blowing seal
and drop-through valve were almost identical for this material.   This
result is not surprising because, unless a mechanical blockage occurred,
it would be reasonable to expect the lumps of coal to discharge easily
from the pockets of a drop-through valve; in which case there would be
no advantage in using a blowing seal.

The final material which was tested in the blowing seal was the
Pulverised Coal.   This also proved to be a problem material because the
pocket filling process restricted the throughput which could be achieved.
This was referred to in section 7.3, where the effect of the size and
shape of a drop-out box were discussed.   Comparing Figure 7.91 with the
results obtained for all the other entrainment configurations used with
the Pulverised Coal shows that they are all similar and that there is a
significant amount of scatter in the results.   Consequently no conclusions
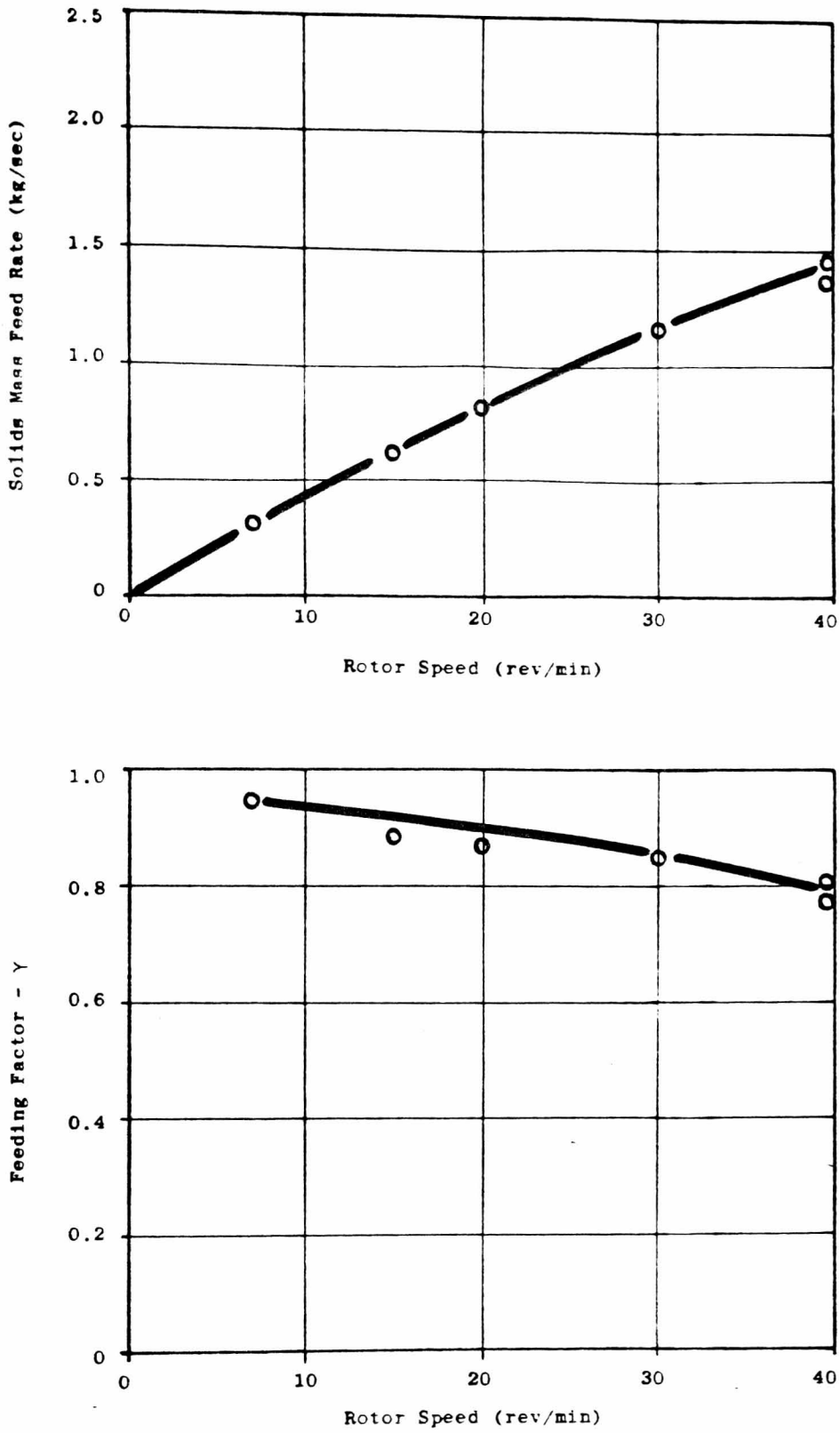
Figure 7.83 Feeding Characteristics of Polyethylene Powder
             with the Blowing Seal.
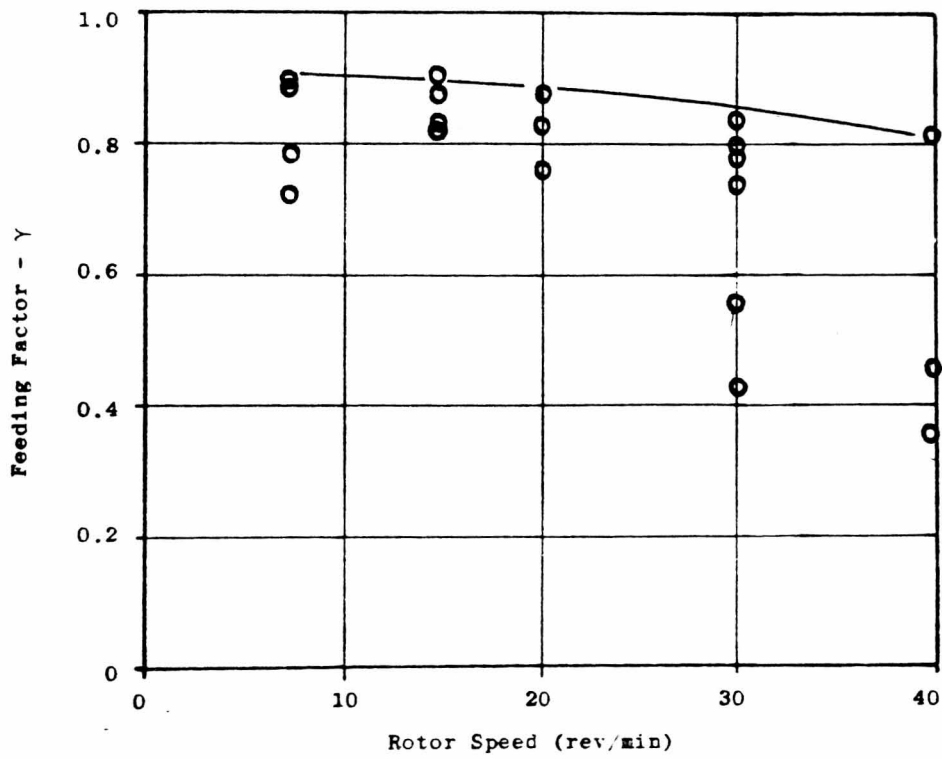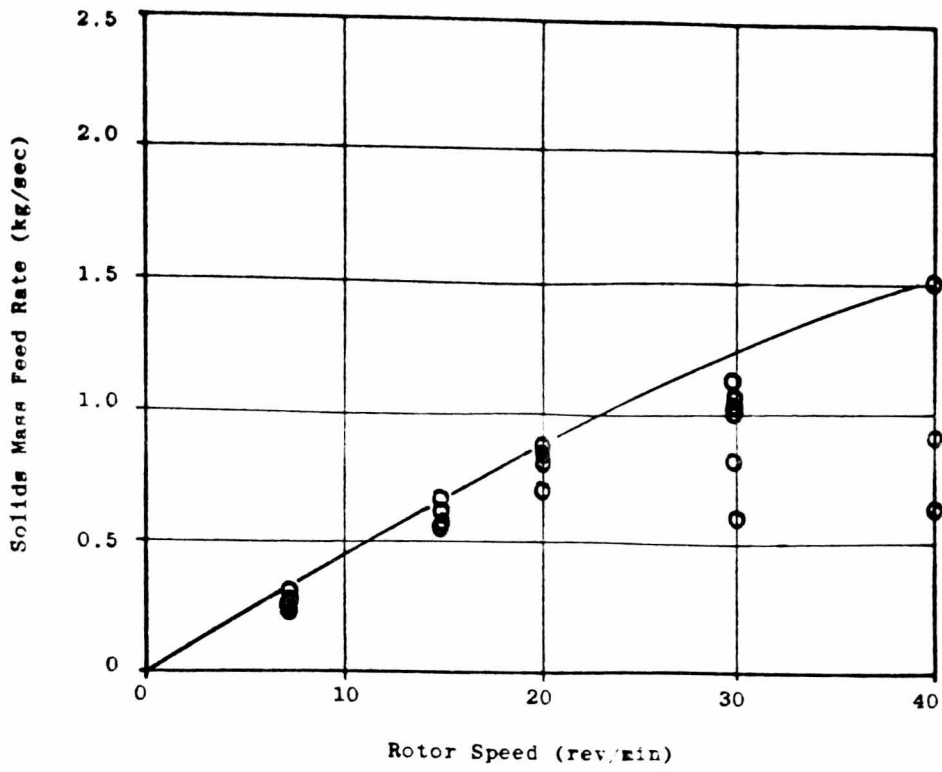
Figure 7.84 Feeding Characteristics of Polyethylene Powder
with Drop-Out Box B and Rotary Valve Orientation c.
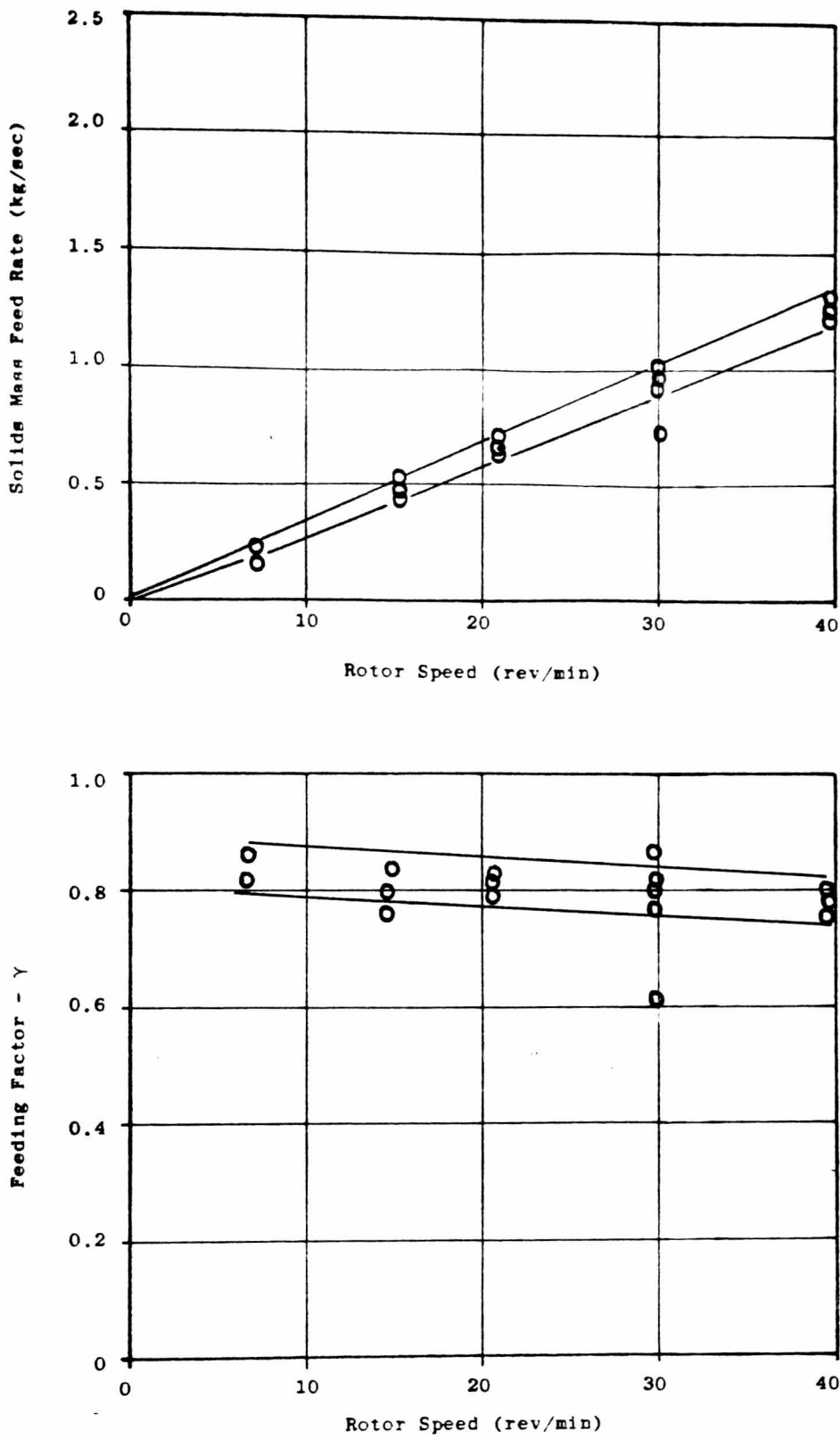
Figure 7.85 Feeding Characteristics of Wheat Flour
            with the Blowing Seal.
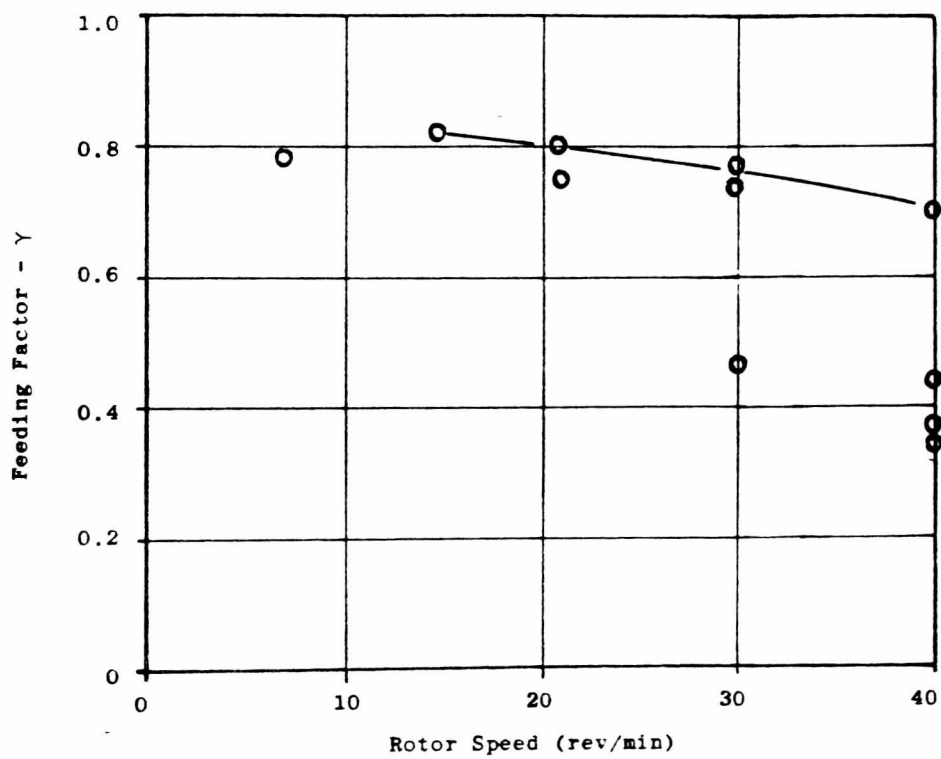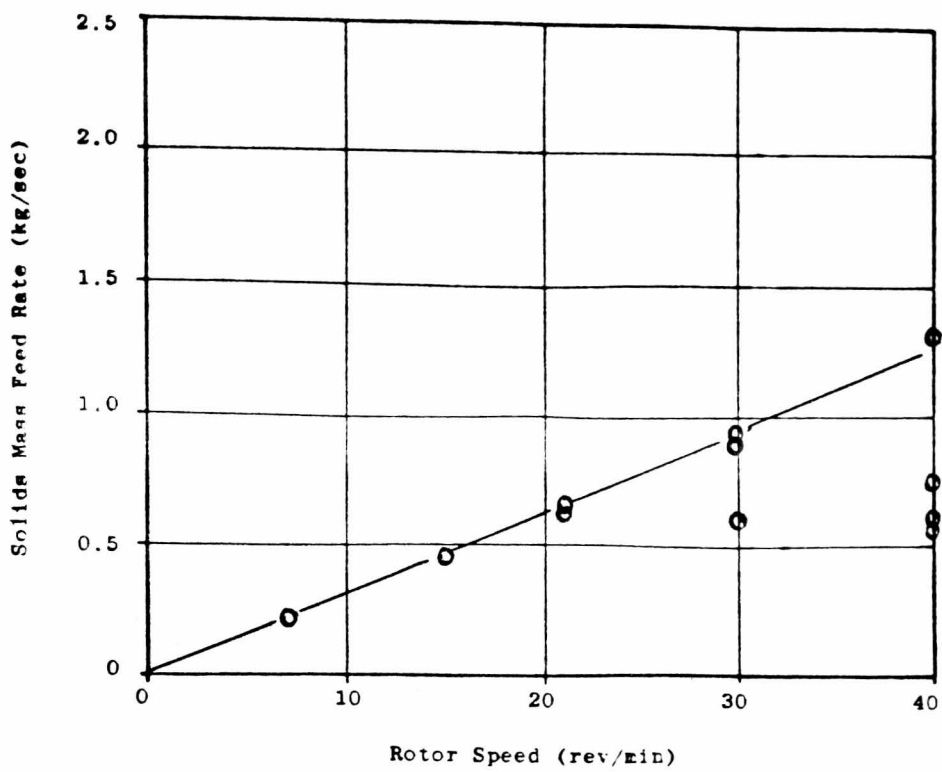
Figure 7.86 Feeding Characteristics of Wheat Flour
with Drop-Out Box B and Rotary Valve Orientation c.
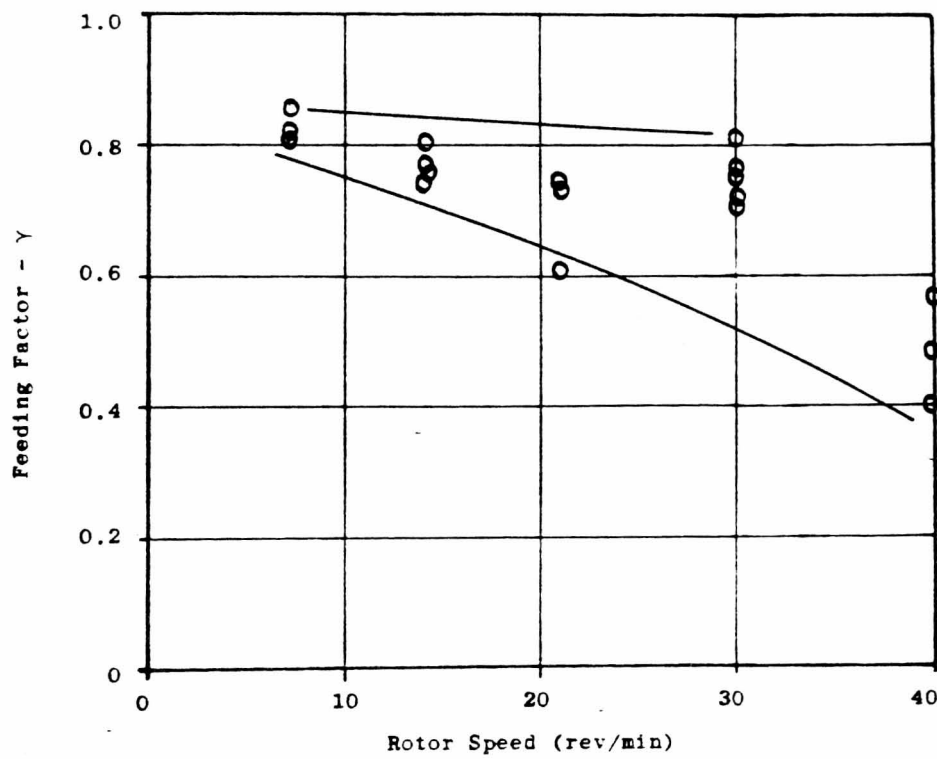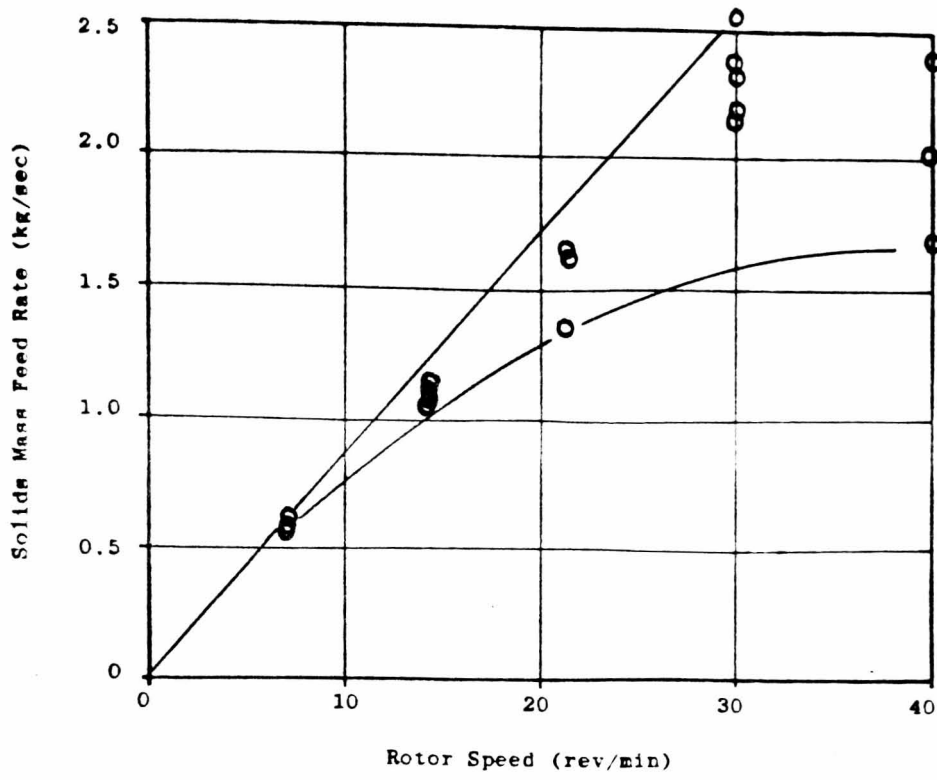
Figure 7.87 Feeding Characteristics of Cement
with the Blowing Seal.
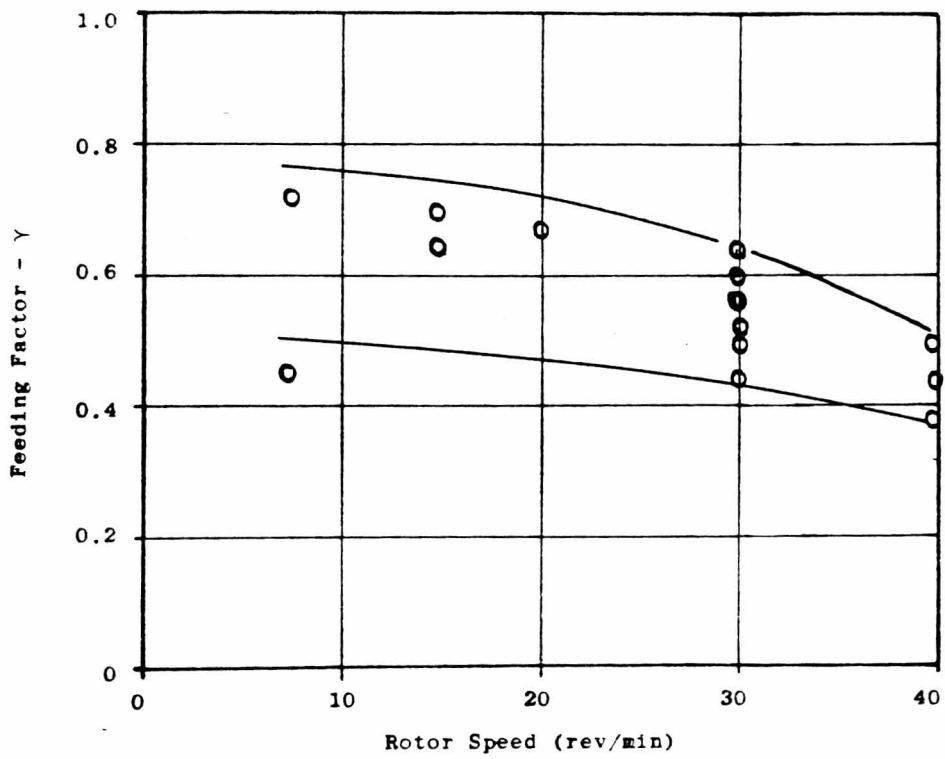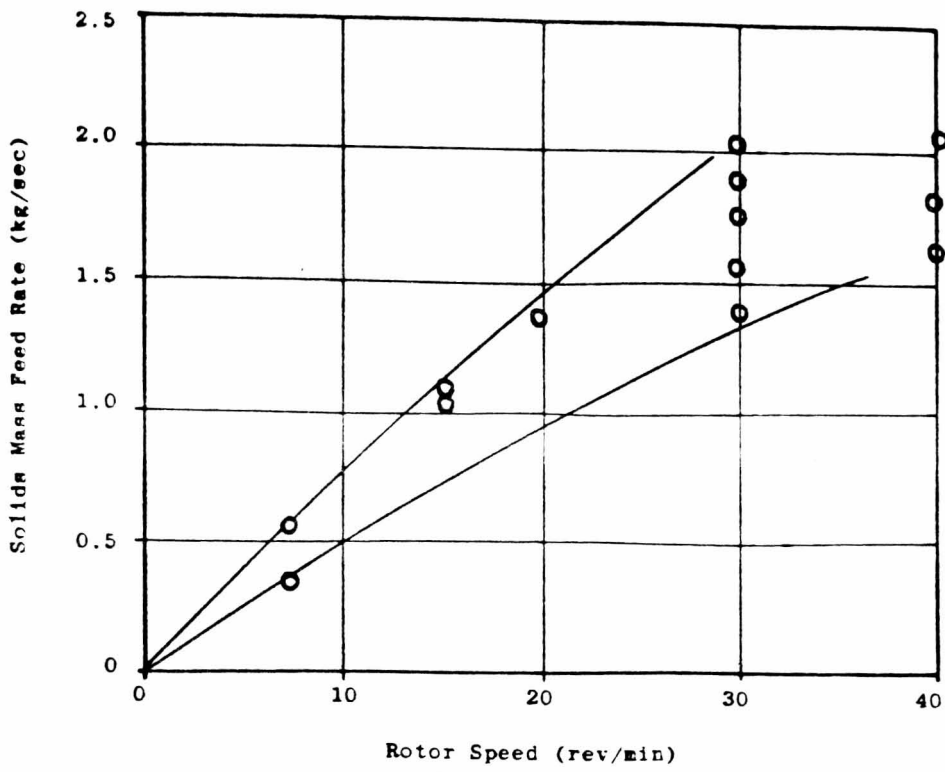
Figure 7.88 Feeding Characteristics of Cement
with Drop-Out Box B and Rotary Valve Orientation c .
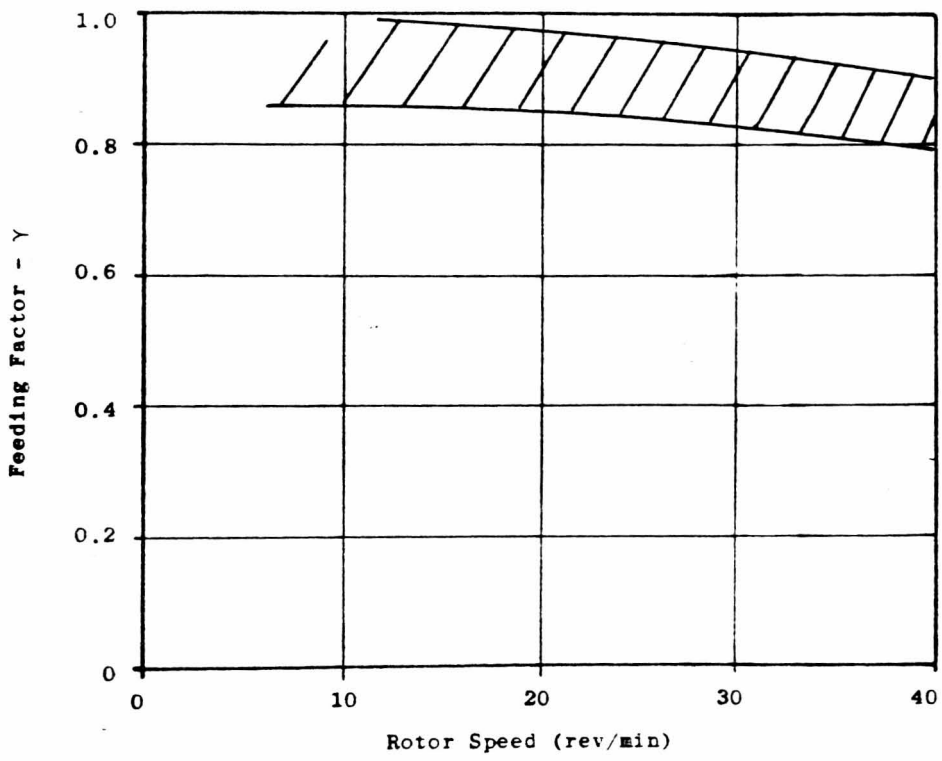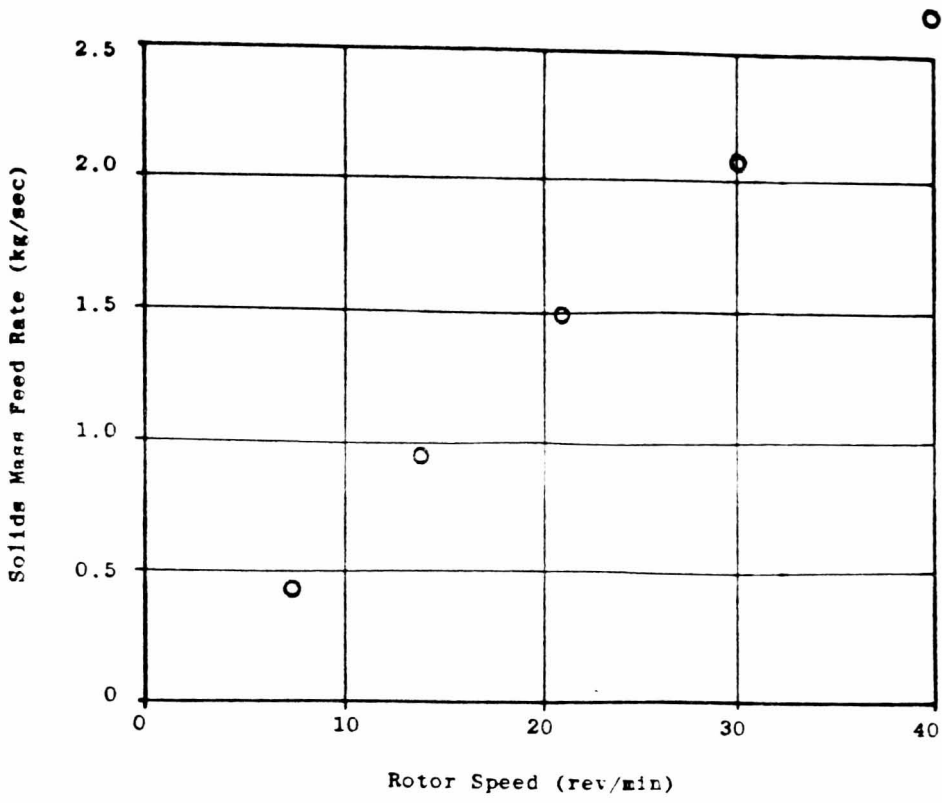
Figure 7.89 Feeding Characteristics of Singles Coal
            with the Blowing Seal.
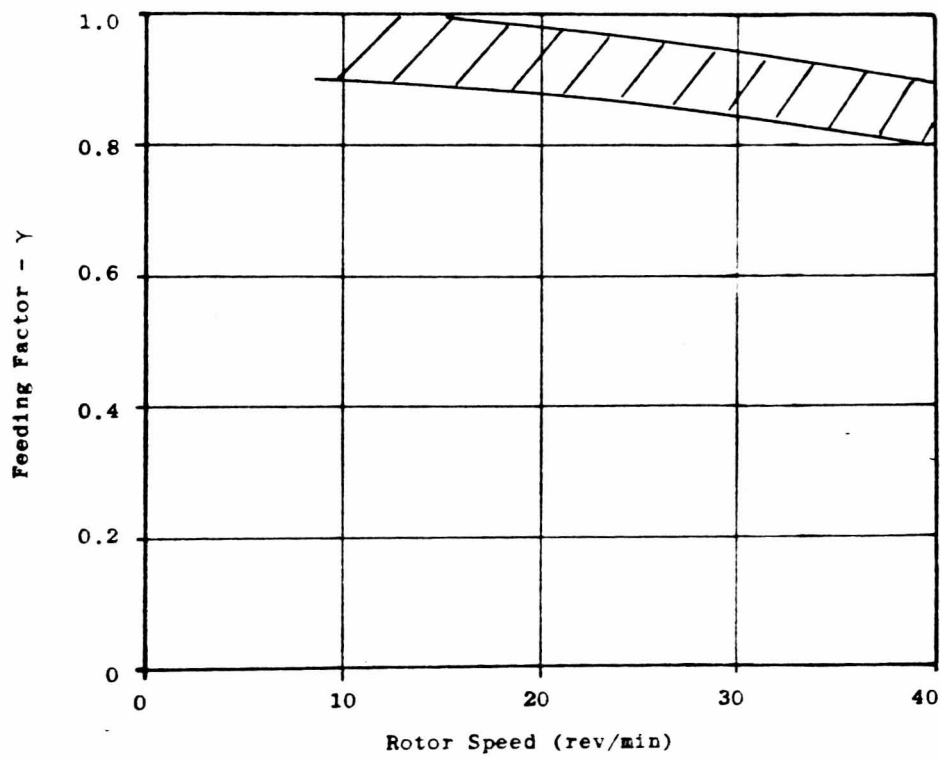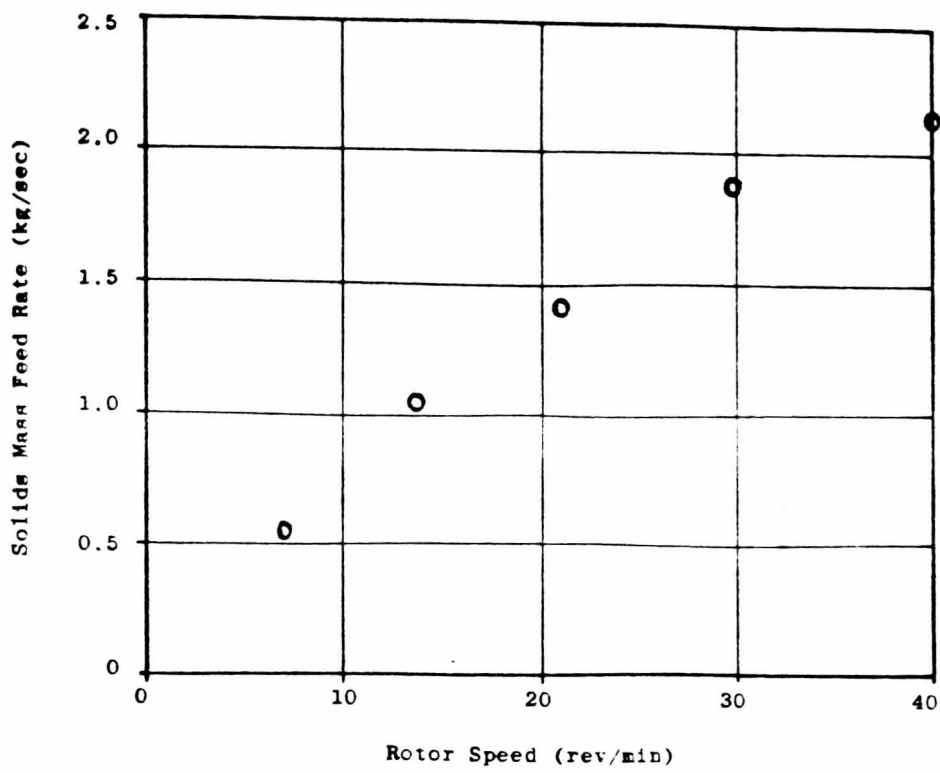
Figure 7.90 Feeding Characteristics of Singles Coal
             with Drop-Out Box B and Rotary Valve Orientation c.
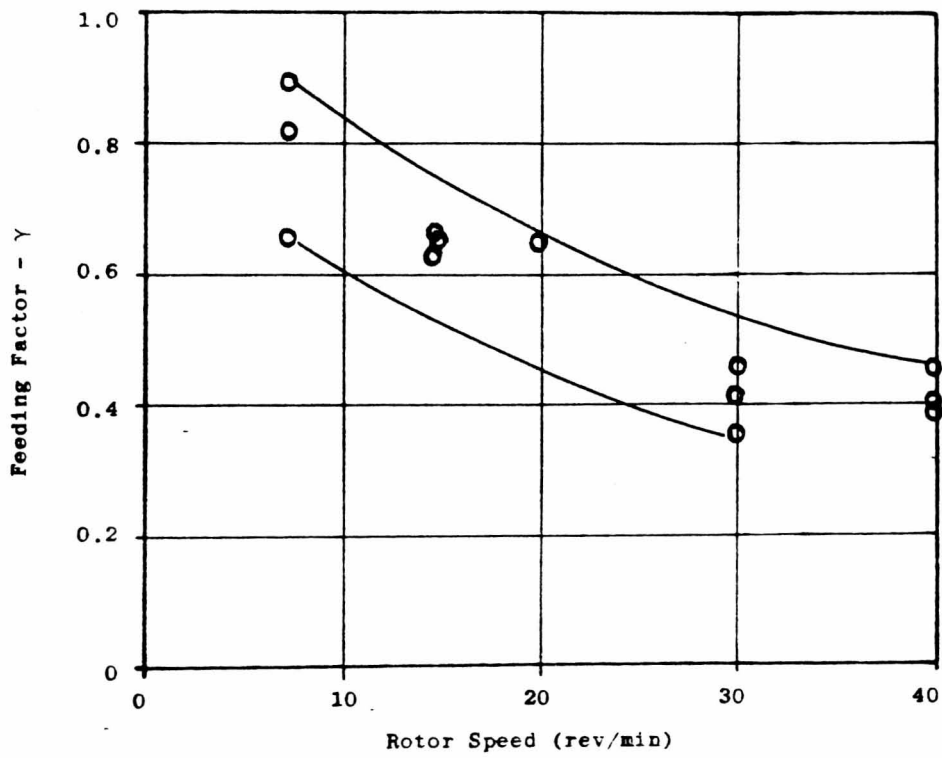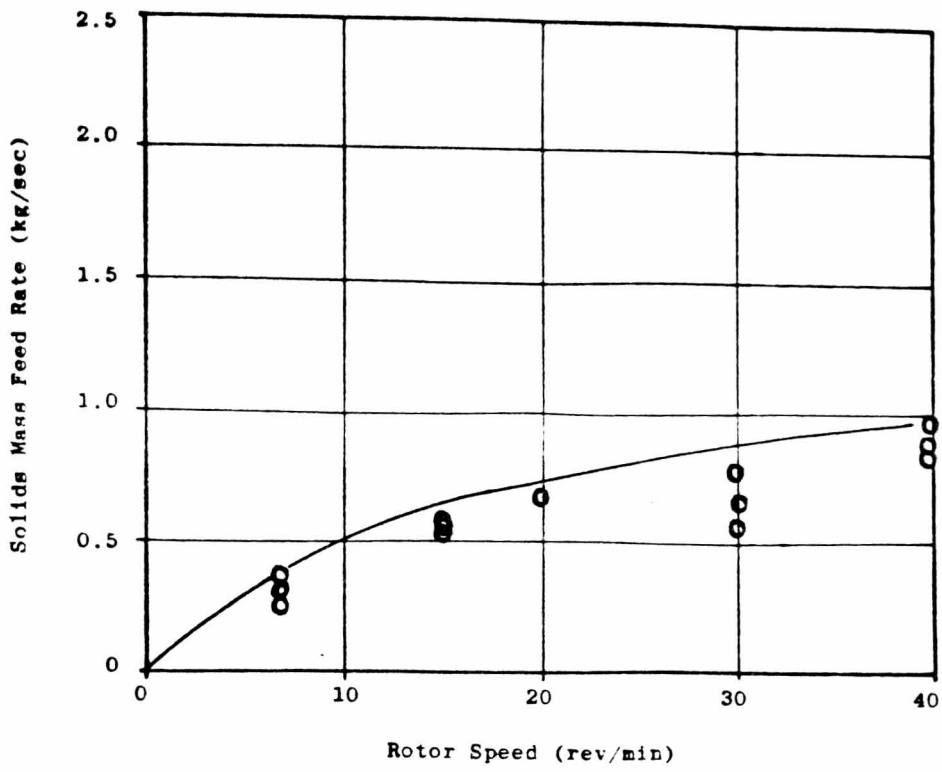
Figure 7.91 Feeding Characteristics of Pulverised Coal
            with the Blowing Seal.
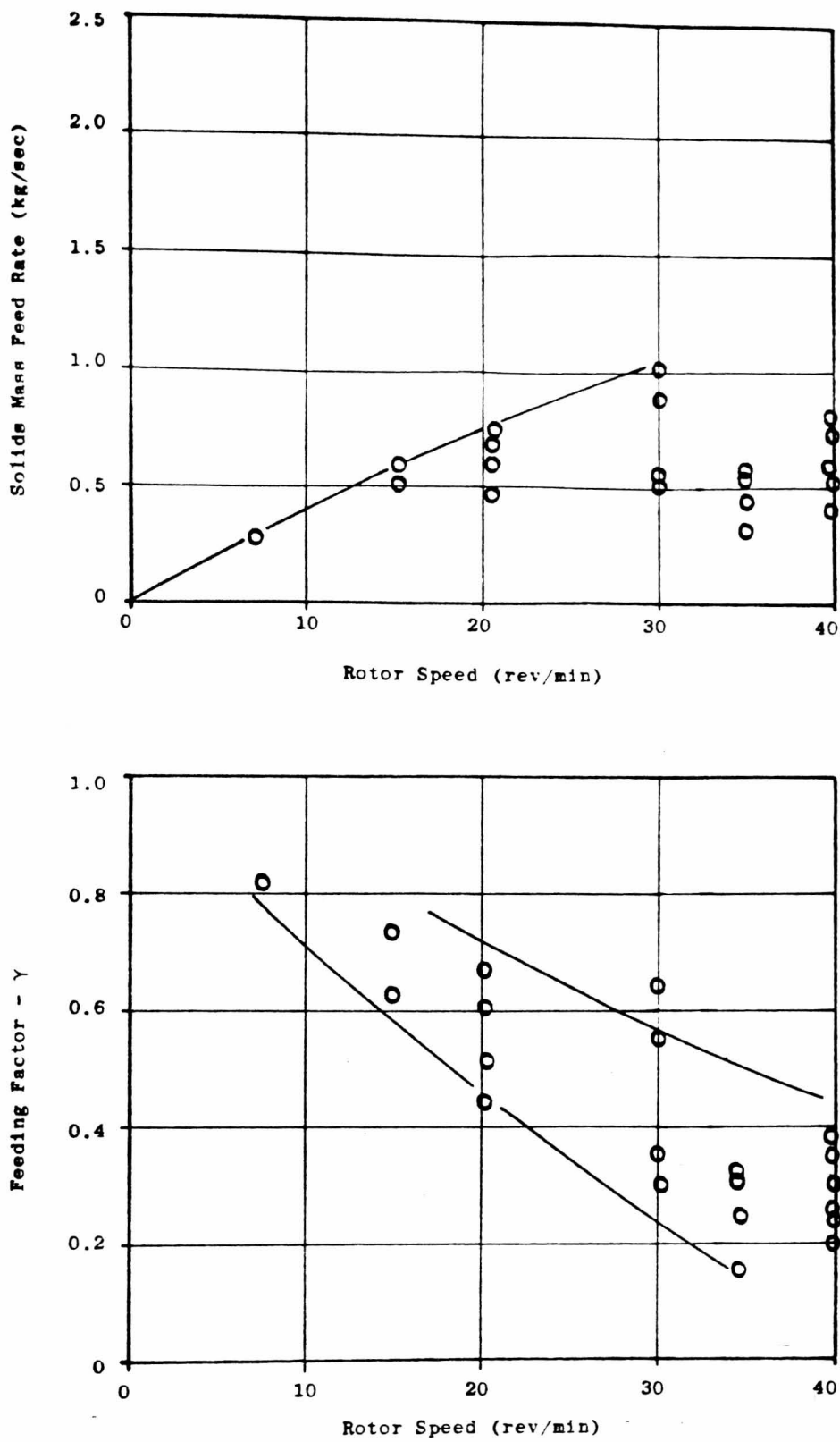
Figure 7.92 Feeding Characteristics of Pulverised Coal
            with Drop-Out Box B and Rotary Valve Orientation c .

can be made about the relative performance of the blow seal and drop-
through valve when handling this material.

The implications of these results are:

i) there are no advantages to be gained by using a blowing
seal if the product being handled is free-flowing; if it
is free-flowing the material is non-cohesive.

ii) in some cases the product throughput may be controlled
more precisely by a blowing seal than by a drop-through
valve; and

iii) for cohesive materials the blowing seal will be more
efficient than the drop-through valve, but the actual
difference between them will depend on the characteristics
of the particular material being handled.

7.6 Air Leakage Measurements

7.6.1 Purpose of Experiment

The purpose of measuring the air leakage through the rotary valve was to
obtain data which could then be used to predict the air leakage for
similar conveying systems. The reason for doing this is that the air
which leaks through a rotary valve can often be a significant proportion
of that needed to convey the product. Consequently, it is of considerable
interest to be able to estimate the air leakage accurately in order that
the air supply may be adequately sized.

In this section the air leakage measurements for four of the test
materials are presented and these are compared with the air leakage rates
predicted by the method developed by Reed (11)[*]. In view of these
results a simple modification to the Reed model is proposed which allows
the air leakage to be predicted more accurately.

7.6.2 Experimental Plan and Method

The experimental plan was to make measurements of the air leakage during
the course of conducting the experiments reported in the previous sections
of this chapter. The method used to measure the air leakage was to duct
the air from the constant head tank and supply hopper to a bank of
rotameters, as previously described in Chapter 5. This bank of rotameters
were connected by a manifold and by opening or closing valves in this
manifold the best combinations of rotameters for the air leakage rate

---

* footnote: See section 2.2.7 of Chapter 2

could be selected, see Figure 5.9 of Chapter 5.

7.6.3 Results

The results obtained from the air leakage measurements are presented in Figures 7.93 to 7.97. These figures consist of graphs which show the variation of the volumetric air leakage rate ($\dot{V}_L$) with the pressure ratio across the rotary valve (ΔP_V). As well as the experimental data points which are plotted on these graphs, the predicted air leakage characteristics obtained by using Reed's model are also shown.

It will be seen from Figures 7.93 to 7.97 that results are not presented for two of the test materials, namely, the Cement and the Pulverised Coal. Results could not be obtained with these products because they carried over into the ducts which connect the constant head tank and supply hopper to the rotameter manifold. Consequently, the rotameters became fouled and it was impossible to take meaningful readings.

7.6.4 Analysis and Discussion of Results

Figure 7.93 shows the relationship between the measured volumetric air leakage rate and the pressure ratio across the rotary valve for the situation where there is no material in the supply hopper or conveying line. This particular data was obtained with the AS-175 rotary valve at a rotor speed of 7 rev/min, but check at other rotor speeds revealed that the air leakage characteristics did not change with this parameter. This finding is in agreement with the work of Reed.

From Figure 7.93 it can be seen that the predicted air leakage is in good agreement with the actual measured air leakage for the range of pressure ratios which were examined. The reason for constructing this graph is that it provides a basis against which to compare the results obtained for the situations where materials were being conveyed.

Figures 7.94 to 7.97 show the results obtained for the Polyethylene Pellets, Polyethylene Powder, Wheat Flour and Singles Coal respectively. The data points shown on these graphs are the combined results for all the different entrainment configurations which were tested, including the blowing seal. The reason for combining the results in this way was that there was no significant difference between the air leakage

characteristics for these different configurations.
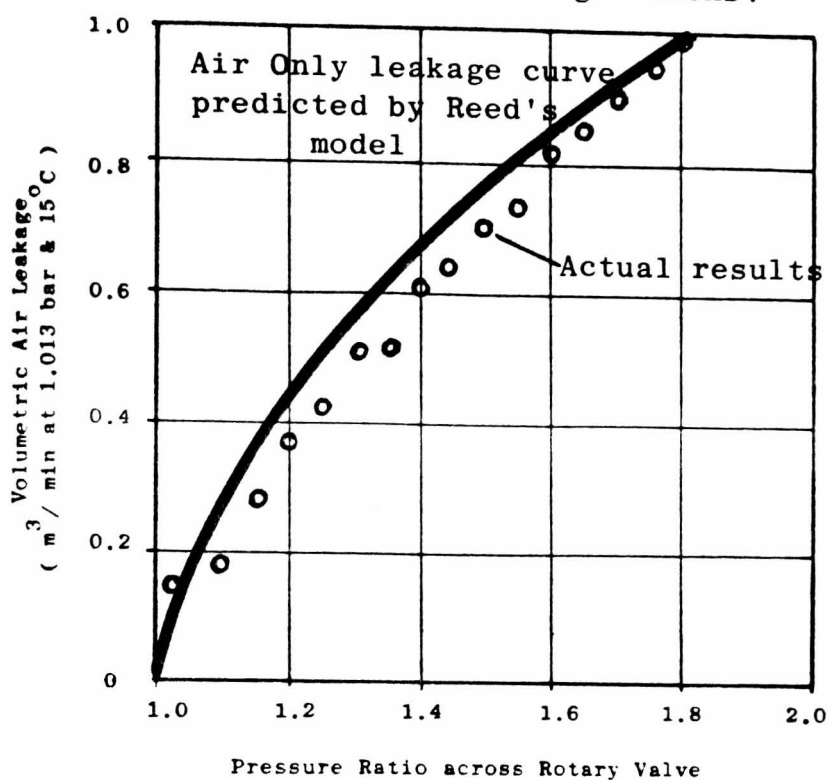
Figure 7.93 Rotary Valve Air Leakage Characteristics
for Air Only.

Figures 7.94 to 7.97 show that the actual measured air leakage was significantly less than that predicted by Reed's model, even when making allowance for the presence of the material as suggested by him. For the two grades of Polyethylene and the Wheat Flour the actual leakage rates were approximately 60% of those which were predicted and for the Singles Coal the actual leakage rate was only about 35% of that predicted. To explain these differences, the difference between the rig used by Reed to obtain his data and the rig used for this study must be considered.

Figure 7.98 is a diagram of the rig used by Reed. From this it can be seen that the rotary valve was not connected to a conveying line but was used to feed material directly into a pressurised receiving vessel. Consequently, the only way for air to excape from the receiving vessel was through the clearances within the rotary valve. Furthermore, because of this arrangement it is reasonable to suppose that there were no significant air currents immediately beneath the discharge port of the rotary valve, such as those that are present when the valve is being used to feed a pneumatic conveying line.
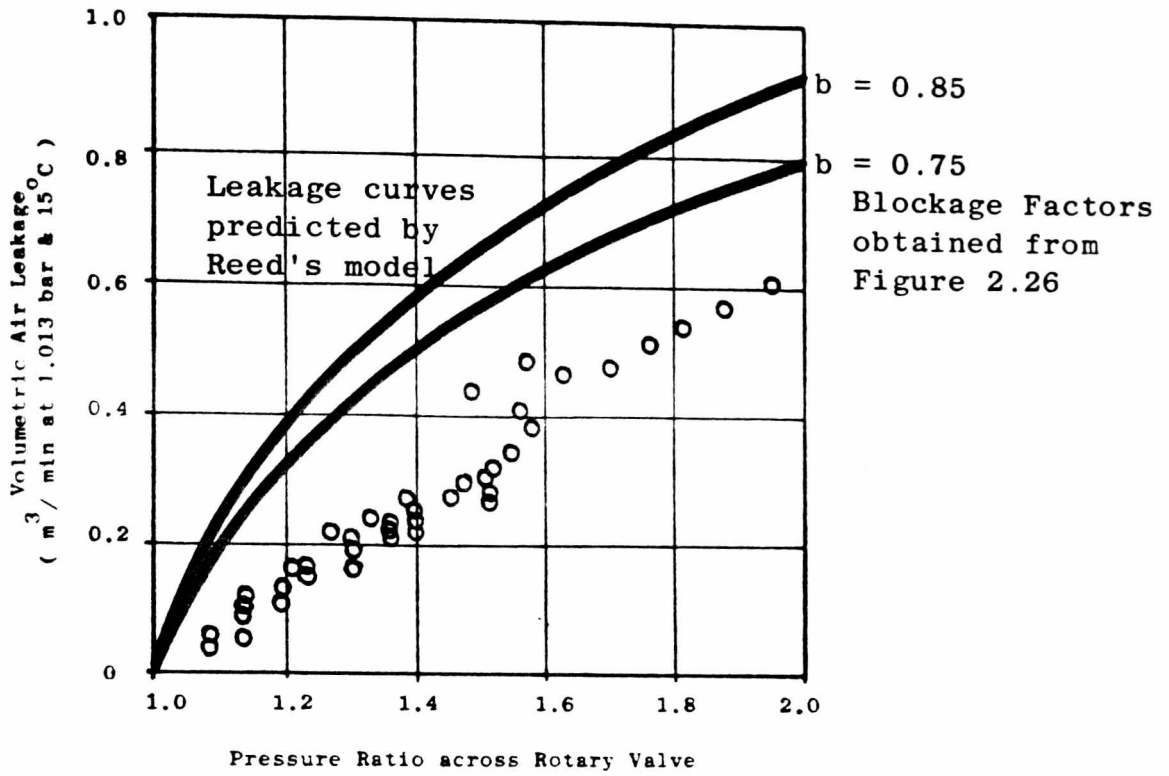
Figure 7.94 Rotary Valve Air Leakage Characteristics
for Polyethylene Pellets.
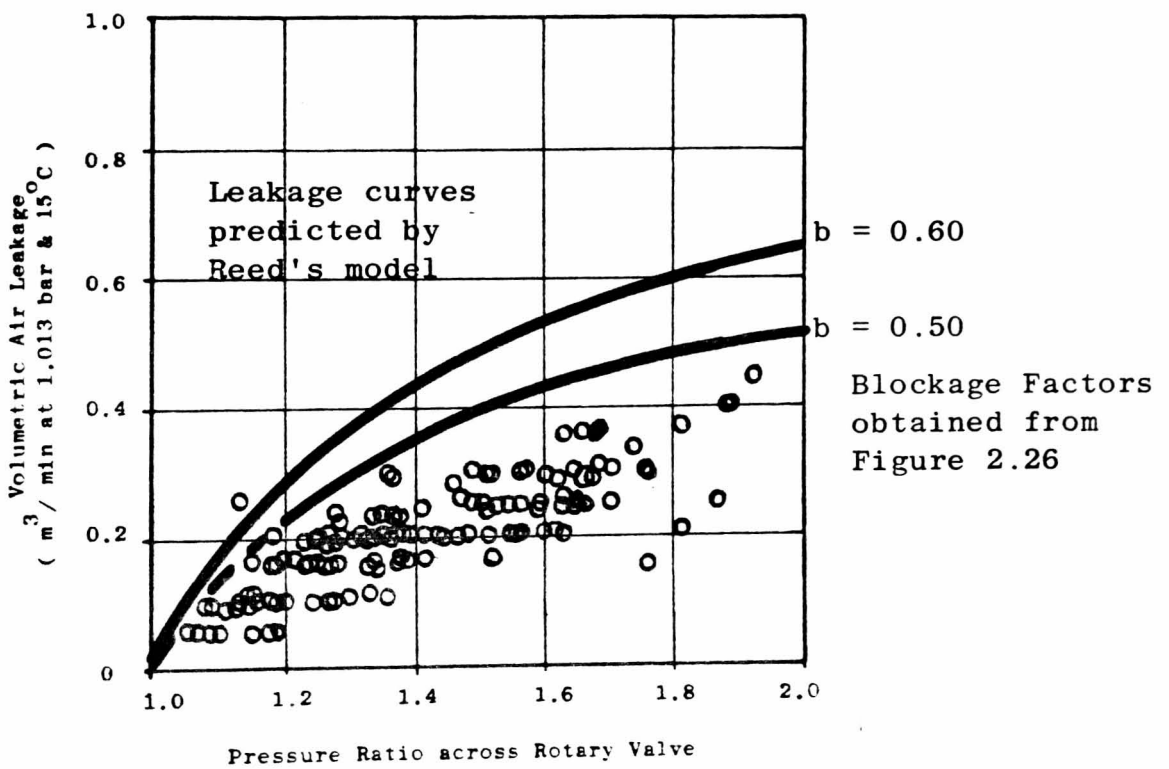
Figure 7.95 Rotary Valve Air Leakage Characteristics
for Polyethylene Powder.
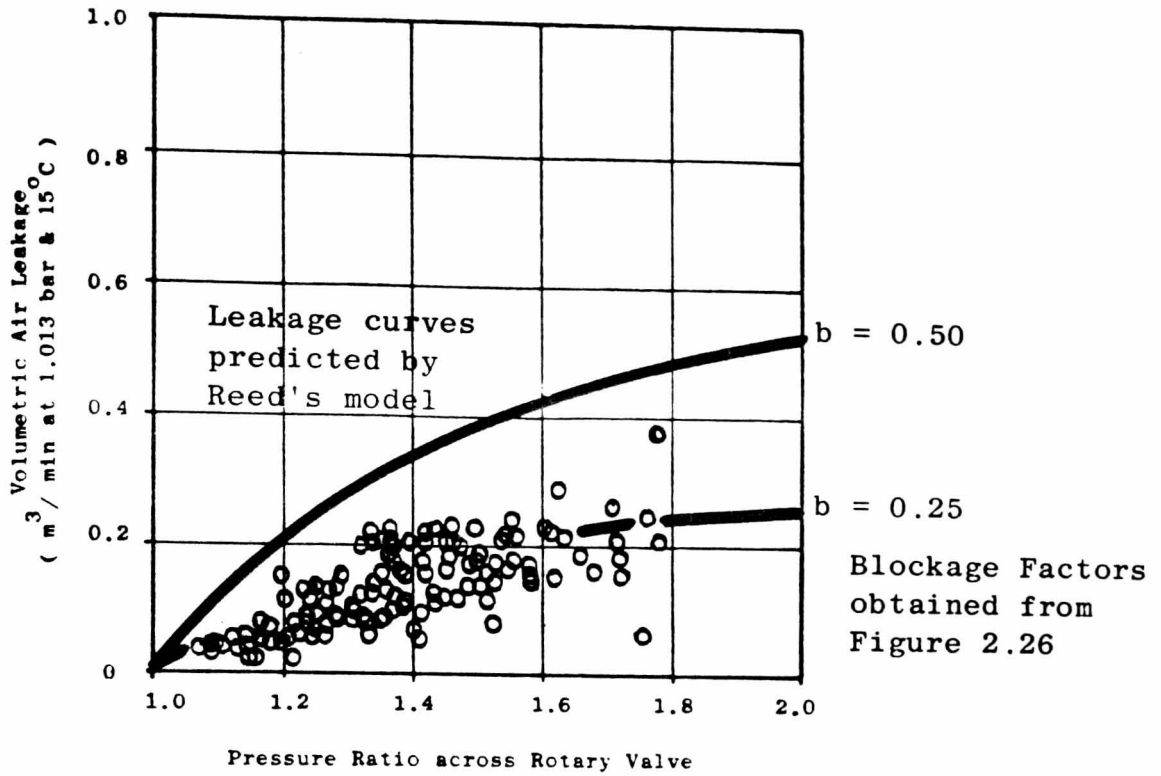
Figure 7.96 Rotary Valve Air Leakage Characteristics
for Wheat Flour.
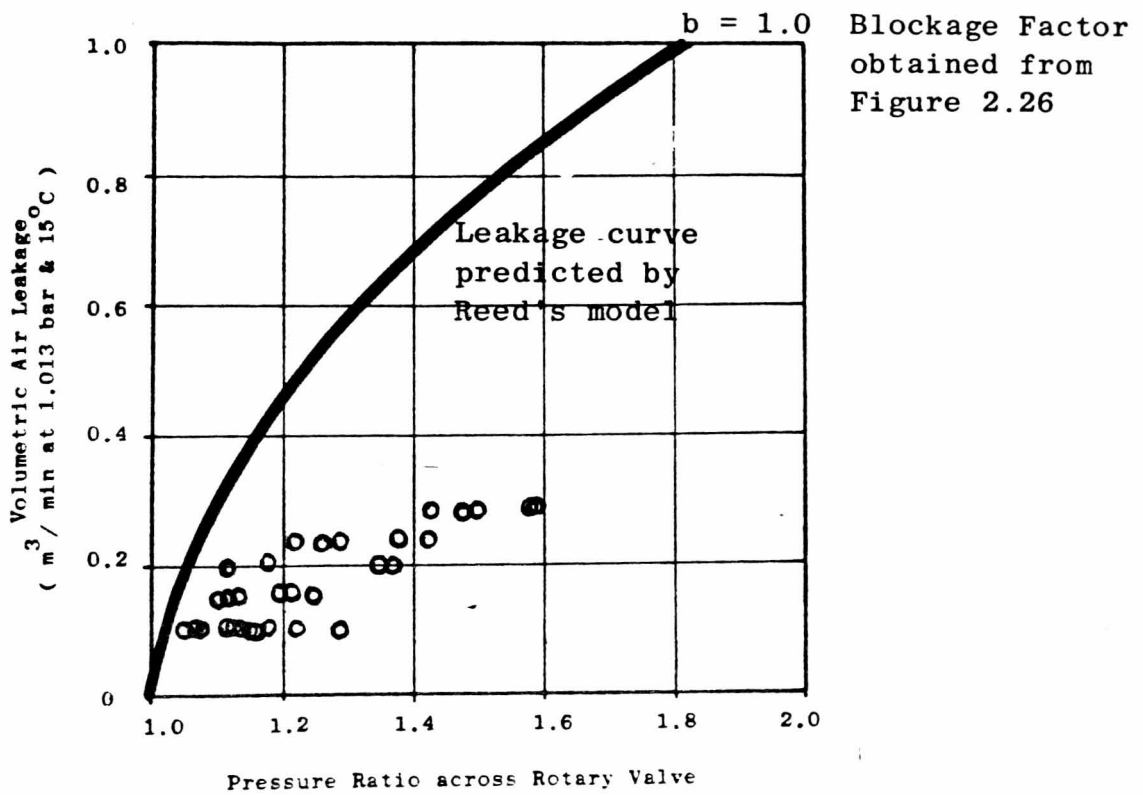
Figure 7.97 Rotary Valve Air Leakage Characteristics
for Singles Coal.
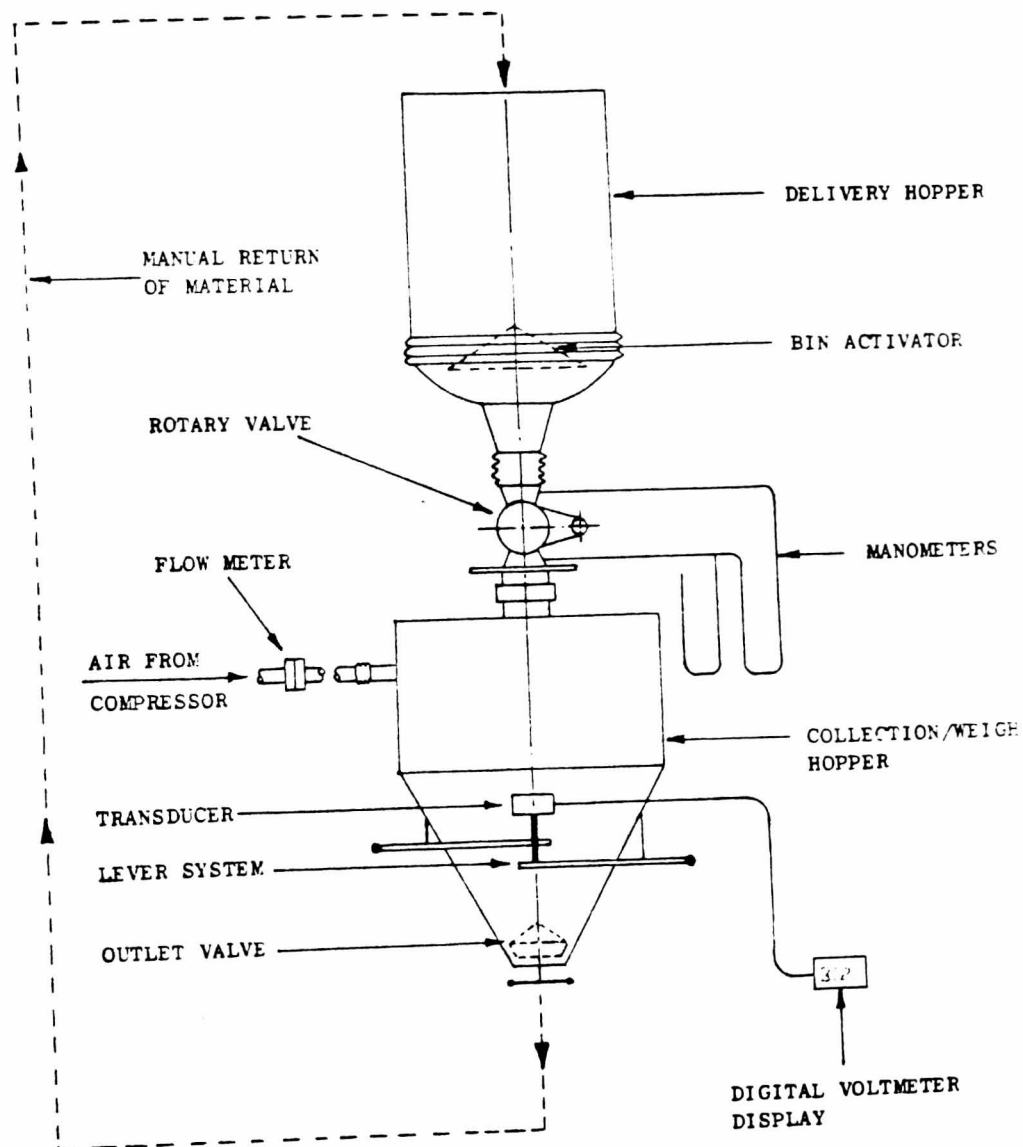
Figure 7.98 Schematic diagram of the rig used by Reed (11).

In contrast, the rig used in this study consisted of a pneumatic conveying system in which the rotary valve was used to feed material into a drop-out box.   Consequently, there were very strong air currents on the discharge side of the rotary valve and an alternative route for the air to take, that is, along the pipeline.

It is proposed that the significant difference between these two systems with regard to the air leakage, is the presence of the strong air currents in the drop-out box of the rig used for this study.   Since the air in the drop-out box has momentum in directions other than towards the discharge port, it is postulated that this will result in a lower air leakage than when the air is stationary and at the same static pressure. If this argument is accepted, then it follows that the air leakage through a rotary valve used to feed a conveying line will be less than that through the same valve when used to feed a simple container at the same pressure as the conveying line.   Blackmore (67) has stated that this conclusion is in agreement with his own practical experience that the air leakage through a rotary valve used to feed material into a dynamic airstream will invariably be less than that through a rotary valve used to feed a static airstream.

When the air only leakage characteristics, presented in Figure 7.93, were obtained, the pipeline had to be blocked in order to generate a significant pressure ratio across the rotary valve.   This would explain the good agreement with the predicted characteristics because the air beneath the rotary valve would have been relatively static and thus similar to the situation in the rig used by Reed.

From the results shown in Figures 7.94 to 7.97, Figure 7.99 was constructed.   This is similar to the figure proposed by Reed for estimating the blockage factor (b) of materials when handled in rotary valves, see Figure 2.26 in Chapter 2.   The blockage factor is the ratio of the air leakage through a rotary valve when material is being conveyed to the air leakage through the same valve when no material is being conveyed.   When used in equation 2.23, which was proposed by Reed for estimating the air leakage rate, it makes allowance for the presence of the material and the effect which this has in blocking the valve clearances.   However, because Reed's data was obtained from the rig shown in Figure 7.98 it was not representative of the leakage

characteristics of a rotary valve used to feed a pneumatic conveying line.

In Figure 7.99 the results obtained from this study are used to suggest a relationship between the blockage factor and the mean particle size of the product which is representative of the leakage characteristics of a rotary valve used to feed a pneumatic conveying line.

The one anomaly in these results is the apparently very low blockage factor obtained with the Singles Coal. This was only 35% of the value suggested by Reed's work, instead of approximately 60% as obtained with the other three materials. The reason for this may be due to the rapid degradation of the Singles Coal which resulted in a significant proportion of fines. It is believed that these blocked the clearances in the rotary valve in the same way as a product with a small mean particle size. This would explain the low air leakage rates which were measured with the coal.

The useful implication of these results is that the method proposed by Reed for estimating the air leakage through a rotary valve used to feed a static airstream may also be applied to the situation where the valve is used to feed a pneumatic conveying line. However, when used for the latter situation the blockage factor should be obtained from Figure 7.99. This will then make an allowance for the effect of the interaction with the pipeline.
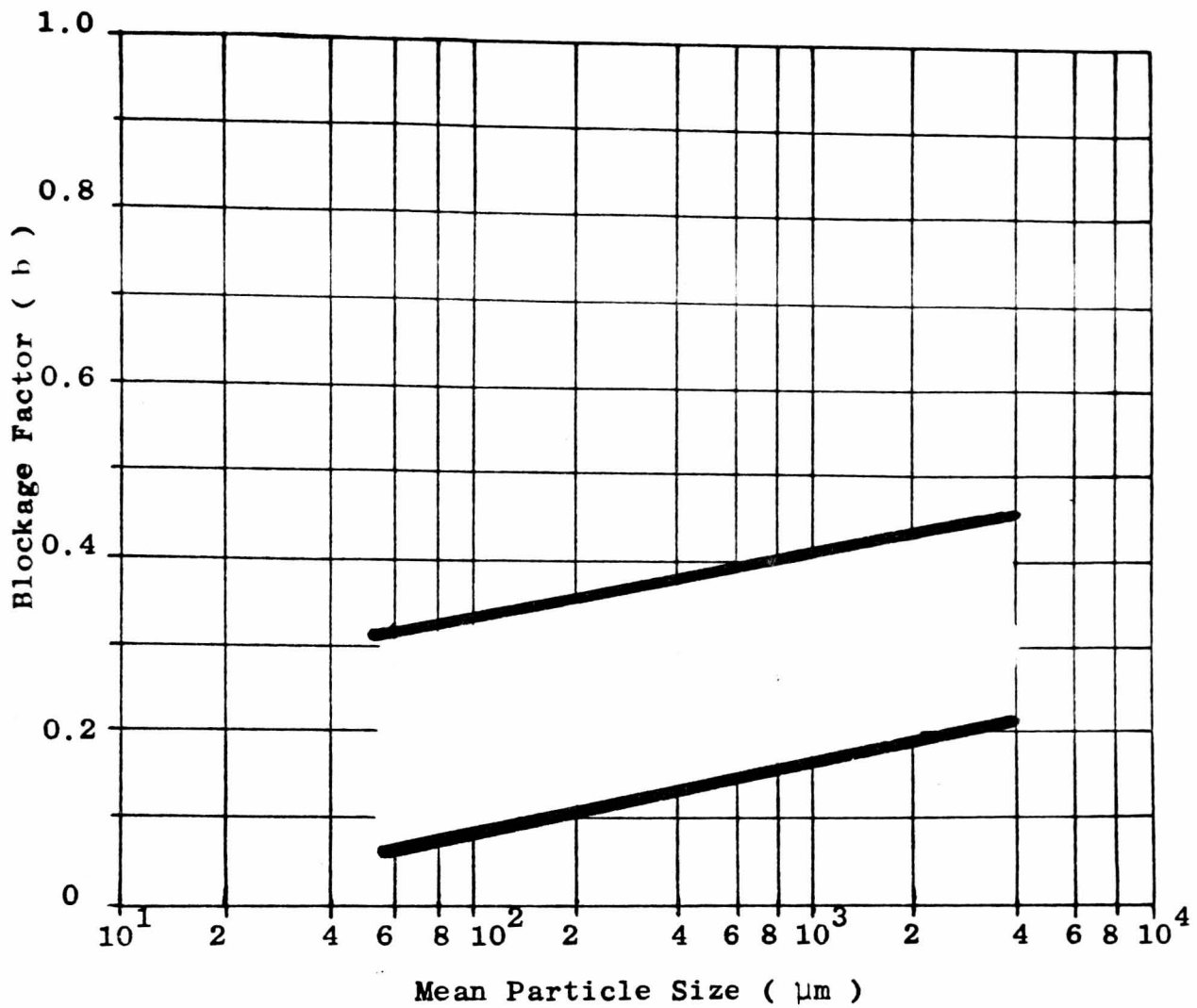
Figure 7.99 The Relationship between the Blockage Factor
            and the Mean Particle Size of a Product for
            a Rotary Valve Feeding a Pneumatic Conveying
            Line.

CHAPTER EIGHT

CONCLUSIONS

8.1 Current Understanding as a Result of this Research

8.1.1 Introduction

Before starting the work reported in this thesis very little information was published about the interaction between rotary valves and pneumatic conveying pipelines. The suppliers of such systems usually have their own ideas and preferences with regard to the way in which these two components should be interfaced, but these are usually based on supposition rather than factual evidence.

It is proposed that this research has led to a better understanding of this interaction and the effect which it can have on the overall system performance. In particular, it is now known that there are two distinctly different modes of flow which can take place in the chamber of the conventional type of drop-out box. The first of these is a turbulent swirling motion caused by the action of the conveying air-stream on the 'captive' volume of air in the drop-out box. This is the most desirable operating condition because it results in the most effective entrainment of material into the conveying line. The other mode of flow is a situation where the drop-out box is effectively 'choked' with product. The cause of this has been identified as a high initial feed rate combined with a high conveying air velocity and is a condition that should be avoided because it can severely restrict the performance of the system.

In addition to identifying these two modes of flow the research has also provided answers to some of the questions posed in Chapter 1, where industrial problems and reasons for the research were discussed.

These questions were:

a) Is there a best orientation of the rotary valve with respect to the pipeline?

b) Is the direction of rotation of the rotor in relation to the pipeline important?

c) Are the size and shape of the drop-out box important?

d) Does the air velocity in the entrainment region affect performance?

e) In what way do the characteristics of the material to be handled affect the answers to the preceding questions?

The following sections summarise the answers to these questions based on the findings of this research.

8.1.2 Valve Orientation and Direction of Rotation of Rotor

The evidence of the research is that the orientation of a rotary valve and the direction of rotation of the rotor have no measurable effect on the rate at which it is possible to feed material into a conveying system. Furthermore, this was found to be the case with all the combinations of material and entrainment configuration tested. The implication of this for practical system design is that it is not necessary to use an specific orientation and/or direction of rotation in order to ensure satisfactory performance.

8.1.3 Size and Shape of the Drop-out Box

The research has shown that the size and shape of a drop-out box can have a measurable effect on the feed rate which can be achieved with a given rotary valve, but the extent of this effect is dependent on the characteristics of the bulk solid being handled.

For large particle, free-flowing materials the feed rate is not perceptibly affected by changes in the size or shape of the box; as demonstrated by the results obtained with the Polyethylene Pellets. The only practical problem which may arise with large products is that of mechanical blockage if the particles are very large in comparison with the size of the box chamber. In this respect, it is somewhat surprising to note that no blockages occurred when the Singles Coal was tested. This had a nominal size distribution between 12.5 and 25 mm and was successfully handled in a drop-out box only 75 mm deep. Nevertheless, the possibility of a mechanical blockage should not be overlooked when

dealing with such materials and the drop-out box should be sized accordingly.

For fine particle products the evidence of the research is that increasing the volume of the drop-out box will lead to a general improvement in the entrainment process. However, it is difficult to quantify this effect and it is unlikely to be significant unless the initial volume of the box was very small, for example, that corresponding to a box depth of less than two pipe diameters.

8.1.4 Volume Ratio and Entrainment Efficiency

In an attempt to categorise different combinations of rotary valve and drop-out box and quantify the effect of drop-out box size on performance a term called the 'volume ratio' (v_R) has been proposed. This was defined as the ratio of the volume of the rotor pocket(s) which engage with the valve discharge port to the overall volume of the drop-out box chamber. In Chapter 4 it was argued that this could be used to determine a theoretical entrainment efficiency (η_e) if a simplified model of the entrainment process was accepted. As a result of this the following expression relating η_e and v_R was proposed:

$$\eta_e = (1 - v_R) \times 100\% \qquad (4.9a)$$

Although the experimental results are not exactly predicted by this relationship the general trends are in the same direction. That is, combinations of rotary valve and drop-out box with a large volume ratio are generally less efficient than those with a small volume ratio. In addition there is some evidence to suggest that increasing the volume of the drop-out box by increasing its depth is more effective than increasing the volume by changing the shape. However, the research has demonstrated that a volume ratio between 0.07 and 0.15 and a drop-out box depth between two and three pipe diameters will usually result in satisfactory performance.

8.1.5 Air Velocity

The research has shown that the air velocity in the drop-out box can have a significant effect on system performance depending on the nature of the product being handled and the type of drop-out box being used. For conventional transition shaped drop-out boxes the air velocity does not

affect the feed rate if it is less than a certain critical value. However, if this velocity is exceeded the drop-out box can become choked with product because the air swirl is then strong enough to prevent it from being entrained into the pipeline. The result of this is a significantly restricted feed rate. In Chapter 7 the following expression for predicting this critical velocity (V_c) was proposed:

$$V_c = C_cP_* \ (ga \ \frac{\rho_s}{\rho_a})^{\frac{1}{2}}$$

(7.1)

where ρ_s is the poured bulk density of the solids, ρ_a is the air density in the drop-out box, a is the length of the box, g is the gravitational constant and C_cP_* is an empirical factor which can be obtained from Figure 7.80.

An important implication of equation 7.1, which is supported by the experimental results, is that materials with a bulk density grater than about 500 kg/m^3 will not choke at pick-up velocities normally used in pneumatic conveying systems. Conversely, although they have not been tested in this work, care should be taken with materials having a bulk density lower than 200 kg/m^3 because the trends suggest that these could choke at normal velocities.

8.1.6 Air leakage

As well as providing information about the entrainment process the research has also demonstrated the importance of considering the effect of air leakage on the pocket filling process. This was best illustrated by the results obtained with the pulverised coal; from which it was impossible to identify any significant differences between the performnces of the various entrainment configurations because of restricted pocket filling. At the present time there is no proven method for predicting the effect of air leakage on pocket filling, but the model proposed in Chapter 4 could provide the basis for achieving this.

The research has also shown that the air leakage itself can be predicted by a method similar to that proposed by Reed (11). The difference being the value of the blockage factor (b) used in equation 2.23, that is:

$$V = b \ u \ L \ c$$

(2.23)

In Reed's model the value of b is determined from Figure 2.26 which was derived from experimental data obtained with a rotary valve feeding a simple pressurised container.   Whilst this gives acceptable results for rotary valves used in such situations, for valves which are used to feed pneumatic conveying pipelines a better estimate of the blockage factor is given by Figure 7.99 which was derived from the results of this research.

8.1.7 Summary

To summarise the various factors which are now known to affect the performance of a rotary valve used to feed a pneumatic conveying line Figure 8.1 has been constructed.   This is similar to Figure 2.33 in Chapter 2 but also considers the influence of the drop-out box and air leakage on valve performance.

In Figure 8.1 curve A represents the typical characteristics of a rotary valuve used to feed a positive pressure pneumatic conveying line. Line B represents the complete pocket filling model and curve C the incomplete pocket filling models of Reed (11) and Jotaki & Tomita (10, 12 & 13).
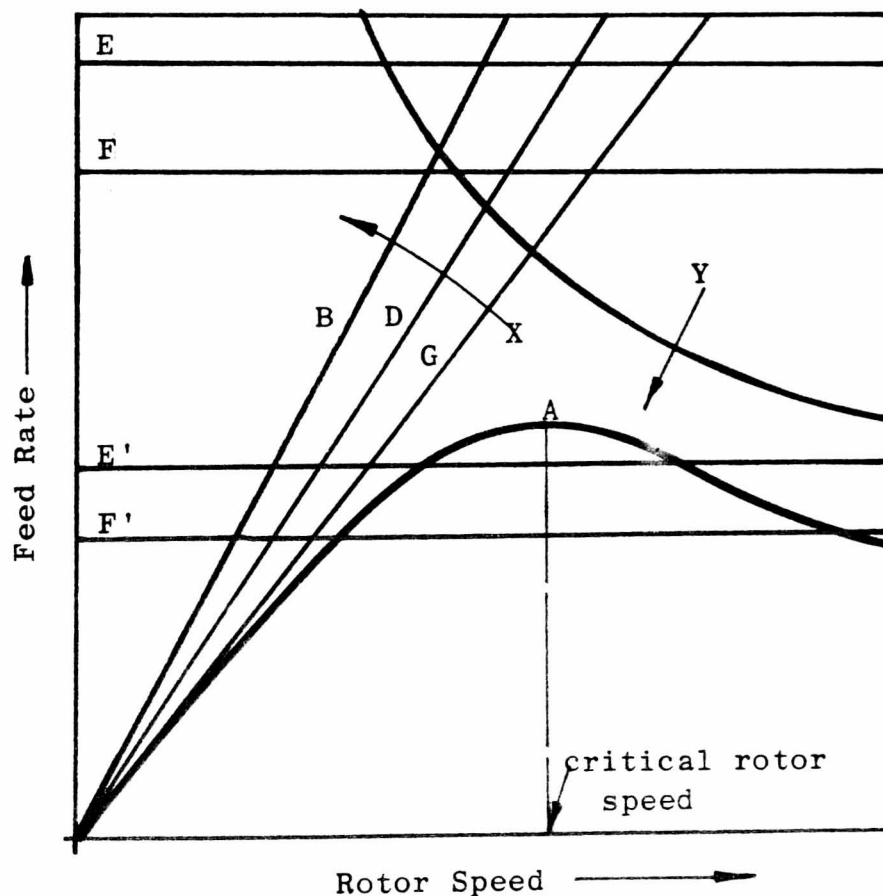
Figure 8.1   Actual and Predicted Characteristics of a Rotary Valve

The intersection of these two curves give a prediction of the 'critical rotor speed' at which the throughput is a maximum.. Below the critical rotor speed the throughput is overestimated by line B and line D gives a better prediction of the performance. Line D is obtained by multiplying the complete pocket filling model by a filling factor (α), such as that obtained from the design curves suggested by Reed, see Figure 2.11. However, this still invariably overestimates the feed rate and so a further correction needs to be made to account for the effect of the drop-out box. This is illustrated by line G and the arrow X, which indicates the effect of increasing the drop-out box volume. Hence line G would approach line D for a box with a large volume.

As already stated, curve C represents the incomplete pocket filling model as suggested by Reed and Jotaki & Tomita. However, in practice this will overestimate the performance of the valve because of the adverse effect of air leakage on pocket filling. Consequently, the actual performance will follow a curve similar to that produced by equation 4.7 of this study, which is similar in form to Reed's equation for incomplete pocket filling but inforporates a 'leakage factor' (K_ℓ) to allow for the effect of air lekage through the internal clearances of the valve. The arrow Y shows the effect of increasing air leakage on curve C.

Lines E and E' show the effect of the hopper discharge characteristics on the overall performance of the feeding system. If the discharge rate of the hopper is greater than the maximum take-away rate of the valve the hopper characteristics will lie above the valve characteristics as indicated by line E. However, if the discharge rate of the hopper is less than the take-away rate of the valve the feed rate will be restricted, as shown by line E'. The choked feed characteristics of the drop-out box will restrict the throughput in a similar way to the hopper characteristics as shown by lines F and F', with the actual feed rate dependent upon the size and shape of the drop-out box.

8.2 Value of the Research to Industry

The value of this research to industry is difficult to quantify in financial terms but, since it is estimated that rotary valves are used in more than 50 per cent of all pneumatic conveying systems, there should be, at the very least, widespread interest in the results. Furthermore, if it is accepted that these results are representative of the performance of industrial systems, it is not unreasonable to use them as the basis for guidelines for interfacing rotary valves with conveying pipelines.   This would then enable systems to be designed with more confidence than was possible previously and thereby satisfy one of the principal objectives of this work.   With this in mind the following guidelines have been produced.

8.3 Guidelines for Interfacing Rotary Valves with Pneumatic Conveying Pipelines

i) Any suitable orientation of the rotary valve with respect to the pipeline may be used without adversely affecting the feed rate which can be achieved.

ii) The direction of rotation of the valve rotor with respect to the direction of the conveying air stream does not affect the feed rate which can be achieved.

iii) Any obstructions, deflection plates or flow constrictions in the drop-out box chamber should be avoided.

iv) For most products there is little point in using drop-out boxes having complex shapes; a simple transition shape two or three pipe diameters deep will usually provide satisfactory performance.

v) The smallest internal dimension of the drop-out box should be at least three times the largest particle size to minimise the risk of mechanical blockage.

vi) To optimise the entrainment efficiency with fine particle products the depth and volume of the drop-out box should be made as large as reasonably possible.

vii) To minimise the risk of choking the drop-out box excessive pick-up velocities should be avoided.

viii) The blowing seal type of rotary valve provides a more consistent feed rate and a better overall volumetric efficiency than the drop-through type for fine cohesive materials.   However, the use of this type of valve should be avoided when handling abrasive and erosive products.

It should be remembered that the above guidelines have been compiled from the results of research conducted with a positive pressure conveying system. In the absence of any other information it is suggested that the same guidelines be used for negative pressure systems with appropriate caution.

8.4 Recommendations for Further Work

8.4.1 Introduction

While it is evident that the work presented in this thesis makes a significant contribution towards the current understanding of the interaction between rotary valves and pneumatic conveying pipelines, it is equally evident that it could be usefully complemented by further investigation.

Since the work presented here was the first to investigate this subject in detail, it was necessary to establish the concept of the 'feeding factor'. This is similar to the 'filling factor' proposed by Reed (11), but quantifies the overall ability of a rotary valve to feed a conveying system and not the performance of a valve in isolation. Consequently it is recommended that this approach is also adopted in the further work suggested here.

8.4.2 Pocket Filling

Both this work and previous investigations have shown that the pocket filling process of a rotary valve is affected by the air leakage resulting from feeding a positive pressure conveying system. This may be considered as an indirect effect of the interaction with the pipeline but, as shown by the results obtained for the pulverised coal, it can severely limit the overall performance. In Chapter 4 a method of modelling this effect was proposed which successfully predicted the correct trends but unfortunately overestimated the reduction in feed rate. Therefore, further work is needed either to improve this model or to develop an alternative. One possible approach could be to use the Ergun equation (56) in the derivation of the pocket filling model rather than the Carman equation (14) used in the model described above. This would take account of the body forces acting on the particle entering the valve as well as the viscous forces, but would not lead to a single simple material characteristic factor.

8.4.3 Air Leakage

The prediction of the air leakage through rotary valves is another area where further work is recommended. When compared with the work of Reed the results of this work appear to show that the air leakage through a rotary valve used to feed a moving airstream is less than that through a similar valve used to feed static air at the same pressure. Consequently, it is suggested that a single rotary valve be tested in both situations and with the same materials in order to obtain a direct comparison.

8.4.4 Drop-out Box Configurations and Other Materials

Since this work has investigated the performance of conventional transition shaped drop-out boxes, a logical development of this would be to examine the performance of other drop-out boxes. The testing of other materials would also be invaluable, particularly with regard to establishing an improved method for predicting the pick-up velocity at which choking occurs.

8.4.5 Vacuum Systems

The work reported in this thesis has been concerned only with the interaction between rotary valves and positive pressure conveying systems. However, it is very common to use rotary valves to feed vacuum conveying systems and at the present time we can only speculate about the entrainment characteristics of such arrangements. Nevertheless, the view of the author is that the entrainment characteristics of vacuum systems will be very similar to those of positive pressure systems because the air swirl which dominates the flow patterns in the drop-out box would still be present. The reason for suggesting this is because the air swirl results from the interaction between the conveying airstream and the 'captive' volume of air in the drop-out box; which would be essentially the same in both types of system. Consequently there is no reason to believe that the overall entrainment characteristics will be significantly different. In particular, it is believed that the phenomenon of choking would still occur in vacuum systems and that the relative sizes of the rotary valve and drop-out box would still have a measurable effect on performance.

In order to test the above reasoning it is recommended that a programme of work be undertaken to investigate the entrainment characteristics of vacuum systems. This would fill a serious gap in our present knowledge and might also lead to a better understanding of entrainment in positive pressure systems.

8.4.6 Multiple Feed Points

It is quite common for there to be more than one feed point into a pneumatic conveyor, and if these are used simultaneously it follows that there will be material in the airstream prior to it entering the downstream drop-out box(es). At the present time the effect of this on the entrainment of material from the downstream box is not known but it seems reasonable to expect that it could be significant. Therefore, an investigation of this subject could provide valuable information.

8.4.7 Bends and Other Downstream Disturbances

In the experimental work conducted for this research the first bend in the conveying pipeline was approximately 12 metres downstream of the rotary valve and drop-out box. This arrangement was used deliberately in order to minimise the effect of the bend on the entrainment process. However, in many industrial systems the first bend is placed immediately after the rotary valve. Consequently it would be very interesting to know the effect of this, or any other downstream disturbances, on the performance of the system and hence provide some guidelines for positioning rotary valves with respect to downstream bends.

References

1. **Dobie W**
    'Letter from W Dobie, ICI Ltd to the British Materials Handling Board', 22nd November 1979.

2. **Johanson J R**
    'Method of Calculating the Rate of Discharge from Hoppers and Bins'. Trans Min Engrs AIME, Vol 232, p 69-80, 1965.

3. **Williams J C**
    'The Rate of Discharge of Coarse Granular Materials from Conical Mass Flow Hoppers'. Chem Eng Sci, Vol 32, p 247-255 1977.

4. **Carleton A J**
    'The Effect of Fluid Drag Forces on the Discharge of Free Flowing Solids from Hoppers'. Power Technology, Vol 6, p 91-96, 1972.

5. **Beverloo W A**
    Lenigen H A
    van de Velde J
    'The Flow of Granular Solids through Orifices'. Chem Eng Sci, Vol 15, p 260-269, 1961.

6. **McLean A G**
    'Flowrate of Simple Bulk Solids from Mass-Flow Bins". PhD thesis, University of Wollongong, Australia, 1979.

7. **Nedderman R M**
    Thorpe R B
    'The Rate of Discharge of Powders". IMechE seminar on 'Bunker/Feeder Interface Problems' 4th October 1983, London UK

8. **Arnold P C**
    McLean A G
    Reed A R
    'The Effect of Bulk Drag Forces on the Discharge Rate of Powders from Mass Flow Bins'. To be published.

9. **Al-Din N**
    Gunn D J
    'Metering of Solids by a Rotary Valve Feeder'. Powder Technology, Vol 36, p 25-31, 1983.

10. **Jotaki T**
    Tomita Y
    'Performance Characteristics of a Rotary Feeder (Part I)'. J Res Assoc of Powder Technology Japan, Vol 7, No 6, p 58-61, December 1970, (in Japanese).

11. **Reed A R**
    'The Effect of Adverse Air Pressure Difference on the Performance of a Rotary Valve used for the Flow Control of Bulk Materials'. PhD thesis CNAA, Thames Polytechnic, London, July 1978.

12. **Jotaki T**
    Tomita Y
    'Feed Rate of a Rotary Feeder', Proc of JSME Conference No 748-3 (74-10 Kagoshima Local Conference) p 82-85 (in Japanese).

13. **Tomita Y**
    Jotaki T
    'Feed Rate of a Rotary Feeder'. Bulletin of JSME Vol 22, No 164, p 213-217, February 1979.

14. **Carman P C**
    'Fluid Flow Through Granular Beds'. Trans Instn Chem Engrs. Vol 15, p 150-166, 1937.

15. Westinghouse   'Derion Bulk Handling Equipment'.   Manufact-
    Systems Ltd   urers' literature.   Westinghouse Brake and
                       Signal Co Ltd.

16. Smoot Co   'Precision-Aire Feeders'.   Manufacturers'
                       trade literature.   Smoot Co. Box 3337,
                       1250 Kansas City, Kan 66103.

17. Finkbeiner T   'The Mechanism of the Rotary Airlock Feeder
                       for Bulk Material'.   VDI - Forschungsheft,
                       563, (1974), (in German).

18. Reed A R   'Estimating Air Leakage Through Rotary Valves'.
    Mason J   Bulk Storage Movement and Control.   January/
                       February 1977.

19. Sprout, Waldron   'Rotary Valves'.   Manufacturers' literature,
    & Co Inc   Bulk Materials Handling Bulletin 2810,
                       Sprout, Waldron & Co Inc.   Penn U SA
                       February 1985.

20. Masuda H   'Characteristics of a Rotary Feeder'.   J Res
                       Assoc of Powder Technology Japan, Vol 11,
                       Special Edition, p 4-14, 1974.

21. Kessel S   'An Investigation into the Flow Behaviour in
    Reed A R   the Entrainment Section of a Rotary Valve Fed
    Mason J   Pneumatic Conveying System'.   Proc Pneumatech I.
                       International Conference on Pneumatic Conveying
                       Technology, Stratford upon Avon, UK, May 1982.

22. Moseman M   'Polypropylene Powder Transfer'.   Proc 6th
                       International Powder and Bulk Solids Handling
                       and Processing Conference, Chicago U S A,
                       May 1980

23. Moseman M   Private Communication, November 1981.

24. Fischer J   'Tips on Choosing Rotary Feeders'.   Plant
                       Engineering, Vol 13, No 2, p 117-118, February
                       1959.

25. Todhunter G T   'Rotary Valves'.   Particulate Matter, p 73-81,
                       March 1973.

26. Wiesselberg E   'Rotary Airlocks'.   Chem Eng Prog. Vol 72, No 3,
                       p 76-77, March 1976.

27. Gerchow F J   'Selecting Rotary Feeder Vane Valves'.   Chem
                       Eng Prog. Vol 72, No 3, p 78-80, March 1976.

28. Widrich W G O   'Rotary Seals'. South African Mech Eng, Vol 26,
    Rose R   p 211-216, May 1976.

29. Perkins D E
    Wood J E

'Rotary Feeders - Operational Factors Affecting their Efficiency'. Bulk, p 47-49, July/August 1978.

30. Pittman E D

'Specifying Rotary Valves'. Chem Eng. p 89-95, July 1985.

31. Atkinson F M

'Pulverulent Material Conveying Apparatus'. US Patent No 2890914. June 1959.

32. CEA Carter Day

'Air Swept Feeder Valve'. Bulletin FV-6, CEA Carter Day, Minneapolis, Minnesota 55432.

33. Rota Val Ltd

'Blowing Seals Valves'. Manufacturers' trade literature DIRV-80/BS. Rota Val Ltd. Industry Park, Cricketts Lane, Chippenham, Wiltshire, SN15 3EQ.

34. Bush & Wilton
    Valves Ltd

Manufacturers' trade literature. Bush & Wilton Valves Ltd, Golden Valley Lane, Bilton, Bristol BS15 6LF.

35. Markham & Co
    Ltd

Manufacturers' trade literature. Markham & Co Ltd, Board Oaks Works, Chesterfield, Derbyshire S41 ODS.

36. Jones R H

'Pneumatic Transport Applied to Structural Concrete'. Paper A5 Pneumotransport I. September 1971.

37. Anon

'Will the "Concrete Cannon" become a Perfect Placer?'. Construction News, May 27th 1971.

38. Tolmachev V
    Kostylev A
    Tsyro V
    Grigoraschenko V
    Tkach K
    Fillipov V

'Improvements in or relating to Rotary Pocket Feeders for Materials'. British Patent 1572755, 1980.

39. Mucon Division
    of BSS Ltd

Drawing No 299508 'Entrainment Pan'. Mucon Division of BSS Ltd, January 1981.

40. Bush & Wilton
    Valves Ltd

Drawing No 0850/SS4 'Entraining Piece'. Bush & Wilton Valves Ltd, March 1973.

41. Bühler Miag
    (England) Ltd

Drawing No 360170-1-004 'Fluidstat Injector'. March 1980.

42. Waeshle

'Feeding Shoe'. Manufacturers' trade literature, Waeshle Maschinenfabrik GmbH, Postfach 2440, D-7980 Ravensburg.

43. Radmark
    Engineering

Drawing No D-1017A '12 inch nominal T-injector'. Radmark Engineering, April 1976.

44. **Tyrrell P**   Private communication, October 1984.

45. **Gerchow F J**   Private communication.

46. **Gerchow F J**   'Conveying of Whole English Walnuts'. Proc Pneumatech 2 International Conference on Pneumatech Conveying Technology, Canterbury, UK, September 1984.   Later published by J of Powder & Bulk Solids Technology Vol 8, No 4, p 10-15, December 1984.

47. Birchenough A   'The Application of Laser Measurement Techniques to the Pneumatic Transport of Fine Particles'. PhD thesis, CNAA, Thames Polytechnic, London, September 1975.

48. Matsumoto S   'Minimum Transport Velocity for Horizontal
    Hara M   Pneumatic Conveying'.   J Chem Eng Japan,
    Saito S   Vol 7, No 6, p 425-430, 1974.
    Maeda S

49. Matsumoto S   'Effect of Particle Size on the Minimum Transport
    Kikuta M   Velocity for Horizontal Conveying of Solids'.
    Maeda S   J Chem Eng Japan, Vol 10, No 4, p 273-279, August 1979.

50. Mills D   'The Influence of Velocity in Pneumatic
    Mason J S   Conveying'.   International Powder and Bulk Solids Handling and Processing Conference, Chicago USA.   Organised by Cahners Exposition Group, May 1982.

51. Stoess H A   'Pneumatic Conveying'.   Wiley-Interscience, John Wiley & Sons Inc, 1970 ISBN 471 82690 4, Chapter 3, p 76-77.

52. Stacey R B   Lecture presented at Short Course in 'Pneumatic Handling of Bulk Materials' Thames Polytechnic, 5th-8th May 1981.

53. Jotaki T   'Feed Stoppage Characteristics of a Rotary
    Tomita Y   Feeder'. Micrometrics, Vol 18, p 61-65, 1973
    Dateki S   (in Japanese).
    Morihata M

54. Woodcock C R   'The Flow of Bulk Solids in an Air-Assisted Gravity Conveyor'.   PhD thesis, CNAA, Thames Polytechnic, London, October 1978.

55. Geldert D   'Types of Gas Fluidization'.   Powder Technology, Volume 7, p 285-292, 1973.

56. Ergun S   'Fluid Flow Through Packed Columns'.   Chem Eng Prog, Vol 49, No 2, p 89-94, February 1952.

57. Simon-Solitec Ltd   'Simon Bin Activator, 600 mm diameter, machine
                           No M97003.' Simon-Solitec Ltd, Bristol Road,
                           Gloucester GL2 6BY.

58. Woodcock C R (Ed)   Intensive Short Course Notes on 'Pneumatic
                           Handling of Bulk Materials'. 5th-8th May
                           1981.

59. Wade Eng Ltd   Crowhurst Road, Brighton BN1 8AJ, England

60. Earles S   'Pulsating Flow Measurement - A Critical
    Jeffery B   Assessment'. ISO/TC 30/WG4 (United Kingdom - 7)
    Williams T   February 1967.
    Zarec J

61. Waters T   'Measurement of Pulsating Air Flow by Means of
                           a Bi-Directional Orifice Meter'. Proceedings
                           of the Inst of Mech Engrs, Vol 182, Part 3H,
                           1967-68.

62. Marcus R   'The Influence of Low Frequency Pressure
                           Pulsations on the Performance Characteristics
                           of a Dilute Phase Pneumatic Conveying System'.
                           Proc Pneumotransport 4. International
                           Conference on the Pneumatic Transport of Solids
                           in Pipes. Paper A5, p 49-60.

63. Jeffery B J   Private communication, September 1982.

64. British Standards   'Methods for the Measurement of Fluid Flow in
    Institution   Pipes'. Part I Orifice Plates, Nozzles and
                           Venturi Tubes. BS 1042: Part I 1964 UCD 532.54.08

65. Kessel S R   'The Relationahip Between Power Consumption and
                           Pick-up Velocity in a Dilute Phase Pneumatic
                           Conveying System'. Proc 9th Annual Powder and
                           Bulk Solids Conference, Chicago USA, 15th-17th
                           May 1984.

66. Kessel S R   'A Review of Methods Used for Predicting the
                           Power Requirements of Dilute Phase Pneumatic
                           Transport Systems'. Proc International
                           Symposium-Workshop and 16th Annual Meeting of
                           the Fine Particle Society, Miami Beach, Florida
                           USA, 22nd-26th April 1985.

67. Blackmore D I   Comments made at the fifth meeting of the Rotary
                           Valve/Pneumatic Conveying Research Project
                           Group. 29th March 1984, Thames Polytechnic,
                           London

PNEUMATIC CONVEYING

Research aims to improve rotary valve performance

With the intention of improving their understanding of rotary valve performance 11 UK companies are jointly guiding and sponsoring a research programme at Thames Polytechnic. This work has generated much interest and ways of making the results of the project more widely available are currently being discussed

Pneumatic conveying systems which consist of a Roots-type blower, rotary valve, pipeline and separator are probably the most common type of pneumatic system for handling bulk solids. Although they are essentially a simple system, it is not uncommon to hear equipment users complain about problems such as insufficient throughput, pipeline blocking, premature wear of pipework, product degradation and excessive power consumption.

These problems are often due to the lack of attention paid to the various factors involved in feeding the product into the pipeline. For example: the installation of the wrong type or size of valve can lead to insufficient throughput, excessive air leakage through the valve to pipeline blocking and high entrainment velocities causing excessive plant wear, undesirable product degradation and high power consumption. A potential user can minimise the likelihood of such problems occurring by employing a reputable and experienced system designer who will seek advice from the rotary valve supplier regarding the most suitable type of feeder for the particular application.

However, despite the vast wealth of experience within industry, many valve manufacturers, system designers and user companies agree that there is still much scope for refining their techniques and products. This can be achieved by improving their knowledge of the way in which the parameters relevant to the feeding zone influence the performance of pneumatic conveyors.

With the intention of improving their understanding of rotary valve performance, eleven British companies, comprising manufacturers of rotary valves, system designers and user companies are jointly sponsoring and guiding a programme of work at the Bulk Solids Handling Unit at Thames Polytechnic. The Unit's involvement in industrially orientated research and consultancy work in the general area of pneumatic conveying is well known, as is its intensive short courses on pneumatic transport, hopper design and bulk solids handling. The sponsoring companies
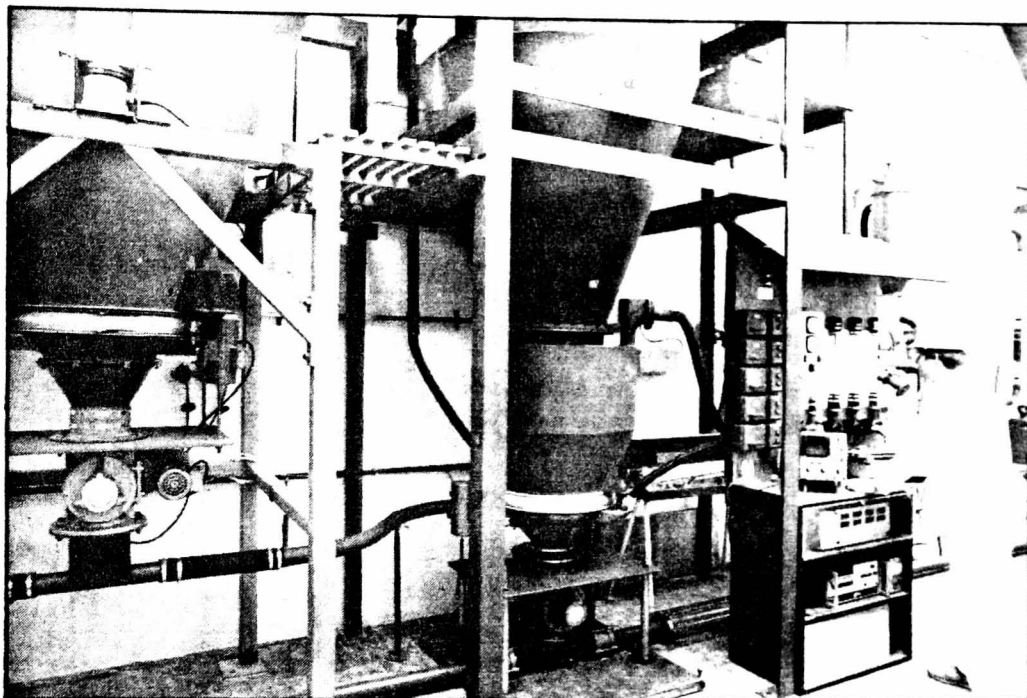
Above. View of the test rig installed in the units laboratories at Woolwich. Below. One type of rotary valve currently undergoing test work
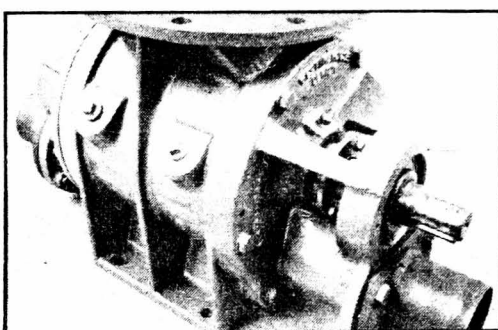
have provided both the equipment and funds needed to build a pilot size rig necessary to generate the all important data.

This rig, which has been installed in the Unit's laboratories at Woolwich, London, is a versatile pneumatic conveying system operating on a recirculatory basis. Means for easily changing the type of rotary valve, its orientation, the drop-out box configuration and for varying the valve speed and air flow rate are incorporated. The instrumentation consists of a range of meters to measure air and product flow rates, air leakage through the rotary valve, conveying line

pressure drop and power consumption. Obviously the results will depend upon the product conveyed and so the rig has been designed to handle products ranging from lump coal to fine flour.

The results of the research programme are received by the sponsoring companies through quarterly progress meetings. To date the work has provided the companies with an improved understanding of the way in which air and products flow through the drop-out box, that is, the important interface between the rotary valve and conveying line. Favourable entrainment configurations and conveying parameters have been identified for a number of materials and this newly acquired technology has already been put to good use in industry. Not surprisingly this work has generated considerable interest with organisations not involved in sponsoring the project and ways of making results more widely available are currently being discussed. **SH 504**

Integration of Equation 4.3

$$\frac{dS}{dt} = g - K(G + S) \qquad\qquad (4.3)$$

By re-arranging equation 4.3 we can write:

$$\frac{dS}{(g - KG) - KS} = dt$$

and hence,

$$-\frac{1}{K} \ln((g - KG) - KS) = t + X_1$$

where X_1 is a constant of integration which may be evaluated by applying the boundary condition $S = 0$ when $t = 0$. Hence:

$$X_1 = -\frac{1}{K} \ln(g - KG)$$

and

$$-\frac{1}{K} \ln((g - KG) - KS) = t - \frac{1}{K} \ln(g - KG)$$

or, alternatively

$$S = \frac{g}{K} - \frac{(g - KG)}{K} \exp(-Kt) - G$$

Now, since $S = \dfrac{dy_b}{dt}$ we may write:

$$dy_b = \frac{g}{K} dt - \frac{(g - KG)}{K} \exp(-Kt) dt - Gdt$$

and hence,

$$y_b = \frac{g}{K} t + \frac{(g - KG)}{K^2} \exp(-Kt) - Gt + X_2$$

where X_2 is a constant of integration which may be evaluated by applying the boundary condition $y_b = 0$ when $t = 0$. Hence:

$$X_2 = \frac{(KG - g)}{K^2}$$

and,

$$y_b = (\frac{g}{K} - G)t - \frac{(g - KG)}{K^2}(1 - \exp(-Kt))$$

By re-arranging this last expression to put it in the same form as that used by Reed (11) in his expression for y_b, equation 2.15, it may be shown that:

$$y_b(t) = \frac{g}{K}(1 - \frac{GK}{g}) \; t - \frac{1}{K}(1 - \exp(-Kt))$$

or, alternatively

$$y_b(t) = \frac{g}{K}K_\ell \; t - \frac{1}{K}(1 - \exp(-Kt)) \qquad (4.5)$$

where K_ℓ is the 'air leakage' factor discussed in Chapter 4.

Calculation of the Minimum Fluidizing Velocity (U_{mf}) for the P.V.C. used by Jotaki et al (53)

For materials with a mean particle size between 50 and 500 μm Woodcock (54) has suggested the following simple correlation for the minimum fluidizing velocity:

$$U_{mf} = 420 \, \rho_p \, d_p^2$$

where U_{mf} is measured in m/s, ρ_b in kg/m^3 and d_p in m.   Since the P.V.C used by Jotaki et al had a mean particle size of 166 μm, this correlation may be used to provide an estimate of U_{mf}.

Mean particle size of the P.V.C. (d_p)   =   166 x 10^{-6} μm

Particle density of the P.V.C (ρ_b)   =   1400 kg/m^3

Hence,

$$\underline{U_{mf} = 0.016 \text{ m/s}}$$

Calculation of the Leakage Factor (K_{ℓ}) corresponding to the Feed Stoppage Condition reported by Jotaki et al (53)

The paper written by Jotaki et al (53) gives the following information about the characteristics of the P.V.C which they used in their experiments.

Mean particle size of the P.V.C (d_p)   =   166 x 10^{-6} μm

Particle density of the P.V.C (ρ_p)   =   1400 kg/m^3

Bulk density of the P.V.C (ρ_p)   =   524 kg/m^3

From this information it may be shown that the voidage of the P.V.C is 0.63.   Then, by assuming a value of 1.8 x 10^{-5} for the dynamic viscosity of the air (μ) and a value of 0.6 for the shape factor of the P.V.C (ϕ), the material characteristic factor (K) may be calculated using equation

2.14, that is:

$$K = \frac{180\mu}{\rho_p} \frac{(1 - \epsilon)}{\epsilon^3 (d_p \phi)^2} \qquad\qquad (2.14)$$

This gives the value of K for the P.V.C as 345.

As well as the above information Jotaki et al also state that the superficial air velocity through the cross-sectional area of the supply hopper was 0.017 m/s when the feed stoppage occurred. Dividing this by the voidage of the P.V.C will give the velocity of the air relative to the rotor pockets (G). The leakage factor K_ℓ may then be calculated by using equation 4.6a, that is:

$$K_\ell = 1 - KG/g$$

where g is the gravitational constant.

Following this procedure gives the value of K_ℓ at the feed stoppage condition reported by Jotaki et al as <u>0.05</u>.